Mechanistic and Phenotypic Characterisation of Rgg/SHP Quorum Sensing System in *Streptococcus pneumoniae*

Thesis submitted for the degree of
Doctor of Philosophy
at the University of Leicester

by

Iman Tajer Abdullah

Department of Infection, Immunity and Inflammation
University of Leicester

May 2019

Statement of Originality

This accompanying thesis submitted for the degree of PhD entitled "**Mechanistic and Phenotypic Characterisation of Rgg/SHP Quorum Sensing System in *Streptococcus pneumoniae***" is based on work conducted by the author in the Department of Infection, Immunity and Inflammation of the University of Leicester during the period between January 2015 and January 2018.

All the work recorded in this thesis is original unless otherwise acknowledged in the text or by references.

None of this work has been submitted for another degree in this or any other University.

Signed ………………………………   Date ………………………………

Mechanistic and Phenotypic Characterisation of Rgg/SHP Quorum Sensing System in *Streptococcus pneumoniae*

Iman Tajer Abdullah

Abstract

The Rgg regulators with their short hydrophobic signalling peptides (SHPs) form part of a quorum sensing system (QS) in Streptococci. They play an important role in stress response, sugar metabolism, and virulence. Therefore, blocking phenotypic manifestations of Rgg/SHP QS system would be an effective strategy to abrogate streptococcal virulence. In this study, I focused on Rgg/SHP144 quorum sensing system in the important human pathogen *Streptococcus pneumoniae* by evaluating the functional importance of SHP144 residues towards the transcriptional activation of the system and Rgg144 binding. This information would allow in depth understanding of the system's operation, and will be useful for developing anti-infectives that target Rgg/SHP144 system.

The results showed that most of selected SHP144 residues are required for *shp144* transcriptional activation, and residues at position I20 and P21 are critically important for mannose utilisation, capsule synthesis and oxidative stress resistance *in vitro* as well as for *in vivo* colonisation. Moreover, transcriptional activation of non-activating modified peptides mimics their binding capabilities, except that while SHP144-C13V17A and SHP144-C13P21A modifications abolished transcriptional activation of *shp144* promoter, these modifications did not affect Rgg binding. SHP144-C13P21A modified peptide could competitively inhibit Rgg144 activation and decrease *shp144* induction in a dose-dependent and sequence-specific manner. This modified peptide has also the capacity to diminish pneumococcal growth on mannose and render pneumococci susceptible to oxidative stress.

QS systems are found widely in bacteria, and they are suggested to be potential anti-infective targets. Thus, this study lays the ground for developing effective inhibitors in future and demonstrates the potential utility of QS systems as anti-infective targets.

Publications

Aggarwal, S.D., Eutsey, R., West-Roberts, J., Domenech, A., Xu, W., **Abdullah, I.T.**, Mitchell, A.P., Veening, J.W., Yesilkaya, H. and Hiller, N.L. (2018). Function of BriC peptide in the pneumococcal competence and virulence portfolio. *PLoS Pathogens*, **14**(10), e1007328.

Glanville, D.G., Han, L., Maule, A.F., Woodacre, A., Thanki, D., **Abdullah, I.T**., Morrissey, J.A., Clarke, T.B., Yesilkaya, H., Silvaggi, N.R. and Ulijasz, A.T. (2018). RitR is an archetype for a novel family of redox sensors in the streptococci that has evolved from two-component response regulators and is required for pneumococcal colonization. *PLoS Pathogens*, **14**(5), e1007052.

Zhi, X., **Abdullah, I.T**., Gazioglu, O., Manzoor, I., Shafeeq, S., Kuipers, O.P., Hiller, N.L., Andrew, P.W. and Yesilkaya, H. (2018). Rgg-Shp regulators are important for pneumococcal colonization and invasion through their effect on mannose utilization and capsule synthesis. *Scientific Reports*, **8**(1), 6369.

Acknowledgments

First and foremost, I thank Almighty ALLAH for giving me the strength, knowledge and ability to persevere and complete this thesis satisfactorily.

I would like to express my sincere gratitude, appreciation and thanks to my supervisors Dr. Hasan Yesilkaya, Prof. Peter Andrew and Prof. Russell Wallis for their intellectual guidance and scientific support throughout this study. Special thanks to Dr. Hasan Yesilkaya for his continuous encouragement, patience and critical reading of this thesis. Without his precious support and guidance this thesis would not have been completed. I would also like to express my sincere gratitude to Prof. Peter Andrew and Prof. Russell Wallis for their invaluable suggestions, helpful advice and guidance throughout this project.

I would also like to thank my colleagues Banaz Kareem, Bayan Faraj, Ozcan Gazioglu, Hasan Kaya, Hastyar Najmuldeen and the members of lab 125 and 218 for their insightful discussions and friendship.

A special word of thanks also goes to Dr. Mohammed El-Mezgueldi in Biochemistry Department at Leicester University for his help in fluorescence spectroscopy experiments.

I wish to extend my gratitude to Ministry of Higher Education and Scientific Research in Iraq for funding my scholarship. I am also grateful to Iraqi Cultural Attaché and Kirkuk University for their assistance and generous support.

Special thanks and gratitude to my beloved husband. Words are never enough to express my sincere thanks and appreciation for his love and support. Last but not the least, I would like to thank my parents, siblings and my beloved family for their love and endless encouragement throughout my study.

Abbreviations

µg	Microgram
µl	Microlitre
µM	Micromolar
ABC	ATP-binding cassette
AHLs	Acyl-homoserine lactones
AIPs	Autoinducing peptides
Asp	Aspartate
BAB	Blood agar base
BHI	Brain heart infusion
bp	Base pair
BSA	Bovine serum albumin
CDM	Chemically defined media
CFU	Colony forming unit
CPS	Capsular polysaccharide
CSP	Competence stimulating peptide
dH_2O	Distilled water
DNA	Deoxyribonucleic acid
dNTP	Deoxynucleotide triphosphate
DTT	Dithiothreitol
FITC	Fluorescein isothiocyanate
FP	Fluorescence polarisation
Fuc	Fucose
g	Gram
Gal	Galactose
GlcNAc	*N*-acetylglucosamine
GalNAc	*N*-acetylgalactosamine
NeuNAc	*N*-acetylneuraminic acid
HK	Histidine kinase
kb	Kilobase
kDa	Kilodalton
L	Litre
LA	Luria Bertani agar
LB	Luria Bertani broth
M	Molar
mg	Milligram
ml	Millilitre
mM	Millimolar
mP	Millipolarisation
ng	Nanogram
nl	Nanolitre
OD	Optical density
ONPG	*O*-Nitrophenyl-β-D-galactopyranoside
PAGE	Polyacrylamide gel electrophoresis
PBS	Phosphate buffered saline
PCR	Polymerase chain reaction
QS	Quorum sensing

Rgg	Regulator gene of glucosyltransferase
RNA	Ribonucleic acid
RNAP	RNA polymerase
ROS	Reactive oxygen species
rpm	revolutions per minute
RR	Response regulator
SHP	Short hydrophobic peptide
TAE	Tris acetic acid EDTA
TFs	Transcription factors
THY	Todd- Hewitt yeast broth
EDTA	Ethylenediaminetetraacetic acid
UV	Ultraviolet
w/v	Weight per volume
x g	Gravity force
NADH	Nicotinamide adenine dinucleotide
SDS	Sodium dodecyl sulphate
Man	Mannose
IPTG	Isopropyl β-D-1-thiogalactopyranoside
TEMED	Tetramethylethylenediamine
TCSs	Two-component regulatory systems
v/v	Volume per volume
Glu	Glutamate

Table of contents

Chapter 1. Introduction

1.1. General features of *Streptococcus pneumoniae*

Streptococcus pneumoniae (known as the pneumococcus) is an anaerobic aerotolerant Gram-positive bacterium belonging to the genus Streptococcus (Bridy-Pappas *et al.*, 2005). It was first discovered in 1881 by George Miller Sternberg in the United States and by Louis Pasteur in France. The former name of *S. pneumoniae* was *Diplococcus pneumoniae* because of its appearance as pairs, and in 1974 this name was changed to *Streptococcus pneumoniae* because it grows in chains in liquid medium (Janoff and Musher, 2015). The pneumococcus is an encapsulated, non-motile, non-spore forming bacterium. It appears as lancet shaped diplococcus or short chains under a microscope with cell size ranging from 0.5 to 1.25 µm. Unlike other streptococcal species, it is sensitive to ethylhydrocupreine (optochin) discs and hydrolyses in bile salts. The pneumococcus is one of the fastidious microorganisms lacking the catalase enzyme, therefore requires a complex media containing a source of catalase such as blood agar for its growth (Tuomanen, 2006). The pneumococcal cells form α-haemolysis (green zone) around the grey-white colonies when grown on blood agar plates (Reller *et al*., 2008). In addition, the presence of 5% carbon dioxide promotes pneumococcal growth, however a fully anaerobic environment is necessary for 20% of newly isolated strains (Tuomanen, 2006). It can grow in a pH range between 6.5-8.3 and temperature between 25-42°C, however the ideal pH and temperature is 7.8 and 37°C, respectively (Terra, 2011). Genetically, *S. pneumoniae* contains 2–2.2 million base pairs and has more than 2000 genes in its genome (Mitchell and Mitchell, 2010), with a 39.7% of guanine–cytosine content (van der Poll and Opal, 2009). It has a distinct cell wall that lies under a capsule sheath, mainly composed of peptidoglycan layer (repeating units of *N*-acetylmuramic acid, *N*-acetylglucosamine, linked together by β1,4 linkages), teichoic acid, which is covalently bound to the peptidoglycan layer and lipoteichoic acid attached to phospholipids of the cell membrane (Maestro and Sanz, 2016).

1.2. Epidemiology of *Streptococcus pneumoniae* infections

Streptococcus pneumoniae is part of the respiratory commensal flora and resides asymptomatically in mucosal surfaces of the nasopharynx and upper airway of healthy individuals (Brooks and Mias, 2018). The nasopharyngeal colonisation rate varies between individuals and commonly depends on geographical area, age, genetic background, and socioeconomic conditions (Bogaert *et al*., 2004). A symptomatic carrier state is the principle reservoir of pneumococcal infections (Kadioglu *et al*., 2008), and considered as a platform for dissemination of pneumococcal infections within the population via direct contact with contaminated respiratory aerosols (Bojang *et al.*, 2015). The highest carriage rate was reported in children at the age of 3 years (55%), and this rate gradually declines with increasing age and stabilises at 8% in children older than 10 years (Bogaert *et al.*, 2004).

The pneumococcus stays as a carrier in the nasopharynx until preferred conditions arises that allows its transmigration to other sites of human body such as lungs, blood or meninges, causing an array of life-threating diseases such as pneumoniae, bacteraemia and meningitis. These diseases are collectively named invasive pneumococcal diseases (IPDs) (Conklin *et al*., 2014). IPDs are more common in children under 2 years, senior over 65 years old and patients with underlying conditions such as asplenia, diabetes mellitus, malignancies and immunodeficiencies (Janoff and Musher, 2015).

Pneumococcal diseases impose an enormous burden on public health in both developing and developed countries (Bogaert *et al*., 2004). According to World Health organization in 2007, the pneumococci are responsible for 14.5 million annual infections worldwide, and two thirds of pneumococcal infections occur in children in developing countries like Asia and Africa (O'Brien *et al*., 2009; Engholm *et al.*, 2017). Pneumococcal infections are also considered as one of a major global health problem in the world by killing more than 1.6 million people each year, and 0.7-1 million of deaths in children under 5 years of age particularly in developing countries (World Health Organization, 2007). More than 90% of deaths occur in developing countries (Johnson *et al*., 2010). This high death rate may be due to malnutrition, lack of appropriate diagnostics tests and treatment facilities in these countries. In addition, widespread HIV and influenza virus infections potentiate secondary pneumococcal infections which often lead to death (Short *et al*., 2012; Shrestha *et al*., 2013).

It has been reported that up to 15%-30% of pneumococcal pneumonia patients have pneumococci in their blood (Musher, 1992), and more than 20% of young infants die from pneumococcal septicaemia in developing countries (World Health Organization, 2012).

The pneumococcus also causes meningitis, the most life-threatening form of invasive pneumococcal diseases (Kastenbauer and Pfister, 2003). It accounts 50% of bacterial meningitis (Uchiyama *et al*., 2009) with global mortality rate around 50% in developing countries (World Health Organization, 2012).

Despite the availability of preventive therapies and improvement in the efficacy of antibiotics, the morbidity and mortality rates of IPDs remains high in industrialised countries (Ogunniyi and Paton, 2015; Chalmers *et al*., 2016). It was reported that each year 44.4/100 000 and 167/100 000 children under 2 year suffer from pneumococcal infections in Europe and the United States (World Health Organization, 2012) with an estimated 40,000 deaths annually in the USA (Obaro and Adegbola, 2002). The annual incidence of pneumococcal bacteraemia in the USA reaches up to 50000 cases, with a mortality rate of 20%. In addition, 15–50% of all community acquired pneumonia in the world are caused by the pneumococci with an estimated 100 per 100,000 adults each year in Europe and the USA (Verma and Khanna, 2012). Pneumococcal meningitis is also widespread in the USA with an estimated incidence of 3000-6000 cases each year with a mortality rate of approximately 30% (Gratz *et al*., 2015). In more than 58% of pneumococcal meningitis survivors, neurological deficits such as deafness, mental retardation and seizures can ensue (World Health Organization, 2012; O'Brien *et al*., 2016).

In addition to invasive diseases, *S. pneumoniae* also causes less serious but more prevalent localised diseases with high medical cost such as otitis media, sinusitis and conjunctivitis (Ogunniyi and Paton, 2015). The pneumococcus is the most prevalent cause of acute otitis media (AOM) accounting for 30%–50% of all acute otitis media cases worldwide (Verma and Khanna, 2012). It was reported that an approximately two thirds of children in the USA get one or more of pneumococcal otitis media episodes in their first years of life (Fletcher and Fritzell, 2012).

1.3. Evolution of antibiotic resistance within pneumococcal population

The β-lactam antibiotics including penicillin have been the first choice for treatment of pneumococcal infections (Cornick and Bentley, 2012), until the emergence of resistance in Australia in 1967. Since then, there is a steady increase in pneumococcal resistance to penicillin and other β-lactams, and currently it exceeds 50% of all pneumococcal isolates in some countries (Liñares *et al.*, 2010). Most important, resistance to penicillin has coincided with a significant increase in resistance to other conventional antibiotics such as macrolides, tetracyclines, chloramphenicol and co-trimoxazole (Cornick and Bentley, 2012). A study published by Active Bacterial Core Surveillance (ABCs) in 2016 showed that 2.2%, 30.7%, 6%, 12.2% of pneumococcal strains isolated from 2,720 cases are resistant to penicillin, erythromycin, co-trimoxazole and tetracycline, respectively (Centers for Disease Control and Prevention, 2016). Of more concern, 40% of pneumococcal isolates are found to be multidrug-resistant, with a high variation in resistance prevalence countries (Reinert, 2009). High resistance rate is attributed to selective pressure originated from widespread use of antimicrobial agents (Hicks *et al.*, 2011).

Resistance to penicillin emerges from mutations in penicillin binding proteins (PBPs), the target site of β-lactams. *S. pneumoniae* possesses six PBPs (1a, 1b, 2x, 2a, 2b, and 3), each with a different molecular weight. PBP membrane proteins are required for peptidoglycan biosynthesis and cell wall integrity (Kaplan, 2004). Thus, modifications in the PBPs, mainly in the transpeptidase domains of PBP1a, PBP2x and PBP2b, reduce the binding affinity of PBPs to penicillin and other βeta-lactams (Liñares *et al.*, 2010; Hakenbeck *et al.*, 2012). Resistance to penicillin requires alteration in PBP2b, whereas modifications in PBP2x and PBP1a are needed for high resistance in expanded spectrum cephalosporins (Coffey *et al.*, 1995). Recent studies have suggested that the high resistance to penicillin is due to the capability of pneumococci to acquire β-lactam resistant genes from other streptococci especially from *S. mitis* and *S. oralis* which reside in the same niche (Jensen *et al.*, 2015; Straume *et al.*, 2015). Such mosaic resistant genes contain sequence blocks that differ from those in susceptible pneumococci by up to 20% at the DNA level or 10% at amino acid sequence level (Hakenbeck *et al.*, 1999). For non-β-lactam antibiotics, the pneumococci have also evolved different resistance mechanisms. For example, macrolide resistance originates from modification in the target site, mediated by the production of 23S rRNA methylase (*erm*B) that adds a methyl group to an adenine nucleoside on the 23S rRNA and prevents macrolides as well as lincosamides and streptogramins B (MLS_B phenotype) from binding to the ribosome. Other macrolide resistance mechanisms include preventing macrolide accumulation by Mef efflux pump, which is encoded by *mef* gene (*mef*A or *mef*E), thereby generating M resistance phenotype, or by the less commonly occurring method, by introducing point mutations in domains II and V of 23S rRNA and in the genes encoding for ribosomal proteins L4 and L22, which confer a variety of macrolide resistance phenotypes (Liñares *et al*., 2010; McGee *et al*., 2015). Similarly, fluoroquinolone resistance arises from point mutations in genes encoding for topoisomerase IV and DNA gyrase in the quinolone resistance-determining regions (QRDRs) or by drug efflux (Eliopoulos, 2004; McGee *et al*., 2015). Other antibiotic resistance mechanisms include resistance to co-trimoxazole by mutations in dihydrofolate reductase gene (DHFR) for trimethoprim or dihydropteroate synthase (DHPS) for sulfamethoxazole (Adrian and Klugman, 1997; Maskell *et al*., 1997), or by acquisition of ribosomal protection proteins Tet(M) and Tet(O) in case of tetracycline (Widdowson *et al*., 1996), and acetyltransferase production in case of chloramphenicol resistance (McGee *et al*., 2015).

As discussed above, treatment of pneumococcal diseases is hampered by the rapid increase of resistance towards conventional antibiotics, therefore implementation of new strategies and discovery of novel drug targets that are effective and less prone to antibiotic resistance mechanisms, would be of great value. Thus, this study focuses on identifying microbial targets that can be utilised to develop effective anti-infectives in the future.

1.4. Vaccination against pneumococcal diseases

Pneumococcal resistance against commonly prescribed antibiotics is continuously increasing and becoming a major global health concern, threatening the treatment success in many countries. Thus, a new strategy is greatly needed to alleviate the burden of pneumococcal diseases. A part of this strategy is to prevent pneumococcal infections through immunisation. Indeed, a tremendous reduction in the incidence of pneumococcal diseases has been observed after the introduction of pneumococcal vaccines into routine immunisation schedules (Izurieta *et al*., 2018; Singh and Dutta, 2018). Plain polysaccharide (PPV23) and conjugate vaccines (PCVs) are the two available vaccines currently for use to eliminate pneumococcal infections (Feldman and Anderson, 2014; Singh and Dutta, 2018). These vaccines provide serotype-specific protection (Durando *et al*., 2013; Miyaji *et al*., 2015).

The 23-valent pneumococcal polysaccharide PPV23 or Pneumovax 23 was firstly licenced in 1983 and was used to vaccinate adults over 65 years of age and children older than 2 years who have underlying conditions such as HIV and severe chronic diseases (Hodder *et al.*, 2010). This vaccine contains 23 serotypes (1, 2, 3, 4, 5, 6B, 7F, 8, 9N, 9V, 10A, 11A, 12F, 14, 15B, 17F, 18C, 19F, 19A, 20, 22F, 23F, and 33F), covering approximately 85-90% of IPDs in the world (World Health Organization, 2008; Daniels *et al.*, 2016). This vaccine can provide protection for young adults against IPDs but has no role for reducing pneumococcal carriage or pneumococcal mucosal infections such as otitis media (Pletz *et al.*, 2008; Daniels *et al.*, 2016). Another concern is the poor immunogenicity of capsular polysaccharides, which provides a short-term protection against pneumococcal diseases. This is because stimulation of mature B cells by capsular polysaccharides produces IgM antibodies without induction of T-cells (Pletz *et al.*, 2008; Sings, 2017). Such immunological response lacks the capability to generate serotype-specific memory B cells, thus it is not recommended for use in younger infants, who have immature immune system and poor response to this vaccine (Pletz and Welte, 2015).

The limitations of PPV23 have been overcome by developing conjugate vaccines, which consist of capsular polysaccharides covalently attached to immunogenic carrier proteins (Singh and Dutta, 2018). The 7 valent capsular polysaccharides PCV7 (Prevnar, Pfizer) is the first conjugated vaccine launched in 2000 for use in young children in the USA and subsequently in other countries (Moffitt and Malley, 2011). This vaccine contains 7 of the most important pneumococcal serotypes (4, 6B, 9V, 14, 18C, 19F, and 23F) conjugated to diphtheria toxoid (CRM197) (Singh and Dutta, 2018). Low serotype coverage by PCV7 has led to the formulation of PCV10 and PCV13.

PCV10 (Synflorix) includes 1, 5, 7F in addition to seven serotypes of PCV7 incorporated to nontypeable *Haemophilus influenzae* protein D (Prymula and Schuerman, 2009), while PCV13 or Prevnar 13 was designed to include serotypes 1, 3, 5, 6A, 7F and 19A along with the 7 included in PCV7 (Jefferies *et al.*, 2011) with coverage reaching nearly 90% in 2011 (Prato *et al.*, 2016). This vaccine confers protection against the six additional serotypes (Shiri *et al.*, 2017) in particular 3 and 19A serotypes which are responsible for half of pneumococcal pneumonia in children (Olarte *et al.*, 2017). Thus, PCV13 has superseded the existing PCV7 and been approved for use in children aged 6 weeks-5 years and adults over 50 years (Sanford, 2012).

Unlike the PPV23, PCVs contain immunogenic proteins which allow activation of both B and T cells and generation of memory-B cells and mucosal immunity (Feldman and Anderson, 2014; Sings, 2017). These vaccines can protect individuals from both invasive bacteraemia, meningitis and mucosal pneumococcal infections, like otitis media (Pletz *et al*., 2008; Reinert *et al*., 2010). PCVs also offer herd immunity through reducing IPDs and carriages among vaccinated and unvaccinated population in all ages (Pletz *et al*., 2008; Yildirim *et al*., 2015) as well as decreasing the prevalence of antibiotic resistance clones (Kyaw *et al*., 2006). However, these effects are largely offset by the appearance of pneumococcal infections due to non-vaccine serotypes. This phenomenon is known as serotype replacement (Kyaw *et al*., 2006; Camilli *et al*., 2017).

Serotype replacement, incomplete serotype coverage and cost represent the main problems threatening the success of current vaccines especially in low-income countries (Kay *et al*., 2016; Wang *et al*., 2018). Therefore, there is a need to develop an efficacious vaccine covering a board range of serotypes, effective in all age groups, and inexpensive (World Health organization, 2008; Lin *et al*., 2015). Protein-based vaccines are currently being explored to be used as an alternative approach to overcome the shortcomings of current conjugated vaccines. One avenue could be to use conserved pneumococcal surface proteins like PspA, pneumolysin, PsaA, or PspC (Moffitt and Malley, 2011) that have been shown to be immunogenic (Zhang *et al*., 2002) and effective against pneumococcal infections in different animal models (Paton, 1998; Brooks-Walter *et al*., 1999). These proteins could be used as chimeric proteins or in conjugation with capsular polysaccharides (Darrieux *et al*., 2015; Lin *et al*., 2015). Another approach that is recently received more attention is whole cell unencapsulated killed vaccine (Moffitt and Malley, 2011). It is hoped that both of these approaches provide broad cross-protection against multiple pneumococcal strains in serotype-independent manner. To achieve these goals, more knowledge about pneumococcal disease pathophysiology is required to generate effective vaccine against life-threating pneumococcal infections.

1.5. Virulence factors and pathophysiology of pneumococcal diseases

One of the important features of pneumococcal biology is its versatility to survive and cause diseases in a variety of host tissues. *In vivo* environments are diverse, ranging from aerobic with low glucose in the respiratory track to fully anaerobic with a high level of glucose in the blood, in addition to different challenges either from the host's immune system or from other microbial inhabitants during attachment and invasiveness. Therefore, adaption to different environmental conditions and survival in various host tissues is a prerequisite for pneumococcal infections. The mechanisms that mediate these adaptions are poorly understood (Trappetti *et al.*, 2013). It is commonly believed that nasopharyngeal colonisation is the first step of pneumococcal diseases and a prelude to spreading the infections to other parts of human body (Koliou *et al.*, 2018). Host immune system and invasive properties of pneumococcal serotypes play a significant role in pneumococcal diseases (Bridy-Pappas *et al.*, 2005). Pneumococcal virulence factors play an important role in immune system evasion and pneumococcal interactions with host tissues (Brooks and Mias, 2018) (Figures 1.1 and 1.2).

Within minutes of entering into the nasal cavity, *S. pneumoniae* confronts several natural barriers such as mucus that hinder pneumococcal binding to the respiratory mucosal surface and its progression into host tissues (Short and Diavatopoulos, 2015). *S. pneumoniae* can protect itself from mucociliary clearance by expressing a negatively charged polysaccharide capsule (CPS), exoglycosidases enzymes and pneumolysin toxin.

Pneumococcal capsule is a major pneumococcal virulence determinant, present in almost all of clinical isolates (de Vos *et al.*, 2015). It consists of repeating units of oligosaccharides and acidic components such as D-glucuronic acid, ribitol, or arabinitol (Alonsodevelasco *et al.*, 1995). It provides protection against the adhesive effect of mucosal secretions by keeping the pneumococcal cells away from mucus by an electrostatic repulsion mechanism, allowing pneumococcal passage through the mucus layer and adherence to epithelial cells (Nelson *et al.*, 2007). Pore-forming toxin pneumolysin (Ply) can also inhibit epithelial cilia movement and disrupt human ciliated epithelium, promoting initial colonisation and subsequent invasion of the lower respiratory tract (Feldman *et al.*, 2002; Mook-Kanamori *et al.*, 2011). In addition, *S. pneumoniae* can also secrete a set of exoglycosidases like neuraminidase A (NanA), β-galactosidase A (BgaA) and β-*N*-acetylglucosaminidase (StrH) to cleave host glycoconjugates covering the mucosal layer and expose host receptors for adherence to epithelial cells (King *et al.*, 2006). Cleavage of host glycoconjugates results in liberation of a set of monosaccharides which can be utilised as a nutrient source in glucose-free mucosal surfaces (Burnaugh *et al*., 2008; King, 2010). In addition, exoglycosidases also deglycosylate mucus glycoconjugates, thus reducing mucus viscosity and protecting the pneumococci from mucus entrapment (Mook-Kanamori *et al*., 2011).

Exoglycosidases provide competitive advantages for pneumococci by cleavage of lipopolysaccharides of other nasopharyngeal inhabitants like *Haemophilus influenzae* and *Neisseria meningitidis* (Shakhnovich *et al*., 2002). It can also modify human host defence proteins such as human lactoferrin and immunoglobulin IgA2 (King *et al*., 2004), providing protection against the innate immune system and facilitate pneumococcal persistence in the respiratory tract. Deletion of neuraminidase impaired pneumococcal colonisation and otitis media in a chinchilla infection model (Long *et al*., 2004; Tong *et al*., 2000). Pneumococcal survival in the nasopharynx, lungs and the blood are also inhibited in mice infected with *nanA* or *nanB* mutants (Manco *et al*., 2006). The *nanA* mutant could not persist in the respiratory tract of infected mice more than 12 h following infection, whereas *nanB* mutant showed some resistance, but without increasing in the bacterial load. In addition, both mutants were unable to survive in the blood of infected mice and to cause sepsis. The involvement of NanA and NanB in nasopharyngeal colonisation was further supported by the report that neuraminidases are required for biofilm formation (Brittan *et al*., 2012; Blanchette *et al*., 2016).

After reaching the nasopharyngeal epithelium, the pneumococci undergo phase variation from opaque (thick capsule) to transparent variants (thin capsule) to facilitate pneumococcal attachment to host epithelial receptors and translocation to bronchi and the lungs (Kim and Weiser, 1998; Bogaert *et al*., 2004). Cell wall associated proteins also play an important role in pneumococcal interaction with host cell receptors. These proteins are anchored to the cell wall surface by one of three sequence motifs: LPxTG motif, a choline-binding domain, or a lipoprotein domain (Henriques-Normark and Tuomanen, 2013). Among cell wall associated proteins, choline binding proteins (CBPs) are the most important family found in all pneumococcal strains. This family includes 13-16 proteins noncovalently attached to cell wall teichoic acid such as pneumococcal surface protein C (PspC), pneumococcal surface protein A (PspA), and hydrolytic enzyme A(LytA). These proteins play important roles in cell-wall physiology, host–pathogen interactions, colonisation and virulence (Galán-Bartual *et al*., 2015).

Penicillin treatment and nutrient depletion in the late growth stationary phase expose the pneumococci to disintegration and lysis (Jedrzejas, 2001; Mellroth *et al*., 2012). Autolysin, LytA (*N*-acetylmuramoyl-L-alanine amidase) is the main enzyme that mediates cell lysis and the release of peptidoglycan, teichoic acids and other cellular components (Kadioglu *et al*., 2008). Cell lysis activates the complement system and stimulates the release of proinflammatory cytokines such as interleukin-1, causing damage to lung tissues and promotion of pneumococcal growth in the lungs and bloodstream. It is thought that such reaction may be responsible for morbidity and mortality of pneumococcal infections (Alonsodevelasco *et al*., 1995). Thus, loss of LytA attenuated pneumococcal pneumonia and bacteraemia in a murine infection model (Berry and Paton, 2000; Orihuela *et al*., 2004) as well as meningitis in rats (Hirst *et al*., 2008).

Additionally, LytA is involved in the release of important intra-cytoplasmic membrane toxin pneumolysin (Ply) (Mitchell *et al*., 1997; Jedrzejas, 2001). This toxin however can be released independently in the absence of autolysin activity (Balachandran *et al*., 2001; Mitchell and Mitchell, 2010). Pneumolysin is a part of pore-forming cytotoxin proteins, cholesterol dependent cytolysin, present in almost all pneumococcal clinical isolates (Kadioglu *et al*., 2008). It plays an important role in invasion and destruction of alveolar and pulmonary endothelial cells, causing edema and haemorrhage in the alveolar space. Disruption of the alveolar-capillary barrier causes alveolar flooding providing nutrients for pneumococcal growth and accelerating pneumococcal penetration into pulmonary interstitium and blood circulation (Rubins and Janoff, 1998; Jedrzejas, 2007). Absence of *ply* caused a significant reduction in pneumococcal load in the upper and lower respiratory tract in the acute pneumoniae murine model (Kadioglu *et al*., 2002), and pneumococcal inability to spread from the lungs to blood to cause sepsis (Orihuela *et al*., 2004). This toxin has also many adverse effects at sublytic concentration on immune system cell functions (Malley *et al*., 2003).

After passage of the respiratory epithelial barrier, the pneumococci encounter another physical barrier which is the extracellular matrix (ECM). The pneumococcal cells produce hyaluronate lyase to destruct hyaluronic acid and facilitate bacterial invasion and dissemination into underlying tissues (Jedrzejas, 2007). This enzyme has capacity to penetrate the blood brain barrier and CSF, and its effect on the development of pneumococcal meningitis has been demonstrated (Kostyukova *et al*., 1995; Zwijnenburg *et al*., 2001). Invasion of basement membrane and underlying ECM is further enhanced by direct interaction of pneumococcal adhesin and virulence factors A (PavA) and B (PavB) with extracellular-matrix components fibronectin and plasminogen (Holmes *et al*., 2001; Jensch *et al*., 2010). Both PavA and PavB are found to be required for full pneumococcal virulence, as deletion of *pavA* or *pavB* impaired pneumococcal colonisation and translocation to other tissues (Kadioglu *et al*., 2010; Paterson and Orihuela, 2010). The pneumococci also express surface proteins enolase, choline-binding protein E (CbpE) and glyceraldehyde-3-phosphate dehydrogenase (GAPDH), which are important for interaction with plasminogen and plasmin and disruption of interepithelial adherence junction proteins like cadherin, thus accelerating pneumococcal migration and invasion into vascular endothelial layer (Attali *et al*., 2008).

After dissemination into blood circulation, the capsule polysaccharide protects the pathogen from phagocytosis and complement-mediated clearance through impeding C3b/iC3b deposition on the pneumococcal surface, mediated by both classical and alternative complement pathways and by inhibiting the binding of immunoglobulin IgG and CRP to bacterial surface (Hyams *et al*., 2010). Most importantly, the pneumococcal capsule varies between strains, and so far, more than 97 capsular polysaccharide serotypes have been identified (Geno *et al*., 2015). Each serotype has distinct biochemical composition and antiphagocytic capability for causing disease. The amount of capsule is also important, as thick capsule confers systemic invasion and phagocytic resistance (Henriques-Normark and Tuomanen, 2013). Thus, loss of capsule results in greater deposition of antibodies and complement system on pneumococcal cells (Bogaert *et al*., 2004) and render them less virulent (Henriques-Normark and Tuomanen, 2013). Pneumococcal surface proteins such as pneumolysin act along with the capsule to prevent phagocytosis and evasion of the host immune system (Mitchell *et al*., 1991). With high titre bacteraemia, the pneumococci breach the blood–brain barrier and penetrate endothelial junctions to access CSF and brain parenchyma (Henriques-Normark and Tuomanen, 2013). Binding of CbpA to laminin receptor (LR) on microvascular endothelial cells (Orihuela *et al*., 2009), and NanA through its laminin G-like lectin domain (Uchiyama *et al*., 2009), would provide further adhesion to endothelial cells and invasion of meningeal cells. Pneumococci with transparent capsule increase pneumococcal invasion into brain endothelial cells up to six-fold (Ring *et al*., 1998). Ply has shown to play an important role in brain damage (Hirst *et al*., 2008).

Although the role of many virulence factors in the pathogenicity of *S. pneumoniae* has been reported (Figures 1.1 and 1.2), the expression kinetics of these factors remain elusive. Limited information is available about virulence gene expression in the presence of different environmental conditions. Therefore, the study of transcriptional proteins in depth are of high importance to fully understand the role of virulence proteins in pneumococcal colonisation and virulence.

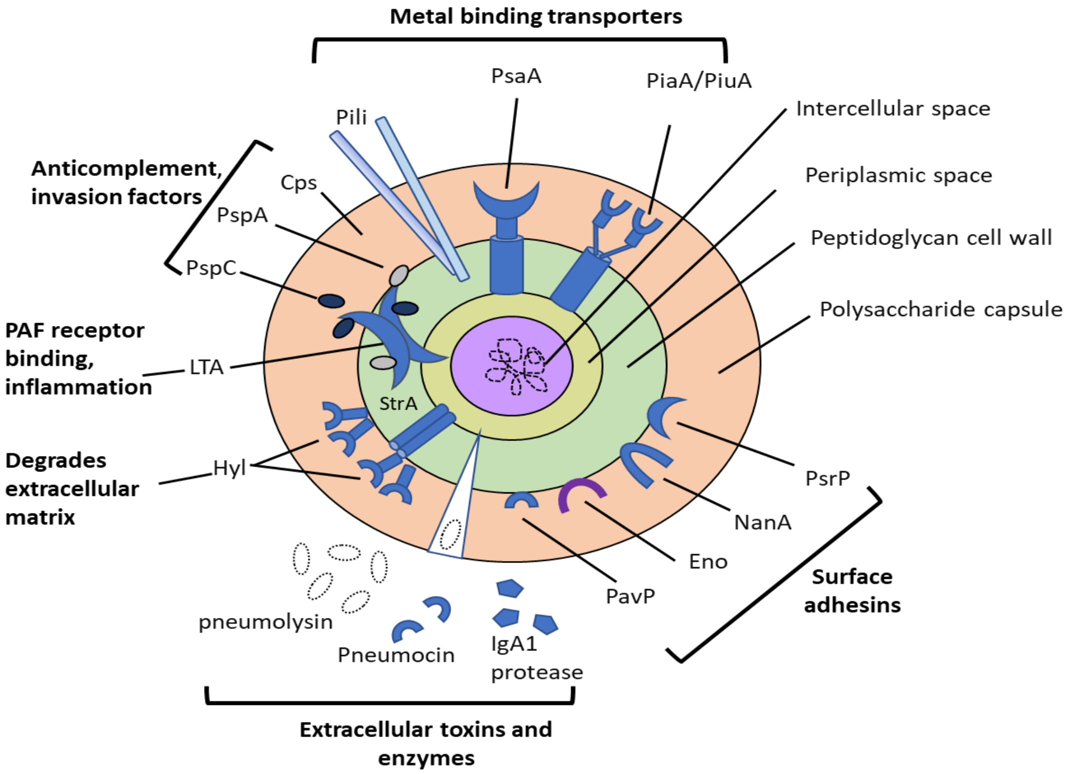

Figure 1.1: Schematic diagram representing virulence factors of *Streptococcus pneumoniae*. PsaA (pneumococcal surface antigen A); NanA (neuraminidase A); Eno (enolase); LytA (autolysin A); Hyl (hyaluronate lyase), PspA and PspC (pneumococcal surface proteins A and C respectively); LTA (lipoteichoic acid); CPS (Capsular polysaccharide). This figure was constructed based on van der Poll and Opal (2009).

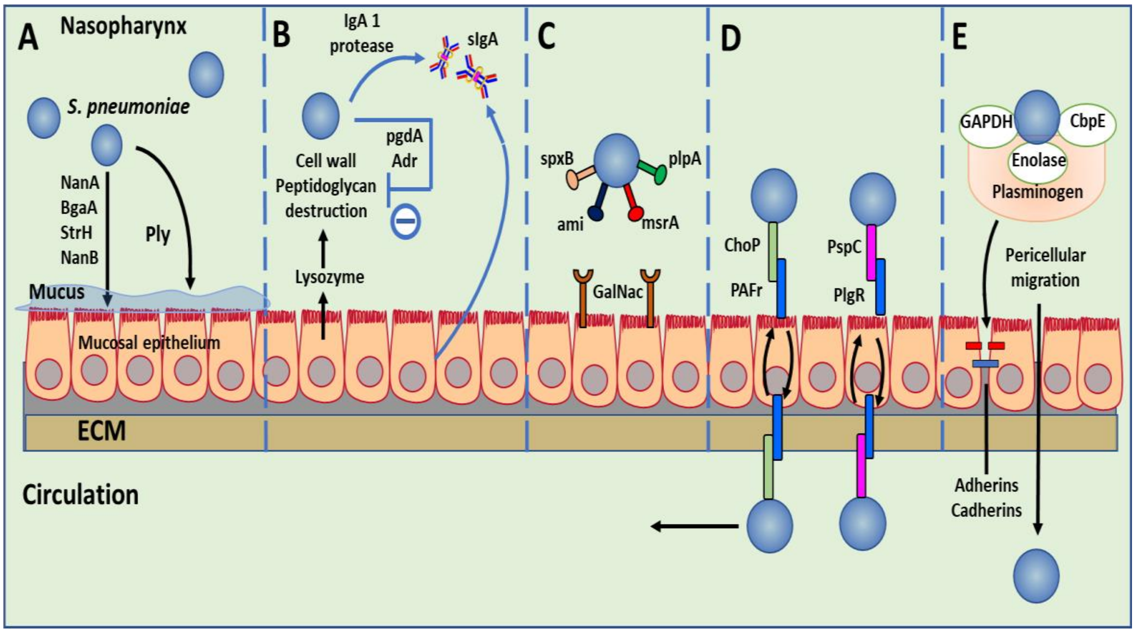

Figure 1.2: Schematic diagram representing colonisation and disease development in *S. pneumoniae*. **(A)** Mucus destruction by pneumococcal enzymes NanA, BgaA, StrH, and NanB, and reduction of epithelium cilia movement by Ply. **(B)** Resistance to lysosome by the activities of *N*-acetylglucosamine deacetylase A (PgdA) and *O*-acetyltransferase (Adr) enzymes, and sIgA by IgA1 protease. **(C)** Binding of pneumococcal cells to epithelial cells by using SpxB, Ami, MsrA, and PlpA proteins. **(D)** Translocation into epithelial cells through interaction of polymeric immunoglobulin receptor (pIgR) with pneumococcal surface protein C (PspC) or platelet-activating factor receptor (PAFr) with pneumococcal phosphorylcholine (ChoP). **(E)** Inter-and pericellular penetration by binding of GAPDH, CbpE, and enolase enzymes to plasminogen facilitating pneumococcal binding to epithelial cells and degradation of interepithelial adherens junctions. This figure was designed based on Mook-Kanamori *et al*. (2011).

1.6. The impact of environmental parameters on pneumococcal biology

1.6.1. Carbohydrates utilisation and its impact on pneumococcal lifestyle

S. pneumoniae is a fermentative microorganism, highly dependent on glycolytic metabolism to gain energy for growth and biosynthesis (Paixão *et al*., 2015a). Carbohydrate metabolism has a crucial role in pneumococcal pathogenesis as it specifically modulates the expression of virulence genes in fluctuating nutritional niche and provides essential nutrients for sustaining growth (Burnaugh *et al*., 2008; Paixão *et al*., 2015a). The pneumococcus differs from other pathogens residing in the same niche, as it has capacity to uptake more than 32 different sugars (Bidossi *et al*., 2012; Buckwalter and King, 2012), and has specific catabolic pathways for utilisation of galactose (Gal), mannose (Man), and *N*-acetylglucosamine (GlcNAc) (Bidossi *et al*., 2012; Paixão *et al*., 2015b). Genomic analysis has shown that approximately one-third of the pneumococcal genome encodes for proteins devoted for carbohydrate catabolism (Hoskins *et al*., 2001; Terra *et al*., 2010). Glucose, the preferential sugar for *S. pneumoniae* is nearly absent in the nasopharynx (initial niche for pneumococcal colonisation), less than 1mM compared with its content in blood (around 4-6 mM) (Philips *et al*., 2003). Thus, the pneumococci must endeavour to exploit other available nutrient resources such as *O*-, *N*-linked glycans and glycosaminoglycan present in airway secretions and decorated respiratory epithelium (Marion *et al*., 2012; Paixão *et al*., 2015b) and utilise them as an energy source during nasopharyngeal colonisation (Burnaugh *et al*., 2008; Yesilkaya *et al*., 2008).

A good example of host glycoproteins is mucin (Yesilkaya *et al*., 2008). Mucins are heavily glycosylated molecules, and the main component of mucus covering the surface of respiratory epithelial cells. Mucins are large molecules, 2-20x10^5 Dalton, mainly composed of *O*-glycans (50–90% carbohydrates) and protein backbone, which contains numerous tandem repeats (TR) enriched with serine, threonine, and proline amino acid residues (Rose and Voynow, 2006). The *O*-glycans contain 1-20 residues that are found as linear or branched structures. Mucins are mainly composed of *N*-acetylglucosamine (GIcNAc), *N*-acetylgalactosamine (GalNAc), sialic acid or *N*-acetylneuraminic acid (NeuNAc), galactose (Gal), fucose (Fuc) and sulphated sugars, which are connected to the protein core via a *N*-acetylgalactosamine moiety (Rose and Voynow, 2006; Lindén *et al*., 2008). Among these carbohydrates, galactose, *N*-acetylgalactosamine and *N*-acetyl glucosamine are the most predominate sugars in mucin structure (Terra *et al*., 2010). The pneumococcus expresses at least 10 genes encoding for glycosidase enzymes. Theses enzymes have a capacity to cleave different range of host substrates (mucin, glycolipids, and glycoproteins) providing sugar residues for bacterial growth, revealing receptors for adherence and colonisation, providing a competitive advantage to pneumococcus over other commensals residing in the same niche, and altering the clearance function of host defence molecules (King, 2010).

The most important exoglycosidases are neuraminidase A, B, and C (NanA, NanB and NanC), β-galactosidase A and C (BgaA and BgaC), *N*-acetylglucosaminidase (StrH), *O*-glycosidase (Eng), endo-β-*N*-acetylglucosaminidase (EndoD) and hyaluronate lyase (Hyl) (King, 2010). The pneumococci produce three distinct neuraminidases A, B and C. NanA and NanB are the most important enzymes, present in 100% and 96% of pneumococcal clinical isolates, respectively, whereas NanC is found in only 51% of pneumococcal strains and usually associated with systemic infection (Pettigrew *et al*., 2006) and haemolytic uraemic syndrome (HUS) in children (Janapatla *et al*., 2013). NanA differs from NanB and NanC, as it has anchoring LPXTG motif at the C-terminus end for binding to the cell surface and is responsible for cleavage of α2-3-, α2-6- and α2-8-linked sialic acid (Xu *et al*., 2008a), whereas NanB and NanC are secreted enzymes with a propensity for cleavage of α 2-3-linked sialic acid (Gut *et al*., 2008; Xu *et al*., 2008b). NanA and B have different pH optima (NanA active at pH 6.5-7.0 while NanB at pH 4.5) (Berry *et al*., 1996), and different molecular size, as NanA is much larger (115 kDa) than NanB (78 kDa) and NanC (82 kDa). NanC shares 50% sequence identity with NanB and 25% with NanA (Xu *et al*., 2008b). All of these provide evidence that these enzymes have different substrates and functions in different biological niches.

In addition, the pneumococcus has capacity for deglycosylation of *O*-linked glycans from mucin through cleavage of sialylated core-1-*O* linked glycans by *O*-glycosidase (Endo-α-*N*-acetylgalactosaminidase, Eng) (Marion *et al*., 2009) and galactose β(1-3) by BgaC (Jeong *et al*., 2009). This provides an indicator that the pneumococci have capacity to utilise both *N*- and *O*- linked glycans from mucin and mucin like proteins for energy requirements (Burnaugh *et al*., 2008; Marion *et al*., 2009).

It is important to mention that the initial cleavage of mucin by NanA is required for efficient sequential degradation of oligosaccharides by other glycosidases (King *et al*., 2006; Terra *et al*., 2010), as deletion of *nanA* impaired pneumococcal growth in media containing mucin (Yesilkaya *et al*., 2008). In addition, mutations of other glycosidases also hinder sequential deglycosylation of host sugars (King, 2010), as loss of *bgaC* decreased pneumococcal capacity to breakdown galactose in media containing mucin (Terra *et al*., 2010).

Recent studies showed that the pneumococci can utilise sialic acid, the most important carbohydrate present on *N*- and *O*-linked glycans as a carbon source for pneumococcal growth *in vivo* (Marion *et al*., 2011), as well as a receptor for adhesion and invasion, and a diffusible signal for enhancing biofilm formation (Trappetti *et al*., 2009; Gualdi *et al*., 2012). In addition, glycosaminoglycans (hyaluronic acid), present on the apical surface of epithelial cells can also be used as an energy source by degradation of hyaluronic acid by the action of hyaluronate lyase (Hyl) (Marion *et al*., 2012). Similarly, the hyaluronic acid capsule of other pathogens and free sugars supplied by host diet can also be utilised as an alternative carbohydrate resource during pneumococcal growth (Buckwalter and King, 2012; Marion *et al*., 2012).

A direct link has been found between carbohydrate metabolism and pneumococcal virulence (Carvalho *et al*., 2013a). Exoglycosidase enzymes have been shown to be important for pneumococcal pathogenesis and *in vivo* fitness. Their roles are supported by the findings that deletion of exoglycosidase enzymes caused a significant reduction in pneumococcal attachment to human epithelial cells, colonisation and invasiveness in mouse infection models (Marion *et al*., 2009; Terra *et al*., 2010; Brittan *et al*., 2012).

Furthermore, *S. pneumoniae* possesses a large number of sugar transporters, and more than 30% of all pneumococcal transporters are predicted to be involved in carbohydrate uptake (Tettelin *et al*., 2001; Bidossi *et al*., 2012). This number is significantly higher compared to those in other prokaryotes. This provides further evidence for importance of carbohydrates in the lifestyle of *S. pneumoniae* (Tettelin *et al*., 2001; Paixão *et al*., 2015a). Carbohydrate transporters in general are classified into three groups: phosphoenolpyruvate: sugar phosphotransferase systems (PTS systems), ATP-binding cassette (ABC) and ion gradient driven transporters. The pneumococci have 21 PTS systems, 7 ATP-binding cassette (ABC) and one sodium: solute symporter and a permease (Bidossi *et al*., 2012). Each of these transporters provides a distinct advantage for pneumococci during colonisation and transmission into other tissues. As mutations in carbohydrate transporter genes cause a significant loss of pneumococcal capacity for colonisation and disease development (Buckwalte and king, 2012).

Carbohydrate metabolic enzymes like pyruvate formate lyase (PFL), lactate dehydrogenase (LDH), and pyruvate oxidase (SpxB) have been found to be important for pneumococcal survival and virulence (Yesilkaya *et al*., 2009; Gaspar *et al*., 2014). PFL plays an important role in galactose metabolism, in particular in the mixed acid fermentation pathway, which is utilised under anaerobic conditions, and in the presence of a non-preferred sugar such as galactose. Deletion of *pflB* caused a significant reduction in ATP production and the amount of acetyl-CoA, which subsequently affect the fatty acid and choline biosynthesis (Yesilkaya *et al.*, 2009). Knockout of *ldh* (homolactic fermentation enzyme) also showed attenuation in pneumococcal pneumoniae and bacteraemia after intranasal and intravenous administration of pneumococci (Gaspar *et al.*, 2014). Similarly, inactivation of *spxB,* encoding for pyruvate oxidase, caused a significant reduction in pneumococcal growth in host tissues and virulence in different murine models for nasopharyngeal colonisation, pneumonia, and sepsis (Spellerberg *et al.*, 1996). This enzyme was found to play an important role in pyruvate oxidase-dependent metabolism through conversion of pyruvate to acetyl phosphate and CO_2. It is assumed that the impact of *spxB* mutation on pneumococcal virulence is due to the reduction in acetyl phosphate production, inhibition of adhesive protein expression, and alteration in sugar utilisation capacity and capsule production (Spellerberg *et al.*, 1996; Carvalho *et al.*, 2013b). The SpxB also plays a role in *in vivo* biofilm biogenesis through production of high amount of hydrogen peroxide that induces bacterial cell lysis and promotes extracellular matrix formation (Blanchette-Cain *et al.*, 2013; Blanchette *et al.*, 2016). It is also thought that attenuation in virulence of the *spxB* mutant might be due to reduction in pneumolysin production during late exponential phase (Bryant *et al.*, 2016). Likewise, deletion of *galK* (galactokinase) and *lacD* (tagatose 1,6-diphosphate aldolase), the key enzymes of Leloir and tagatose 6-phosphate galactose catabolic pathways, render the pneumococci unable to grow on galactose *in vitro* and abrogate virulence in respiratory infection model (Paixão *et al.*, 2015b). In spite of these studies, many other catabolic pathways remain functionally elusive and more work is needed to characterise their importance in pneumococcal biology.

Robb and his colleagues provide evidence for capability of pneumococci to depolymerise the mannose portion of high-mannose *N*-glycans through cleavage of terminal α-(1,2)-linked mannose residues by α-(1,2)-mannosidase and EndoD enzymes generating Man5GlcNAc2 and Man5GlcNAc respectively. The released molecules are bound to solute binding protein named NgtS (part of ABC transporter) for importing inside the bacterial cell. Both α-(1,2)-mannosidase and EndoD showed their contribution in host-pathogen interaction through destruction of high mannose *N*-glycans, covering the most important complement component C3, thus protecting the pneumococci from the host immune response and facilitating their transition within host tissues (Robb *et al.*, 2017).

Given the importance of carbohydrate metabolism and its correlation with pneumococcal virulence, additional studies are required to understand pneumococcal sugar metabolism and its relation to pneumococcal adaption during colonisation and infection. All of these might provide clues for identification of new drug targets to combat pneumococcal diseases. Thus, in this study I attempted to study the effect of mannose on Rgg/SHP144 QS.

1.6.2. Pneumococcal adaptation to oxidative stress

Streptococcus pneumoniae is a part of human nasopharyngeal microbiota, colonises asymptotically in the human nasopharynx and can also cause various diseases in different host tissues. During infection, the pneumococci encounter multiple challenges that hinder their growth and virulence. One of these detriments is exposure to a significant amount of reactive oxygen species (ROS), generated from bacterial metabolism during respiration and from recruitment of immunological cells to the site of infection. *S. pneumoniae* encounters variant levels of oxygen during infection process. It has been suggested that the pneumococcus is usually exposed to normal air (20% O_2) in the top of nasopharynx, microaerobic condition in the lung (around 5% O_2), and anaerobic in the blood and brain (Yesilkaya *et al.*, 2013). Reactive oxygen species (ROS) are typically formed due to electron transfer to oxygen molecule, generating superoxide anion ($O_2^{\bullet-}$), hydrogen peroxide (H_2O_2) and hydroxyl radicals ($OH^{\bullet}$) or through energy transfer to O_2 and formation of singlet oxygen (Saleh *et al.*, 2013; Yesilkaya *et al.*, 2013). The ROS can cause mutation in DNA, damage protein, and can cause lipid peroxidation (Kashmiri and Mankar, 2014).

The pneumococci have capacity to produce prodigious amounts of H_2O_2 (up to 1mM) resulting from the activity of the pneumococcal pyruvate oxidase (SpxB) encoded by *spxB* (Pericone *et al.*, 2003). This enzyme is able to convert pyruvate to acetyl phosphate, CO_2, and H_2O_2 in the presence of oxygen (Spellerberg *et al.*, 1996). Besides its function in oxidative stress, it plays a prominent role in pneumococcal metabolism and virulence (Pericone *et al.*, 2003; Orihuela *et al.*, 2004). It is noteworthy to mention that the toxic effects of H_2O_2 is potentiated in the presence of iron ions, as it interacts with H_2O_2 via the Fenton reaction and generates a massive amount of highly toxic and damaging reactive hydroxyl radical molecules (Yesilkaya *et al.*, 2013). The Fenton reaction occurs in *S. pneumoniae*, but with less adverse effects, this is because of the presence of a very limited number of pneumococcal proteins with iron-sulphur clusters, which are usually targeted by ROS (Pericone *et al.*, 2003), and the presence of an excellent regulatory mechanism for iron uptake (Ulijasz *et al*., 2004).

The impact of H_2O_2 on *S. pneumoniae* appears to be a double-edged sword. On the one hand, H_2O_2 offers competitive advantages for the pneumococci through inhibiting the growth of other nasopharyngeal colonisers such *as Haemophilus influenzae*, *Neisseria meningitidis* and *Moraxella catarrhalis* (Pericone *et al*., 2000), H_2O_2 also plays a crucial role in pneumococcal pathogenesis, possibly through activation of the genes responsible for host inflammatory response and cytotoxic effects on human epithelial cells (Duane *et al*., 1993; Loose *et al*., 2015). On the other hand, *S. pneumoniae* cannot entirely overcome the harmful effects of H_2O_2 derived from endogenous reactions or host immune cells. As the presence of high amounts H_2O_2 activates *spxB* expression which causes an increase in the mutation rate, defects in bacterial morphology and plasma membrane composition, and inhibition of pneumococcal growth in stationary phase (Pericone *et al*., 2002; Regev-Yochay *et al*., 2007; Yesilkaya *et al*., 2013). Thus, the pneumococci should have an efficient defence mechanism for dealing with toxic effects of ROS.

Unlike other bacteria, the pneumococci lack the proteins which are usually used by other bacteria to relieve the deleterious effects of oxidative stress such as H_2O_2 scavengers and H_2O_2 detoxifying enzymes like catalase and NADH-peroxidase (Hoskins *et al*., 2001; Tettelin *et al*., 2001; Hajaj *et al*., 2017). Instead, the pneumococci rely on other enzymes such as manganese-dependent superoxide dismutase (SodA) (Yesilkaya *et al*., 2000), NADH oxidase (Nox) (Auzat *et al*., 1999), alkyl hydroperoxidase (AhpD) (Paterson *et al*., 2006a) and thiol peroxidase (TpxD) (Hajaj *et al*., 2012).

Numerous studies have indicated the importance of these enzymes in alleviation of ROS toxicity and promoting pneumococcal survival (Auzat *et al*., 1999;Yesilkaya *et al*., 2000). For example, SodA has been shown to be required for conversion of superoxide radicals to H_2O_2 and O_2 (Liochev and Fridovich, 2007), and its deletion caused a significant inhibition of pneumococcal growth in aerobic conditions, and virulence attenuation in an intranasal murine model (Yesilkaya *et al*., 2000). Pneumococcal NADH oxidase (Nox) also participates in the oxidative stress process through converting O_2 to H_2O and reducing the harmful effects of O_2 and its by-products (Auzat *et al*., 1999). Loss of *nox* renders the pneumococci more sensitive to oxidative stress, and less virulent in murine respiratory tract and otitis media infection models (Yu *et al*., 2001).

In addition, the AhpD enzyme is also involved in oxidative stress response, as this enzyme has capability to cleave toxic peroxide compounds to alcohol and water (Paterson *et al*., 2006a). Finally, thiol peroxidase TpxD, a part of ABC-manganese permease complex (PsaBCA) which is able to reduce toxic effects of H_2O_2 and allow the pneumococci to grow in aerobic environment such as nasopharynx (Hajaj *et al*., 2012).

The pneumococcus also lacks the global peroxide regulator OxyR, peroxide response regulator PerR, Mar, RpoS and superoxide stress SoxRS. However, it has other transcriptional regulators such as TCS04, SpxR , PsaR, CiaRH, Rgg, MerR/NlmR, RitR, which are found to be implicated in oxidative stress response. Two component system TCS04 and PsaR modulate the expression of *psaBCA*, and SpxR responsible for regulation of *spxB* (Yesilkaya *et al*., 2013). HtrA regulated by CiaRH plays a significant role in the removal of damaged and misfolded proteins produced during stress condition. Both *ciaR* and *htrA* mutants showed similar defect in resistance capability against oxidative stress (Ibrahim *et al*., 2004a). NmlR also contributes in protection against hydrogen peroxide (Potter *et al*., 2010), and nitric oxide stress response in highly oxygenated environment (Stroeher *et al*., 2007), more likely by the activation of *adhC*, which is important for thiol peroxidase activity. Orphan regulator RitR represses the expression of the *piu* iron uptake operon and activates the genes responsible for oxidative stress resistance and DNA damage repair system (Ulijasz *et al*., 2004; Yesilkaya *et al*., 2013). Finally, the Rgg transcriptional regulator has found to be induced under aerobic conditions. Inactivation of Rgg accelerated pneumococcal killing by paraquat but not by H_2O_2, and dramatically attenuated pneumococcal virulence in both pneumonia and septicaemia murine models (Bortoni *et al*., 2009).

Based on this available evidence, sensing and responding to oxidative compounds are crucial for pneumococcal fitness and *in vivo* survival. However, little is known about the role of transcriptional regulators like Rgg family in oxidative stress resistance. Hence, in this study it was decided to investigate the involvement of Rgg/SHP144 QS in pneumococcal oxidative stress resistance and identify SHP144 amino acids which are important for oxidative stress function and in turn in virulence.

1.7. Transcriptional regulation in bacteria

Regulation of the gene expression profile is a fundamental process for optimising the amount of gene products produced in response to the changes in environmental stimuli and the internal cellular state (Engstrom and Pfleger, 2017). This process enables the bacteria to adapt and survive in different host niches. The main component of the transcription regulatory network in bacteria is multi-subunit DNA dependent RNA polymerase (RNAP) (Browning and Busby, 2004) responsible for transcribing DNA templates into RNA molecules (Raineri, 2001). The core enzyme is composed of the two large β polypeptide chains (β and β′), two identical α subunits (αI and αII), omega subunit (ω) plus dissociable alternate sigma factor (σ factor), which is required only for initiation and separation from RNAP during transcription (Snyder *et al.*, 2013). Each of the two α units is composed of two independently folded domains [amino-terminal domain (αNTD) and carboxy-terminal domain (αCTD), joined together by a short linker of an approximately 20 amino acid] (Figure 1.3A). Each domain has a distinct function, the αNTD domains are responsible for the assembly of the core subunits (β and β′ subunits), while the αCTD are the DNA binding module at specific promoters (Browning and Busby, 2004). The β subunits are considered as the catalytic site of RNAP, responsible for binding to both the DNA template and RNA product during transcription (Govindarajan and Amster-Choder, 2014). The last subunit is ω (omega) which has a role in recruitment of the β′-subunit to the core enzyme complex (Snyder *et al.*, 2013).

DNA transcription is initiated by the recruitment of RNAP to a specific locus upstream of the gene on DNA, which is called the promoter region. This process can be carried out by binding of RNA polymerase to σ-factor to form the holoenzyme (Browning and Busby, 2004; Snyder *et al.*, 2013). The σ-subunit plays a significant role in recognition of the correct nucleotide motifs in the promoter region, the position of RNA polymerase at the target promoter and prevention of the winding of DNA duplex near the transcription start site (Govindarajan and Amster-Choder, 2014). Most bacteria have several different sigma factors which enable RNA polymerase holoenzyme to recognise different sets of promoters. Sigma factors in general consist of four or more domains joined together by flexible linkers. The domains 2, 3 and 4 are important for promoter recognition, while domain 1 has unknown function (Browning and Busby, 2004).

Four DNA sequence elements within each specific promoter have a crucial role in docking the RNA polymerase within the promoter region. These elements are -10,-35,-10 extended and UP element (Browning and Busby, 2016). The first two elements -10 and -35 hexamers are short regions centred 10 and 35 bp respectively upstream from the transcription start site (TSS), and are recognised by RNA polymerase σ-subunit 2 and 4 domains, respectively (Engstrom and Pfleger, 2017), while the other two important promoter elements are the extended -10 element and UP element. The extended -10 element is a small locus present on some bacterial promoter regions (Haugen *et al*., 2008), and consists of 3-4 bp located immediately upstream of -10 hexanucleotides and can be recognised by domain 3 of the RNA polymerase σ-factor (Browning and Busby, 2004). The last element is upstream or UP element, is AT-rich region, consists of 20 bp, situated upstream of the -35 hexamer and can directly interact with α-subunits of RNA polymerase (Govindarajan and Amster-Choder, 2014).

The RNA polymerase holoenzyme then starts interacting with well-defined DNA promoter regions to form an open complex, in which a short section of two DNA chains around the transcription start site are separated (Browning and Busby, 2004). From this point, the RNA chain synthesis starts from the DNA template by formation of phosphodiester bond between the initiating and adjacent nucleoside triphosphates. This is followed by dissociation of RNAP from sigma factor and moving into the elongation complex to extend the RNA strand. RNA synthesis continues until the transcription is terminated at a specific sequence region on the DNA, resulting the release of RNA transcript from DNA template (Browning and Busby, 2004; Govindarajan and Amster-Choder, 2014).

Transcription regulation occurs under the control of regulatory proteins called transcription factors (TFs). TFs can act as a repressor or activator according to environmental signals and/or intracellular triggers (Perez-Rueda *et al*., 2018). TFs play a crucial role for correct distribution of the limited amount of RNAP among the huge number of competing promoters (Browning and Busby, 2004). These proteins carry specific DNA-binding domains (DBDs) in their structure, which allow the attachment to the DNA recognition site and determine the direction of the RNA polymerase along the DNA. These regulatory proteins are responsible for regulation of one or sets of genes under different conditions (Browning and Busby, 2004; Seshasayee *et al.,* 2011).

Transcriptional activators (TA) usually bind to a specific region located upstream of the promoter called an activator site to increase the binding affinity of RNA polymerase towards target promoter (Snyder *et al.*, 2013). There are three mechanisms used by bacterial cells for activation of the target promoter. Firstly, the activator protein binds to a target sequence located upstream of the promoter –35 element and recruits RNA polymerase to the promoter through direct binding with αCTD domains of the RNA polymerase. Secondly, the activator interacts with the promoter in the region overlapping -35 element, and the bound activator then interacts with domain 4 of the σ-subunit of RNA polymerase. This interaction attracts the RNA polymerase to the correct promoter region. The last mechanism occurs when the activator introduces conformational changes in the target promoter sequence which allow the binding of the RNA polymerase with -10 and/or -35 elements of target promoter. In this activation, the TF should bind at, or very close to the promoter elements (Browning and Busby, 2004).

In contrast, some of TFs act as repressors of transcription through impeding the binding of the RNA polymerase to promoter elements. This repression occurs either by occupying core promoter elements, or through formation of DNA looping. In certain cases, the repressor works as an anti-activator, in this case the repressor binds to the activator and shuts off its function for binding to RNA polymerase and so inhibits the transcription (Browning and Busby, 2004). Activation and repression mechanisms are shown in Figure 1.3B.

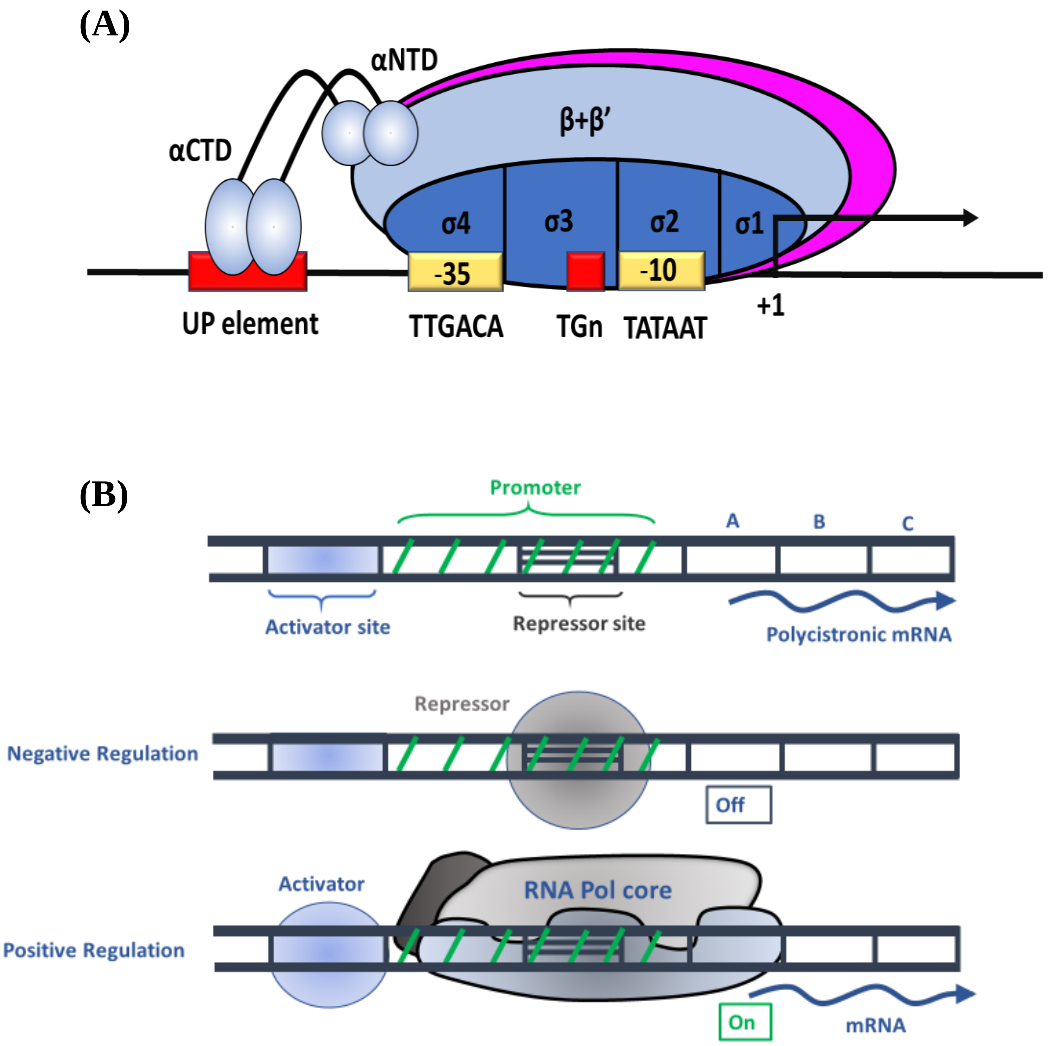

Figure 1.3: (A) Diagram showing the interaction of RNA polymerase with promoter elements in bacteria. The most important components involved in RNAP-promoter interaction are consensus sequences for the -35 (TTGACA), extended –10 (TGn), -10 (TATAAT), σ -factor domains (1-4 σ), UP element, αNTD represents N-terminal domain of RNAP responsible for the assembly of the core subunits (β and β′ subunits), αCTD are the DNA binding module at specific promoters and (+1), is a transcription start site and arrow above it represents the direction of transcription. **(B)** Diagram illustrating the two general types of transcriptional regulation (positive and negative regulation). In negative regulation, the repressor binds to a repressor-binding site (or operator) and represses the expression of gene or operon. While in positive regulation, the activator binds to upstream of the promoter and initiates gene expression. Figures **(A)** and **(B)** were constructed based on Browning and Busby (2004) and Snyder *et al*. (2013) respectively.

1.8. Pneumococcal regulatory mechanisms

Streptococcus pneumoniae asymptomatically colonises the nasopharynx of humans, but under unknown conditions invades host tissues and causes an array of diseases ranging from mild localised infections like otitis media and sinusitis to invasive life threating diseases including bacteraemia, pneumoniae or even meningitis (Gamez and Hammerschmidt, 2012). The pneumococcus encounters various environmental conditions in various host tissues, such as oxidative stress, temperature fluctuations, metal ions limitations, pH variation and nutrient availability (Aprianto *et al*., 2018) which might affect the expression of virulence genes. Thus, sensing and responding to environmental signals are important for adapting to changing habitats, bacterial fitness and survival (Harapanahalli *et al*., 2015; Nguyen *et al*., 2015).

It is still unclear how *S. pneumoniae* adapts to different external stimuli and how it can move from a colonisation to pathogenic state. It is commonly believed that the presence of several regulatory mechanisms enables this microbe to orchestrate its virulence genes expression and provide adaptive capabilities to the new conditions (Hendriksen, 2010). *S. pneumoniae* has several multifunctional regulatory proteins which are shown to be important for sensing and responding to internal or external environmental signals and for successful host adaption (Kietzman and Rosch, 2015; Nguyen *et al*., 2015). The pneumococcus possesses three gene regulatory pathways which are stand-alone regulators, two-component regulatory systems (TCSs) and a quorum sensing pathway (Kietzman and Rosch, 2015; Gómez-Mejia *et al*., 2018). It is believed that these regulatory systems play vital roles in pneumococcal adaptation to various niches. Hence, each regulatory system will be addressed in detail in the following sections.

1.8.1. Two-component regulatory systems (TCSs)

Two-component systems are the most widespread regulatory system in bacteria, commonly used to link environmental signals to adaptive responses (Monedero *et al*., 2017). These systems usually rely on two proteins: a membrane-bound sensor, called histidine kinase (HK), and a cognate cytoplasmic response regulator (RR) containing DNA binding domain (Beier and Gross, 2006). Both TCS components (HK and RR) have well-defined domains responsible for modulating the input signal and output product for appropriate biological function. HKs are membrane proteins, responsible for sensing external stimuli and transferring the signal to response regulator. These proteins are anchored on the cell membrane by transmembrane domains (TMD) (Mascher *et al*., 2006), and mainly consist of three important components: the diverse sensing region located in the N-terminal end, commonly exposed to external signal, followed by a transmembrane linker region which connects the N-terminal domain with the highly conserved C-terminal cytoplasmic kinase domain. The latter domain involves in dimerisation and histidine phosphotransfer system (DHp). Similar to HK, the response regulator (RR) has N and C-terminal domains, which are joined together by a linker. The N-terminal domain contains a conserved aspartate residue (Asp) important for the phosphorylation event (Gómez-Mejia *et al*., 2018).

Upon sensing a specific external stimulus such as temperature, pH or difference in nutrient composition, the histidine kinase phosphorylates its histidine residue then transfers this phosphoryl group to a conserved aspartate residue of its cognate response regulator protein (RR). Once the aspartate residue is phosphorylated, it induces conformational change in the C-terminal domain of the RR, facilitating the interaction with target DNA and regulation of the transcription of target genes either by activation or repression (Blue and Mitchell, 2003) (Figure 1.4A).

S. pneumoniae interacts with its environment by using 13 putative TCSs (13 HK: RR pairs) plus orphan response regulator (RitR) (Lange *et al*., 1999; Throup *et al*., 2000). The 13 pneumococcal TCSs proteins are annotated from TCS01 to TCS13, independent of their location on the genome (Lange *et al*., 1999). These TCSs are commonly organised as a group in operons and localised close to their target promoter regions (Gómez-Mejia *et al*., 2018). Most of TCS regulatory systems have been shown to be important for pneumococcal fitness and virulence in a murine pneumoniae model (Throup *et al*., 2000; Paterson *et al*., 2006b). However, their contributions in virulence are varied and mainly dependent on pneumococcal strains and infection model used (Paterson *et al*., 2006b).

ComDE (TCS12), CiaR/CiaH (TCS05), are the two well-studied TCS in *S. pneumoniae* responsible for competence, antibiotic resistance and pneumococcal survival under stress conditions (Gómez-Mejia *et al*., 2018). TCS12 plays a significant role in the competence process, in which the bacteria take up exogenous DNA from the environment and incorporate into its genome, acquiring new genetic properties and pathogenic features (Hendriksen, 2010). The competence process is mediated by competence stimulating peptide CSP encoded by *comC*, exported and processed to mature peptide with the aid of ATP-binding cassette protein encoded by *comAB*. When the concentration of CSP peptide reaches the threshold level, it phosphorylates the histidine kinase ComD, which exists on the cell membrane and transfers the phosphate group to its cognate cytoplasmic response regulator ComE (Hendriksen, 2010; Martin *et al*., 2010; Cortes *et al*., 2015), which in turn activates 24 early competence genes *comAB*, *comCDE* including the gene encoding the alternative sigma factor ComX. The latter involves regulation of 80 of late competence genes, crucial for DNA uptake and transformation (Zhu *et al*., 2015). A clear link has been found between the virulence and competence regulon. Using pneumoniae and bacteremia models, it was found that deletion of *comD* attenuated pneumococcal virulence in serotype 2 strain D39 (Bartilson *et al*., 2001), serotype 3 (Lau *et al*., 2001), and serotype 4 TIGR4 strain (Hava and Camilli, 2002). Recent studies have also reported the involvement of the competence regulon in the lysis of non-competent cells and the release of DNA content and virulence factor pneumolysin (Guiral *et al*., 2005; Claverys *et al*., 2007). By using microarray analysis, it has also been found that some of the stress responsive genes are positively regulated by CSP-ComDE cascade, indicating the importance of the competence regulon in pneumococcal fitness (Peterson *et al*., 2004).

TCS05 or CiaRH (competence induction and altered cefotaxime susceptibility) is another TCS implicated in regulation of diverse functions such as competence, antibiotic resistance, virulence (Guenzi *et al*., 1994; Throup *et al*., 2000; Mascher *et al*., 2003), stress response, autolysis, polysaccharide metabolism and bacteriocin production (Dagkessamanskaia *et al*., 2004; Halfmann *et al*., 2007a). CiaRH appears to play a role in the pneumococcal stress response and infection process through activating the expression of chaperones and heat shock proteins such as HtrA (High temperature requirement A) (Dagkessamanskaia *et al*., 2004; Gómez-Mejia *et al*., 2018). HtrA commonly contains chaperone and protease domains for degradation of undesired or mis-folded proteins and confer pneumococcal growth at elevated temperatures (Ibrahim *et al*., 2004b; Gómez-Mejia *et al*., 2018). A link between CiaRH and HtrA was further confirmed in colonisation and systemic infection models (Sebert *et al*., 2002; Ibrahim *et al*., 2004a, 2004b). Reduction of virulence phenotype in the CiaR mutant was possibly due to the inhibition of HtrA expression, as deletion of CiaR and HtrA exerts similar attenuation properties in a murine infection model (Ibrahim *et al*., 2004a). CiaRH has also been found to minimise the stress of competence development through degradation of the competence signalling peptide CSP (Cassone *et al*., 2012).

TCS02 also termed as WalRK, VicRK, YycFG and MicAB, is a well characterised system that is important for cell wall biosynthesis, fatty acid metabolism and activation of the important virulence factor PspA (Mohedano *et al*., 2005; Ng *et al*., 2005). TCS02 is considered to be the only system that was shown to be essential for pneumococcal viability, and the response regulator RR02 is the most important component (Clausen *et al*., 2003). The essential role of TCS02 in cell viability is more likely due to the regulation of the expression of murein hydrolase gene *pcsB*, and the two other important surface proteins (Spr0096 and Spr1875), which are required for murein biosynthesis and membrane integrity (Ng *et al*., 2005), as deletion of VicRK (RR02) caused severe defects in pneumococcal cell morphology and cell wall synthesis (Ng *et al*., 2004).

TCS09 was shown to play a role in pneumococcal virulence. The contribution of this regulatory system in virulence varies between pneumococcal strains and infection site. For example, in *S. pneumoniae* D39 serotype 2, inactivation of response regulator *rr09* renders the pneumococci avirulent in both pneumoniae and bacteremia murine models. Conversely deletion of *rr09* in a serotype 4 (TIGR4) and serotype 3 (0100993) attenuated pneumococcal virulence only in the pneumonia model, suggesting inability of mutants to disseminate to the blood rather than inability to grow in the lungs (Blue and Mitchell, 2003). In addition, deletion of *rr09* repressed the expression of significant numbers of PTS genes responsible for sugar transport in D39, while in TIGR4 only three PTS genes are affected by *rr09* mutation (Hendriksen *et al*., 2007). All these findings provide overwhelming evidence for the involvement of TCS09 in pneumococcal pathogenesis in a strain dependent manner.

Pneumococcal orphan two-component response regulator RitR, referred to as Repressor of Iron Transport Regulator, differs from the other 13 TCS, as the orphan response regulator RitR lacks a cognate HK and a conserved aspartate residue, important for the signalling relay. Recent studies have shown that RitR can be phosphorylated through interaction with serine-threonine phosphatase kinase StkP (Ulijasz *et al*., 2009). RitR acts to regulate iron uptake by repressing the expression of the *piuABC* transport system and activation of a wide variety of genes involved in oxidative stress resistance and DNA damage repair (Ulijasz *et al*., 2004; Yesilkaya *et al*., 2013). Inactivation of *ritR* increased pneumococcal susceptibility to killing by H_2O_2 and impaired its growth in iron enriched media. This seems to be due to accumulation of high amounts of free iron in mutant *ritR,* which increases the opportunity of binding to H_2O_2 and induces oxidative stress by the Fenton reaction. This assumption was further confirmed by the finding that the treatment of the *ritR* mutant with manganese in high iron media reconstitutes pneumococcal growth and reduces the amount of H_2O_2 produced by bacterial cells (Ong *et al*., 2013). RitR was also found to be important for virulence in a lung infection model (Ulijasz *et al*., 2004). Recent study conducted by Glanville *et al*. (2018) has found that RitR can regulate pneumococcal iron homeostasis, through sensing high level of peroxide presenting in the environment through oxidation of single cysteine residue in the linker domain. This oxidation facilitates RitR binding to the iron uptake (Piu) promoter and represses the transcription of *piu* and iron transport system, thereby protecting the bacteria from the detrimental effect of peroxide and promoting an efficient colonisation.

Finally, it is worth mentioning that the presence of a direct link between pneumococcal pathogenesis and two-component systems, and their absence in mammals make them potential anti-infective targets (Casino *et al*., 2009).

1.8.2. Stand-alone regulators

Streptococcus pneumoniae differs from other pathogenic bacteria as it lacks the typical sigma factor in its genome. Instead, it has alternative sigma factor ComX with limited regulatory capability (Luo and Morrison, 2003). Therefore, the pneumococci rely on stand-alone response regulators and TCS regulatory systems for modulation of their virulence gene expression. Stand-alone regulators are cytoplasmic proteins that lack the sensor histidine kinase and contain signal recognition and DNA binding domains in the same protein (Figure 1.4B). However, the exact mechanism of action of these regulators is still obscure (Gómez-Mejia *et al*., 2018) since their sensory elements remain unidentified (Kreikemeyer *et al*., 2003; McIver, 2009). These regulators modulate virulence regulon expression through sensing and responding to changing environmental conditions.

The pneumococci possess several stand-alone transcriptional regulators that are implicated in pneumococcal adaption and virulence (Gómez-Mejia *et al*., 2018). One of these regulators is MgrA (Mga-like repressor A). This protein has homology to the stand-alone transcriptional regulator of *Streptococcus pyogenes* Mga (multiple gene regulator), which contributes in regulation of various virulence genes essential for nasopharyngeal colonisation and pneumonia in a mouse infection model (Hemsley *et al*., 2003). Pneumococcal CodY is another global nutritional regulator, which plays a key role in repression of the genes involved in synthesis and metabolism of carbon and amino acid uptake (Hendriksen *et al*., 2008a). Recent studies have indicated the involvement of CodY in ROS scavenging through activation of the transcription of H_2O_2 detoxifying enzyme TpxD and the repression of the iron transport system (Johnston *et al*., 2015; Hajaj *et al*., 2017). Defect in CodY function results in attenuation in pneumococcal adherence, mainly by repression of the transcription of choline-binding protein PcpA, and colonisation in a murine model (Hendriksen *et al*., 2008a). Another transcriptional repressor is GlnR, which acts in combination with GlnA to repress the transcription of two operons *glnRA* and *glnPQ-zwf* as well as the *gdhA* involved in glutamine and glutamate metabolism (Kloosterman *et al*., 2006a). Several genes of the GlnR regulon are required for pneumococcal colonisation and survival in different animal tissues (Hendriksen *et al*., 2008b).

The pneumococcal stand-alone transcriptional regulator CcpA (catabolite control protein A) coordinates the most important regulatory pathway named carbon catabolite repression regulatory pathway (CCR) (Iyer *et al*., 2005). This regulatory pathway has been studied in detail in many Gram-positive bacteria (Titgemeyer and Hillen, 2002; Warner and Lolkema, 2003). It represses the expression of genes involved in transport and metabolism of secondary carbon source (non-preferred), until the cell has finished the preferred sugar (Deutscher, 2008). By this way, the bacteria would use its energy effectively and achieve optimal growth in complex carbohydrate environments (Deutscher, 2008; Fleming *et al*., 2015). CcpA has been reported to contribute in numerous pneumococcal physiological processes, including carbohydrate metabolism (Carvalho *et al*., 2011), capsule synthesis (Giammarinaro and Paton, 2002), and in nasopharyngeal colonisation and lung infection in mice (Iyer *et al*., 2005; Al-Bayati *et al*., 2017).

CcpA belongs to the LacI/GalR family transcriptional regulators and modulates the expression of a large number of catabolic operons in *B. subtilis* and many other streptococcal species including *S. pneumoniae* (Henkin, 1996; Iyer *et al*., 2005; Willenborg *et al*., 2014). CcpA binds to DNA promoters of CCR-sensitive genes at specific regulatory sites called catabolite responsive elements (*cre*) (Lulko *et al*., 2007; Görke and Stülke, 2008), and this binding is potentiated in the presence of histidine phosphocarrier protein (HPr). HPr is the main component of phosphoenolpyruvate dependent phosphotransferase system (PTS), responsible for transmission of high energy phosphate from phosphoenolpyruvate (PEP) to the sugar-specific enzyme II complex during sugar uptake (Postma and Lengeler, 1985; Kaufman and Yother, 2007). In the presence of a favourable carbon source such as glucose, HPr is phosphorylated on a conserved serine residue at position 46 by the aid of HPr kinase/phosphorylase (HPrK/P). The activity of HPrK/P is further stimulated in the presence of glycolytic intermediates named fructose-1, 6-bisphosphate (FBP) resulting the HPr-Ser~P (Görke and Stülke, 2008; Fleming *et al*., 2015). HPr-Ser~P is not a preferred substrate for EI-dependent phosphorylation, resulting in a reduced production of HPr-His~P and restriction of PTS transport of other sugars. At the same time, HPr-Ser~P can bind to CcpA and form a complex for stimulation of CcpA-*cre* binding and repression of the expression of non-preferred carbohydrate metabolism genes (Deutscher *et al*., 2006; Fleming *et al*., 2015). Moreover, CcpA can act as activator or repressor, which is mainly dependent on the *cre* location relative to promoter region in catabolite regulated genes (Lulko *et al*., 2007; Zomer *et al*., 2007). When the amount of preferred sugar is reduced in the environment, the effect of CCR is relieved by dephosphorylation of HPr-Ser~P and activation of non-preferred carbohydrate transport (Fleming *et al*., 2015).

It is clear that multiple studies have been done to define regulatory pathways in pneumococci, however, further work is required to understand the exact connection between environmental signals, gene expression profiles, and virulence.

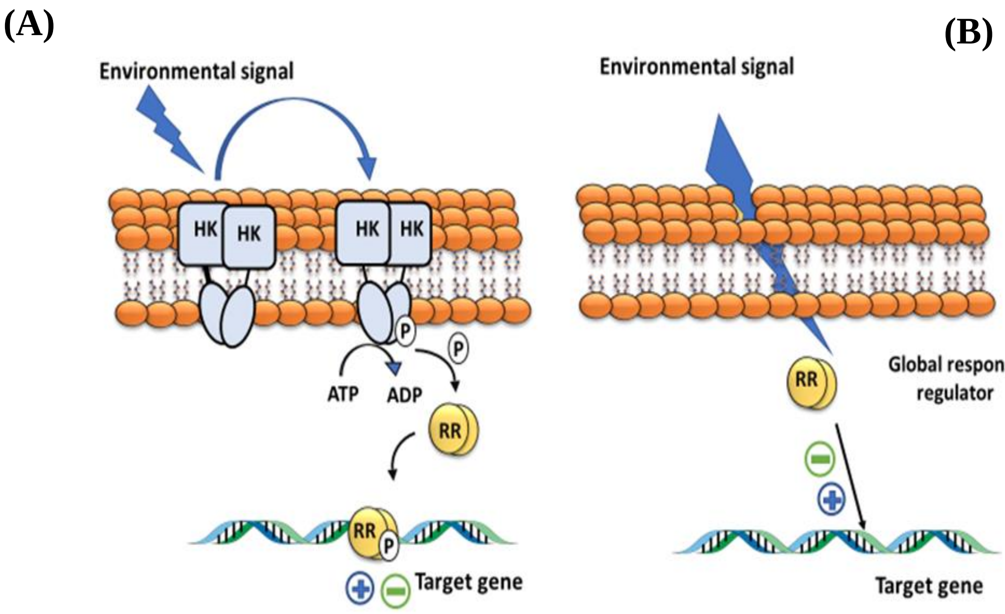

Figure 1.4: Transcriptional regulatory systems in *S. pneumoniae*. **(A)** Two-component regulatory system (TCS). Following detection of external signal by the N-terminal domain of histidine kinase (HK), the ATP is used to autophosphorylate histidine residue within the cytoplasmic domain of HK. The phosphoryl group is then transferred to a conserved aspartate residue in its cognate cytoplasmic regulator (RR). Once the aspartate residue is phosphorylated, it induces conformational change in the C-terminal domain of response regulator (RR), facilitating its interaction with target promoters and regulation of the transcription of target genes. **(B)** Stand-alone transcriptional regulators. This type of regulators lack sensor histidine kinase and can modulate virulence regulon expressions through sensing and responding to changing environmental conditions. Figures **(A)** and **(B)** were adapted from Solano-Collado (2014).

1.9. Quorum sensing system (QS)

When the size of the bacterial population increases, they manifest different phenotypic traits and these traits at high cell density are regulated by systems called quorum sensing (QS) or cell-to-cell communication systems (Kalia, 2013). QS allows the bacterial population to switch behaviour collectively, thereby regulating the important physiological processes including bioluminescence, virulence, biofilm development and antibiotic resistance (Li and Nair, 2012). Thus, some opportunistic pathogens exploit the characteristic features of QS to overwhelm host's defence mechanisms and facilitate host infections (Kalia, 2013).

In general, all bacterial QS circuits rely on four basic elements: (1) production of signalling molecules; (2) excretion of the signals into the extracellular environment; (3)

detection by cognate receptors once the signals concentrations reach a threshold level leading to (4) alteration in target gene expression (Sifri, 2008). These signalling molecules are initially synthesised inside the bacterial cells, secreted to the extracellular milieu by passive or active diffusion and detected either by two-component regulatory system on the cell surface or through direct interaction with transcriptional regulators in the cytoplasm. Their detection leads the bacterial cells to coordinate the transcription of QS regulon including those encoding for signalling molecules, generating a positive feedback regulation (Rutherford and Bassler, 2012; Papenfort and Bassler, 2016). Some bacterial species can produce more than one signal molecule and they might have multiple quorum-sensing circuits. For example, Gram-negative bacterium *P. aeruginosa* possesses multiple QS systems and has a complex hierarchical transcription network (Jimenez *et al*., 2012).

The QS system was discovered first in Gram negative marine bacterium *Vibrio fischeri* and was called LuxI/LuxR. This system is responsible for coordinating the expression of luciferase genes, essential for light production (Ruby, 1996; Rutherford and Bassler, 2012). This system became a prototypical model for most QS systems in Gram-negative bacteria (Fuqua *et al*., 2001; Federle, 2009; Bai and Rai, 2011). Acyl-homoserine lactones (AHLs) are the most dominant signalling molecules utilised by Gram-negative bacteria (Ng and Bassler, 2009; Fetzner, 2015). They are typically synthesised by LuxI synthases by the aid of two substrates, S-adenosyl-methionine (SAM) and an acylated acyl carrier protein (acyl-ACP). These substrates are important to form an amide bond between SAM and acyl groups and for lactonisation of the autoinducer signal (Parsek *et al*., 1999). AHLs are mainly composed of homoserine lactone (HSL), which is conserved among all AHL molecules attached to variable acyl chain group. The AHL structure varies between Gram-negative bacteria, and this variation is mainly due to difference in length of the acyl side chain, ranging between 4-18 carbons, saturation level, and oxidation at C3 position of acyl chain (Marketon *et al*., 2002; LaSarre and Federle, 2013). Variation in AHL structure offers some specificity for bacteria to differentiate their own AHLs from those produced by other species (Frederix and Downie, 2011). At a critical concentration, AHL interacts with its cognate LuxR-receptor and induces the transcription of QS dependent genes (Sifri, 2008; Kalia, 2013).

Quorum-sensing systems in Gram-positive bacteria differ from those found in Gram-negative bacteria in terms of composition and structure of the signal molecules, and mechanism of recognition and sensing of autoinducing signals. In Gram-positive bacteria, QS systems are regulated by autoinducing peptides (AIPs), in contrast to organic molecules like AHLs signals which are used by Gram-negative bacteria (Waters and Bassler, 2005). The AIPs are synthesised as pre-peptides, secreted, processed to small peptides (5-17 amino acids), and then re-imported inside the cell by oligopeptide transporters (Rutherford and Bassler, 2012). While, AHL molecules can freely diffuse in and out of the cell without processing because of their small sizes and lipophilic characteristics (Sifri, 2008). Recently, a group of signalling molecules named autoinducer 2 (AI-2) has been discovered. This family contains a group of interconvertible furanones derived from 4,5-dihydroxy-2,3-pentanedione (DPD) (Schauder *et al*., 2001). DPD is produced by the LuxS enzyme, and detected by AI-2/LuxS systems, recently found in a wide range of Gram-negative and Gram-positive bacteria. Thus, it is predicted that AI-2 acts as an interspecies signal among different bacterial species (LaSarre and Federle, 2013; Park *et al*., 2017). The involvement of AI-2 in virulence of different pathogens was reported such as *E. coli*, *H. influenzae*, *H. pylori*, *S. pneumoniae* and *V. cholerae* (Pereira *et al*., 2013). This study aims to characterise Rgg family QS systems in Gram positive *Streptococcus pneumoniae*, therefore Rgg and homologues regulatory pathways will be discussed in a greater detail in the following sections.

1.9.1. Quorum sensing in Gram positive bacteria

The LuxI/LuxR pairs are absent in Gram positive bacteria, thus they rely on small modified oligopeptides known as pheromones or autoinducing peptides (AIPs) to modulate the expression of their target genes. These peptides are ribosomally synthesised as pre-peptides within the cell, and actively transported out by the aid of specific transporters. At this point, signalling peptides are exposed to certain modification events, including processing and/or cyclisation (LaSarre and Federle, 2013) prior to detection either by (i) membrane-bound sensor kinase on the cell surface such as Agr system in *Staphylococcus aureus,* Fsr in *Enterococcus* faecalis (Nakayama *et al*., 2001; Thoendel *et al*., 2011), and competence circuit in *S. pneumoniae* (Håvarstein *et al*., 1995), or by (ii) importation into the cell by oligopeptide permeases (Opp or Ami) and direct interaction with their cognate receptors belonging to RRNPP family QS systems (Jimenez and Federle, 2014; Do and Kumaraswami, 2016) (Figure 1.5A).

Based on differences in peptide structure and sensory system architectures among bacterial species, the signaling peptides have been divided into four groups in Gram positive QS systems: Agr cyclic peptides, double glycine peptides (Gly-Gly), RNPP family and Rgg-like regulatory family. Gram-positive bacteria have capacity to utilise different types of QS pathways within the same species to coordinate a variety of crucial behaviors like competence, conjugation, biofilm development and virulence factors synthesis (Cook and Federle, 2014).

Agr family refers to accessory gene regulator, which is encoded by *agr* locus. Agr network plays a significant role in control of adhesion and virulence factors production in *Staphylococcus aureus* (Thoendel *et al*., 2011; Rutherford and Bassler, 2012). The *agr* locus is mainly composed of 2 divergent promoters P2 and P3. The P2 (RNAII) activates *agr* operon genes (*agrA agrB*, *agrC*, *agrD*), while P3 (RNAIII) stimulates α-toxin production such as hemolysin and downregulates cell surface associated proteins like protein A (Queck *et al*., 2008; Canovas *et al*., 2016). Activation of RNAIII leads to alternation of *S. aureus* phenotype from adhesion state to invasion (Karathanasi *et al*., 2018). The fundamental feature of this pathway is the utilisation of cyclic peptides as autoinducer molecules. These peptides are characterised by the presence of cyclic thiolactone in their structure, which is important for their activity (Novick and Geisinger, 2008). Cyclic peptides are synthesised as precursor 46 amino acid peptides, encoded by the *agrD* gene, modified and secreted out of the cell by the aid of a dedicated transport protein named AgrB (Thoendel and Horswill, 2009; Thoendel *et al*., 2011). AgrD peptides are processed at both N and C terminus by signal peptidase SpsB and transmembrane endopeptidase AgrB respectively to introduce a unique thiolactone ring between highly conserved cysteine residue and the carboxyl terminus (Kavanaugh *et al*., 2007; Bai and Rai, 2011). It is thought that AgrB possesses a putative cysteine endopeptidase domain (Qiu *et al*., 2005), which involves in peptide processing and transport of AgrD peptide. The resulting mature peptide induces two-component system (membrane-bound histidine kinase AgrC and cytoplasmic response regulator AgrA) and subsequently activates the expression of RNAII and RNAIII via P2 and P3, respectively (Novick, 2003; Sifri, 2008; Queck *et al*., 2008).

Gly-Gly peptide family is another QS pathway in Gram positive bacteria, characterised by the presence of double glycine motif in their conserved leader sequence

(LSX$_2$ELX$_2$IXGG) (Håvarstein *et al*., 1994) such as competence stimulating peptides (CSPs) of streptococci and class II bacteriocins. These peptides are exported through a transporter containing an accessory domain important for proteolysis of the polypeptide at the site located immediately following the conserved Gly-Gly motif (Håvarstein *et al*., 1995). Similar to Agr family, double glycine peptides are identified by TCS and the signal is transported via phosphorylation of cognate response regulators.

Specific emphasis is given to RRNPP family (RNPP and Rgg regulators) due to their relevance to the hypothesis of this thesis. The RRNPP proteins share some characteristic features: (i) they have homologues in different Gram-positive genera like Bacilli, Streptococci, or Enterococci (ii) they have oligopeptide quorum sensors that interact directly with their receptors in the responder cell, (iii) genes encoding for regulatory proteins and their signaling peptides form a cassette located in the bacterial chromosome or in plasmids (Rocha-Estrada *et al*., 2010; Perez-Pascual *et al*., 2016). This family includes Rgg (regulator gene of glucosyltransferase), Rap (aspartyl phosphate phosphatases), NprR (neutral protease regulator), PlcR (phospholipase C regulator) and PrgX (sex pheromone receptor) regulators.

Rap (aspartyl phosphate phosphatases) proteins with their inhibitory oligopeptides Phr form a QS cassette in *Bacillus subtilis* (Parashar *et al*., 2013). Eleven Rap proteins and eight putative Phr have been identified (Hayashi *et al*., 2006; Rocha-Estrada *et al*., 2010). Rap proteins consist of approximately 375 amino acids, with >25% identity among the homologs (Pottathil and Lazazzera, 2003). They also have six helix-turn-helix repeats or tetratricopeptide repeats (TPR) domains at their C-terminus, which facilitate protein-peptide and protein–protein interactions (Perego and Brannigan, 2001; Core and Perego, 2003). The Rap proteins carry different functions, for example, RapA, RapB and RapE act as negative regulators, inhibit phosphorelay signal transduction systems (essential for initiation of sporulation) and stimulate dephosphorylation of response regulator Spo0F (Perego *et al*., 1994; Jiang *et al*., 2000), while RapC and RapF are involved in competence development through modulating the activity of transcription factor ComA (Core and Perego, 2003; Bongiorni *et al*., 2005). Raps dephosphorylation capabilities are diminished upon binding to mature Phr signaling peptides. The Phr peptides are produced as precursors, processed to mature five amino acid by proteases and reimported into the cell by Opp transport system (Pottathil and Lazazzera, 2003). At high cell density, the Phr binds to Rap phosphatases and induces conformational changes in the TPR domains which disrupts Rap interaction to response regulator Spo0F and initiates sporulation and competence (Rocha-Estrada *et al*., 2010).

The transcriptional regulator NprR has been characterised in *Bacillus cereus*, *B. thuringiensis*, *B. anthracis*, and other Bacillus species. In the presence of signalling peptide NprX, NprR can regulate the expression of neutral protease NprA in *B. cereus* and *B. thuringiensis* (Perchat *et al*., 2011), and 41 genes encoding for other degradative enzymes like lipases, peptidases and chitinases as well as lipopeptide (kurstakin), which is important for swarming mobility and biofilm formation (Dubois *et al*., 2012). For *B. anthracis,* a little information is available about the role of NprR/NprX system in bacterial pathogenesis. A recent study conducted by Bergman *et al*. (2007) showed that the expression of *nprR* is upregulated during the outgrowth of *B. anthracis* spores within murine macrophages. In addition, NprR/NprX circuit was found to be modulated by PlcR and CodY regulators (Dubois *et al*., 2013). Similar to other RRNPP signalling peptides, NprX peptide is produced as precursor peptide with 43 residues, processed to mature peptide and re-imported back into the cell by Opp (Rice *et al*., 2016). The imported NprX peptide interacts with NprR and induces conformational changes allowing the shift from the inactive NprR dimer to an active tetramer facilitating DNA binding (Zouhir *et al*., 2013).

PlcR (phospholipase C regulator) is firstly identified as a pleiotropic regulator in *B. thuringiensis* and found to be involved in activation of the expression of phosphatidylinositol-specific phospholipase C gene (Lereclus *et al*., 1996). PlcR activity is regulated by PapR, encoded by *papR* gene, that is located immediately downstream of *plcR* forming PlcR/PapR quorum-sensing cassette (Pottathil and Lazazzera, 2003; Rocha-Estrada *et al*., 2010). PapR peptide is similar to other RRNPP signaling peptides, which is expressed as pre-peptide with 48-aa peptide and exported to extracellular milieu by secretory pathway (Slamti and Lereclus, 2002). Once outside the cell, the pro-PapR is processed to mature heptapeptide by the help of secreted neutral protease B (NprB) (Pomerantsev *et al*., 2009). The processed peptide is re-imported into the cell by oligopeptide permease system and directly interacts with PlcR at the PlcR box in the upstream of PlcR regulated genes (Slamti and Lereclus, 2002). PlcR-PapR binding leads to conformational changes in the DNA binding domain, PlcR oligomerisation, and regulation of the PlcR regulon (Declerck *et al*., 2007; Grenha *et al*., 2013). It has been found that PlcR associated PapR activates the transcription of 45 genes in *B. cereus* group, most of them encoding for extracellular virulence proteins such as enterotoxins, hemolysins, phospholipases and proteases (Lereclus *et al*., 1996; Bouillaut *et al*., 2008; Gohar *et al*., 2008). In *S. pneumoniae* D39 serotype 2, two homologues of PlcR regulators (SPD_1745 and SPD_1786) have been identified, and SPD_1745 has been characterised (Hoover *et al*., 2015; Motib *et al*., 2017). Pneumococcal SPD_1745 encodes TprA transcriptional regulator with its cognate peptide PhrA. This system has been found in 60% of sequenced pneumococcal strains (Hoover *et al*., 2015). Pneumococcal TprA/PhrA differs from other Phr-signalling circuits, in that *tprA* and *phrA* genes are transcribed divergently in opposite direction, in contrast to all known Phr-signaling genes which have the same orientations (Pottathil and Lazazzera, 2003; Pomerantsev *et al*., 2009) (Figure 1.5B). TprA/PhrA function as the activator of the lantibiotic gene cluster, encoding for antimicrobial peptides important for pneumococcal competition during colonisation (Hoover *et al*., 2015). Furthermore, TprA/PhrA was found to be essential for pneumococcal growth on galactose, mannose and mucin (Motib *et al*., 2017), the most important carbon source for pneumococcal survival *in vivo* (Kahya *et al*., 2017; Robb *et al*., 2017). Furthermore, TprA/PhrA regulates genes involved in carbohydrate metabolism. It was found that TprA/PhrA QS system is activated by galactose and repressed by glucose (Hoover *et al*., 2015). Disruption of TprA or PhrA or both of them abolished pneumococcal virulence in pneumonia and septicemia murine models as well as in the chinchilla otitis media model (Motib *et al*., 2017). Recently, Kadam *et al*. (2017) have identified another pair of TprA/PhrA in multidrug-resistant pneumococcal lineage PMEN1 named TprA2/PhrA2. Phr2 peptide in PMEN1 can regulate its own cognate transcriptional regulator TprA2 and *S. pneumoniae* D39 TprA.

PrgX is a sex pheromone receptor, encoded in the tetracycline resistance plasmid pCF10 in *Enterococcus faecalis*. This regulator coordinates conjugation and plasmid transfer within and between enterococcal species (Dunny and Berntsson, 2016). Unlike the other RRNPP pathways, the PrgX QS system occurs between two different types of cells (donor cell carries conjugative plasmid and plasmid-free recipient cell) (Kozlowicz *et al*., 2006; Rocha-Estrada *et al*., 2010). Through this pathway, donor cell binds to peptide pheromone molecule cCF10 produced by recipient and initiates activation of the genes responsible for transfer functions such as aggregation substance (AS). The AS molecule promotes the attachment of donor cell to recipients through using a complementary receptor called enterococcal binding substance (EBS). Binding of AS to EBS allows the formation of the mating channel between the two cells and transition of the plasmid to recipient cell (Wardal *et al.*, 2010). The pCF10 containing cell expresses both chromosomal activator peptide cCF10 and inhibitor peptide iCF10. The latter is encoded by the *prgQ* on pCF10 plasmid, acts as inhibitor to prevent conjugation occurrence between two cells carrying the same conjugative plasmid (Kozlowicz *et al.*, 2006; Cook and Federle, 2014). More interesting, both donor and recipient cells produce cCF10 pheromone, but most of cCF10 pheromone from the donor cells are sequestered by PrgY, which is present on the cell membrane allowing the donor cells to respond only to the pheromone produced by the recipient cell. Following production of the precursor signaling peptides cCF10 and iCF10, they are secreted to the extracellular milieu and exposed to cleavage by a metalloprotease system (Chandler *et al.*, 2005). The cCF10 and iCF10 mature peptides are then re-imported into the cytosol with the aid of oligopeptide permease Opp and PrgZ (Leonard *et al.*, 1996). cCF10 competes with iCF10 for binding to PrgX (Kozlowicz *et al.*, 2006). Binding of iCF10 to PrgX stabilizes a tetrameric form of PrgX and form a DNA loop, which restricts RNA polymerase access to *prgQ* promoter and the transcription of conjugation genes. While displacement of iCF10 by cCF10 induces conformational changes in the C-terminal domain of PrgX causing disruption of PrgX tetramer and activation of *prgQ* conjugation operon expression (Shi *et al.*, 2005). The ratio of the inhibitor and inducer peptides plays a significant role in determination of the conjugative state of the cell (Kozlowicz *et al.*, 2006; Chatterjee *et al.*, 2013). The importance of aggregation substances is not limited to facilitating enterococcal conjugation, but also extends to the regulation of a variety of important virulence behaviors such as stimulation of fibrin adhesion (Hirt *et al.*, 2000), vegetation formation of enterococcal endocarditis (Chuang *et al.*, 2009) and biofilm development on heart valve tissues (Chuang-Smith *et al.*, 2010).

Another member of RRNPP is Rgg regulators. Rggs are also known as MutR and GadR, and are common in AT rich Gram-positive bacteria, found in Streptococcaceae, Lactobacillales and Listeriaceae (Cook and Federle, 2014; Monnet and Gardan, 2015). Rggs are stand-alone transcriptional regulators, firstly discovered in *Streptococcus gordonii* and designated as regulator genes of glucosyltransferase (*rgg*) (Sulavik *et al.*, 1992). Rggs are described as global transcriptional regulators, contribute in different physiological functions such as regulation of the transcription of glucosyltransferases in *S. gordonii* (Sulavik and Clewell, 1996; Vickerman and Minick, 2002) and *S. oralis* (Fujiwara *et al*., 2000), and the secreted cysteine proteinase virulence factor (SpeB) in *S. pyogenes* (Chaussee *et al*., 1999; Neely *et al*., 2003). Rggs also contribute in oxidative stress resistance in *S. thermophilus* (Fernandez *et al*., 2006), *S. pyogenes* (Chaussee *et al*., 2004), *S. pneumoniae* (Bortoni *et al*., 2009) as well as in bacteriocin production of *S. mutans* (Qi *et al*., 1999) and *Lactobacillus sakei* (Rawlinson *et al*., 2002; Skaugen *et al*., 2002), glutamate-dependent acid stress resistance in *Lactococcus lactis* (Sanders *et al*., 1998), thermal adaptation in *S. thermophilus* (Henry *et al*., 2011), virulence and pathogenesis of *S. pyogenes* (Chaussee *et al*., 2003), *S. agalactiae* (Samen *et al*., 2006) and *S. suis* (Zheng *et al*., 2011), and non-carbohydrate metabolism of *S. suis* (Zheng *et al*., 2011).

Recent genomic analysis revealed that *rgg* genes are located in close vicinity to the ORF expressing short linear signaling peptides named SHP. The *rgg*/*shp* loci have been found in the majority of streptococci (Ibrahim *et al*., 2007a; Fleuchot *et al*., 2011; Cook *et al*., 2013) with one or several paralogs within each species (Ibrahim *et al*., 2007a). These pairs of genes are overlapped at putative promoters or coding sequence regions in a convergent orientation.

The SHP signalling peptides were firstly identified by Ibrahim *et al*. (2007a) and categorised as short coding sequences. These genes code for peptides of 20–23 aa in length and are characterised by the abundance of hydrophobic amino acid residues. They also possess basic residues at the N-terminus (lysine or arginine) and glutamate or aspartate at their C-terminus. In addition, SHPs are located upstream of the *rgg* genes and divergently transcribed. Further genomic analysis by Fleuchot *et al*. (2011) identified 484 *rgg*-like genes along with 61 adjacent *shp* genes from analysis of 90 genomes in Streptococcae, Lactobacillale and Listeriaceae. Furthermore, phylogenetic analysis of Rgg amino acid sequences in streptococci revealed the presence of 68 *rgg*/*shp* homologs, 28 of them carrying different amino acid sequences, suggesting the widespread distribution of Rgg/SHP pairs in the streptococci (Fleuchot *et al*., 2011; Cook and Federle, 2014). Based on this analysis, streptococcal SHPs have been classified into three groups. In first and second groups (I and II), the SHPs contain a conserved glutamate and aspartate residues at the C-terminal end, respectively, and both *shp* and *rgg* genes are transcribed divergently. While in the third group (III), *shp* genes are situated downstream of *rgg* genes and transcribed in the opposite direction with an overlap at the 3’-ends (Figure 1.5B). SHPs in this group contain either a glutamate or an aspartate residue in their C-terminus These conserved residues are believed to be important for the peptide maturation (Fleuchot *et al*., 2013).

The working mechanism of this QS system relies on the synthesis of SHP, which is produced as a pre-peptide, and released to the extracellular environment by a specific peptide transporter (Sec pathway or the ABC-type transporters). They are processed either during transport or in the extracellular milieu by the pheromone-specific peptidase (Eep). Once they reach to sufficient concentration, they are imported back into the bacterial cell by the aid of an oligopeptide permease Opp, and subsequently interact with the cognate cytoplasmic receptor Rgg. As a result, the imported peptides modulate the activity of the Rgg regulon including the *shp,* which encodes for SHP, generating a positive-feedback regulation (Chang *et al*., 2011).

The first interaction between Rgg and SHP was identified in *S. thermophilus* LMD-9 (*rgg1358*), in which *rgg1358* regulatory functions rely on the adjacent *shp1358* gene and two transport systems (*eep,* codes protease and *ami,* codes oligopeptide permease) (Ibrahim *et al*., 2007b; Fleuchot *et al*., 2011). Similar regulatory mechanisms such as Rgg0182/SHP, RovS/SHP1520, Rgg2/SHP2 and Rgg3/SHP3 have been recognised in the *S. thermophilus* strain LMG18311 (Henry *et al*., 2011), in *S. agalactiae* (Cook *et al*., 2013), and two in *S. pyogenes* (Chang *et al*., 2011; LaSarre *et al*., 2012), respectively. Additionally, a cross-talk has been observed among streptococcal Rgg/SHP QS systems. For example, SHP3 of *S. pyogenes* was found to induce the expression of *shp* of other streptococcal species like *S. agalactiae* and *S. mutans* (Fleuchot *et al*., 2013), and SHP1520 of *S. agalactiae* could induce the expression of *shp2* and *shp3* in *S. pyogenes* and vice versa (Cook *et al*., 2013).

Despite the similarity in mechanisms of production and processing of SHPs, the transcriptional regulation and effect of each peptide are widely different. For example, in *S. pyogenes* Rgg2 acts as activator while, Rgg3 as a repressor for their adjacent *shp* genes. Both are involved in streptococcal aggregation and biofilm formation which are important for colonisation, antibiotic resistance and necrotic infections (Chang *et al.,* 2011). In addition, Rgg/SHP systems enable *S. pyogenes* to survive in different environmental conditions such as in the presence of non-preferred sugars like mannose and in a metal depleted environment. It also increases streptococcal resistance capability against lysozyme, an important human antimicrobial enzyme that exists in mucosal secretions and immunological cells and promotes streptococcal colonisation and persistence within the host (Chang *et al*., 2015). All these data provide evidence that the Rgg/SHP systems are involved in regulation of different social behaviors, thus each Rgg/SHP circuit requires individual examination to understand the mechanism by which each protein regulates transcription in response to peptide.

Recent studies have also characterised the involvement of Rgg proteins in regulation of the *shp* genes through the use of transcriptional reporter constructs. The results have shown that the presence of Rgg and SHP are essential for *shp* induction as disruption of one of them, resulted in a significant reduction in reporter induction (Fleuchot *et al*., 2011; Pérez-Pascual *et al*., 2015). In addition, using different synthetic versions of SHP peptides in the reporter assay, a strong correlation between SHP length and ability to induce *shp* transcription was reported (Aggarwal *et al*., 2014). For example, in *S. pyogenes* the SHP synthetic peptide comprising a C-terminal eight amino acids was sufficient for *shp* expression whereas synthetic peptides carrying full length SHP had lacked this ability. It is reasoned that unfavourable intramolecular interaction between Rgg and full-length SHP prevented *shp* transcription. This is consistent with the model, suggesting that pre-SHP peptides require processing and modification in order to be active and able to interact properly with Rgg (Aggarwal *et al*., 2014). Thus, it was suggested that the C-terminal region of Rgg-associated SHP peptide contains a domain necessary to transmit the cellular responses. Furthermore, it was also found that the intact C-terminal domain of SHP peptide is also important for Rgg activation as changing one residue by substitution or deletion resulted in a significant reduction in *shp* induction (Chang *et al*., 2011). In spite of these observations, the natural composition and length of mature SHP-signalling pheromones remain elusive and need to be investigated (Aggarwal *et al*., 2014).

1.10. Rgg/SHP cassette in *S. pneumoniae* D39

In pneumococcal genomes, the number of Rgg homologs range from 3 to 6. Type 2 D39 strain contains five putative Rgg homologs (SPD_0144, SPD_0939, SPD_0999, SPD_1518, and SPD_1952). A study conducted by Zhi *et al*., (2018) showed that three clusters, represented by SPD_0144, SPD_0999, and SPD_1952, are found in all the analysed pneumococcal strains, while SPD_0939 and SPD_1518 are present only in 54% and 38% of selected pneumococcal strains, respectively. Off these, SPD_0144 and SPD_0939 are associated with *shp* genes, whereas for other Rggs, there is no peptide pheromone, hence they are considered as stand-alone regulators. Recent study conducted by Junges *et al*. (2017) have characterised the pneumococcal Rgg/SHP0939 QS system and its regulatory role on capsule biosynthesis. The authors showed that a pneumococcal operon containing 12 genes is upregulated by Rgg/SHP system, leading to an increase in capsule size and inhibition of biofilm formation on epithelial lung cells. Additionally, Cuevas *et al*. (2017) have also revealed the involvement of Rgg/SHP in biofilm synthesis and pneumococcal pathogenesis through regulation of the expression of Gly-Gly virulence peptide 1 (*vp1*). This peptide is highly expressed in the chinchilla model of middle ear infection and plays a role in biofilm development on chinchilla middle ear epithelial cells. Our recent work has also showed the involvement of pneumococcal Rggs in regulation of the genes responsible for important physiological functions and virulence such as capsule synthesis and cell division. Inactivation of the Rgg/SHP144 QS system attenuated pneumococcal utilisation of mannose and abrogated pneumococcal virulence and colonisation in an experimental animal model (Zhi *et al*., 2018). Due to the importance of Rgg systems in pneumococcal biology, and their potential utility as a drug target, here, I focused on studying Rgg/SHP144. I characterised the functional importance of SHP144 amino acid residues for Rgg-mediated transcription, binding and pneumococcal pathogenesis in order to understand the molecular basis of Rgg/SHP144 mediated transcriptional control, and for designing anti-infective drug leads.

1.11. Structural characterisation of RRNPP family

All RRNPP family proteins (Rgg, NprR, PlcR, and PrgX) are DNA-binding transcription factors except Rap proteins which are phosphatases and transcriptional anti-activators (Parashar *et al*., 2015). All the RRNPP family have a tetratricopeptide (TPR)-like repeat domain at the C-terminal end, consisting of 5-9 repeated motifs, responsible for protein oligomerisation and peptide binding (LaSarre *et al.*, 2012). The RRNPP family, except Rap proteins, have helix turn-helix (HTH) motif in their N-terminus, probably for interaction with the promoter region of their target genes (Do and Kumaraswami, 2016). Thus, it is reasonable to suggest that all these QS systems are derived from the same ancestor (Declerck *et al.*, 2007). So far, only the molecular structure of enterococcal transcription regulator PrgX with its cognate peptide PrgX:cCF10 (Shi *et al.*, 2005), PlcR/PapR in *Bacillus cereus* (Declerck *et al.*, 2007), Rap/Phr in *Bacillus subtilis* (Gallego del Sol and Marina, 2013; Parashar *et al.*, 2013) and NprR:NprX in *Bacillus cereus* (Zouhir *et al.*, 2013) have been revealed. Based on structural analysis, it was found that RRNPP members share a common fold and operate via a peptide-mediated switch, however their modes of action are different. For example, the two members of RRNPP (PlcR of *Bacillus cereus* and PrgX from *Enterococcus faecalis*), showed significant difference in their interactions with DNA promoters and conformational changes. For example, PrgX binds to its target promoters as a tetramer through its HTH domains forming a loop in the DNA that prevents transcription (Shi *et al.*, 2005). Upon interaction with its peptide, a conformational change disrupts the tetramer and the PrgX dimers fall off the DNA through loss of avidity thereby allowing transcription to proceed. By contrast, PlcR is a transcription activator that cannot bind to DNA without its peptide. Peptide binding repositions the HTH domains to enable DNA binding and promote transcription (Grenha *et al.*, 2013). A remarkable feature of the PlcR and PrgX systems is that the conformational changes that regulate transcription are different.

To our knowledge, Rggs with their cognate peptide SHPs have not been yet characterised structurally in *S. pneumoniae*. Recently, Prof Russell Wallis and Dr Hasan Yesilkaya (personal communication) obtained the structure of the Rgg144 protein and generated a model of Rgg/SHP144 interaction in *S. pneumoniae* D39. Pronounced grooves have been identified at C-terminus of Rgg144, which are predicted to be the binding site for the SHP. Regarding Rgg binding to SHP, it has been established that different versions of SHP have different affinity to bind to Rgg proteins, and more importantly, their binding affinities are correlated with Rgg transcriptional activity. For instance, incapability of SHP to bind with Rgg is associated with its inability to induce *shp* expression (Aggarwal *et al.*, 2014). It is predicted that Rgg/SHP binding at C-terminal regions enhances intermolecular rearrangements that enables the HTH domain of Rgg to bind properly to its DNA–binding sites located at *shp* promoter region, thus allowing transcriptional activation or suppression to occur (LaSarre *et al.*, 2012). In spite of identification of Rgg/SHP binding, it is still unknown which SHP residue is critical for Rgg binding.

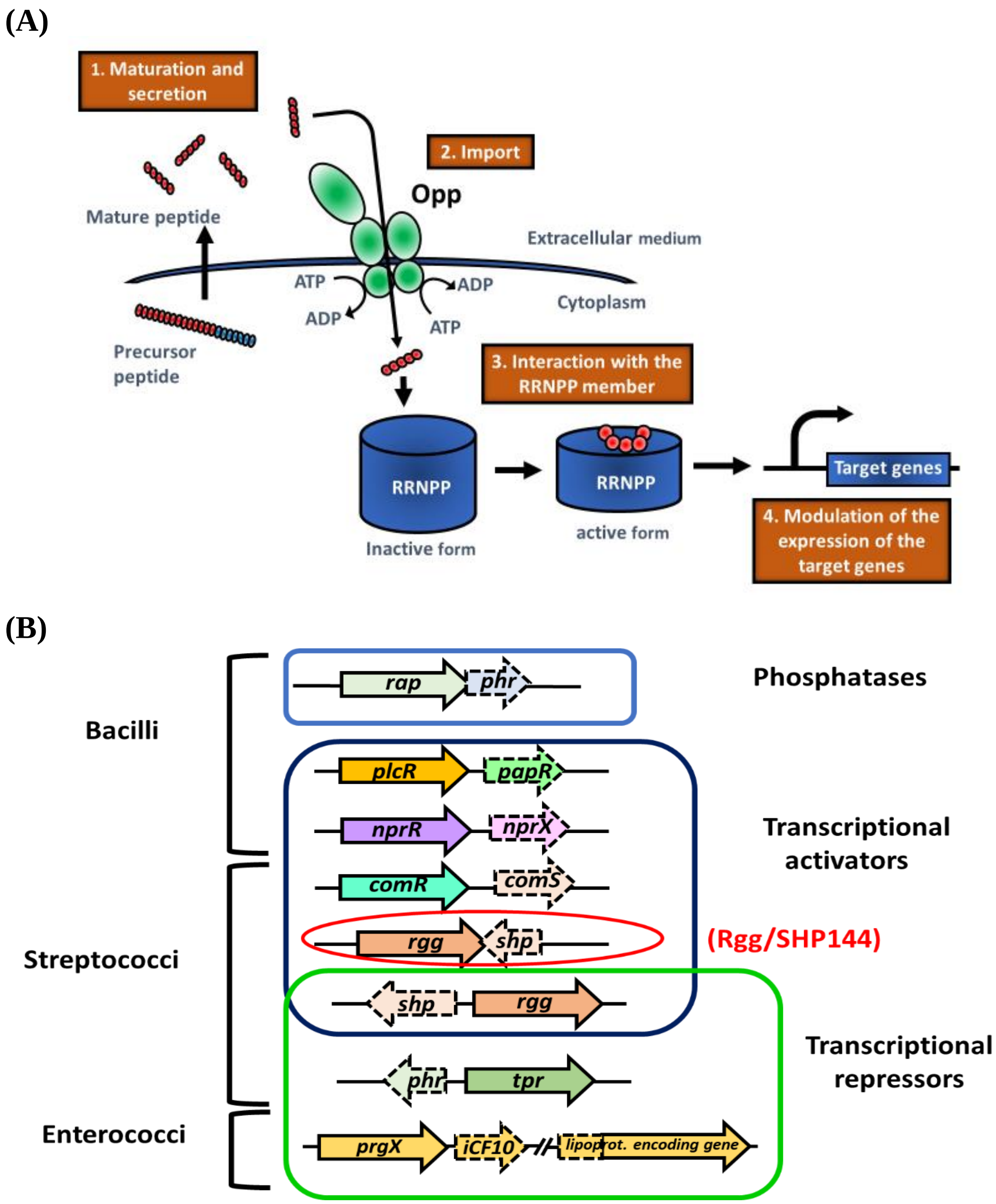

Figure 1.5: RRNPP quorum sensing pathways in Gram positive bacteria. **(A)** Signalling peptides are initially synthesised as precursor peptides inside the cell, and then exported to the extracellular environment. Once they reach threshold concentration, they are reimported inside the cell by the aid of Opp system and interact with cytoplasmic transcriptional regulators to coordinate the QS regulated genes. **(B)** Genetic organisation

of the loci encoding RRNPP members (plain arrows) and their cognate peptides (dotted arrows). Highlighted in red colour represents pneumococcal Rgg/SHP144 which will be studied in detail in this project. Figures **(A)** and **(B)** were constructed based on Monnet and Gardan (2015).

1.12. Utilisation of quorum sensing pathways as anti-virulence drugs

Antibiotic resistance is one of the top threats to global health around the world (Brooks and Brooks, 2014). Thus, there is an urgent need to develop new antibiotics that are effective, less prone to microbial resistance, and cheap to produce (Wohlleben *et al*., 2016). Unfortunately, the pace of developing new antibiotics is slower than the rapid increase in the prevalence of antibiotic resistant strains. While financial constraints are important considerations, there are also biological and methodological reasons that hinder antibiotic development programs.

Methodologies utilised for antimicrobial drug discovery has significant impact on the outcome of drug development programs. There are three well-established methodologies for anti-infective discovery. These include (i) bioactive-guided screening using substances in crude or purified forms for biological activity mainly in whole cell assays without knowledge on drug target, (ii) chemical screening (from biological sources or from chemical libraries) to identify novel, chemically diverse molecules without consideration to biological activity, and (iii) the target-orientated screening, which aims to identify compounds that hit a known and validated molecular target (Wohlleben *et al*., 2016). The main drawback of these approaches is that they are expensive, laborious and they do not make use of the existing knowledge of the biological target or the advantages inherent within the system.

In this study, I focused on bacterial communication systems as potential anti-infective targets (Kalia, 2013), and my approach to drug discovery is based on the knowledge gathered from the system under study. As mentioned above a wide range of microbial phenotypes are modulated by QS systems including biofilm formation, competence, sporulation, microbial competition and virulence expression (Rocha-Estrada *et al*., 2010; Rutherford and Bassler, 2012). QS system homologs are absent in mammalian hosts and conserved among pathogenic bacteria decreasing the possibility of host-toxicity and ensuring targets in human pathogens, respectively. Moreover, unlike drugs targeting the essential cellular functions such as DNA replication, protein and cell wall biosynthesis (Dong *et al*., 2007; Allen *et al*., 2014), those targeting virulence factors is expected to impose less selective pressure due to their non-essential nature for microbial survival, hence, the likelihood of antibiotic resistance would be lower (Clatworthy *et al*., 2007; Brooks and Brooks, 2014).

In this study, I focused on studying pneumococcal Rgg/SHP144 and potential ability to utilise this system to create inhibitors for pneumococcal diseases. I hypothesised that by preventing the interaction between SHP144 and its cognate cytoplasmic receptor Rgg144, the pneumococcal phenotypes mediated by this system could be switched off, reducing the adaptive capability of the microbe. My results showed that SHP144 residues have different roles in activation and binding. Using this knowledge, I found that P21A replacement in active 13 aa long SHP144 representing the C-terminal end of the peptide (SHP144-C13) led to the competitive inhibition of Rgg144 activation, and diminished pneumococcal growth on mannose and resistance ability against oxidative stress induced by paraquat and H_2O_2. Here, my results present an alternative way of developing an inhibitor for Rgg/SHP144 systems that can be utilised for other QS systems.

1.13. Aims and objectives

The central hypothesis underlying this study was that SHP144 binding and Rgg144 transformation leading to transcription are mediated, at least in part, by distinct subsets of interacting amino acid residues. Decoupling Rgg binding from transcription regulation would convert the SHP from an allosteric activator to an inhibitor, thus preventing the Rgg from changing the behaviour of the pneumococcus. Thus, the ultimate aims of this study were to establish a drug discovery platform using the inherent capabilities of Rgg/SHP system. To achieve these aims, several synthetic peptides representing the C-terminal end of SHP144 were synthesised to identify active SHP144 using reporter strains P_{shp144}::*lacZ*-Wt and P_{shp144}::*lacZ*-Δ*shp144* (‘P’-promoter). Site directed mutagenesis was used for systemic substitution of selected individual amino acids residues of SHP144 with alanine, and the effect of each amino acid replacement on Rgg144-mediated transcription was studied using a transcriptional reporter assay. Furthermore, the binding affinity of native and mutant SHP144-C13 peptides to Rgg144 were also measured using fluorescence polarisation assay. Different modified SHP144 synthetic peptides labelled with Fluorescein isothiocyanate were synthesised and tested for their ability to bind to purified recombinant full length Rgg144 protein using fluorescence polarisation assay. Crystallisation of Rgg144 with its ligand (modified and non-modified SHP144) was also trialled using different commercial crystallisation kits and sitting-drop vapor diffusion technique. The phenotypic impacts of mutations were determined by oxidative stress induced by paraquat and H_2O_2, by growth assays in the presence of different sugars, capsule synthesis, and *in vivo*.

Chapter 2. Materials and Methods

2.1. Chemicals and reagents

Unless otherwise indicated all reagents and chemicals used for media preparation were purchased from Oxoid and Sigma-Aldrich, UK. Restriction endonuclease enzymes and DNA ladder were ordered from New England Biolabs, UK. For protein purification, centrifugal protein concentrators were ordered from Millipore, complete protease inhibitor tablets from Roche, Switzerland. Ni-affinity resin and Superdex 200 16/60 columns were purchased from GE Healthcare, UK. BugBuster protein extraction reagent was from Merck Millipore and Isopropyl β-D-1-thiogalactopyranoside (IPTG) from Sigma.

2.2. Culture media and antibiotics used in this study

Different culture media were used for growth of *S. pneumoniae* D39 and *E. coli*. Culture media were prepared according to manufacturer's specifications, and sterilised by autoclaving at 121°C at 15 psi pressure for 15 min.

For *S. pneumoniae,* Brain Heart Infusion broth (BHI), Todd-Hewitt broth supplemented with 0.5% (w/v) yeast extract (THY) and Blood agar base (BAB) supplemented with 5% (v/v) sterilised defibrinated horse blood were used for growing of pneumococcal strains at 37°C in candle jar (5% CO_2) to provide anaerobic environment. BAB was prepared according to manufacturer's instructions and autoclaved. After sterilisation, the media was cooled down to 45°C before adding 5% (v/v) of defibrinated horse blood. The media was mixed well, and 20 ml was dispensed into sterile petri plates and kept at 4°C. When necessary, appropriate amount of antibiotics were added to culture media (100 µg/ml spectinomycin, 250 µg/ml kanamycin, 3 µg/ml tetracycline and 1 µg/ml gentamicin). The antibiotic stocks and working solutions are listed in Table 2.1.

Table 2.1: Antibiotic stock solutions and working concentrations used in this study.

Antibiotics	**Stock concentration (mg/ml)**	**Solvent**	**Working concentration (µg/ml)**	
			E. coli	***S. pneumoniae***
Ampicillin	100	dH_2O	100	-
Kanamycin	50	dH_2O	50	250
Tetracycline	15	50% (v/v) ethanol	-	3
Spectinomycin	100	dH_2O	-	100
Gentamicin	5	dH_2O	-	1

All antibiotics were dissolved either in distilled water or in 50% ethanol and sterilised using 0.22 µm syringe filter (Millipore, UK). After sterilisation, the antibiotics solutions were aliquoted into 500 µl in sterile Eppendorf tubes and kept at -20°C for further use.

Chemically defined medium (CDM) supplemented with desired sugar (van de Rijn and Kessler, 1980; Kloosterman *et al*., 2006b) was also used for growing of *S. pneumoniae* to study phenotypic characterisations of wild type and its isogenic mutants. This media consists of mixture of solutions (basal solution, amino acids, vitamins, micronutrients, nitrogenous bases, sodium pyruvate and choline-HCl). The composition of each solution is given in Table 2.2. Basal solution was prepared in 870 ml deionised water, and pH was adjusted to 6.5. The solution was then sterilised by autoclaving at 121°C for 15 min and kept at -20°C until use. Micronutrients and amino acids were prepared by dissolving in deionised water and the pH was adjusted to 6.5 for amino acids solution, filter sterilised before storage at 4°C. For vitamin supplements, riboflavin was dissolved in 75% of total volume of the solution and heated up to 70°C. D-biotin and folic acid were dissolved in 2 M NaOH. Once riboflavin solution is cooled to 30°C, other vitamins were added, and pH was adjusted to 6.5. The vitamin solution was then filtered and kept at 4°C for further use. All nitrogenous bases were dissolved in 0.1 M NaOH, sterilised through a 0.22 µm membrane filter and kept at 4°C. Pyruvate and choline-HCl solutions were prepared as indicated in Table 2.2. The selected sugars (glucose, galactose, mannose, *N*-acetylglucosamine and maltose) were also prepared in deionised water, filtered and stored at 4°C.

Finally, CDM was prepared by mixing appropriate amount from each solution as shown in Table 2.3. When required, appropriate amount of selected sugar (Table 2.2) was added to the medium as a main source of carbon to a final concentration 250 µM for maltose and 55 mM of other sugars.

Table 2.2: List of chemicals used for preparation of chemically defined medium.

Components	Stock (g/L)	Components	Stock (g/L)
Basal solution (pH 6.5)		**Vitamins (pH 6.5)**	
Na_2-β-glycerophosphate	26.0	Na-p-Aminobenzoate	0.5
$(NH_4)_3$ citrate	0.6	D-Biotin	0.25
KH_2PO_4	1.0	Folic acid	0.1
Na-Acetate	1.0	Nicotinic acid	0.1
Cysteine-HCl	0.4	Ca (D+) Pantothenate	0.1
Amino acids (pH 6.5)		Pyridoxamine-HCl	0.25
Alanine	3	Pyridoxine-HCl	0.2
Arginine	1.55	Riboflavin	0.1
Asparagine	4.4	Thiamine-HCl	0.1
Aspartate	5.25	DL-6,8-Thioctic acid	0.15
Glutamate	6.25	Vitamin B12	0.1
Glutamine	4.9	**Nitrogenous bases**	
Glycine	2.2	Adenine	1.0
Histidine	1.9	Uracil	1.0
Isoleucine	2.65	Xanthine	1.0
Leucine	5.7	Guanine	1.0
Lysine	5.5	**Micronutrients**	
Methionine	1.55	$MgCl_2$	20
Phenylalanine	3.45	$CaCl_2$	3.8
Proline	8.45	$ZnSO_4$	0.5
Serine	4.25	**Sugars (when required)**	
Threonine	2.8	Glucose	500

Tryptophan	0.65	Mannose	500
Valine	4.05	Galactose	250
Other components		*N*-acetylglucosamine	222
Pyruvate	10	Maltose	1
Choline- HCl	2.5		

Table 2.3: Volume of prepared solutions in Table 2.2 used for preparation of CDM.

Ingredients	**Volume (ml)**
Basal solution	870
Amino acids	80
Micronutrients	10
Nitrogenous bases	10
Vitamins	10
Choline-HCl	4
Pyruvate	1

E. coli strains were used for plasmid propagation and were grown either in Luria Bertani Broth (LB) (10 g/L of NaCl, 5 g/L of yeast extract and 10 g/L trypticase peptone) in a shaking incubator (220 rpm) (New Brunswick Scientific, USA) at 37°C or on Luria agar (LA) (LB supplemented with 1.5% (w/v) bacteriological agar). When required, ampicillin and kanamycin were added to *E. coli* culture at 100 µg/ml and 50 µg/ml respectively (Table 2.1).

2.3. Bacterial strains and plasmids used in this study

All bacterial strains, reporter constructs and plasmids used and constructed in this study are listed in Tables 2.4, 2.5 and 2.6, respectively.

Table 2.4: Pneumococcal strains used in this study.

Strains	Description	Source
***S. pneumoniae* D39**	Serotype 2 virulent strain	Dr Hasan Yesilkaya
Δ*shp144*	D39; shp0144:Spec^R	Dr Hasan Yesilkaya
Δ*rgg144*	D39; SPD0144:Spec^R	Dr Hasan Yesilkaya
Δ*rgg144/shp144*	D39; SPD0144:Spec^R; shp0144:Spec^R	Dr Hasan Yesilkaya
Δ*rgg144*Com	D39; *rgg144* + Δ*rgg144*:Spec^R; Kan^R	Dr Hasan Yesilkaya
Δ*shp144*Com	D39; *shp144* + Δ*shp144*:Spec^R; Kan^R	This study
Δ*shp144*ComS14A	D39; *shp144*S14A + Δ*shp144*:Spec^R; Kan^R	This study
Δ*shp144*ComE15A	D39; *shp144*E15A + Δ*shp144*:Spec^R; Kan^R	This study
Δ*shp144*ComW16A	D39; *shp144*W16A + Δ*shp144*:Spec^R; Kan^R	This study
Δ*shp144*ComV17A	D39; *shp144*V17A + Δ*shp144*:Spec^R; Kan^R	This study
Δ*shp144*ComI18A	D39; *shp144*I18A + Δ*shp144*:Spec^R; Kan^R	This study
Δ*shp144*ComV19A	D39; *shp144*V19A + Δ*shp144*:Spec^R; Kan^R	This study
Δ*shp144*ComI20A	D39; *shp144*I20A + Δ*shp144*:Spec^R; Kan^R	This study
Δ*shp144*ComP21A	D39; *shp144*P21A + Δ*shp144*:Spec^R; Kan^R	This study
Δ*shp144*ComF22A	D39; *shp144*F22A + Δ*shp144*:Spec^R; Kan^R	This study

Δ*shp144*ComL23A	D39; *shp144*L23A + Δ*shp144*:Spec^{R}; Kan^{R}	This study
Δ*shp144*ComT24A	D39; *shp144*T24A + Δ*shp144*:Spec^{R}; Kan^{R}	This study
Δ*shp144*ComN25A	D39; *shp144*N25A + Δ*shp144*:Spec^{R}; Kan^{R}	This study
Δ*shp144*ComL26A	D39; *shp144*L26A + Δ*shp144*:Spec^{R}; Kan^{R}	This study

Table 2.5: Pneumococcal reporter (*lacZ*-fusion) strains constructed in this study

Strains	Description	Source
P$_{shp144}$::*lacZ*-Wt	D39; Δ*bgaA*::P$_{shp144}$-*lacZ*; Tet^{R}	This study
P$_{shp144}$::*lacZ*-Δ*shp144*	Δ*shp144*:Spec^{R}; Δ*bgaA*::P$_{shp144}$-*lacZ*; Tet^{R}	This study
P$_{shp144}$::*lacZ*-Δ*shp144*Com	Δ*shp144*Com:Spec^{R}; Kan^{R}; Δ*bgaA* ::P$_{shp144}$-*lacZ*; Tet^{R}	This study
P$_{shp144}$::*lacZ*-Δ*shp144*ComS14A	Δ*shp144*ComS14A:Spec^{R}; Kan^{R}; Δ*bgaA*::P$_{shp144}$-*lacZ*; Tet^{R}	This study
P$_{shp144}$::*lacZ*-Δ*shp144*ComE15A	Δ*shp144*ComE15A:Spec^{R}; Kan^{R}; Δ*bgaA*::P$_{shp144}$-*lacZ*; Tet^{R}	This study
P$_{shp144}$::*lacZ*-Δ*shp144*ComW16A	Δ*shp144*ComW16A:Spec^{R}; Kan^{R}; Δ*bgaA*::P$_{shp144}$-*lacZ*; Tet^{R}	This study
P$_{shp144}$::*lacZ*-Δ*shp144*ComV17A	Δ*shp144*ComV17A:Spec^{R}; Kan^{R}; Δ*bgaA*::P$_{shp144}$-*lacZ*; Tet^{R}	This study
P$_{shp144}$::*lacZ*-Δ*shp144*ComI18A	Δ*shp144*ComI18A:Spec^{R}; Kan^{R}; Δ*bgaA*::P$_{shp144}$-*lacZ*; Tet^{R}	This study
P$_{shp144}$::*lacZ*-Δ*shp144*ComV19A	Δ*shp144*ComV19A:Spec^{R}; Kan^{R}; Δ*bgaA*::P$_{shp144}$-*lacZ*; Tet^{R}	This study
P$_{shp144}$::*lacZ*-Δ*shp144*ComI20A	Δ*shp144*ComI20A:Spec^{R}; Kan^{R}; Δ*bgaA*::P$_{shp144}$-*lacZ*; Tet^{R}	This study

P$_{shp144}$::*lacZ*-Δ*shp144*ComP21A	Δ*shp144*ComP21A:Spec^{R}; Kan^{R}; Δ*bgaA*::P$_{shp144}$-*lacZ*; Tet^{R}	This study
P$_{shp144}$::*lacZ*-Δ*shp144*ComF22A	Δ*shp144*ComF22A:Spec^{R}; Kan^{R}; Δ*bgaA*::P$_{shp144}$-*lacZ*; Tet^{R}	This study
P$_{shp144}$::*lacZ*-Δ*shp144*ComL23A	Δ*shp144*ComL23A:Spec^{R}; Kan^{R}; Δ*bgaA*::P$_{shp144}$-*lacZ*; Tet^{R}	This study
P$_{shp144}$::*lacZ*-Δ*shp144*ComT24A	Δ*shp144*ComT24A:Spec^{R}; Kan^{R}; Δ*bgaA*::P$_{shp144}$-*lacZ*; Tet^{R}	This study
P$_{shp144}$::*lacZ*-Δ*shp144*ComN25A	Δ*shp144*ComN25A:Spec^{R}; Kan^{R}; Δ*bgaA*::P$_{shp144}$-*lacZ*; Tet^{R}	This study
P$_{shp144}$::*lacZ*-Δ*shp144*ComL26A	Δ*shp144*ComL26A:Spec^{R}; Kan^{R}; Δ*bgaA*::P$_{shp144}$-*lacZ*; Tet^{R}	This study
P$_{shp144}$::*lacZ*-Δ*rgg144*	Δ*rgg144*:Spec^{R}; Δ*bgaA*::P$_{shp144}$-*lacZ*; Tet^{R}	This study
P$_{shp144}$::*lacZ*-Δ*rgg144*Com	Δ*rgg144*Com:Spec^{R}; Kan^{R}; Δ*bgaA*::P$_{shp144}$-*lacZ*; Tet^{R}	This study
P$_{shp144}$::*lacZ*-Δ*rgg144/shp144*	Δ*rgg144/shp144*:Spec^{R}; Δ*bgaA*::P$_{shp144}$-*lacZ*; Tet^{R}	This study
pPP2-Wt	D39; Δ*bgaA*::pPP2-*lacZ*; Tet^{R}	This study

Table 2.6: List of plasmids and competent *E. coli* strains used in this study.

Plasmids/Strains	Description	Source
pLEICS-01	6His-Tag for protein expression; Amp^R	PROTEX, UK
pCEP	Genetic complementation; Kan^R	Guiral *et al.*, 2006
pPP2	Promoterless *lacZ* for transcriptional fusions; Amp^R Tet^R	Halfman *et al.*, 2007b
***E. coli* BL21 (DE3)**	Protein expression	Agilent Technology Ltd., UK
***E. coli* TOP10**	Plasmid propagation	Laboratory collection
***E. coli* DH5α**	Plasmid propagation	In-Fusion® HD Cloning Kit, Clontech, USA

2.4. Preparation of bacterial glycerol stock

Pneumococcal glycerol stock was prepared by streaking a single colony on a blood agar plate and incubated overnight at 37°C in 5% CO_2. The next day, a sweep of colonies was transferred to 10 ml of BHI and harvested at 37°C to mid-exponential phase OD_{600} ~0.6. The bacterial culture was spun down at 3500 rpm for 10 min (Sorvall legend T, Thermo Scientific), and the supernatant was discarded. The bacterial pellet was resuspended in 1 ml of BHI supplemented with 15% (v/v) glycerol, aliquoted in 1.5 ml microcentrifuge tubes and kept at -80° C for further use.

For *E. coli*, the bacterial strains were initially plated on LA agar plates and transferred to 10 ml of LB broth. The culture was then incubated aerobically in shacking incubator at 37°C until OD_{600} had reached ~0.6. At this stage, the culture was centrifuged at 3500rpm for 10 min and the pellet was diluted in LB broth containing 15% (v/v) glycerol. The bacterial sample was distributed into small aliquots and kept at -80°C until needed.

2.5. Colony forming unit count (CFU/ml)

Miles and Misra method were used to count viable cell in bacterial culture. An aliquot of 20 µl of bacterial suspension was mixed with 180 µl of sterile PBS, pH 7.0 in 96 well microtiter plate, and followed by a 10-fold serial dilution. Forty microliters were taken from each dilution and plated onto fresh blood agar plates. The plates were dried at room temperature and left at 37°C for overnight incubation in a candle jar. The sections which had 30-300 colonies were counted, and colony forming unit per ml (CFU/ml) was calculated according to the following formula (Miles *et al*., 1938).

CFU/ml= number of colonies X dilution factor X 1000/40

2.6. Pneumococcal DNA extraction

Pneumococcal DNA was isolated using phenol/chloroform extraction method (Saito and Maiura, 1963). The overnight pneumococcal culture was centrifuged at 3500 rpm for 10 minutes (Sorvall Legend RR, Thermo Scientific). The pellet was then resuspended in 400 µl of TE buffer (1 M Tris-HCl and 500 mM EDTA, pH 8.0) containing 25% (w/v) sucrose, 60 µl of 500 mM EDTA, 40 µl of 10% (w/v) sodium dodecyl sulphate SDS (1g of SDS was dissolved in 10 ml of dH_2O) and 2 µl of proteinase K (12.5 mg/ml). This mixture was transferred to 1.5 ml microcentrifuge tube and incubated at 37°C for 1-2 hours until a clear lysate was formed. After incubation, the sample was centrifuged at 13000 rpm for 5 minutes in a bench top centrifuge (Microfuge, Sigma). The upper aqueous phase was transferred to a fresh 1.5 ml tube without disturbing the white protein layer and mixed with an equal volume of phenol: chloroform: isoamyl alcohol (25:24:1, v/v) (Invitrogen, UK). The sample was gently mixed until an emulsion was formed, and then centrifuged at 13000 rpm for 10 min, and upper aqueous phase was transferred to a fresh tube without disturbing the white protein layer formed between the two phases. The previous step was repeated by mixing the sample with an equal volume of liquid phenol (Sigma-Aldrich) and centrifuged as before. The 500 µl of clear aqueous phase of bacterial sample was mixed with 2.5 ml of 100 % ethanol (v/v) and 25 µl of 3 M sodium acetate pH 5.2, then spun down at 13000 rpm for 5 min. The supernatant was discarded, and the pellet was washed with 500 µl of 70% (v/v) ethanol. The sample was centrifuged again at 13000 rpm for 5 min and the supernatant was discarded. The pellet was left to dry for few minutes at room temperature before resuspending with 250 µl of TE buffer pH 7.0. The concentration of extracted DNA was measured at OD_{260} using a NanoDrop^{TM} spectrophotometer (Thermo Scientific, UK), and kept at -20°C until use.

2.7. Purification of DNA fragments from agarose gel and PCR product

A Wizard® SV Gel and PCR clean-Up kit (Promega, USA) was used to purify DNA fragments either from dissolved gel slices or directly from PCR product by following supplier's instructions. This system relies on binding of DNA to silica membrane in the presence of chaotropic salts and allowing the impurities to pass with flow through.
To purify DNA recovered from agarose gel, the band of interest was excised with a minimal amount of gel by a clean scalpel and transferred to a pre-weighed 1.5 ml microcentrifuge tube. The slice was then weighed and mixed with membrane binding solution (4.5 M guanidine isothiocyanate, 0.5 M potassium acetate, pH 5.0) at a ratio of 10 µl of membrane binding solution per 10 mg of gel slice. The mixture was vortexed and incubated at 50-65°C for 10 min in a thermo-shaker (Grant-Bio) or until the gel slice was fully molten. The dissolved gel was then transferred to SV mini column and incubated for 1 min at room temperature. The column was centrifuged at 16000 x g for 1 min in bench top microcentrifuge, and the flow through was discarded. The SV Mini column was reinserted again into collection tube, washed with 700 µl of membrane wash solution (10 mM potassium acetate pH 5.0, 80% ethanol, 16.7 µM EDTA pH 8.0) and centrifuged at 16000 x g for 1 min. The recovered DNA was washed again with 500 µl of wash buffer and spun down at 16000 x g for 5 min. The centrifugation process was repeated for another 1 min without lid to eliminate residual ethanol. The SV Mini column was transferred to a fresh 1.5 ml tube, and the bound DNA was eluted in 50 µl of nuclease-free water. The column was incubated for 1 min at room temperature and centrifuged at 16000 x g for 1 min. The SV Mini column was removed, and tube containing purified DNA was kept at –20°C until needed.

To purify DNA from PCR amplification product, an equal volume of membrane binding solution was directly added to the PCR sample and the PCR mixture was transferred to the SV mini column by following the same procedure as described above. The purified DNA was run on ethidium bromide-stained agarose gel and visualised under a UV transilluminator system (UVP, USA) to confirm the successful recovery of purified DNA.

2.8. Extraction of plasmid DNA

A QIAprep Spin Miniprep Kit (Qiagen, UK) was used to extract plasmid DNA from *E. coli* culture by following manufacturer's instructions. Briefly, *E. coli* harbouring a desired plasmid or construct was inoculated into 10 ml of LB broth supplemented with appropriate antibiotic and incubated overnight at 37°C in a shaking incubator. The overnight culture was centrifuged at 3500 rpm for 10 min, and the supernatant was discarded. The pellet was resuspended in 250 µl of Buffer P1 (50 mM Tris-HCl, pH 8.0, 10 mM EDTA, 100 µg/ml RNase A), followed by addition of 250 µl lysis Buffer P2 (200 mM NaOH, 1% SDS). The cell lysate was then neutralized by adding 350 µl of neutralization Buffer N3 (4.2 M guanidine-HCl, 0.9 M potassium acetate, pH 4.8), and thoroughly mixing by inverting the tube 4-6 times until a cloudy suspension had formed. The sample was then pelleted at 13000 rpm for 10 min in a bench top microcentrifuge (Microfuge, Sigma), and the supernatant was transferred to a clean QIAprep spin column without disturbing the pelleted protein layer. The column was spun down again for 1 min and the flow-through was discarded. Then column was reinserted into collection tube and washed with 500 µl of Buffer PB (5 M guanidine-HCl, 30% isopropanol) to remove any trace of nucleases. The sample was then spun down at 13000 rpm for 1 min and washed again with 750 µl of Buffer PE (10 mM Tris-HCl pH 7.5, 80% ethanol) to remove buffers and residual ethanol that could interfere with the subsequent enzymatic reactions. The washed column was centrifuged twice for 1 min at 13000 rpm. Finally, the QIAprep column was transferred to a clean 1.5 ml centrifuge tube, and the recovered plasmid was eluted with 50 µl of Buffer EB (10 mM Tris-HCl, pH 8.5). The column was left to stand for 1 min at room temperature prior to centrifugation at 13000 rpm for 1 min. The concentration of resulting plasmid was quantified using a NanoDrop^{TM} (Thermo Scientific, UK), and kept at -20°C for further use.

2.9. Agarose gel electrophoresis

Gel electrophoresis was used to analyse the size and integrity of genomic DNA/PCR products using previously described method (Sambrook *et al.*, 1989). The DNA sample was electrophoretically separated on a 1% (w/v) agarose gel, which was prepared by dissolving 1g of agarose (Bioline, UK) in 100 ml of 1X TAE buffer (40 mM Tris-acetate, 1 mM EDTA, pH 8.0) (Sigma). The suspension was heated in microwave until the gel was completely dissolved, and left to cool down to 55°C. The gel was then mixed with ethidium bromide (10 mg/ml) to a final concentration 0.5 µg/ml and poured into gel-casting tray. Once the gel was solidified, DNA samples were loaded into wells after mixing with 5 µl of 6x loading dye (New England Biolabs, UK). The 1 kb or 100 bp ladder was also loaded along in the same gel to estimate the size and concentration of DNA. The electrophoresis was run at 100 volts for approximately 1 h and DNA was visualized under UV light using a long-wave UV transilluminator.

2.10. Preparation of cell lysate by sonication

Cell free lysate was prepared from pneumococcal constructs to study enzymatic activity of pneumococcal strains. Briefly, *S. pneumoniae* wild type and its isogenic mutants were inoculated into 10 ml of BHI and incubated overnight at 37°C. The overnight culture was centrifuged at 3500 rpm for 10 min and the supernatant was discarded. The pelleted cells were washed once with 10 ml of PBS and re-suspended in 2 ml of PBS pH 7.0. The cells were lysed by sonication (Sanyo soniprep 150, Japan) at an amplitude of 8 microns, 15 sec pulse followed by 45 sec intervals on ice container to avoid protein denaturation due to overheating. Sonication process was repeated for at least 6-8 times to ensure the complete disruption of bacterial cells. The sample was then transferred to 1.5 ml microcentrifuge tube and pelleted at 14000 rpm for 15 min at 4°C (Heraeus^{TM} Fresco^{TM} 21, Thermo Scientific). The supernatant was transferred to a clean tube, aliquoted and kept at -80°C until required.

2.11. Quantification of protein concentration

Bradford assay was used to measure total protein concentration in the pneumococcal cell lysates using Bradford dye-protein binding method (Bradford, 1976). Bio-Rad protein reagent (Bio-Rad Laboratories Inc., Hercules, CA) with a set of bovine serum albumin (BSA) standards (0-1000µg/ml) were used to generate Bradford standard curve through measuring the absorbance of standards at 595 nm using a microplate reader model infinite F50 (TECAN). Standard curve was created as shown in Figure 2.1 by plotting the absorbance of each standard against its concentration (µg/ml). The slop of standard curve was determined using linear regression fitting and was used to measure unknown protein concentration.

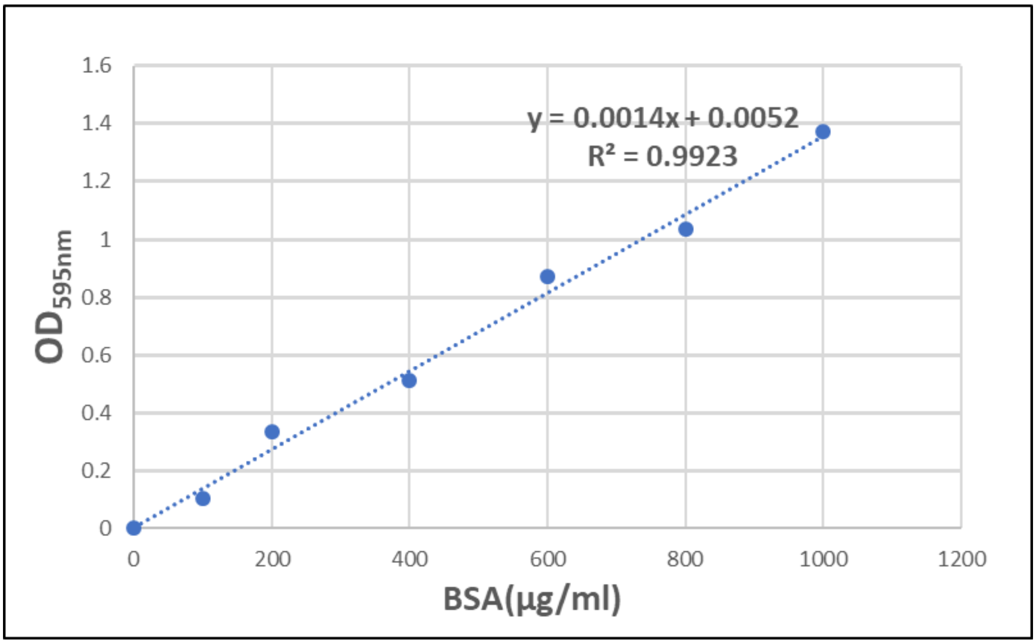

Figure 2.1: A typical Bradford standard curve using different concentrations of BSA.

2.12. Haemolytic activity assay

Haemolytic activity of pneumococcal strains was determined as described previously (Pan *et al*., 2009; Kimaro Mlacha *et al*., 2013) with slight modifications. To perform this assay, 4% (v/v) sheep red blood cells (RBC) were prepared by washing twice in cold phosphate buffered saline (PBS). Serial two-fold dilutions (50 µl) of pneumococcal lysates (Section 2.10) were prepared in 96 well microtiter plate, and then 50 µl of washed RBC was added to cell lysate to yield a final 2% (v/v) concentration. The plate was then incubated for 30 min at 37°C and centrifuged at 1000 x g for 10 min using Jouan C4i benchtop centrifuge (Thermo Scientific, UK). After centrifugation, the supernatant was transferred to a clean microtiter plate and absorbance of released haemoglobin was measured at 540 nm using Multiskan^{TM} GO Microplate Spectrophotometer (Thermo Scientific, UK). A blank reaction containing 50 µl of PBS instead of the cell lysate was also included. This assay was done for three independent biological samples and each with three replicates.

2.13. Neuraminidase activity assay

Neuraminidase activity of pneumococcal strains was quantified using 2-*O*-(p-Nitrophenyl)-α-D-*N*-acetylneuraminic acid (pNP-NANA) as a substrate (Sigma, UK) as described before (Manco *et al.*, 2006). Neuraminidase cleaves substrate pNP-NANA and releases free *p*-nitrophenol (pNP), the latter can be detected at a wavelength of 405 nm. The 25 µl of prepared cell lysate (Section 2.10) was mixed with 25 µl of 0.3 mM pNP-NANA dissolved in phosphate buffered saline (PBS), pH 7.0 in 96 well flat bottom plate. The plate was then incubated statically at 37°C for 2 hours and the reaction was stopped by adding 100 µl of ice cold 0.5 M Na_2CO_3 (pH 9.6) into each well. The amount of pNP released was measured spectrophotometrically by reading at 405 nm using Multiskan^{TM} GO Microplate Spectrophotometer (Thermo Scientific, UK). The absorbance values were corrected from blank containing 25 µl of PBS instead of the sample. This assay was done in triplicates and repeated for three independent cell lysates. Finally, neuraminidase activity was calculated using a standard curve prepared from known concentrations of *p*-nitrophenol (Sigma). One unit of enzyme activity was defined as the amount of enzyme that produced 1nmol *p*-nitrophenol per min per microgram of protein under assay condition.

2.14. Pneumococcal growth assay

Multiskan^{TM} GO Microplate Spectrophotometer (Thermo Scientific, UK) was used to characterise the growth properties of wild type and its isogenic mutants. The 198 µl of BHI or CDM supplemented with 55 mM of desired sugar, with or without synthetic peptide (Section 2.15) was placed into 96 well flat bottom microtiter plate and was mixed with 2 µl of bacterial suspension containing approximately 5 x 10^9 CFU/ml. The microtiter plate was placed inside the spectrophotometer, and optical density (OD) of bacterial cells was measured at a wavelength of 600 nm every hour over 18 hours at 37°C. This experiment was done in triplicate and repeated with three independent cultures. The growth yield of each strain was calculated by measuring the highest optical density during the bacterial growth. Maximum growth rate (µ) was also calculated by using the following equation (Neidhardt *et al.*, 1990; Widdel, 2007).

$(\mu)\ h^{-1} = \ln OD_2 - \ln OD_1 / t_2\text{-}t_1$

In= natural logarithm of a number

t_2-t_1= Time of growth in late and early exponential phase

OD_1= Cell density at t_1

OD_2= Cell density at t_2

2.15. Synthetic SHP144 peptides

Several synthetic SHP144 peptides representing the C-terminal end with or without Fluorescein isothiocyanate (FITC) were purchased from CovalAb, UK with a high purity (>98%). All stocks were prepared by dissolving lyophilised peptides in DMSO (Dimethyl sulfoxide) to a final concentration of 6 mM and were kept at -20°C for further use. Labelled peptides were sealed with aluminium foil to protect from the light. The sequence of each SHP144 peptide is presented in Tables 2.7, 2.8 and 2.9.

Table 2.7: SHP144 variants used in this study.

SHP144	Peptide sequence
SHP144-C8	NH_2-VIPFLTNL-COOH
SHP144-C9	NH_2-IVIPFLTNL-COOH
SHP144-C10	NH_2-VIVIPFLTNL-COOH
SHP144-C11	NH_2-WVIVIPFLTNL-COOH
SHP144-C12	NH_2-EWVIVIPFLTNL-COOH
SHP144-C13	NH_2-SEWVIVIPFLTNL-COOH
SHP144-C14	NH_2-ISEWVIVIPFLTNL-COOH
SHP144-C15	NH_2-LISEWVIVIPFLTNL-COOH
SHP144-C13Rev	NH_2-LNTLFPIVIVWES-COOH

Table 2.8: Modified SHP144-C13 synthetic peptides used in this study. Red bold letter represents the replacement of individual amino acid of SHP144-C13 with alanine.

Modified SHP144-C13	Peptide sequence
SHP144-C13S14A	NH_2-**A**EWVIVIPFLTNL-COOH
SHP144-C13E15A	NH_2-S**A**WVIVIPFLTNL-COOH
SHP144-C13V19A	NH_2-SEWVI**A**IPFLTNL-COOH
SHP144-C13P21A	NH_2-SEWVIVI**A**FLTNL-COOH

Table 2.9: List of FITC-SHP144-C13 peptides used for fluorescence polarisation assay. Red bold letters indicate the modification site of each selected peptide.

FITC-SHP144-C13	Peptide sequence
FITC-SHP144-C13	FITC-SEWVIVIPFLTNL-COOH
FITC-SHP144-C13S14A	FITC-**A**EWVIVIPFLTNL-COOH
FITC-SHP144-C13E15A	FITC-S**A**WVIVIPFLTNL-COOH
FITC-SHP144-C13W16A	FITC-SE**A**VIVIPFLTNL-COOH
FITC-SHP144-C13V17A	FITC-SEW**A**IVIPFLTNL-COOH
FITC-SHP144-C13I18A	FITC-SEWV**A**VIPFLTNL-COOH
FITC-SHP144-C13V19A	FITC-SEWVI**A**IPFLTNL-COOH
FITC-SHP144-C13I20A	FITC-SEWVIV**A**PFLTNL-COOH
FITC-SHP144-C13P21A	FITC-SEWVIVI**A**FLTNL-COOH
FITC-SHP144-C13F22A	FITC-SEWVIVIP**A**LTNL-COOH
FITC-SHP144-C13L23A	FITC-SEWVIVIPF**A**TNL-COOH
FITC-SHP144-C13T24A	FITC-SEWVIVIPFL**A**NL-COOH
FITC-SHP144-C13N25A	FITC-SEWVIVIPFLT**A**L-COOH
FITC-SHP144-C13L26A	FITC-SEWVIVIPFLTN**A**-COOH
FITC-NSP-C13	FITC-SE**YSATH**PFLTNL-COOH

2.16. Polymerase Chain Reaction (PCR)

A Prime thermo cycler machine (Techne, UK) was used for DNA amplification, genetic modification and sequencing analysis. PrimeSTAR HS premix (Clontech, USA) and HotStarTaq *Plus* Master Mix (Qiagen, UK) were used for setting PCR reactions. PrimeSTAR HS Premix contains a high-fidelity DNA Polymerase, which provides a high proof-reading activity and an excellent amplification efficiency. Thus, this enzyme was used for DNA cloning and genetic mutations purposes. A typical PCR reaction contained 25 µl of 2x PrimeSTAR HS premix (1.25 U/25 µl PrimeSTAR HS DNA Polymerase, 2X dNTP mixture 0.4 mM each, 2X PrimeSTAR buffer including 2 mM Mg^{2+}), 2 µl of DNA template (20 ng/µl), 2 µl of gene specific forward and reverse primers mix (1 pmol each/reaction) and 21 µl of nuclease-free water to a final volume of 50 µl. The PCR reaction was carried out with initial denaturation at 98°C for 10 sec, followed by 30 amplification cycle. Each cycle consisted of three fundamental steps: denaturation of double stranded DNA template at 98°C for 10 sec, annealing at 55°C for 5 sec (depends on primer’s temperature) and extension at 72°C for 1min /1 kb of DNA target, and hold at 4°C.

Routinely, HotStarTaq *Plus* Master Mix was used for confirmation of successful cloning of target gene. The PCR reaction was prepared in a final volume of 20 µl including 10 µl 2X HotStarTaq *Plus* Master Mix (HotStarTaq *Plus* DNA Polymerase, PCR Buffer with 3 mM $MgCl_2$, and 400 µM of each dNTP), 2 µl of gene specific primers (1 pmol each/reaction), 2 µl genomic DNA or plasmid template (20 ng/µl) and 6 µl of nuclease-free water. The PCR machine was set to run initial activation for 10 min at 95°C followed by 30 cycles for amplification: denaturation at 95°C for 45 sec, annealing at 55°C for 45 sec, extension at 72°C for 1 min/kb, final extension at 72°C for 10 min, and hold at 4°C. All Primers used for cloning and genetic complementation are listed in Table 2.10.

Table 2.10: Oligonucleotides primers used in this study.

Primers	Nucleotide sequence (5'- 3')
Shp144Com/F	CATG**CCATGG**CAAGTACAGTATAACACGAAA
Shp144Com/R	ACG**GGATCC**CCTTTTTGAATTGCGTTTTCAGCA
Shp144S14A/F	CCTACTTATTGCGGAGTGGGTTATT

Shp144S14A/R	AATAACCCACTCCGCAATAAGTAGG
Shp144E15A/F	CTTATTTCGGCGTGGGTTATTGTCA
Shp144E15A/R	TGACAATAACCCACGCCGAAATAAG
Shp144W16A/F	TATTTCGGAGGCGGTTATTGTCATTC
Shp144W16A/R	GAATGACAATAACCGCCTCCGAAATA
Shp144V17A/F	TCGGAGTGGGCTATTGTCATTCCAT
Shp144V17A/R	ATGGAATGACAATAGCCCACTCCGA
Shp144I18A/F	GGAGTGGGTTGCTGTCATTCCATTTT
Shp144I18A/R	AAAATGGAATGACAGCAACCCACTCC
Shp144V19A/F	TGGGTTATTGCCATTCCATTTTTAA
Shp144V19A/R	TTAAAAATGGAATGGCAATAACCCA
Shp144I20A/F	GGTTATTGTCGCTCCATTTTTAAC
Shp144I20A/R	GTTAAAAATGGAGCGACAATAACC
Shp144P21A/F	TATTGTCATTGCATTTTTAACTAAT
Shp144P21A/R	ATTAGTTAAAAATGCAATGACAATA
Shp144F22A/F	TGTCATTCCAGCTTTAACTAATCT
Shp144F22A/R	AGATTAGTTAAAGCTGGAATGACA
Shp144L23A/F	CATTCCATTTGCAACTAATCTATAAG
Shp144L23A/R	CTTATAGATTAGTTGCAAATGGAATG
Shp144T24A/F	TCCATTTTTAGCTAATCTATAAGTT
Shp144T24A/R	AACTTATAGATTAGCTAAAAATGGA
Shp144N25A/F	TTTTTAACTGCTCTATAAGTTCTT
Shp144N25A/R	AAGAACTTATAGAGCAGTTAAAAA
Shp144L26A/F	TAACTAATGCATAAGTTCTTTATATTG
Shp144L26A/R	CAATATAAAGAACTTATGCATTAGTTA
NcoI-shp144	*AACACACGAGGTGCTA***CCATGG**CAACTCAGCTTCTGTCAATTCC
BamHI-shp144	*CCATTAAAAATCAAAC***GGATCC**CTTATCAGAACTCATGGAGCGA
Mal/F	GCTTGAAAAGGAGTATACTT
pCEP/R	AGGAGACATTCCTTCCGTATC

Bold typeface refers to the incorporated restriction sites of *NcoI* and *BamHI*, respectively, whereas italicised letters represent the homologous regions of pCEP. Red colour is amino acid codon that was replaced with alanine, and underlined letters are the base pairs that had been changed.

2.17. Restriction and ligation of DNA fragments

Generation of compatible ends for vector and insert gene is considered as an essential element for performing an efficient cloning so that using appropriate restriction endonuclease enzymes are necessary for cleavage DNA molecules at specific sites. In this study, pCEP plasmid (Guiral *et al.*, 2006) was used for construction of genetically modified and unmodified complemented stains. *BamHI* and *NcoI* enzymes were used for double digestion of pCEP plasmid and target insert. The digestion mixture contained ~1 µg DNA fragment (plasmid/insert), 1 µl (10 U/µl) from each enzyme, 5 µl of the corresponding 10X CutSmart® buffer (NEB, UK) and nuclease-free water to a total volume of 50 µl. The mixture was incubated in a water bath for 3 hours at 37°C. The digested DNA was purified using Wizard® SV Gel and PCR clean-up system (Section 2.7) and visualized on an ethidium bromide-stained agarose gel. Finally, the digested insert was ligated into linearised pCEP. The ligation reaction was prepared in 20 µl by mixing 2 µl of 10X T4 DNA ligase reaction buffer (50 mM Tris-HCl, 10 mM $MgCl_2$, 1 mM ATP, 10 mM DTT, pH 7.5) (NEB, UK), 2 µl (400 U/µl) of T4 DNA ligase enzyme (NEB, UK), and 1:2 molar ratio of purified plasmid to insert. The reaction was incubated in a PCR machine for 16 hours at 16°C followed by inactivation of T4 ligase activity at 65°C for 10 min. The ligated product was then transformed into competent *E. coli* TOP10 as shown in section 2.19.

2.18. Preparation of chemically competent *E. coli*

Chemically competent *E. coli* was prepared according to the protocol described before (Green and Rogers, 2013) with some modifications. Briefly, *E. coli* TOP10 from the frozen stock was streaked on LA plate, and incubated overnight at 37°C. Then, a single colony was picked and inoculated into 5 ml LB broth containing 20 mM $MgSO_4$. The bacterial culture was incubated at 37°C for 16-18 h in a shaking incubator. Next day, 1 ml of the overnight culture was transferred to 100 ml LB broth and incubated for 2.5-3 hours or until OD_{550} was reached ~0.7-0.8. At this stage, the culture was harvested by centrifugation at 3000 rpm for 10 min (Sorvall legend T, Thermo Scientific). The cell pellet was re-suspended in 30 ml of sterile ice-cold Tfb I buffer [(K-acetate 3 mM, $MnCl_2$ 50 mM, KCl 100 mM, $CaCl_2$ 10 mM, glycerol 15% (v/v)] and cooled down on ice for 5-30 min. Bacterial cells were spun down at 3000 rpm for 10 min at 4°C and the supernatant was discarded. The pellet was re-suspended in a total volume of 4 ml of Tfb II buffer [(Na-MOPS 10 mM, $CaCl_2$ 75 mM, KCl 10 mM, glycerol 15% (v/v)]. The bacterial suspension was aliquoted into 60 µl in sterile microcentrifuge tubes and stored at -80°C for further use.

2.19. Transformation into chemically competent *E. coli*

Recombinant plasmid carrying gene of interest was transferred to chemically competent *E. coli* TOP10 or BL21 (DE3) by conventional heat-shock protocol. An aliquot of competent *E. coli* cells was thawed on ice, and 50 µl was transferred to a prechilled 14 ml BD Falcon polypropylene round bottom tube. The competent cells were then mixed with 5 µl of plasmid and incubated on ice for 30 min to allow the plasmid to be close contact with the bacterial cell. Then, plasmid-cell mixture was heated to 42°C for 45 sec in water bath and placed on ice bucket for 2 min to facilitate the uptake of the DNA. Finally, 500 µl of pre-warmed LB was added to the transformation reaction and incubated for 90 min at 37°C in a shaking incubator to promote the recovery of bacteria. After incubation, 250 µl of transformation mixture was plated onto duplicate LA agar plates supplemented with appropriate antibiotic, and incubated overnight at 37°C. The successful transformation was confirmed by colony PCR using HotStarTaq *Plus* Master Mix and plasmid specific primers. One of the positive transformants was selected for plasmid extraction and for DNA sequencing.

2.20. Transformation into *S. pneumoniae*

The insert in recombinant plasmid was transformed into pneumococcal strains following the method previously described (Bricker and Camilli, 1999). To do this, *S. pneumoniae* was initially inoculated into 10 ml of BHI and incubated overnight at 37°C in a static incubator. The overnight culture was then centrifuged at 3500 rpm for 10 min, and the pellet was resuspended in 1 ml of fresh BHI. The bacterial suspension was diluted in 10 ml of fresh BHI at a ratio of 1:100 (v/v), and then incubated at 37°C until OD_{600} had reached ~0.06-0.08. At this point, 860 µl of bacterial culture was transferred to 1.5 ml sterile microcentrifuge tube, and mixed with 100 µl of 100 mM NaOH, 10 µl of 20% (w/v) bovine serum albumin (BSA), 10 µl of 100 mM $CaCl_2$, 2 µl of 50 ng/µl competence stimulating peptide (CSP) and 5-10 µl of extracted plasmid. The mixture was then incubated at 37°C for 3 hours, and 330 µl of mixture was plated out each hour on blood agar plates containing appropriate antibiotics. The plates were incubated overnight at 37°C. The successful integration of insert into pneumococcal genome was confirmed by colony PCR using pneumococcal DNA as a template and two sets of primers (gene and vector specific primers) (Table 2.10). The DNA template was extracted by inoculating a single transformant into 10 ml of BHI containing appropriate antibiotic and harvested overnight at 37°C. After overnight incubation, 1ml of culture was transferred to sterile Eppendorf tube and centrifuged at 13000 rpm for 2 min. The pellet was then resuspended in 500 µl of PBS, and heated on a hot plate to 95°C for 5 min. The heated mixture was cooled down on ice for 2 min and centrifuged at 13000 rpm for 1 min using a bench-top microcentrifuge. Subsequently, the supernatant was transferred to fresh tube without disturbing the pellet and was used for PCR reaction.

2.21. Genetic complementation of Δ*shp144*

To eliminate the possibility of polar effects of genes located downstream of *shp144*, an intact copy of *shp144* (150351-150581) was introduced into transcriptionally silent site using non-replicative plasmid pCEP as previously described (Guiral *et al.*, 2006). This plasmid (9540 bp) is characterised by its ability to replicate in *E. coli*, but not in *S. pneumoniae*. Although it is non-replicative in *S. pneumoniae*, but it has about 2 kb DNA fragment homologous to pneumococcal genome. For this reason, the recombinant pCEP carrying the gene of interest can be directly integrated into downstream of *amiA* operon, which is considered as a transcriptionally silent site, hence the integration of exogenous gene does not cause any detrimental effects on pneumococcal cellular functions (Alloing *et al.*, 1990). pCEP has also a maltosaccharide-inducible promoter separated from kanamycin cassette gene by multiple cloning sites. Therefore, cloned gene expression could be driven by its own native promoter or by maltosaccharide-inducible promoter in the plasmid.

2.21.1. Cloning of *shp144* gene into pCEP

Plasmid pCEP was extracted from *E. coli* using the QIAprep spin Miniprep kit as previously described in section 2.8. The *shp144* gene and its putative promoter region were amplified using proof reading PrimeSTAR HS premix enzyme (Section 2.16) and set of gene specific primers (Shp144Com/F and Shp144Com/R) containing *NcoI and BamHI* restriction sites (Table 2.10). After amplification, the PCR product was purified using Wizard® SV Gel and PCR clean-up system and analysed on 1% (w/v) agarose gel electrophoresis. The pCEP plasmid and amplified gene were double digested with high fidelity *NcoI* and *BamHI* restriction enzymes (Section 2.17) and purified using the Wizard® SV Gel and PCR clean-up purification kit. Linearised pCEP was subjected to agarose gel electrophoresis and was compared with uncut pCEP to confirm the successful digestion. Finally, digested insert was ligated to pCEP by PCR using T4 DNA ligase (Section 2.17) and transformed into competent *E. coli* TOP10. The transformants were selected on LA plates containing 50 µg/ml kanamycin (Section 2.19).

2.21.2. Confirmation of successful transformation into *E. coli*

Following transformation into *E. coli*, kanamycin-resistant clones were screened for successful incorporation of entire gene into pCEP by colony PCR using HotStarTaq *Plus* Master Mix (Section 2.16) and plasmid dependent primers (Mal/F and pCEP/R) (Table 2.10), whose recognition sites are located directly up and downstream of the cloning site. Further conformation was done by DNA sequencing to rule out the presence of unwanted mutation(s).

2.21.3. DNA sequencing and transformation into Δ*shp144*

The successful genetic complementation was confirmed by DNA sequencing. The extracted recombinant pCEP was amplified using PrimeSTAR HS Premix and plasmid-based primers (Table 2.10). The amplified fragments were then purified using Wizard® SV Gel and PCR purification kit and sent for sequencing at the Protein Nucleic Acid Chemistry Laboratory (PNACL), University of Leicester. DNA sequence data were aligned with complete genome sequence of *S. pneumoniae* D39 (Accession no. NC_008533.1) by using NCBI Blast.

The sequenced plasmid carrying the gene of interest was transformed into *shp144* knock out mutant using the protocol previously mentioned in section 2.20. Transformants were selected on blood agar plates containing 250 μg/ml Kanamycin and 100 μg/ml spectinomycin respectively and were screened for successful incorporation of *shp144* into pneumococcal genome by PCR using HotStarTaq *Plus* MasterMix (Section 2.16) with vector and gene specific primers (Table 2.10). The construct was designated as Δ*shp144*Com.

2.22. Construction of genetically modified *shp144* strains using overlap extension method

To assess the involvement of each amino acid residue of SHP144 in Rgg144 regulation, each residue in active SHP144 was replaced with alanine by using overlap extension PCR (SOEing PCR) method (Lee *et al.*, 2004). This method is simple and efficient; however, several difficulties had been encountered during cloning of modified *shp144* gene into cloning plasmid pCEP (Guiral *et al.*, 2006). This was due to inefficient cleavage of DNA fragments. This problem was overcome by designing primers containing 16 base pairs extensions homologous to cloning sites of pCEP. This homologous sequence was added at 5′ end of external primers in front of restriction sites (Table 2.10). Therefore, all genetically modified strains were successfully constructed using two-PCR steps, and strategy of cloning is depicted in Figure 2.2. In the first PCR reaction, right and left flanks of modified *shp144* were individually amplified using pneumococcal DNA as a template and PrimeSTAR HS premix (Section 2.16). The primers used were external primers containing *NcoI* and *BamHI* restriction sites respectively, and mutagenic primers containing mutated region. The left flank region was generated using primer pairs *NcoI*-shp144 and Shp144XA/R, whereas right flank was set up by using *BamHI*-shp144 and Shp144XA/F (where XA refers to an amino acid in SHP codon is replaced with alanine codon). The PCR product was purified using Wizard® SV Gel and PCR clean-up purification kit as previously described in section 2.7 and used as template for the next round of PCR amplification.

In the second PCR, the purified flanking regions carrying homologous sequences for each other were overlapped and joined together to produce linear fused product using proof reading PrimerSTAR HS premix enzyme (Section 2.16) and outermost primers pair (*NcoI*-shp144 and *BamHI*-shp144). The fused fragment representing a full-length modified *shp144* was subjected into 1% (w/v) agarose gel electrophoresis, and band of interest was excised and purified using Wizard® SV Gel and PCR Clean-Up System. The compositions of two-PCR reactions are presented in Table 2.11.

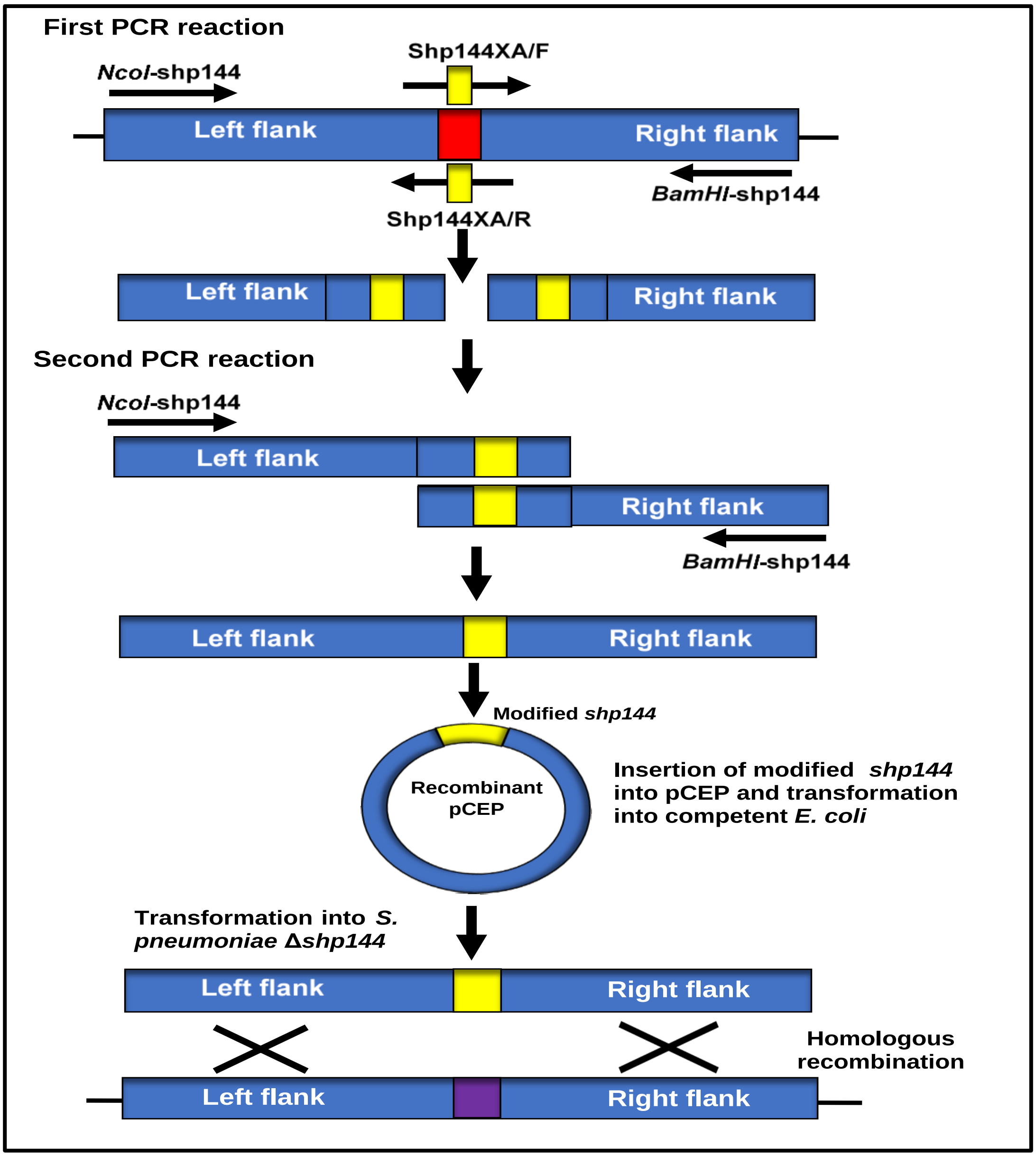

Figure 2.2: Schematic diagram showing steps of introducing point mutation into *shp144* sequence using overlap extension method. The red box represents D39 wild type nucleotides which are replaced with modified nucleotides (yellow box). The *NcoI*-shp144 and *BamHI*-shp144 refer to external primers carrying *NcoI* and *BamHI* restriction sites respectively whereas Shp144XA/F and Shp144XA/R represent mutagenic primers containing the intended mutation. The XA indicates the replaced amino acid codon of *shp144* with alanine. The purple box represents transcriptionally silent site in S. pneumoniae Δ*shp144*. This figure was adapted from Horton *et al*. (1993).

Table 2.11: The stages of PCR reactions for construction of modified *shp144.*

First PCR reaction

Components	**Volume (concentration)**
Template pneumococcal DNA	2 µl (20 ng/µl)
Primers Left flank (*NcoI*-shp144 and Shp144XA/R) Right flank (*BamHI*-shp144 and Shp144XA/F)	2 µl (1 pmol each/reaction)
Enzyme (PrimeSTAR HS premix)	25 µl (2X)
Nuclease-free water	21 µl
Total	50 µl

Second PCR reaction

Components	**Volume (concentration)**
Template Purified right and left flanks (1st PCR reaction)	4 µl (2 µl from each flank) (20 ng/µl)
Primers *NcoI*-shp144 and *BamHI*-shp144	2 µl (1 pmol each/reaction)
Enzyme (PrimeSTAR HS premix)	25 µl (2X)
Nuclease-free water	19 µl
Total	50 µl

Subsequently, purified DNA fragments were double digested with *NcoI* and *BamHI* (Section 2.17) and purified using Wizard® SV Gel and PCR Clean-Up System. Linearised DNA fragment was ligated into cut pCEP using T4 ligase (Section 2.17). Next, an aliquot of ligation mixture was transformed into competent *E. coli* TOP10 and transformants were selected on LA agar plates containing 50 µg/ml kanamycin. After 16 hours incubation, transformants were checked for correct assembly by colony PCR using HotStarTaq *Plus* Master Mix and pCEP based primers (Mal/F and pCEP/R). One of the positive transformants was selected for plasmid preparation and DNA sequence analysis (Section 2.21.3). The sequenced plasmid was then transformed into downstream of *amiA* operon at a transcriptionally silent site in *S. pneumoniae* Δ*shp144* following the procedure previously described in section 2.20. The colonies were selected on blood agar plates supplemented with appropriate antibiotics (100 µg/ml spectinomycin and 250 µg/ml kanamycin). Antibiotic resistant *S. pneumoniae* clones were screened for the presence of the insert in the correct position by PCR using gene specific primers (*NcoI*-shp144 and *BamHI*-shp144) and vector dependent primers (Mal/F and pCEP/R).

2.23. Construction of pneumococcal transcriptional reporter strains

To better understand the involvement of selected SHP144 residues in transcriptional regulation, several pneumococcal *lacZ* fusion constructs were generated following the protocol previously reported (Halfmann *et al*., 2007b). After *in silico* identification of promoter region of *shp144* (P_{shp144},"P" indicates promoter) using bacterial promoter recognition software BPROM (Softberry, USA) (Solovyev and Salamov, 2011; Maidin *et al*., 2014), the putative promoter region of *shp144* gene was amplified by PCR using proof reading PrimeSTAR HS premix enzyme (Section 2.16). The amplified PCR product was double digested and fused into promoterless *lacZ* gene in an integrative reporter plasmid pPP2. The fused product was then transformed into competent *E. coli* TOP10 by heat shock (Section 2.19). The transformants were selected on LA plates supplemented with 100 µg/ml of ampicillin. The successful cloning was confirmed by colony PCR and DNA sequencing using set of primers (Fusion-Seq-F and Fusion-Seq-R) as shown in Table 2.12. The cloned plasmid carrying P_{sh144} was transformed into different pneumococcal backgrounds via double crossover in the *bgaA* gene following the protocol mentioned in section 2.20. The transformants were selected on blood agar plates supplemented with

3 μg/ml tetracycline for wild type, and with 100 μg/ml spectinomycin and 3 μg/ml tetracycline for mutant background, respectively. The successful integration of *lacZ*-fusion into wild type and mutant genomes was confirmed by colony PCR using primer pairs Fusion-Seq-F and Fusion-Seq-R, whose recognition sites are located immediately up and downstream of the cloning site. Transcriptional reporter strains constructed in this study are provided in Table 2.5.

Table 2.12: Primers used for confirmation of successful construction of pneumococcal *lacZ*-fusions.

Primers	Nucleotide sequence (5'- 3')
Fusion-Seq-F	CTACTTGGAGCCACTATCGA
Fusion-Seq-R	AGGCGATTAAGTTGGGTAAC

2.24. Determination β-galactosidase activity of pneumococcal reporter strains

β-galactosidase assay was used to assess P_{shp144} induction level in different pneumococcal backgrounds using previously published protocol with slight modifications (Miller, 1972; Zhang and Bremer, 1995). The induced *shp144* promoter transcriptionally drive the expression of the promoterless *lacZ* gene resulting in production of β-galactosidase enzyme. This enzyme hydrolyses the colourless substrate *O*-Nitrophenyl-β-D-galactopyranoside (ONPG) generating galactose and *O*-Nitrophenyl, a soluble yellow product. The β-galactosidase activity in the cell-free extract can be quantified by measuring the amount of *O*-Nitrophenyl released over time spectrophotometrically at 420 nm.

The pneumococcal *lacZ*-fusion constructs or "reporter strains" were grown in 10 ml of CDM supplemented with selected sugar to late exponential phase. When synthetic SHP144 peptide (Tables 2.7 and 2.8) was used, the pneumococcal culture was grown to an early exponential phase. The 3 ml of each culture was centrifuged at 3500 rpm for 15 min and the supernatant was discarded. The pellet was then resuspended in 3 ml of chilled Z buffer (0.80 g $Na_2HPO_4.7H_2O$, 0.28 g $NaH_2PO_4.H_2O$, 0.5 ml 1M KCl, 0.05 ml 1M $MgSO_4$, 0.175 ml β-mercaptoethanol (BME), 40 ml dH_2O, pH 7.0) and the absorbance was measured at 600 nm wavelength by using Z buffer as blank. Then, the cells were further diluted in Z buffer at a ratio of 1:10 (100 µl bacterial cell: 900 µl Z buffer) and permeabilised with one drop of Triton^{TM} X-100 (Sigma-Aldrich, UK). After incubation for 5-10 min at 30°C, 200 µl of ONPG (4 mg/ml) was added to the mixture and incubated for 90 min at 30°C. When a sufficient yellow colour had developed, the reaction was stopped by adding 500 µl of 1 M Na_2CO_3, and incubation time was recorded. Finally, the sample was centrifuged at 14000 rpm for 5-10 min (Microfuge, Sigma), and absorbance of the supernatant was measured at 420 nm. This experiment was done in triplicate and repeated at least for three times. The enzymatic activity was calculated using the following equation and expressed in Miller units (nmol *p*-nitrophenol/min/ml).

Miller units =1000x OD_{420}/ (TxVxOD_{600})
OD_{600} and OD_{420} = Density of cells at different wavelengths
T =Time of the reaction in minutes
V =Volume of the culture used in ml

2.25. Detection of Rgg/SHP144 inhibitor using spent culture supernatant

To test the capability of modified SHP144 peptides to competitively inhibit endogenous SHP144 produced by wild type D39, the cell-free culture supernatants were collected from wild type D39 and genetically complemented native and modified *shp144* strains. To perform this, the pneumococcal cultures were inoculated into 30 ml of CDM supplemented with 55 mM mannose and incubated at 37°C until late-exponential phase. The complemented *shp144* cultures were also supplemented with 250 µM maltose to induce pCEP maltose promoter. All bacterial cultures were spun down at 4000 rpm for 30 min at 4°C, and the supernatants were collected and sterilised using 0.22 µm syringe filter. The collected supernatants were kept at -20°C for further analysis.

The inhibitory assay was done by growing wild type reporter strain P_{shp144}::*lacZ*-Wt to an OD_{600} ~0.6 and centrifugation at 3500 rpm for 15 min. The pellet was resuspended with wild type, native or modified *shp144* collected supernatants, and allowed to grow to an OD_{600} ~0.5-0.6. At this stage, the culture was centrifuged at 3500 rpm for 15 min and the impact of modification on P_{shp144} transcription was examined using β-galactosidase assay as previously mentioned in section 2.24. The inhibitory effect of modified peptide was also confirmed by the addition of a mixture of wild type and mutant supernatants to the pellet of P*shp144*::*lacZ*-Δ*shp144* deficient SHP144, and assessing P*shp144* activity using β-galactosidase assay.

2.26. Pneumococcal survival assay in the presence of oxidising agents

2.26.1. Paraquat susceptibility assay

To determine whether the mutant SHP144 variants have any impact on pneumococcal resistance ability against toxic effect of paraquat, superoxide generator, the pneumococcal inoculum was prepared as described before (Bortoni *et al*., 2009) with some modifications. Wild type D39, Δ*shp144* Com and mutant strains (Δ*shp144* and Δ*rgg144*) were grown in 10 ml THY broth supplemented with 0.5% yeast extract with or without SHP144 peptide to an early exponential phase (OD_{600} ~0.3-0.4). At this point, 10 µl of the bacterial culture was mixed with 50 µl of paraquat to a final concentration of 1 mM and topped up with PBS to 1 ml. The mixture was then incubated at 37°C for one hour. The bacterial culture without paraquat was used as control. The sample and control were then serially diluted and plated onto blood agar plates. The number of viable cells was counted (Section 2.5), and survival percentages were calculated relative to the control without paraquat.

2.26.2. H_2O_2 survival assay

The pneumococcal inoculum was prepared as described above, and the bacterial cells were treated with varying concentrations of H_2O_2 (10 mM and 20 mM) (Sigma) and incubated for 20 min at 37°C. The CFU/ml was determined by serial dilution and plating on blood agar plates (Section 2.5). The results were expressed as percent survival of treated sample relative to control, which had not been treated with H_2O_2.

2.27. Quantification of glucuronic acid amount in the pneumococcal strains

Capsular polysaccharide (CSP) was extracted and glucuronic acid was quantified using the protocol previously described (Favre-Bonte *et al*., 1999; Lai *et al*., 2003) with slight modifications. The pneumococcal strains were inoculated into 10 ml of CDM supplemented with 55 mM of selected sugar and incubated at 37°C to late exponential phase. At this stage, 500 µl of bacterial culture was transferred to sterile 1.5 ml microcentrifuge tube and mixed with 100 µl of 1 % (v/v) Zwittergent 3-14 detergent (Sigma-Aldrich, UK) in 100 mM citric acid (pH 2.0). After 20 min incubation at 50°C in thermo-shaker (Bio-Grant, UK), the sample was pelleted at 14000 rpm for 5 min, and 300 µl of supernatant was precipitated with 1200 µl of absolute ethanol to a final concentration of 80% (v/v). The bacterial mixture was then placed at 4°C for 20 min, recovered by centrifugation at 14000 rpm for 5 min and resuspended in 200 µl of distilled water.

The amount of glucuronic acid in the isolated capsular polysaccharide was quantified using carbazole method (Cho *et al.*, 2009). The 125 µl of CPS was mixed with 750 µl of 0.025 M sodium tetracarbonate solution (Borax) dissolved in 93% (v/v) H_2SO_4 (Sigma-Aldrich, UK), vigorously vortexed and incubated for 10 min at 100°C in a thermo-shaker. The mixture was cooled down to room temperature on ice box and mixed with 25 µl of 0.125% (w/v) carbazole solution in absolute ethanol (Sigma-Aldrich, UK). The sample was then heated again to 100°C for 10 min and cooled down to room temperature. The absorbance of the mixture was measured at 530 nm. The concentration of glucuronic acid was measured using a standard curve prepared with the known concentrations of glucuronic acid (0, 10, 20, 40, 60, 80, and 100 µg/ml) (Sigma-Aldrich, UK) and the resulting data was expressed as µg of glucuronic acid per 10^7 CFU/ml.

2.28. Biofilm assay

Biofilm formation assay was carried out using method described before (Muñoz-Elías *et al.*, 2008; Hussey *et al.*, 2017). The pneumococcal cells were grown in 10 ml THY supplemented with 0.5% yeast extract and incubated overnight at 37°C. After centrifugation for 15 min at 4000 rpm at 4°C, the pellet was resuspended with 2 ml of fresh THY and cell density was measured at 600 nm. The culture was further diluted with 10 ml of fresh THY to an OD_{600} ~0.05. The bacterial culture (3 ml) was placed in each well of 12 well flat bottom microplate and incubated in a static incubator for 24 hours at 37°C in a candle jar. Next, liquid media was aspirated from the wells and transferred to a new plate. The content of each well was washed with 3 ml of PBS and aspirated. Finally, 1 ml of PBS was added to wells, and biofilm forming cells were detached by cell scraper (Biologix, UK). The CFU/ml of biofilm cells was detected by serial dilution and plating on blood agar plates as described in section 2.5.

2.29. Expression and purification of full length and truncated Rgg144 proteins

2.29.1. Amplification of target gene and cloning into pLEICS-01

The *rgg144* (SPD_0144) representing full length gene or truncated, lacking 216 base pairs, was amplified using PrimeSTAR HS premix and set of specific primers containing 15-18 nucleotides complementary to cloning site of pLEICS-01 (Table 2.13). The PCR amplicon was electrophoresed on 1% (w/v) agarose gel, and the band of expected size was excised and purified to remove salts and primer-dimers using Wizard® SV Gel and PCR Clean-Up System as shown in section 2.7. Next, the targeted PCR fragment was cloned into pLEICS-01 expression vector carrying an N-terminal His-6 tag in collaboration with Protein Expression Laboratory (PROTEX), University of Leicester. The cloning procedure was carried out by following In-Fusion® HD Cloning Kit instructions (Clontech, USA). The overview of the cloning procedure is given in Figure 2.3. Briefly, appropriate amount of purified PCR amplicons was mixed with linearised pLEICS-01 in the presence of 2 µl of 5X In-Fusion HD enzyme premix. The mixture was incubated at 37°C for 20 min followed by heating to 50°C for 20 min. The mixture was then transformed into *E. coli* DH5α, and the transformant cells were selected on LA plates supplemented with 100 µg/ml of ampicillin.

2.29.2. Transformation of recombinant pLEICS-01 into BL21 (DE3)

Following transformation of recombinant plasmid into *E. coli* DH5α, the bacterial colonies were screened by PCR using insert-based primers (Table 2.13). One of the positive clones was selected for further plasmid extraction using QIAprep spin Miniprep kit. The extracted plasmid was verified by DNA sequencing at PNACL using plasmid sequencing primers (T7- Promoter-F and pLEICS-01-Seq-R) as indicated in Table 2.14 to eliminate the possibility of undesirable mutations and confirm the complete coverage of insert sequence. The sequenced plasmid carrying intended gene was subsequently transformed into *E. coli* BL21 (DE3) competent cells using heat shock method (Section 2.19). The successful cloning was confirmed by PCR using HotStarTaq *Plus* Master Mix and insert specific primers (Table 2.13). Glycerol stock was prepared for one of positive transformants and stored at -80°C for further use.

Table 2.13: Primers used for cloning of *rgg144* gene into pLEICS-01 vector.

Primers	Nucleotide sequence (5'- 3')
SPD0144-Full/F	**TACTTCCAATCCATG**ATTGAAAAAATGGAACTGGG
SPD0144-Full/R OR SPD0144-Trun/R	**TATCCACCTTTACTGTCA**ATCTATAAGTTCTTTATATT
SPD0144-Trun/F	**TACTTCCAATCCATG**GAATCTCCACATATGCGAATCGG

Bold typeface nucleotides refer to regions of homology with pLEICS-01, supplied by PROTEX for ligase-independent cloning.

Table 2.14: pLEICS-01 sequencing primers for protein expression.

Primers	Nucleotide sequence (5'- 3')
T7-Promoter-F (PNACL)	TAATACGACTCACTATAGGG
pLEICS-01-Seq-R (PNACL)	ATTAACATTAGTGGTGGTGGT

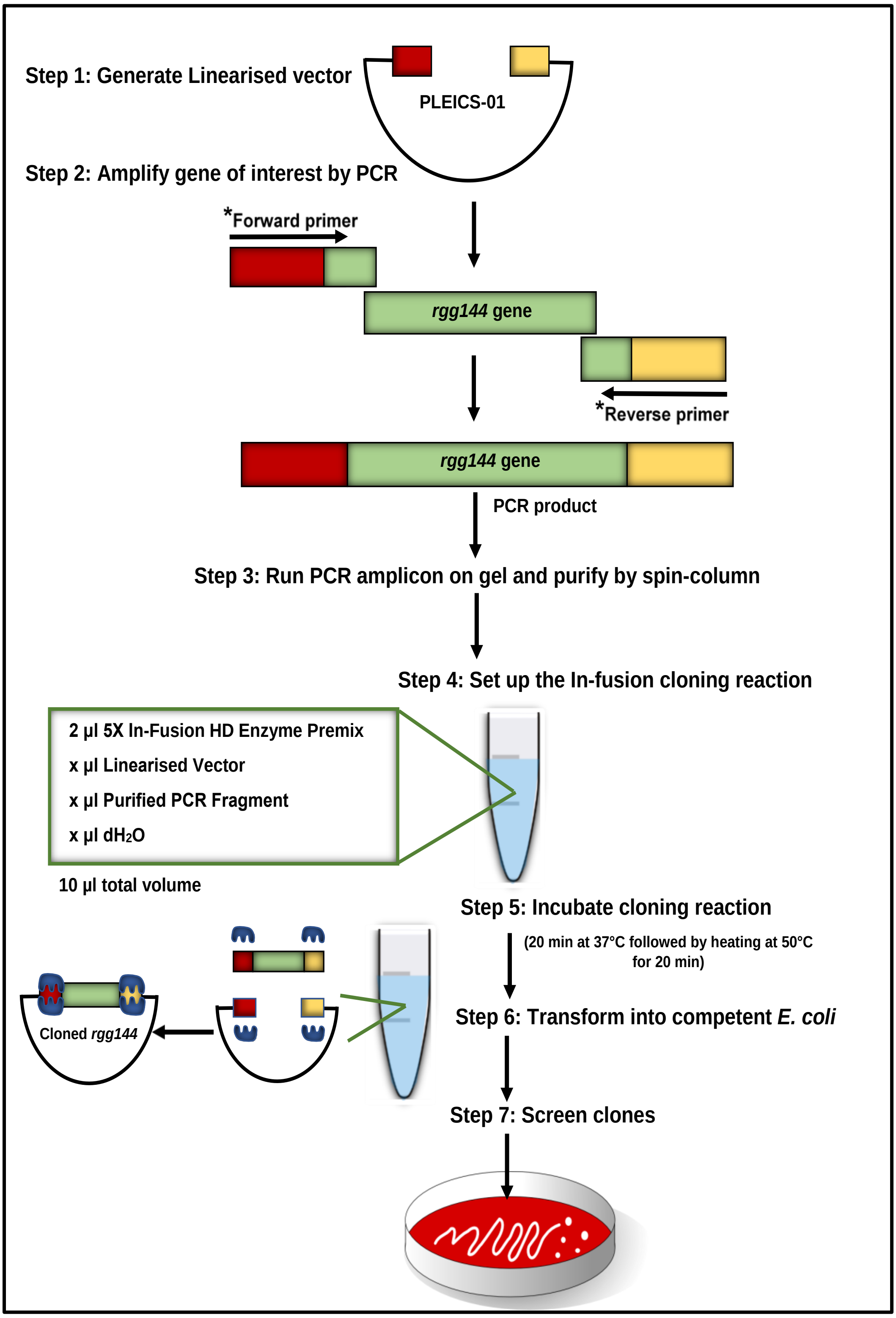

***Gene specific primers with 15-18 bp extensions homologous to pLEICS-01 vector ends.**

Figure 2.3: In-Fusion® HD EcoDry™ Cloning Kit protocol used for cloning *rgg144* gene into pLEICS-01 vector for protein expression. This diagram was constructed using an online tool provided by the Clontech Laboratories, Inc (Takara Bio Company).

2.29.3. Small-scale Rgg144 expression

To determine whether the protein is expressed as soluble or insoluble state (inclusion bodies), and to find out the optimal conditions for protein expression and purification, a single colony of *E. coli* BL21 (DE3) carrying the desired construct was inoculated into 10 ml power prime broth (AthenaES, USA) containing 100 µg/ml ampicillin and incubated overnight at 37°C with constant shaking (220 rpm). The overnight culture was diluted 1:10 into a new power prime broth with 100 µg/ml ampicillin and incubated at 37°C in a shaking incubator until the OD_{600} was reached ~1.2-1.6. After incubation, the bacterial culture was induced with 0.5 or 1 mM of IPTG (Isopropyl β-D-1-thiogalactopyranoside) (Sigma) and left for overnight incubation at different temperatures (18, 24 and 37°C). At this point, the samples were centrifuged at 4000 x g for 15 min at 4°C in a precooled Allegra^{TM} X-22R centrifuge (Beckman Coulter, USA), and the pellets were resuspended in 300 µl of PBS, pH 7.0. The resuspended samples were sonicated (at 8 amplitude) eight times for 15 sec each with 45 sec rest on ice bucket to prevent overheating. The cell lysates were transferred to 1.5 ml microcentrifuge tubes, and pelleted at 14000 rpm for 15 min at 4°C. Both the pellet and supernatant were analysed on a 15% (w/v) sodium dodecyl sulphate polyacrylamide gel electrophoresis (SDS-PAGE) to check protein expression level. The procedure for preparation of SDS-PAGE gel is provided in section 2.30.

2.29.4. Large-scale Rgg144 expression and purification

Accumulation of the target protein as inclusion bodies (IBs) in host cell makes the recovery of bioactive protein challenging. Therefore, inclusion body purification and subsequent steps (solubilisation and refolding) should be properly achieved to recover functionally active protein (Singh and Panda, 2005; Singh *et al.*, 2015). To accomplish this, four major steps were followed:

2.29.4.1. Isolation of inclusion bodies (IBs)

After transformation of the desired construct into *E. coli* BL21 (DE3), the overnight culture carrying the gene of interest was inoculated into 500 ml power prime broth containing 100 µg/ml ampicillin and incubated at 37°C in a shaking incubator (220 rpm) to an OD_{600} ~1.4. At this stage, the bacterial cells were induced with 1 mM IPTG, and the growth was continued overnight at 37°C with constant shaking. The overnight culture was spun down at 20000 x g for 20 min at 4°C in a precooled Allegra^{TM} X-22R centrifuge (Beckman Coulter, USA) and followed by washing the pellet with 100 ml of PBS. The bacterial suspension was centrifuged at 20000 x g at 4°C for 20 min, and the pellet was kept at -80°C until use. Later, the pellet was resuspended with 40 ml of lysis buffer (25 mM Tris pH 8.0, 150 mM NaCl, 0.5% (v/v) Triton^{TM} X-100, 1 mM EDTA, 0.5 mg/ml lysozyme) with one tablet of complete EDTA free protease inhibitor cocktail. The mixture was then harvested at room temperature for 20 min with shaking, followed by the addition of DNase (5 µg/ml) and $MgCl_2$ (5 mM) and incubated for an additional 20 min to digest the DNA. The bacterial cells were lysed by sonication as above (Section 2.29.3). The cell lysate was cleared by centrifugation at 20000 x g for 20 min at 4°C. The pellet was added with 40 ml resuspension solution (25 mM Tris pH 8.0, 0.5 M NaCl, 1 mM EDTA and 0.5% (v/v) Triton^{TM} X-100), sonicated and centrifuged as mentioned above. Washing step was repeated by the use of 40 ml solution containing 1 M urea, 0.5 M NaCl, and 1 mg/ml sodium deoxycholate in 25 mM Tris pH 8.0. These washing steps are useful to remove impurities that might interfere with protein during solubilisation and refolding processes. The resulting pellet was then resuspended in 40 ml of 1:10 diluted BugBuster® Master Mix containing Benzonase® Nuclease and rLysozyme™ Solution (Merck Millipore, UK), and centrifuged at 14000 rpm for 10 min to obtain pellet, which was resuspended with 10 ml of 25 mM Tris pH 8.0. The sample was then aliquoted into 1 ml fractions and centrifuged at 14000 rpm for 10 min. The supernatants were discarded, purified IBs were snap frozen in liquid nitrogen, and kept at -80°C for solubilisation and refolding processes. The SDS-PAGE gel was run to check the purity of IBs.

2.29.4.2. Solubilisation and refolding of inclusion bodies

Purified inclusion bodies were solubilised in buffer containing guanidine hydrochloride along with a reducing agent DTT (25 mM Tris pH 8.0, 6 M guanidine-HCl and 5 mM DTT) to keep all cysteines in the reduced state, and to break down disulphide bonds formed during purification process (Singh *et al.*, 2015). The protein sample was then incubated at 37°C for 10 min to facilitate the solubilisation process, and then centrifuged at 14000 rpm for 10 min to remove insoluble cell debris. After centrifugation, supernatant was collected, and protein concentration was determined by measuring the UV absorbance at 280 nm using a NanoDrop™ Spectrophotometer. The solubilised protein was then refolded by diluting the sample to 2 mg/ml using solubilisation buffer as mentioned above, and was further diluted 1:20 in refolding buffer (50 mM MES(2-(N-morpholino) ethanesulfonic acid, 9.6 mM NaCl, 0.4 mM KCl, 2 mM $MgCl_2$, 2 mM $CaCl_2$, 0.5 M arginine, 0.05% Polyethylene glycol 3550, and 1 mM DTT, pH 6.0) by adding the protein in small drops slowly into the refolding buffer using an injection needle at 4°C with rapid stirring. Finally, the refolded protein was filtered through a 0.22 μm stericup™ filter units (Millipore, UK) to remove insoluble aggregations, and the clear solution was used for protein dialysis.

2.29.4.3. Protein dialysis

To remove solubilising buffer and to allow the protein to refold efficiently, the protein was transferred to dialysis membrane (Fisher Scientific, UK), and incubated overnight in dialysis buffer at a 1:10 ratio (protein sample: dialysis buffer containing 25 mM Tris pH 7.4 and 150 mM NaCl) at 4°C with constant stirring. The dialysis buffer was changed twice and then clarified by 0.22 μm filter to remove aggregations.

2.29.4.4. Metal affinity and size exchange chromatography

Metal affinity chromatography was performed by passing refolded protein through a 2 ml Ni-NTA affinity column pre-equilibrated with 10 ml of buffer containing low concentration of imidazole (25 mM Tris-HCl pH 7.4, 150 mM NaCl and 20 mM imidazole). After loading protein sample, the column was washed again with low imidazole buffer and the protein was eluted in 1ml aliquots using of 25 mM Tris-HCl pH 7.4, 150 mM NaCl and 500 mM imidazole. Further purification was carried out by loading protein sample on Superdex 200 16/60 HiLoad column equilibrated with the gel filtration buffer (50 mM Trizma® base, pH 7.5 and 150 mM NaCl). Once equilibration was finished, 5 ml protein sample was injected slowly into loading loop of the AKTA purifier (GE Health life sciences, UK), and run at a flow rate of 1 ml/minute according to the manufacturers' protocol. The peak-fractions were collected and analysed on 15% (w/v) SDS-PAGE to confirm the successful recovery of eluted protein. Finally, the selected fractions were concentrated in an Amicon Ultracel-10K centrifuge concentrator (Millipore, UK), then snap frozen in liquid nitrogen, and stored at -80ºC for further use.

2.30. Sodium dodecyl-polyacrylamide gel electrophoresis (SDS-PAGE)

SDS-PAGE gel was used to separate recombinant proteins according to their electrophoretic mobility by following Bio-Rad Mini-PROTEAN II gel electrophoresis system. SDS-PAGE consisted of two gels (resolving and stacking), and compositions of each gel are given in Table 2.15. The resolving gel was initially prepared, poured between two glass plates in a gel cassette and overlaid with isopropanol to remove air bubbles and ensure the flat surface between resolving and stacking gels. When the gel was solidified, isopropanol was removed from the gel cassette, and stacking gel was casted on top of the resolving gel. A comb was immediately inserted into gel to create the sample wells and left to polymerise for 30 min before loading the sample. The protein sample was prepared by mixing 20 µl from each protein sample with 5 µl of 5X loading buffer (250 mM Tris-HCl pH 6.8, 50% (v/v) glycerol, 10% (w/v) SDS, 500 mM DTT, 0.25% (w/v) bromophenol blue) and heated to 95°C for 5 min on hot plate to denature the protein. Then, 10 µl of denatured protein was loaded on the gel along with standard protein marker (Bio-Rad, UK), and run on 1X SDS running buffer (25 mM Tris-HCl, 192 mM glycine, 0.1% (w/v) SDS) in the mini protein tetra system tank (Bio-Rad, UK). Electrophoresis was carried out at 200 volts at room temperature for approximately 50 min or until the dye front reached the bottom of the gel. Once the electrophoresis was completed, the gel cassette was gently separated, and carefully transferred to a petri dish. The gel was then stained with Coomassie blue stain (0.4% (w/v) in 10% (v/v) acetic acid and 50% (v/v) methanol) for 20 minutes. The staining solution was discarded, and the gel was de-stained with 7% (v/v) acetic acid and 30% (v/v) methanol solution and left overnight with gentle agitation. Finally, the stained gel was scanned using HP Scanjet G4010, and protein molecular weight was also determined.

Table 2.15: Solutions used for preparation of SDS-PAGE gel.

Reagents	15% Resolving gel	5% Stacking gel
30% Acrylamide	5 ml	670 µl
1.5 M Tris pH 8.8	2.5 ml	-
1.0 M Tris pH 6.8	-	0.5 ml
10% SDS	100 µl	40 µl
TEMED	4 µl	4 µl
10% ammonium persulphate	120 µl	60 µl
H_2O	2.3 ml	2.7 ml

2.31. Confirmation of protein identity by MALDI-TOF mass spectrometry

The purified recombinant proteins were sent for sequencing at PNACL, Leicester University to verify the identity of isolated proteins by Matrix-Assisted Laser Desorption Ionization–Time of Flight (MALDI-TOF) mass spectrometry. This analysis depends on trypsin digestion by cleavage of carboxyl terminus of amino acids arginine and lysine generating mixture of peptides with different molecular weights. The latter can be easily analysed by mass spectrometry and compared with protein database to find the best match with target protein. The molecular weight of full length and truncated Rgg144 recombinant proteins was also determined by using Electrospray LC-MS at PNACL.

2.32. Investigation of Rgg/SHP144 binding

2.32.1. Intrinsic fluorescence spectroscopy

Intrinsic fluorescence of proteins, originating from three aromatic amino acids (tryptophan, tyrosine and phenylalanine) have been widely used to study protein dynamics and conformational changes (Munishkina and Fink, 2007; Ghisaidoobe and Chung, 2014). Among three fluorescent amino acids, tryptophan is the most dominant source of UV absorbance at ~280 nm and emission at ~350 nm. As Rgg144 protein has multiple aromatic amino acid residues (3 tryptophan, 19 phenylalanine and 11 tyrosine) in its structure, therefore this method was exploited to monitor the interaction between Rgg144 and its ligand using fluorescence spectrofluorometer (Horbia-Max 4). This assay was performed by mixing a fixed amount of Rgg144 protein (1 μM) and increasing amounts of SHP144 variants (0-100 μM) in black quartz cuvette (Table 2.7). The fluorescence was then measured at an excitation and emission wavelengths (295 nm and 320-350 nm respectively) with spectral slit width 3/3 at constant temperature 20°C. Protein or peptide with buffer was served as a negative control. Maximum fluorescence intensity value of each reading was obtained and plotted against SHP144 concentration using GraphPad Prism version 7.02.

2.32.2. Fluorescence polarisation assay (FP)

Fluorescence polarisation is another fluorescence spectroscopy method was extensively used for analysing molecular interactions (protein-small ligand, protein-protein and protein-DNA) and for quantifying enzymatic activity (Moerke, 2009; Lea and Simeonov, 2011). This technique is rapid, accurate and inexpensive as it requires only one labelled species. Therefore, this method was also exploited to investigate the binding affinity of native or mutant SHP144-C13 peptides with its receptor Rgg144. The basic principle of this assay is depicted in Figure 2.4. To do this assay, purified full length or truncated Rgg144 protein was serially diluted (0.09-182 µM) in protein storage buffer containing 150 mM NaCl, 50 mM Trizma® base pH 7.5 using OptiPlate 96 well black opaque polystyrene microplate. Diluted protein was incubated with constant amount of native or modified FITC-SHP144-C13 (10 nM) (Table 2.9) to a final volume 60 µl for 20 min at 20°C. Protein and peptide dilution buffers were used as assay blank. Millipolarisation values (mP) were measured at 485 nm excitation and 520 nm emission spectra using Hidex Sense Microplate Reader. Similar experiment was repeated by the use of bovine serum albumin (BSA) instead of Rgg144 and non-specific fluorescein-labelled same sized peptide FITC-NSP-C13 to confirm the specificity of binding assay. The fluorescence values were plotted against protein concentrations, and K_d were calculated using non-linear regression stimulation dose-response curve (Graph Pad Prism version 7.02).

For competition FP binding assay, a serial dilution of unlabelled peptide SHP144-C13 was mixed with Rgg/SHP144 complex (10 nM of FITC-SHP144-C13 and 6.6 µM protein representing half-maximal Rgg144-SHP144 interaction determined from direct FP binding) in 96 well black microplate. The plate was incubated at 20°C for 30 min. As a negative control, competence stimulating peptide (CSP) known not to interact with Rgg144, was serially diluted into the reaction, and its ability to compete with FITC-SHP144-C13 was also assayed. The millipolarisation values were measured as previously described in direct binding assay, and IC_{50} was determined using non-linear regression inhibition dose-response curve (Graph Pad Prism version 7.02).

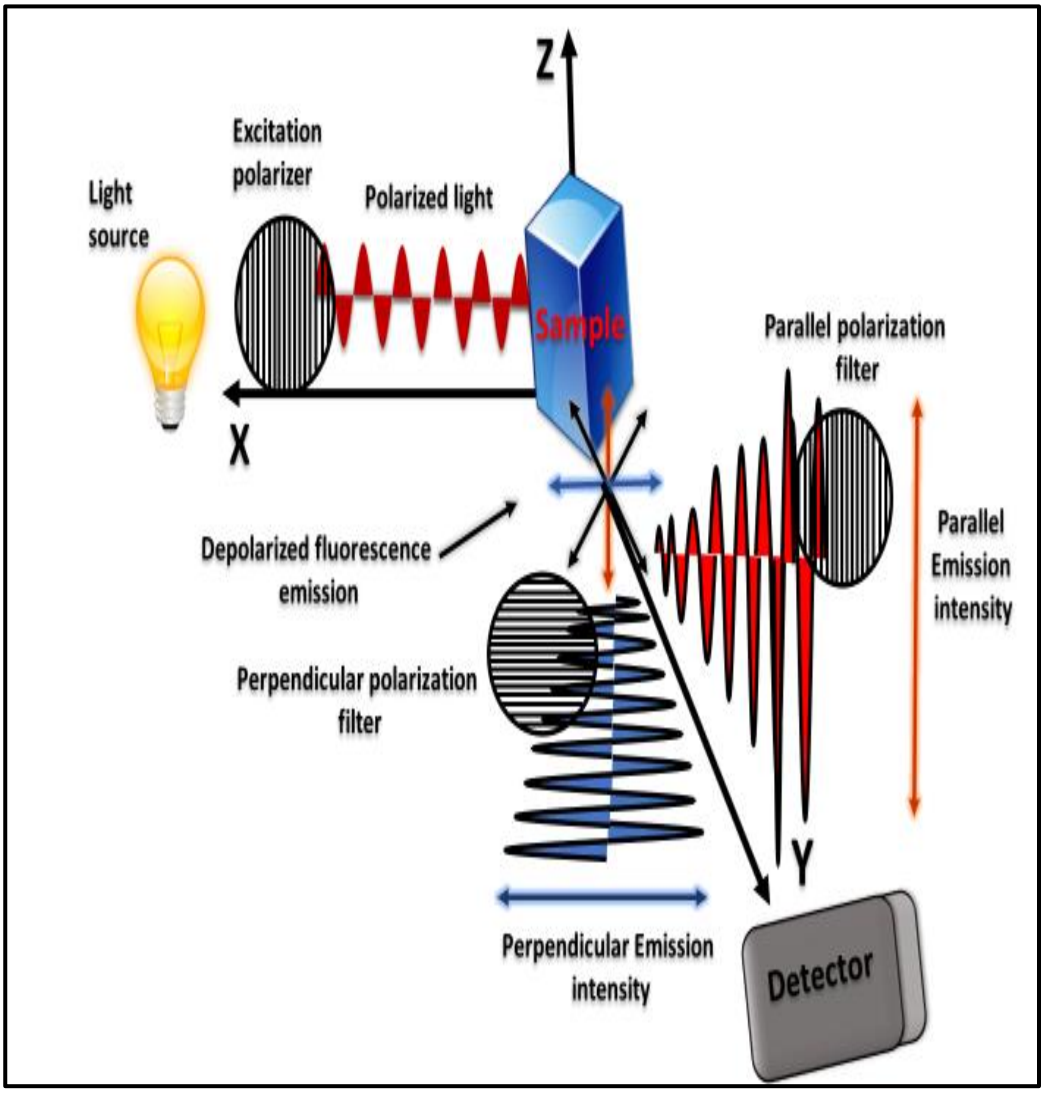

Figure 2.4: Schematic diagram representing the basic principle of fluorescence polarisation assay. A fluorescent molecule in sample solution is excited by polarised light after passing through an excitation polarising filter. The emitted light from excited molecule depends on its rotational motion in the solution. The emission light passes through emission polarisation filters, which are parallel (Red signals) and perpendicular (Blue signals) relative to excitation plane prior determination of emission intensity by detector. The parallel and perpendicular intensity measurements are used to calculate fluorescence polarisation values. This figure was constructed based on Hall *et al.* (2016).

2.33. Identification of SHP144 peptides by mass spectrometry

Wild type D39 and Δ*shp144* strains were inoculated into 100 ml of CDM supplemented with mannose or BHI and incubated statically at 37°C until the growth was reached to the late exponential phase. The bacterial cells were then separated from the liquid phase via centrifugation at 4000 rpm for 15 min and sterilised using a 0.22 µm filter membrane. Filtered spent culture was frozen in liquid nitrogen and dried in vacuo in a Labconco freeze dryer. The dried fractions were sent to PNACL (University of Leicester) and biOMICS (Biological Mass Spectrometry Facility, University of Sheffield) for mass spectrometry analysis.

2.34. Crystallisation Rgg144 with its ligand

Several spare-matrix commercial crystallisation kits (PACT Premier, JCSG+, ProPlex and Morpheus) from Molecular Dimensions were trialled to find out the optimal condition for crystallisation Rgg144 with its ligand SHP144 using the sitting-drop vapour diffusion method (Dessau and Modis, 2011). Initially, 80 µl of each screen condition was placed in corresponding reservoir well on triple sitting drop 96 well crystallisation plate (TTP Labtech, UK). Then, 100 nl reservoir solution was mixed with 100 nl of mixture containing SHP144 and Rgg144 at a 1:20 ratio (purified protein: selected SHP144 peptide) using a mosquito nanolitre crystallisation robot (TTP Labtech, UK). Two plates were prepared for each screen, sealed with transparent tape and kept at desired temperature (generally between 4°C and room temperature). The plates were daily monitored and examined under microscope to check the crystal growth.

2.35. Murine colonisation experiments

2.35.1. Preparation of pneumococcal inoculum

Pneumococcal strains were initially streaked on blood agar plates and incubated overnight at 37°C in the presence of 5% CO_2. Next day, a sweep of colonies was inoculated into 10 ml of BHI and incubated at 37°C until OD_{500} had reached ~1.4-1.6. The cultures were then centrifuged at 3000 rpm for 15 min, and the supernatant was discarded. The cell pelleted was then resuspended in 1 ml of 80% (v/v) BHI and 20% (v/v) sterilised fetal calf serum. The 700 µl of the resuspended pellet was inoculated into 10 ml of fresh warmed BHI serum broth, and the culture OD_{500} was adjusted to ~0.7. Then, the growth was continued until OD_{500} had reached ~1.6. At this stage, the culture was aliquoted into 500 µl and kept at -80°C until needed. After 24 hours, the number of viable cells were determined by thawing an aliquot of each pneumococcal culture to room temperature and centrifugation at 13000 rpm for 5 min. The pellet was then resuspended in 400 µl of PBS and the CFU/ml was counted as described in section 2.5.

2.35.2. Nasopharyngeal colonisation model

Eight to ten-week-old female CD1 mice (Charles & Rivers, UK) were used for colonisation experiments. Mice were housed in individually ventilated cages and left for one week to acclimatise prior to use. All *in vivo* work was carried out in accordance with regulations of Animal Scientific Procedure Act 1986 of the United Kingdom under project and personal licence numbers (P7B01C07A and I7E217691), respectively. The standardised inoculum was prepared as described in section 2.35.1. Colonisation experiment was set up into two groups (0 and 7 days post infection) by following the procedure described before (Richards *et al.*, 2010). Both sets of mice were deeply anaesthetised with 5% (v/v) isoflurane over oxygen (1.4 to 1.6 litres/min) in an anaesthetic box. A 20-µl volume of PBS containing approximately $1x10^5$ CFU/mouse of pneumococcal inoculum was administered gradually to both nostrils of mice held horizontally to ensure that the pneumococci do not spread to the lower respiratory tract. Following infection, the animals were immediately placed on their backs inside the cage to allow for recovery from anaesthesia and to prevent the release of the inoculum from nostrils. The viable cells of inoculum were also checked by plating after infection. The infected mice were sacrificed by cervical dislocation on days 0 and 7 after inoculation. The number of pneumococci colonised the nasopharynx was determined by washing nasopharyngeal cavity with 500 µl of sterile PBS using 18 G needle. CFU/ml was determined by serially diluting 20 µl of washed PBS with 180 µl of PBS and plating onto blood agar plates supplemented with 1 µg/ml gentamicin to suppress the growth of non-pneumococcal organisms. The results are expressed as log_{10} CFU/ml of each nasopharyngeal wash.

2.35.3. Evaluation the impact of modified and native SHP144-C13 peptides on pneumococcal virulence *in vivo*

The competitive inhibition effect of modified SHP144-C13P21A peptide on pneumococcal virulence *in vivo* was studied using murine colonisation model. For this, mice were infected intranasally either with $2.5x10^5$ CFU/mouse of pneumococcal D39 wild type in 20 µl PBS as a control, or with the inoculum containing 200 µM modified peptide SHP144-C13P21A in 20 µl PBS. The same dose supplemented with 200 µM of unmodified peptide SHP144-C13 was given to a third group as a control to test the specificity of peptide inhibitor. The cohorts infected with modified or unmodified peptides received additional doses of peptide (200 µM) at predetermined times (24, 48 and 72 h post infection) whereas control group received only 20 µl PBS. The mice were then sacrificed by cervical dislocation on day 5 and nasal washes were obtained as described before.

To assess the ability of native SHP144-C13 to complement the known virulence defect of *shp144* mutant, similar colonisation experiment was repeated over a 5-day period by infecting the mice with 20 µl inoculum containing $2.5x10^5$ Δ*shp144* supplemented with or without 200 µM of SHP144-C13 unmodified peptide. Mice were sacrificed by cervical dislocation and nasal washes were obtained as previously mentioned (Section 2.35.2).

2.36. Statistical analysis

Graph Pad Prism software version 7.02 (GraphPad, California, USA) was used to analyse all data presented in this study. All experiments were repeated with at least three independent biological replicates, and data were expressed as means ± standard error of the mean (SEM). One-way or two-way analysis of variance (ANOVA) followed by multiple comparison tests and two-tailed unpaired student's *t*-test were used to check significant differences between data sets for growth studies, enzymatic activity and *in vivo* colonisation. For direct and indirect fluorescence polarisation analysis, non-linear regression stimulation and inhibition dose-response curves were used to determine K_d and IC_{50} respectively. Statistical significance was considered as *p<0.05, **p<0.01, ***p<0.001 and ****p<0.0001.

Chapter 3. Results

Section A: Identification of a new quorum sensing system in *S. pneumoniae*

3.1. Rgg/SHP quorum sensing system

Gram positive bacteria utilise small hydrophobic peptides as a signal for QS. The Rgg/SHP system is an example of peptide mediated QS systems and found widely among Gram positive bacteria. Through search on *S. pneumoniae* D39 genome, five *rgg*-like genes (*rgg144* (SPD_0144), *rgg939* (SPD_0939), *rgg999* (SPD_0999), *rgg1518* (SPD_1518) and *rgg1952* (SPD_1952) have been found homologues to prototypical Rgg from *Streptococcus gordonii* (SGO0496) with a sequence identity over 17% at the amino acid sequence level (Zhi *et al*., 2018). Off these SPD_0144 and SPD_0939 are predicted to be associated with unannotated ORFs, coding for a short hydrophobic peptide (SHP), whereas for other Rggs, there is no peptide pheromone gene, hence they are considered as stand-alone regulators. The *shp* genes are small in size and originally unannotated. They are designated according to their proximity from *rgg* genes, and the presence of double lysine residues in their N-terminus (Ibrahim *et al*., 2007a). The *rgg* and *shp* genes are transcribed divergently with an overlap at their promoters or coding sequence regions. Thus, pneumococcal *shp* genes are named as *shp144* and *shp939* because of the hydrophobicity of peptides they encode.

The Rgg144 crystal structure has been characterised in collaboration with Prof Russell Wallis. Hence this study was designed to characterise the Rgg/SHP144 signalling pathway in *S. pneumoniae* D39 through studying the intermolecular interaction between Rgg144 and SHP144. Specifically, the aim was to quantify the functional importance of individual SHP residues for Rgg binding and transcription activation in order to establish the mechanism of Rgg144's phenotypic manifestation. Modified SHP144 peptides with high binding and low transcription ability were assayed for their ability to competitively inhibit Rgg/SHP144 mediated transcription and consequently change the phenotypes of *S. pneumoniae*. To perform these aims, the Δ*rgg144*, Δ*shp144,* and double mutants (Δ*rgg144/shp144*) were kindly provided by Dr Hasan Yesilkaya whereas genetically complemented Δ*shp144*Com and thirteen modified *shp144* strains (in which selected amino acid residues were replaced with alanine) were constructed in this study. These strains were tested by growth studies, in their resistance to oxidising agents, and for synthesis of capsule.

In addition, several transcriptional reporter strains harbouring P$_{shp144}$::*lacZ* fusion in wild type and mutant backgrounds were constructed to determine the activity of Rgg/SHP144 in the presence of native and modified signalling peptide SHP144, and establish environmental conditions for stimulation of this system.

3.2. Construction and evaluation of pneumococcal *lacZ* fusions

Transcriptional fusions are commonly used to study changes in gene expression and promoter activity in response to different cellular and environmental signals in many different organisms (Uliczka *et al*., 2011). Multiple reporter genes have been developed to evaluate the transcriptional activity of various genes by fusing the putative promoter region of the gene of interest with a reporter gene whose product is easily assayed, making the quantification of the activity of the gene of interest easier under defined environmental conditions. The available reporter genes are *E. coli* β-galactosidase *lacZ* (Hand and Silhavy, 2000; Oster and Phillips, 2011), the green fluorescent protein *gfp* from the jelly fish *Aequorea victoria* (Phillips, 2001; Southward and Surette, 2002), the luciferase, *lux*, from the fire fly *Photinus pyralis* (Stewart and Williams, 1992; Bronstein *et al*., 1994), the *E. coli* chloramphenicol acetyl transferase, *cat,* (Gorman *et al*., 1982), and the *E. coli* β-glucuronidase *gus* (Jefferson *et al*., 1987; Oster and Phillips, 2011).

Among the available reporters, the *lacZ* gene from *E. coli* is the most commonly used reporter system, as it is simple, does not require specialised equipment, and its product is stable and easily quantified using the β-galactosidase assay (Miller, 1972; Liang *et al*., 1998; Hayes *et al*., 2010). Therefore, this reporter gene was used to construct pneumococcal *lacZ* fusions using integrative promoter probe plasmid pPP2 (Halfmann *et al*., 2007b). This plasmid contains a promoterless *lacZ* gene encoding for β-galactosidase from *E. coli*, ampicillin *(bla*) and tetracycline (*tetM*) resistance genes, which can be used for selection of *E. coli* and pneumococcal transformants, respectively. In addition, pPP2 carry two homologues regions to *S. pneumoniae* D39 (SPD_0562 (*bgaA* gene) encoding for β-galactosidase, and SPD_0561), meaning that upon integration of recombinant pPP2 into the *S. pneumoniae* genome, promoter-*lacZ* fusion is directed to the endogenous *bga*A gene resulting in disruption of *bga*A, hence leading to reduction of endogenous β-galactosidase activity. In the same manner, the *tetM* gene, which confers resistance to tetracycline, is also integrated into the *S. pneumoniae* D39 genome (Halfmann *et al.*, 2007b). This strategy was followed to generate pneumococcal reporter strains for studying the activity of Rgg/SHP144 using β-galactosidase assay as shown in Figure 3.1.

The expression of signal peptide genes in quorum sensing most frequently is controlled by positive feedback regulation by their cytoplasmic regulators. To investigate whether the SHP144 forms an active autoinducing peptide of Rgg/SHP144 QS and to find out the amino acid residues involved in transcriptional activation, the *lacZ* transcriptional fusion was constructed by fusing the upstream region of *shp144* gene (P_{shp144}, P indicates promoter) to the *lacZ* using pPP2 plasmid.

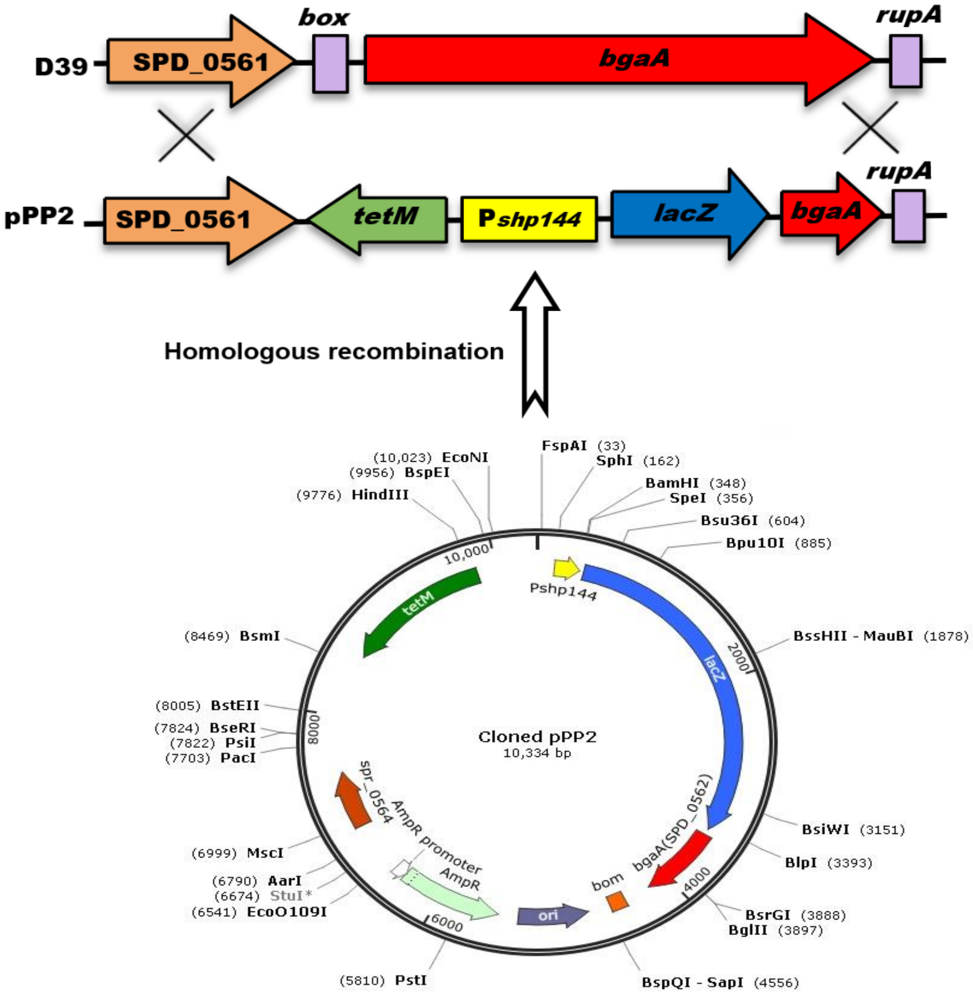

Figure 3.1: Schematic diagram illustrating the insertion of putative promoter region of *shp144* into pPP2, and integration of recombinant pPP2 into *S. pneumoniae* D39 genome by homologous recombination. Upon integration, the native *bgaA* gene (red box) and its flanking regions (*box*, *rupA*) (purple boxes) are deleted. This figure was constructed according to Halfmann *et al.* (2007b).

After *in silico* identification using software BPROM (Softberry, USA) (Solovyev and Salamov, 2011; Maidin *et al*., 2014), the putative promoter region of *shp144* was amplified and fused to promoterless *lacZ* in an integrative reporter plasmid pPP2. The recombinant plasmid carrying the correct insert was extracted and sequenced using pPP2 primers (Fusion-Seq-F and Fusion-Seq-R). The sequencing results showed that the construct had the correct putative promoter region of *shp144* (Appendix 1). The sequenced fusion construct carrying P_{shp144}::*lacZ* fusion was then integrated in a single copy on wild type D39 and its respective isogenic mutants at *bgaA* site via double cross-over following the protocol described previously in Materials and Methods (Section 2.20).

The transformants were selected on blood agar plates containing 3 μg/ml tetracycline for wild type, and tetracycline plus 100 μg/ml spectinomycin for the mutant strains. The integration of recombinant plasmid into the pneumococcal genome was verified by PCR using Fusion-Seq-F and Fusion-Seq-R primers whose recognition sites are localised immediately up and downstream of the cloning site, respectively. The strategy of PCR amplification is shown in Figure 3.2A. The agarose gel electrophoresis analysis showed that P_{shp144}::*lacZ* fusion was incorporated successfully into wild type D39, Δ*rgg144*, Δ*shp144* and double Δ*rgg144/shp144* mutant as shown in lanes 1-4 of Figure 3.2B. As expected, the size of DNA fragments was similar to that obtained with recombinant P_{shp144} plasmid (384 bp) as shown in lane 5, which served as a positive control. For negative control, promoterless native pPP2 plasmid was amplified and a fragment of the correct size (200 bp) was obtained by using the same set of primers as indicated in lane 6. The resulting reporter strains were designated as P_{shp144}::*lacZ*-Wt, P_{shp144}::*lacZ*-Δ*rgg144,* P_{shp144}::*lacZ*-Δ*shp144* and P_{shp144}::*lacZ*-Δ*rgg144/shp144*.

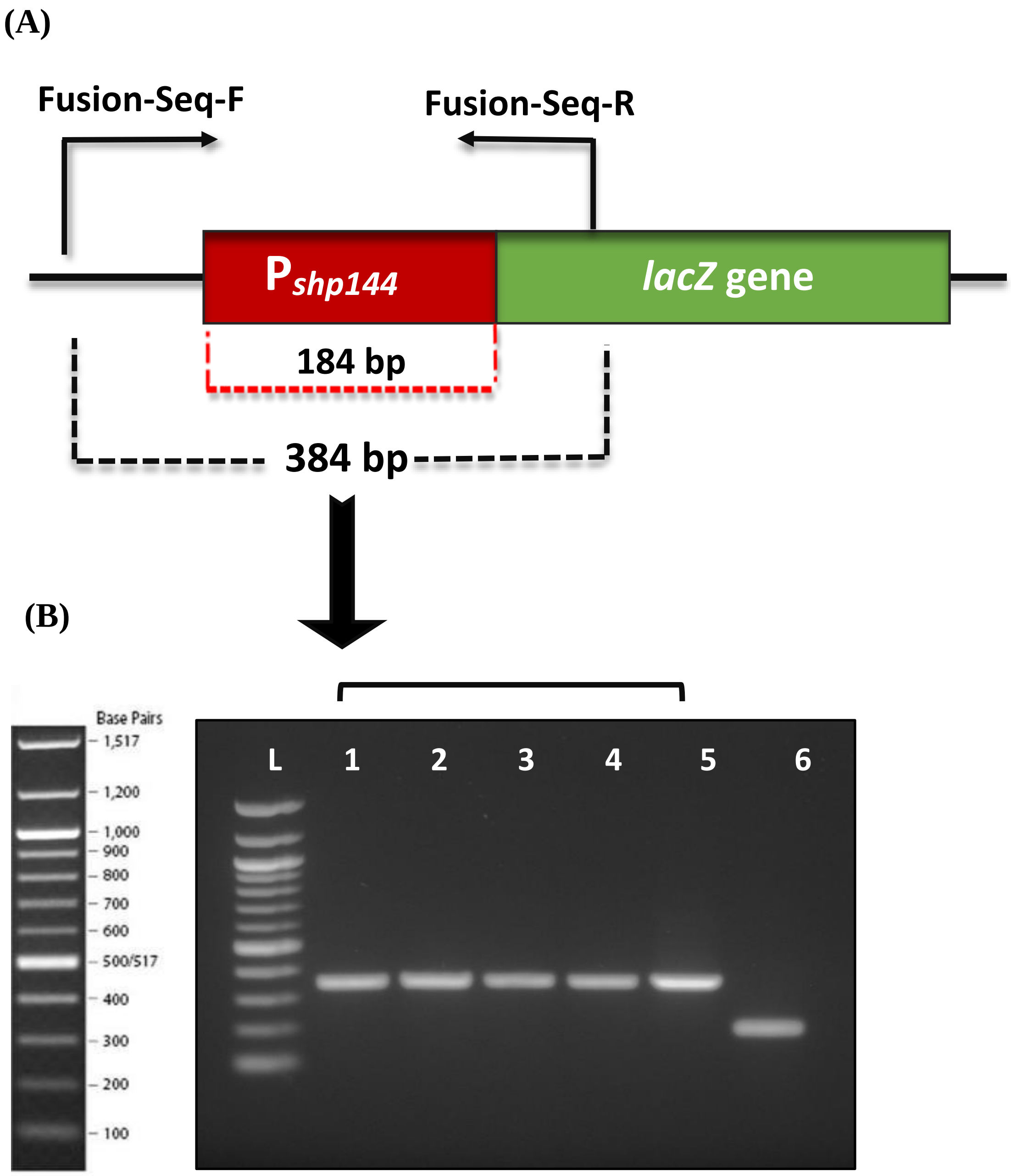

Figure 3.2: (A) PCR strategy used to confirm the successful integration of transcriptional fusion P_{shp144}::*lacZ* within the pneumococcal genome. Fusion-Seq-F and Fusion-Seq-R primers were used to amplify putative promoter region of *shp144* resulting a product of an approximately 384 bp in size, while the empty pPP2 plasmid produced PCR products of 200 bp using the same set of primers. **(B)** Agarose gel electrophoresis showing successful transformation of P_{shp144}::*lacZ* into wild type and its isogenic mutants. Lane L, 100 bp DNA marker (New England Biolabs, UK); lane1, P_{shp144}::*lacZ*-Wt; lane 2, P_{shp144}::*lacZ*-Δ*rgg144*; lane 3, P_{shp144}::*lacZ*-Δ*shp144*; lane 4, P_{shp144}::*lacZ*-Δ*rgg144/shp144*; lane 5, P_{shp144} plasmid (positive control); lane 6, empty pPP2 plasmid (negative control).

To test the role of Rgg144 and SHP144 in stimulation of P$_{shp144}$ expression, the reporter strains were analysed in chemically defined medium containing glucose. When P$_{shp144}$ is induced, it drives the expression of promoterless *lacZ* gene resulting in production of β-galactosidase enzyme. This enzyme hydrolyses *O*-Nitrophenyl β-D-galactopyranoside (ONPG) substrate and produces a yellow colour. The *lacZ* activity (Miller Unit, MU) was normalised to CFU/ml and expressed in nmol *p*-nitrophenol/min/ml. As shown in Figure 3.3. the *shp144* expression in wild type reporter strain P$_{shp144}$::*lacZ*-Wt (135 ± 5.0 MU, n=3) was significantly higher compared with mutant strains P$_{shp144}$::*lacZ*-Δ*rgg144* (1.2 ± 0.2 MU, n=3) and P$_{shp144}$::*lacZ*-Δ*shp144* (2.3 ± 0.2 MU, n=3) ($p<0.0001$). A similar trend was seen with examination of double mutant P$_{shp144}$::*lacZ*-Δ*rgg144*/*shp144* strain as the β-galactosidase activity was 1.6 ± 0.1 MU, significantly lower than that of wild type ($p<0.0001$). These results demonstrate that *shp144* activation is dependent on the presence of Rgg144 and SHP144, and the absence of either of these resulted in markedly reduced *shp144* expression. As expected, a weak enzymatic activity was seen with pPP2-Wt (2.25 ± 0.25 MU), which does not have any promoter. As mentioned earlier, the promoterless pPP2 disrupts the native β-galactosidase *bgaA* gene after integration into pneumococcal genome. Therefore, this lower β-galactosidase activity is very likely originating from other pneumococcal β-galactosidase gene, *bgaC*.

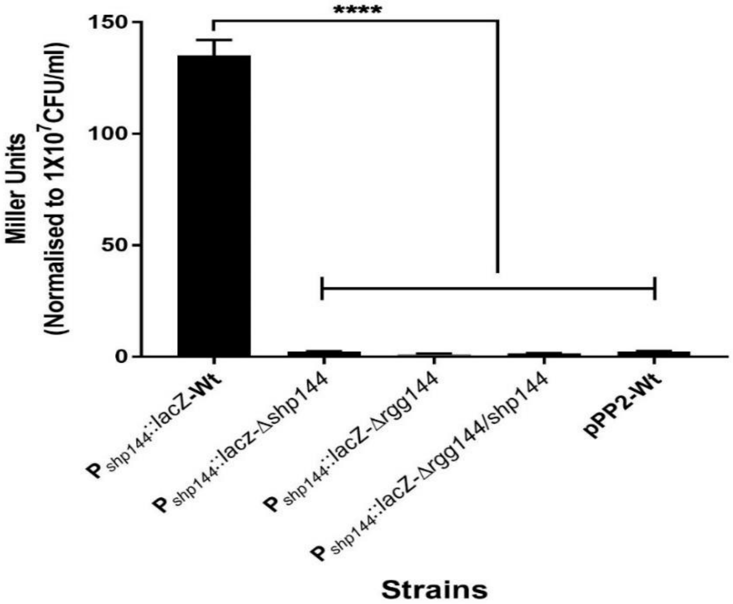

Figure 3.3: β-galactosidase activity of pneumococcal reporter strains grown in CDM supplemented with 55 mM glucose. The error bars represent the standard error of the mean for each set. Values are average of three independent experiments, each with three replicates. The activity is normalised to 1x10^7 CFU/ml and expressed in Miller units. ****$p<0.0001$ compared to wild type reporter strain P$_{shp144}$::*lacZ*-Wt.

3.3. Identification of mature SHP144 in the supernatants of *S. pneumoniae* cultures

Identification of the Rgg/SHP144 interaction promoted an investigation focussing on whether the SHP144 signalling pheromone produced by *shp144* is secreted into the extracellular milieu. To perform this goal, cell-free culture supernatant was collected from late exponential wild type culture, which contains an intact copy of *shp144* as well as from mutants lacking either Rgg144 or SHP144. The collected supernatants were mixed with the pellet of a reporter strain containing P_{shp144}::*lacZ* fusion in the Δ*shp144* background. This mutant strain was used to eliminate induction by the endogenously produced SHP144. Fresh uninoculated CDM (vehicle) served as negative control. The P_{shp144} expression level was examined using β-galactosidase assay. As expected, the *shp144*-deficient reporter strain showed a high level of induction when incubated with the wild type supernatant (161.24 ± 4.9 MU, n=3) compared with the supernatants from deletion mutants (14.04 ± 1.5 and 15.3 ± 1.4 MU for Δ*rgg144* and Δ*shp144*, n=3, respectively) ($p<0.0001$) (Figure 3.4). In addition, the β-galactosidase activity in the presence of wild type supernatant was nearly 13-fold higher than that of uninoculated media ($p<0.0001$). Thus, the wild type supernatant but not the mutants contains a secreted SHP144 molecule capable of inducing its own expression.

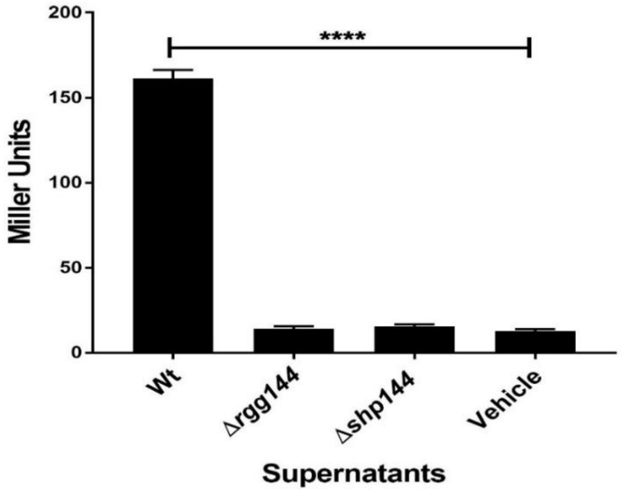

Figure 3.4: β-galactosidase activity level of P_{shp144}::*lacZ*-Δ*shp144* reporter strain treated with wild type (Wt), Δ*rgg144* and Δ*shp*144 supernatants. Vehicle represents uninoculated media. The error bars are standard error of the mean for each set. Values are the average of three independent experiments, each with three replicates.****$p<0.0001$ compared with reporter strain treated with wild type supernatant.

To validate the previous observation that SHP144 is the secreted molecule and to identify the active form of the secreted peptide, a synthetic form of this peptide was utilised. The *shp144* encodes 26 amino acids residues (MKKRKIQLILLLISEWVIVIPFLTNL) and based on the studies of similar systems in other streptococci showing that the active SHP is represented in the C-terminal end of the processed peptide and multiple variants, each with different lengths, have been identified (Aggarwal *et al.*, 2014; Cook and Federle, 2014). Therefore, different versions of SHP144 synthetic peptide 8 to 15 amino acid residues long, representing the C-terminal were synthesised, and added independently to P_{shp144}::*lacZ*-Δ*shp144* reporter strain culture. Their effect on P_{shp144} expression was assessed using β–galactosidase assay. The selected peptides were designated as SHP144-C8, SHP144-C9, SHP144-C10, SHP144-C11, SHP144-C12, SHP144-C13, SHP144-C14 and SHP144-C15 respectively. The peptide composed of the reversed sequence (SHP144-C13Rev) was also included in the assay to confirm the specificity of induction. As indicated in Figure 3.5(A) a dramatic increase in P_{shp144} induction was seen in reporter culture treated with synthetic peptides corresponding to the C-terminal 12 and 13 amino acid residues compared with other versions of peptide ($p<0.0001$). The SHP144-C12 and C13 induce 54 and 49-fold changes in reporter induction relative to untreated culture ($p<0.0001$). In contrast, no induction was observed when an equal concentration of SHP144-C13Rev was added to reporter culture ($p<0.0001$). A similar expression pattern was seen in reporter culture in wild type background treated with SHP144 variants as shown in Figure 3.5B. The results suggest the SHP144-C13 and C12 are possibly the most active variants derived from native SHP144.

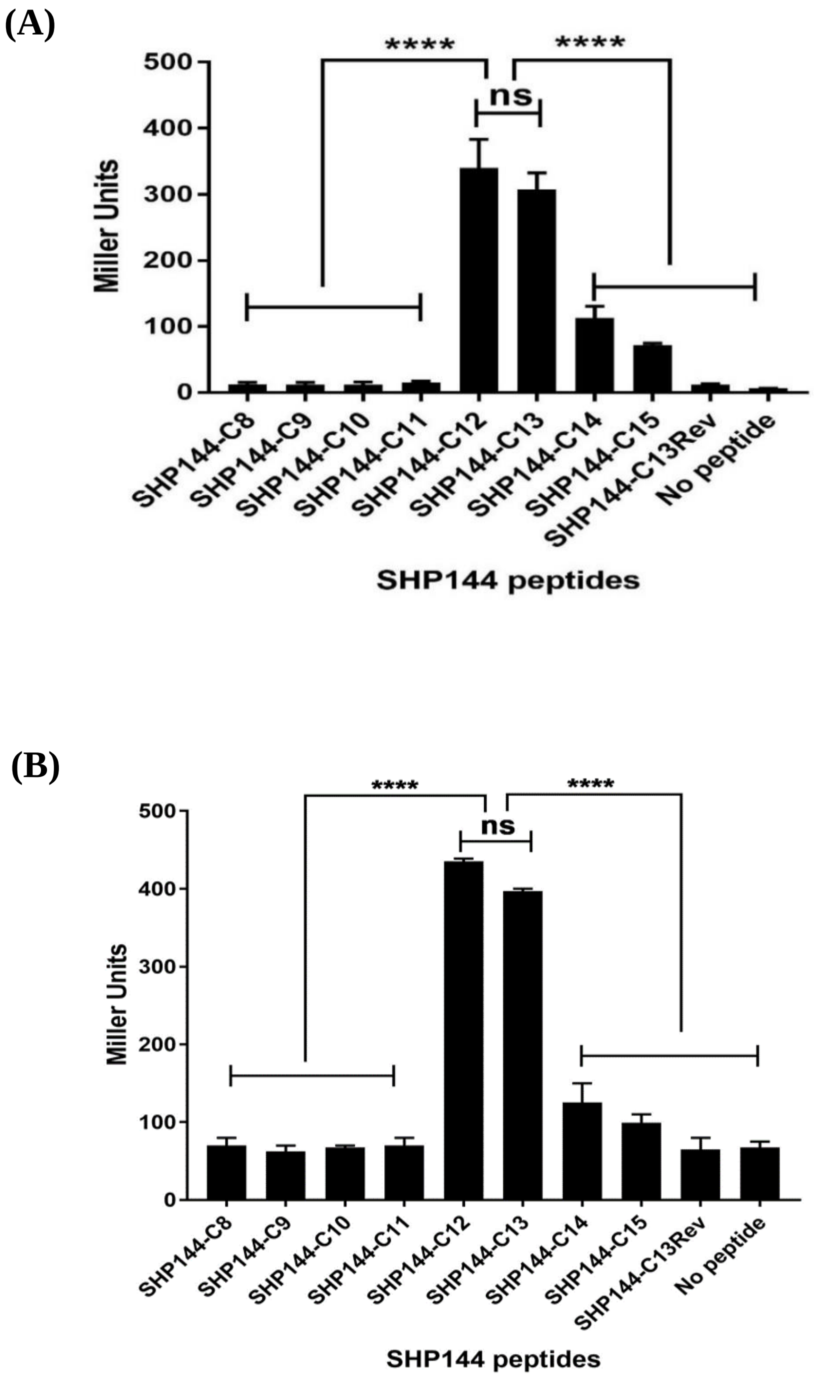

Figure 3.5: Addition of exogenous SHP144-C12 and C13 synthetic peptides stimulate P_{shp144} expression. The reporter strains P_{shp144}::*lacZ*-Δ*shp144* **(A)** and P_{shp144}::*lacZ*-Wt **(B)** were grown in CDM-glucose, with or without different length SHP144 variants. The pneumococcal cultures were incubated microaerobically to early exponential phase and the β-galactosidase activity was assayed. The reporter strains without peptide were used as a negative control. The activity is expressed in Miller Units (nmol *p*-nitrophenol/min/ml). The values indicate the average of three independent experiments, each with three replicates. The error bars represent SEM (****p<0.0001, 'ns' no significant) compared to reporter culture with maximum activity.

3.4. The *shp144* induction in response to SHP144 concentration

It is well known that quorum sensing systems are responsive to the level of signalling molecules for their operation (Podbielski and Kreikemeyer, 2004; Siehnel *et al*., 2010). It was of interest to check if this applies to Rgg/SHP144 QS. To this end, the reporter strain P_{shp144}::*lacZ*-Wt was incubated individually with varying concentrations of SHP144-C13 (50-500 nM) to an early exponential phase. The SHP144-C13 was selected as no significant difference in P_{shp144} induction could be detected between SHP144-C12 and C13. Untreated reporter culture was served as a negative control for the assay. The results showed a significant increase in P_{shp144} induction with the increasing SHP144-C13 concentration in culture media. The highest induction was seen with 500 nM synthetic peptide (599.2 ± 9.2 MU, n=3), then by 250 nM (408.7 ± 18.7 MU, n=3), 100 nM (210.1 ± 10.0 MU, n=3) and the lowest induction was seen with 50 nM peptide (104.2 ± 14.2 MU, n=3) (Figure 3.6). Furthermore, a similar experiment was conducted using transcriptional reporter strain in mutant *shp144* background to eliminate the induction caused by endogenously produced SHP144. The induction pattern was similar to that was seen with the wild type (Figure 3.6). On the other hand, several attempts have been made to measure the concentration of native and synthetic SHP144-C13 peptides using mass spectrometry, but their concentrations were below the level of detection (Section 3.20).

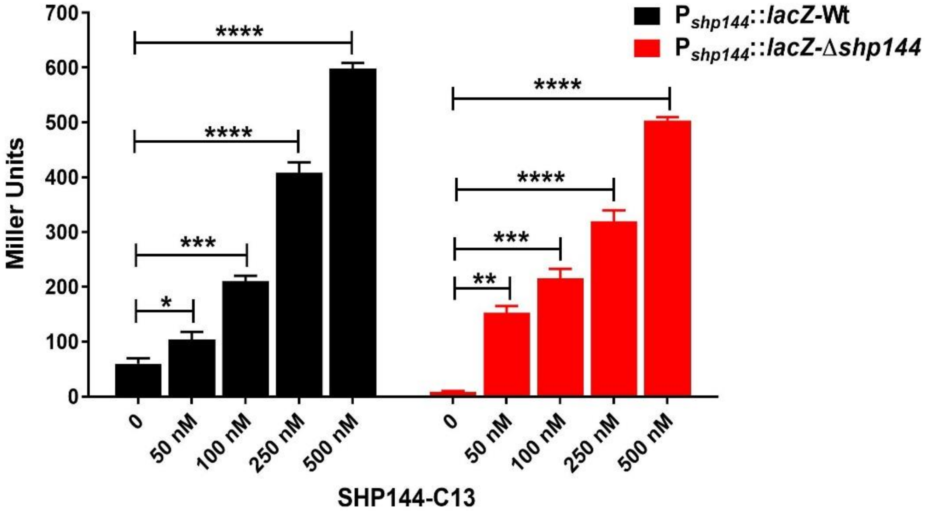

Figure 3.6: Dose dependent stimulation of P_{shp144} expression. The pneumococcal reporter strains grown in CDM containing 55 mM glucose and in the presence of varying concentrations of SHP144-C13 (50-500 nM). The error bars represent standard error of the mean for each set. Values are average of three independent experiments, each with three replicates. *p<0.05, **p<0.01, ***p<0.001, ****p<0.0001 compared with reporter cultures in the absence of peptide.

To further confirm that the expression of *shp144* is dependent on the SHP144 concentration in culture media, the reporter strain carrying P_{shp144}::*lacZ*-Δ*shp144* fusion was treated with wild type supernatants collected at different cell densities (early, mid and late logarithmic phase) in CDM supplemented with glucose. The induction mediated by high-cell density (210.5 ± 1.5 MU, n=3) was significantly higher than those seen by early and mid-exponential culture supernatants (52.5 ± 1.5 and 161.24 ± 4.9 MU, n=3 respectively) ($p<0.0001$ and $p<0.01$). This response was specific, as the mutant supernatants (Δ*shp144* and Δ*rgg144*) did not induce *shp144* expression regardless of growth phase and therefore used as a negative control for the experiment (Figure 3.7). These results support my hypothesis that the SHP144 production and secretion are dependent on bacterial population density.

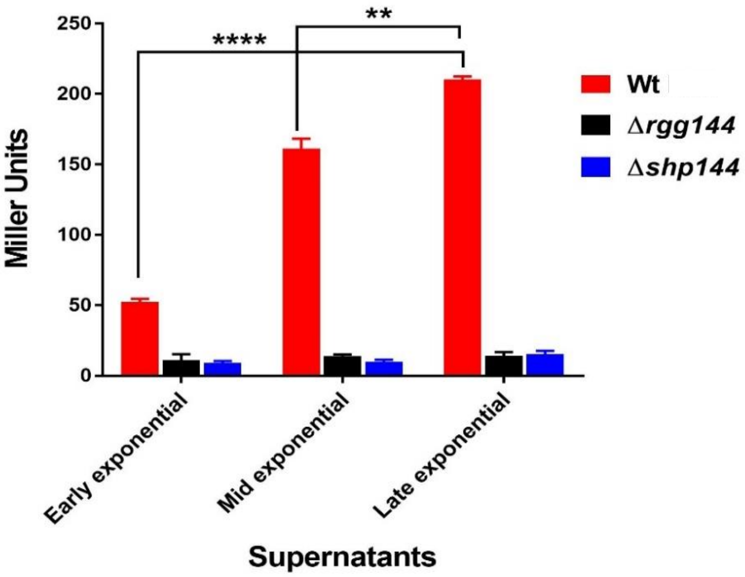

Figure 3.7: Expression levels of pneumococcal *lacZ* fusions upon treatment with wild type (Wt) and mutant supernatants (Δ*rgg144* and Δ*shp144*). The pellet of P_{shp144}::*lacZ*-Δ*shp144* was mixed with supernatants collected at different growth points (early, mid and late exponential phase), and the cultures were incubated to an early exponential phase for β-galactosidase analysis. Values are the average of three independent experiments, each with three replicates. Comparisons are made relative to reporter culture treated with late exponential culture supernatant of wild type (**$p<0.01$, ****$p<0.0001$).

3.5. Rgg/SHP144 quorum sensing system is induced by mannose and galactose

Streptococcus pneumoniae largely depends on host carbohydrates as a carbon source for growth and survival. The nature and availability of carbohydrates are widely varied between tissues (Paixão *et al*., 2015a). For instance, free sugars like glucose are nearly absent in the upper respiratory tract including nasopharynx, thus pneumococci rely on other abundant sugars like galactose and mannose present in mucosal glycans (Pericone *et al*., 2000; Rose and Voynow, 2006). Here, the responsiveness of P_{shp144} to different carbon sources (glucose, galactose, mannose and *N*-acetylglucosamine) was assessed. The P_{shp144} driven β-galactosidase activity was determined in reporter strain P_{shp144}::*lacZ*-Wt grown to different growth points (early, mid and late exponential phase) in the presence of the selected sugar. Of the carbohydrates tested, the reporter strain in CDM supplemented with 55 mM mannose or galactose revealed significantly higher induction than in cells grown with 55 mM glucose or *N*-acetylglucosamine (Figure 3.8). Maximum expression was achieved in culture grown on mannose to late exponential phase (759 ± 20 MU, n=3) followed by galactose (610 ± 21 MU, n=3), which are statistically different from the expression in the presence of glucose (267 ± 27 MU, n=3) or *N*-acetylglucosamine (251.5 ± 13.5 MU, n=3) ($p<0.001$). The same trend was observed for reporter cultures growing to mid-log phase ($p<0.01$), but the induction level was low compared with that in late exponential cultures. While, no difference in induction could be observed in pneumococcal cultures incubated to early exponential phase regardless of carbon source ($p>0.05$). These results suggest that the induction of *shp144* promoter is influenced by the type of sugars used, and mannose and galactose play a significant role in activation of P_{shp144}::*lacZ* expression particularly at late exponential cultures, in which the amount of produced SHP144 is high.

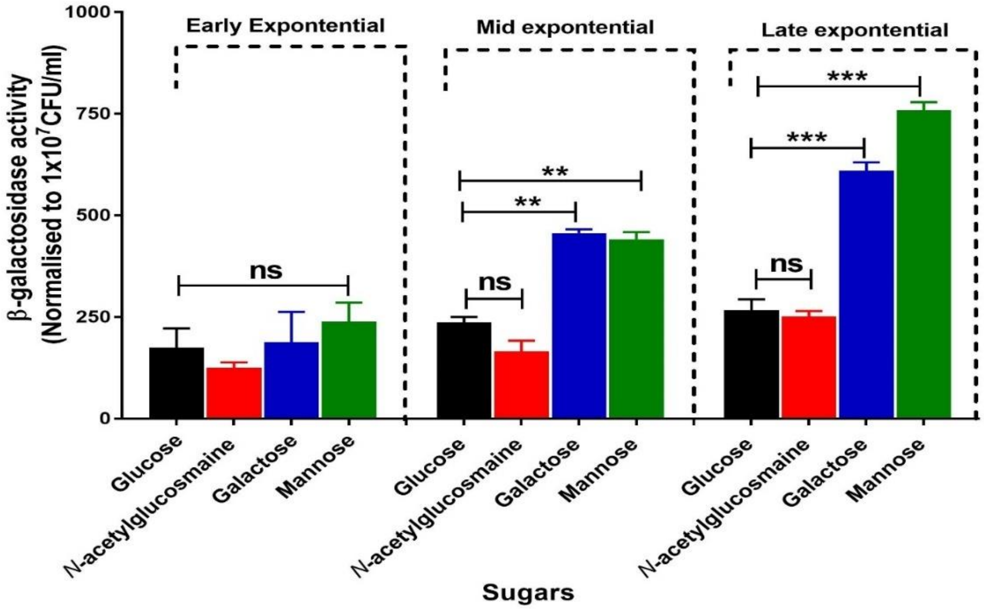

Figure 3.8: Expression level of P$_{shp144}$::*lacZ* in reporter culture P$_{shp144}$::*lacZ*-Wt supplemented with different types of sugars (glucose, mannose, galactose and *N*-acetylglucosamine). The reporter cultures were grown microaerobically in selected sugar to different growth points (early, mid and late-log phase) and the P$_{shp144}$ induction was measured by β-galactosidase assay. The activity was normalised to $1x10^7$ CFU/ml and expressed in Miller Units. Each data point represents the mean of three independent experiments, each with three replicates. **$p<0.01$, ***$p<0.001$, 'ns' not significant compared with reporter culture grown on glucose.

Section B: Construction of genetically complemented *shp144*

3.6. Genetic complementation of mutant *shp144*

Genetic complementation is one of the techniques that has been widely used in the field of molecular biology for several purposes. For example, studying the relationship between the genes that are responsible for a particular phenotype and in analysis of gene functions (gene-protein relationship) (Srivastava and Srivastava, 2003). In addition, it is also used for evaluating phenotypic characterisation of mutant genes through reintroducing an intact copy of gene of interest into mutant strains for eliminating the possibility of polar effects that can occur for genes located downstream of the mutation (Reyrat *et al.*, 1998). Introduction of insertion-deletion mutation into a bacterial genome might cause polar effects for the genes located downstream of the mutation particularly if they do not have their own promoters in an operon organisation (Shapiro, 1969; Reyrat *et al*., 1998) as well as if the mutated gene is the first gene of a predicted operon (Guiral *et al*., 2006). In this study, the *shp144* mutant strain was complemented with an intact copy of *shp144* to study the self-regulation of SHP144 (feedback regulation) and to rule out the possibility of polar effects of the mutation.

3.6.1. Amplification of *shp144* gene for genetic complementation

A region of approximately 266 bp encompassing the *shp144* coding sequence and its putative promoter region was amplified from chromosomal D39 using primer pairs Shp144Com/F and Shp144Com/R, which are designed to introduce *BamHI* and *NcoI* restriction sites into the 5’ and 3’ ends of the amplicon (Table 2.10). The resulting product was purified using Wizard® SV Gel and PCR Clean-Up System (Promega, UK), and analysed on agarose gel electrophoresis. It is apparent from lanes 1 and 2 of Figure 3.9 that the amplification had been successfully done by obtaining a DNA fragment corresponding to the expected size (266 bp).

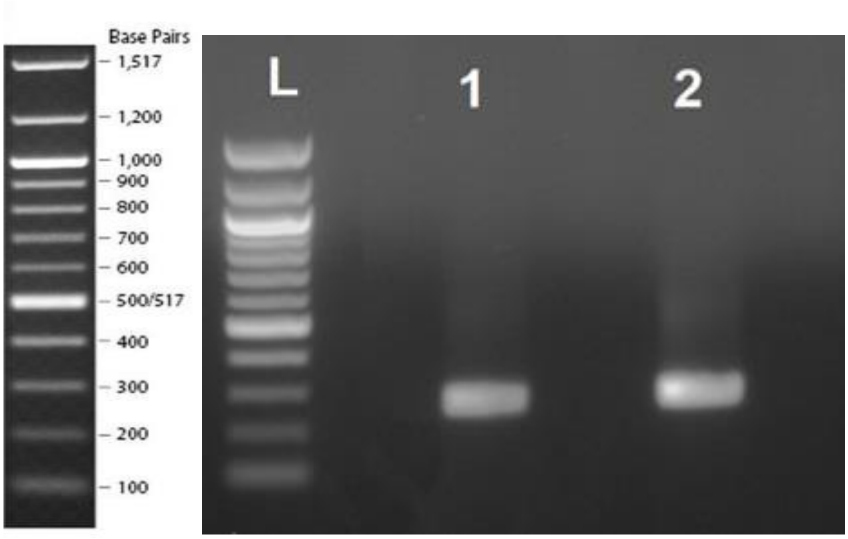

Figure 3.9: Agarose gel electrophoresis showing successful amplification of *shp144* gene using PCR reaction. Lane L, 100 bp DNA ladder (New England Biolabs, UK); lanes 1 and 2 PCR amplicons containing the coding sequence and putative promoter region of *shp144* gene (266 bp) using Shp144Com/F and Shp144Com/R primers.

3.6.2. Extraction and digestion of plasmid pCEP

Plasmid pCEP was used for *cis*-complementation of the mutant *shp144* strain (Guiral *et al*., 2006). This plasmid is a 9540 bp single copy plasmid, unable to replicate in *S. pneumoniae*, but it has around 2 kb DNA surrounding its multiple cloning site homologous to pneumococcal genome and this site is known to be transcriptionally silent. For this reason, the recombinant pCEP carrying *shp144* gene can be integrated successfully into downstream of *amiA* operon of *S. pneumoniae* via homologous recombination without any harmful effects on the pneumococcal physiological functions (Figure 3.10).

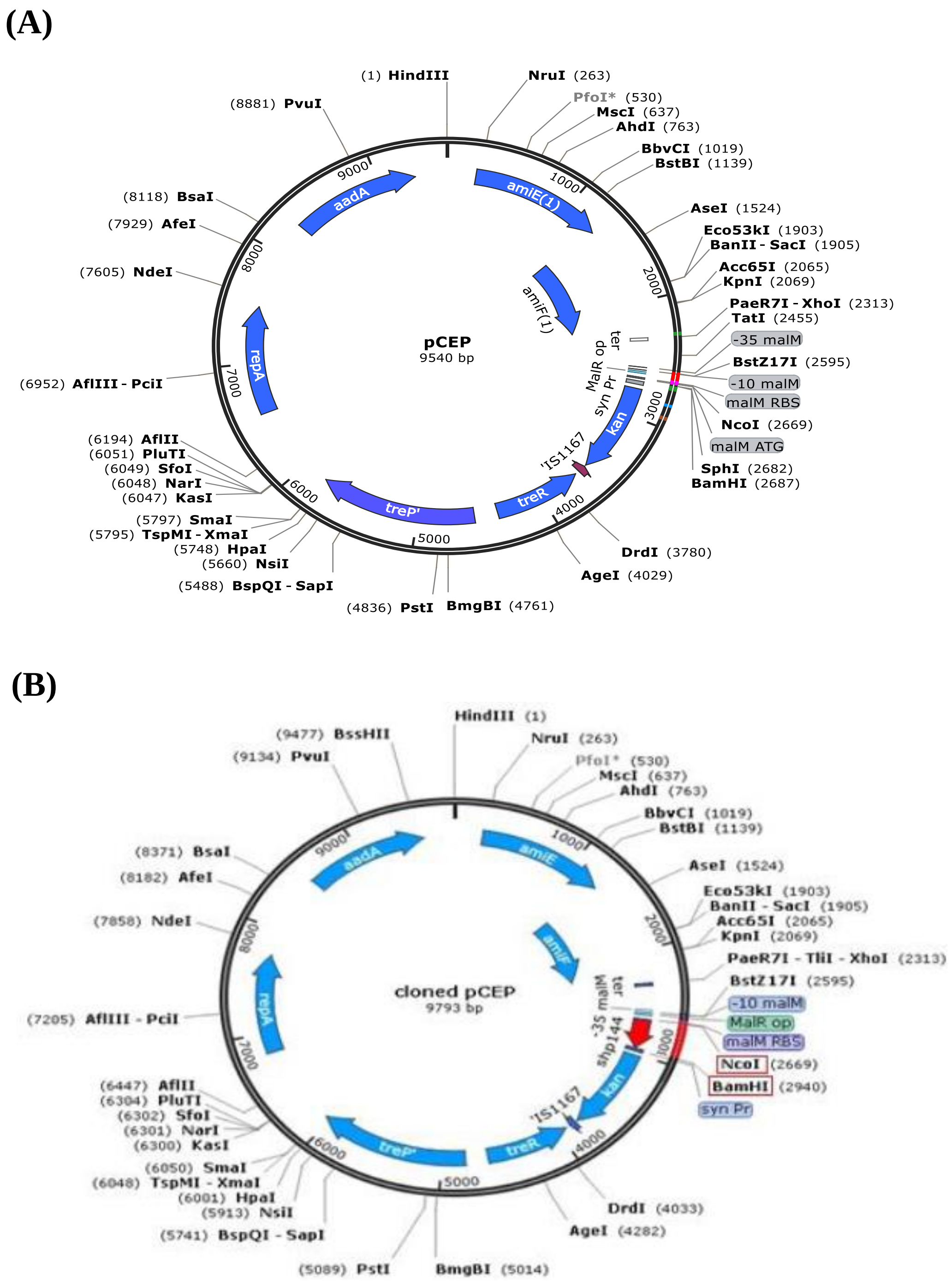

Figure 3.10: **(A)** Genetic map showing the main features of pCEP plasmid. *treR*: Trehalose operon repressor, *amiF*, *amiE*: oligopeptide ABC transporters, *treR* and *treP*: trehalose-utilisation system, *kan*: kanamycin resistance cassette, *ter*, transcription terminator and *malR*: maltosaccharide-inducible promoter. The pCEP contains a cluster of restriction sites: *BstZ17I*, *NcoI*, *SphI* and *BamHI*. **(B)** pCEP plasmid harbouring *shp144* gene. The red arrow indicates the target gene (*shp144)* whereas the red boxes refer to *NcoI* and *BamHI* restriction sites used for digestion of insert and pCEP plasmid (Based on Guiral *et al.*, 2006).

The pCEP was extracted from *E. coli* using QIAprep spin Miniprep kit and double digested with *NcoI* and *BamHI* enzymes as previously described in Materials and Methods (Section 2.17). The successful digestion was confirmed by agarose gel electrophoresis. It is clear from lane 1 of Figure 3.11 that the pCEP was digested successfully by appearance of single linear band with 9.5 kb whereas the lane 2 showed uncut pCEP with multiple bands.

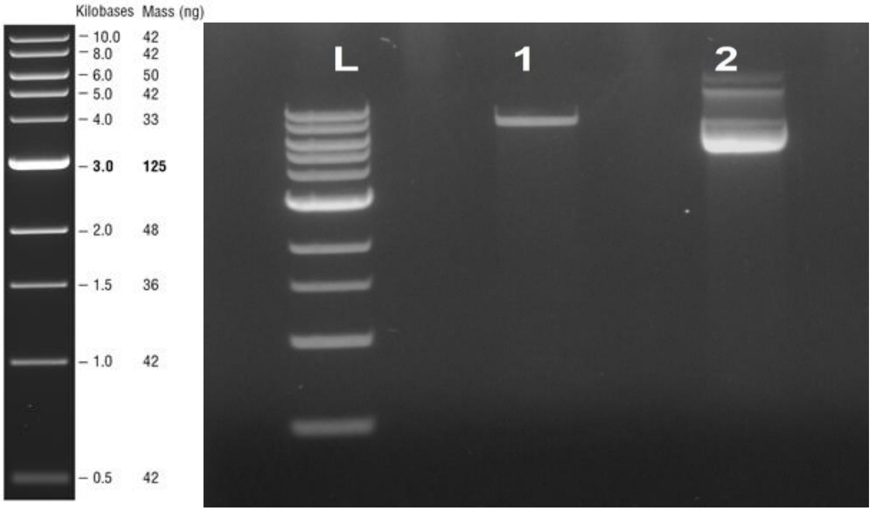

Figure 3.11: Confirmation of successful digestion of pCEP using an agarose gel electrophoresis. Lane L, 1 kb DNA ladder (New England Biolabs, UK); lane 1, digested pCEP (double digestion with *NcoI* and *BamHI* enzymes); lane 2, uncut pCEP.

3.6.3. Construction of recombinant pCEP for genetic complementation

After double digestion of insert and pCEP with *NcoI* and *BamHI* restriction enzymes, the digested insert was ligated into pCEP using T4 ligase as mentioned in section 2.17. The resulting ligation product was transformed into *E. coli* TOP10 chemically competent cells and selected on LA plates containing appropriate concentration of kanamycin as previously indicated in Materials and Methods (Section 2.19). Kanamycin transformants were analysed for the presence of recombinant plasmid using Mal/F and pCEP/R primers, that anneal to either side of cloning site. The amplified PCR products were then analysed by agarose gel electrophoresis. As expected, the positive transformants produced amplicons of approximately 529 bp as depicted in lanes 1 and 2 of Figure 3.12. This size corresponds to the estimated insert size, which is approximately 266 bp plus the size of up and down streams of multiple cloning site of pCEP, which is approximately 263 bp (lane 3 of Figure 3.12). The successful construction of recombinant pCEP was further confirmed for the presence of *shp144* by DNA sequencing using Mal/F and pCEP/R primers. The sequencing data confirmed successful cloning of *shp144* without mutations (Appendix 2A).

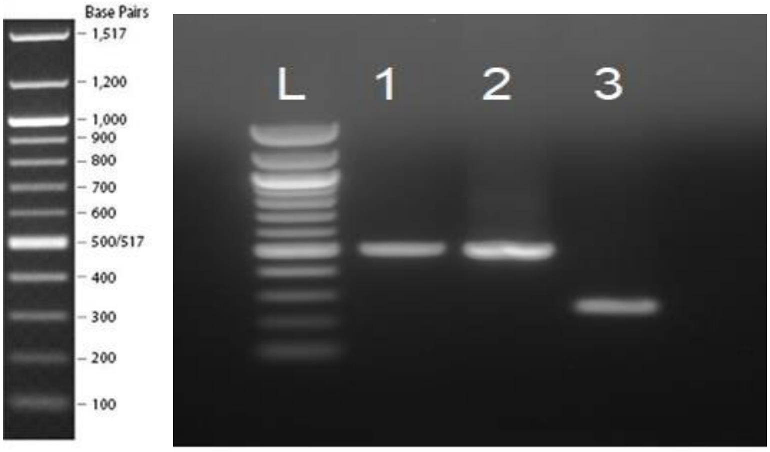

Figure 3.12: Gel electrophoresis analysis showing the successful construction of recombinant pCEP for genetic complementation. Lane L, 100 bp DNA ladder (New England Biolabs, UK); lanes 1-2, PCR amplicons containing *shp144* coding sequence and its putative promoter region plus upstream and downstream of cloning site which are approximately 529 bp obtained using Mal/F and pCEP/R primers; lane 3, empty pCEP without insert (263 bp).

3.6.4. Transformation of recombinant pCEP into mutant *shp144*

The sequenced plasmid was further transformed into *S. pneumoniae* knock out *shp144* gene strain following the protocol of Bricker and Camilli (1999) as described in section 2.20. The successful integration of an intact copy of *shp144* with its putative promoter into pneumococcal genome was verified by colony PCR using pCEP based primers Mal/F and pCEP/R (529 bp) and insert specific primers Shp144Com/F and Shp144Com/R (266 bp) as shown in Figure 3.13A and B.

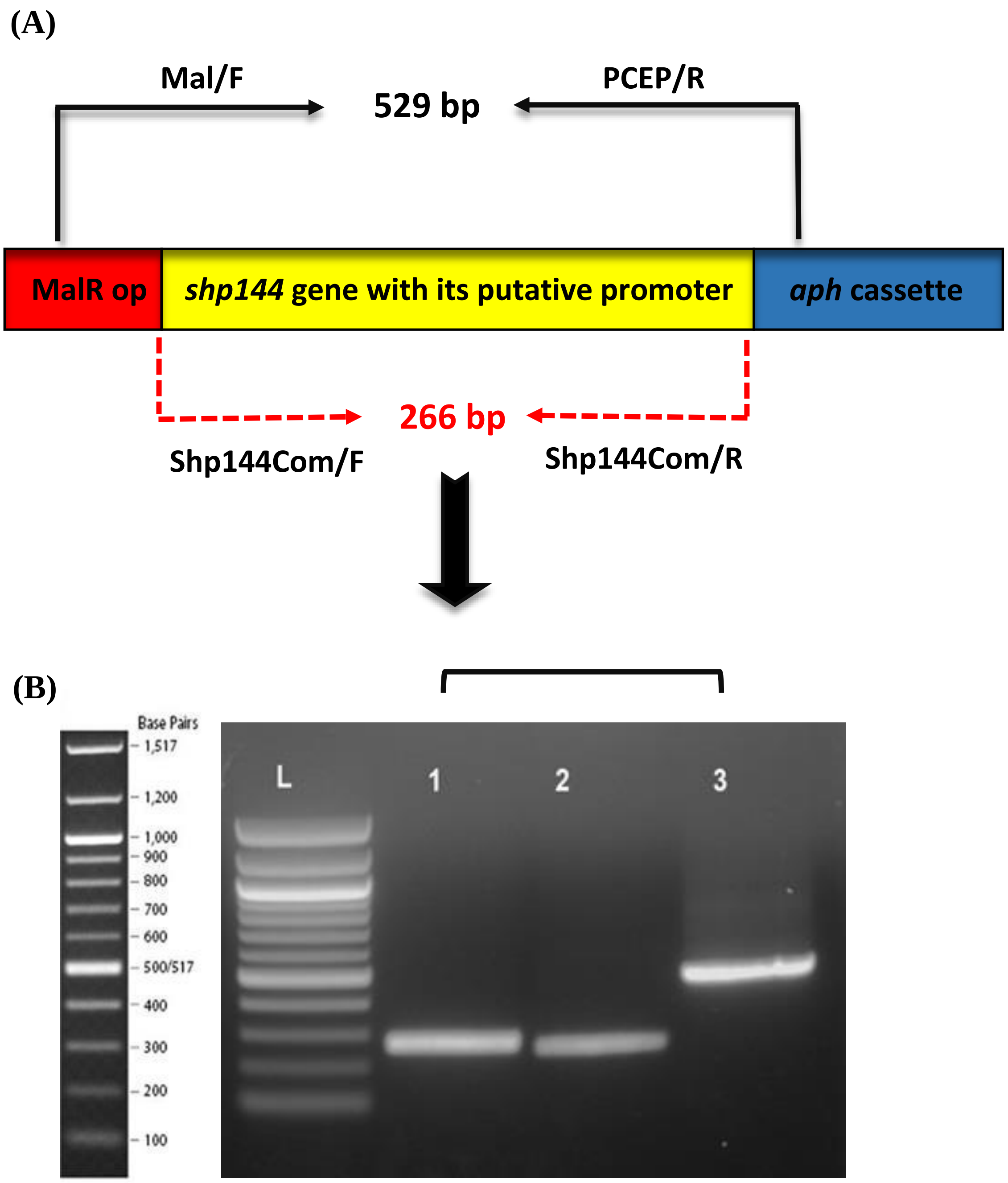

Figure 3.13: (A) PCR strategy used to confirm successful incorporation of the insert carrying the intact copy of *shp144* with its putative promoter within the pneumococcal genome. Primers Mal/F and pCEP/R were designed to amplify the entire insert along with the region surrounding the cloning site generating a fragment of 529 bp. **(B)** Confirmation of the successful transformation of *shp144* into the mutant *shp144* genome using agarose gel electrophoresis. Lane L, 100 bp DNA ladder (New England Biolabs, UK); lanes 1, PCR amplicon represents the insert, which is about 266 bp; lane 2, empty pCEP without insert (263 bp); lane 3 recombinant pCEP carrying the entire gene of *shp144*.

3.7. Construction of genetically modified strains by site-directed mutagenesis

The results in the current study showed that Rgg144 drives *shp144* transcription, and 12 and 13 aa long synthetic SHP are sufficient to stimulate P_{shp144} expression. The length of SHP144 is longer than other active peptide pheromones in the RRNPP family, which generally vary between 5 to 8 aa long (Aggarwal *et al.*, 2014). This is very likely due to the deep binding groove in Rgg144. In this study, SHP144-C13 was selected as a basis to introduce point mutations into coding sequence of *shp144*. Thirteen-point mutations were introduced to systemically replace each amino acid coded by *shp144* with alanine using splicing overlap extension PCR (SOEing-PCR) method (Horton, 1995; Lee *et al.*, 2004). The overlapping PCR approach offers several advantages over other methods of site-directed mutagenesis such as plasmid-based mutation and mariner mutagenesis (Horton *et al.*, 1993; Akerley *et al.*, 2002). The SOEing-PCR introduces a mutation in a target gene via combining two DNA fragments without the need for restriction sites or ligase generating a clustered set of base pair changes such as deletions, substitution or insertions of any length at defined position in chromosomal DNA molecule (Heckman and Pease, 2007). This is in contrast to mariner mutagenesis, which allows random insertion of a DNA fragment by transposons. Therefore, SOEing-PCR is considered as an ideal and efficient method for introducing mutations in pneumococcal genome since it is naturally competent and can accept exogenous DNA molecule from the environment and incorporate directly into its genome (Seitz and Blokesch, 2014). Alanine was selected for substitution as it has an inert structure, non-bulky and non-reactive side chain (Betts and Russell, 2003). Full details for construction of modified *shp144* are shown in Figure 3.14.

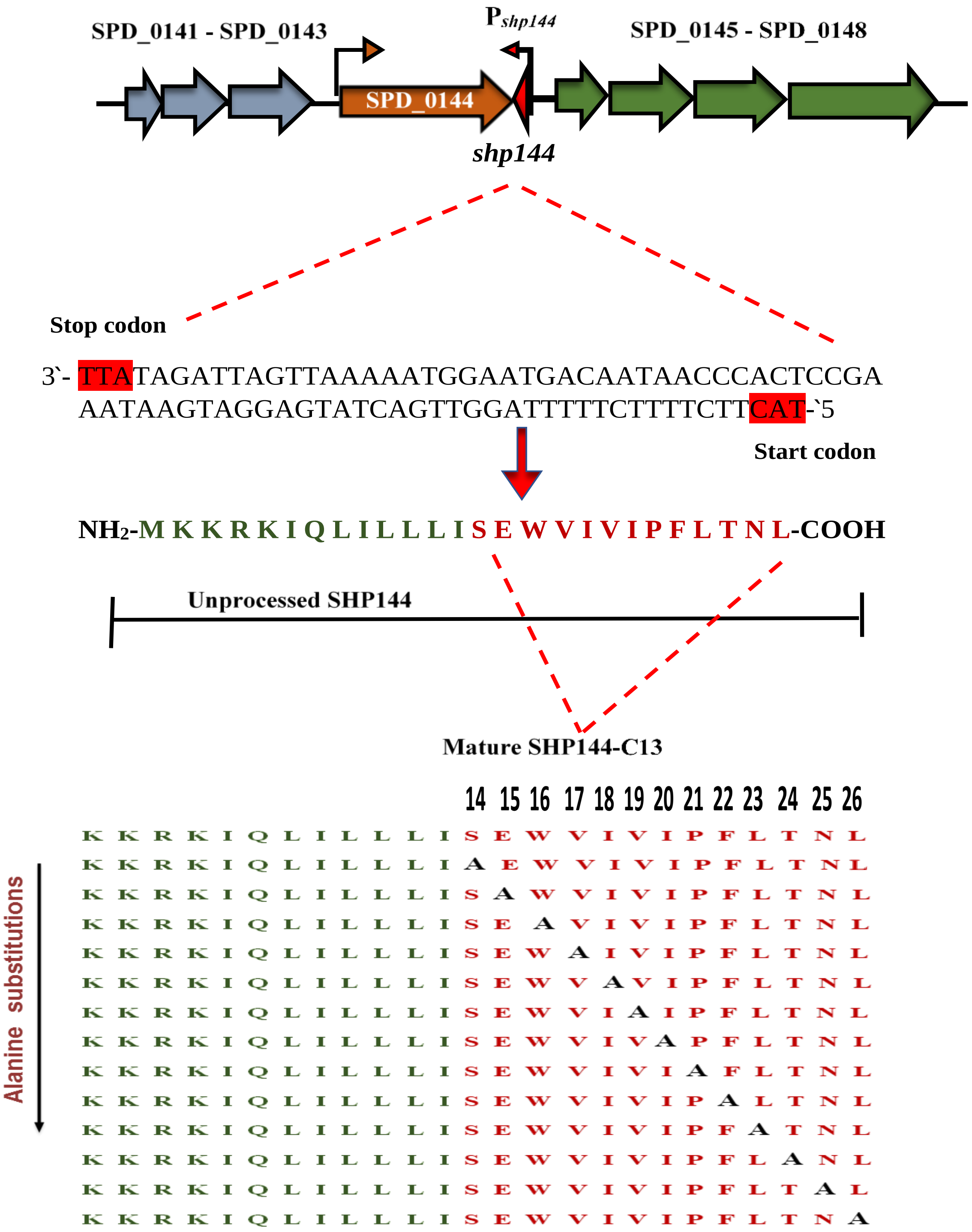

Figure 3.14: Diagram representing alanine scanning of selected SHP144 amino acids residues. CAT and TTA represents the start and stop codons of *shp144*, respectively. Brown and red boxes indicate the *rgg144* and *shp144* genes, which are transcribed divergently. Grey and green boxes refer to genes located upstream and downstream of *rgg144*. The residues in red typeface represent the active form of SHP144 and were selected for alanine replacement.

3.7.1. Amplification of flanking regions and SOEing fragments of modified *shp144* genes

To substitute each amino acid of *shp144* with alanine, two consecutive PCR reactions were set up as shown previously in Materials and Methods (Figure 2.2). In the first PCR, left and right flanking regions of *shp144* were individually amplified from D39 genomic DNA using the primers that incorporated restriction sites for *NcoI* and *BamHI* enzymes (*NcoI*-shp144 and *BamHI*-shp144 primers, respectively), and the mutagenic primers containing desired mutation (Shp144XA/F and Shp144XA/R), where XA indicate the replaced amino acid codon with alanine as illustrated in Figure 2.2. The resulting PCR products were analysed on agarose gel electrophoresis. The results in Figure 3.15 show the successful amplification of left and right flanking regions of modified *shp144*. In Figure 3.15, the PCR amplicons in lanes 1 and 4 represent the expected approximate sizes of left flank for shp144L26A, shp144N25A, shp144T24, shp144L23, shp144F22A, shp144P21A, shp144I20A, shp144V19A, shp144I18A, shp144V17A, shp144W16A, shp144E15A and shp144S14A, which ranged between approximately 348 to 384 bp. On the other hand, the lanes 2 and 5 of the same figure show the expected amplicon sizes for the right flank, approximately 292 to 328 bp, for shp144L26A, shp144N25A, shp144T24A, shp144L23A, shp144F22A, shp144P21A, shp144I20A, shp144V19A, shp144I18A, shp144V17A, shp144W16A, shp144E15A, and shp144S14A. The PCR amplicons were then purified from the agarose gel using Wizard® SV Gel and PCR Clean-Up System (Section 2.7) to remove impurities like dimers, dNTPs, enzymes and salts from the PCR products.

In the second PCR, the purified flanking fragments sharing the compatible ends were joined together to produced full-length mutated *shp144* using outermost flanking primers as listed in Table 2.10. The fused amplicons were separated electrophoretically on agarose gel. The successful amplifications of SOEing products are shown in lanes 3 and 6 of Figure 3.15, as evidenced by the amplification of approximately 603 bp product. Subsequently, the band corresponding to expected size of each modified gene was excised and purified to avoid introducing any nonspecific DNA products into the pneumococcus.

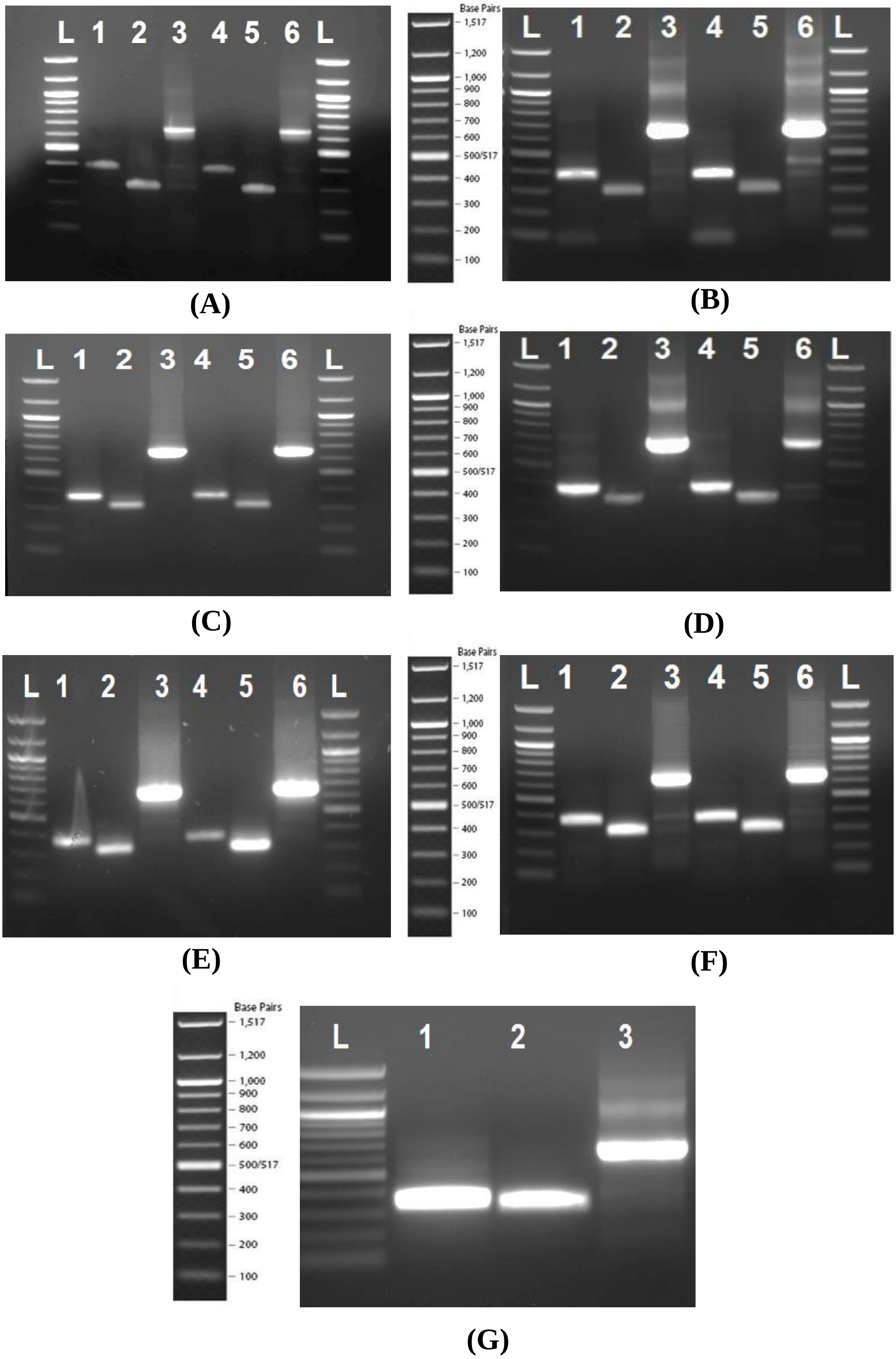

Figure 3.15: Agarose gel electrophoresis analysis confirming the successful amplification of flanking regions (left and right) and SOEing products of 13 modified *shp144* alleles by using site directed mutagenesis. Lane L, 100 bp DNA ladder (New England Biolabs, UK); Lanes 1 and 4 show amplification of left flanks of shp144L26A and shp144N25A **(A)**;

shp144T24A and shp144L23A **(B)**; shp144F22A and shp144P21A **(C)**; shp144I20A and shp144V19A **(D)**; shp144I18A and shp144V17A **(E)**; shp144W16A and shp144E15A **(F)** and shp144S14A **(G)**. The amplicons size ranged between (348-384 bp). Lanes 2 and 5 refer to the right flanking regions of shp144L26A and shp144N25A **(A)**; shp144T24A and shp144L23A **(B)**; shp144F22A and shp144P21A **(C)**; shp144I20A and shp144V19A **(D)**; shp144I18A and shp144V17 **(E)**; shp144W16A and shp144E15A **(F)** and shp144S14A **(G)** with an estimated band size between (292-328 bp). Lanes 3 and 6 show the overlapping PCR products containing the entire region of each modified *shp144* (putative promoter region and coding sequence with desired modification) with the expected size of 603 bp.

3.7.2. Cloning of *in vitro* mutagenised *shp144* alleles and transformation into *E. coli* and DNA analysis

pCEP plasmid was used for introducing the mutant alleles to pneumococcal genome (Figure 3.10). This plasmid and the PCR amplicons containing entire region of each modified *shp144* (Section 3.7.1) were double digested with *BamHI* and *NcoI*. The resultant fragments were purified using Wizard® SV Gel and PCR Clean-Up System and ligated into the restricted pCEP using T4 DNA ligase as indicated in section 2.17. The ligation mixtures were transformed into *E. coli* TOP10 chemically competent cells for propagation and cloning confirmation. The transformants were selected on LA plates in the presence of kanamycin. The putative recombinant pCEP constructs were extracted from selected clones, and the successful cloning was confirmed by PCR using pCEP based primers Mal/F and pCEP/R (Table 2.10). The PCR amplicons were run on agarose gel electrophoresis and successful cloning was confirmed by appearance of a DNA fragment of corresponding size, which is about 866 bp as depicted in lanes 1-9 of Figure 3.16A and lanes 1-4 of Figure 3.16B. This size represents the estimated insert size, which is approximately 603 bp (coding sequence and putative promoter region of each modified gene), and genomic region surrounding the multiple cloning sites of pCEP, which is around 263 bp). In addition, lanes 10 and 5 of Figure 3.16A and B, respectively show the PCR amplicons of empty pCEP without insert (263 bp) using the same set of Mal/F and pCEP/R primers.

The positive pCEP constructs containing the desired insert region was further verified by DNA sequencing using Mal/F and pCEP/R primers. Sequence analysis demonstrated the successful replacement of selected nucleotides in all examined clones as provided in Appendix 2 (B-N).

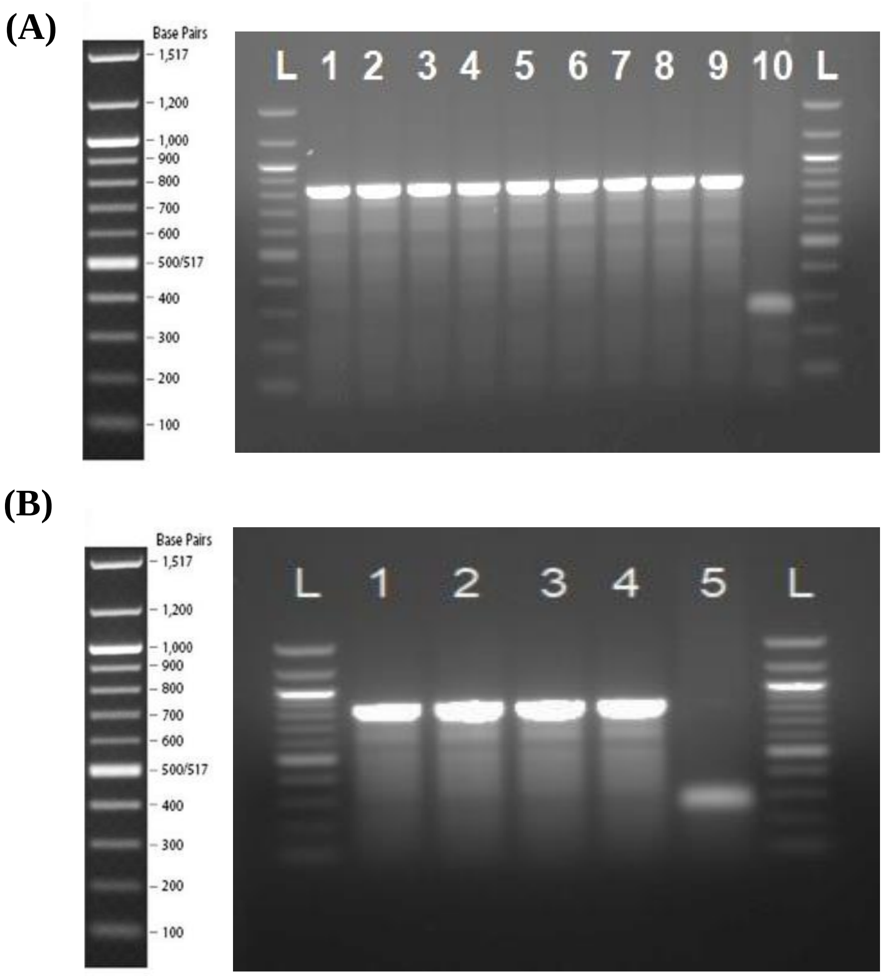

Figure 3.16: Confirmation of successful construction of recombinant pCEP constructs harbouring modified *shp144* alleles**.** Lane L, 100 bp DNA ladder (New England Biolabs, UK). Lanes (1-9) **(A)** and (1-4) **(B)** PCR fragments amplified from recombinant pCEP carrying putative promoter region and modified coding sequence of *shp144*; **(A)** *shp144*L26A, *shp144*N25A, *shp144*T24A, *shp144*L23A, *shp144*F22A, *shp144*P21A, *shp144*I20A, *shp144*V19A, *shp144*I18A; **(B)** *shp144*V17A, *shp144*W16A, *shp144*E15A and *shp144*S14A using Mal/F and pCEP/R primers. Amplicons had the expected sizes (866 bp). Lane 10 **(A)** and Lane 5 **(B)** show the amplification of empty pCEP lacking the insert (263bp) by using the same set of primers Mal/F and pCEP/R.

3.7.3. Transformation of recombinant pCEP into pneumococcal genome

Upon confirmation of mutations by DNA sequencing, the pCEP constructs carrying modified *shp144* alleles were transformed independently into *S. pneumoniae* Δ*shp144* strain following the procedure described in section 2.20. The transformants were selected on blood agar plates containing kanamycin and spectinomycin. The successful integration of the mutant’s alleles was confirmed by colony PCR using Mal/F and pCEP/R and insert specific *NcoI*-shp144 and *BamHI*-shp144 primers (Table 2.10). The resulting PCR fragments were analysed by agarose gel electrophoresis. As can be seen from Lanes 2, 4, 6, 8 of Figure 3.17 B-E, DNA fragments of approximately 603 bp, which are the correct expected size of each modified *shp144*, were generated by using insert specific primers. Plasmid primers (Mal/F and pCEP/R) were also used to confirm the correct location of inserted alleles within pneumococcal genome. An 866-bp fragment containing the insert (603 bp) plus up and downstream flanking regions of cloned gene (263 bp) was obtained as shown in lanes 1, 3, 5, and 7 of Figure 3.17 B-E. For positive controls, bands of estimated sizes of 603 and 866 bp were achieved when recombinant pCEP was used as template and *NcoI*-shp144 and *BamHI*-shp144 and Mal/F and pCEP/R primers respectively (lanes 9-10 of 3.17 B-D and 3-4 of 3.17E).

Following the successful confirmation by DNA sequencing and PCR, the complemented modified strains were designated as Δ*shp144*ComL26A, Δ*shp144*ComN25A, Δ*shp144*ComT24A, Δ*shp144*ComL23A, Δ*shp144*ComF22A, Δ*shp144*ComP21A, Δ*shp144*ComI20A, Δ*shp144*ComV19A, Δ*shp144*ComI18A, Δ*shp144*ComV17A, Δ*shp144*ComW16A, Δ*shp144*ComE15A and Δ*shp144*ComS14A.

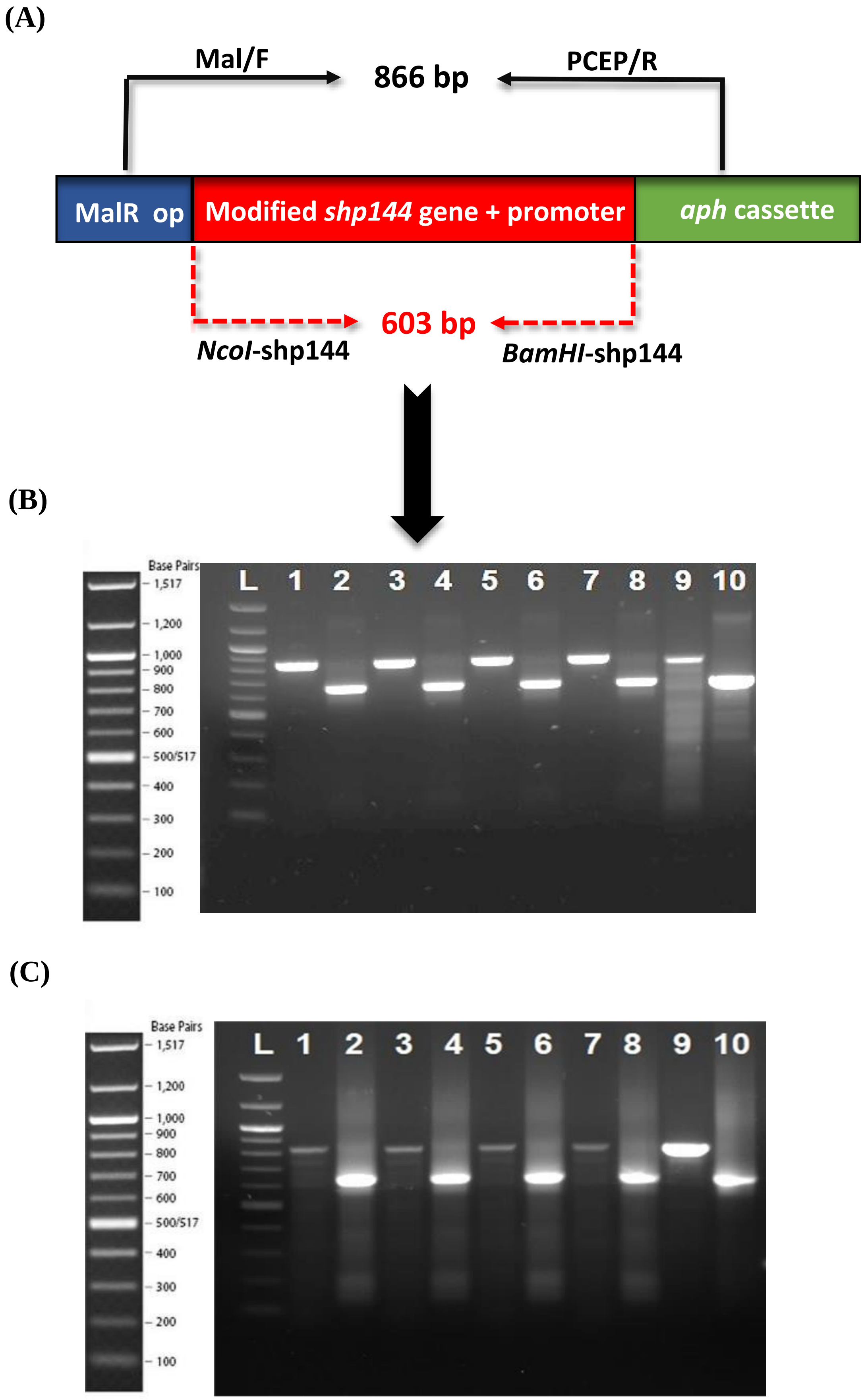
(A)
Mal/F
866 bp
PCEP/R
MalR op
Modified shp144 gene + promoter
aph cassette
603 bp
NcoI-shp144
BamHI-shp144
(B)
Base Pairs
1,517
1,200
1,000
900
800
700
600
500/517
400
300
200
100
L 1 2 3 4 5 6 7 8 9 10
(C)
Base Pairs
1,517
1,200
1,000
900
800
700
600
500/517
400
300
200
100
L 1 2 3 4 5 6 7 8 9 10

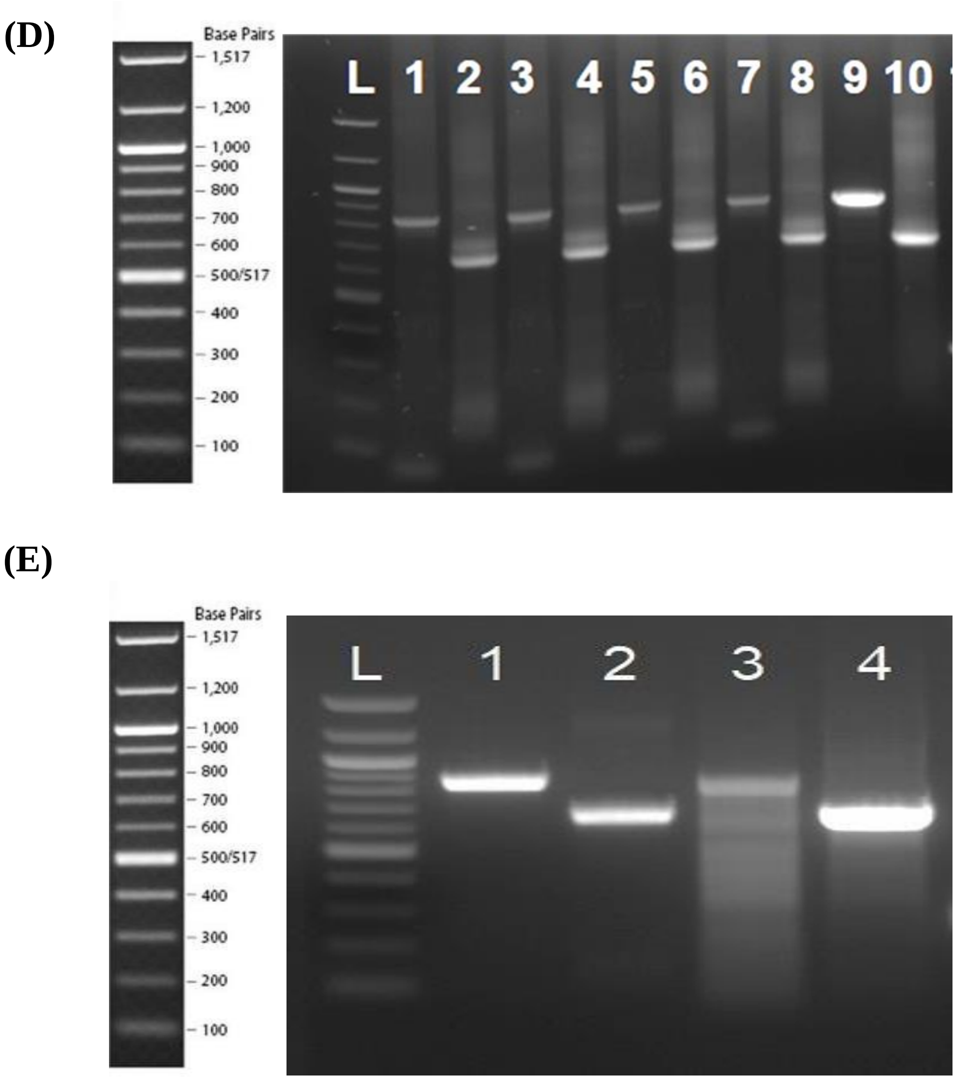

Figure 3.17: **(A)** PCR reaction used for amplification of complemented modified *shp144* genes from pneumococcal genome using insert specific primers and plasmid-based primers. **(B-E)** Agarose gel electrophoresis showing the successful insertion of modified *shp144* alleles and their putative promoter regions within Δ*shp144*. Lane L, 100 bp DNA ladder (New England Biolabs, UK); lanes 1, 3, 5, 7 **(B-E)** show the successful amplification of entire region of modified *shp144* with flanking regions of pCEP (866 bp) for *shp144*L26A, *shp144*N25A, *shp144*T24A and *shp144*L23A **(B)**; *shp144*F22A, *shp144*P21A, *shp144*I20A and *shp144*V19A **(C)**; *shp144*I18A, *shp144*V17A, *shp144*W16A, *shp144*E15A **(D)** and *shp144*S14A in lane 1 of **(E)** by using Mal/F and pCEP/R primers. While PCR products with approximate sizes of 603 bp were obtained by using insert specific *NcoI*-shp144 and *BamHI*-shp144 primers as shown in lanes 2, 4, 6, 8 for *shp144*L26A, *shp144*N25A, *shp144*T24A and *shp144*L23A **(B)**; *shp144*F22A, *shp144*P21A, *shp144*I20A and *shp144*V19A **(C)**; *shp144*I18A, *shp144*V17A *shp144*W16A, *shp144*E15A **(D)** and *shp144*S14A in lane 2 **(E)**. Positive controls were also included in analysis as shown in lanes 9-10 **(B-D)** and 3-4 **(E)** by using recombinant pCEP as template and the Mal/F and pCEP/R and *NcoI*-shp144 and *BamHI*-shp144 primers respectively.

3.8. Assessment the P_{shp144}::*lacZ* activity in genetically complemented strains

To determine whether the reduction in *shp144* promoter induction in the mutants caused by deficiency of the mutant genes (*shp144* and *rgg144*) rather than polar effects of the mutations, a transcriptional *lacZ* fusion in complemented backgrounds (Δ*shp144*Com and Δ*rgg144*Com) were constructed by transforming P_{shp144}::*lacZ* fusion into complemented strains and analysing by PCR using Fusion-Seq-F and Fusion-Seq-R primers, and by agarose gel electrophoresis. Lanes 1-2 of Figure 3.18 revealed the successful transformation, and a DNA fragment of the expected size was obtained (384 bp for both Δ*shp144*Com and Δ*rgg144*Com). The resulting reporter strains were designated as P_{shp144}::*lacZ*-Δ*shp144*Com and P_{shp144}::*lacZ*-Δ*rgg144*Com. The P_{shp144} expression level was measured in complemented reporter strains using β-galactosidase assay. As shown in Figure 3.19 the *lacZ* activity of complemented strains closely resembles that of parental strain ($p>0.05$). The β-galactosidase activity was 228 ± 2, 215 ± 5 and 210 ± 10 MU (n=3) for P_{shp144}::*lacZ*-Wt and the complemented reporter strains, P_{shp144}::*lacZ*-Δ*rgg144*Com and P_{shp144}::*lacZ*-Δ*shp144*Com, respectively. Further, the complemented strains showed a higher β-galactosidase activity relative to their respective mutants ($p<0.0001$). The data presented above rule out the possibility of polar effect of the mutations, and potential ability to reconstitute *shp144* activity by introducing a single copy of *rgg144* or *shp144* into their respective mutants.

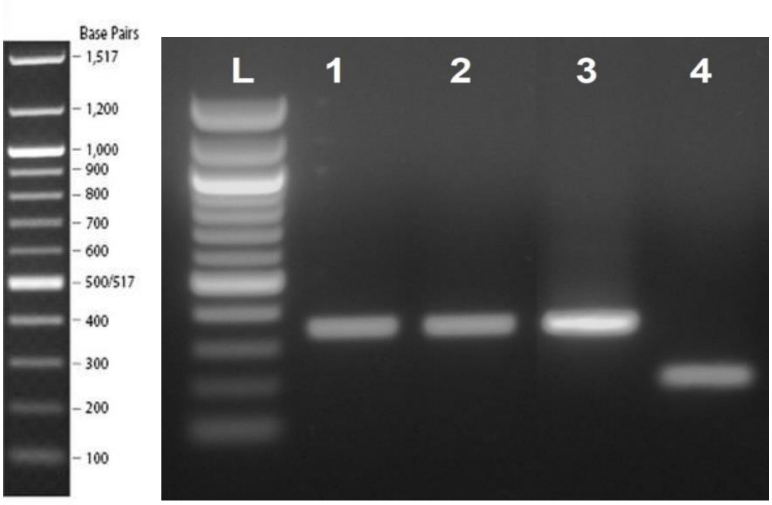

Figure 3.18: Agarose gel electrophoresis analysis confirming successful transformation of P_{shp144}::*lacZ* fusion into complemented strains. Lane L,100 bp DNA ladder (New England Biolabs, UK); lane 1, P_{shp144}::*lacZ*-Δ*rgg144*Com; lane 2, P_{shp144}::*lacZ*-Δ*shp144*Com; lane 3, P_{shp144} plasmid (positive control); lane 4, empty pPP2 plasmid (negative control).

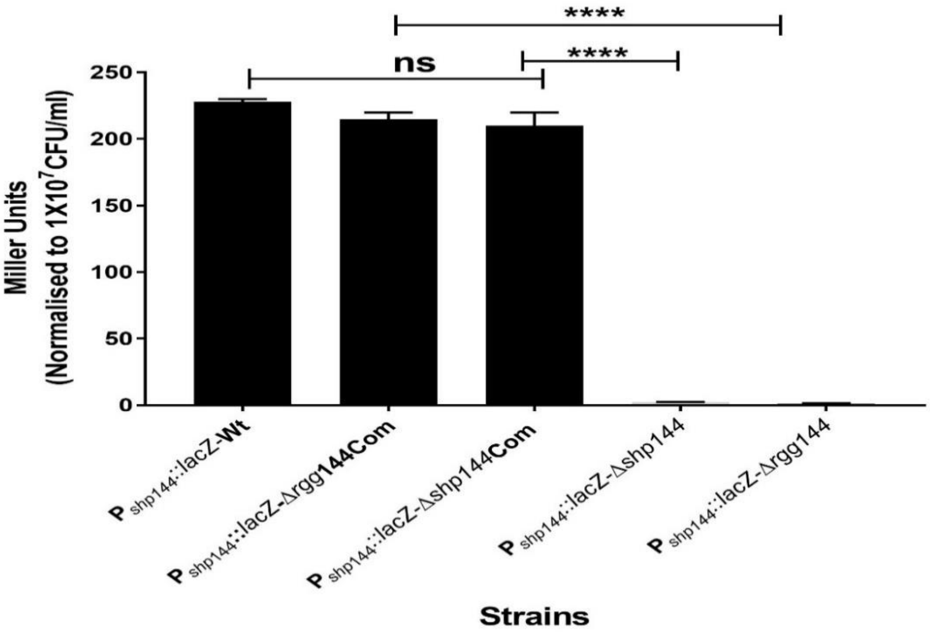

Figure 3.19: β-galactosidase activity of P_{shp144}::*lacZ* fusion in complemented backgrounds (P_{shp144}::*lacZ*-Δ*shp144*Com and P_{shp144}::*lacZ*-Δ*rgg144*Com). The enzyme activity is expressed in Miller Units (nmol *p*-nitrophenol/min/ml). **** $p<0.0001$, ‘ns’ not significant compared to wild type and complemented strains.

3.9. Quantifying the functional importance of SHP144 amino acid residues for transcriptional activation of Rgg/SHP144 QS

It was hypothesised that each SHP144 residue would have a different role in Rgg144 binding and transcriptional activation. Certain SHP144 residues would have a role in binding to Rgg144 and their mutation would lead to decrease in transcriptional activation of *shp144*, while the mutation of other residues would prevent activation of Rgg144 by the bound SHP144, which also leads to reduction in transcriptional activation. On the other hand, some residues would have no role either in binding or in activation, therefore, their mutations would not affect the *shp144* transcription.

Based on the knowledge that the 13 aa long synthetic SHP144 is sufficient to stimulate P_{shp144} expression in the presence of mannose, thus the role of each one of these thirteen amino acids of SHP144 in transcriptional activation of the system was screened and utilised to develop inhibitors to abolish phenotypic manifestations of Rgg/SHP144. A set of transcriptional *lacZ* reporter strains were constructed through incorporation of the P_{shp144}::*lacZ* fusion into genome of Δ*shp144* strains that were genetically complemented with different variants of *shp144* following the protocol mentioned in Materials and Methods (Section 2.20). The transformants were selected on blood agar plates supplemented with tetracycline and kanamycin. The successful transformation was analysed for the presence of correct insert using Fusion-Seq-F and Fusion-Seq-R primers. These primers amplify about 200 bp DNA fragment when empty pPP2 plasmid was used as template (lanes 9 (A) and 8 (B) of Figure 3.20), however, the insertion of *shp144* promoter into cloning site of pPP2 increases the amplicon size to 384 bp as shown in lanes 1-7 (A) for Δ*shp144*ComL26A, Δ*shp144*ComN25A, Δ*shp144*ComT24A, Δ*shp144*ComL23A, Δ*shp144*ComF22A, Δ*shp144*ComP21A, Δ*shp144*ComI20A and lanes 1-6 (B) for Δ*shp144*ComV19A, Δ*shp144*ComI18A, Δ*shp144*ComV17A, Δ*shp144*ComW16A, Δ*shp144*ComE15A and Δ*shp144*ComS14A strains.

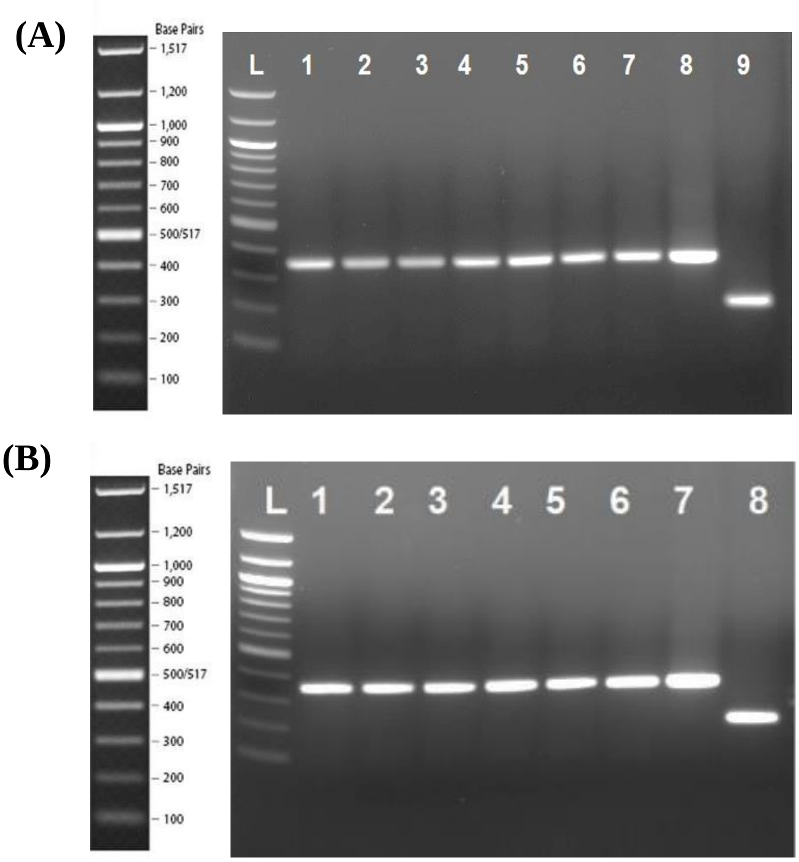

Figure 3.20: Gel electrophoresis analysis confirming the successful incorporation of P_{shp144}::*lacZ* fusion into chromosomal DNA of complemented modified *shp144* strains. Lane L ,100 bp DNA ladder (New England Biolabs, UK); Lanes 1-7 **(A)** and 1-6 **(B)** PCR amplicons with 384 bp in size amplified from the genomic DNA of Δ*shp144*ComL26A, Δ*shp144*ComN25A, Δ*shp144*ComT24A, Δ*shp144*ComL23A, Δ*shp144*ComF22A, Δ*shp144*ComP21A and Δ*shp144*ComI20A strains **(A)**; and from Δ*shp144*ComV19A, Δ*shp144*ComI18A, Δ*shp144*ComV17A, Δ*shp144*ComW16A, Δ*shp144*ComE15A and Δ*shp144*ComS14A **(B)** using Fusion-Seq-F and Fusion-Seq-R primers. Lanes 8 **(A)** and 7 **(B)** show the amplification of recombinant pPP2 plasmid (384 bp positive control) whereas

lanes 9 **(A)** and 8 **(B)** amplification of promoterless fragment of the empty pPP2 plasmid (200 bp negative control) using the same set of primers (Fusion-Seq-F and Fusion-Seq-R).

The reporter strains were designated as P_{shp144}::*lacZ*-Δ*shp144*ComL26A, P_{shp144}::*lacZ*-Δ*shp144*ComN25A, P_{shp144}::*lacZ*-Δ*shp144*ComT24A, P_{shp144}::*lacZ*-Δ*shp144*ComL23A, P_{shp144}::*lacZ*-Δ*shp144*ComF22A, P_{shp144}::*lacZ*-Δ*shp144*ComP21A, P_{shp144}::*lacZ*-Δ*shp144*ComI20A, P_{shp144}::*lacZ*-Δ*shp144*ComV19A, P_{shp144}::*lacZ*-Δ*shp144*ComI18A, P_{shp144}::*lacZ*-Δ*shp144*ComV17A, P_{shp144}::*lacZ*-Δ*shp144*ComW16A, P_{shp144}::*lacZ*-Δ*shp144*ComE15A and P_{shp144}::*lacZ*-Δ*shp144*ComS14A.

The resulting reporter constructs grown on mannose were used to study the effect of each replacement on *shp144* transcription using a promoter reporter assay. Of the 13 modified *shp144* reporter strains, five were completely unable to induce P_{shp144} driven *lacZ* activity, as their *lacZ* activity were 7.5 ± 2.5, 6 ± 1.0, 7.5 ± 1.5, 8.5 ± 0.5 and 7.5 ± 2.5 MU (n=3) respectively for P_{shp144}::*lacZ*-Δ*shp144*ComW16A, P_{shp144}::*lacZ*-Δ*shp144*ComV17A, P_{shp144}::*lacZ*-Δ*shp144*ComI18, P_{shp144}::*lacZ*-Δ*shp144*ComI20A and P_{shp144}::*lacZ*-Δ*shp144*ComP21A, respectively, which was similar to the reporter strain in mutant *shp144* background (11.935 ± 1.815 MU, n=3). On the other hand, seven mutations P_{shp144}::*lacZ*-Δ*shp144*ComS14A (105 ± 5 MU), P_{shp144}::*lacZ*-Δ*shp144*ComE15A (107.5 ± 2.5 MU) P_{shp144}::*lacZ*-Δ*shp144*ComF22A (90 ± 10 MU), P_{shp144}::*lacZ*-Δ*shp144*ComL23A (95 ± 5 MU), P_{shp144}::*lacZ*-Δ*shp144*ComT24A (175 ± 5 MU), P_{shp144}::*lacZ*-Δ*shp144*ComN25A (185 ± 5 MU) and P_{shp144}::*lacZ*-Δ*shp144*ComL26A (187.5 ± 2.5 MU) resulted in a significant reduction in β-galactosidase activity compared to the strain containing intact copy of *shp144* (215 ± 5 MU, n=3) (Figure 3.21A). In these seven strains, while the mutations reduced the activity significantly, these strains still retained around 50% or more of β galactosidase activity, showing their contributions in transcriptional activation of Rgg/SHP144 QS system. On the other hand, P_{shp144}::*lacZ*-Δ*shp144*ComV19A substitution did not have any impact on transcriptional activation of *shp144* (215 ± 5 MU, n=3) indicating that this residue is not essential for *shp144* transcription. A similar enzymatic trend was obtained when glucose was used instead of mannose as the carbon source in culture media, however the induction level was lower compared to that on mannose (Figure 3.21B).

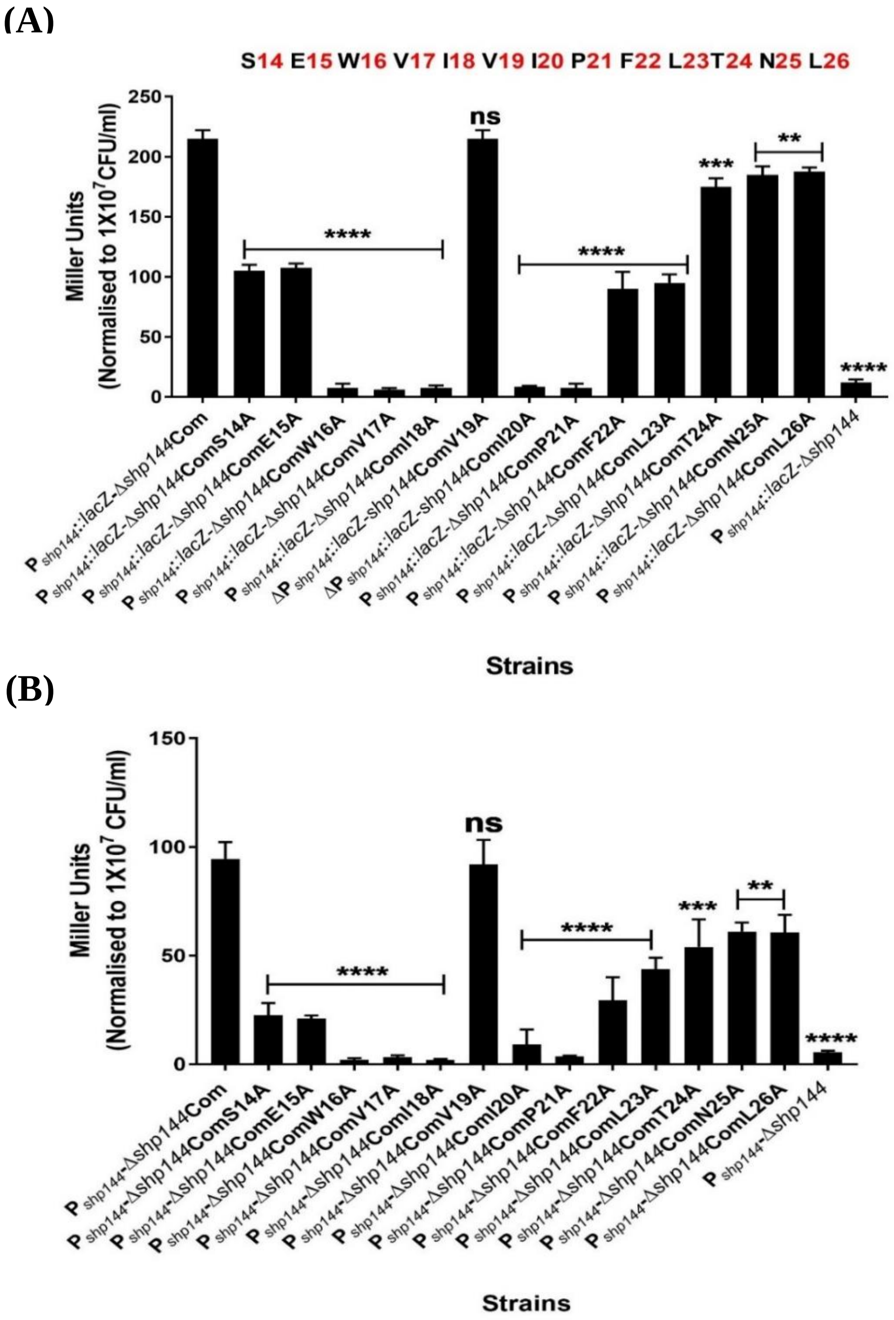

Figure 3.21: Assessing the effect of each SHP144-C13 residue on transcriptional activation of Rgg/SHP144 system by *lacZ* reporter assay. The reporter strains in *shp144* mutant background genetically complemented either with unmodified or modified *shp144* strains, and they were grown either in CDM supplemented with 55 mM mannose **(A)** or glucose **(B)** to late exponential phase. The P_{shp144} expression was assessed using β-galactosidase activity. Comparisons are made relative to P_{shp144}::*lacZ*-Δ*shp144*Com, which expresses wild type SHP144. **p<0.01, *** p<0.001, **** p<0.0001, 'ns' non-significant. Reporter strain in the mutant background was included as a control for assay. Error bars represent the standard error of the mean for each set. The values represent the average of three independent experiments, each with three replicates.

After detecting the importance of each residue in endogenous induction, the ability of supernatant containing the modified SHP in induction of *shp* expression was also determined. For this assay, the Δ*shp144*Com and *shp* modified strains were grown on mannose, where the system is induced, and the supernatants were collected at late exponential phase. The P_{shp144} expression was determined using the β-galactosidase assay in P_{shp144}::*lacZ*-Δ*shp144*. As shown in Figure 3.22A the induction levels by modified *shp144* supernatants were nearly identical to those obtained with endogenously modified *shp144* strains as shown before in Figure 3.21A, except those achieved with E15A or V19A modifications. The inability to induce the reporter strain was more likely due to the insufficient peptide production under assay conditions, or due to the lack of export of these peptides to extracellular milieu. However, exogenous addition of modified synthetic E15A and V19A peptides led to increase in the level of P_{shp144} driven β-galactosidase activity by over 25 and 18-folds compared to culture without peptide (Figure 3.22B). These findings strongly support the hypothesis that the modified *shp144* gene products are exported to extracellular milieu as native SHP144 peptide, and each residue plays a different role in activation.

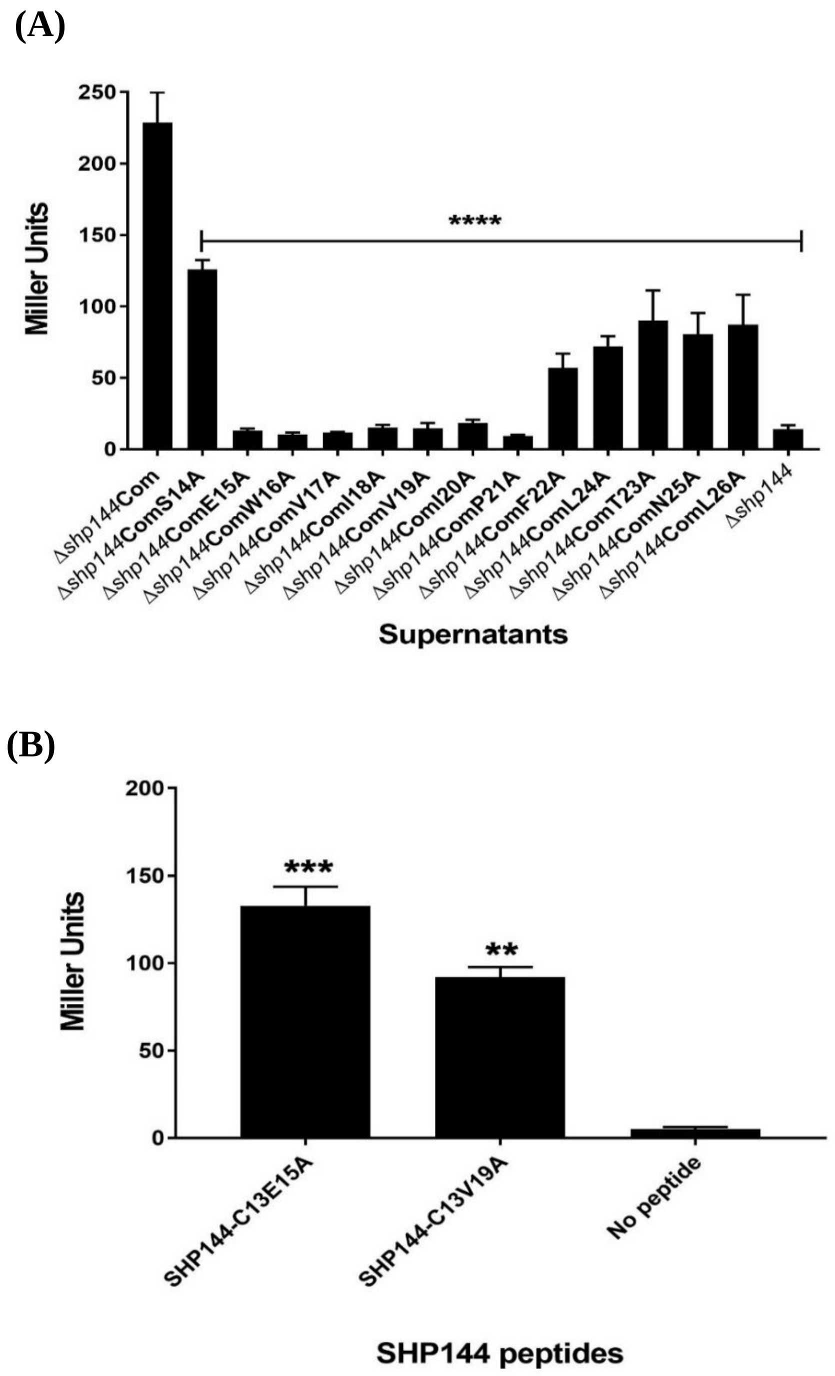

Figure 3.22: **(A)** β-galactosidase activity level of P$_{shp144}$::*lacZ*-Δ*shp144* reporter strain in the presence of late exponential culture supernatants collected from Δ*shp144*Com and modified *shp144* cultures on mannose. The pellet of P$_{shp144}$::*lacZ*-Δ*shp144* was incubated with collected supernatants to an early exponential phase and the expression was analysed using β-galactosidase assay. Comparisons are made relative to Δ*shp144*Com supernatant, which contains wild type SHP144. **(B)** Stimulation of P$_{shp144}$ expression by using 1000 nM of SHP144-C13V19A or SHP144-C13E15A peptide. The results were compared with reporter culture in the absence of peptide. Values are the average of three independent experiments, each with three replicates. The activity is expressed in nmol *p*-nitrophenol/min/ml. Error bars indicate the SEM (**p<0.01, *** p<0.001, **** p<0.0001).

Section C: Phenotypic characterisation of Rgg/SHP144 system

The Rgg/SHP quorum sensing systems play a significant role in physiological functions of many pathogenic streptococci (Fleuchot *et al*., 2011; Cook *et al*., 2013). They are involved in aggregations and biofilm formation in *Streptococcus pyogenes* (Aggarwal *et al*., 2014) and in pathogenicity of *S. agalactiae* (Pérez-Pascual *et al*., 2015). They are also implicated in the non-glucose carbohydrate metabolism and lysosome resistance of *S. pyogenes* (Chang *et al*., 2015). A recent study in our research group showed the importance of Rgg regulons in oxidative stress and carbohydrate utilisation in *S. pneumoniae* (Zhi *et al*., 2018). In this study, the involvement of Rgg/SHP144 in pneumococcal biology was defined in more detail by determining the effect of each amino acid residue of SHP144 on growth profile, resistance to oxidative stress (paraquat and H_2O_2), capsule synthesis and in *in vivo* survival of the microbe. The contribution of *rgg144* and *shp144* in pneumococcal growth was determined by growing the wild type D39 strain and its isogenic mutants in BHI or in media containing different sugars (glucose, mannose, galactose and *N*-acetylglucosamine). Mannose and galactose were used as they induce the system (Section 3.5). Any defect in pneumococcal growth on selected sugar would provide an indicator about the involvement of Rgg/SHP144 QS in metabolism of a particular sugar.

3.10. Haemolytic activity of pneumococcal strains

Pneumolysin is an important virulence determinant in *S. pneumoniae,* responsible for haemolytic activity and cytotoxic properties (Shak *et al*., 2013; Marshall *el al*., 2015). The impact of deletion of Rgg144 and SHP144 on haemolytic activity was tested in the cell lysates of wild type and its isogenic mutants using 4% sheep red blood cells as described in section 2.12. PBS instead of cell lysate was included as a negative control of assay. As indicated in Figure 3.23. The haemolytic activity of wild type was comparable with those found with the mutants (Δ*shp144* and Δ*rgg144*) and complemented strain Δ*shp144*Com, suggesting that the pneumococcal haemolytic activity was not affected by deletion of Rgg144 or SHP144.

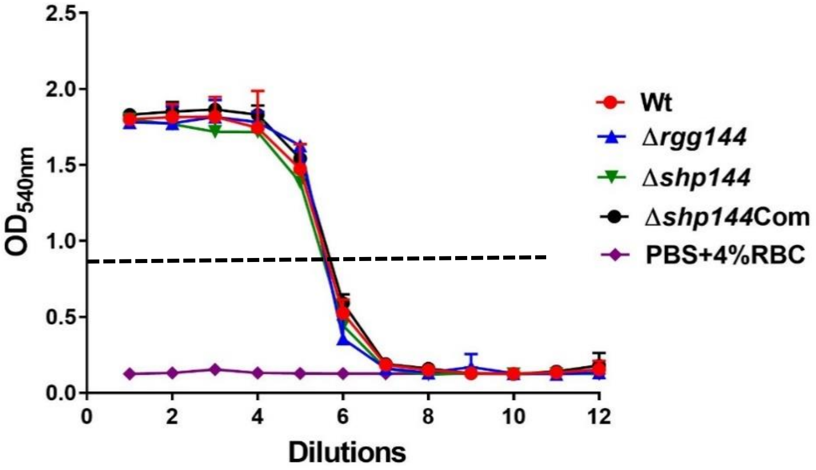

Figure 3.23: The haemolytic activity of the wild type and its isogenic mutants using 4% sheep RBC. No difference could be detected in haemolytic activity between pneumococcal cell lysates. The horizontal line represents the highest dilution of cell-free supernatant exhibits at least 50% of RBC lysis. This experiment was repeated using three independent cell lysates. Error bars indicate standard error of the mean (SEM).

3.11. Detection of neuraminidase activity in pneumococcal strains

S. pneumoniae produces three types of neuraminidase (NanA, NanB and NanC). These enzymes are involved in deglycosylation of complex carbohydrates such as mucin releasing utilizable growth substrates, which can be a source of nutrient during colonisation and invasion of host tissues (Yesilkaya *et al*., 2008; Brittan *et al*., 2012). To test the impact of Rgg/SHP144 system on neuraminidase activity, the mutants (Δ*rgg144* and Δ*shp144*), complemented *shp144* and parental wild type strains were assayed using the chromogenic substrate pNP-NANA as described previously in Materials and Methods (Section 2.13). As can be seen from Figure 3.24 there was no significant change in neuraminidase activity between the wild type, complemented and mutant strains ($p>0.05$). The level of neuraminidase activity was 60.18 ± 1.35, 60.19 ± 1.86, 59.66 ± 1.59 and 60.1 ± 1.84 for wild type, Δ*shp144*Com, Δ*rgg144* and Δ*shp144* respectively. These data suggest that the Rgg/SHP144 QS system does not involve in regulation of the genes responsible for neuraminidase activity.

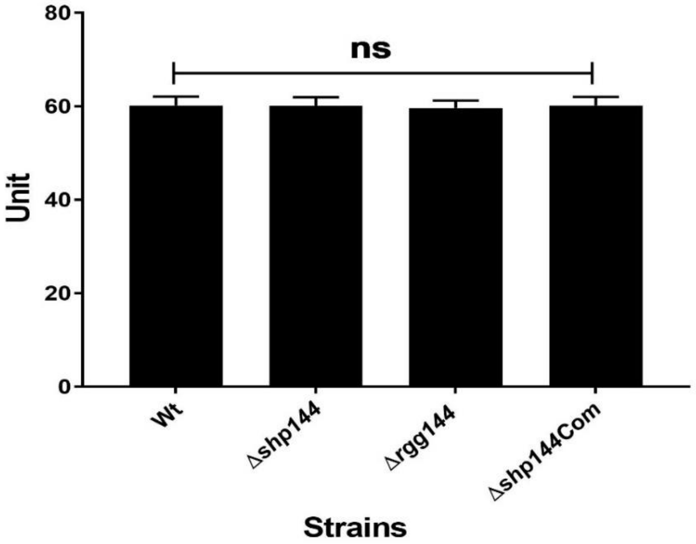

Figure 3.24: Neuraminidase activity of pneumococcal strains using chromogenic substrate pNP-NANA. The enzymatic activity was expressed as nmol *p*-nitrophenol/min/µg total cell protein. Values represent the average of three independent experiments each with triplicates. Error bars refer to standard error of the mean (SEM). 'ns' not significant compared with wild type.

3.12. Growth of pneumococcal strains in BHI

Results in Figure 3.25 show that all pneumococcal strains exhibited a similar growth pattern and rates in BHI under microaerobic conditions ($p>0.05$). The growth features (growth rate and yield) were determined for each strain and provided in Table 3.1. The growth rates (µ) ranged between 0.257 to 0.268 h^{-1} and pneumococcal yield (maximal OD_{600}) was between 1.251 to 1.261. These data suggest that mutation of *rgg144* and *shp144* can be tolerated in rich liquid media.

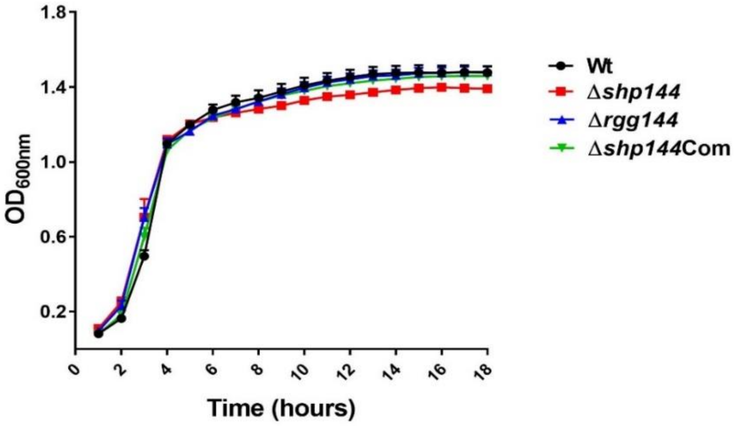

Figure 3.25: Growth profiles of wild type D39 and its isogenic mutants in BHI broth. Error bars refer to the standard error of the mean for three individual measurements each with three replicates.

Table 3.1: Calculation of growth rate (µ) and yield (maximal OD_{600}) of pneumococcal strains grown microaerobically in rich media (BHI) at 37°C. Values are average of three independent experiments each with three replicates. '±' indicates standard error of means (SEM). No significant differences could be seen when the growth rates and yields of mutants were compared with the wild type D39 using one-way ANOVA and Dunnett's multiple comparisons test.

Strains	**BHI**	
	Growth rate (h^{-1})	**Growth yield**
Wt	0.268 ± 0.010	1.261 ± 0.022
Δ*rgg144*	0.264 ± 0.005	1.254 ± 0.026
Δ*shp144*	0.257 ± 0.011	1.253 ± 0.025
Δ*shp144*Com	0.266 ± 0.011	1.251 ± 0.040

3.13. Growth profile of pneumococcal strains in CDM supplied with different sugars

It was hypothesised that each amino acid residue of SHP144 would have a different role in carbohydrate utilisation. To investigate this hypothesis, initially, the effect of deletion of the *rgg144* and *shp144* on growth behaviour was tested in CDM containing 55 mM of selected sugar (glucose, mannose, *N*-acetylglucosamine and galactose), and the growth rates and yields were calculated following the procedure previously described in section 2.14. These sugars were selected as they are the predominant carbohydrates present either in the structure of mucins in the respiratory tract or in circulatory glycoproteins. The results showed that wild type and its isogenic mutants had identical growth profiles in media containing glucose, galactose or *N*-acetylglucosamine ($p>0.05$) [Figure 3.26 (A-C) and Tables (3.2 and 3.3)]. It seems that the deletion of *rgg144* and *shp144* genes did not affect the pneumococcal growth properties on glucose, galactose and *N*-acetylglucosamine under growth conditions.

Consistent with previously reported data (Zhi *et al.*, 2018), deletion of *rgg144* and *shp144* caused a substantial decrease in the pneumococcal growth rate and maximal OD_{600} compared with parental wild type strain in CDM supplemented with mannose (Table 3.3). The mutant strain *rgg144* had the lowest growth rate (0.017 ± 0.0007 h^{-1}), followed by Δ*shp144* (0.019 ± 0.0007 h^{-1}) relative to wild type growth rate (0.025 ± 0.0006 h^{-1}, n=3) ($p<0.0001$ and $p<0.001$, respectively). Similarly, the Δ*rgg144* and Δ*shp144* mutants showed a significant reduction in growth yield (0.195 ± 0.004 and 0.205 ± 0.006, n=3, respectively) compared with wild type (0.241 ± 0.003) ($p<0.0001$) (Figure 3.26D and Table 3.3). These results indicate that *rgg144* and *shp144* contribute in mannose metabolism, and their presence support pneumococcal growth on mannose. On the other hand, this defect in pneumococcal growth rates and yields were fully restored by complementation of mutants with an intact copy of the respective gene (*shp144* and *rgg144*) as represented in Figure 3.26D and Table 3.3. As their growth rates were (0.023 ± 0.0015 h^{-1} and 0.024 ± 0.0009 h^{-1}, respectively) and yields were (0.240 ± 0.007 and 0.237 ± 0.005, respectively) similar to that of the wild type strain demonstrating that the observed phenotypes in the mutants were not due to polar effect of insertion mutations.

(A)

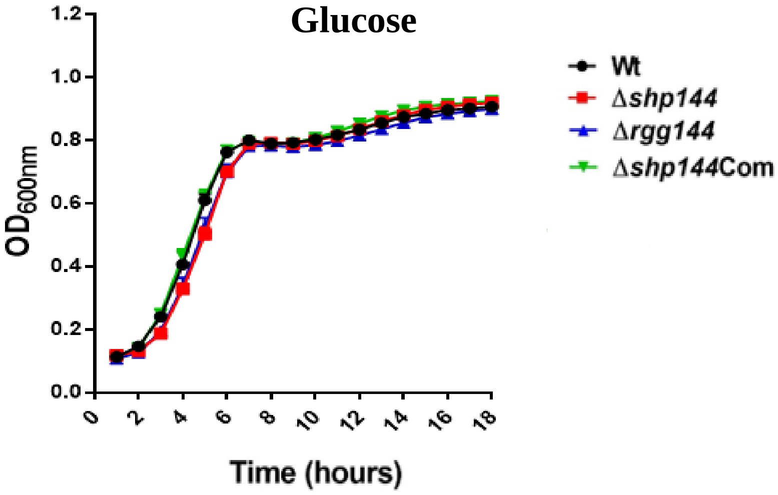

(B)

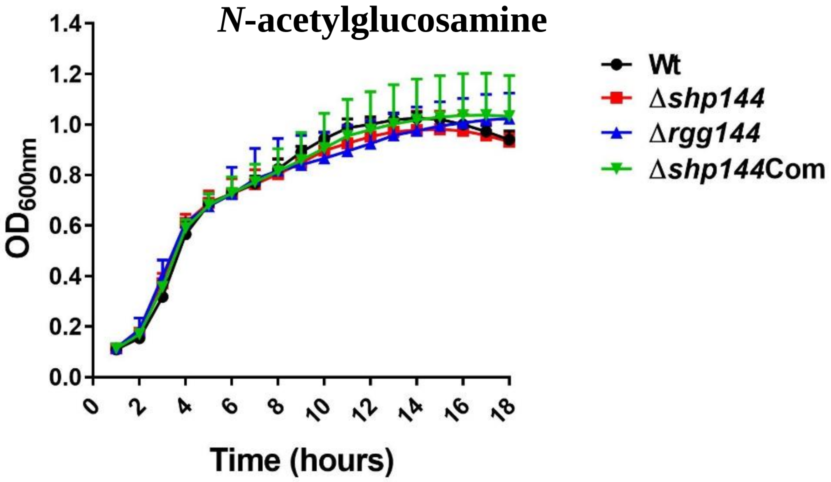

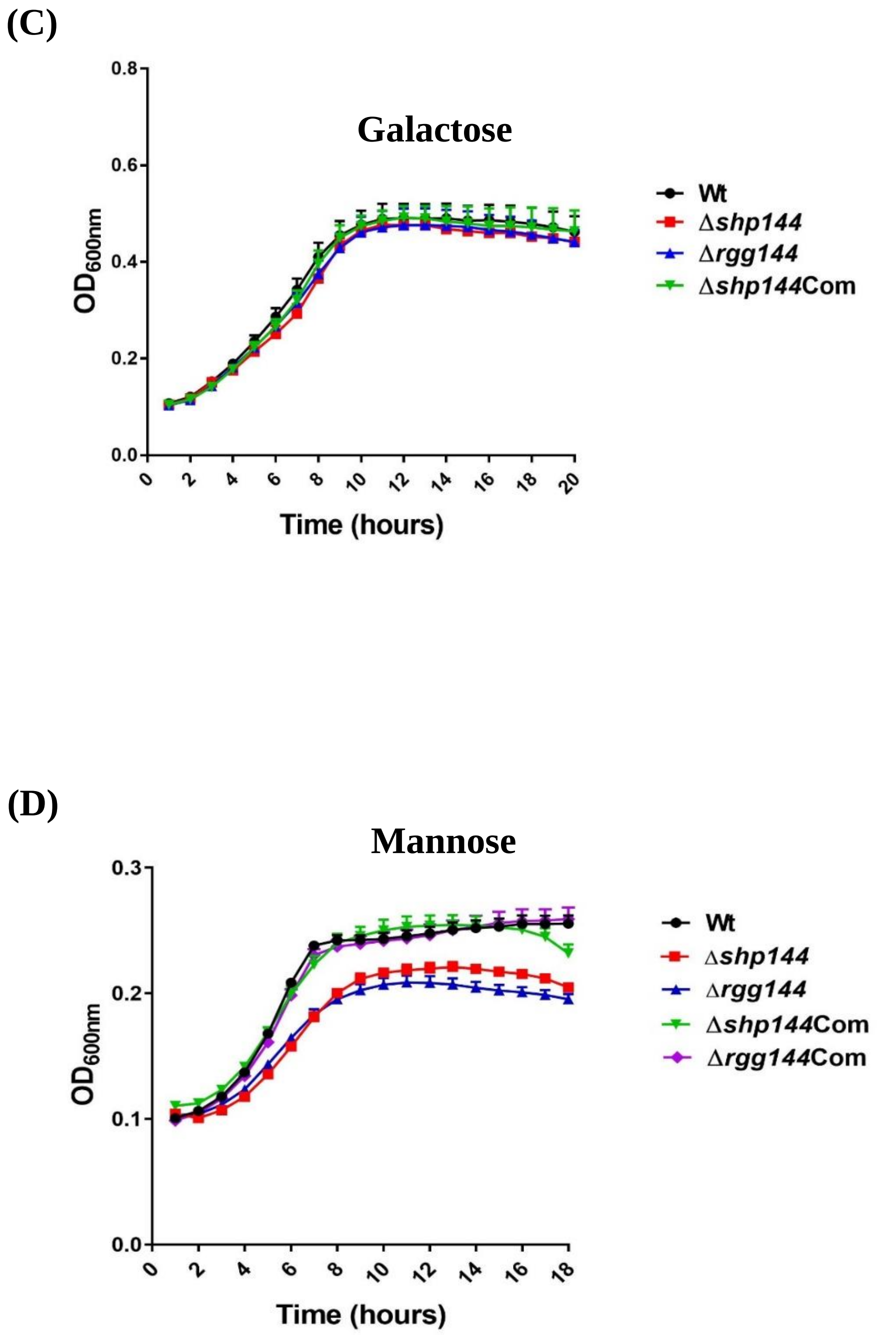

Figure 3.26: Pneumococcal growth performed microaerobically in CDM supplemented with 55 mM glucose **(A)**, *N*-acetylglucosamine **(B)**, galactose **(C)** and mannose **(D)**. The *rgg144* and *shp144* deficient mutants showed significant growth impairment in media supplemented with mannose. The growth measurements were carried out at a wavelength of 600 nm for 18 h at 37°C. This experiment was done in triplicate and repeated at least for three times.

Table 3.2: Growth rate (µ) and yield (maximal OD_{600}) of pneumococcal strains grown microaerobically in CDM containing 55 mM of glucose or *N*-acetylglucosamine. Values are average of three independent experiments each with three replicates. '±' indicates standard error of means (SEM). One-way ANOVA and Dunnett's multiple comparisons test were used for calculation of growth parameters.

Strains	**CDM-glucose**		**CDM-*N*-acetylglucosamine**	
	Growth rate (h^{-1})	**Growth yield**	**Growth rate (h^{-1})**	**Growth yield**
Wt	0.131 ± 0.002	0.799 ± 0.010	0.144 ± 0.004	0.729 ± 0.023
Δ*rgg144*	0.131 ± 0.002	0.781 ± 0.014	0.134 ± 0.015	0.724 ± 0.106
Δ*shp144*	0.132 ± 0.002	0.789 ± 0.008	0.138 ± 0.019	0.726 ± 0.059
Δ*shp144*Com	0.131 ± 0.001	0.794 ± 0.0007	0.140 ± 0.014	0.729 ± 0.064

Table 3.3: Growth rate (µ) and yield of mutants and parental wild type strains grown microaerobically in CDM containing 55 mM of galactose or mannose. The growth rates and yields were calculated and expressed as average ± standard error of means (SEM). Values are average of three independent experiments each with three replicates. One-way ANOVA and Dunnett's multiple comparisons tests were used for calculation of growth parameters. ***p<0.001, ****p<0.0001 compared with wild type.

Strains	**CDM-galactose**		**CDM-mannose**	
	Growth rate (h^{-1})	**Growth Yield**	**Growth rate (h^{-1})**	**Growth yield**
Wt	0.048 ± 0.003	0.477 ± 0.029	0.025 ± 0.0006	0.241 ± 0.003
Δ*rgg144*	0.045 ± 0.004	0.461 ± 0.033	**0.017 ± 0.0007******	**0.195 ± 0.004******
Δ*shp144*	0.045 ± 0.001	0.465 ± 0.009	**0.019 ± 0.0007*****	**0.205 ± 0.006******
Δ*shp144*Com	0.048 ± 0.002	0.474 ± 0.022	0.023 ± 0.0015	0.240 ± 0.007
Δ*rgg144*Com	-	-	0.024 ± 0.0009	0.237 ± 0.005

These observations led to investigate the amino acid residues in active SHP144 that are involved in mannose utilisation. A set of modified strains were grown in CDM supplemented with 55 mM mannose, and their effects on pneumococcal growth kinetics were determined. As indicated in Figure 3.27A and Table 3.4, modified strains with alanine substitution at positions P21, I18 and I20 had lower growth yields compared with strain containing native peptide ($p<0.05$, $p<0.01$, $p<0.001$), since their growth yields were (0.267 ± 0.017, 0.235 ± 0.015, 0.210 ± 0.016 for Δ*shp144*Com21A, Δ*shp144*ComI18A and Δ*shp144*ComI20A respectively) lower than the strain with a wild type copy of *shp* (0.358 ± 0.025).

Strain with I18 modification exhibited statistically significant reduction in growth rate (0.020 ± 0.001 h^{-1}) compared with strain complemented with intact copy of *shp144* (0.031 ± 0.003 h^{-1}) ($p<0.001$), whereas the other modified strains did not show any difference in terms of growth rate and yield ($p>0.05$). No obvious difference in the growth parameters between the strains complemented with intact or modified copy of *shp144* could be seen when glucose was used as a primary carbon source (Figure 3.27B). These observations suggest the involvement of these residues in SHP144 function as their modifications remarkably affect the SHP144 activity to utilise mannose, which are in accordance with transcriptional activation results of modified *shp144* strains.

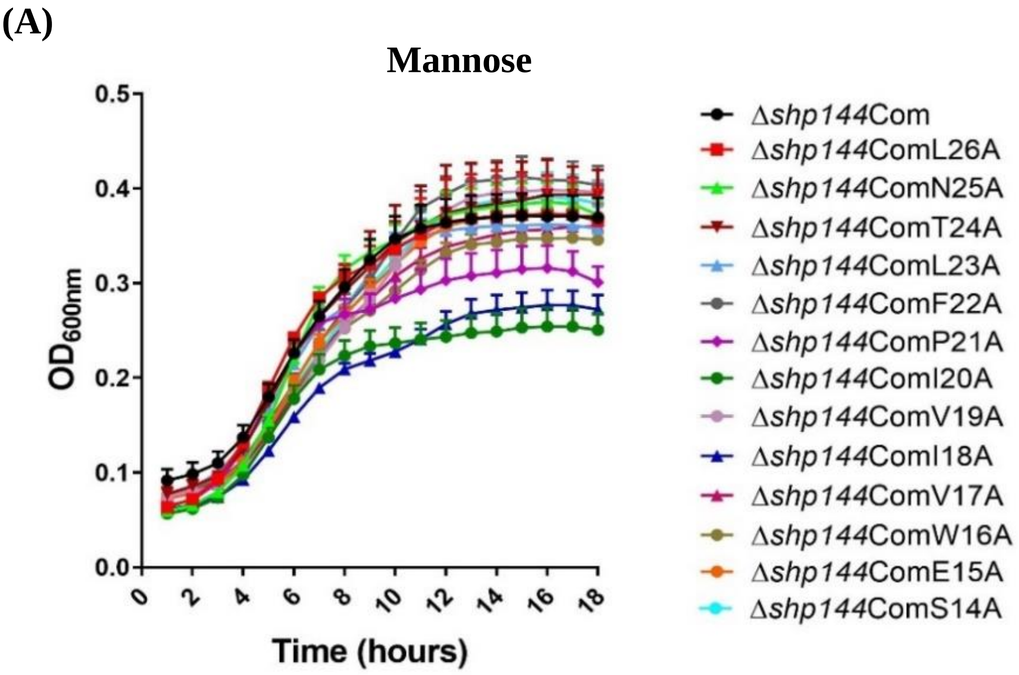

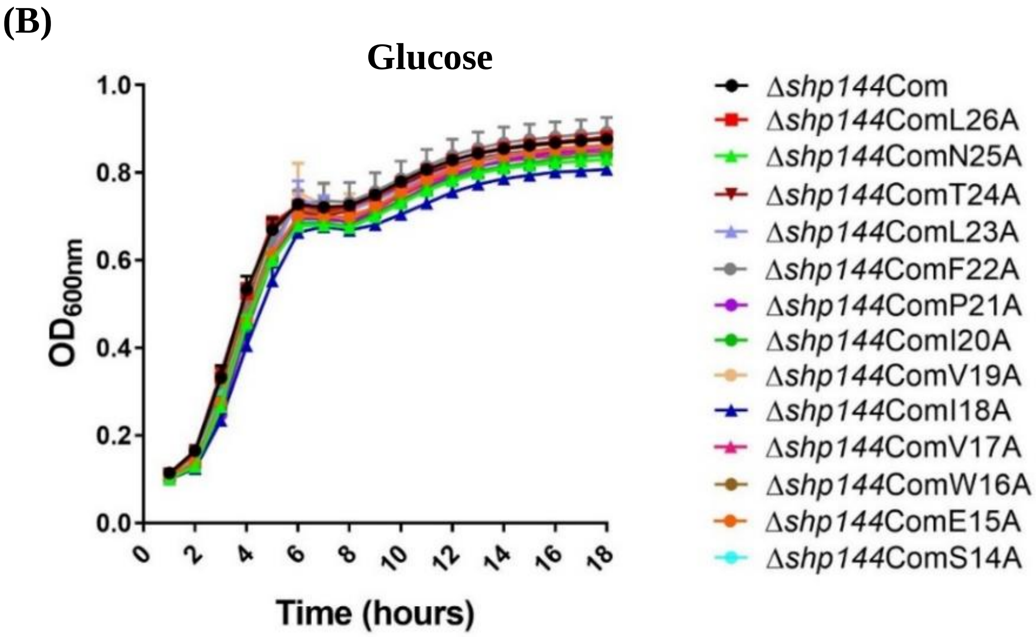

Figure 3.27: Growth profiles of modified *shp144* strains grown in the presence of 55 mM of mannose **(A)** or glucose **(B)**. The growth measurements were recorded at 600 nm at 37°C. These experiments were done in triplicate and repeated for at least three times.

Table 3.4: Growth rates (μ) and yields of modified *shp144* strains grown in CDM supplemented with 55 mM mannose. Values are average of three independent experiments each with three replicates. '±' indicates standard error of means (SEM). Comparisons were made relative to complemented *shp144* strain using one-way ANOVA and Dunnett's multiple comparisons test. *p<0.05, **p<0.01 and ***p<0.001.

Strains	**CDM-mannose**	
	Growth rate (h^{-1})	**Growth yield**
Δ*shp144*Com	0.031 ± 0.003	0.358 ± 0.025
Δ*shp144*ComL26A	0.032 ± 0.005	0.352 ± 0.038
Δ*shp144*ComN25A	0.035 ± 0.002	0.362 ± 0.020
Δ*shp144*ComT24A	0.033 ± 0.005	0.360 ± 0.043
Δ*shp144*ComL23A	0.031 ± 0.002	0.351 ± 0.018
Δ*shp144*ComF22A	0.036 ± 0.002	0.379 ± 0.018
Δ*shp144*ComP21A	0.036 ± 0.003	**0.267 ± 0.017***
Δ*shp144*ComI20A	0.030 ± 0.003	**0.210 ± 0.016*****
Δ*shp144*ComV19A	0.033 ± 0.001	0.352 ± 0.014
Δ*shp144*ComI18A	**0.020 ± 0.001*****	**0.235 ± 0.015****
Δ*shp144*ComV17A	0.029 ± 0.002	0.326 ± 0.012
Δ*shp144*ComW16A	0.028 ± 0.001	0.314 ± 0.010
Δ*shp144*ComE15A	0.032 ± 0.001	0.344 ± 0.010
Δ*shp144*ComS14A	0.033 ± 0.003	0.352 ± 0.023

3.14. Inactivation Rgg/SHP144 inhibits pneumococcal resistance against paraquat

To investigate whether introducing a modification into SHP144 sequence would have an impact on pneumococcal resistance against superoxide-generating agent paraquat, the effect of the deletion of Rgg144 and SHP144 on pneumococcal oxidative stress resistance was initially examined. Pneumococcal strains (wild type, Δ*rgg144*, Δ*shp144* and complemented strains Δ*rgg144*Com and Δ*shp144*Com) grown in THY to exponential phase were exposed to 1 mM paraquat for one hour at 37°C. Survival percentages were determined by serial dilution on blood agar plates and compared with culture that had not been treated with paraquat. As shown in Figure 3.28A, deletion of Rgg144 or SHP144 significantly attenuated the pneumococcal capability to deal with toxic effects of paraquat. In comparison with wild type (91%), the survival percentage decreased to 52% and 65% in cultures lacking *rgg144* or *shp144*, respectively ($p<0.01$). However, no difference in survival was observed between the complemented strain and the wild-type D39 ($p>0.05$) (Figure 3.28A) .

Having demonstrated the involvement of both Rgg144 and SHP144 in the superoxide resistance, it was imperative to identify the amino acids residues of SHP144 that would involve in oxidative stress response. A collection of modified *shp144* strains were screened for the superoxide resistance by challenging the pneumococci with 1 mM paraquat. The results showed that the complemented strains carrying mutations (E15, I20 and P21) render pneumococci more susceptible to paraquat (Figure 3.28B). The survival rates of mutants were 52.5%, 53% and 52.5%, respectively, significantly lower than that producing an intact SHP144 (87.5%) ($p<0.05$). On the other hand, the remaining modified strains were as resistant to superoxide as the wild type. Taken together, these results suggest the involvement of Rgg144 and SHP144 in protection against paraquat, and more interestingly, some of SHP144 mutant strains with alanine replacement showed a similar phenotypic impact as *shp144* deficient strain.

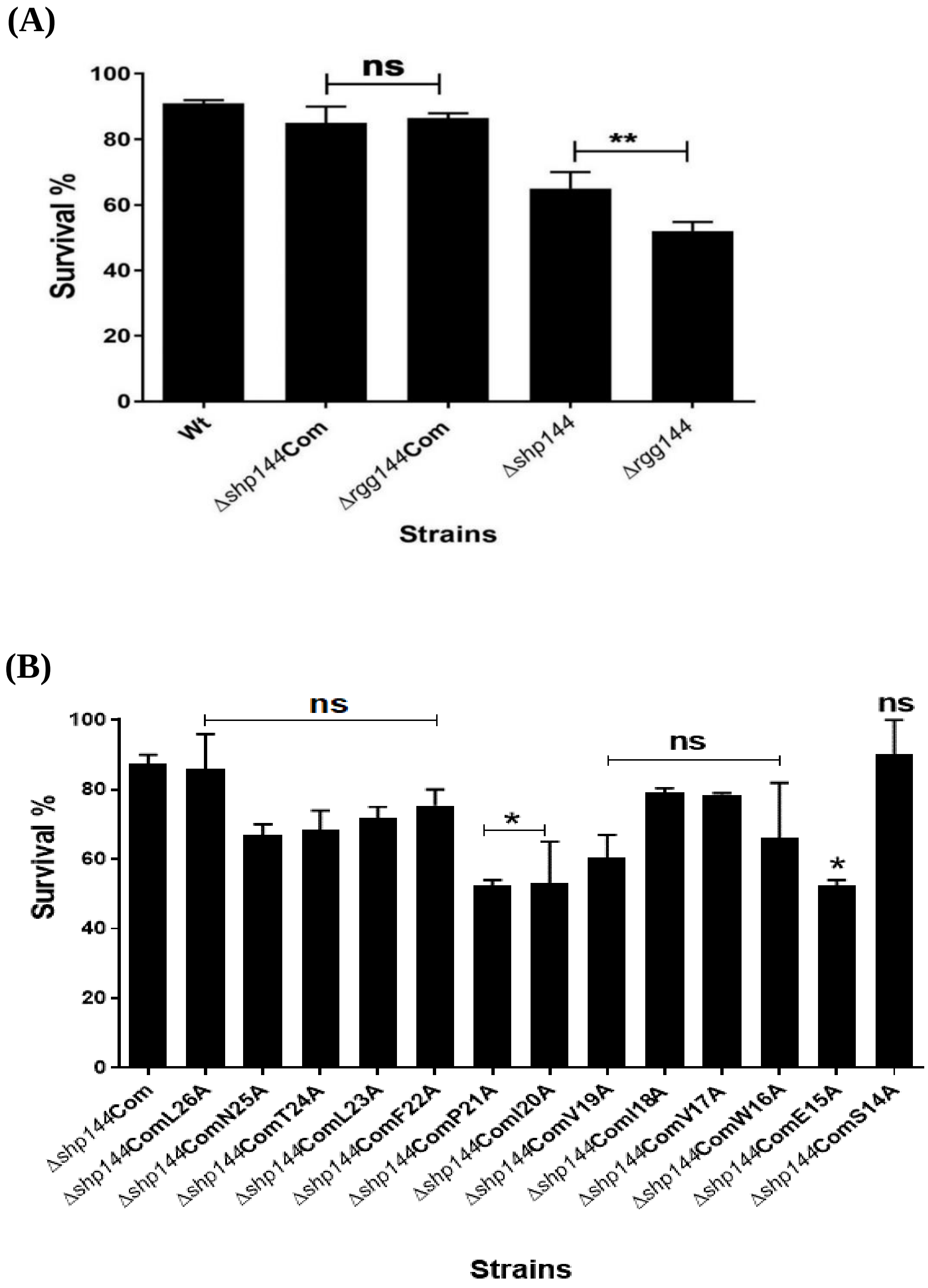

Figure 3.28: Survival percentages of pneumococcal strains after treatment with 1 mM paraquat. The survival percentages were calculated for each strain [wild type, mutants, genetically complemented strains **(A)**, and modified *shp144* strains **(B)**], and were compared with wild type or genetically complemented strain Δ*shp144*Com. Data represent the average of three independent experiments, each with triplicates (*p<0.05, ** p<0.01, 'ns' non-significant).

3.15. Rgg/SHP144 affords protection against H_2O_2

S. pneumoniae encounters large amount of H_2O_2, produced mainly by the activity of the pyruvate oxidase under aerobic conditions, and from host metabolism and immune response. The pneumococci can deal with high levels of H_2O_2 that would normally cause damage to various components such as DNA and proteins causing mutagenesis or death of bacterial cell (Andisi *et al*., 2012; Yesilkaya *et al*., 2013). The Rgg family is involved in oxidative stress resistance, for example, in *S. pyogenes*, disruption of *rgg144* increased susceptibility of bacteria to killing by paraquat (Chaussee *et al*., 2004). Moreover, loss of *rgg1952* gene renders the pneumococci more sensitive to oxidative stress (Bortoni *et al*., 2009).

The results found that the challenge of mutants (Δr*gg144* and Δ*shp144*) with 20 mM H_2O_2 resulted in remarkably decreased survival (53.5% and 64%, respectively) compared with wild type D39 ($p<0.01$) (Figure 3.29A) supporting my hypothesis that Rgg/SHP144 QS plays a crucial role against H_2O_2. In addition, the complemented strains had similar phenotypes as the wild type D39 ($p>0.05$) excluding the possibility of polar effects originated from mutations. On the other hand, challenging the mutants with 10 mM H_2O_2 does not cause changes in pneumococcal survival ($p>0.05$).

To gain insight into the involvement of selected SHP144 residues in H_2O_2 scavenging, modified *shp144* strains in which amino acid residues were replaced with alanine were treated with 20 mM of exogenous H_2O_2. After 20 min incubation, the survival percentages were determined in the H_2O_2 treated cultures and compared with unchallenged pneumococci. As shown in Figure 3.29B the mutants carrying modification at positions I20 and P21 were more susceptible to H_2O_2 (52.5% and 55%, respectively) compared with that carrying an intact copy of SHP144 ($p<0.05$), while no difference could be observed with other SHP144 mutants ($p>0.05$). This means that these residues play a significant role in SHP144 function, as their replacements with alanine led to a significant reduction in pneumococcal resistance against oxidative stress.

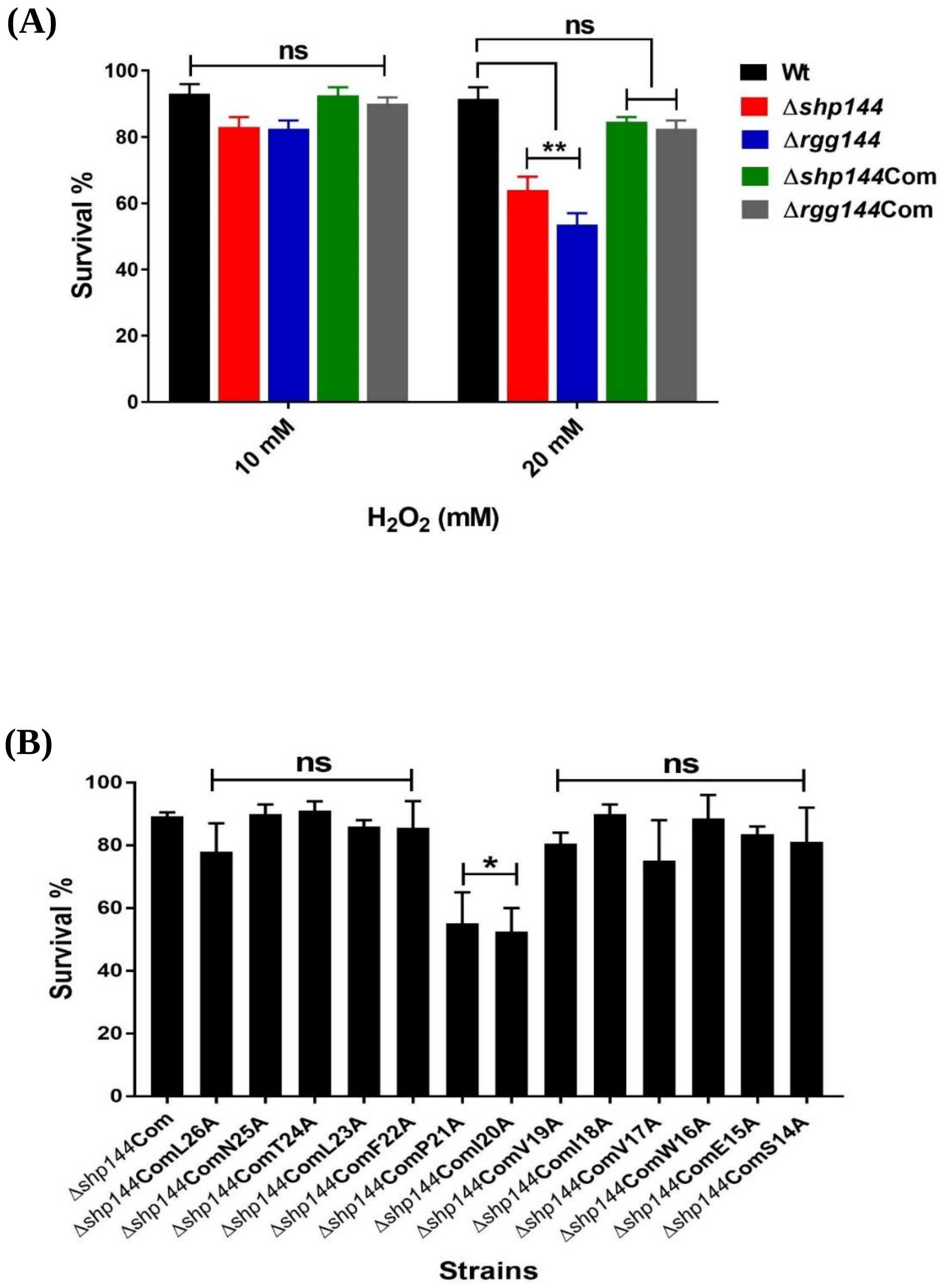

Figure 3.29: The susceptibility of pneumococcal strains to 20 mM H_2O_2. The survival percentages for wild type and its respective mutants **(A)**, and for modified *shp144* strains **(B)** were determined by colony counting and compared with cultures that were not treated with H_2O_2. Error bars indicate the SEM. *p<0.05, **p<0.01 and 'ns' not significant compared with wild type and complemented *shp144* strains.

3.16. Determination the effect of Rgg/SHP144 system on capsule biosynthesis

Capsular polysaccharide (CPS) is the major pathogenicity factor of *S. pneumoniae*. It plays a critical role in pneumococcal adhesion, biofilm formation, resistance to host immune response and survival in different host environment (Qin *et al*., 2013; de Vos *et al*., 2015). To elucidate the influence of Rgg/SHP144 QS system in capsule synthesis, the capsular polysaccharide was extracted from pneumococcal strains grown in CDM mannose or glucose to late exponential phase and followed by quantification of glucuronic acid (the main component of *S. pneumoniae* serotype 2 type capsule) using phenol-sulfuric acid extraction method as described in Materials and Methods (Section 2.27). The glucuronic acid quantification results were normalised to $1x10^7$ CFU/ml. From Figure 3.30A, a significant increase of glucuronic acid content was observed in *rgg144* and *shp144* deficient cultures on mannose (32.95 ± 3.95 and 26 ± 1.0 µg per $1x10^7$ CFU/ml, n=3 respectively) compared with wild type (12.9 ± 1.2 µg per $1x10^7$ CFU/ml, n=3) ($p<0.05$ and $p<0.01$). However, no significant difference in capsule production was seen between the wild type and complemented strains ($p>0.05$). As the amount of glucuronic acid were 13.5 ± 0.5 and 14.8 ± 1.2 µg per $1x10^7$ CFU/ml (n=3) for Δ*rgg144*Com and Δ*shp144*Com, respectively.

As expected, all pneumococcal strains produced the same amount of glucuronic acid in the presence of glucose ($p>0.05$) (Figure 3.30B). This demonstrates that Rgg/SHP144 QS downregulates the genes putatively involved in capsular polysaccharide biosynthesis.

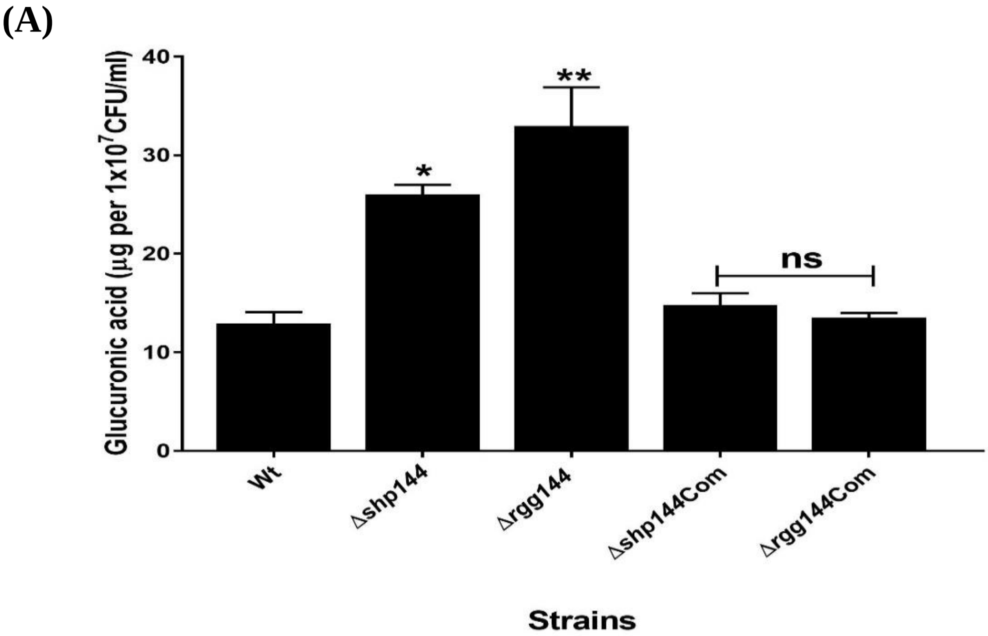

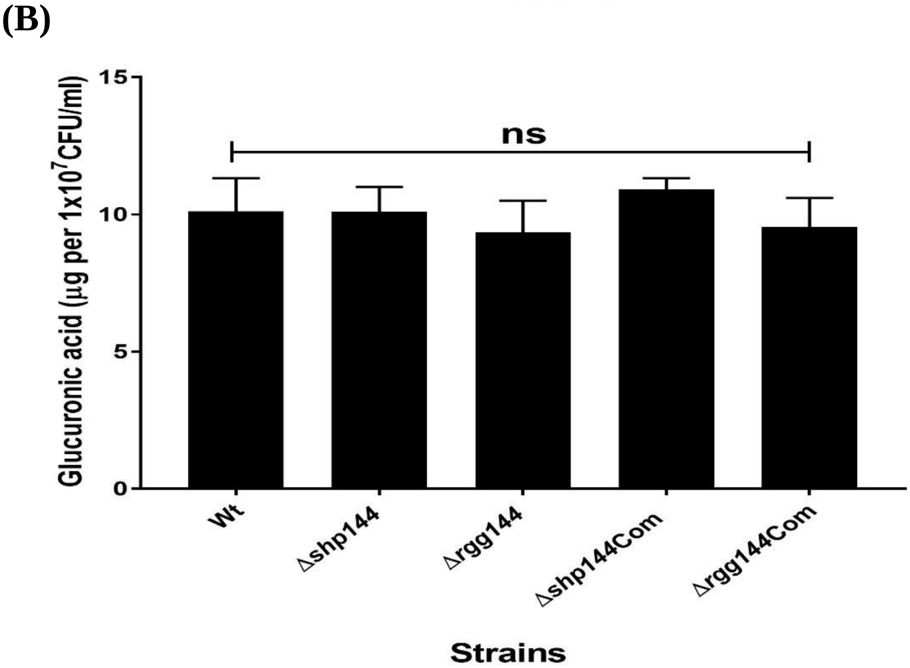

Figure 3.30: Amount of glucuronic acid produced in pneumococcal strains grown on 55 mM mannose **(A)** or glucose **(B)**. The pneumococcal capsule was extracted from cultures grown to late exponential phase and glucuronic acid was extracted from each strain using phenol-sulfuric acid method. Values represent the average of three independent experiments each with triplicates. Error bars are the standard error of the mean (SEM). *$p<0.05$, **$p<0.01$ ‘ns’ not significant compared with wild type.

Having found the involvement of Rgg/SHP144 in capsule synthesis, the influence of non-activating modified SHP144 peptides on capsule production was also tested. Capsular polysaccharide was extracted from modified strains (Δ*shp144*ComW16A, Δ*shp144*ComV17A, Δ*shp144*ComI18A, Δ*shp144*ComI20A and Δ*shp144*ComP21A) by using the same method mentioned above. Glucuronic acid was detected in the isolated capsule and compared with that of mutant *shp144* strain. All modified *shp144* cells form similar levels of capsule as mutant *shp144* on mannose ($p>0.05$). The amount of glucuronic acid for Δ*shp144*ComW16A, Δ*shp144*ComV17A, Δ*shp144*ComI18A, Δ*shp144*ComI20A and Δ*shp144*ComP21A (32.6 ± 5.9, 31.2 ± 4.6, 29.6 ± 5.5, 28.1 ± 6.7 and 30.1 ± 3.5 µg per $1x10^7$ CFU/ml, n=3, respectively) was similar to Δ*shp144* (26.7 ± 1.5 µg per $1x10^7$ CFU/ml, n=3) (Figure 3.31). These data indicate that selected modified *shp144* strains behave as mutant strain in terms of regulation of capsule biosynthesis.

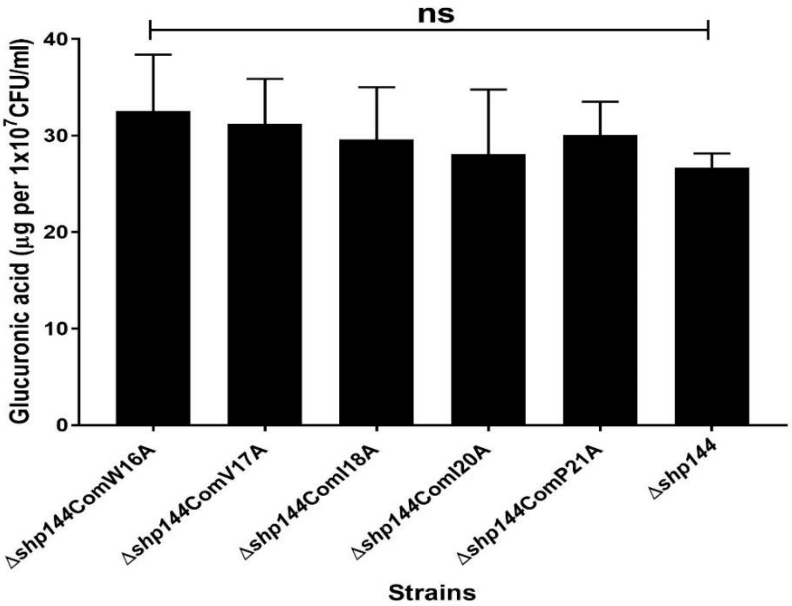

Figure 3.31: Measurement of the amount of glucuronic acid isolated from modified *shp144* strains on mannose. The capsule was extracted from cultures grown to late exponential phase and glucuronic acid was detected using phenol-sulfuric acid method. Values represent the average of three independent experiments each with triplicates. Error bars represent the standard error of the mean (SEM). 'ns' not significant compared with mutant *shp144* strain.

3.17. Inactivation of Rgg/SHP144 QS inhibits biofilm formation

Biofilm development is a complex process that is commonly regulated by quorum sensing system (Karatan and Watnick, 2009). The involvement of Rgg/SHP signalling pathway in biofilm formation was reported in group A streptococci (Chang *et al.*, 2011; Aggarwal *et al.*, 2014). To test whether Rgg/SHP144 played the same role in biofilm formation, the biofilm forming in wild type D39 and deletion mutants (*shp144* and *rgg144*) was quantified. As indicated in Figure 3.32, wild type D39 formed significantly more biofilm forming cell

($\log_{10}$ 5.65 ± 0.35 CFU/ml, n=3) than that of mutants ($\log_{10}$ 4.15 ± 0.35 and 4.10 ± 0.1 CFU/ml, n=3 for Δ*rgg144* and Δ*shp144*, respectively) ($p<0.05$). However, wild type and complemented *shp144* strains showed similar capability to produce biofilm ($p>0.05$).

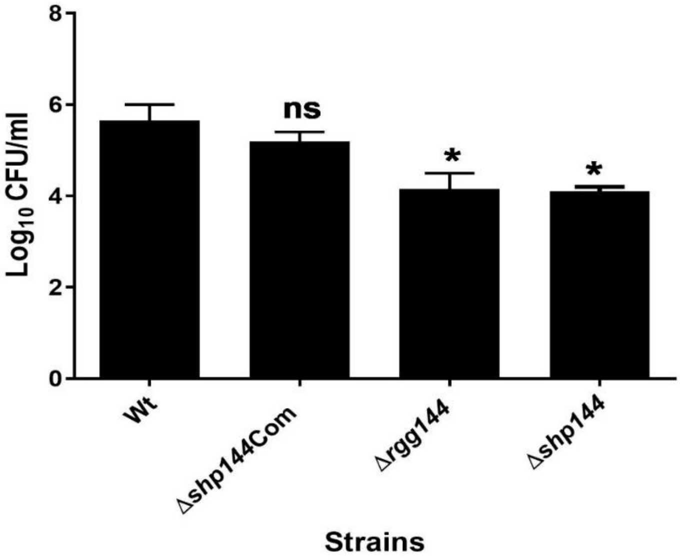

Figure 3.32: Biofilm formation of wild type and its isogenic mutants grown in 12 well polystyrene plate for 24 h at 37°C. After incubation, the biofilm cells were assessed by counting the number of viable cells on blood agar plates. Error bars indicate standard errors of three independent experiments. *P<0.05,'ns' not significant compared with wild type.

Section D: Purification of Rgg144 proteins and binding analysis

3.18. Overexpression and purification of Rgg144 recombinant proteins

In this study, Rgg144 and SHP144 pair have shown their involvement in regulation of *shp144* transcription, and 13-aa long synthetic peptide is sufficient to induce Rgg/SHP144 system. Further, each amino acid residue of SHP144 has a distinct role in transcription of its own gene expression. Therefore, it is noteworthy to characterise the direct binding between SHP144-C13 and its cognate Rgg144 and quantify the contribution of each amino acid residue of SHP144 towards Rgg144 binding using fluorescence spectrophotometer. To perform all these assays, the protein encoded by SPD_0144 was cloned, expressed and purified following Vallejo and Rina's protocol (2004). The purified protein was also used for crystallisation of Rgg144 with its cognate peptide SHP144 using sitting-drop vapour diffusion method (Dessau and Modis, 2011).

3.18.1. Amplification and cloning of *rgg144* gene into pLEICS-01

Full length and truncated Rgg144 proteins were utilised to investigate the interaction between Rgg144 and its cognate SHP144. The Rgg144 is much larger than its ligand therefore it was envisaged that deletion of some amino acid residues from the N-terminus region of Rgg144 will increase the binding efficiency as the Rgg binding site for SHP has been reported to be localised at the C-terminus of the protein (Parashar *et al.*, 2015). Therefore, *rgg144* (SPD_0144) variants, full length and truncated *rgg144* lacking 216 bp, were amplified using PrimeSTAR HS premix and the gene specific primers listed in Table 2.13. This enzyme was used to reduce the possibility of introducing unwanted mutations as this enzyme has a proof-reading feature. The PCR amplicons were separated by agarose gel electrophoresis analysis. The results showed the successful amplification of target genes by obtaining the bands of expected sizes (about 864 bp for full length and 648 bp for truncated Rgg144) as shown in Figure 3.33 A-B. The PCR products were then purified from the agarose gel using Wizard® SV Gel and PCR Clean-Up System (Section 2.7).

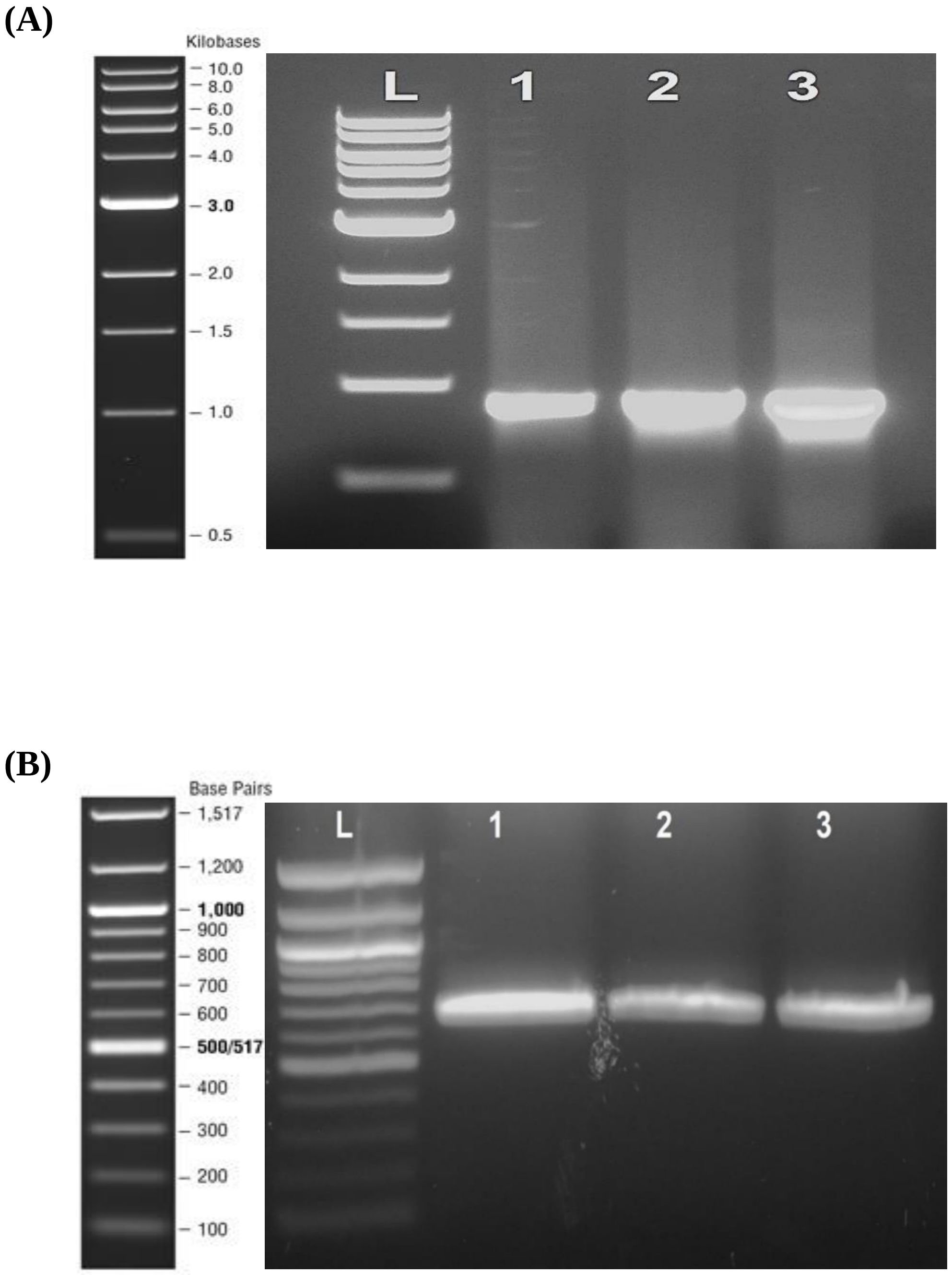

Figure 3.33: Agarose gel electrophoresis showing the successful amplification of *rgg*144 variants. Lane L **(A)** and **(B)**, 1 kb and 100 bp DNA ladder respectively (New England Biolabs, UK); lanes 1-3, PCR amplicons containing an intact copy of *rgg144* **(A)** or truncated *rgg144* **(B)** using gene specific primers.

3.18.2. Cloning of *rgg144* genes and transformation into *E. coli*

The purified amplicons were cloned into hexa histidine-tagged, ampicillin resistant plasmid pLEICS-01 at PROTEX, University of Leicester. The genetic map of pLEICS-01 is shown in Appendix 3. The His-tag was selected for several reasons: (i) it is small in size and charge rarely interferes with the structure or function of the fusion protein, (ii) it can be placed on either the N or the C terminus of recombinant proteins, (iii) it can be used for purification of proteins under native or denaturing conditions, (iv) His-tag fusion proteins are highly expressed in the plasmid containing a strong promoter such as T7 promoter, and easily purified using immobilized metal affinity chromatography (Gopal and Kumar, 2013; Costa *et al*., 2014).

After the cloning of the target gene into pLEICS-01, the recombinant plasmid was then extracted from one of the positive colonies using Miniprep kit (Section 2.8). The extracted plasmid was verified by DNA sequencing using T7-Promoter-F and pLEICS-01-Seq-R primers as indicated in Table 2.14. The DNA sequencing data confirmed the successful cloning of target genes and the absence of mutations as indicated in Appendix 4A and B. Following DNA sequencing, the recombinant plasmid was then transformed into *E. coli* BL21 (DE3) competent cells using heat shock as described in section 2.19. This strain is genetically modified for protein expression purposes, it has a copy of T7 RNA polymerase gene that can direct the expression of cloned genes under the control of the T7 promoter-IPTG induction system. This strain is also deficient in outer membrane and cytoplasm proteases (*ompT* and *lon* respectively), which increase the recombinant protein stability (Jia and Jeon, 2016). After transformation of recombinant plasmid into the BL21 (DE3) strain, the identity of the transformants was confirmed by PCR analysis using the gene specific primers (Table 2.13) and agarose gel electrophoresis. The PCR products in lanes 1-2, of Figure 3.34 (A-B) had the expected approximate size for full length Rgg144 (864 bp) and truncated Rgg144 (648 bp), respectively. The positive transformants were then kept in 15% (v/v) LB glycerol at -80°C for further protein expression.

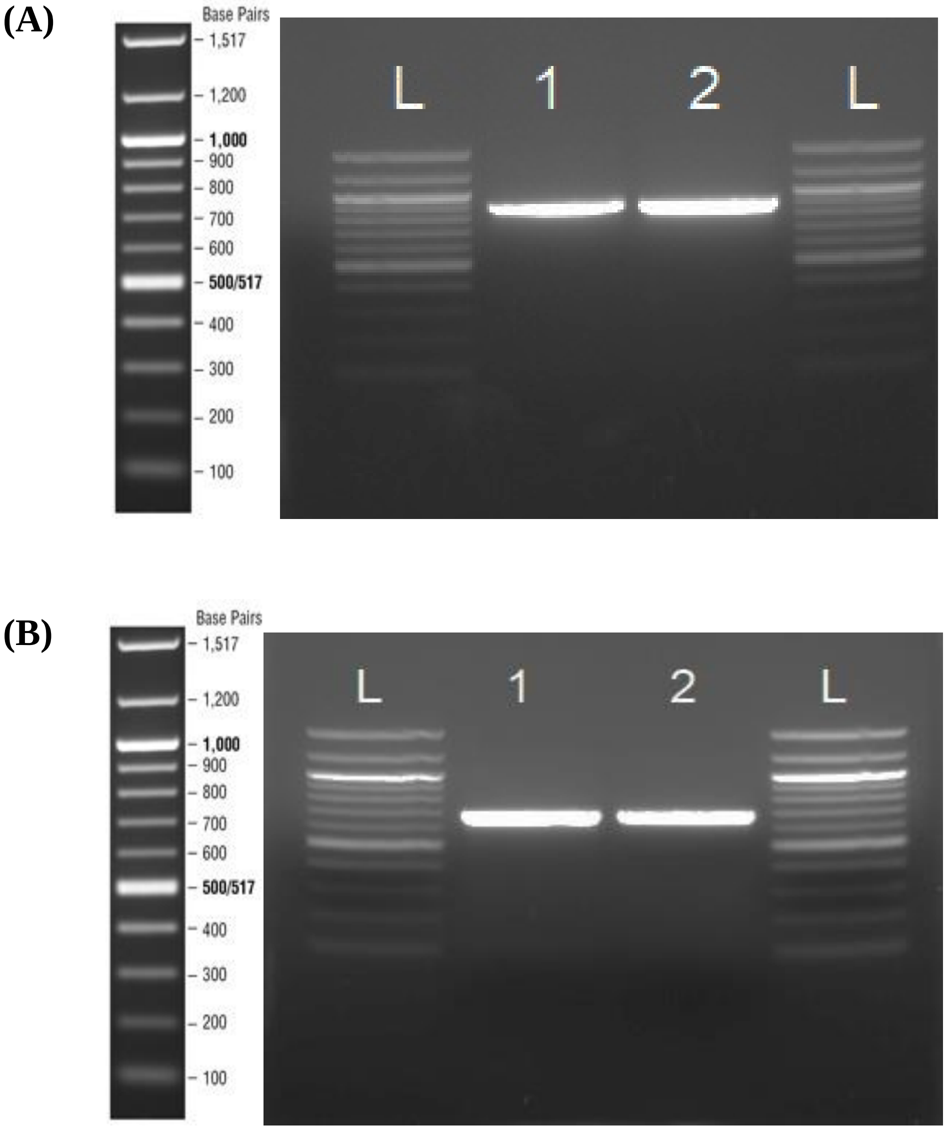

Figure 3.34: Confirmation of successful transformation of recombinant pLEICS-01 plasmid into *E. coli* BL21 (DE3) using agarose gel electrophoresis analysis. Lane L **(A-B)**, 100 bp DNA ladder (New England Biolabs, UK); lanes 1-2 PCR fragments amplified from recombinant plasmids carrying full length *rgg144* **(A)** or truncated *rgg144* **(B)** construct.

3.18.3. Small-scale purification

Small-scale expression was set up to identify the best expression conditions for full length and truncated Rgg144, and to investigate whether the protein of interest is expressed as soluble or inclusion bodies. The bacterial strains *E. coli* BL21 (DE3) harbouring the desired constructs were induced either with 0.5 or 1 mM IPTG at different growth phases (when OD_{600} was ~1.2-1.6) in power prime broth and incubated at different temperatures (18, 24 and 37°C). The results showed that the recombinant proteins (full length and truncated

Rgg144) were successfully induced with 1 mM IPTG when the OD_{600} of culture was 1.4, and further overnight incubation carried out at 37°C in shaking incubator at 220 rpm. SDS-PAGE gel analysis showed that both proteins are produced in an insoluble state by appearance of visible bands in the pellet indicating the presence of inclusion bodies (data not shown).

3.18.4. Large-scale purification

The optimal conditions used in small-scale expression were applied for large-scale protein expression and purification. Inclusion bodies (IBs) of full length and truncated Rgg144 were isolated from bacterial cells using a combination of mechanical and chemical cell disruption techniques as described previously in Materials and Methods (Section 2.29.4.1). The IBs purity was checked on SDS-PAGE gel stained with Coomassie blue. Lanes 1-3 (Figure 3.35A) and 1-2 (Figure 3.35E) show the successful purification of inclusion bodies by appearance of massive bands with an approximate molecular size (~35.7 kDa for full length and ~27.7 kDa for truncated Rgg144)**,** which includes the molecular weight of each recombinant protein plus the histidine tag (0.84 kDa) and TEV (Tobacco Etch Virus) cleavage site (0.957 kDa).

The purified inclusion bodies were successfully solubilised at alkaline pH in the presence of 6 mM guanidine-HCl solution and refolded in the buffer supplemented with numerous additives such as amino acids, salts and polymers (Section 2.29.4.2). The protein sample was then dialysed and passed through a Ni-NTA column, extensively washed with buffer containing 20 mM imidazole, and eluted using 500 mM imidazole. The eluted fractions were collected and analysed on SDS-PAGE gels. The results confirmed the successful elution of protein samples by obtaining the bands which are in line with the predicted molecular mass of the full length and truncated Rgg144 (Figure 3.35B and F). For further purification, the imidazole fractions were applied to 200 16/60 superdex Hiload gel filtration column, and peak fractions were collected as shown in Fig.3.35C and G. SDS-PAGE gel analysis of purified fractions showed the presence of a single band corresponding to the expected molecular weight for Rgg144 proteins and the absence of contaminating protein bands (Figure 3.35D and H).

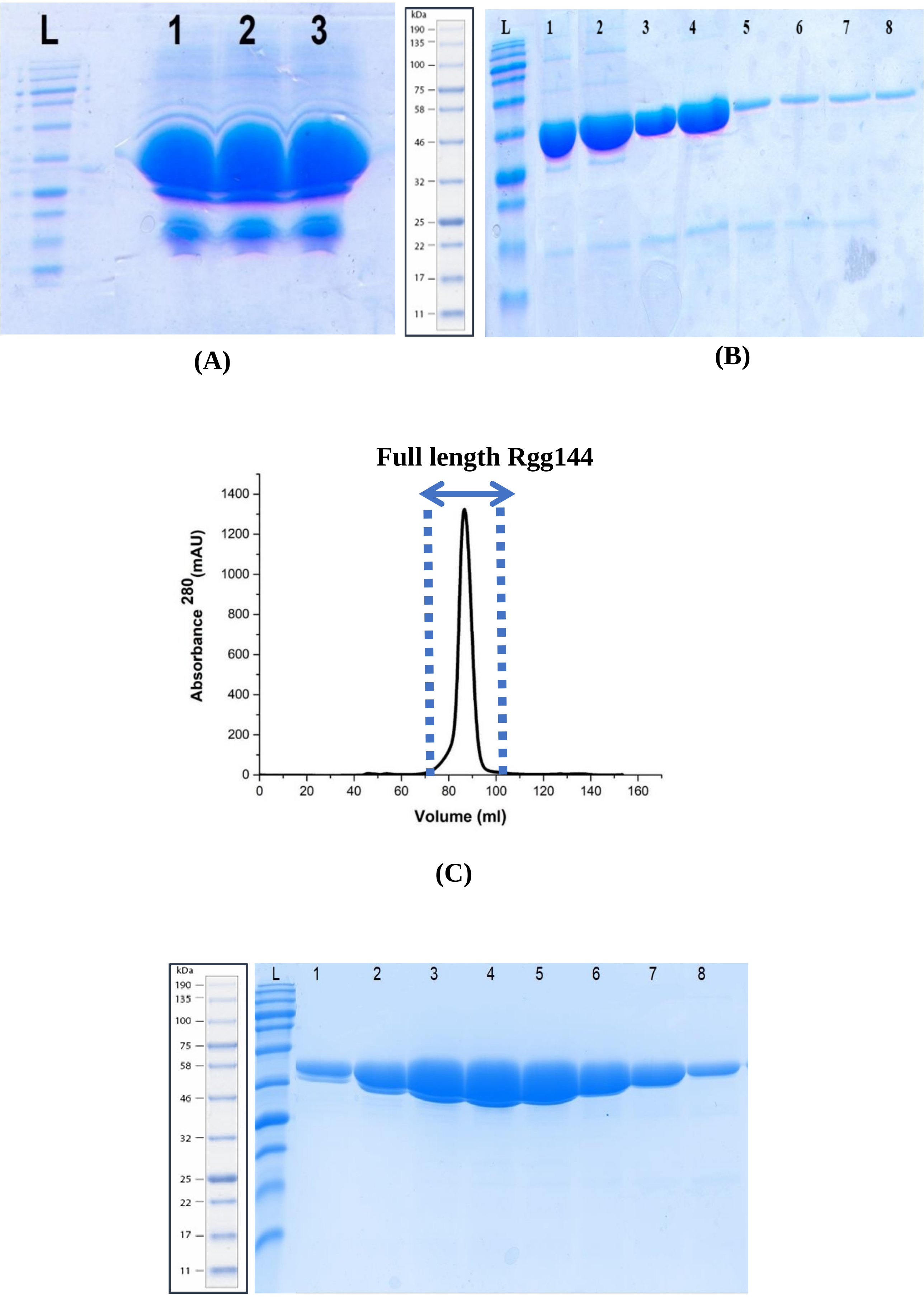
L
1
2
3
kDa
190
135
100
75
58
46
32
25
22
17
11
L
1
2
3
4
5
6
7
8
Full length Rgg144
Absorbance 280 (mAU)
1400
1200
1000
800
600
400
200
0
0
20
40
60
80
100
120
140
160
Volume (ml)
kDa
190
135
100
75
58
46
32
25
22
17
11
L
1
2
3
4
5
6
7
8

(A) (B)

(C)

(D)

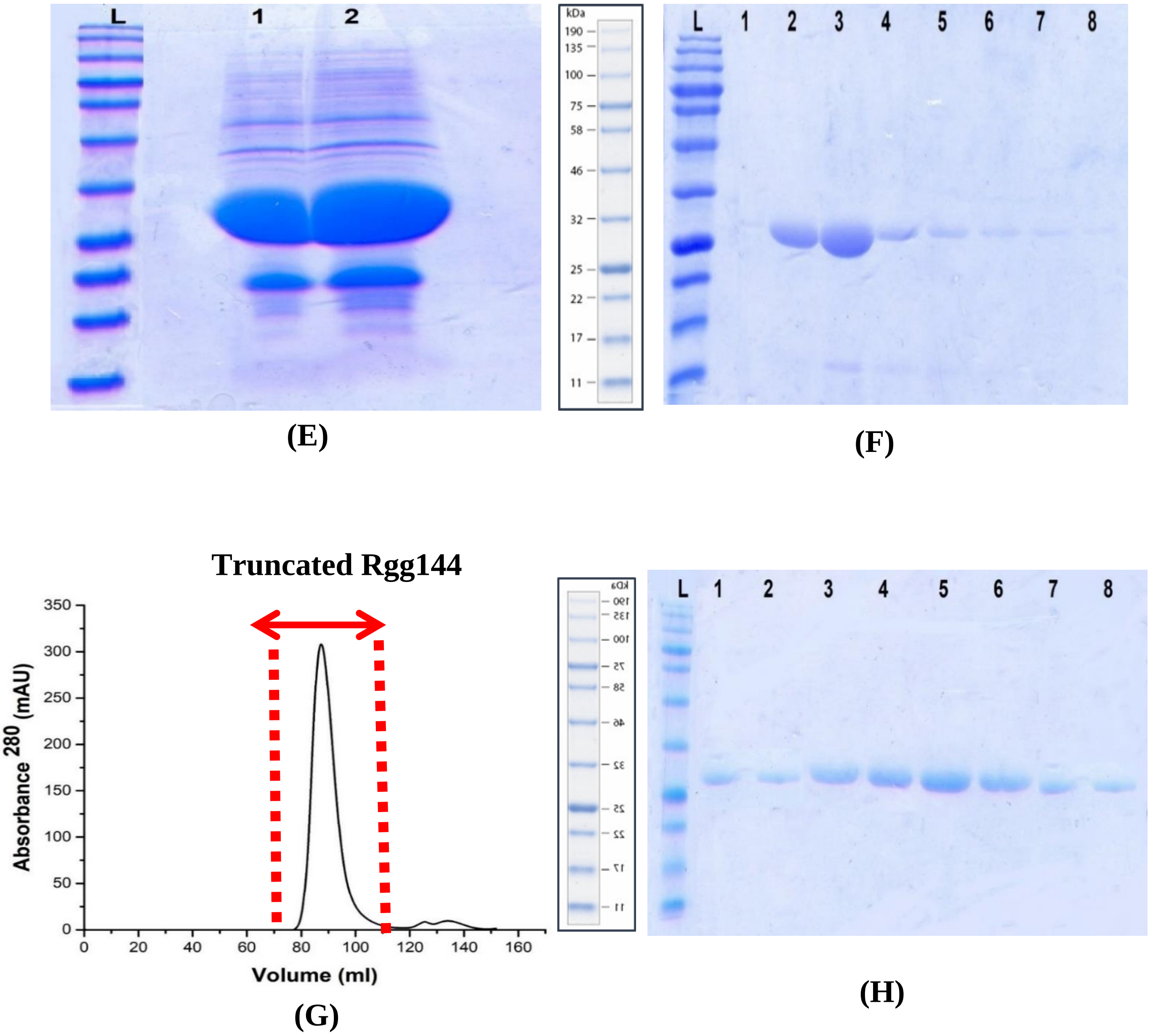

(E) (F)

(G) (H)

Figure 3.35: Confirmation of successful purification of recombinant full length and truncated Rgg144 proteins by SDS-PAGE gel and gel filtration analysis. Lane L, Blue Prestained Protein Standard, Broad Range ladder (New England Biolabs, UK); **(A)** and **(E)** purified inclusion bodies of full length and truncated Rgg144 respectively; **(B)** and **(F)** eluted Nickle column fractions in 500 mM imidazole; **(C)** and **(G)** gel filtration of full length and truncated Rgg144 proteins on superdex 200 16/60 column, **(D)** and **(H)** gel filtration fractions analysed on 15% SDS-PAGE gel, and bands of the expected sizes (approximately 35.7 kDa and 27.7 kDa for full length and truncated Rgg144) were obtained. The overall yield of pure full length Rgg144 protein was approximately 14 mg/1000 ml of bacterial culture and 6 mg/500 ml for truncated Rgg144 protein.

3.18.5. Identification of recombinant proteins by MALDI-TOF mass spectrometry

To confirm the identity of isolated proteins, the gel slices containing the protein of interest were cut and sent for sequencing at PNACL, Leicester University. Sequence analysis was done by digestion of purified protein with trypsin and generation of a set of peaks. Each peak represents a particular peptide from the protein. The masses of resulting peptides were analysed simultaneously by Matrix-Assisted Laser Desorption Ionization–Time of Flight (MALDI-TOF) mass spectrometry and compared with database results. The sequence data confirmed the identity of full length and truncated Rgg144 recombinant proteins (Appendix 5A and B). In addition, the molecular mass of each recombinant protein was also verified by Electrospray LC-MS. The results indicated that the molecular weight of each protein was nearly similar to predicted molecular weight as provided in Appendix 6 (A and B).

3.19. Analysis of Rgg/SHP144 interaction by fluorescence spectroscopy

Attempts were made to elucidate the interaction between Rgg144-SHP using a fluorescence spectrophotometer to identify the SHP144 amino acid residues important for binding. Fluorescence techniques are one of the most powerful methods used for studying of protein-ligand interactions because of their versatility, ease of application and high sensitivity (Lakowicz, 2006; Chan *et al.*, 2014). Fluorescence spectroscopy commonly relies on either intrinsic fluorophores, which are part of protein structure, or extrinsic markers, which are created by linking the fluorescent probe to the molecule structure (Albani, 2007).

3.19.1. Intrinsic fluorescence for detection Rgg/SHP144 interaction

In proteins, aromatic amino acids [phenylalanine (F), tyrosine (Y), and tryptophan (W)] can be used as a marker for studying protein structure, folding and binding interactions (Munishkina and Fink, 2007; Lakowicz, 2006; Chan *et al.*, 2014). These amino acids absorb light at a specific wavelength and fluoresce in the UV range between (250 – 400 nm) (Lakowicz, 2006; Chan *et al.*, 2014). Tryptophan fluorescence is the most valuable method for studying protein conformational changes since its fluorescence properties (emission wavelengths and intensity) are highly sensitive to the local environment (Ghisaidoobe and Chung, 2014). Thus, this method was selected for initial screening of Rgg/SHP144 binding as its inexpensive method, no need for labelling and easy to perform. To achieve this, Rgg144 recombinant protein was mixed with synthetic SHP144-C13 peptide in a black cuvette, and the binding measurements were detected by tryptophan fluorescence spectroscopy as previously described in Materials and Methods (Section 2.32.1). Peptide or protein with buffer served as a control of assay. Based on the Rgg144 protein structure and our knowledge of similar allosteric systems in other streptococci (Chang *et al*., 2011; Aggarwal *et al*., 2014), we hypothesised that binding of SHP144-C13 to Rgg144 would induce conformational changes in the target protein which allows the transcription activation to occur. This conformational transition may lead to changes in fluorescence intensity of tryptophan. Unfortunately, the results did not show any noticeable changes in total fluorescence intensity of Rgg144 treated with peptide in comparison with reaction without peptide (Fig.3.36F). It was thought that the other versions of SHP144 with varying sizes could be able to bind to Rgg144. A parallel set of experiments by treating Rgg144 separately with SHP144-C8, SHP144-C9, SHP144-C10, SHP144-C11, SHP144-C12, SHP144-C14 and SHP144-C15 was performed. Similarly, no difference in fluorescence intensity could be identified for any of the peptides tested (Figure 3.36A, B, C, D, E, G and H). This is more likely due to the presence of multiple tryptophan residues in both the protein and most of the selected peptides, making the interpretation of the results complicated. To overcome unfavourable conditions arisen from intrinsic fluorescence, another fluorescence technique called fluorescence polarisation was employed.

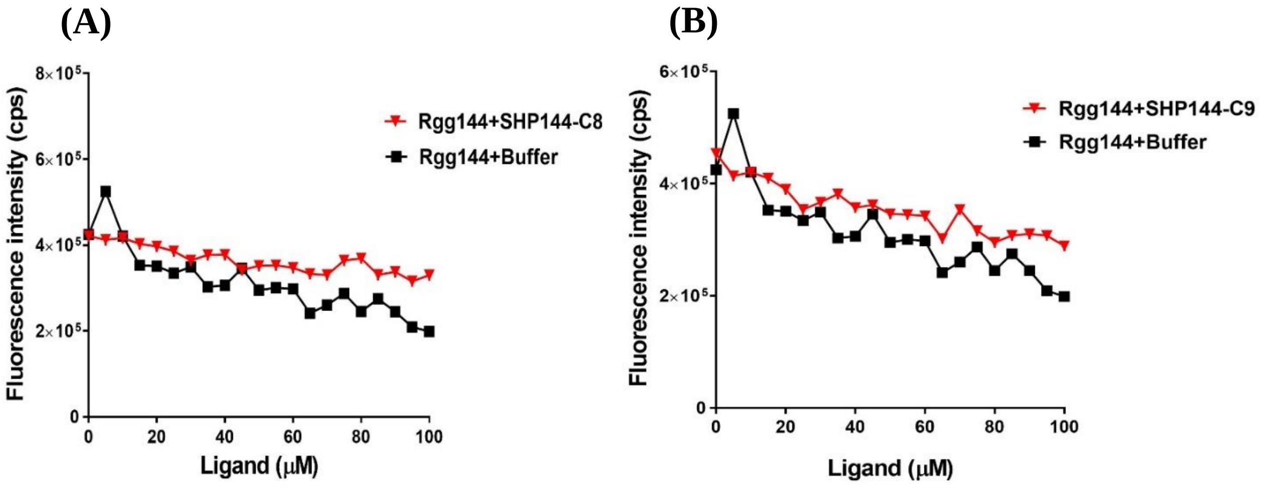

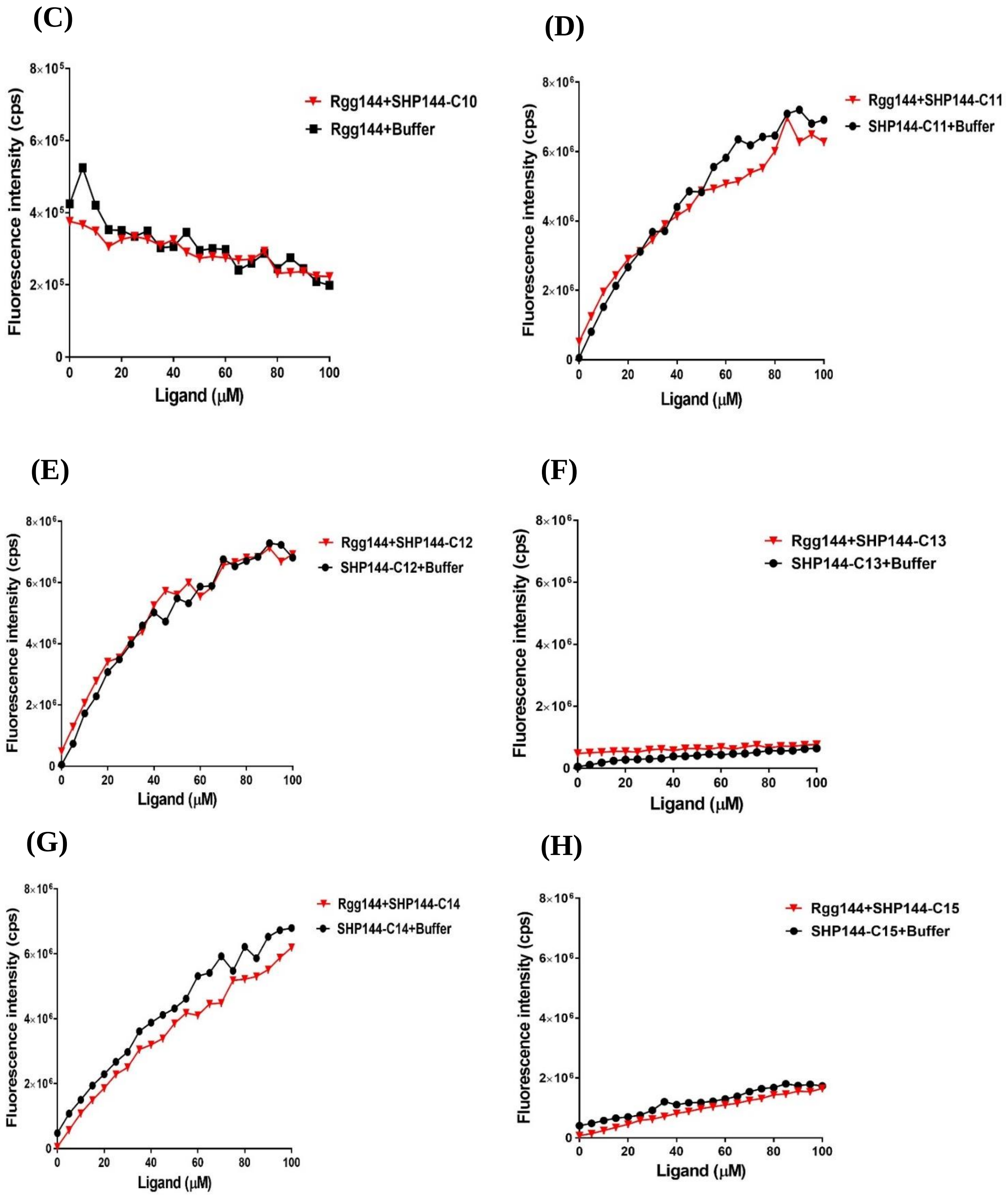

Figure 3.36: Diagrams showing the interaction of 1 µM purified Rgg144 protein with different concentrations (0-100 µM) of SHP144 variants. **(A)** SHP144-C8; **(B)** SHP144-C9; **(C)** SHP144-C10; **(D)** SHP144-C11; **(E)** SHP144-C12; **(F)** SHP144-C13; **(G)** SHP144-C14 and **(H)** SHP144-C15 using fluorescence spectroscopy. The fluorescence intensity values were expressed in counts per second (cps).

3.19.2. Detection of Rgg/SHP144 binding using fluorescence polarisation (FP)

It is clear from Figure 3.36 that the Rgg/SHP144 binding measurements by intrinsic fluorescence were unsuccessful. Therefore, another fluorescence technique, called fluorescence polarisation was used to study Rgg/SHP144 binding affinity. This method offers numerous advantages over other binding techniques. It is simple, fast and can be performed in a homogeneous solution without solid supports, allowing true equilibrium analysis down to the low picomolar range. FP measurements can be directly utilised without separation of the bound and free ligand, allowing the detection of binding with low affinity (Rossi and Taylor, 2011). Further, FP is a non-destructive technique and the same sample can be treated and reanalysed in order to ascertain the effect on binding of changes in parameters such as pH, temperature and salt. Further, non-radioactive substances are involved in the FP assay making it safer than radioligand binding assays. Finally, the FP values are mainly based on measuring the polarisation of light caused by changes in molecular size rather than the fluorophore concentration as intrinsic fluorescence, thus providing more accurate data (Owicki, 2000; Burke *et al*., 2003; Moerke, 2009).

Fluorescence polarisation assay was set up as previously described in section 2.32.2 using Rgg144 protein and synthetic peptide corresponding to 13 amino acid residues (active peptide) conjugated with FITC. The fluorescence values (mP) were measured at 485 nm excitation and 520 nm emission wavelengths using Hidex Sense Microplate Reader. The K_d was calculated using a non-linear regression stimulation dose-response curve (Graph Pad Prism version 7.02). The basic principle of Rgg/SHP144 interaction using fluorescence polarisation is given in Figure 3.37. This method is generally based on the observation that when the fluorescent ligand like FITC-SHP144-C13 is excited by polarised light, the emitted light will be mostly depolarised due to rapid tumbling of the labelled molecule during the excited state, resulting a low level of polarisation signals. While if this ligand is bound to a large molecule like Rgg144 protein, the rotation of the complex will be much slower than that of the peptide alone, and the emitted light will still be polarised (Moerke, 2009).

The results showed that FITC-SHP144-C13 was able to bind to full length Rgg144 with binding affinity of 6.60 µM as shown in Figure 3.38A. It was hypothesised that using truncated Rgg144 protein would increase the interaction efficiency. A similar experiment was repeated using the truncated Rgg144. The results showed a similar binding affinity (10.40 µM) (Figure 3.38A). This data suggests that deletion some of Rgg144 amino acid residues does not improve the binding capability of Rgg144 and SHP144-C13. Similar binding assay was repeated by the use of non-specific fluorescein peptide FITC-NSP-C13 to confirm the specificity of binding assay. As can be seen from Figure 3.38A, no binding could be detected by using a non-specific peptide. In addition, when Rgg144 is replaced with bovine serum albumin (BSA), no FITC-SHP144-C13 binding could be observed (Figure 3.38B).

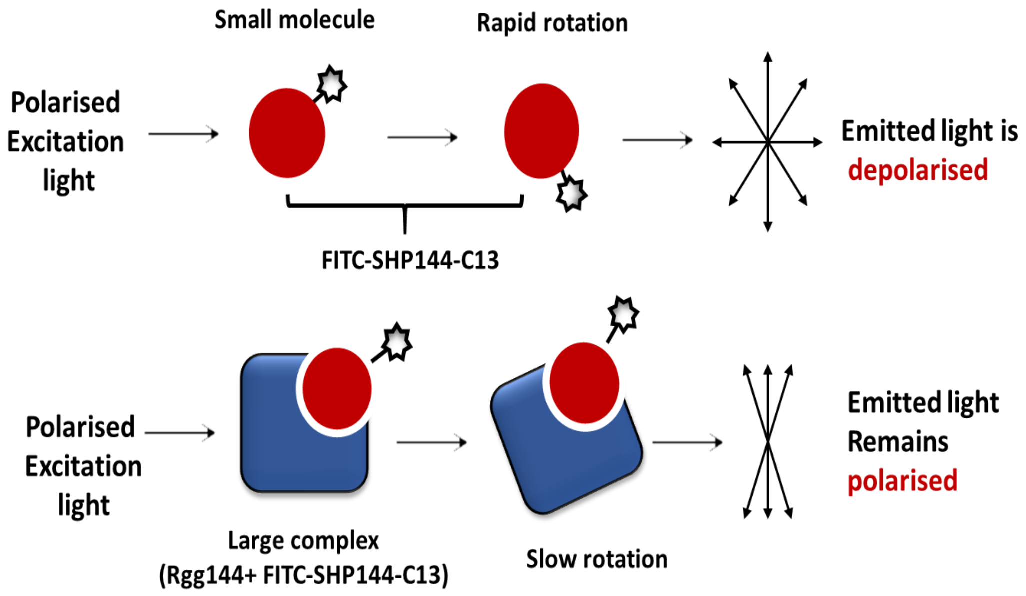

Figure 3.37: Schematic diagram showing the basic principle of binding the Rgg144 to its ligand SHP144-C13 using fluorescence polarisation. When labelled peptide SHP144-C13 (Red circle) is excited by polarised light at excitation wavelength of FITC (485 nm), the ligand rotates faster during the excited state making the emitted light to be largely depolarised. When this ligand binds to a large molecule like Rgg144 (blue square), the resulting complex rotates slowly due to their size and retains its polarised light. This figure was constructed based on Moerke (2009).

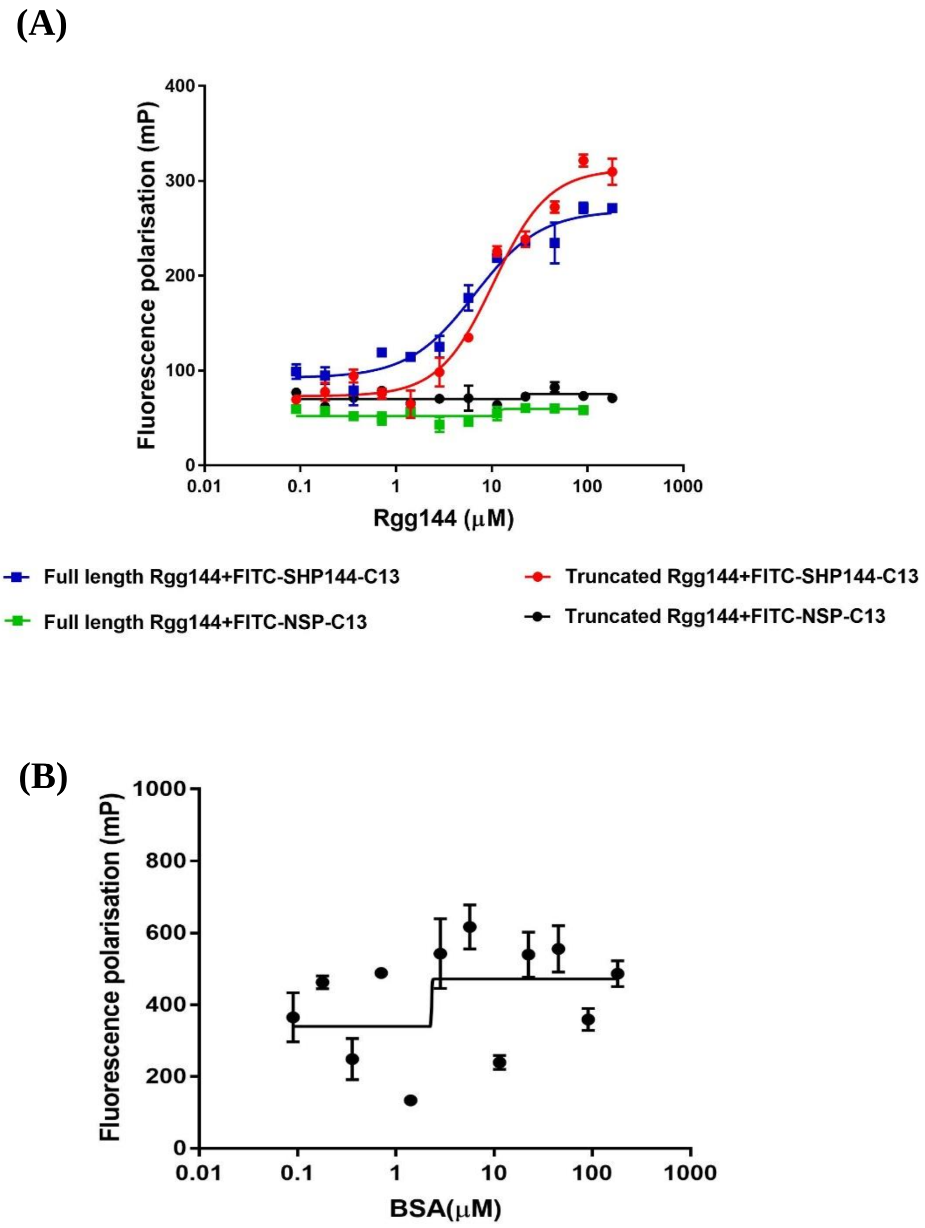

Figure 3.38: Direct binding of Rgg144 and FITC-SHP144-C13 using fluorescence polarisation technique. **(A)** Blue and red sigmoid curves indicate the binding of FITC-SHP144-C13 to full length and truncated Rgg144 respectively, whereas flat curves represent the interaction of same sized non-specific FITC-NSP-C13 to full length Rgg144 (green colour) and truncated Rgg144 (black colour). **(B)** The interaction of bovine serum albumin and FITC-SHP144-C13. Millipolarisation values were monitored at 485 nm excitation and 520 nm emission spectra using Hidex Sense Microplate Reader in 96 well black opaque plate. Each value was normalised and plotted against protein concentration. A linear scale on Y axis represents mP values whereas concentration of protein is presented as logarithmic scale on X axis. Equilibrium dissociation constant (K_d) values were calculated by fitting to a sigmoidal dose-response curve with variable slope in Prism GraphPad 7.02.

In addition, a relative binding affinity of SHP144-C13 was also determined by a FP competition assay using unlabelled SHP144-C13 peptide (SEWVIVIPFLTNL). This assay is generally based on measuring the reduction in FP signals upon addition of competitor to the ligand /protein reaction. The FP competition assay was done by mixing serially diluted unlabelled SHP144-C13 peptide with Rgg/SHP144 complex (10 nM of FITC-SHP144-C13 and 6.60 µM protein representing half-maximal Rgg/SHP144 interaction determined from direct FP binding) (Figure 2.38A). This mixture was incubated at 20ºC for 30 min and fluorescence polarisation was measured. As a negative control in a separate reaction, competence stimulating peptide (CSP) known not to interact with Rgg144, was serially diluted, and its ability to compete with FITC-SHP144-C13 was also assayed. The results showed that unlabelled SHP144-C13 peptide was able to displace Rgg144-FITC-SHP144-C13 complex. It was found that IC_{50} (the concentration of competitor required to disrupt 50% FITC-SHP144 binding to Rgg144) of unlabelled SHP144-C13 was 86.80 µM, whereas no competition has been seen by using nonspecific competence stimulating peptide (CSP) as FP values remained constant around 172 mP (Figure 3.39).

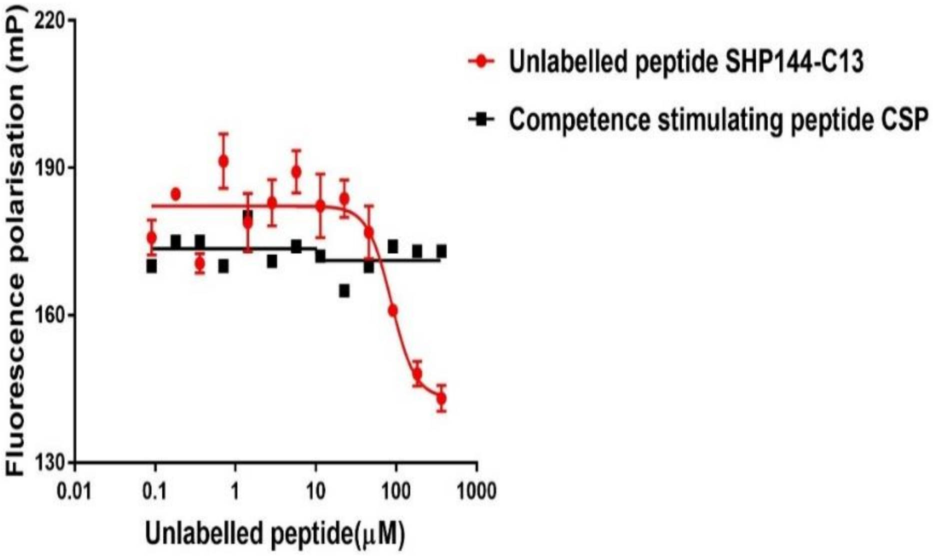

Figure 3.39: Assessing the capability of unlabelled peptide SHP144-C13 to competitively displace Rgg144-FITC-SHP144-C13 complex. The 10 nM FITC-SHP144-C13 was initially mixed with 6.60 µM Rgg144 (K_d value was taken from previous direct binding assay), and then incubated with serially diluted unlabelled SHP144-C13 (0.09-364 µM) peptide for 30 min at 20°C. Millipolarisation values (mP) were measured at 485 nm excitation and at 520 nm emission using Hidex Sense Microplate Reader. The mP values were dropped with increasing the concentration of unlabelled peptide SHP144-C13 whereas the fluorescence values were still constant by adding control peptide CSP. The IC_{50} values were obtained by fitting polarisation values versus total concentration of competitor to a dose-response model.

3.19.3. Assessing the role of SHP144 residues in binding to Rgg144 using fluorescence polarisation

Having established the binding conditions using the unmodified labelled SHP144-C13, next, it was hypothesised that each SHP144-C13 residue would have a different role in binding to recombinant Rgg144. As expected, three binding patterns were identified: some amino acid substitutions did not have any effect on binding (S14A, E15A, V17A, V19A, P21A, F22A, L23A, T24A, N25A, L26A), as their binding affinities were (8.06, 3.31, 9.67, 4.14, 1.67, 7.11, 4.27, 3.30, 3.34 and 3.44 µM, respectively), which is similar to that of unmodified peptide (6.60 µM). On the other hand, certain residues had a role in binding as their replacements with alanine led to reduce the binding affinity [W16A (50.04 µM) and I20A (23.54 µM)] or completely abolished binding (I18A) compared with unmodified peptide (Figure 3.40 A-F). The binding pattern of non-activating modified peptides (W16A, V17, I18, I20 and P21) was consistent with their transcriptional activation capability, except that while V17A and P21A modifications abolished transcriptional activation of *shp144*, but did not affect the Rgg/SHP144 binding (Figure 3.40B and D and Table 3.5). These results suggest that the V17A and P21A substitutions can be utilised to design competitive inhibitors of Rgg144 activation by SHP144-C13. Similar experiments were done with BSA to confirm the specificity of binding, as shown in Figure 3.41 (A-F). As expected, there was no specific binding with BSA.

(A)

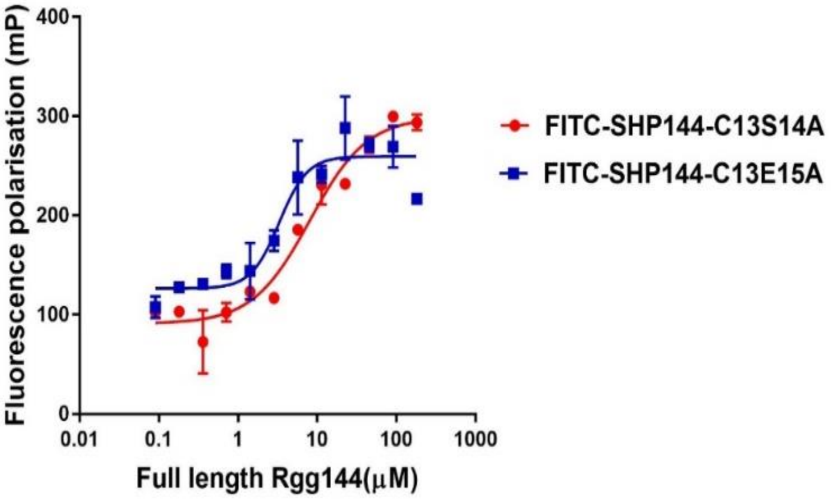

(B)

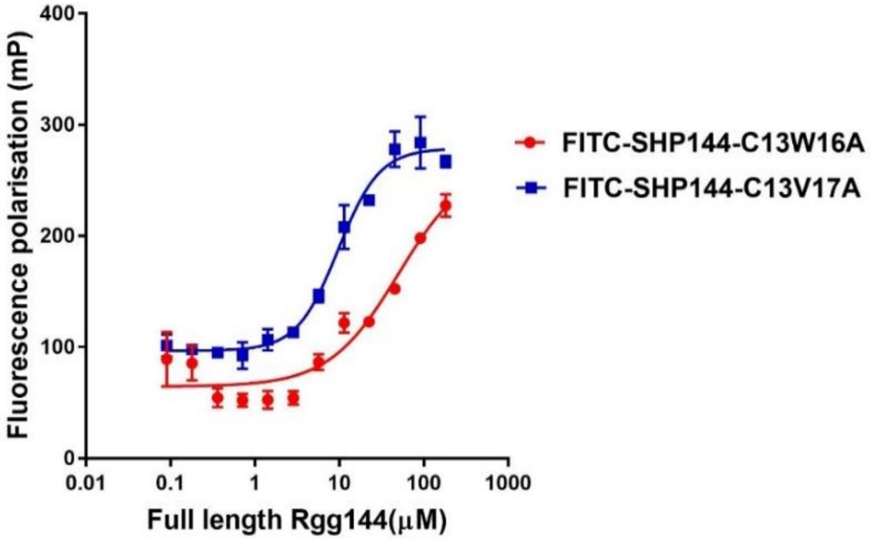
Fluorescence polarisation (mP)
400
300
200
100
0
0.01
0.1
1
10
100
1000
Full length Rgg144(μM)
FITC-SHP144-C13W16A
FITC-SHP144-C13V17A

(C)

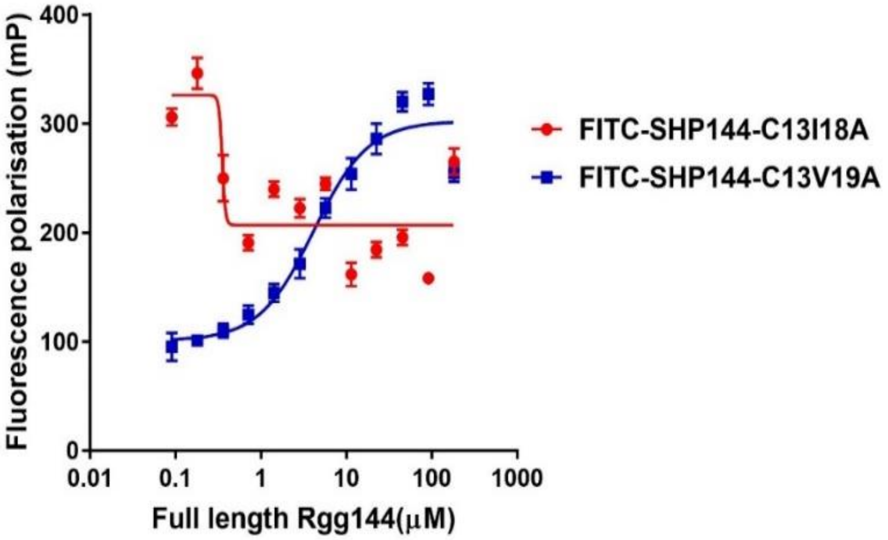
Fluorescence polarisation (mP)
400
300
200
100
0
0.01
0.1
1
10
100
1000
Full length Rgg144(μM)
FITC-SHP144-C13I18A
FITC-SHP144-C13V19A

(D)

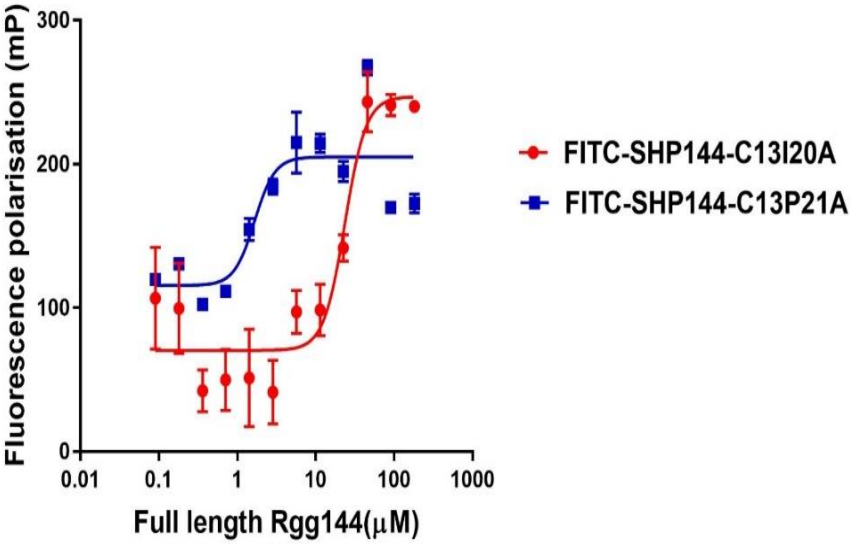
Fluorescence polarisation (mP)
300
200
100
0
0.01
0.1
1
10
100
1000
Full length Rgg144(μM)
FITC-SHP144-C13I20A
FITC-SHP144-C13P21A

(E)

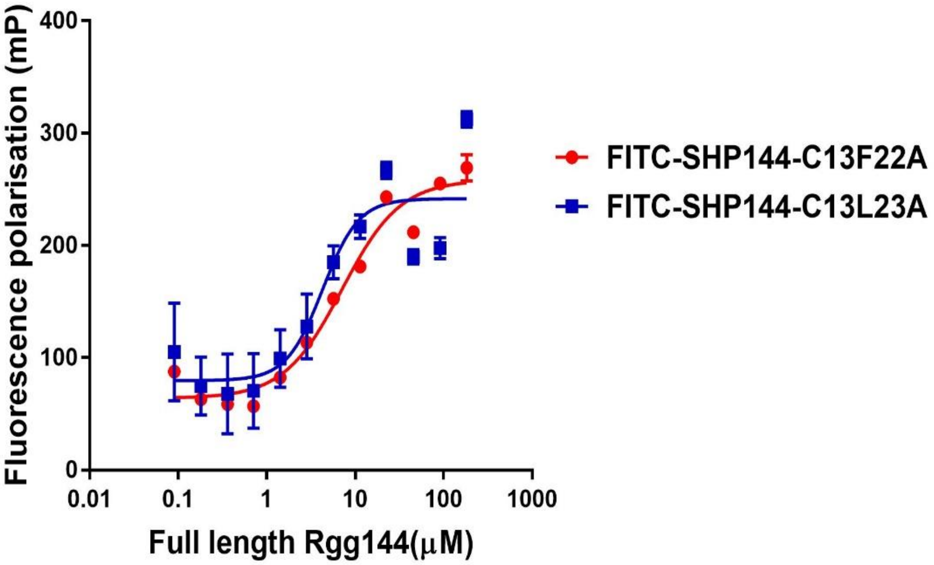

(F)

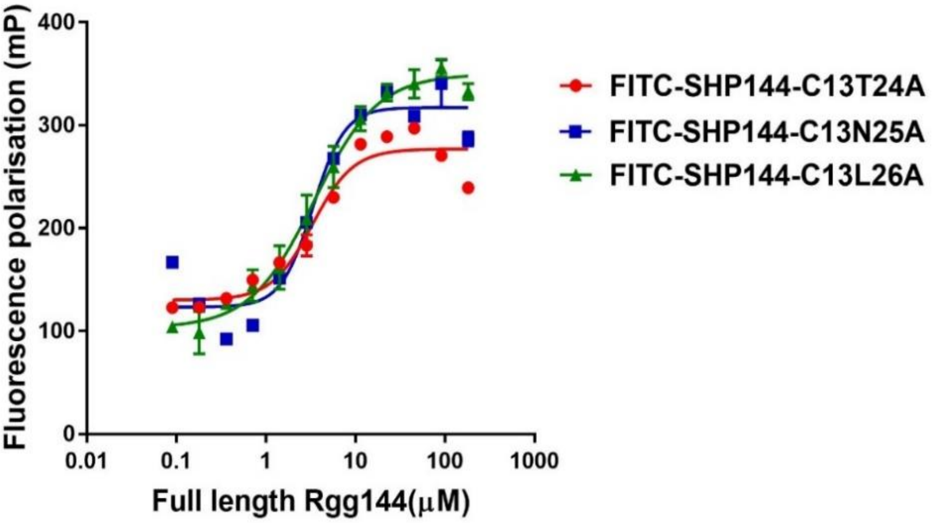

Figure 3.40: The effect of introducing a modification into SHP144 structure on its binding capability to Rgg144. Constant amount (10 nM) of modified FITC-SHP144-C13 variants [**(A)** FITC-SHP144-C13S14A, FITC-SHP144-C13E15A; **(B)** FITC-SHP144-C13W16A, FITC-SHP144-C13V17A; **(C)** FITC-SHP144-C13I18A, FITC-SHP144-C13V19A; **(D)** FITC-SHP144-C13I20A, FITC-SHP144-C13P21A; **(E)** FITC-SHP144-C13F22A, FITC-SHP144-C13L23A; **(F)** FITC-SHP144-C13T24A, FITC-SHP144-C13N25A and FITC-SHP144-C13L26A] was incubated with serially diluted recombinant Rgg144, ranging from 0.09 to 182 µM for 20 min at 20°C. The binding affinity (K_d) for each peptide was measured using fluorescence polarisation (Hide Sense Microplate Reader). Fluorescence values were then plotted against protein concentration for three independent experiments.

Table 3.5: Showing transcriptional activation of pneumococcal reporter strains carrying native or modified SHP144, and the binding affinities of FITC-SHP144-C13 variants.

Strains	**Transcriptional activation* (Miller units)**	**Peptides**	**Binding affinities (K_d in μM) ****
P_{shp144}::*lacZ*-Δ*shp144*Com	215 ± 5	FITC-SHP144-C13	6.60
P_{shp144}::*lacZ*-Δ*shp144*ComS14A	105 ± 5	FITC-SHP144-C13S14A	8.06
P_{shp144}::*lacZ*-Δ*shp144*ComE15A	107 ± 2.5	FITC-SHP144-C13E15A	3.31
P_{shp144}::*lacZ*-Δ*shp144*ComV19A	215 ± 5	FITC-SHP144-C13V19A	4.14
P_{shp144}::*lacZ*-Δ*shp144*ComF22A	90 ± 10	FITC-SHP144-C13F22A	7.11
P_{shp144}::*lacZ*-Δ*shp144*ComL23A	95 ± 5	FITC-SHP144-C13L23A	4.27
P_{shp144}::*lacZ*-Δ*shp144*ComT24A	175 ± 5	FITC-SHP144-C13T24A	3.30
P_{shp144}::*lacZ*-Δ*shp144*ComN25A	185 ± 5	FITC-SHP144-C13N25A	3.34
P_{shp144}::*lacZ*-Δ*shp144*ComL26A	187.5 ± 2.5	FITC-SHP144-C13L26A	3.44
P_{shp144}::*lacZ*-Δ*shp144*ComV17A	6 ± 1.0	FITC-SHP144-C13V17A	9.67
P_{shp144}::*lacZ*-Δ*shp144*ComP21A	7.5 ± 2.5	FITC-SHP144-C13P21A	1.67
P_{shp144}::*lacZ*-Δ*shp144*ComW16A	7.5 ± 2.5	FITC-SHP144-C13W16A	50.04
P_{shp144}::*lacZ*-Δ*shp144*ComI18A	7.5 ± 1.5	FITC-SHP144-C13I18A	ND
P_{shp144}::*lacZ*-Δ*shp144*ComI20A	8.5 ± 0.5	FITC-SHP144-C13I20A	23.54

ND means not determined

* represents (mean ± SEM) of three independent experiments

** Dissociation constant between the Rgg144 and its ligands (FITC-SHP144-C13 variants).

(A)

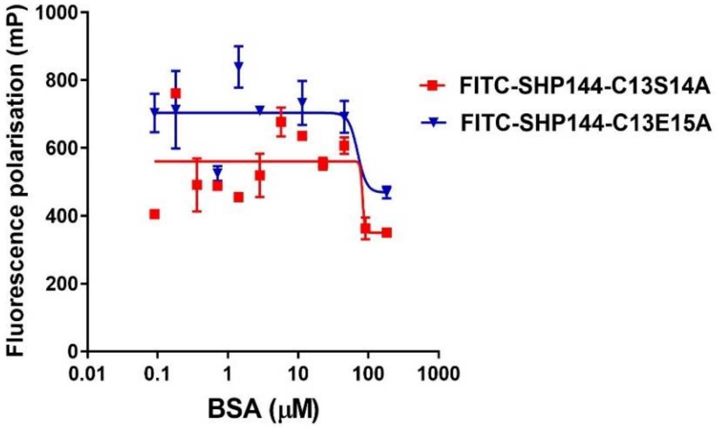
Fluorescence polarisation (mP)
1000
800
600
400
200
0
0.01
0.1
1
10
100
1000
BSA (μM)
FITC-SHP144-C13S14A
FITC-SHP144-C13E15A

(B)

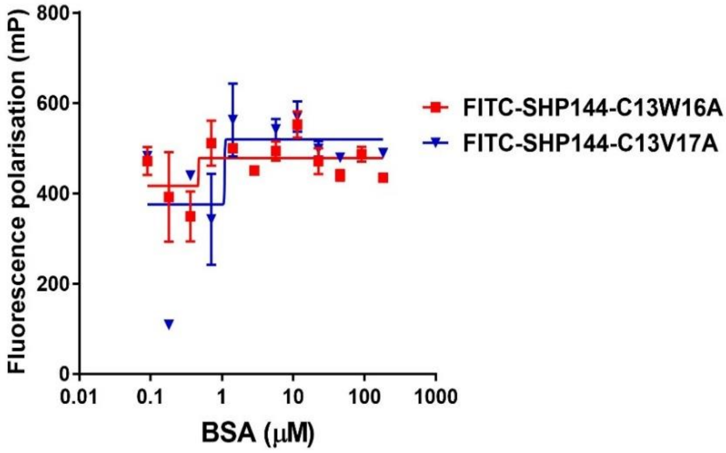
Fluorescence polarisation (mP)
800
600
400
200
0
0.01
0.1
1
10
100
1000
BSA (μM)
FITC-SHP144-C13W16A
FITC-SHP144-C13V17A

(C)

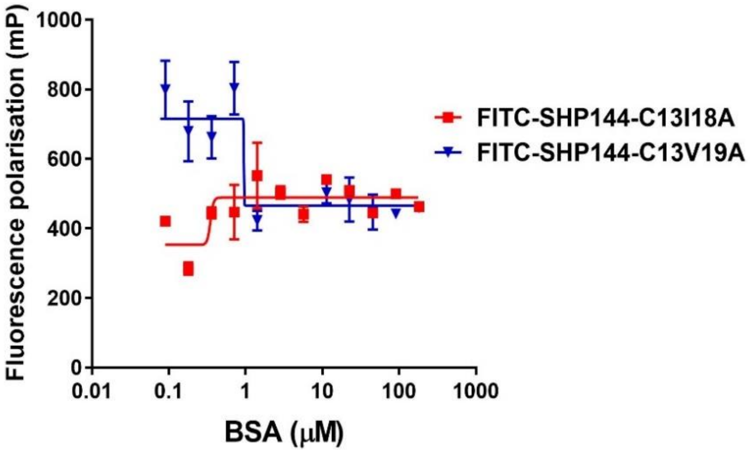
Fluorescence polarisation (mP)
1000
800
600
400
200
0
0.01
0.1
1
10
100
1000
BSA (μM)
FITC-SHP144-C13I18A
FITC-SHP144-C13V19A

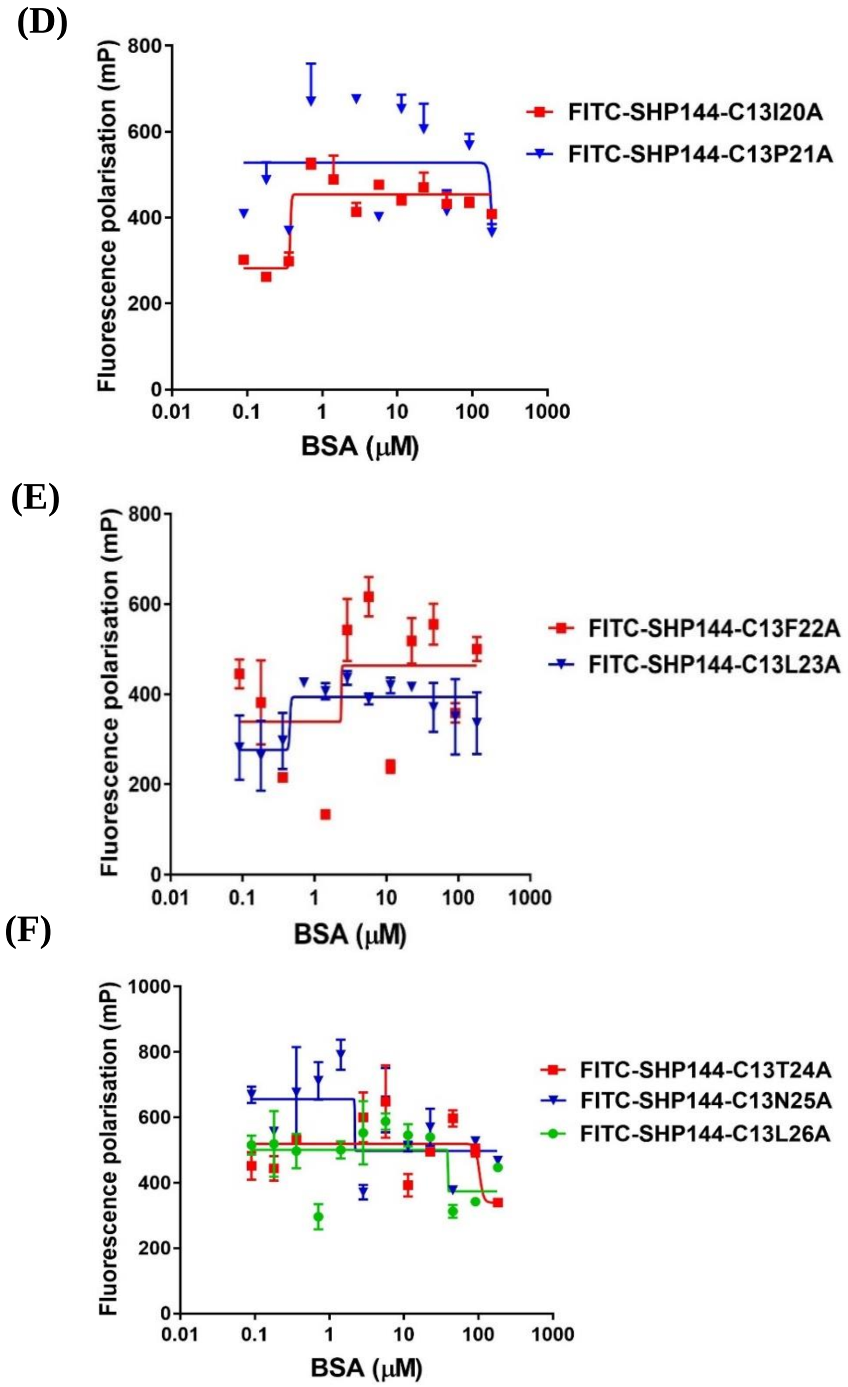

Figure 3.41: (A-F) Diagrams showing the lack of intermolecular interaction between bovine serum albumin (BSA) and modified FITC-SHP144-C13 peptides. **(A)** FITC-SHP144-C13S14A, FITC-SHP144-C13E15A; **(B)** FITC-SHP144-C13W16A, FITC-SHP144-C13V17A; **(C)** FITC-SHP144-C13I18A, FITC-SHP144-C13V19A; **(D)** FITC-SHP144-C13I20A, FITC-SHP144-C13P21A; **(E)** FITC-SHP144-C13F22A, FITC-SHP144-C13L23A and **(F)** FITC-SHP144-C13T24A, FITC-SHP144-C13N25A and FITC-SHP144-C13L26A using fluorescence polarisation technique. Polarisation values (mP) were measured using Hidex Sense Microplate Reader at excitation 485 nm and emission at 520 nm, and each value was plotted against BSA concentration. The values represent the average of three independent experiments.

Section E: Structural analysis of Rgg/SHP144

In collaboration with Prof Russell Wallis, the full length Rgg144 of *S. pneumoniae* was crystallised using PACT screen (Molecular Dimensions) at 6 mg/ml. Samples were mixed with an equal volume of buffer using the sitting-drop vapor diffusion method. Crystals grew at room temperature in 0.1M Bis-Tris propane pH 7.5 and 8.5 containing 0.2 M Potassium sodium tartrate tetrahydrate or 0.2 M Sodium malonate dibasic monohydrate. Diffraction data were collected at Diamond Light Source and were processed with iMosflm. Phases were determined using seleneomethionine-enriched Rgg. The best crystals of native Rgg diffracted to 2.2 Å resolution. Models were optimised using cycles of manual refinement with Coot and refinement in Refmac5 (Murshudov *et al.*, 1997), part of the CCP4 software suite (Collaborative Computational Project, 1994), and in Phenix (Adams *et al.*, 2010). Rgg144 is a homodimer in solution (by gel filtration) and in the crystal, with a tetratricopeptide-like fold. Each polypeptide comprises a HTH domain and a C-terminal regulatory domain featuring a pronounced groove that forms the binding site for the SHP as shown in Figure 3.42A. This well-defined groove is much more amenable for selective targeting than most protein interfaces, which are often relatively featureless, rendering Rgg a good drug target.

In this study, crystallisation of the Rgg144 with its ligands SHP144-C13 and C12 was done by mixing an equal volume of Rgg/SHP144 complex and reservoir solution, and incubation at room temperature or 4°C. Crystallisation procedures were repeated several times using different molecular dimension screens, however without success. It was thought that binding of SHP144 to its receptor Rgg144 induces conformational changes preventing the crystal to grow. Thus, it was expected that the use of modified peptides (SHP144-C13V17A and SHP144-C13P21A) could resolve this problem through binding to Rgg144 without producing conformational alterations. Unfortunately, no crystal could be detected. Therefore, the Rgg/SHP144 complex was modelled using Rosetta Flex Pep Dock, a programme that refines coarse peptide–protein models, allowing significant changes in both peptide backbone and side chains using the Monte-Carlo with minimisation approach. Modelling suggests that a SHP13-mer fits into the binding groove of Rgg144 (Figure 3.42B) to form a variety of polar and hydrophobic interactions. This model was tested using site-directed mutagenesis of the SHP144 as mentioned in previous sections.

The transcriptional activation and binding results demonstrated the involvement of three amino acids at positions W16, I18 and I20 in the binding with Rgg144 as their replacements with alanine completely abolished the transcriptional activation and reduced binding capabilities. However, further work is required to optimise the conditions for crystallisation of Rgg144 with its ligand.

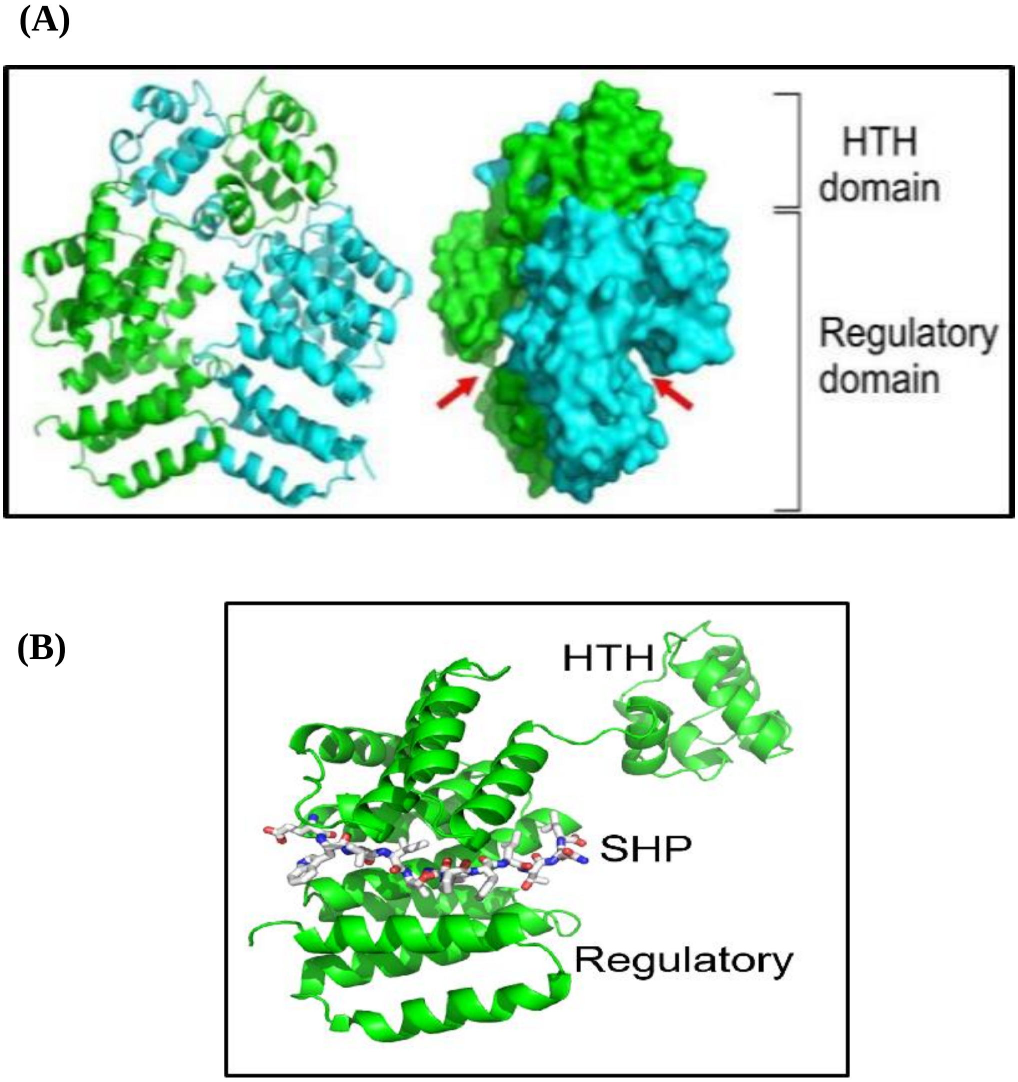

Figure 3.42: (A) Structure of the Rgg144 dimer. The binding grooves are indicated by red arrows. **(B)** A model of Rgg/SHP144 interaction in *S. pneumoniae* D39 using Rosetta Flex Pep Dock software. SHP144 13-mer docked into the peptide binding groove of Rgg144.

3.20. Identification of the SHP144 secreted peptides from pneumococcal culture supernatants

Mass spectrometry was used to identify the sequence and amount of SHP144 peptide naturally present in *S. pneumoniae* D39 supernatant collected from culture grown to late exponential phase, in which SHP144 is maximally expressed. The Δ*shp144* supernatant lacking SHP144 was used as a negative control. The collected supernatants were processed as described previously in section 2.33 and sent to PNACL, University of Leicester, and biOMICS, University of Sheffield, for mass spectrometry analysis. Synthetic peptides with varying sizes were used as an internal standard. Despite several attempts we were unable to identify the active SHP144 in supernatants of wild type D39 grown in either BHI or CDM-mannose. This is very likely because of the low concentration of secreted peptides in a highly complex background containing a large complex mixture of proteins making proteomic approach virtually impossible. Therefore, for future analysis, the supernatant sample should be handled in the manner that makes it compatible for mass spectral analysis or use other detection methods such as bare boron-doped diamond electrode or capillary electrophoresis (Verbeke *et al*., 2017).

Section F: Competitive inhibition phenotypic manifestations of Rgg/SHP144 QS system

3.21. Competitive inhibition of Rgg/SHP144 system

After establishing the importance of modified peptides SHP144V17A and P21A in *shp144* transcriptional activation and binding, it was aimed to test their contributions to the phenotypic manifestation of Rgg/SHP144 QS. To do that, the spent culture supernatants of strains producing SHP144 with V17A or P21A modifications were collected at late exponential phase and were added to bacterial pellets of reporter P_{shp144}::*lacZ*-Wt strain, capable of producing native SHP144. Wild type and complemented *shp144* supernatants were included as a control. In addition, the supernatants of complemented strains carrying different modifications (L26A or N25A) were also used to confirm the specificity of the inhibition assay. Mannose was used for stimulation the *shp144* expression as demonstrated previously in section 3.5. In addition, maltose was also included in complemented *shp144* cultures to activate the maltosaccharide-inducible promoter (PM) of pCEP to express more SHP144 peptides. The expression of *shp144* would be under the control of its own constitutive promoter and maltosaccharide-inducible promoter of pCEP following ectopic integration of recombinant pCEP carrying the *shp144* into pneumococcal genome. This promoter is regulated by the MalR repressor, and the binding of MalR to PM is relieved when pneumococcal cells are grown in media containing the appropriate amount of maltose (Guiral *et al*., 2006). To do this, various concentrations of maltose (25-250 µM) were firstly added to complemented *shp144* fusion culture expressing native SHP144, and the activity of P_{shp144} was then determined using β-galactosidase assay. Reporter cultures were also supplied with glucose as a main carbon source and as a control. As indicated in Figure 3.43, the β-galactosidase activity was increased from 191.7 ± 1.5 MU (n=3) in the control culture without maltose to 314.47 ± 9.94 MU (n=3) in the presence of 250 µM maltose ($p<0.001$). This change however could not be detected in culture treated with other concentrations of maltose ($p>0.05$). Data indicate that *shp144* activity in the complemented strain could be modulated by pCEP promoter when a sufficient amount of maltose is present in the culture media. The expression of *shp144* was further stimulated by mixing 250 µM maltose with 55 mM non-glucose carbon source (mannose or galactose). The results showed 3-fold change in the reporter activity compared with media containing glucose and maltose ($P<0.001$) (Figure 3.44). Thus, a mixture of 250 µM maltose and 55 mM mannose was used in the inhibition assays for stimulation *shp144* expression in native and modified complemented *shp144* strains.

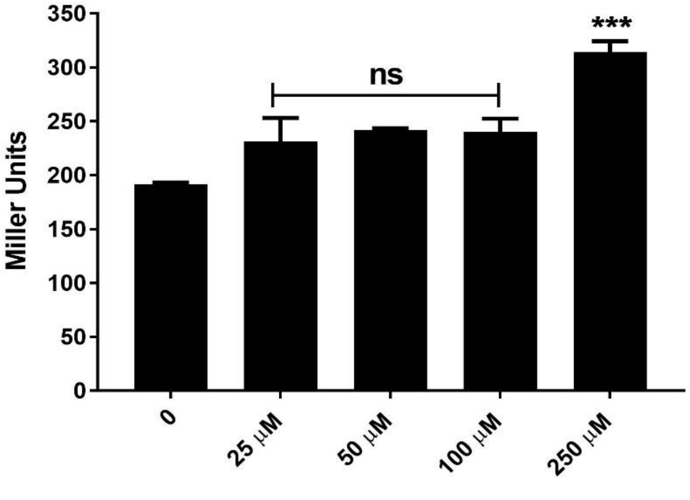

Figure 3.43: β-galactosidase levels in P$_{shp144}$::*lacZ*-Δ*shp144*Com in the presence or absence of maltose. Varying concentrations of maltose were added to pneumococcal culture and incubated to late exponential phase. The P$_{shp144}$ expression was measured using β-galactosidase assay. Values are the average of three independent experiments, each with triplicates. Error bars indicate the SEM (*** p<0.001, 'ns' not significant compared with culture free of maltose).

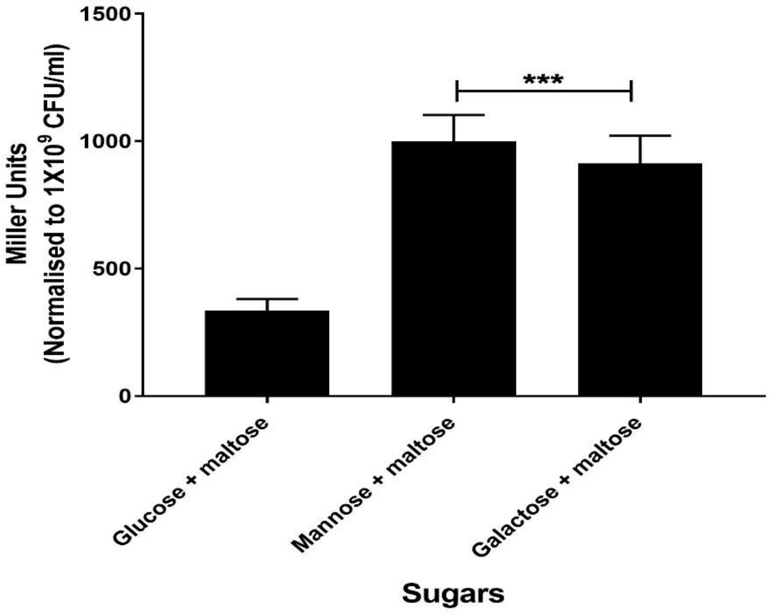

Figure 3.44: β-galactosidase activity of reporter strain P$_{shp144}$::*lacZ*-Δ*shp144*Com grown microaerobically in CDM supplemented with 250 µM maltose and other primary carbon sources (glucose, mannose or galactose). The activity is expressed in nmol *p*-nitrophenol/min/ml using late exponential phase cultures. Values represent the average of three independent experiments each with three replicates. Error bars indicate the SEM. *** p<0.001 compared with culture containing maltose and glucose.

It was expected that the addition of culture supernatants containing V17A or P21A modified SHP144 peptide would diminish the activation of P_{shp144} by endogenously produced SHP144 peptide. The strategy of inhibition is shown in Figure 3.45. The results showed, indeed, that culture supernatant with P21A modified peptide significantly decreased P_{shp144} transcriptional activity. The β-galactosidase activity was 98.64 ± 45.39 MU (n=3) compared with that achieved with wild type, 394.98 ± 30.03 MU (n=3) and complemented supernatants (347.64 ± 37.39 MU, n=3) ($p<0.05$) (Figure 3.46). Moreover, a slight reduction in β-galactosidase activity was observed by using culture supernatant containing V17A modified peptide (240.23 ± 60.04 MU, n=3). However, this change did not reach statistical significance ($p>0.05$). The inhibition by P21A was specific because the use of supernatants with L26A and N25A modifications (319.35 ± 47.63 and 340.01 ± 32.25 MU, n=3, respectively) did not have any significant impact on the induction mediated by the wild type peptide ($p>0.05$).

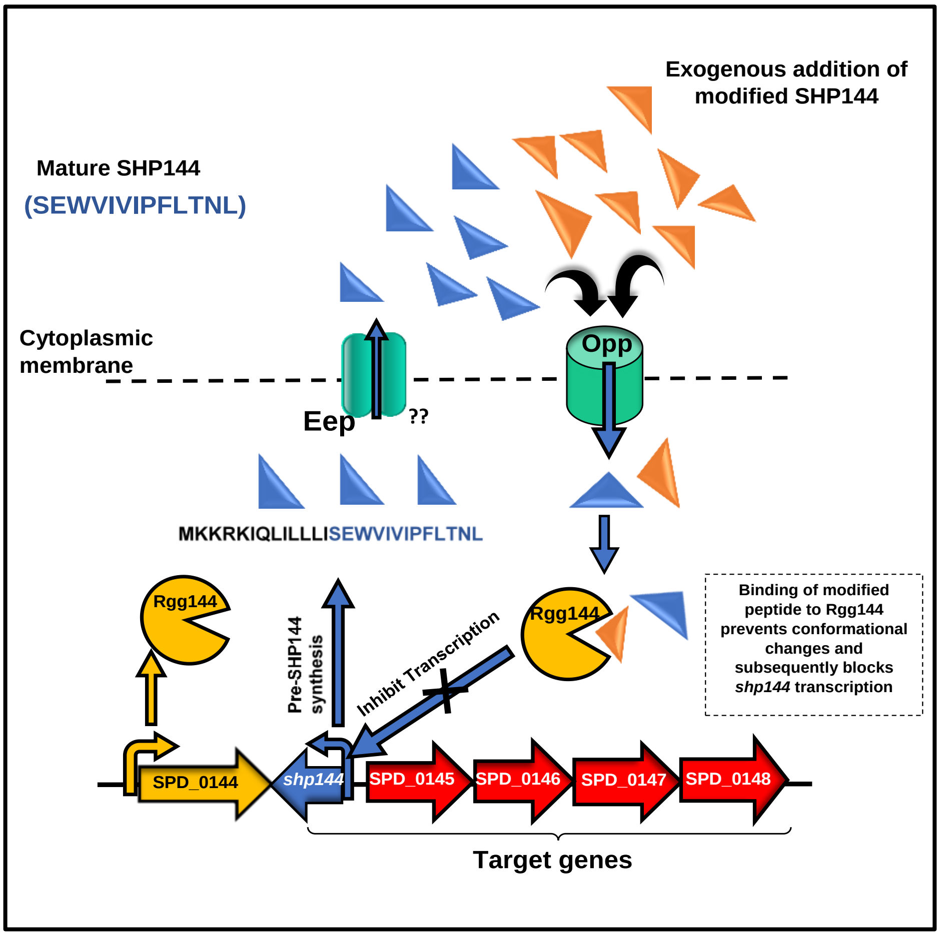

Figure 3.45: Suggested model of regulation of Rgg/SHP144 signalling pathway of *S. pneumoniae* D39 in the presence of native (Blue triangle) and modified SHP144 peptide (Brown triangle). The native pre-SHP144 is processed by Eep and released to the extracellular milieu by an unknown transporter. Once the threshold concentration is

reached, the peptide is imported inside the cell by an oligopeptide permease and directly binds to its cognate receptor Rgg144. This binding facilitates transcription activation of *shp144* and downstream genes. On the other hand, when modified SHP144 peptide was added to culture media, it competes with the native SHP144 peptide for binding to Rgg144, resulting in the inhibition of Rgg/SHP144 QS activation.

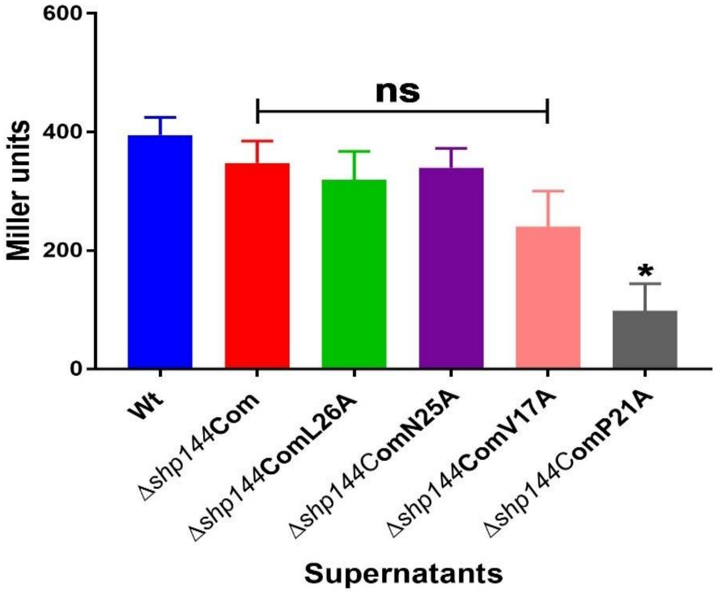

Figure 3.46: Inhibition of P_{shp144} transcription by using supernatant containing modified SHP144. The pellet of P_{shp144}::*lacZ*-Wt reporter was incubated with the supernatant of wild type, or *cis*-complemented *shp144* strains generating modified or native SHP144. The supernatant was obtained when the cultures reached late exponential phase. The P_{shp144} activity was measured by β-galactosidase assay. The error bars represent the standard error of the mean. *p<0.05, 'ns' not significant compared to wild-type supernatant producing native SHP144.

3.22. Dose dependent inhibition of *shp144* expression

To confirm that the *shp144* inhibition by P21A modified peptide is concentration dependent, a similar experiment was repeated by using serially diluted P21A modified peptide supernatants. As shown in Figure 3.47, the lowest *lacZ* induction was obtained when the reporter culture was treated with neat supernatant containing a high amount of inhibitor (61.89 ± 3.62 MU, n=3). The level of induction was gradually increased with decreasing concentration of inhibitor in diluted supernatants. The β-galactosidase activity was 285.71 ± 11.7, 641.09 ± 12.63, 664.96 ± 8.60 and 845.42 ± 9.62 MU, (n=3) for 1/2, 1/4, 1/8 and 1/16 dilutions respectively, and the activity levels were significantly different from that obtained with undiluted neat supernatant (p<0.5 and p<0.01 for 1/2, 1/4, 1/8 and

1/16 dilutions, respectively). This pattern however was not seen when the D39 wild type diluted supernatants were used. These data clearly establish the concentration-dependent inhibition of *shp144* expression by P21A peptide.

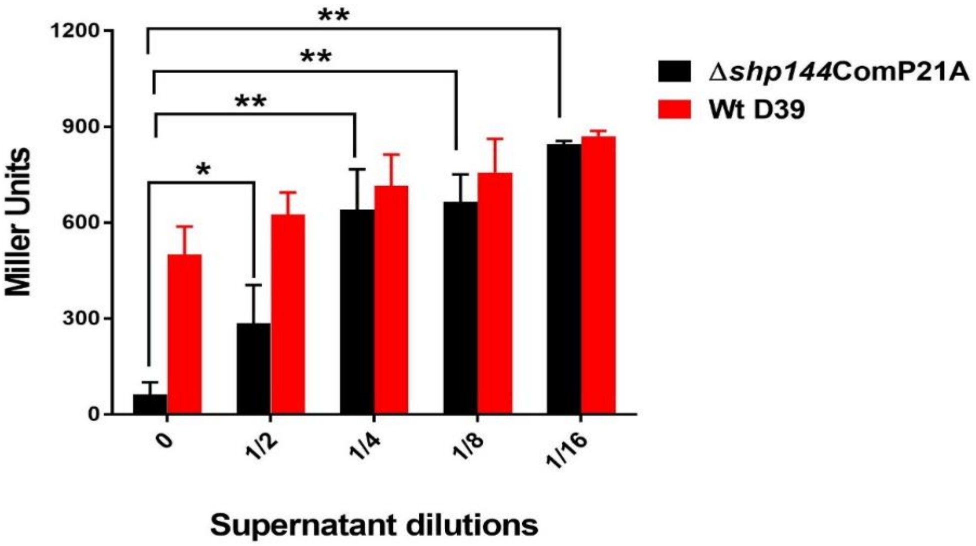

Figure 3.47: Dose-dependent inhibition of P_{shp144} transcription using diluted SHP144-C13P21A supernatants. Wild type reporter strain was incubated with the neat and diluted supernatants to an OD_{600} (~0.6) and *lacZ* activity of each culture was determined using β-galactosidase assay. Wild type D39 supernatant containing native SHP144 peptide was used as a control. The error bars represent the standard error of the mean. $*p<0.05$, $**p<0.01$ compared to P21A undiluted supernatant.

3.23. Confirmation of the inhibition of *shp144* expression by using a mixture of spent culture supernatants

The inhibitory effect of P21A peptide was further verified by a mixture of supernatants collected from wild type D39 and mutant P21A grown exponentially in media containing a combination of 55 mM mannose and 250 µM maltose. To perform this assay, different ratios of wild type and mutant P21A supernatants (wild type: mutant 1:1, 1:4, and 1:10) were mixed with the pellet of reporter strain P_{shp144}::*lacZ*-Δ*shp144*. In this assay, mutant *shp144* background was used to eliminate the induction by endogenously produced SHP144. A mixture of mutant *shp144* and wild type D39 supernatants was served as a control of assay. The results showed that at 1:10 ratio, the mutant P21A supernatant was able to significantly decrease the transcriptional activation of the system (Figure 3.48). In this setting, the β-galactosidase activity was (16.05 ± 1.05 MU, n=3), which was significantly lower than that of control culture (1:10 dilution of wild type D39 supernatant with the spent culture supernatant of Δ*shp144*) (40.12 ± 1.12 MU, n=3). No inhibition could be observed with other ratios suggesting the presence of insufficient amount of modified peptide to inhibit *shp144* expression. Hence a high load of modified P21A peptide is required to obtain a sufficient level of inhibition.

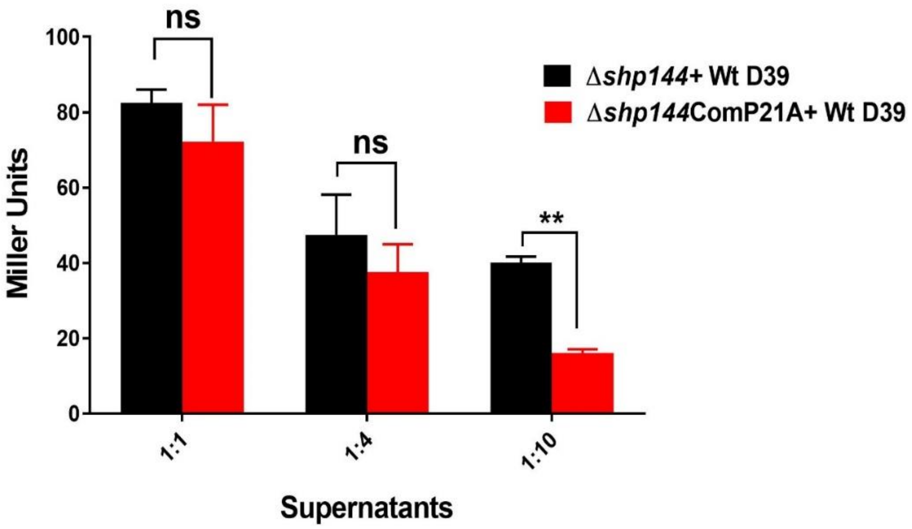

Figure 3.48: SHP144-C13P21A competitively inhibits transcriptional activation of *shp144*. Decreasing ratios of Δ*shp144*ComP21A and wild type D39 supernatants were incubated with pellet of reporter strain P$_{shp144}$::*lacZ*-Δ*shp144*, and the P$_{shp144}$ driven β-galactosidase activity was assessed (red columns). As a control the dilutions of wild type D39 supernatant in Δ*shp144* supernatant was used (black columns). Comparisons were made relative to *shp144* transcription level in culture containing mixture of Wt D39 and Δ*shp144* supernatants. **p<0.01 and 'ns 'non-significant.

Section G: The impact of inhibitor peptide on Rgg/SHP144 conferred phenotypes

Having established the capacity of modified peptide SHP144-C13P21A to abolish transcriptional activation of Rgg/SHP144, it was hypothesised that this modified peptide would abrogate the phenotypic manifestation of Rgg/SHP144 quorum sensing system, namely utilisation of mannose and oxidative stress resistance, which have been established in our group and repeated in this study.

3.24. Effect of modified SHP144-C13P21A peptide on pneumococcal growth

As demonstrated in Figure 3.26D, the pneumococcal growth in the absence of SHP144 is attenuated in CDM supplemented with 55 mM mannose relative to the wild type but no effect was observed on other sugars (Figure 3.26 A-C). To restore the growth defect of Δ*shp144* on mannose, different concentrations of modified and unmodified SHP144-C13 peptide ranging between 50-1000 nM were added to the mutant *shp144* culture, and the growth parameters were measured as described previously in Materials and Methods (Section 2.14). The growth rates and yields are presented in Table 3.6. The growth rate of all mutant *shp144* cultures were identical, regardless of the presence of peptide ($p>0.05$). While, the maximum OD_{600} of mutant *shp144* was reconstituted when 1000 nM and 500 nM of SHP144-C13 were added to the culture medium. As their growth yields were (0.391 ± 0.015 and 0.320 ± 0.019, n=3 respectively), statistically higher than that in the absence of peptide ($p<0.0001$ and $p<0.01$ for 1000 nM and 500 nM) (Figure 3.49 D-E). This difference, however, could not be observed when other concentrations of SHP144-C13 (50-250 nM) were used ($p>0.05$) (Figure 3.49 A-C). On the other hand, this complementation could not be observed by the addition of the same concentrations of peptide carrying either S14A or P21A modifications on mannose, showing the specificity of peptide for functional complementation (Figure 3.49 and Table 3.6). Furthermore, no effect was seen by using other sugars (glucose or galactose) as a main source of carbon (Figure 3.50 A-B and Table 3.7) ($p>0.05$). This data supports my hypothesis that the SHP144-C13 peptide can reconstitute the growth profile of mutant *shp144* in the media containing mannose.

(A)

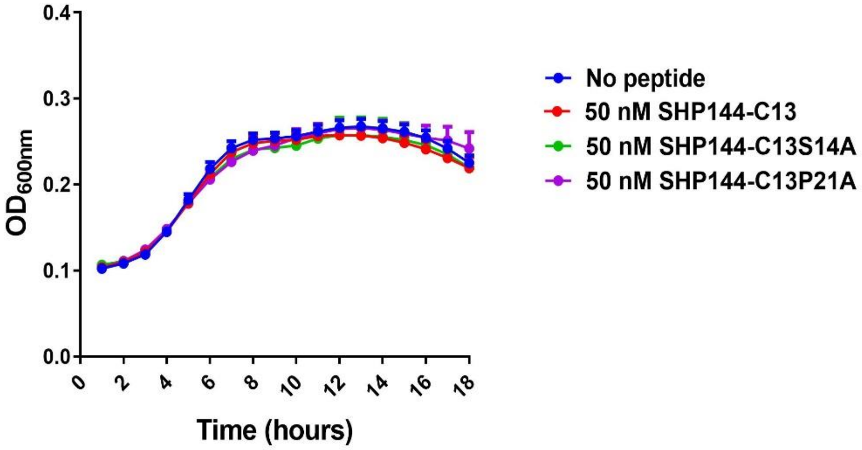
0.4
0.3
0.2
0.1
0.0
OD_{600nm}
0
2
4
6
8
10
12
14
16
18
Time (hours)
No peptide
50 nM SHP144-C13
50 nM SHP144-C13S14A
50 nM SHP144-C13P21A

(B)

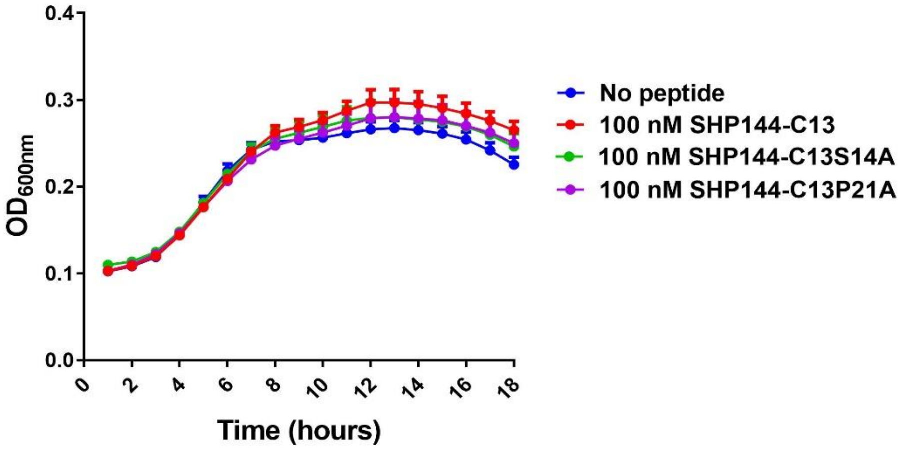
0.4
0.3
0.2
0.1
0.0
OD_{600nm}
0
2
4
6
8
10
12
14
16
18
Time (hours)
No peptide
100 nM SHP144-C13
100 nM SHP144-C13S14A
100 nM SHP144-C13P21A

(C)

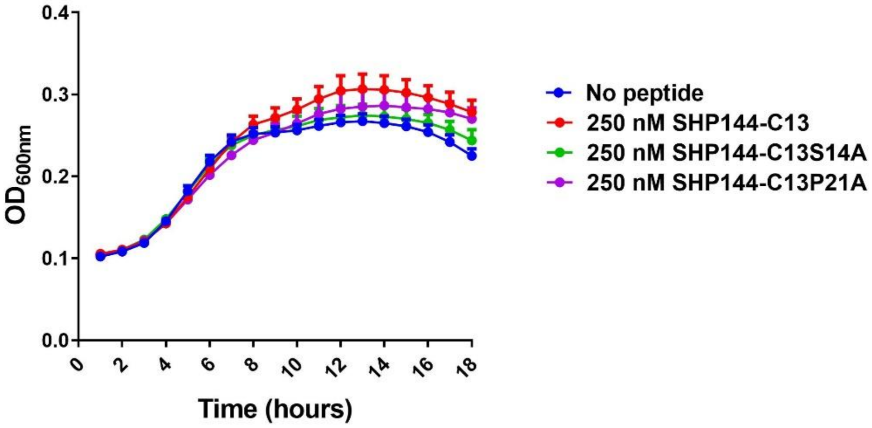
0.4
0.3
0.2
0.1
0.0
OD_{600nm}
0
2
4
6
8
10
12
14
16
18
Time (hours)
No peptide
250 nM SHP144-C13
250 nM SHP144-C13S14A
250 nM SHP144-C13P21A

(D)

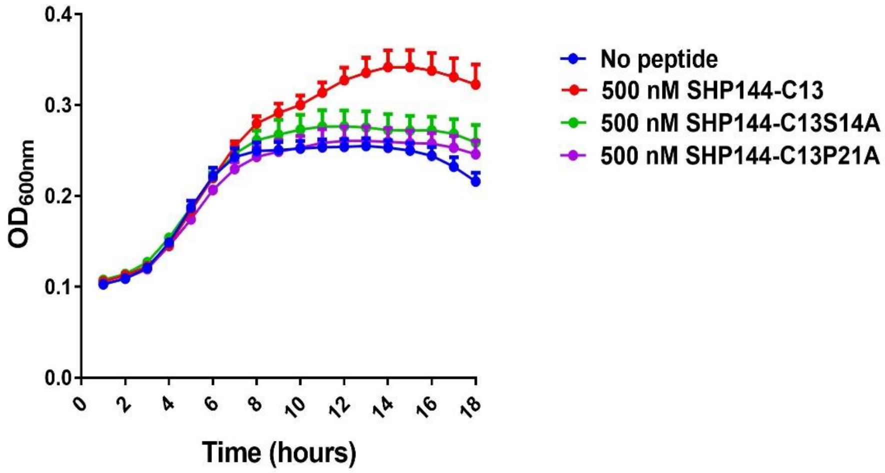

(E)

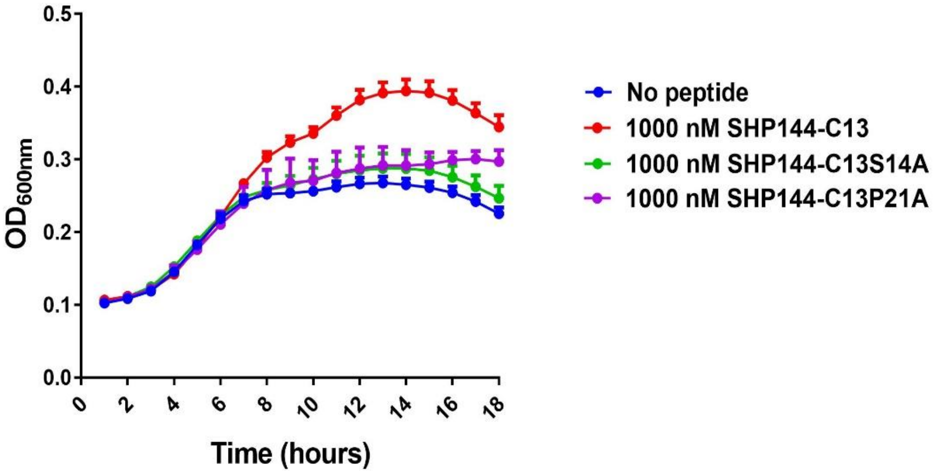

Figure 3.49: (A-E) Exogenous addition of different concentrations of SHP144-C13 synthetic peptide reconstitutes mutant *shp144* growth. Various concentrations of native and modified SHP144-C13P21A or S14A were added to Δ*shp144* culture to reconstitute the pneumococcal growth defect on mannose. No growth complementation could be observed by using modified peptides. This experiment was repeated for three independent biological samples and each with three replicates.

Table 3.6: Showing growth rate (µ) and yield (maximal OD_{600}) of Δ*shp144* strain grown microaerobically in CDM supplemented with 55 mM mannose, and in the presence of different concentrations of modified or unmodified SHP144-C13 peptide. Values are average of three independent experiments each with three replicates. '±' indicates standard error of means (SEM). Comparisons are made relative to mutant *shp144* culture lacking peptide using one-way ANOVA and Dunnett's multiple comparisons test. **p<0.01 and ****p<0.0001.

Peptide concentration	**CDM-mannose**	
	Growth rate (h^{-1})	**Growth yield**
No peptide	0.027 ± 0.001	0.252 ± 0.008
50 nM SHP144-C13	0.025 ± 0.002	0.248 ± 0.008
50 nM SHP144-C13P21A	0.023 ± 0.002	0.240 ± 0.008
50 nM SHP144-C13S14A	0.024 ± 0.002	0.241 ± 0.009
No peptide	0.022 ± 0.001	0.254 ± 0.007
100 nM SHP144-C13	0.025 ± 0.001	0.269 ± 0.009
100 nM SHP144-C13P21A	0.022 ± 0.002	0.255 ± 0.010
100 nM SHP144-C13S14A	0.023 ± 0.002	0.262 ± 0.013
No peptide	0.023 ± 0.0009	0.260 ± 0.007
250 nM SHP144-C13	0.024 ± 0.0039	0.262 ± 0.023
250 nM SHP144-C13P21A	0.022 ± 0.0018	0.254 ± 0.011
250 nM SHP144-C13S14A	0.022 ± 0.0020	0.257 ± 0.013
No peptide	0.026 ± 0.002	0.249 ± 0.009
500 nM SHP144-C13	0.021 ± 0.002	**0.320 ± 0.019****
500 nM SHP144-C13P21A	0.025 ± 0.002	0.243 ± 0.011
500 nM SHP144-C13S14A	0.027 ± 0.002	0.261 ± 0.011
No peptide	0.027 ± 0.001	0.252 ± 0.008
1000 nM SHP144-C13	0.027 ± 0.002	**0.391 ± 0.015******
1000 nM SHP144-C13P21A	0.027 ± 0.002	0.258 ± 0.012
1000 nM SHP144-C13S14A	0.027 ± 0.002	0.288 ± 0.020

(A)

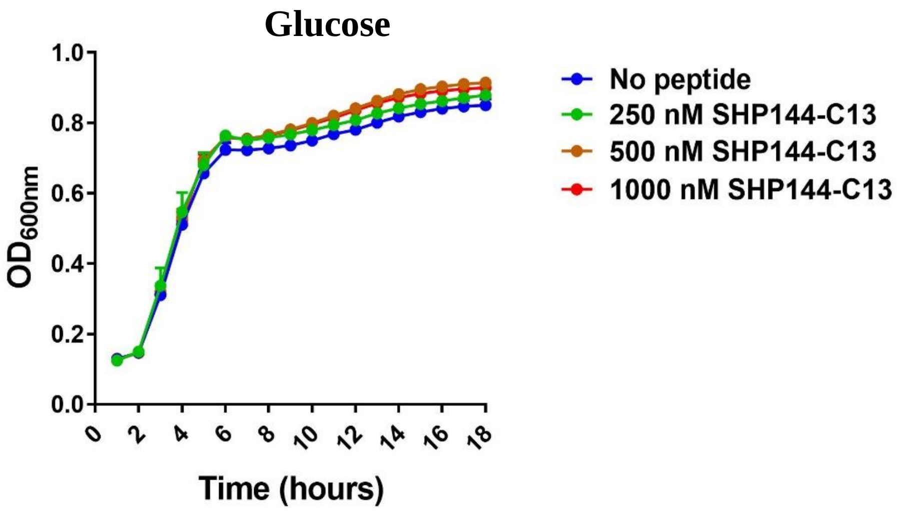

(B)

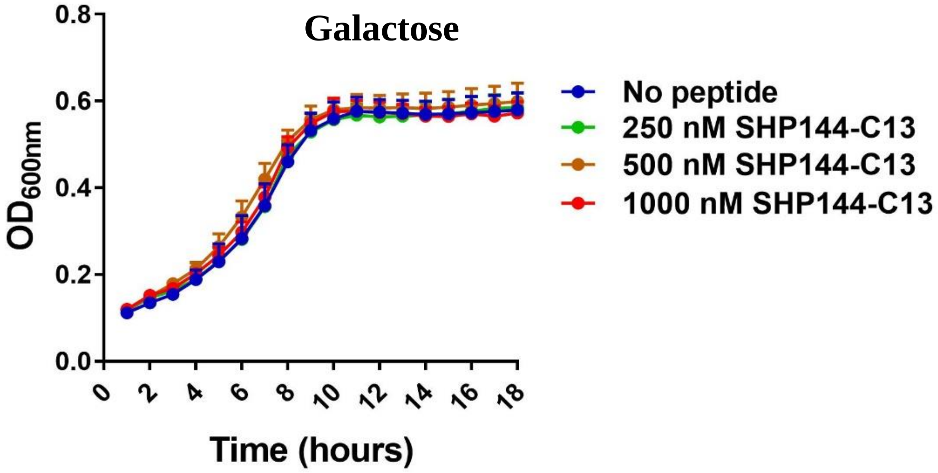

Figure 3.50: Identification the impact of SHP144-C13 synthetic peptide on Δ*shp144* growth in media containing either glucose **(A)** or galactose **(B)**. No effect could be observed in both culture media . Comparisons are made relative to Δ*shp144* culture without peptide. Error bars indicate the standard error of the mean (SEM). The values were averaged from three independent experiments each with three replicates.

Table 3.7: Growth rate (µ) and yield (maximal OD_{600}) of Δ*shp144* strain grown microaerobically in CDM containing 55 mM glucose or galactose with 250-1000 nM of SHP144-C13. Values are average of three independent experiments each with three replicates. '±' indicates standard error of means (SEM).

SHP144-C13	**CDM-glucose**		**CDM-galactose**	
	Growth rate (h^{-1})	**Growth yield**	**Growth rate (h^{-1})**	**Growth yield**
No peptide	0.144 ± 0.005	0.723 ± 0.020	0.058 ± 0.004	0.559 ± 0.039
250 nM	0.154 ± 0.002	0.769 ± 0.009	0.056 ± 0.002	0.557 ± 0.017
500 nM	0.153 ± 0.002	0.759 ± 0.007	0.057 ± 0.003	0.580 ± 0.027
1000 nM	0.153 ± 0.001	0.758 ± 0.007	0.055 ± 0.005	0.569 ± 0.055

Next, the peptide with the P21A modification was used to determine its impact on growth of wild type *S. pneumoniae* on mannose. Various concentrations of modified peptide ranging from 50 to 1000 nM were individually added to the wild type D39 culture, and their effects on growth profile (growth rate and yield) were monitored as described previously in section 2.14. As expected, SHP144-C13P21A reduced the pneumococcal growth, very likely through competitive inhibition of wild type SHP144 peptide in CDM supplemented with mannose and in a dose dependent manner (Figure 3.51). As shown in Figure 3.51B and Table 3.8, addition of 500 nM modified peptide resulted in a significant reduction in both growth rate (0.015 ± 0.0007 h^{-1}, n=3) ($p<0.01$) and yield (0.209 ± 0.005, n=3) ($p<0.0001$) relative to culture without peptide. In addition, further reduction was seen in culture treated with 1000 nM of modified peptide (Figure 3.51C and Table 3.8), as the growth rate was 0.009 ± 0.0006 h^{-1} and yield 0.167 ± 0.004, n=3 ($p<0.0001$). This inhibition, however, could not be seen by using 250 nM of SHP144-C13P21A (Figure 3.51A and Table 3.8). In addition, inhibition by modified peptide was specific because the use of the same concentrations of peptides with different modifications (SHP144-C13V19A and SHP144-C13E15A) had no effect on pneumococcal growth. It can conclude from these results that SHP144-C13P21A has capacity to diminish pneumococcal growth on mannose through competitive inhibition of Rgg144 activation.

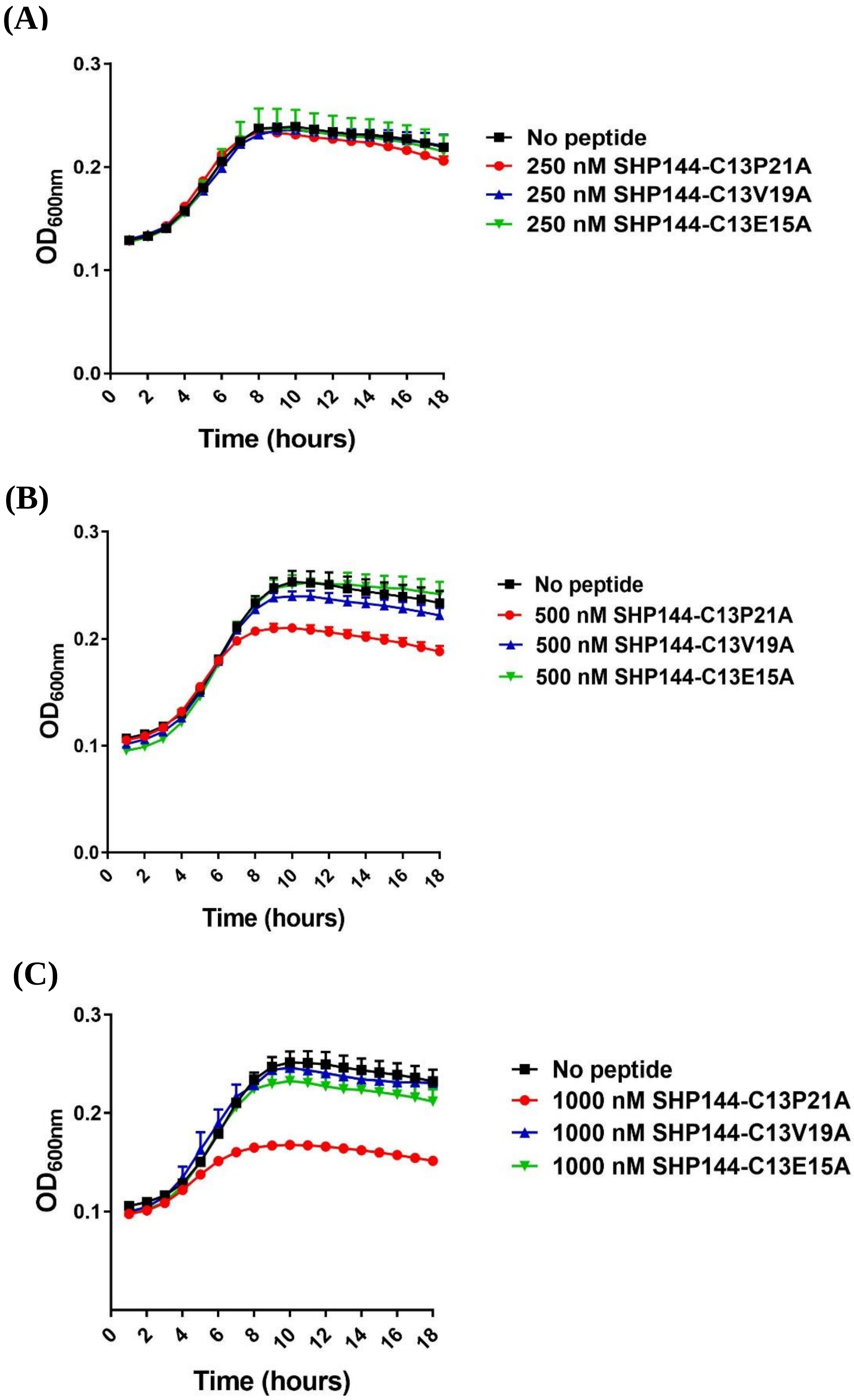

Figure 3.51: Effect of SHP144-C13P21A on pneumococcal growth in media supplemented with mannose. Addition of 500 nM **(B)** and 1000 nM **(C)** of SHP144-C13P21A attenuate wild type growth, whereas no impact could be observed by using 250 nM **(A)**. In addition, peptides with different modifications (SHP144-C13V19A and SHP144-C13E15A) had no influence on the growth compared to cultures that did not receive peptide. Each experiment was performed three times in triplicates.

Table 3.8: Growth rate (µ) and yield (maximal OD_{600}) of wild type D39 strain grown microaerobically in CDM supplemented with 55 mM mannose and in the presence of different concentrations of modified SHP144-C13P21A peptide. Values are average of three independent experiments each with three replicates. '±' indicates standard error of means (SEM). One-way ANOVA and Dunnett's multiple comparisons tests were used for calculation of growth parameters. **p<0.01, ****p<0.0001 compared with wild type culture did not receive modified peptide.

Peptide concentration	**CDM-mannose**	
	Growth rate (h^{-1})	**Growth yield**
No peptide	0.017 ± 0.0003	0.238 ± 0.003
250 nM SHP144-C13P21A	0.017 ± 0.0007	0.234 ± 0.004
250 nM SHP144-C13V19A	0.016 ± 0.0008	0.231 ± 0.006
250 nM SHP144-C13E15A	0.017 ± 0.0030	0.237 ± 0.020
No peptide	0.020 ± 0.0012	0.254 ± 0.008
500 nM SHP144-C13P21A	**0.015 ± 0.0007****	**0.209 ± 0.005******
500 nM SHP144-C13V19A	0.021 ± 0.0013	0.238 ± 0.005
500 nM SHP144-C13E15A	0.019 ± 0.0009	0.247 ± 0.008
No peptide	0.020 ± 0.006	0.249 ± 0.009
1000 nM SHP144-C13P21A	**0.009 ± 0.0006******	**0.167 ± 0.004******
1000 nM SHP144-C13V19A	0.018 ± 0.0017	0.244 ± 0.003
1000 nM SHP144-C13E15A	0.020 ± 0.0008	0.230 ± 0.010

3.25. Impact of modified SHP144-C13P21A peptide on pneumococcal oxidative stress resistance

The phenotypic impact of SHP144-C13P21A on pneumococcal oxidative stress resistance was determined following the protocol previously described in section 2.26.1. When the pneumococci were treated with 1 mM of the superoxide radical generator paraquat, a significant adverse impact on Δ*shp144* survival was seen relative to the wild type (p<0.01). For example, after 1-hour incubation while 91% of wild type survived, only 65% of Δ*shp144* CFU/ml could be recovered (Figure 3.28A). As expected, the addition of SHP144-C13 to Δ*shp144* reconstituted the pneumococcal resistance to paraquat (Figure 3.52A). The survival percentage of mutant *shp144* in the presence of 1 µM SHP144-C13 (92.5%) was significantly higher than that without peptide (p<0.05). This response was specific for

SHP144-C13, as using the same concentration of SHP144-C13S14A had no effect on pneumococcal survival (p>0.05).

Furthermore, the use of 10 µM SHP144-13P21A, but not SHP144-C13S14A, rendered the wild type *S. pneumoniae* susceptible to killing by 1 mM paraquat. The survival percentage of wild type D39 (94.5%) dropped to 72.5% when pneumococci were treated with 10 µM of SHP144-C13P21A (p<0.05) (Figure 3.52B). These data clearly show the inhibitory effect of SHP144-C13P21A on pneumococcal oxidative stress induced by paraquat.

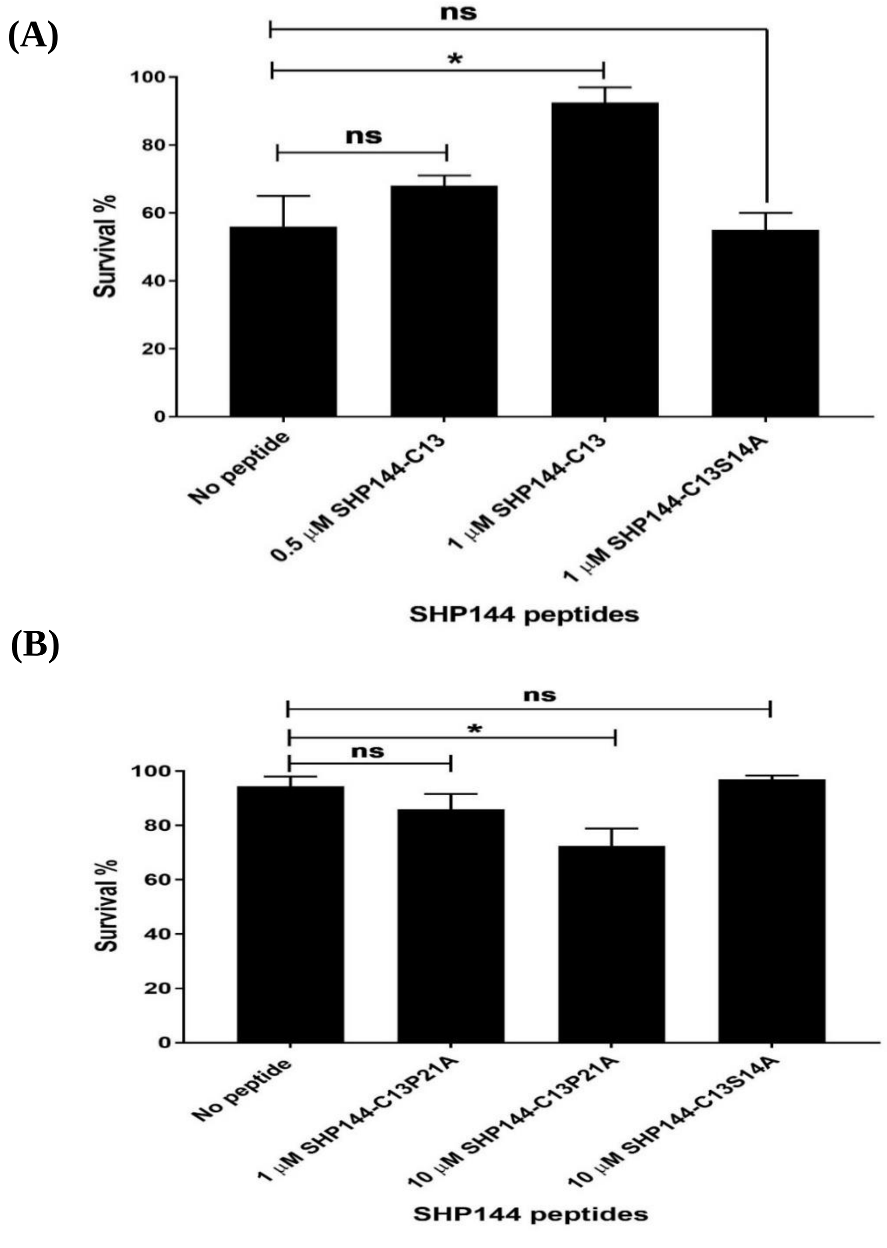

Figure 3.52: Survival of pneumococcal strains following treatment with 1 mM paraquat. **(A)** Addition of 1 µM of SHP144-C13 reconstitutes Δ*shp144* oxidative stress resistance,

but not the peptide with S14A modification. **(B)** Inhibition of pneumococcal oxidative stress resistance by using 10 µM of SHP144-C13P21A. This inhibition could not be seen by using S14A modified peptide. The survival percentages were calculated for each strain grown in THY, and in the presence or absence of selected peptide. Comparisons are made relative to wild type or Δ*shp144*. Data represent the average of three independent experiments, each with triplicates. $^*p<0.05$, 'ns' non- significant.

The inhibitory effect of P21A modified peptide on pneumococcal oxidative stress was further confirmed by challenging wild type D39 treated with 10 µM inhibitor with 20 mM H_2O_2. Approximately 93.5% of wild type D39 cells survived after treatment with 20 mM H_2O_2, while this number reduced to 68.5% when pneumococcal cells were treated with the inhibitor peptide ($p<0.05$) (Figure 3.53A). However, this effect could not be observed when peptide with S14 modification was employed ($p>0.05$) supporting the conclusion that the presence of SHP144-C13P21A in culture media impaired pneumococcal resistance to toxic effects of H_2O_2.

Finally, addition of 10 µM SHP144-C13 to mutant *shp144* culture increased the survival percentage of pneumococcal cells challenged with 20 mM H_2O_2. Without peptide, the survival rate was 56.5%, and this rate increased to 95% in culture treated with unmodified peptide ($p<0.05$) (Figure 3.53B). The findings confirm my previous data that the SHP144-C13 reconstitutes pneumococcal tolerance against reactive oxygen species.

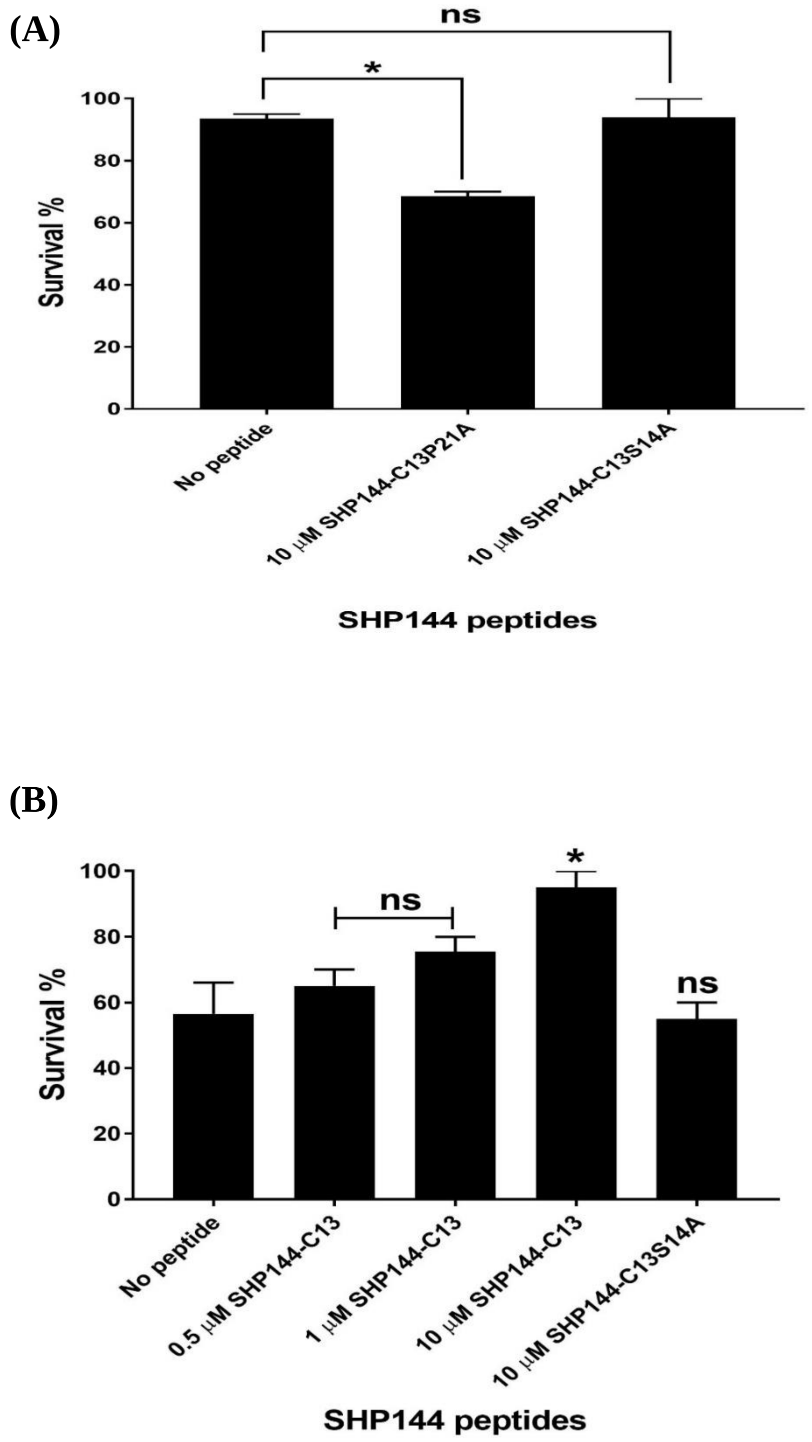

Figure 3.53: The effect of SHP144-C13P21A **(A)** and SHP144-C13 **(B)** peptides on pneumococcal resistance after exposure to 20 mM H_2O_2. The survival percentages were calculated for each strain grown in THY, and in the presence or absence of selected peptide. Comparisons are made relative to wild type or Δ*shp144*. Data represent the average of at least three independent experiments, each with triplicates. *p<0.05, ‘ns’ non- significant.

Section H: *In vivo* studies

In line with our previous study (Zhi *et al*., 2018), the data obtained in this study showed the involvement of SHP144 and Rgg144 in regulation of *shp144* expression. Rgg/SHP144 QS plays a significant role in pneumococcal survival *in vitro,* as mutation of these genes attenuate pneumococcal growth on mannose and decrease the oxidative stress resistance against reactive oxygen species as well as biofilm formation. Furthermore, most of the SHP144 residues showed their involvements in Rgg144-mediated transcription using transcriptional fusions. Moreover, some of modified strains (Δ*shp144*ComI18A, I20A and P21A) displayed lower growth in media containing mannose (one of the prominent carbohydrates in the respiratory tract involved in pneumococcal colonisation) (Robb *et al*., 2017). Likewise, strains with E15, I20, P21 modifications revealed lower resistance to toxic effects of paraquat and H_2O_2. Thus, based on data provided above it was hypothesised that the peptides with these modifications will have a significant role in pneumococcal virulence *in vivo*. To test this hypothesis, modified *shp144* strains (Δ*shp144*ComE15A, Δ*shp144*ComI20A and Δ*shp144*ComP21A) were selected to test in murine colonisation model.

Animal models are widely used to study the pathogenesis of infectious diseases and efficacy of drugs and vaccines. Mouse is a well-established experimental model, because of genetic similarity between mice and human. It is inexpensive and easy to breed and can be manipulated compared with other large animals (Ernst, 2016), which allow the scientists to use high number of mice in a single study to obtain significant results (Mohawk and O'Brien, 2011). Inbred strains are largely used to examine the efficacy of vaccines and drugs as they have tightly controlled immune systems making their responses to experimental treatment more uniform, while outbred strains are employed to study the pathogenicity mechanisms of infectious diseases like pneumonia, sepsis and meningitis as outbred mice are characterised by genetic diversity (Chiavolini *et al*., 2008). For *S. pneumoniae,* mouse models are considered the most important tools for examination of the key features of pneumococcal virulence and the host immune responses to infection (Kadioglu and Andrew, 2005). Intranasal administration is the most popular route for pneumococcal pneumonia as it is fast, easy to perform, there is no need for surgical procedures, and it mimics the natural route of infection in humans (Chiavolini *et al*., 2008).

3.26. Colonisation model

Nasopharyngeal colonisation by *S. pneumoniae* is a prerequisite to spread the infection to the lungs or bloodstream (Bogaert *et al*., 2004; Ramos-Sevillano *et al*., 2011). To study the effect of *shp144* deletion or introducing a modification into the coding sequence of *shp144* on nasopharyngeal colonisation, the *shp144* mutant, the genetically complemented mutants with native or modified *shp144* (Δ*shp144*Com, Δ*shp144*ComE15A, Δ*shp144*ComI20A and Δ*shp144*ComP21A) strains, and the wild type D39 strain were examined as previously described in section 2.35.2. These modified strains were selected for *in vivo* work, as they are involved in *shp144* transcriptional activation and the Rgg/SHP144 phenotypic characterisations. The Δ*shp144*ComE15A was also selected based on previous studies showing that the glutamate residue at the C-terminus is highly conserved among the SHP family, and predicted to be important for SHP maturation and activation (Chang *et al*., 2011; Fleuchot *et al*., 2013).

Pneumococci were administered intranasally and viable cells were enumerated by serial dilution of nasopharyngeal washes of infected mice at the time of infection and 7 days after infection. The density of colonisation was expressed as mean $\log_{10}$ CFU/ml of nasopharyngeal wash ± SEM. One hour after intranasal administration, the bacterial load in the nasopharyngeal wash for Δ*shp144*, Δ*shp144*ComE15A, Δ*shp144*ComI20A and Δ*shp144*ComP21A ($\log_{10}$ 3.85 ± 0.23, $\log_{10}$ 4.28 ± 0.16, $\log_{10}$ 4.25 ± 0.12 and $\log_{10}$ 3.78 ± 0.15 CFU/ml respectively, n =5) was similar to that of wild type and complemented *shp144* strain ($\log_{10}$ 3.80 ± 0.23 and $\log_{10}$ 3.90 ± 0.15 CFU/ml, n =5 respectively) ($p>0.05$) (Figure 3.54A). On the other hand, at 7-day post-infection the colony count for Δ*shp144* ($\log_{10}$ 1.02 ± 0.63 CFU/ml, n =5) was significantly lower than the count of wild type strain ($\log_{10}$ 4.18 ± 0.21 CFU/ml, n=5) ($p<0.01$). Similarly, the colony counts for Δ*shp144*ComI20A and Δ*shp144*ComP21A ($\log_{10}$ 1.48 ± 0.88 and $\log_{10}$ 1.43 ± 0.84 CFU/ml respectively, n=5), were less than those for complemented strain ($\log_{10}$ 4.33 ± 0.13 CFU/ml, n=5) ($p<0.05$) (Figure 3.54B). But no significant difference in the bacterial load of modified strain Δ*shp144*ComE15A could be seen ($p>0.05$). In addition, reintroduction of an intact copy of *shp144* into Δ*shp144* reconstituted the virulence of mutant strain ($\log_{10}$ 4.33 ± 0.13 CFU/ml, n=5), not significantly different from the wild type count ($p>0.05$). The results obtained with the complemented strain indicate that the observed *in vivo* attenuation is due to the *shp144* deletion rather than a polar effect of the mutation.

These results strongly suggest that insertional inactivation of the *shp144* gene in the type 2 strain D39 significantly reduced pneumococcal colonisation in mouse model. Similarly, introducing a modification into coding sequence of *shp144* particularly at positions I20 and P21 makes pneumococcal cells less able to colonise the nasopharynx of mice.

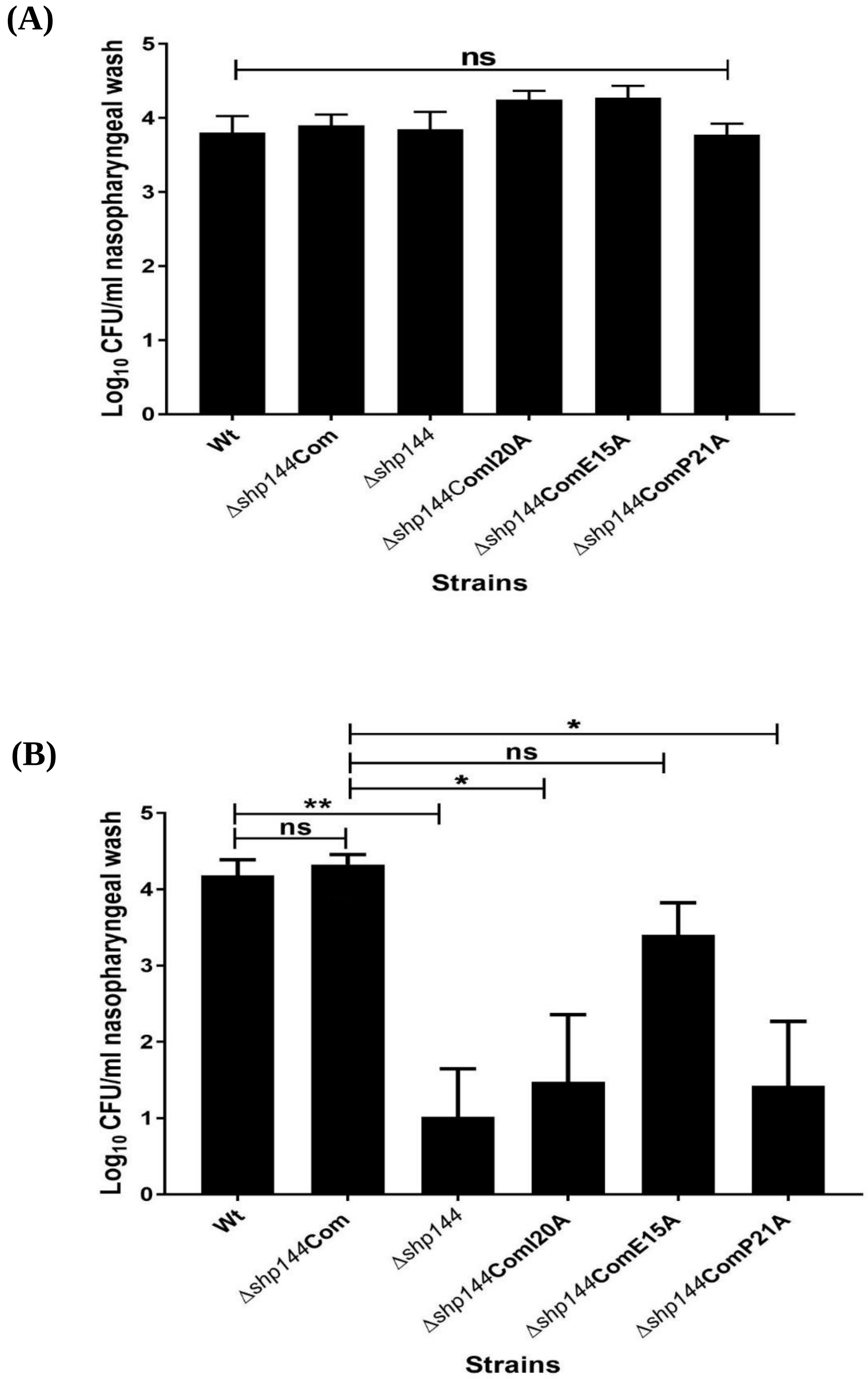

Figure 3.54: Pneumococcal strains lacking *shp144* or having modified *shp144* are less able to colonise nasopharynx**.** Mice were challenged with approximately $1x10^5$ CFU

pneumococci. Infected mice were culled at day 0 **(A)** and day 7 **(B)**, and CFU/ml of bacteria were calculated by serial dilutions of nasopharyngeal wash. Each bar represents the mean of data collected from five mice. Error bars show the standard error of the mean. Significance changes in bacterial counts are compared with wild type and complemented strains using one-way ANOVA and Tukey's multiple comparisons test (*p<0.05, **p<0.01, ‘ns’ not significant).

3.27. The inhibitory effect of modified SHP144 on pneumococcal colonisation

Following demonstration of the inhibitory effect of the peptide with the P21 modification on Rgg/SHP144 conferred phenotypes *in vitro* (growth parameters and oxidative resistance), it was hypothesised that this peptide might have a role in pneumococcal colonisation when added exogenously. Prior to commencing the *in vivo* experiments, synthetic peptides were checked for their toxicity on the host. Four mice were inoculated intranasally with 200 µM of synthetic peptide (SHP144-C13P21A or SHP144-C13) at different time points (0, 24, 48 and 72 h) and signs of illness was monitored for 5 days following administration. The results demonstrated that the synthetic peptides lacked toxicity.

To examine the inhibitory effect of modified peptide on pneumococcal virulence *in vivo*, the 2.5×10^5 CFU of pneumococcal D39 wild type with or without 200 µM modified peptide SHP144-C13P21A were administered to mice as described previously (Section 2.35.3). Another group received the same dose supplemented with 200 µM of unmodified peptide SHP144-C13. The cohorts infected with modified or unmodified peptides received additional doses of peptide (200 µM) in 20 µl PBS at predetermined times (24, 48 and 72 h post infection) whereas the control group received only 20 µl PBS. The counts for all the groups were determined in nasopharyngeal wash at the time of infection, and at 5 days after infection. All the mice had the same bacterial load in nasopharyngeal washes immediately after infection (Figure 3.55A). Likewise, no significant differences were observed in colony counts between infected cohorts at day 5 post infection for wild type (Wt + PBS), Wt + SHP144-C13 and Wt + SHP144-C13P21A ($\log_{10}$ 4.62 ± 0.22, $\log_{10}$ 4.24 ± 0.24 and $\log_{10}$ 4.58 ± 0.04 CFU/ml respectively, n=5) ($p>0.05$) (Figure 3.55B). These data indicate that modified SHP144-C13P21A did not impaired the virulence of D39 in these conditions.

To investigate whether exogenous addition of synthetic peptide SHP144-C13 reconstitutes the capacity of Δ*shp144* to colonise the nasopharynx. A parallel colonisation experiment was done as above by infecting the mice with 20 µl inoculum containing $2.5x10^5$ Δ*shp144* with or without 200 µM SHP144-C13 synthetic peptide as previously mentioned in section 2.35.3. The CFU counts of infected mice are shown in Figure 3.55C and D. No phenotypic difference could be observed in the number of Δ*shp144* in the presence or absence of synthetic peptide at days 0 and 5 days post inoculation ($p>0.05$). As the colony counts for Δ*shp144* + PBS and Δ*shp144* + SHP144-C13 at the time of infection ($\log_{10}$ 4.46 ± 0.24 and $\log_{10}$ 4.18 ± 0.08 CFU/ml respectively, n =5) and 5 days post-infection ($\log_{10}$ 3.09 ± 0.18 and $\log_{10}$ 3.18 ± 0.17 CFU/ml respectively, n =5) were the same. The results suggest that SHP144-C13 peptide was unable to restore the virulence defect of Δ*shp144*.

While these initial experiments did not show any impact of synthetic peptides on pneumococcal colonisation, more work beyond this study is required to optimise the dose of peptide, time, route of infection in addition to determination of ADME (absorption, distribution, metabolism, and elimination) of peptide.

(A)

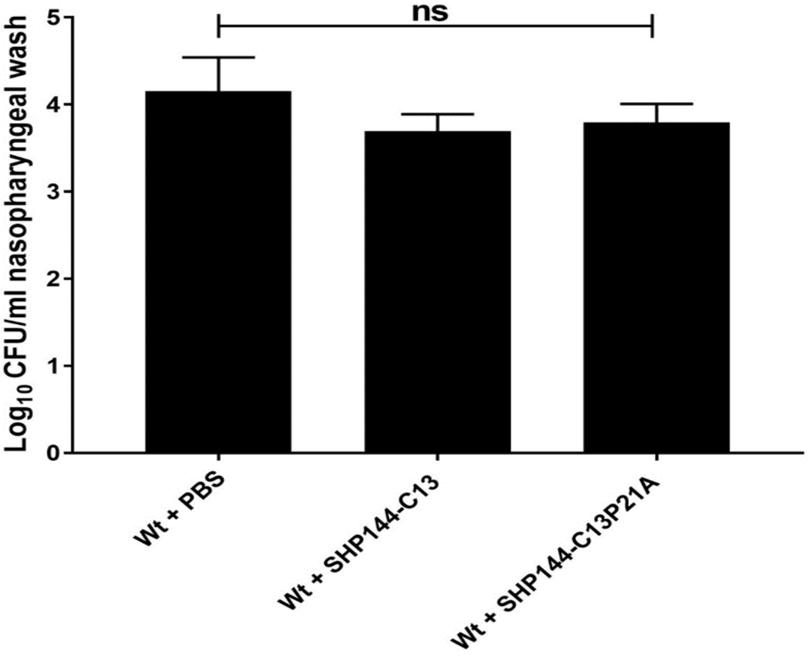

(B)

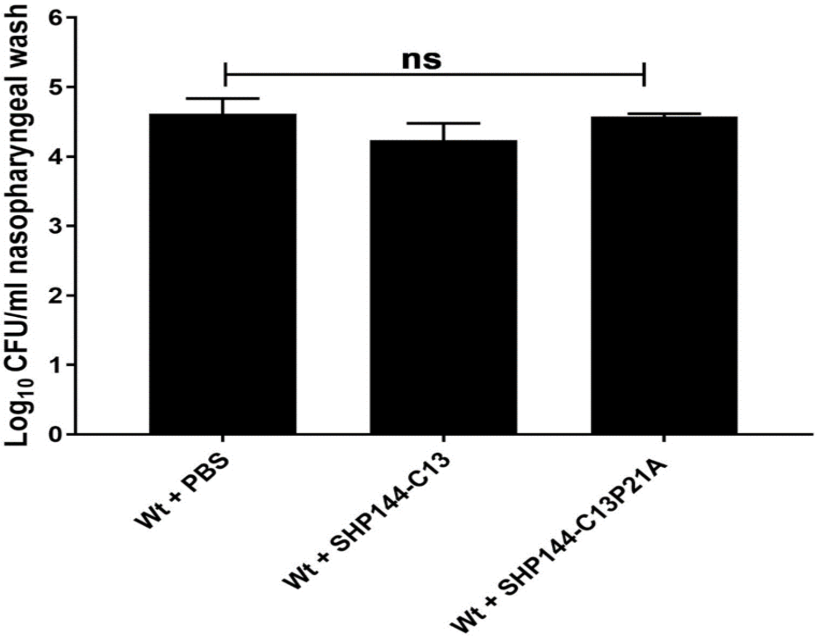
Log$_{10}$ CFU/ml nasopharyngeal wash
6
5
4
3
2
1
0
ns
Wt + PBS
Wt + SHP144-C13
Wt + SHP144-C13P21A

(C)

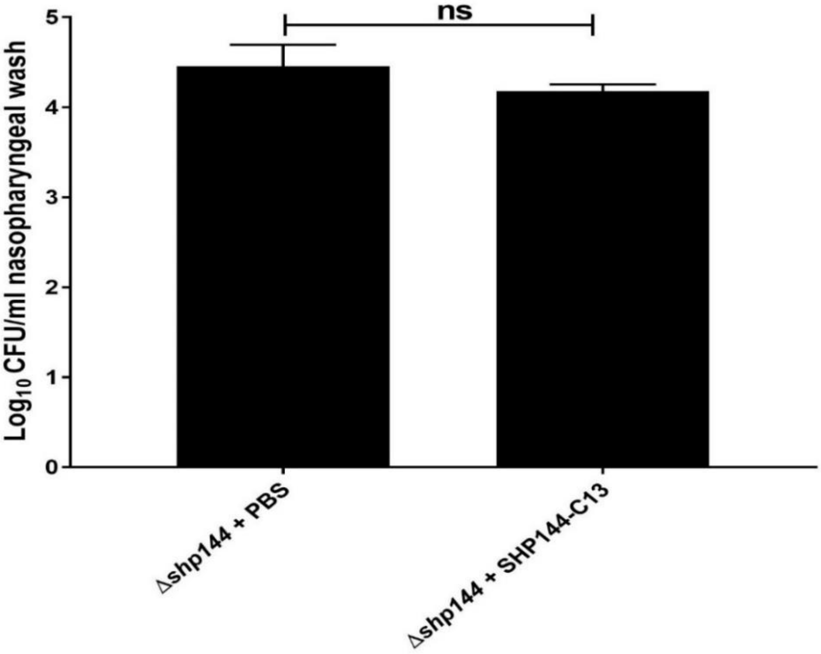
Log$_{10}$ CFU/ml nasopharyngeal wash
5
4
3
2
1
0
ns
Δshp144 + PBS
Δshp144 + SHP144-C13

(D)

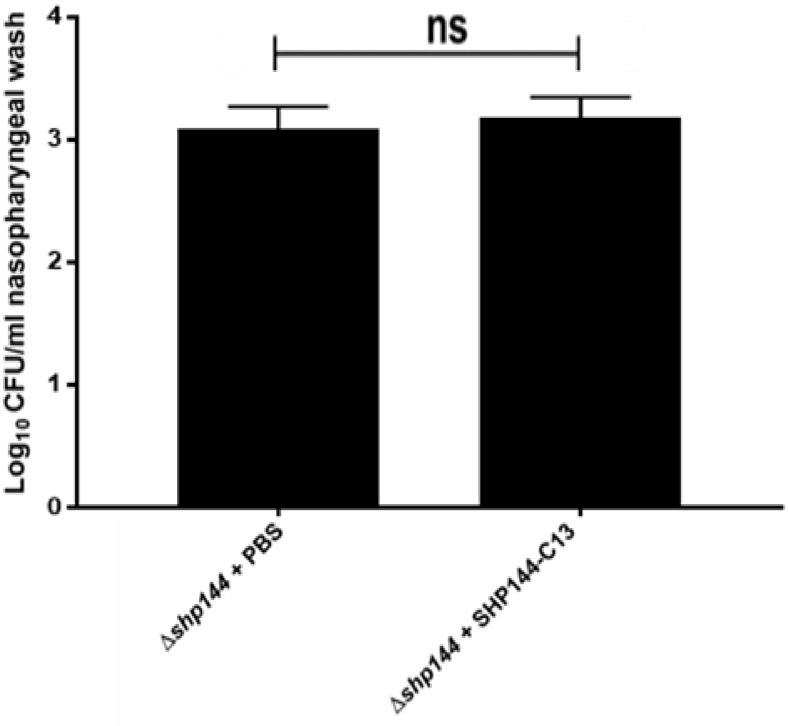

Figure 3.55: Identification the impact of SHP144 synthetic peptides on pneumococcal colonisation in murine model. **(A-B)** mice infected intranasally either with 2.5x10^5 CFU/mouse of pneumococcal D39 wild type (control) or the inoculum containing 200 µM of SHP144-C13P21A or SHP144-C13. The latter peptide was used to check the specificity of assay. While **(C-D)** groups of mice received 2.5x10^5 CFU/Δ*shp144* supplemented with or without 200 µM of SHP144-C13. The cohorts infected with modified or unmodified peptides received additional doses of peptide (200 µM) at predetermined times (24, 48 and 72 h post infection) whereas control group received only 20 µl PBS. The mice at day 0 and 5 were sacrificed by cervical dislocation and nasal washes were obtained and processed as described before. Error bars show the standard error of the mean. One-way ANOVA followed by Tukey’s multiple comparison tests, and two-tailed unpaired student’s *t*-test were applied to compare the bacterial counts with control groups (n=5 for each group, ‘ns’ not significant).

Chapter 4. Discussion

Streptococcus pneumoniae resides asymptomatically in the nasopharynx of healthy individuals, but under certain circumstances it converts its lifestyle from a commensal to parasitic one, causing moderate to severe infections like pneumonia, bacteremia, meningitis, and otitis media (Shak *et al*., 2013). The pneumococci encounter variable environmental conditions during colonisation and invasion of host tissues such as exposure to oxidative stress, fluctuating temperature, and nutrient limitation (Aprianto *et al*., 2018). Thus, sensing and responding to these environmental cues are of utmost importance for bacterial fitness and survival (Hendriksen, 2010). However, molecular mechanisms that mediate these adaptions in pneumococci remain largely unknown (Ogunniyi *et al*., 2012).

Transcriptional regulators have been known to play a significant role in microbial detection and response to environmental signals. This adaption can occur at a single cell-or at the population level by the action of extracellular signaling peptides in the process known as quorum sensing (QS) (Cook and Federle, 2014). QS allows the population to switch behavior collectively and respond to environmental changes in a coordinated and an efficient manner, similar to multicellular organisms (Syvitski *et al*., 2007; Monnet *et al*., 2016). A wide range of microbial phenotypes are modulated by QS systems including biofilm biogenesis, competence, antibiotic production, microbial competition, sporulation and virulence expression (Syvitski *et al*., 2007; Ng and Bassler, 2009; Rutherford and Bassler, 2012). Therefore, disruption of the QS system would be ideal for preventing bacteria from synchronizing their virulent behaviors and thus reducing their fitness.

The Rgg proteins are one of the recently identified transcriptional regulators that are found in low G+C Gram positive bacteria, and their roles in streptococcal pathogenesis have been extensively investigated (Kreikemeyer *et al*., 2003; Chaussee *et al*., 2004). Rggs exert control over a wide range of physiological functions, including oxidative stress response, non-glucose sugar metabolism, biofilm formation, competence, quorum sensing and virulence (Kreikemeyer *et al*., 2003; Chaussee *et al*., 2004; Bortoni *et al*., 2009; Jimenez and Federle, 2014). The Rggs operate in tandem with their hydrophobic cognate peptides SHP to modulate Rgg/SHP regulated genes in a cell-density dependent manner. The Rgg/SHP QS circuits have recently been identified in nearly all of streptococcal species by *in silico* analysis (Cook *et al*., 2013; Fleuchot *et al*., 2013; Pérez-Pascual *et al*., 2015). The involvement of Rgg systems in regulation of different social behaviors such as virulence and pathogenicity of opportunistic pathogen *S. agalactiae* (Pérez-Pascual *et al*., 2015), and sugar metabolism, lysosome resistance and biofilm formation in *S. pyogenes* (Chang *et al*., 2015; Gogos *et al*., 2018; Pérez Morales *et al*., 2018) have been reported. In *S. pneumoniae* D39 strain, Rgg/SHP systems control the genes encoding for SHP and those important for cellular processes such as capsule synthesis, biofilm formation and non-glucose metabolism (Cuevas *et al*., 2017; Junges *et al*., 2017; Zhi *et al*., 2018). These observations were further supported by the results obtained from the current study through characterisation of one of the Rgg/SHP circuits in *S. pneumoniae* D39 strain 2 (Rgg/SHP144). It was found that Rgg/SHP144 has a significant contribution in regulation of the genes responsible for sensing and detoxifying of oxygen radicals and those responsible for mannose utilisation, one of the most prominent carbohydrates in the respiratory tract encountered by pneumococci during colonisation (Robb *et al*., 2017). In addition, Rgg/SHP144 was found to be important for biofilm formation (Cuevas *et al*., 2017), the complex microbial structure important for antibiotic resistance, host immune response evasion, pneumococcal persistence in the nasopharynx and the development of infectious diseases (Marks *et al*., 2012; Trappetti and Oggioni, 2015; Aggarwal *et al*., 2018).

All these data provide insights into the importance of the Rgg/SHP system in pneumococcal adaptation and survival. Thus, it is plausible to hypothesise that Rgg/SHP144 system can be utilised as an anti-infective target for attenuation of *S. pneumoniae* adaptive capability through modulation of the Rgg144 activity. Most importantly, Rgg144 was found in all pneumococcal strains and other related species, such as *S. pseudopneumoniae*, *S. mitis*, and *S. oralis* strains (Zhi *et al*., 2018). Thus, it is important to further characterise Rgg/SHP144 system. In this study, it was attempted to characterise the importance of SHP144 amino acid residues in transcriptional activation, binding to Rgg144 receptor and then examined the effect of these modifications on Rgg/SHP144 regulated phenotypes.

4.1. Impact of SHP144 modifications on Rgg144 transcriptional activation and its phenotypic traits

Bacterial pheromone systems usually form a positive feedback regulation with their regulators, generating a fast response and high expression of the pheromone (Junges *et al*., 2017). Through analysis of the expression level of *shp144* in transcriptional reporter strains carrying P_{shp144}::*lacZ*-Wt, it was found that SHP144 regulates its own expression, and Rgg144 is required for *shp144* expression. Consistent with recent published data, disruption of *shp* or *rgg* resulted in a complete loss of reporter induction (Chang *et al*., 2011; Fontaine *et al*., 2010; Pérez-Pascual *et al*., 2015). The Rgg/SHP144 activation pattern mimics the operation of other quorum sensing systems in terms of sensing and responding to extracellular peptide in concert with high population density, and in the presence of high amount of peptide in the culture media. This observation is clearly seen in my results, as maximal activity of reporter strain was obtained by using wild type D39 late exponential cell-culture supernatant or a high amount of synthetic SHP144 peptide.

Nutritional composition of the culture medium was found to play a role for stimulation of Rgg/SHP systems and their target genes like RovS/SHP in *S. agalactiae* (Pérez-Pascual *et al*., 2015) and SHP1358/Rgg1358 in *S. thermophilus* (Ibrahim *et al*., 2007b). The authors in these studies reported a high expression level of QS systems in chemically defined medium free of peptides relative to low expression in a peptide-rich medium. In this study, sugars were found to have a significant role for activation of pneumococcal Rgg/SHP144. Mannose and galactose showed a high capacity for activation of this system compared with other carbohydrates such as glucose or *N*-acetylglucosamine. Previously, published data from a study performed in *S. pyogenes* showed the importance of mannose in stimulation of Rgg/SHP (Chang *et al*., 2015). Another pneumococcal regulatory circuit TprA/PhrA was also found to be induced in culture media containing galactose but not glucose (Hoover *et al*., 2015). This suggests that these sugars play an important role in the activation of signaling pathways of pneumococcal cells. This high induction in the presence of mannose or galactose is presumably due to activity of a carbon-catabolite control mechanism, in which the regulator protein CcpA binds to *cre* binding site in promoters of target genes in the presence of glucose (Sonenshein, 2007). The TprA/PhrA of *S. pneumoniae* D39 was found to be under the control of carbon-catabolite repressor of CcpA, as the promoter of the signaling peptide gene *phrA* was found to have a *cre* site for

CcpA binding (Carvalho *et al*., 2011; Hoover *et al*., 2015). In addition, transcriptomic studies were also shown to upregulate of *tprA* and *phrA* expression in the *ccpA* mutant (Carvalho *et al*., 2011). On the other hand, an inducible mannose transporter PTS of *S. pyogenes* strain NZ131 was found to be involved in activation of the Rgg/SHP signaling system in the presence of mannose. This transporter acts as an intermediary transcriptional factor of genes regulated by the PTS system rather than directly being responsible for mannose import (Chang *et al*., 2015). Other evidence for involvement of Rgg in nutritional response is that Rgg144 was found to be modulated by CodY and GntR (Hendriksen *et al*., 2008a, 2008b; Cuevas *et al*., 2017). CodY, GntR and CcpA are the most important pneumococcal regulators that contribute in amino acid and carbohydrate metabolism as well as iron uptake (Hendriksen *et al*., 2008a, 2008b; Carvalho *et al*., 2011). It appears that there is a link between nutritional response and cell–cell communication pathways including Rgg/SHP. Further studies are required to understand the full extent of this regulation.

Furthermore, it was found that synthetic SHP144 peptide with 13 amino acid residues is the functional autoinducing peptide, that has a greatest ability to induce the system activity. This activation is specific, as using a reversed peptide with identical length was unable to activate the system. This 13 aa long active peptide, however, is longer than other active peptides in other streptococci, which generally vary between 5 to 8 aa long (Aggarwal *et al*., 2014). The PhrA, a signaling peptide of TprA/PhrA in *S. pneumoniae* was also shorter than SHP144, as the active peptide ranges between 7-10 residues (Hoover *et al*., 2015). This discrepancy in the peptide length is very likely due to differences in the processing cascade and binding site for each signaling peptide. The SHP144 length is still consistent with the idea that the functional activity of the mature peptide is located in its C-terminus, and potential capability of re-entering the active peptide into the cell using a specific peptide transporter Opp (Chang *et al*., 2011; Jimenez and Federle, 2014), which has capability to transport peptides with a different size (4-18 residues) (Detmers *et al*., 2000). Furthermore, it is predicted that this length would fit properly into the binding interface of the Rgg144 receptor, and this hypothesis was strengthened by computational docking studies, which showed appropriate fitting of the SHP 13-mer into the binding groove of Rgg144. It can conclude that the size of signaling peptide is important for activation of Rgg mediated regulation, as SHP144 variants other than C12 or C13 did not show detectable stimulation of *shp144*, and this agreed with the results of Federle group (Chang *et al*., 2011).

Furthermore, the composition of the signaling peptide was found to be important for activation of the system (Chang *et al*., 2011). The chemical features of each amino acid residue, including charges, acidity, polarity and hydrophobicity were found to have a role in activation of the signalling peptide (Duan *et al*., 2012). Based on these observations, a set of modified *shp144* strains in which each amino acid of SHP144 was replaced with alanine were constructed using alanine scanning mutagenesis, and the contribution of each amino acid residue to Rgg144 mediated transcription was quantified using β-galactosidase assays. Knockout *shp144* strain was used as a background for construction of modified *shp144* strains. This mutant was initially complemented with an intact copy of *shp144* by using non-replicative plasmid pCEP (Guiral *et al*., 2006) to eliminate the possibility of polar effects. The complementation of Δ*shp144* was successfully achieved, and phenotypic traits of *shp144* were fully restored, indicating that the observed phenotypes in the *shp144* mutant were due to mutation rather than polar effects of the mutation.

Alanine-scanning mutagenesis was used in this study as it is a powerful method to determine the importance of individual amino acid residues within a peptide (MDowell *et al*., 2001), and to identify their contributions to peptide-protein interactions (Boersma *et al*., 2008). Alanine substitutions altered the regulatory function of SHP144 and generated peptides with various activity, such as reduction, no effect or complete loss of activation. This was also associated with varying binding affinities to the Rgg144 receptor using a fluorescence polarisation assay as shown in Table 3.5. All replaced residues significantly altered SHP144 dependent Rgg activation except one modification at position V19, which had no effect on SHP144 activity, signifying the importance of selected residues for activation of Rgg144-mediated transcription. This finding is consistent with previous studies, which showed that the specificity of signal peptide is greatly dependent on amino acid sequence, as single residue modification causes loss of signal activity (MDowell *et al*., 2001; Fontaine *et al*., 2013). In a similar manner, Perego (1997) also reported the importance of amino acid sequence in determination of peptide activity and specificity for target recognition, as single amino acid substitutions greatly affect signalling peptide PhrA function. Further evidence for the importance of C-terminal end comes from Chang's study (2011), which showed that the intact C-terminal domain of the SHP peptide is important for *shp* activation in *S. pyogenes*, as changing one residue by substitution or deletion resulted in a significant reduction in *shp* induction. Similar to Rgg/SHP144 activation, the enzymatic activity of modified reporter strains was remarkably higher in media containing mannose rather than in glucose.

Furthermore, the results of reporter assays using strains with modified SHP144 were nearly similar to that induced by modified *shp144* supernatants, indicating that the modifications in SHP144 structure did not affect the diffusion of peptide across the bacterial cells except for the supernatant collected from strains with E15A or V19A modification. However, when synthetic peptides with E15A or V19A modification were used at 1000 nM, the effect of each peptide was demonstrated, hence their importance for transcriptional activation. This discrepancy can be explained by different scenarios. Firstly, the assay conditions were not the optimal for peptide production in the modified strain background, which generates a small amount of modified peptide, which could be below the threshold concentration for *lacZ* reporter assay. It has been previously reported that pheromone accumulation and diffusion might be affected by growth condition, as an increase in media viscosity limits signal diffusion, and inhibits bacterial population level at which QS system is stimulated (Yang *et al.*, 2010; Monnet *et al.*, 2016). In addition, pheromone integrity and activity might be also reduced due to accumulation of proteolytic activity in bacterial cells at stationary phase as demonstrated in *E. faecalis* (Monnet *et al.*, 2016), as opposed to synthetic peptide, which is more stable and exposed less to proteolytic activity. Secondly, poor capacity of pneumococcal cells to secret peptides into extracellular milieu, presumably due to modification of peptide sequence which might hinder peptide's export and subsequent uptake by the peptide transporter. As replacement of polar negative charge glutamate with a non-polar hydrophobic residue like alanine might increase the peptide's hydrophobicity, this may lead to the peptide's adhesion to the cell membrane rather than secretion to extracellular environment.

Very little is known about the processing and maturation of SHP peptides in almost all streptococci including *S. pneumoniae*. It is commonly believed that the peptide is secreted to the extracellular medium by the Sec-dependent export pathway or ABC transporters, processed inside or outside the cell by membrane-associated peptidase Eep, and actively reimported into the cell by the oligopeptide permease, *opp* or *ami* operon (Fleuchot *et al.*, 2011; Aggarwal *et al.*, 2014). The ABC-type transporter called PpTAB was recently identified to export signalling peptides in *S. pyogenes* (Chang and Federle, 2016) and *S. agalactiae* (Pérez-Pascual *et al.*, 2015). It was also demonstrated that PpTAB is essential for signal production rather than signal detection (Chang and Federle, 2016). Recent studies have found that the metalloprotease Eep is also required for production of mature Rgg-associated peptides by *S. thermophilus* (Fleuchot *et al.*, 2011), *S. pyogenes* (Chang *et al.*, 2011) and *S. agalactiae* (Pérez-Pascual *et al.*, 2015). The Eep-encoding genes were identified in all streptococcal genomes, suggesting the same role for Eep in all streptococci. Moreover, oligopeptide permease is involved in maturation and importation of SHP signalling peptides in streptococci (Chang *et al.*, 2011; Fleuchot *et al.*, 2011; Pérez-Pascual *et al.*, 2015) as well as the Phr peptide of *B. subtilis* (Lazazzera *et al.*, 1997), PhrA of S. *pneumoniae* (Hoover *et al.*, 2015), PapR of *B. cereus* and *B. thuringensis* (Slamti and Lereclus, 2002), plasmid conjugation pheromones of *Enterococcus faecalis* (Leonard *et al.*,1996) and competence inducing peptides ComS and XIP in *S. thermophilus* and *S. mutans* (Fontaine *et al.*, 2010; Mashburn-Warren *et al.*, 2010), suggesting the importance of Opp in peptide associated signalling pathways in most of Gram positive bacteria. In *S. pneumoniae* D39 strain, an ortholog of an ABC transporter (SPD_0464) sharing 76.8% identity with PptAB, *ami* operon including a cluster of genes (SPD_1667 - SPD_1671) and an *eep* ortholog (SPD_0245) with DNA similarity 62.9% to spy49_1620c of S. *pyogenes* have been reported (Zhi, 2017). This analysis has been done *in silico*, therefore the role of each element in pneumococcal biology should be addressed experimentally in the future.

Several attempts are made in this study to isolate SHP144 variants from pneumococcal supernatants in order to use these natural fractions for stimulation of the reporter fusion, P_{shp144}::*lacZ*-Δ*shp144*. Unfortunately, the mass spectrometry analysis was unsuccessful. This is probably due to a low concentration of the secreted peptides in a highly complex sample which makes a proteomic approach virtually impossible. This hypothesis is further supported by previous studies reporting the presence of low concentration of signalling peptide in the supernatants, which ranged between 7 nM for SHP of *S. thermophilus* and 4 nM for CSP in *S. pneumoniae* (Fleuchot *et al.*, 2013; Yang *et al.*, 2010; Monnet *et al.*, 2016). Similarly, GBAP of *E. faecalis* (Nakayama *et al.*, 2001) and AgrD of *S. aureus* were found in the low nanomolar range (Mayville *et al.*, 1999), or even in picomolar range (Verbeke *et al.*, 2017). It seems that such signalling peptides operate at very low concentrations, thus their isolation require more attention during sample preparation, and much more sensitive techniques for identification and characterisation of their properties (Turan *et al.*, 2017; Verbeke *et al.*, 2017). In spite of this, SHP peptides of other streptococci have successfully been recovered from supernatants of *S. pyogenes* (Aggarwal *et al.*, 2014), *S. thermophilus* LMD-9, *S. agalactiae* NEM316 and *S. mutans* UA159 (Fleuchot *et al.*, 2011, 2013). The sequence of pneumococcal SHP144 is generally divergent from other related streptococci and predicted to have a specific mode of processing. This is apparent from difference in the length of active peptide, which is 12 or 13 residues in pneumococcal SHP144, in contrast to 8 residues in other streptococci (Aggarwal *et al.*, 2014). Furthermore, media composition, sample preparation and type of mass spectrometry used for identification in this study were largely different than the other studies.

The interaction between signalling molecule and cognate receptor is the fundamental step in any cell-cell communication circuit including Rgg/SHP. In this study, a fluorescence polarisation assay was successfully applied for detection of the direct interaction between fluorescently labelled modified or unmodified SHP144 with recombinant Rgg144 protein receptor. The binding of Rgg and FITC-SHP144-C13 was at micromolar affinity (6.60 µM). This binding was specific, as using non-specific fluorescent peptide with identical length (FITC-NSP-C13), or receptor other than Rgg144 such as bovine serum albumin had no detectable binding. More importantly, FITC-SHP144-C13 was successfully replaced with unlabelled SHP144-C13, but not with competence stimulating peptide CSP in a competitive binding assay. It is thought that using truncated Rgg144 lacking the N-terminus would promote Rgg/SHP144 binding. Interestingly, full length and truncated Rgg144 have equivalent binding affinities, indicating that both proteins have the same propensity for binding, and the N-terminus of Rgg144 as expected had no role in binding. By using modified SHP144-C13 peptides, various binding affinities for Rgg144 protein were identified, highlighting the importance of SHP144 sequence and the geometry of amino acid side chains in Rgg144 binding and its functional activities. More strikingly, the binding affinities of non-activating modified peptides linked to their transcriptional activation measured by bioreporter β-galactosidase assay, except those at position V17 and P21, which were found to be important for the activity of SHP144, but dispensable for binding to Rgg144. This suggests that these modified peptides can be utilised to design an inhibitor against *S. pneumoniae*.

The results of the current study also showed that hydrophobic residues at positions I18, I20 and W16 are the most critical ones for SHP144 bioactivity and receptor binding, as their substitutions led to complete loss of transcriptional activation, and inhibition or elimination of SHP144 binding. Previous *in silico* analysis of SHPs from various strains of streptococcus (Ibrahim *et al.*, 2007a; Fleuchot *et al.*, 2011) showed that SHP is highly hydrophobic, and isoleucine is largely distributed in the C terminus end. In addition, protein multiple sequence alignment in the current study showed that isoleucine at position 20 is conserved among streptococcal SHPs peptides (Appendix 7). Thus, it is reasonable to assume that isoleucine substitution with another residue changes the peptide's specificity and receptor recognition. Similarly, substitution of bulky amino acid such as tryptophan with small side chain alanine undoubtedly affects peptide binding and impairs its regulatory function.

There are several factors that are critical for peptide selectivity, which include anchoring contacts, hydrophobic interactions conferring shape complementarity between the two molecules, peptide backbone interactions for stability, and side chain-specific hydrogen bonding contacts. Usually, the carboxylate oxygen of the C terminus of the signal peptides interact with the polar and charged amino acids found at the deep end of the binding pocket. These contacts play a vital role in anchoring for alignment of the peptides within the binding pocket. A second level of interactions appears between the aromatic or hydrophobic side chains of the signal peptides and the polar pockets of the receptor proteins. These interactions are required for shape complementarity between the two molecules and mediate a tight fit for the cognate pheromone peptides in target binding pocket (Do and Kumaraswami, 2016). Therefore, it was speculated that the local structural changes due to single alanine substitutions weakens the structural integrity of the dimer interface, which results in destabilisation of the dimerisation interactions and/or interference with peptide-mediated allosteric alterations in Rgg144. Additional work is needed to verify these results and characterise ligand-binding pocket in Rgg.

The activation of Gram-positive RRNPP QS receptors, on the other hand, results from an allosteric mechanism, which is initiated by the interaction with its respective AIP. The receptor oligomerisation is modulated by AIP binding, where it may either lead to separation, as seen in PrgX, or multimerisation, as seen in PlcR, and this regulation indicates a specific interaction of these receptors with their DNA (Lixa *et al.*, 2015).

It was noticed that there is a variation between *shp144* activation and manifestation of phenotypes conferred by Rgg/SHP144 in modified strains, except those carrying modification at position I20A and P21A, including mannose utilisation and oxidative stress resistance. This might be due to different reasons: (i) difference in the sensitivity of assay platform: bacterial phenotypes arise due to involvement and interaction of multiple proteins (Alper and Stephanopoulos, 2007), thus characterisation of a specific phenotype in highly complex metabolic background is expected to be less sensitive compared with β-galactosidase reporter assay, which is more sensitive and specific, as it measures the activity of single gene such as *shp144* (ii) substantial overlap between genes regulated by Rgg homologs under the same environmental condition. This means that Rggs have capability to respond to the same stimuli and control the function of the same set of genes (Zhi *et al.*, 2018), which might allow the compensation of Rgg144 function in the absence of functional peptide.

On the other hand, modification at position I20A as well as P21A affect the phenotypic traits of *shp144* in both *in vitro* and *in vivo* assays. It seems that both of these residues are also essential for SHP144 activity and functions, as their modifications caused a remarkable change in binding with Rgg144 and in turn switch the Rgg/SHP144 system off. Indeed, a weak interaction was observed with modified SHP144-C13I20A synthetic peptide (23.54 µM) and a strong binding with high affinity with SHP144-C13P21A (1.67 µM), compared with binding affinity of unmodified peptide (6.60 µM). These results suggest that the modifications at I20A might lead to inefficient binding of SHP144 to the binding pocket in the Rgg144, causing failure to form Rgg/SHP144complex, as opposed to tight binding in the case of SHP144-C13P21A. This might be due to unfavourable conformational changes in the target protein, blocking the activation of the system and DNA transcription. This interference with receptor binding caused attenuation in the expression of genes under the control of Rgg/SHP144 system. Further support for this explanation comes from *in vivo* results, which showed a significant reduction in bacterial burden in the nasopharynx of mice infected intranasally with these modified strains, which resemble the phenotype obtained with *shp144* deficient strain.

The reduction in nasopharyngeal colonisation in mutant and modified strains is more likely due to the inability to utilise mannose efficiently, which is abundantly found in the *N*- and *O*-linked glycans of host respiratory tract (King, 2010; Robb *et al.*, 2017). The host glycans represent the main carbon resource for pneumococci during nasopharyngeal colonisation in which there is a limited amount of free glucose (Burnaugh *et al*., 2008; Paixão *et al*., 2015b). The inability to utilise mannose might reduce pneumococcal capacity for competition with other inhabitants residing in the same niche for space and nutrient resource. This explanation is substantiated by results obtained from the current study which showed a substantial stimulation of *shp144* by mannose and galactose, and the absence or modification in *shp144* gene (Δ*shp144*ComP21A and Δ*shp144*ComI20A) caused a significant reduction in mannose utilisation.

The results of this study reconfirm earlier observations, which showed the involvement of Rgg/SHP in mannose metabolism in *S. pyogenes* (Chang *et al*., 2015) and *S. pneumoniae* (Zhi *et al*., 2018). The pneumococci have a large repertoire of glycosidases responsible for cleavage of host glycans and liberation of monosaccharides such as mannose and galactose (King, 2010; Paixão *et al*., 2015b). NanA represents the most important glycosidases required for initial cleavage of host glycoprotein and facilitate the exposure of oligosaccharides such as galactose and mannose to the activity of other glycosidases such as galactosidases and mannosidases (King, 2010). Defects in NanA or other glycosidases might hinder the sequential cleavage of host glycans and the release of monosaccharides (King, 2010; Terra *et al*., 2010). Limiting the access of pneumococcus to these sugars might lead to the inability to activate *shp144* expression, hence SHP144 synthesis, resulting in inhibition of Rgg/SHP144 expression and its associated genes. However, the full mechanism of this regulation in *in vivo* context still is not entirely clear and needs to be characterised in the future.

Another reason for attenuation of nasopharyngeal colonisation for the mutant and modified *shp144* strains is the high production of capsule. A significant increase in glucuronic acid production was observed in both mutant and modified strains. High production of capsule might hinder pneumococcal attachment to epithelial cells, and subsequent invasion of host tissues as demonstrated by Kimaro Mlacha *et al.* (2013). Previous study has shown that Rgg/SHP systems act as a direct repressor for capsule synthesis loci in the presence of mannose, and this was demonstrated by microarray analysis and EMSA (Zhi *et al*., 2018). Thick capsule is usually accompanied with reduction in the expression of cell-wall associated proteins and carbohydrates involved in cell wall structure (Bogaert *et al*., 2004) as well as inhibition of NanA, the important exoglycosidase required for pneumococcal adherence and colonisation (King *et al*., 2006). However, no effect was observed for Rgg/SHP144 regarding NanA activity, as both wild type and mutants (Δ*rgg144* or Δ*shp144*) showed similar enzymatic activity. On the other hand, it was found that thick capsule of *S. pneumoniae* is usually accompanied with a low level of biofilm (Moscoso *et al.,* 2006). Indeed, an elevated level of capsule production in the *shp144* mutant associated with low production of biofilm formation was observed. Biofilms are the most important component of pneumococcal biology, they play a role in drug resistance, bacterial transmission, maintenance of asymptomatic colonisation, and development of disease. Bacterial cells dispersed from nasopharyngeal biofilms facilitate pneumococcal transmission between individuals through incorporation into nasal secretions (Aggarwal *et al*., 2018). In addition, biofilm associated pneumococci have a higher tendency for dissemination to tissues than planktonic pneumococci, suggesting that chronic biofilms mediate the stimulation of virulence upon release of biofilms (Marks *et al*., 2013; Chao *et al*., 2015). The inhibition of biofilm formation by the capsule is more likely due to the abrogation of the attachment of pneumococcal surface associated proteins to host epithelial cells (Hammerschmidt *et al*., 2005). The reduction in biofilm formation might also be due to downregulation of virulence peptide VP1, which is under the control of Rgg/SHP144 as demonstrated recently (Cuevas *et al*., 2017).

Another reason for attenuation of strains lacking Rgg/SHP144 during colonisation is the high sensitivity to oxidative stress. This phenotype is important for enhancing pneumococcal colonisation and for competitively inhibiting the survival of other inhabitants (Pericone *et al*., 2000). The results showed a profound reduction in pneumococcal survival following exposure to 20 mM of H_2O_2 and 1mM paraquat. The Rgg involvement in oxidative stress resistance has been reported in *S. pneumoniae* (Bortoni *et al*., 2009; Zhi *et al*., 2018) and *S. pyogenes* (Chaussee *et al*., 2004). These data suggest that the involvement of Rgg/SHP144 in oxidative stress resistance might be due to regulation of oxygen detoxifying enzymes or genes involved in other cellular processes such as capsule thickness and efficient ATP production, which is required for oxidative stress resistance (Carvalho *et al*., 2013b). Our previous microarray data clearly showed the involvement of *rgg144* in regulation of glutathione reductase (coded by *gor*), the key enzyme required for conversion of the glutathione from oxidised form to the reduced state (Potter *et al*., 2012). Glutathione can be imported inside the pneumococcal cells by the aid of ABC transporter and is involved in oxidative stress tolerance through its disulphide reductase activity. Disruption of *gor* renders the pneumococcal cells more susceptible to superoxide and reduces colonisation and the development of invasive diseases in the murine infection model (Potter *et al*., 2012). Moreover, microarray data also showed upregulation of genes encoding for ABC transporters in mutant *rgg144*. These transporters are known to be important for nutrient uptake and removal of toxins and antibiotics (Ulijasz *et al*., 2004; Yesilkaya *et al*., 2013). On the other hand, ABC transporters were shown to be important for inorganic ion transport and metabolism, hence repressing these ion transporters would preserve the pneumococci from toxic effects of intracellular iron and reduce the chance of hydroxyl ion formation by the Fenton reaction (Pericone *et al*., 2003). Additional investigations are required to elucidate the mechanism by which Rgg/SHP regulates oxidative stress genes, and the impact of this regulation on colonisation.

Modified strain carrying a modification at position E15A was also included *in vivo* assays to investigate the impact of this residue on pneumococcal colonisation. Recent genomic analysis showed that all mature SHP have the negatively charged amino acid residues, Asp or Glu, at the first position, exception being Rgg Stu0182-associated SHP in *S. thermophilus* strain LMG18311 and Rgg Str0182-associated SHP in *S. thermophilus* strain CNRZ1066, which have cysteine at this position (Fleuchote *et al*., 2011, 2013). These residues are predicted to be important for recognition of the precursor SHP by protease and subsequent maturation and activity of SHP (Fleuchot *et al*., 2013). In addition, it was found that aspartate Asp is important for activation of SHP2 in *S. pyogenes*, as its substitution with an amide-bearing residue such as asparagine led to a significant reduction in peptide activity, whereas substitution with glutamate retained full activity (Chang *et al*., 2011). The results in this study showed a significant reduction in *shp144* transcriptional activation and pneumococcal survival following treatment with superoxide-generating agent paraquat in strain with E15A modification.

Despite this, no effect of modification could be observed *in vivo*. This disparity might be due to difference in environmental conditions between *in vitro* and *in vivo* assays. For example, *in vivo,* there is a strong competition between the pneumococci and other inhabitants living in highly mixed microbiota such as nasopharynx, while this competition is absent in *in vitro* experiments.

The defect in the *shp144* mutant was fully complemented by extracellular addition of wild type D39 supernatant, or by exogenous addition of synthetic peptide corresponding to the last 12 or 13 residues. It appears that peptide length and primary amino acid sequence determine the outcome of functional complementation, as peptides with other lengths or with reversed sequence were unable to activate *shp144* expression in mutant *shp144* or even wild type strain. Similar complementation approaches have been applied for other Rgg/SHP circuits such as activation of *shp1358* promoter in the reporter strain lacking *shp1358* by using *S. thermophilus* LMD-9 supernatant (Fleuchot *et al*., 2011). Likewise, addition 1 µM of synthetic peptide corresponding to active SHP peptide (DILIIVGG), or co-culturing with WT-pTCVlac strain expressing native SHP was able to restore *shp* expression in mutant *shp* reporter strain of *S. agalactiae* strain NEM316 (Pérez-Pascual *et al*., 2015). Moreover, synthetic peptide SHP144-C13 in this study rescued the defects *in vitro* of virulence-related phenotypes including mannose utilisation and oxidative stress resistance in a dose-dependent manner. This finding is in agreement with my previous results, which showed that mannose is the activating signal of Rgg/SHP. Furthermore, this functional complementation was sequence specific, as modified peptides were unable to reconstitute pneumococcal phenotypes of Rgg/SHP144.

Despite this, native SHP144-C13 failed to restore the virulence of mutant *shp144* when administered simultaneously with Δ*shp144* in the murine infection model. This is presumably because the peptide’s concentration did not reach the activation level, peptide instability and susceptibility to degradation by host proteases, which need to be tested in the future. In addition, recent study also reported the presence of aminopeptidase on the surface of streptococci which might increase the chance of peptide cleavage (Fleuchot *et al*., 2013). The final possibility is route of administration. Peptide in this study was administrated intranasally, and this might not be the most optimal route. Thus, other alternative routes of administration should be tested to validate the effect of this peptide.
Structural analysis of Rgg144 protein in *S. pneumoniae* D39 showed a similar structure to other RRNPP proteins (Parashar *et al*., 2015; Do and Kumaraswami, 2016), as it is a dimer, contains HTH motif at N-terminus end for DNA binding, connected by a short linker to repeat binding motif at C-terminus, important for peptide recognition and binding. Several binding grooves have been characterised at the C-terminus of Rgg144 which are predicted to be the binding site for SHP144. The purified full length Rgg144 protein was trialled to crystallise with its ligand SHP144 by using sitting-drop vapor

diffusion method. Unfortunately, co-crystallisation was unsuccessful, presumably due to conformational changes in the C-terminus of Rgg144 upon peptide binding, which might cause change in protein structure and prevent crystal formation. It is important to note that there are multiple parameters, which might affect crystal growth such as pH, temperature, types of precipitant, ionic strength and concentration of the protein (Navarro *et al.*, 2009). To increase the possibility of crystal production, the truncated form of Rgg144 lacking the N-terminus was used. This approach was successfully applied for crystallisation of NprR HTH deleted domain (member of RRNPP) in complex with its signalling peptide NprX. Truncated Rgg144 peptide failed to produce crystal. In spite of structural similarity between Rgg and NprR, there are differences in binding mode of each peptide. Thus, further optimisation of experimental conditions is required, and this can be achieved in the future.

Accumulating evidence from this study suggests that Rgg/SHP144 is important for pneumococcal biology, and modification in its inducing signal SHP144 affects the system activation and function. Some of these modified peptides are unable to activate the system but have capability to bind to Rgg receptor and block Rgg-mediated transcription, such modified peptides can be used as a competitive inhibitor for Rgg/SHP system to alleviate pneumococcal infections, and this will be discussed in the following section.

4.2. Inhibition of Rgg/SHP144 quorum sensing system by modified peptide

In recent years, bacterial resistance against conventional antibiotics has been increasing dramatically and the resistance is becoming a major issue that needs resolving. Bacteria have developed various resistance mechanisms such as inactivation of antibiotics, modification of drug targets or alteration of cell membrane permeability and drug efflux. These resistance mechanisms can be inherited or acquired by mutation in the bacterial chromosome or through acquisition of resistance plasmids or transposons. Alternatively, the resistance can occur through adaptative mechanisms by switching from planktonic to sessile biofilm existence. Therefore, effective antimicrobial drugs are required to combat bacterial infections, avoid known resistance mechanisms and preserve the natural microbiome of the host (Brooks and Brooks, 2014). Current antibiotics target cell viability by interfering with essential cellular processes such as cell wall synthesis, DNA replication, RNA transcription and protein synthesis. This places selective pressure on bacteria to acquire mutations or other adaptive mechanisms to survive, giving rise to the development of drug resistant strains (Clatworthy *et al*., 2007). Thus, search for new alternative approach targeting virulence factors, that are important for host damage and disease progression would be better than killing or inhibition of pathogen growth (Allen *et al*., 2014; Heras *et al*., 2015).

Quorum sensing systems have been indicated as a viable anti-infective target because the inhibitors of QS systems can change the behavior of a population of bacteria collectively preventing efficient microbial adaptation to environmental change, thus being unable to thrive and being more susceptible to destruction by the host’s immune system (Hentzer and Givskov, 2003; Rasmussen and Givskov, 2006). As QS inhibitors do not kill bacteria, but switch off the adaptive and virulence capabilities of target microbe, their impact on microbiota would be less than the broad-spectrum traditional antibiotics. Furthermore, it is expected that the possibility of bacterial resistance to QS inhibitors to be lower than traditional antibiotics not least because QS systems are not essential for microbial survival but also escaping the inhibitory effects of a drug that blocks the peptide binding groove, in the case of Gram positive QS systems, would require complementary changes to both the cytoplasmic receptor protein as well as its signal peptide, making adaptive mutations less likely.

There are three mechanisms for disrupting QS circuits: (1) inactivation of QS molecules (2) prevention of QS signal biosynthesis (3) inhibition of ligand/receptor interactions (Brooks and Brooks, 2014). Enzymatic and non-enzymatic strategies have successfully been applied for disruption of bacterial QS systems in Gram negative bacteria. Three classes of enzymes have been identified to hydrolyse or modify signalling acyl-homoserine lactone (AHLs) molecules, including lactonases to hydrolase the lactone bond of AHLs (Dong *et al*., 2001), acylases breakdown the acyl-amide bond of AHLs and release of fatty acid and homoserine lactone (Lin *et al*., 2003), and finally oxidoreductases which oxidise or reduce the acyl side chain of AHL (Uroz *et al*., 2005; Chen *et al*., 2013). Non-enzymatic methods can be achieved by the production of monoclonal antibodies to sequester AHLs (Mookherjee *et al*., 2018) such as RS2–1G9 targeting 3OC12HSL signalling peptide in *P. aeruginosa* (Kaufmann *et al*., 2006; LaSarre and Federle, 2013). While AHL biosynthesis can be inhibited by targeting NADH-dependent enoyl-ACP reductase, required for acyl-ACP synthesis, the most important substrate involved in AHL production (LaSarre and Federle, 2013), such as triclosan which suppresses enoyl-ACP reductase and inhibits C4-HSL synthesis in *P. aeruginosa* (Hoang and Schweizer, 1999).

The most popular approach relies on interference with signal/receptor interaction through modifications in the normal conformation of signal/receptor complex, which prevents dimerisation or interaction with target promoter (Grandclément *et al*., 2016). QS inhibitors in Gram negative bacteria work directly on LuxR receptor such as halogenated furanones which interact with receptor protein and induce rapid proteolytic degradation (Manefield *et al*., 2002). Isothiocyanate iberin, a natural product extracted from horse radish, acts as inhibitor through preventing the C4-HSL interaction with RhlR regulator in *P. aeruginosa* (Jakobsen *et al*., 2012).

For Gram positive bacteria, several approaches have been taken to switch the QS systems off. These included screening of combinatorial libraries to identify competitive peptidomimetic inhibitors. For example, linear peptidomimetics inhibit *S. aureus agr* system by disrupting the interaction between native cyclic peptide AgrD and response regulator AgrC (Karathanasi *et al*., 2018). Another example includes the use of chemical and natural virulence inhibitors such as savarin and solonmides, which can interfere with the *S. aureus agr* signalling pathway and inhibit the expression of virulence factors of *S. aureus* (Mansson *et al*., 2011; Sully *et al*., 2014). Ambic acid, a fungal metabolite, has been reported to inhibit the production of cyclic peptide in *E. faecalis, S. aureus* and *Listeria innocua* (Nakayama *et al*., 2009). Our group in Leicester has demonstrated the use of molecularly imprinted polymers such as linear molecularly imprinted polymers to modulate TprA/PhrA system in *S. pneumoniae* (Motib *et al*., 2017). Park *et al*. (2007) has adapted an immune pharmacotherapeutic approach to identify monoclonal antibodies to neutralise the signal peptide via sequestration such as AP4-24H11 targeting (AIP)-4 of *S. aureus* RN4850. Unfortunately, these approaches do not use the existing knowledge of the biological target or the advantages inherent within the system. My approach, on the other hand, uses the knowledge derived from the system, and it could be modified to target other systems involving transcription regulators that are controlled by peptide ligands. Prevention of ligand/receptor interactions has been attempted recently to target a Rgg/SHP system in *Streptococcus dysgalactiae* by screening an inhibitor library, and cyclosporine, was identified as the inhibitor of the system (Parashar *et al*., 2015). However, it is unlikely that cyclosporine would be used as an anti-infective as it is an immunosuppressive (Calne, 2004).

By attributing a function to each residue either in transcription or binding, the peptide that contained the P21A replacement showed a significant inhibitory activity against the Rgg/SHP144 system. This peptide competitively inhibited the induction of the system in a concentration dependent manner as demonstrated in spent culture supernatant experiments. It also abrogated the phenotypic manifestation of Rgg/SHP144 QS system, such as the ability to utilise mannose and the oxidative stress resistance. The inhibitory effect of modified peptide was clear at 1:10 (wild type: mutant) ratio, suggesting that the high load of modified P21A peptide is required to obtain an efficient inhibition. Therefore, combining multiple mutations would potentially generate a strong inhibitor against Rgg/SHP144 system such as mutated residue at position V17A, which showed a slight inhibition activity. In addition, a slight increase in binding affinity of modified peptide FITC-SHP144-C13P21A (1.67 µM) was found compared with native FITC-SHP144 peptide (6.60 µM), suggesting that alanine substitution at position P21 converts peptide activity from agonist to antagonist of the Rgg/SHP144 system. This is probably due to a specific role of proline in protein folding and protein-protein interactions (Deber *et al*., 2010), as its unique side chain forms ring structure by connecting to protein backbone twice (Betts and Russell, 2003). Thus, it is reasonable to suggest that proline substitution would impede an allosteric conformational change in the C-terminal domain of Rgg144, which is essential for Rgg/SHP144 activation.

In spite of the strong inhibitory effect of P21A modified peptide in *in vitro* assays, it was unable of exert a significant attenuation of bacterial loads in intranasal colonisation assay in mice. It is thought that this might be due to the insufficient concentration used in *in vivo* assay, which was not enough to inhibit endogenous Rgg/SHP144. It is also possible that time of peptide administration and route of injection might have affected the outcome. In this study, intranasal inoculation was used to check the effect of inhibitor only once, however, a single experiment is not enough to judge the efficacy of peptide thus more experiments are required to verify these results using several different parameters.

Peptide drugs are increasingly being used for treatment of various disease manifestations including for infectious diseases due to their relative safety, tolerability, specificity and for their efficacious nature. Consequently, there is an increased interest in peptides in pharmaceutical research and development, and approximately 140 peptide therapeutics are currently being evaluated in clinical trials (Fosgerau and Hoffmann, 2015). Such synthetic peptides have successfully been applied for inhibition of competence development, and virulence factor expression in *S. pneumoniae* (Zhu and Lau, 2011). Similarly, truncated peptide (AIP) was used as cross inhibitor for QS of different *S. aureus* species (Lyon *et al*., 2000). In addition to their direct use, these peptides can be used as templates for the development of small molecule inhibitors for the treatment of pneumococcal disease in the future. Understanding the structural basis of transcriptional activation by Rggs will facilitate the design of inhibitors for these regulators that can be used as lead compounds, and eventually therapeutics, for the treatment of pneumococcal disease. This is what we aim to achieve in future.

Conclusion and Final Remarks

In this study, it was demonstrated that Rgg/SHP144 is one of the most important QS circuits in *S. pneumoniae* D39. It plays a crucial role in sugar metabolism, oxidative stress, capsule synthesis, biofilm formation and virulence. The Rgg/SHP144 QS is a highly inducible system in the presence of mannose and galactose, but not in glucose or *N*-acetylglucosamine, and in cell-density dependent fashion. The signalling molecule SHP144-C13 plays an important role in the activation of this system, and its functional activity is dependent on size, composition and peptide concentration. Single amino acid substitution drastically affects peptide' capacity for binding to its cognate receptor Rgg144 and stimulation of the system. This binding, however, was weakened or abolished when amino acid resides W16, I18 and I20 were replaced with alanine. This inhibition was associated with inability to stimulate transcriptional activation of the system. Peptides with V17A and P21A modifications abolished transcriptional activation but retained binding capacity to the level closer or higher than native SHP144-C13 peptide. Finally, the strain carrying I20A or P20A modification caused a significant attenuation in pneumococcal growth on mannose, ROS resistance and nasopharyngeal colonisation.

This study also showed successful activation and reconstitution of Rgg/SHP144 phenotypes in *shp144* mutant by addition of unmodified synthetic SHP144-C13 peptide or wild type D39 supernatant. On the other hand, peptide with modification at position P21A showed a potent inhibitory capacity against Rgg/SHP144 through inhibition of *shp144* expression and abrogation of phenotypic manifestations mediated by the system including mannose utilisation and resistance to toxic effect of H_2O_2 and paraquat. These effects however could not be observed when native or modified peptides were administrated with the bacterial inoculum in the nasopharynx of mice. Despite this, finding an inhibitor by using this inherent knowledge of Rgg/SHP144 system provides a starting point for discovery of a new anti-infective target.

Future Plan

Interference of signalling between Rgg144 and SHP144 can offer a viable strategy for anti-infective drug design. However more detailed analysis is required to understand the complete picture of how Rgg/SHP144 complexes control DNA transcription. By using the existing knowledge of the biological target or the advantages inherent within the system, namely the presence of a deep peptide-binding groove to which the SHP binds specifically, we generated inhibitors by modifying the SHP144-C13, such that the potential inhibitors could still bind to the Rgg144 but no longer activate the transcription i.e. the SHP144 is converted to an inhibitor of Rgg/SHP144 QS. Despite the promising results obtained with using one inhibitor generated in this study in *in vitro* experiments, the results of *in vivo* experiments were insufficient to determine the efficacy of this inhibitor. Therefore, more in-depth experiments are required to evaluate the appropriate dose of the inhibitor and dosing regimen that will inhibit the Rgg/SHP144 QS and reduce the pneumococcal fitness in murine infection model. It will also be interesting to determine the potential capacity to use this inhibitor as prophylactic agent to alleviate the detrimental effects of pneumococcal infections. As it is well known that the bacteria produce signalling peptides continuously throughout their growth, but QS circuit becomes active only at a high cell density (Banerjee and Ray, 2017). Intranasal administration route was the only method used to evaluate the impact of modified peptide on pneumococcal fitness in this study, thus, using other alternative administration routes such as intravenous or intraperitoneal injection would be valuable.

While one inhibitor was generated in this study, further work is required to determine its ADME parameters (Absorption, Distribution, Metabolism, Excretion) as well as toxicity before proceeding its development as a drug lead. Understanding of these parameters will provide information about the behaviour, pharmacological activity and safety of this compound. This can be conducted by *in vitro* and *in vivo* experimental models (Zhang *et al.*, 2012).

Furthermore, the inhibitory effect of this peptide can be improved using a rational approach by replacing those residues that mainly contribute towards transcription activation such as V17 with alanine that is likely to enhance binding. The Rgg/SHP144 binding can also be improved by the addition of non-biological amino acids to create a synthetic peptide inhibitor. Such strategies have been used effectively for a wide variety of inhibitors (Fosgerau and Hoffmann, 2015) including cytotoxic T-cell inhibitors (Tretiakova *et al.*, 2000), complement inhibitors (Qu *et al.*, 2013), HIV fusion inhibitors (Eggink *et al.*, 2010) and protease inhibitors (Hong *et al.*, 2000).

Structural analysis of Rgg/SHP/DNA complexes will provide a complete picture of how Rgg/SHP complexes control transcription. This can be achieved by crystallisation of Rgg144 with its SHP144, and with respective DNA. This would elucidate the molecular network underlying Rgg144/SHP144 activation and might bring new insights about SHP144 peptide binding mode and its effect on Rgg144 transcription. The preliminary experiments for Rgg144 crystallisation with its SHP144 peptide were unsuccessful. Thus, more attention and numerous experiments are required to determine the appropriate conditions for crystal growth. A large number of commercial crystallisation kits are available to produce successful crystals. These kits contain hundreds of solutions with various combinations of pH, ionic strength, salts and precipitants (such as polyethylene glycol, dextran, polyvinyl alcohol, and polyvinyl pyrrolidone) as well as various additives and metal ions, which might maximise the chance of getting complex crystal. In addition, optimisation of the concentration of protein, ligand or DNA in the solution would facilitate the crystal to grow. Furthermore, soaking protein crystals with ligand might assist protein-ligand crystal formation. On the other hand, using other binding techniques such as NMR spectroscopy would be beneficial for detailed characterisation of protein/ligand interaction under specific physiological conditions. Additionally, quantitative gel-shift and DNA footprinting assays would be useful to study the interaction of Rgg144 with its target promoter in the presence of native or modified SHP144 peptide.

According to our published microarray data (Zhi *et al.*, 2018), a set of genes responsible for diversity of functions such as capsule synthesis, cell division and iron transport are under Rgg/SHP144 QS control. Therefore, it would be interesting to study the impact of inhibitor peptide on Rgg144 regulon using quantitative reverse transcriptase PCR and microarray analysis. In this case, the RNA will be extracted from wild-type D39 cells treated with or without modified peptide, cDNA will be analysed, and relative expression will be determined.

The results in this study suggest the presence of a link between Rgg/SHP144 QS and sugar metabolism. As addition of mannose or galactose to culture media stimulates the Rgg/SHP144 system whereas this induction was undetectable in the presence of glucose or *N*-acetylglucosamine. It would be interesting to test the impact of sugars as well as other environmental signals such as temperature, pH and metal ions on the Rgg/SHP144 regulated genes. This can be achieved by using reporter strains constructed in this study to determine the inducing conditions. Once the inducing conditions are determined, further analysis can be done by using DNA microarray and RNA sequence analysis for wild type and mutants (Δ*shp144* and Δ*rgg144*) under selected condition. The impact of selected genes on pneumococcal biology and virulence will then be examined.

S. pneumoniae type 2 D39 strain encodes five members of the Rgg family. Our recent published data have shown a cross talk between pneumococcal Rgg systems (Rgg/SHP144 and Rgg/SHP939) (Zhi *et al*., 2018). Thus, it would be reasonable to check if the inhibitor generated in this study could be applied to abolish phenotypic manifestations of other pneumococcal Rgg-dependent quorum sensing systems. To test this hypothesis, transcriptional reporter P_{shp939}::*lacZ* fused to the wild type D39 will be constructed, and then exposed to cell-culture supernatant of strain producing inhibitor peptide (Δ*shp144*ComP21A), or synthetic inhibitor peptide. The activity of *shp939* will then be determined using β-galactosidase assay. If the inhibitor works as hypothesised, the experiments similar to Rgg/SHP144 will be done to characterise the effect of inhibitor on phenotypic characterisations of Rgg939 QS system.

Finally, recent studies have pointed out the synergistic inhibitory activities of co-administration of QS-interfering agent with traditional antibiotics (Grandclément *et al*., 2016). QS inhibitors obstruct the bacterial signals which are responsible for drug resistance and bacterial persistence in the host, thus allowing antimicrobial agents influx into bacterial cells. Christensen *et al*. (2012) revealed that combination of tobramycin with one of QS inhibitors (such as furanone C-30, ajoene or iberin) accelerates *P. aeruginosa* biofilm dispersal and bacterial clearance in infected mice. Combination of baicalin hydrate, hamamelitannin, or cinnamaldehyde with different set of antibiotics have been studied in different pathogens such as Burkholderia spp., *S. aureus*, and *P. aeruginosa* in various *in vitro* and *in vivo* biofilm model systems (Brackman *et al*., 2011). Thus, in future studies, treatment of pneumococcal diseases with a mixture of antibiotic and SHP144 inhibitor might disrupt pneumococcal biofilm and increase their susceptibility against resistant antibiotic.

Appendix 1

Schematic diagram and DNA sequencing analysis of recombinant pPP2 carrying fusion construct (P$_{shp144}$::*lacZ)* for transcriptional *lacZ*-fusion analysis.

Alignment with Fusion-Seq-F primer

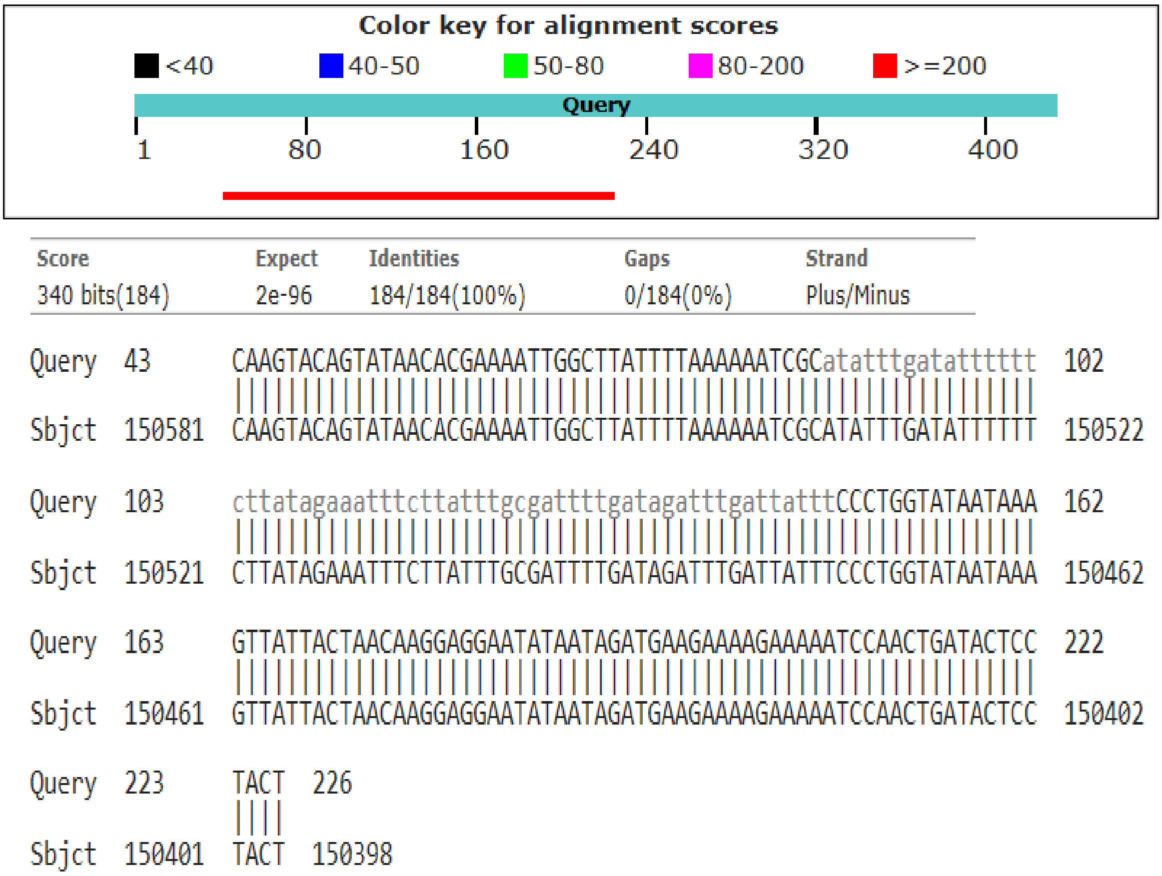

```
Score           Expect  Identities       Gaps       Strand
340 bits(184)   2e-96   184/184(100%)    0/184(0%)  Plus/Minus

Query  43      CAAGTACAGTATAACACGAAAATTGGCTTATTTTAAAAAATCGCatatttgatatttttt  102
               ||||||||||||||||||||||||||||||||||||||||||||||||||||||||||||
Sbjct  150581  CAAGTACAGTATAACACGAAAATTGGCTTATTTTAAAAAATCGCATATTTGATATTTTTT  150522

Query  103     cttatagaaatttcttatttgcgattttgatagatttgattatttCCCTGGTATAATAAA  162
               ||||||||||||||||||||||||||||||||||||||||||||||||||||||||||||
Sbjct  150521  CTTATAGAAATTTCTTATTTGCGATTTTGATAGATTTGATTATTTCCCTGGTATAATAAA  150462

Query  163     GTTATTACTAACAAGGAGGAATATAATAGATGAAGAAAAGAAAAATCCAACTGATACTCC  222
               ||||||||||||||||||||||||||||||||||||||||||||||||||||||||||||
Sbjct  150461  GTTATTACTAACAAGGAGGAATATAATAGATGAAGAAAAGAAAAATCCAACTGATACTCC  150402

Query  223     TACT  226
               ||||
Sbjct  150401  TACT  150398
```

Appendix 2

(A-N) Schematic diagrams and DNA sequencing data of fourteen recombinant pCEP constructs carrying the intact or modified copy of *shp144* gene with its putative promoter region.

(A) Intact copy of *shp144* with its putative promoter region

Alignment with Mal/F primer

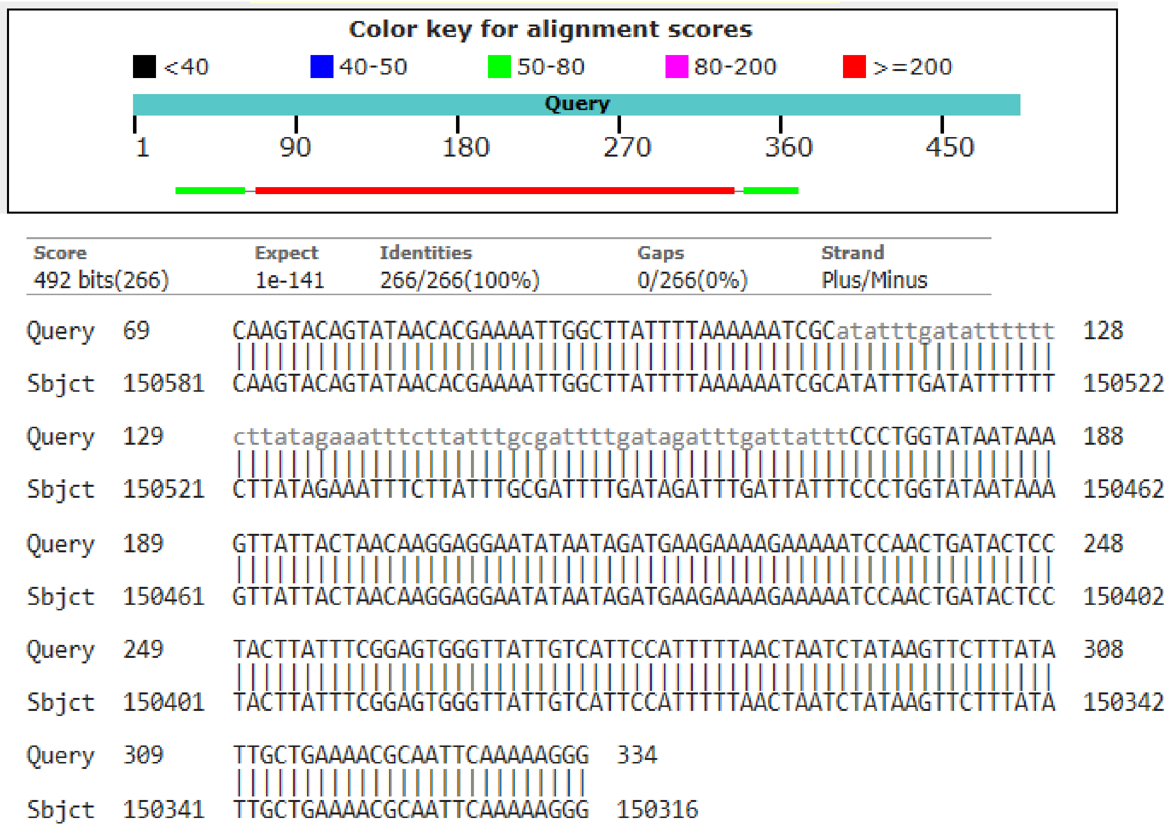

```
Score          Expect    Identities       Gaps       Strand
492 bits(266)  1e-141    266/266(100%)    0/266(0%)  Plus/Minus

Query  69      CAAGTACAGTATAACACGAAAATTGGCTTATTTTAAAAAATCGCatatttgatatttttt  128
               ||||||||||||||||||||||||||||||||||||||||||||||||||||||||||||
Sbjct  150581  CAAGTACAGTATAACACGAAAATTGGCTTATTTTAAAAAATCGCATATTTGATATTTTTT  150522

Query  129     cttatagaaatttcttatttgcgattttgatagatttgattatttCCCTGGTATAATAAA  188
               ||||||||||||||||||||||||||||||||||||||||||||||||||||||||||||
Sbjct  150521  CTTATAGAAATTTCTTATTTGCGATTTTGATAGATTTGATTATTTCCCTGGTATAATAAA  150462

Query  189     GTTATTACTAACAAGGAGGAATATAATAGATGAAGAAAAGAAAAATCCAACTGATACTCC  248
               ||||||||||||||||||||||||||||||||||||||||||||||||||||||||||||
Sbjct  150461  GTTATTACTAACAAGGAGGAATATAATAGATGAAGAAAAGAAAAATCCAACTGATACTCC  150402

Query  249     TACTTATTTCGGAGTGGGTTATTGTCATTCCATTTTTAACTAATCTATAAGTTCTTTATA  308
               ||||||||||||||||||||||||||||||||||||||||||||||||||||||||||||
Sbjct  150401  TACTTATTTCGGAGTGGGTTATTGTCATTCCATTTTTAACTAATCTATAAGTTCTTTATA  150342

Query  309     TTGCTGAAAACGCAATTCAAAAAGGG  334
               ||||||||||||||||||||||||||
Sbjct  150341  TTGCTGAAAACGCAATTCAAAAAGGG  150316
```

---

* ***shp144*** **modified nucleotides are highlighted with yellow colour.**

(B) Modified *shp144*L26A with its putative promoter [Leucine (CTA) changed to alanine (GCA)]

Alignment with Mal/F primer

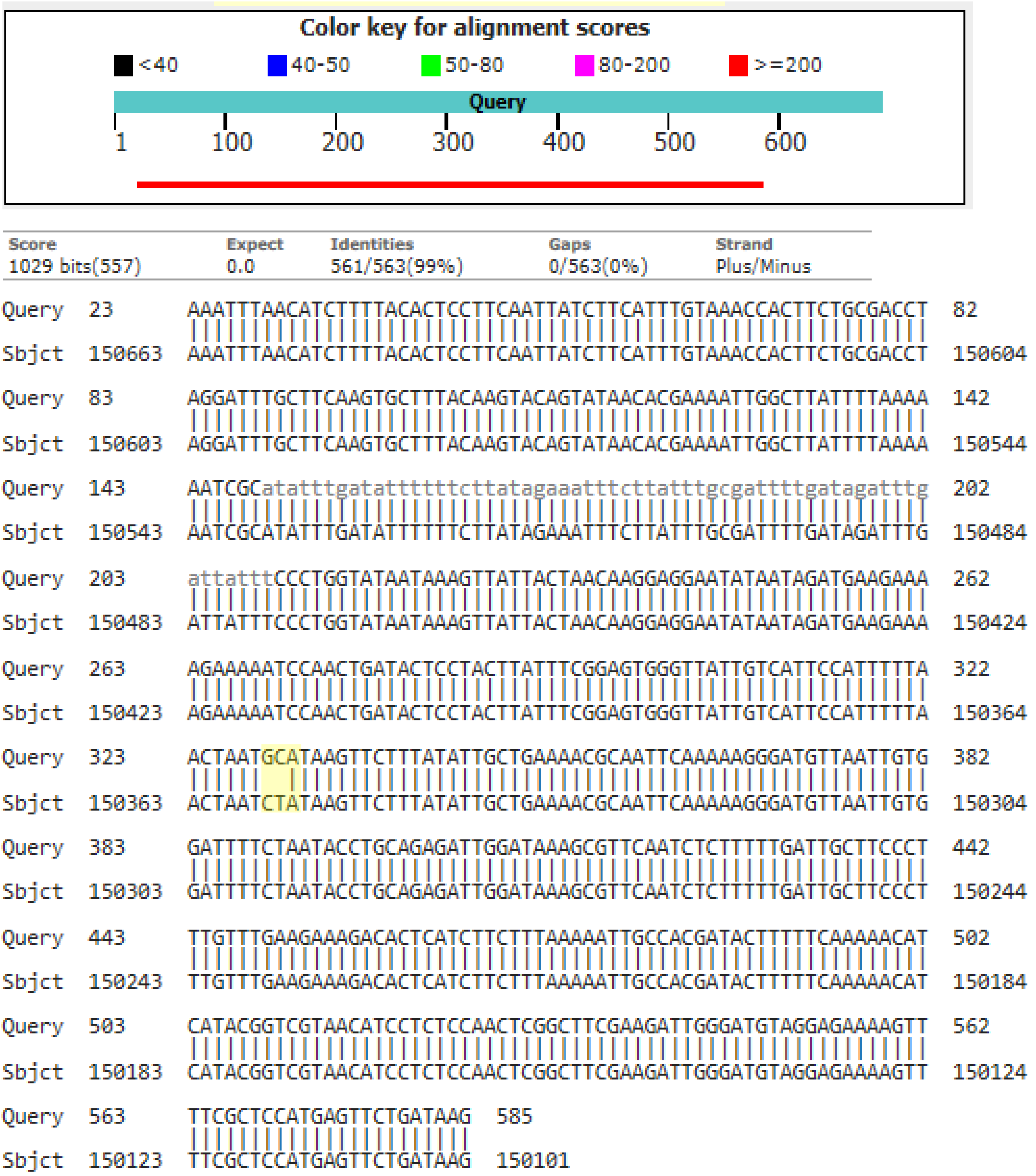

```
Score            Expect  Identities      Gaps          Strand
1029 bits(557)   0.0     561/563(99%)    0/563(0%)     Plus/Minus

Query  23      AAATTTAACATCTTTTACACTCCTTCAATTATCTTCATTTGTAAACCACTTCTGCGACCT  82
               ||||||||||||||||||||||||||||||||||||||||||||||||||||||||||||
Sbjct  150663  AAATTTAACATCTTTTACACTCCTTCAATTATCTTCATTTGTAAACCACTTCTGCGACCT  150604

Query  83      AGGATTTGCTTCAAGTGCTTTACAAGTACAGTATAACACGAAAATTGGCTTATTTTAAAA  142
               ||||||||||||||||||||||||||||||||||||||||||||||||||||||||||||
Sbjct  150603  AGGATTTGCTTCAAGTGCTTTACAAGTACAGTATAACACGAAAATTGGCTTATTTTAAAA  150544

Query  143     AATCGCatatttgatatttttttcttatagaaatttcttatttgcgattttgatagatttg  202
               ||||||||||||||||||||||||||||||||||||||||||||||||||||||||||||
Sbjct  150543  AATCGCATATTTGATATTTTTTCTTATAGAAATTTCTTATTTGCGATTTTGATAGATTTG  150484

Query  203     attatttCCCTGGTATAATAAAGTTATTACTAACAAGGAGGAATATAATAGATGAAGAAA  262
               ||||||||||||||||||||||||||||||||||||||||||||||||||||||||||||
Sbjct  150483  ATTATTTCCCTGGTATAATAAAGTTATTACTAACAAGGAGGAATATAATAGATGAAGAAA  150424

Query  263     AGAAAAATCCAACTGATACTCCTACTTATTTCGGAGTGGGTTATTGTCATTCCATTTTTA  322
               ||||||||||||||||||||||||||||||||||||||||||||||||||||||||||||
Sbjct  150423  AGAAAAATCCAACTGATACTCCTACTTATTTCGGAGTGGGTTATTGTCATTCCATTTTTA  150364

Query  323     ACTAATGCATAAGTTCTTTATATTGCTGAAAACGCAATTCAAAAAGGGATGTTAATTGTG  382
               ||||||  ||||||||||||||||||||||||||||||||||||||||||||||||||||
Sbjct  150363  ACTAATCTATAAGTTCTTTATATTGCTGAAAACGCAATTCAAAAAGGGATGTTAATTGTG  150304

Query  383     GATTTTCTAATACCTGCAGAGATTGGATAAAGCGTTCAATCTCTTTTTGATTGCTTCCCT  442
               ||||||||||||||||||||||||||||||||||||||||||||||||||||||||||||
Sbjct  150303  GATTTTCTAATACCTGCAGAGATTGGATAAAGCGTTCAATCTCTTTTTGATTGCTTCCCT  150244

Query  443     TTGTTTGAAGAAAGACACTCATCTTCTTTAAAAATTGCCACGATACTTTTTCAAAAACAT  502
               ||||||||||||||||||||||||||||||||||||||||||||||||||||||||||||
Sbjct  150243  TTGTTTGAAGAAAGACACTCATCTTCTTTAAAAATTGCCACGATACTTTTTCAAAAACAT  150184

Query  503     CATACGGTCGTAACATCCTCTCCAACTCGGCTTCGAAGATTGGGATGTAGGAGAAAAGTT  562
               ||||||||||||||||||||||||||||||||||||||||||||||||||||||||||||
Sbjct  150183  CATACGGTCGTAACATCCTCTCCAACTCGGCTTCGAAGATTGGGATGTAGGAGAAAAGTT  150124

Query  563     TTCGCTCCATGAGTTCTGATAAG  585
               |||||||||||||||||||||||
Sbjct  150123  TTCGCTCCATGAGTTCTGATAAG  150101
```

(C) Modified *shp144*N25A with its putative promoter [Asparagine (AAT) changed to alanine (GCT)]

Alignment with Mal/F primer

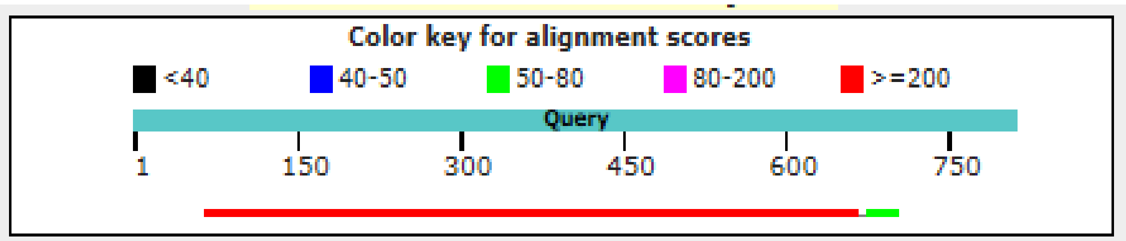

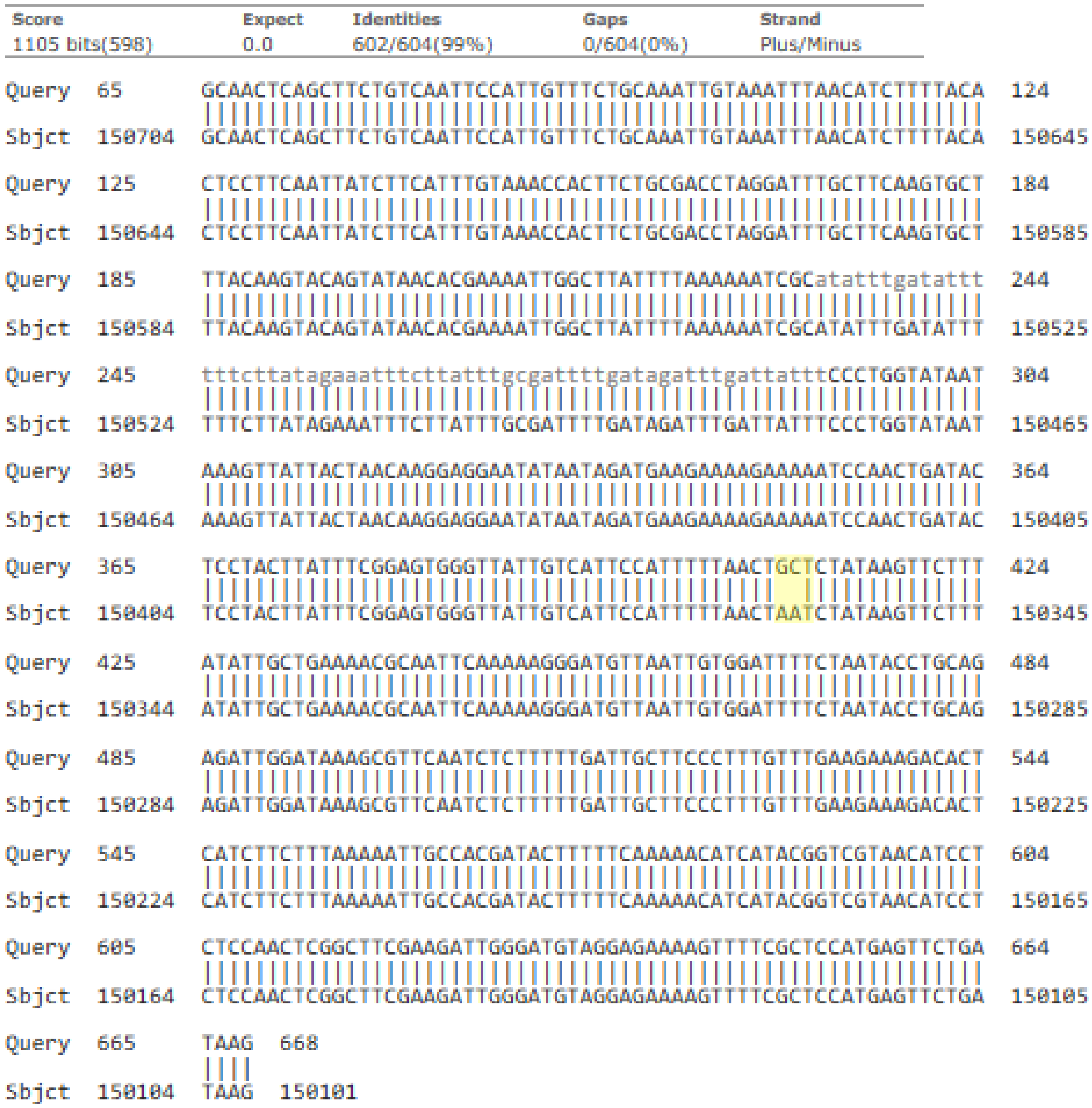

```
Score              Expect    Identities        Gaps          Strand
1105 bits(598)     0.0       602/604(99%)      0/604(0%)     Plus/Minus

Query  65      GCAACTCAGCTTCTGTCAATTCCATTGTTTCTGCAAATTGTAAATTTAACATCTTTTACA  124
               ||||||||||||||||||||||||||||||||||||||||||||||||||||||||||||
Sbjct  150704  GCAACTCAGCTTCTGTCAATTCCATTGTTTCTGCAAATTGTAAATTTAACATCTTTTACA  150645

Query  125     CTCCTTCAATTATCTTCATTTGTAAACCACTTCTGCGACCTAGGATTTGCTTCAAGTGCT  184
               ||||||||||||||||||||||||||||||||||||||||||||||||||||||||||||
Sbjct  150644  CTCCTTCAATTATCTTCATTTGTAAACCACTTCTGCGACCTAGGATTTGCTTCAAGTGCT  150585

Query  185     TTACAAGTACAGTATAACACGAAAATTGGCTTATTTTAAAAAATCGCatatttgatattt  244
               ||||||||||||||||||||||||||||||||||||||||||||||||||||||||||||
Sbjct  150584  TTACAAGTACAGTATAACACGAAAATTGGCTTATTTTAAAAAATCGCATATTTGATATTT  150525

Query  245     tttcttatagaaatttcttatttgcgattttgatagatttgattatttCCCTGGTATAAT  304
               ||||||||||||||||||||||||||||||||||||||||||||||||||||||||||||
Sbjct  150524  TTTCTTATAGAAATTTCTTATTTGCGATTTTGATAGATTTGATTATTTCCCTGGTATAAT  150465

Query  305     AAAGTTATTACTAACAAGGAGGAATATAATAGATGAAGAAAAGAAAAATCCAACTGATAC  364
               ||||||||||||||||||||||||||||||||||||||||||||||||||||||||||||
Sbjct  150464  AAAGTTATTACTAACAAGGAGGAATATAATAGATGAAGAAAAGAAAAATCCAACTGATAC  150405

Query  365     TCCTACTTATTTCGGAGTGGGTTATTGTCATTCCATTTTTAACTGCTCTATAAGTTCTTT  424
               ||||||||||||||||||||||||||||||||||||||||||||  ||||||||||||||
Sbjct  150404  TCCTACTTATTTCGGAGTGGGTTATTGTCATTCCATTTTTAACTAATCTATAAGTTCTTT  150345

Query  425     ATATTGCTGAAAACGCAATTCAAAAAGGGATGTTAATTGTGGATTTTCTAATACCTGCAG  484
               ||||||||||||||||||||||||||||||||||||||||||||||||||||||||||||
Sbjct  150344  ATATTGCTGAAAACGCAATTCAAAAAGGGATGTTAATTGTGGATTTTCTAATACCTGCAG  150285

Query  485     AGATTGGATAAAGCGTTCAATCTCTTTTTGATTGCTTCCCTTTGTTTGAAGAAAGACACT  544
               ||||||||||||||||||||||||||||||||||||||||||||||||||||||||||||
Sbjct  150284  AGATTGGATAAAGCGTTCAATCTCTTTTTGATTGCTTCCCTTTGTTTGAAGAAAGACACT  150225

Query  545     CATCTTCTTTAAAAATTGCCACGATACTTTTTCAAAAACATCATACGGTCGTAACATCCT  604
               ||||||||||||||||||||||||||||||||||||||||||||||||||||||||||||
Sbjct  150224  CATCTTCTTTAAAAATTGCCACGATACTTTTTCAAAAACATCATACGGTCGTAACATCCT  150165

Query  605     CTCCAACTCGGCTTCGAAGATTGGGATGTAGGAGAAAAGTTTTCGCTCCATGAGTTCTGA  664
               ||||||||||||||||||||||||||||||||||||||||||||||||||||||||||||
Sbjct  150164  CTCCAACTCGGCTTCGAAGATTGGGATGTAGGAGAAAAGTTTTCGCTCCATGAGTTCTGA  150105

Query  665     TAAG  668
               ||||
Sbjct  150104  TAAG  150101
```

(D) Modified *shp144*T24A with its putative promoter [Threonine (ACT) changed to alanine (GCT)]

Alignment with Mal/F primer

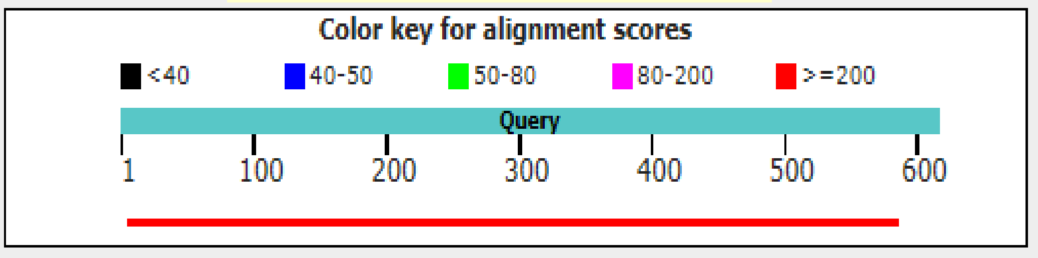

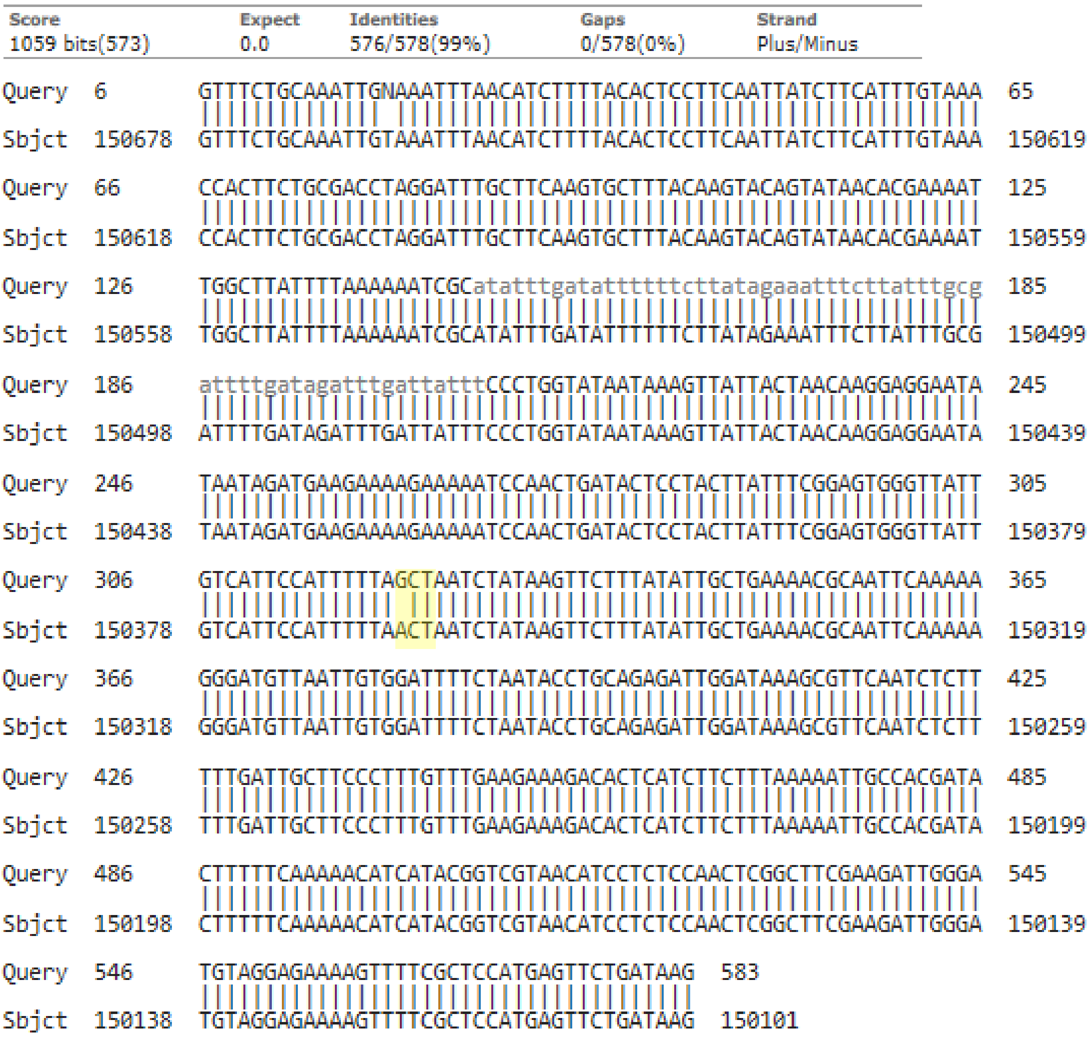

```
Score            Expect  Identities     Gaps       Strand
1059 bits(573)   0.0     576/578(99%)   0/578(0%)  Plus/Minus

Query  6       GTTTCTGCAAATTGNAAATTTAACATCTTTTACACTCCTTCAATTATCTTCATTTGTAAA  65
               |||||||||||||| |||||||||||||||||||||||||||||||||||||||||||||
Sbjct  150678  GTTTCTGCAAATTGTAAATTTAACATCTTTTACACTCCTTCAATTATCTTCATTTGTAAA  150619

Query  66      CCACTTCTGCGACCTAGGATTTGCTTCAAGTGCTTTACAAGTACAGTATAACACGAAAAT  125
               ||||||||||||||||||||||||||||||||||||||||||||||||||||||||||||
Sbjct  150618  CCACTTCTGCGACCTAGGATTTGCTTCAAGTGCTTTACAAGTACAGTATAACACGAAAAT  150559

Query  126     TGGCTTATTTTAAAAAATCGCatatttgatattttttcttatagaaatttcttatttgcg  185
               ||||||||||||||||||||||||||||||||||||||||||||||||||||||||||||
Sbjct  150558  TGGCTTATTTTAAAAAATCGCATATTTGATATTTTTTCTTATAGAAATTTCTTATTTGCG  150499

Query  186     attttgatagatttgattatttCCCTGGTATAATAAAGTTATTACTAACAAGGAGGAATA  245
               ||||||||||||||||||||||||||||||||||||||||||||||||||||||||||||
Sbjct  150498  ATTTTGATAGATTTGATTATTTCCCTGGTATAATAAAGTTATTACTAACAAGGAGGAATA  150439

Query  246     TAATAGATGAAGAAAAGAAAAATCCAACTGATACTCCTACTTATTTCGGAGTGGGTTATT  305
               ||||||||||||||||||||||||||||||||||||||||||||||||||||||||||||
Sbjct  150438  TAATAGATGAAGAAAAGAAAAATCCAACTGATACTCCTACTTATTTCGGAGTGGGTTATT  150379

Query  306     GTCATTCCATTTTTAGCTAATCTATAAGTTCTTTATATTGCTGAAAACGCAATTCAAAAA  365
               ||||||||||||||| ||||||||||||||||||||||||||||||||||||||||||||
Sbjct  150378  GTCATTCCATTTTTAACTAATCTATAAGTTCTTTATATTGCTGAAAACGCAATTCAAAAA  150319

Query  366     GGGATGTTAATTGTGGATTTTCTAATACCTGCAGAGATTGGATAAAGCGTTCAATCTCTT  425
               ||||||||||||||||||||||||||||||||||||||||||||||||||||||||||||
Sbjct  150318  GGGATGTTAATTGTGGATTTTCTAATACCTGCAGAGATTGGATAAAGCGTTCAATCTCTT  150259

Query  426     TTTGATTGCTTCCCTTTGTTTGAAGAAAGACACTCATCTTCTTTAAAAATTGCCACGATA  485
               ||||||||||||||||||||||||||||||||||||||||||||||||||||||||||||
Sbjct  150258  TTTGATTGCTTCCCTTTGTTTGAAGAAAGACACTCATCTTCTTTAAAAATTGCCACGATA  150199

Query  486     CTTTTTCAAAAACATCATACGGTCGTAACATCCTCTCCAACTCGGCTTCGAAGATTGGGA  545
               ||||||||||||||||||||||||||||||||||||||||||||||||||||||||||||
Sbjct  150198  CTTTTTCAAAAACATCATACGGTCGTAACATCCTCTCCAACTCGGCTTCGAAGATTGGGA  150139

Query  546     TGTAGGAGAAAAGTTTTCGCTCCATGAGTTCTGATAAG  583
               ||||||||||||||||||||||||||||||||||||||
Sbjct  150138  TGTAGGAGAAAAGTTTTCGCTCCATGAGTTCTGATAAG  150101
```

(E) Modified *shp144*L23A with its putative promoter [Leucine (TTA) changed to alanine (GCA)]

Alignment with Mal/F primer

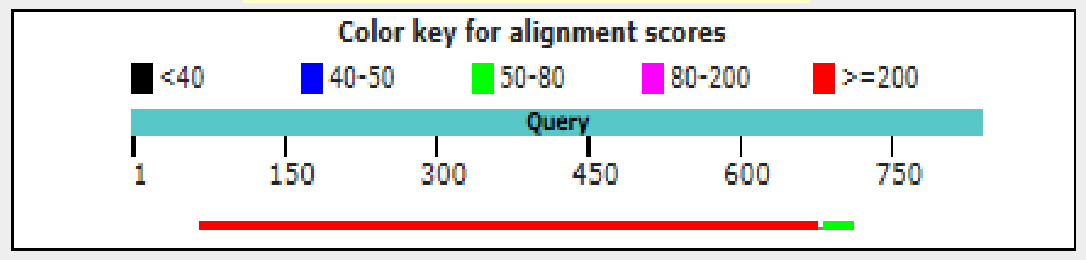

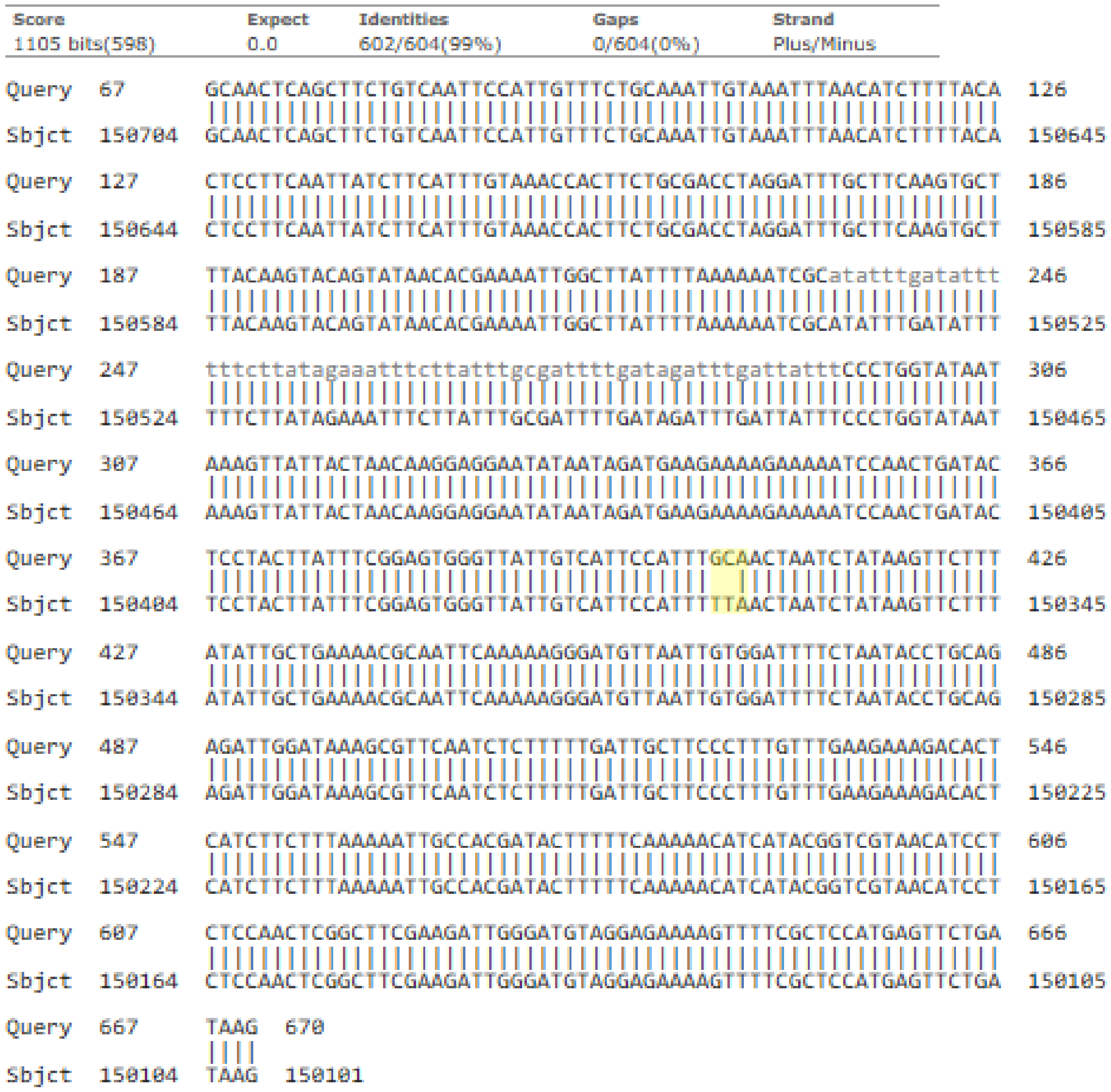

```
Score            Expect   Identities       Gaps         Strand
1105 bits(598)   0.0      602/604(99%)     0/604(0%)    Plus/Minus

Query  67      GCAACTCAGCTTCTGTCAATTCCATTGTTTCTGCAAATTGTAAATTTAACATCTTTTACA  126
               ||||||||||||||||||||||||||||||||||||||||||||||||||||||||||||
Sbjct  150704  GCAACTCAGCTTCTGTCAATTCCATTGTTTCTGCAAATTGTAAATTTAACATCTTTTACA  150645

Query  127     CTCCTTCAATTATCTTCATTTGTAAACCACTTCTGCGACCTAGGATTTGCTTCAAGTGCT  186
               ||||||||||||||||||||||||||||||||||||||||||||||||||||||||||||
Sbjct  150644  CTCCTTCAATTATCTTCATTTGTAAACCACTTCTGCGACCTAGGATTTGCTTCAAGTGCT  150585

Query  187     TTACAAGTACAGTATAACACGAAAATTGGCTTATTTTAAAAAATCGCatatttgatattt  246
               ||||||||||||||||||||||||||||||||||||||||||||||||||||||||||||
Sbjct  150584  TTACAAGTACAGTATAACACGAAAATTGGCTTATTTTAAAAAATCGCATATTTGATATTT  150525

Query  247     tttcttatagaaatttcttatttgcgattttgatagatttgattatttCCCTGGTATAAT  306
               ||||||||||||||||||||||||||||||||||||||||||||||||||||||||||||
Sbjct  150524  TTTCTTATAGAAATTTCTTATTTGCGATTTTGATAGATTTGATTATTTCCCTGGTATAAT  150465

Query  307     AAAGTTATTACTAACAAGGAGGAATATAATAGATGAAGAAAAGAAAAATCCAACTGATAC  366
               ||||||||||||||||||||||||||||||||||||||||||||||||||||||||||||
Sbjct  150464  AAAGTTATTACTAACAAGGAGGAATATAATAGATGAAGAAAAGAAAAATCCAACTGATAC  150405

Query  367     TCCTACTTATTTCGGAGTGGGTTATTGTCATTCCATTTGCAACTAATCTATAAGTTCTTT  426
               ||||||||||||||||||||||||||||||||||||||  ||||||||||||||||||||
Sbjct  150404  TCCTACTTATTTCGGAGTGGGTTATTGTCATTCCATTTTTAACTAATCTATAAGTTCTTT  150345

Query  427     ATATTGCTGAAAACGCAATTCAAAAAGGGATGTTAATTGTGGATTTTCTAATACCTGCAG  486
               ||||||||||||||||||||||||||||||||||||||||||||||||||||||||||||
Sbjct  150344  ATATTGCTGAAAACGCAATTCAAAAAGGGATGTTAATTGTGGATTTTCTAATACCTGCAG  150285

Query  487     AGATTGGATAAAGCGTTCAATCTCTTTTTGATTGCTTCCCTTTGTTTGAAGAAAGACACT  546
               ||||||||||||||||||||||||||||||||||||||||||||||||||||||||||||
Sbjct  150284  AGATTGGATAAAGCGTTCAATCTCTTTTTGATTGCTTCCCTTTGTTTGAAGAAAGACACT  150225

Query  547     CATCTTCTTTAAAAATTGCCACGATACTTTTTCAAAAACATCATACGGTCGTAACATCCT  606
               ||||||||||||||||||||||||||||||||||||||||||||||||||||||||||||
Sbjct  150224  CATCTTCTTTAAAAATTGCCACGATACTTTTTCAAAAACATCATACGGTCGTAACATCCT  150165

Query  607     CTCCAACTCGGCTTCGAAGATTGGGATGTAGGAGAAAAGTTTTCGCTCCATGAGTTCTGA  666
               ||||||||||||||||||||||||||||||||||||||||||||||||||||||||||||
Sbjct  150164  CTCCAACTCGGCTTCGAAGATTGGGATGTAGGAGAAAAGTTTTCGCTCCATGAGTTCTGA  150105

Query  667     TAAG  670
               ||||
Sbjct  150104  TAAG  150101
```

(F) Modified *shp144*F22A with its putative promoter [Phenylalanine (TTT) changed to alanine (GCT)]

Alignment with Mal/F primer

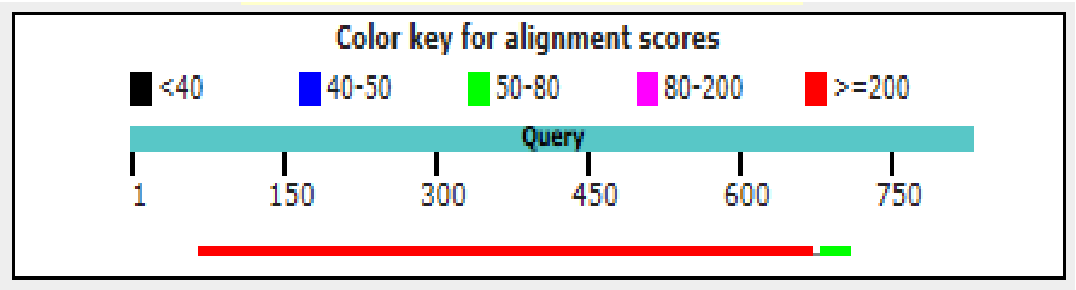

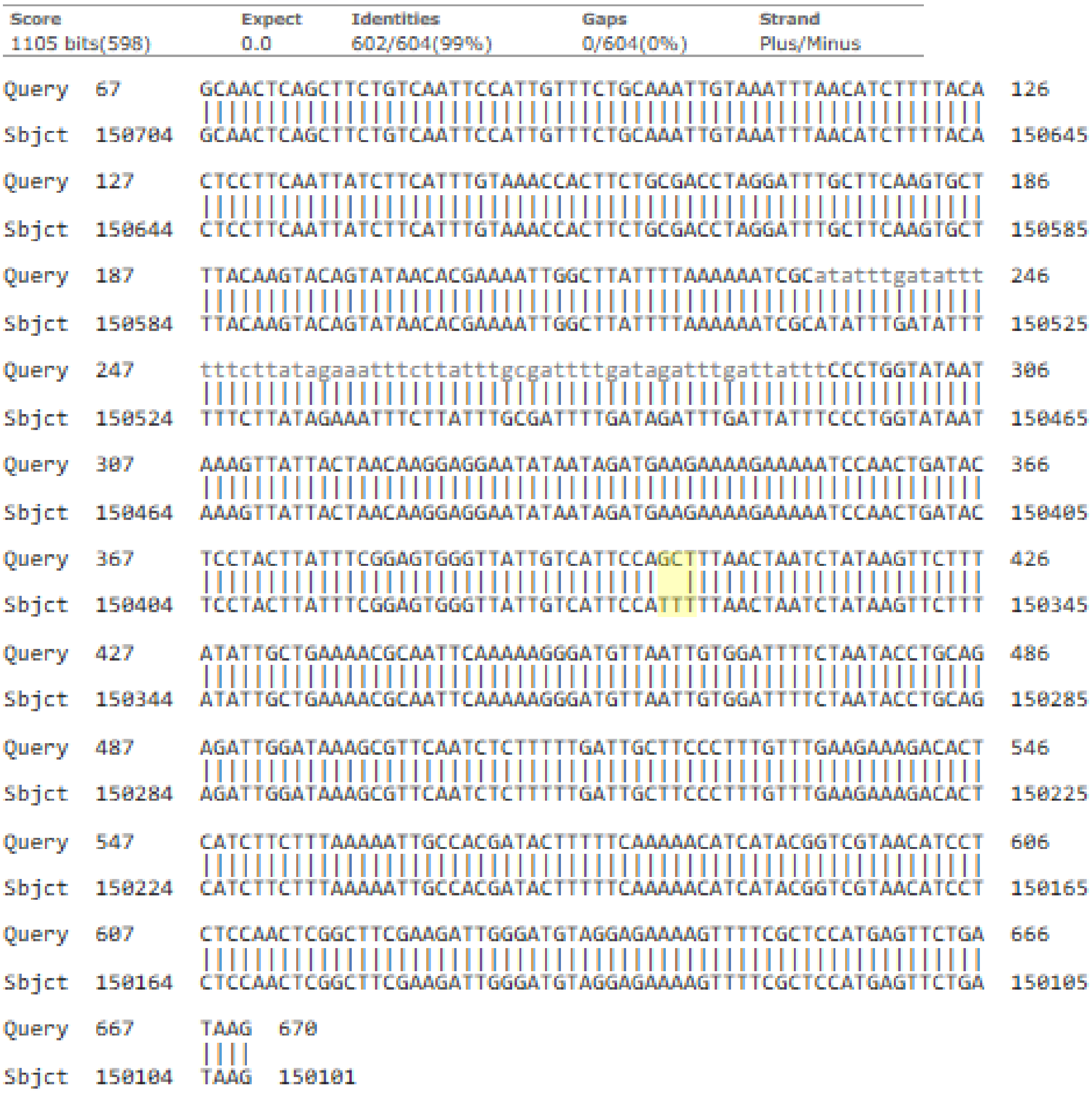

```
Score            Expect   Identities      Gaps        Strand
1105 bits(598)   0.0      602/604(99%)    0/604(0%)   Plus/Minus

Query  67      GCAACTCAGCTTCTGTCAATTCCATTGTTTCTGCAAATTGTAAATTTAACATCTTTTACA  126
               ||||||||||||||||||||||||||||||||||||||||||||||||||||||||||||
Sbjct  150704  GCAACTCAGCTTCTGTCAATTCCATTGTTTCTGCAAATTGTAAATTTAACATCTTTTACA  150645

Query  127     CTCCTTCAATTATCTTCATTTGTAAACCACTTCTGCGACCTAGGATTTGCTTCAAGTGCT  186
               ||||||||||||||||||||||||||||||||||||||||||||||||||||||||||||
Sbjct  150644  CTCCTTCAATTATCTTCATTTGTAAACCACTTCTGCGACCTAGGATTTGCTTCAAGTGCT  150585

Query  187     TTACAAGTACAGTATAACACGAAAATTGGCTTATTTTAAAAAATCGCatatttgatattt  246
               ||||||||||||||||||||||||||||||||||||||||||||||||||||||||||||
Sbjct  150584  TTACAAGTACAGTATAACACGAAAATTGGCTTATTTTAAAAAATCGCATATTTGATATTT  150525

Query  247     tttcttatagaaatttcttatttgcgattttgatagatttgattatttCCCTGGTATAAT  306
               ||||||||||||||||||||||||||||||||||||||||||||||||||||||||||||
Sbjct  150524  TTTCTTATAGAAATTTCTTATTTGCGATTTTGATAGATTTGATTATTTCCCTGGTATAAT  150465

Query  307     AAAGTTATTACTAACAAGGAGGAATATAATAGATGAAGAAAAGAAAAATCCAACTGATAC  366
               ||||||||||||||||||||||||||||||||||||||||||||||||||||||||||||
Sbjct  150464  AAAGTTATTACTAACAAGGAGGAATATAATAGATGAAGAAAAGAAAAATCCAACTGATAC  150405

Query  367     TCCTACTTATTTCGGAGTGGGTTATTGTCATTCCAGCTTTAACTAATCTATAAGTTCTTT  426
               |||||||||||||||||||||||||||||||||||  |||||||||||||||||||||||
Sbjct  150404  TCCTACTTATTTCGGAGTGGGTTATTGTCATTCCATTTTTAACTAATCTATAAGTTCTTT  150345

Query  427     ATATTGCTGAAAACGCAATTCAAAAAGGGATGTTAATTGTGGATTTTCTAATACCTGCAG  486
               ||||||||||||||||||||||||||||||||||||||||||||||||||||||||||||
Sbjct  150344  ATATTGCTGAAAACGCAATTCAAAAAGGGATGTTAATTGTGGATTTTCTAATACCTGCAG  150285

Query  487     AGATTGGATAAAGCGTTCAATCTCTTTTTGATTGCTTCCCTTTGTTTGAAGAAAGACACT  546
               ||||||||||||||||||||||||||||||||||||||||||||||||||||||||||||
Sbjct  150284  AGATTGGATAAAGCGTTCAATCTCTTTTTGATTGCTTCCCTTTGTTTGAAGAAAGACACT  150225

Query  547     CATCTTCTTTAAAAATTGCCACGATACTTTTTCAAAAACATCATACGGTCGTAACATCCT  606
               ||||||||||||||||||||||||||||||||||||||||||||||||||||||||||||
Sbjct  150224  CATCTTCTTTAAAAATTGCCACGATACTTTTTCAAAAACATCATACGGTCGTAACATCCT  150165

Query  607     CTCCAACTCGGCTTCGAAGATTGGGATGTAGGAGAAAAGTTTTCGCTCCATGAGTTCTGA  666
               ||||||||||||||||||||||||||||||||||||||||||||||||||||||||||||
Sbjct  150164  CTCCAACTCGGCTTCGAAGATTGGGATGTAGGAGAAAAGTTTTCGCTCCATGAGTTCTGA  150105

Query  667     TAAG  670
               ||||
Sbjct  150104  TAAG  150101
```

(G) Modified *shp144*P21A with its putative promoter [Proline (CCA) changed to alanine (GCA)]

Alignment with Mal/F primer

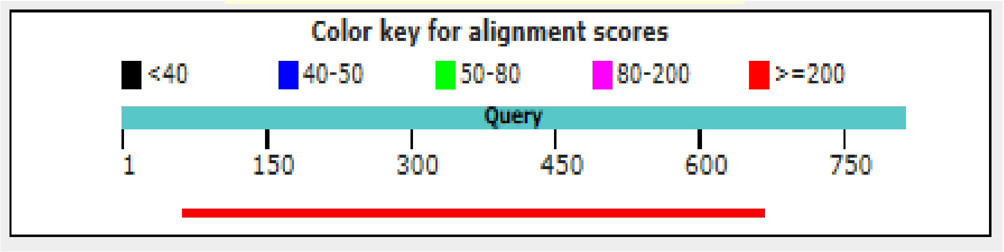

```
Score           Expect  Identities      Gaps        Strand
1110 bits(601)  0.0     603/604(99%)    0/604(0%)   Plus/Minus

Query  65      GCAACTCAGCTTCTGTCAATTCCATTGTTTCTGCAAATTGTAAATTTAACATCTTTTACA  124
               ||||||||||||||||||||||||||||||||||||||||||||||||||||||||||||
Sbjct  150704  GCAACTCAGCTTCTGTCAATTCCATTGTTTCTGCAAATTGTAAATTTAACATCTTTTACA  150645

Query  125     CTCCTTCAATTATCTTCATTTGTAAACCACTTCTGCGACCTAGGATTTGCTTCAAGTGCT  184
               ||||||||||||||||||||||||||||||||||||||||||||||||||||||||||||
Sbjct  150644  CTCCTTCAATTATCTTCATTTGTAAACCACTTCTGCGACCTAGGATTTGCTTCAAGTGCT  150585

Query  185     TTACAAGTACAGTATAACACGAAAATTGGCTTATTTTAAAAAATCGCatatttgatattt  244
               ||||||||||||||||||||||||||||||||||||||||||||||||||||||||||||
Sbjct  150584  TTACAAGTACAGTATAACACGAAAATTGGCTTATTTTAAAAAATCGCATATTTGATATTT  150525

Query  245     tttcttatagaaatttcttatttgcgattttgatagatttgattatttCCCTGGTATAAT  304
               ||||||||||||||||||||||||||||||||||||||||||||||||||||||||||||
Sbjct  150524  TTTCTTATAGAAATTTCTTATTTGCGATTTTGATAGATTTGATTATTTCCCTGGTATAAT  150465

Query  305     AAAGTTATTACTAACAAGGAGGAATATAATAGATGAAGAAAAGAAAAATCCAACTGATAC  364
               ||||||||||||||||||||||||||||||||||||||||||||||||||||||||||||
Sbjct  150464  AAAGTTATTACTAACAAGGAGGAATATAATAGATGAAGAAAAGAAAAATCCAACTGATAC  150405

Query  365     TCCTACTTATTTCGGAGTGGGTTATTGTCATTGCATTTTTAACTAATCTATAAGTTCTTT  424
               |||||||||||||||||||||||||||||||| |||||||||||||||||||||||||||
Sbjct  150404  TCCTACTTATTTCGGAGTGGGTTATTGTCATTCCATTTTTAACTAATCTATAAGTTCTTT  150345

Query  425     ATATTGCTGAAAACGCAATTCAAAAAGGGATGTTAATTGTGGATTTTCTAATACCTGCAG  484
               ||||||||||||||||||||||||||||||||||||||||||||||||||||||||||||
Sbjct  150344  ATATTGCTGAAAACGCAATTCAAAAAGGGATGTTAATTGTGGATTTTCTAATACCTGCAG  150285

Query  485     AGATTGGATAAAGCGTTCAATCTCTTTTTGATTGCTTCCCTTTGTTTGAAGAAAGACACT  544
               ||||||||||||||||||||||||||||||||||||||||||||||||||||||||||||
Sbjct  150284  AGATTGGATAAAGCGTTCAATCTCTTTTTGATTGCTTCCCTTTGTTTGAAGAAAGACACT  150225

Query  545     CATCTTCTTTAAAAATTGCCACGATACTTTTTCAAAAACATCATACGGTCGTAACATCCT  604
               ||||||||||||||||||||||||||||||||||||||||||||||||||||||||||||
Sbjct  150224  CATCTTCTTTAAAAATTGCCACGATACTTTTTCAAAAACATCATACGGTCGTAACATCCT  150165

Query  605     CTCCAACTCGGCTTCGAAGATTGGGATGTAGGAGAAAAGTTTTCGCTCCATGAGTTCTGA  664
               ||||||||||||||||||||||||||||||||||||||||||||||||||||||||||||
Sbjct  150164  CTCCAACTCGGCTTCGAAGATTGGGATGTAGGAGAAAAGTTTTCGCTCCATGAGTTCTGA  150105

Query  665     TAAG  668
               ||||
Sbjct  150104  TAAG  150101
```

(H) Modified *shp144*I20A with its putative promoter [Isoleucine (ATT) changed to alanine (GCT)]

Alignment with Mal/F primer

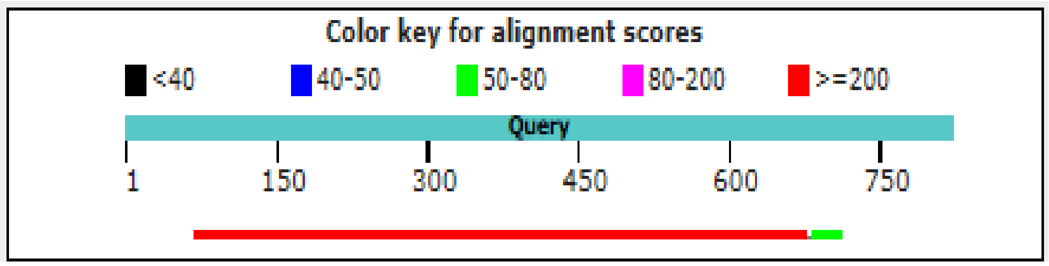

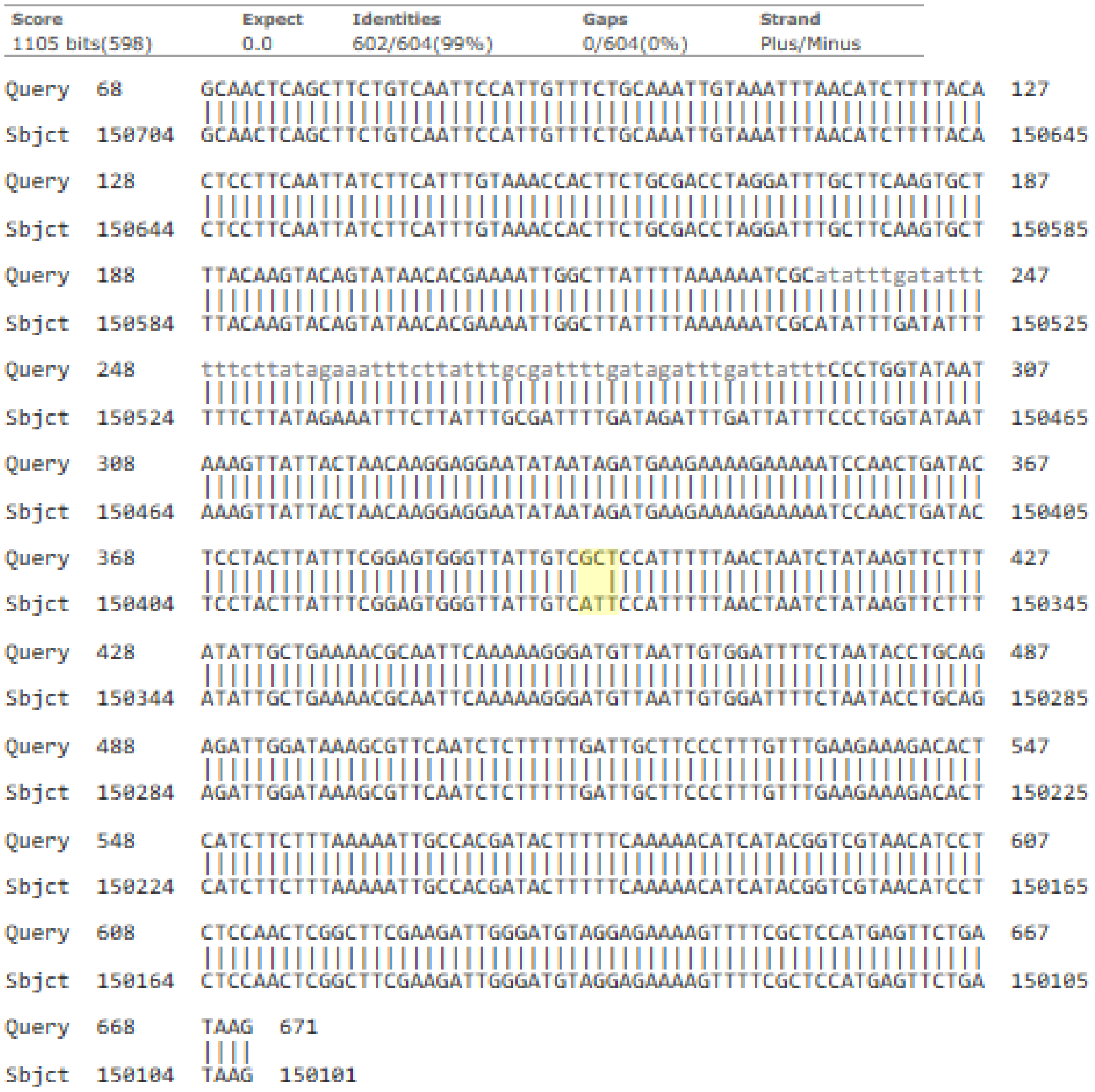

```
Score            Expect   Identities      Gaps        Strand
1105 bits(598)   0.0      602/604(99%)    0/604(0%)   Plus/Minus

Query  68      GCAACTCAGCTTCTGTCAATTCCATTGTTTCTGCAAATTGTAAATTTAACATCTTTTACA  127
               ||||||||||||||||||||||||||||||||||||||||||||||||||||||||||||
Sbjct  150704  GCAACTCAGCTTCTGTCAATTCCATTGTTTCTGCAAATTGTAAATTTAACATCTTTTACA  150645

Query  128     CTCCTTCAATTATCTTCATTTGTAAACCACTTCTGCGACCTAGGATTTGCTTCAAGTGCT  187
               ||||||||||||||||||||||||||||||||||||||||||||||||||||||||||||
Sbjct  150644  CTCCTTCAATTATCTTCATTTGTAAACCACTTCTGCGACCTAGGATTTGCTTCAAGTGCT  150585

Query  188     TTACAAGTACAGTATAACACGAAAATTGGCTTATTTTAAAAAATCGCatatttgatattt  247
               ||||||||||||||||||||||||||||||||||||||||||||||||||||||||||||
Sbjct  150584  TTACAAGTACAGTATAACACGAAAATTGGCTTATTTTAAAAAATCGCATATTTGATATTT  150525

Query  248     tttcttatagaaatttcttatttgcgattttgatagatttgattatttCCCTGGTATAAT  307
               ||||||||||||||||||||||||||||||||||||||||||||||||||||||||||||
Sbjct  150524  TTTCTTATAGAAATTTCTTATTTGCGATTTTGATAGATTTGATTATTTCCCTGGTATAAT  150465

Query  308     AAAGTTATTACTAACAAGGAGGAATATAATAGATGAAGAAAAGAAAAATCCAACTGATAC  367
               ||||||||||||||||||||||||||||||||||||||||||||||||||||||||||||
Sbjct  150464  AAAGTTATTACTAACAAGGAGGAATATAATAGATGAAGAAAAGAAAAATCCAACTGATAC  150405

Query  368     TCCTACTTATTTCGGAGTGGGTTATTGTCGCTCCATTTTTAACTAATCTATAAGTTCTTT  427
               |||||||||||||||||||||||||||||  |||||||||||||||||||||||||||||
Sbjct  150404  TCCTACTTATTTCGGAGTGGGTTATTGTCATTCCATTTTTAACTAATCTATAAGTTCTTT  150345

Query  428     ATATTGCTGAAAACGCAATTCAAAAAGGGATGTTAATTGTGGATTTTCTAATACCTGCAG  487
               ||||||||||||||||||||||||||||||||||||||||||||||||||||||||||||
Sbjct  150344  ATATTGCTGAAAACGCAATTCAAAAAGGGATGTTAATTGTGGATTTTCTAATACCTGCAG  150285

Query  488     AGATTGGATAAAGCGTTCAATCTCTTTTTGATTGCTTCCCTTTGTTTGAAGAAAGACACT  547
               ||||||||||||||||||||||||||||||||||||||||||||||||||||||||||||
Sbjct  150284  AGATTGGATAAAGCGTTCAATCTCTTTTTGATTGCTTCCCTTTGTTTGAAGAAAGACACT  150225

Query  548     CATCTTCTTTAAAAATTGCCACGATACTTTTTCAAAAACATCATACGGTCGTAACATCCT  607
               ||||||||||||||||||||||||||||||||||||||||||||||||||||||||||||
Sbjct  150224  CATCTTCTTTAAAAATTGCCACGATACTTTTTCAAAAACATCATACGGTCGTAACATCCT  150165

Query  608     CTCCAACTCGGCTTCGAAGATTGGGATGTAGGAGAAAAGTTTTCGCTCCATGAGTTCTGA  667
               ||||||||||||||||||||||||||||||||||||||||||||||||||||||||||||
Sbjct  150164  CTCCAACTCGGCTTCGAAGATTGGGATGTAGGAGAAAAGTTTTCGCTCCATGAGTTCTGA  150105

Query  668     TAAG  671
               ||||
Sbjct  150104  TAAG  150101
```

(I) Modified *shp144*V19A with its putative promoter [Valine (GTC) changed to alanine (GCC)]

Alignment with Mal/F primer

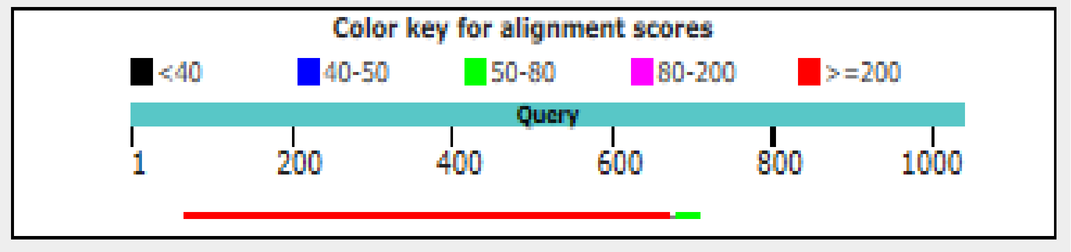

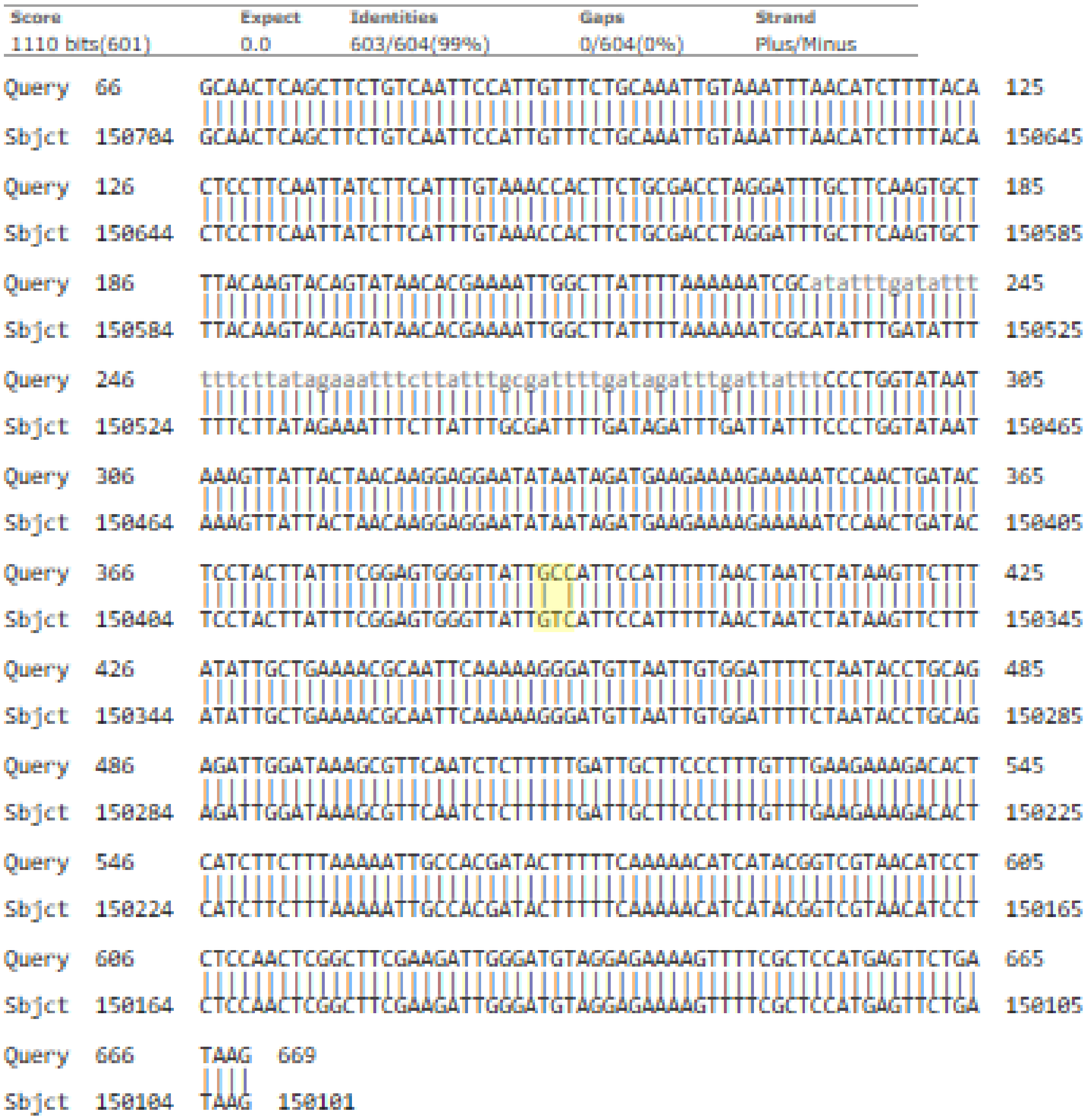

```
Score           Expect  Identities     Gaps       Strand
1110 bits(601)  0.0     603/604(99%)   0/604(0%)  Plus/Minus

Query  66      GCAACTCAGCTTCTGTCAATTCCATTGTTTCTGCAAATTGTAAATTTAACATCTTTTACA  125
               ||||||||||||||||||||||||||||||||||||||||||||||||||||||||||||
Sbjct  150704  GCAACTCAGCTTCTGTCAATTCCATTGTTTCTGCAAATTGTAAATTTAACATCTTTTACA  150645

Query  126     CTCCTTCAATTATCTTCATTTGTAAACCACTTCTGCGACCTAGGATTTGCTTCAAGTGCT  185
               ||||||||||||||||||||||||||||||||||||||||||||||||||||||||||||
Sbjct  150644  CTCCTTCAATTATCTTCATTTGTAAACCACTTCTGCGACCTAGGATTTGCTTCAAGTGCT  150585

Query  186     TTACAAGTACAGTATAACACGAAAATTGGCTTATTTTAAAAAATCGCatatttgatattt  245
               ||||||||||||||||||||||||||||||||||||||||||||||||||||||||||||
Sbjct  150584  TTACAAGTACAGTATAACACGAAAATTGGCTTATTTTAAAAAATCGCATATTTGATATTT  150525

Query  246     tttcttatagaaatttcttatttgcgattttgatagatttgattatttCCCTGGTATAAT  305
               ||||||||||||||||||||||||||||||||||||||||||||||||||||||||||||
Sbjct  150524  TTTCTTATAGAAATTTCTTATTTGCGATTTTGATAGATTTGATTATTTCCCTGGTATAAT  150465

Query  306     AAAGTTATTACTAACAAGGAGGAATATAATAGATGAAGAAAAGAAAAATCCAACTGATAC  365
               ||||||||||||||||||||||||||||||||||||||||||||||||||||||||||||
Sbjct  150464  AAAGTTATTACTAACAAGGAGGAATATAATAGATGAAGAAAAGAAAAATCCAACTGATAC  150405

Query  366     TCCTACTTATTTCGGAGTGGGTTATTGCCATTCCATTTTTAACTAATCTATAAGTTCTTT  425
               ||||||||||||||||||||||||||| ||||||||||||||||||||||||||||||||
Sbjct  150404  TCCTACTTATTTCGGAGTGGGTTATTGTCATTCCATTTTTAACTAATCTATAAGTTCTTT  150345

Query  426     ATATTGCTGAAAACGCAATTCAAAAAGGGATGTTAATTGTGGATTTTCTAATACCTGCAG  485
               ||||||||||||||||||||||||||||||||||||||||||||||||||||||||||||
Sbjct  150344  ATATTGCTGAAAACGCAATTCAAAAAGGGATGTTAATTGTGGATTTTCTAATACCTGCAG  150285

Query  486     AGATTGGATAAAGCGTTCAATCTCTTTTTGATTGCTTCCCTTTGTTTGAAGAAAGACACT  545
               ||||||||||||||||||||||||||||||||||||||||||||||||||||||||||||
Sbjct  150284  AGATTGGATAAAGCGTTCAATCTCTTTTTGATTGCTTCCCTTTGTTTGAAGAAAGACACT  150225

Query  546     CATCTTCTTTAAAAATTGCCACGATACTTTTTCAAAAACATCATACGGTCGTAACATCCT  605
               ||||||||||||||||||||||||||||||||||||||||||||||||||||||||||||
Sbjct  150224  CATCTTCTTTAAAAATTGCCACGATACTTTTTCAAAAACATCATACGGTCGTAACATCCT  150165

Query  606     CTCCAACTCGGCTTCGAAGATTGGGATGTAGGAGAAAAGTTTTCGCTCCATGAGTTCTGA  665
               ||||||||||||||||||||||||||||||||||||||||||||||||||||||||||||
Sbjct  150164  CTCCAACTCGGCTTCGAAGATTGGGATGTAGGAGAAAAGTTTTCGCTCCATGAGTTCTGA  150105

Query  666     TAAG  669
               ||||
Sbjct  150104  TAAG  150101
```

(J) Modified *shp144*I18A with its putative promoter [Isoleucine (ATT) changed to alanine (GCT)]

Alignment with Mal/F primer

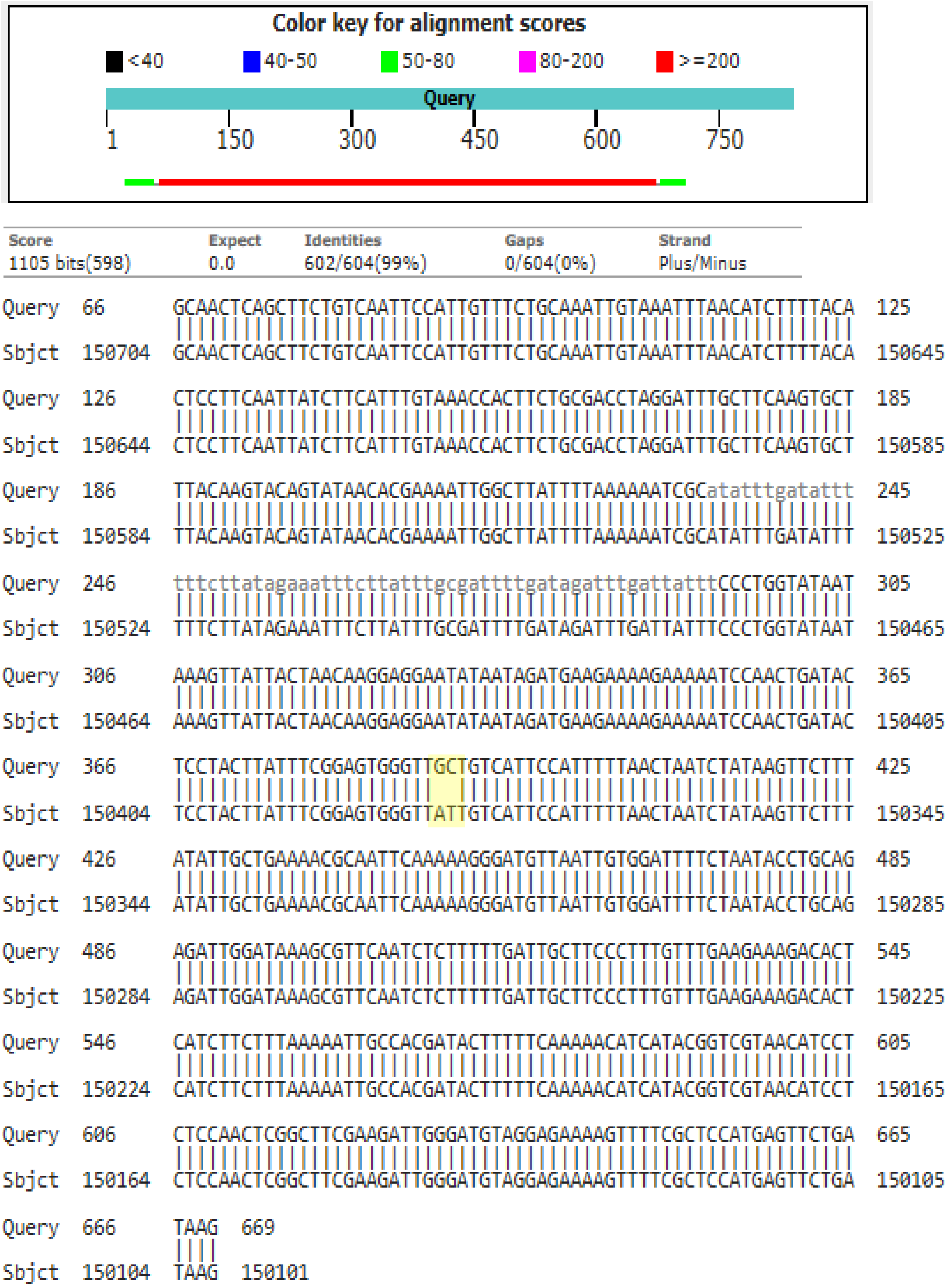

```
Score             Expect   Identities      Gaps       Strand
1105 bits(598)    0.0      602/604(99%)    0/604(0%)  Plus/Minus

Query  66      GCAACTCAGCTTCTGTCAATTCCATTGTTTCTGCAAATTGTAAATTTAACATCTTTTACA  125
               ||||||||||||||||||||||||||||||||||||||||||||||||||||||||||||
Sbjct  150704  GCAACTCAGCTTCTGTCAATTCCATTGTTTCTGCAAATTGTAAATTTAACATCTTTTACA  150645

Query  126     CTCCTTCAATTATCTTCATTTGTAAACCACTTCTGCGACCTAGGATTTGCTTCAAGTGCT  185
               ||||||||||||||||||||||||||||||||||||||||||||||||||||||||||||
Sbjct  150644  CTCCTTCAATTATCTTCATTTGTAAACCACTTCTGCGACCTAGGATTTGCTTCAAGTGCT  150585

Query  186     TTACAAGTACAGTATAACACGAAAATTGGCTTATTTTAAAAAATCGCatatttgatattt  245
               ||||||||||||||||||||||||||||||||||||||||||||||||||||||||||||
Sbjct  150584  TTACAAGTACAGTATAACACGAAAATTGGCTTATTTTAAAAAATCGCATATTTGATATTT  150525

Query  246     tttcttatagaaatttcttatttgcgattttgatagatttgattatttCCCTGGTATAAT  305
               ||||||||||||||||||||||||||||||||||||||||||||||||||||||||||||
Sbjct  150524  TTTCTTATAGAAATTTCTTATTTGCGATTTTGATAGATTTGATTATTTCCCTGGTATAAT  150465

Query  306     AAAGTTATTACTAACAAGGAGGAATATAATAGATGAAGAAAAGAAAAATCCAACTGATAC  365
               ||||||||||||||||||||||||||||||||||||||||||||||||||||||||||||
Sbjct  150464  AAAGTTATTACTAACAAGGAGGAATATAATAGATGAAGAAAAGAAAAATCCAACTGATAC  150405

Query  366     TCCTACTTATTTCGGAGTGGGTTGCTGTCATTCCATTTTTAACTAATCTATAAGTTCTTT  425
               |||||||||||||||||||||||  |||||||||||||||||||||||||||||||||||
Sbjct  150404  TCCTACTTATTTCGGAGTGGGTTATTGTCATTCCATTTTTAACTAATCTATAAGTTCTTT  150345

Query  426     ATATTGCTGAAAACGCAATTCAAAAAGGGATGTTAATTGTGGATTTTCTAATACCTGCAG  485
               ||||||||||||||||||||||||||||||||||||||||||||||||||||||||||||
Sbjct  150344  ATATTGCTGAAAACGCAATTCAAAAAGGGATGTTAATTGTGGATTTTCTAATACCTGCAG  150285

Query  486     AGATTGGATAAAGCGTTCAATCTCTTTTTGATTGCTTCCCTTTGTTTGAAGAAAGACACT  545
               ||||||||||||||||||||||||||||||||||||||||||||||||||||||||||||
Sbjct  150284  AGATTGGATAAAGCGTTCAATCTCTTTTTGATTGCTTCCCTTTGTTTGAAGAAAGACACT  150225

Query  546     CATCTTCTTTAAAAATTGCCACGATACTTTTTCAAAAACATCATACGGTCGTAACATCCT  605
               ||||||||||||||||||||||||||||||||||||||||||||||||||||||||||||
Sbjct  150224  CATCTTCTTTAAAAATTGCCACGATACTTTTTCAAAAACATCATACGGTCGTAACATCCT  150165

Query  606     CTCCAACTCGGCTTCGAAGATTGGGATGTAGGAGAAAAGTTTTCGCTCCATGAGTTCTGA  665
               ||||||||||||||||||||||||||||||||||||||||||||||||||||||||||||
Sbjct  150164  CTCCAACTCGGCTTCGAAGATTGGGATGTAGGAGAAAAGTTTTCGCTCCATGAGTTCTGA  150105

Query  666     TAAG  669
               ||||
Sbjct  150104  TAAG  150101
```

(K) Modified *shp144*V17A with its putative promoter [Valine (GTT) changed to alanine (GCT)]

Alignment with Mal/F primer

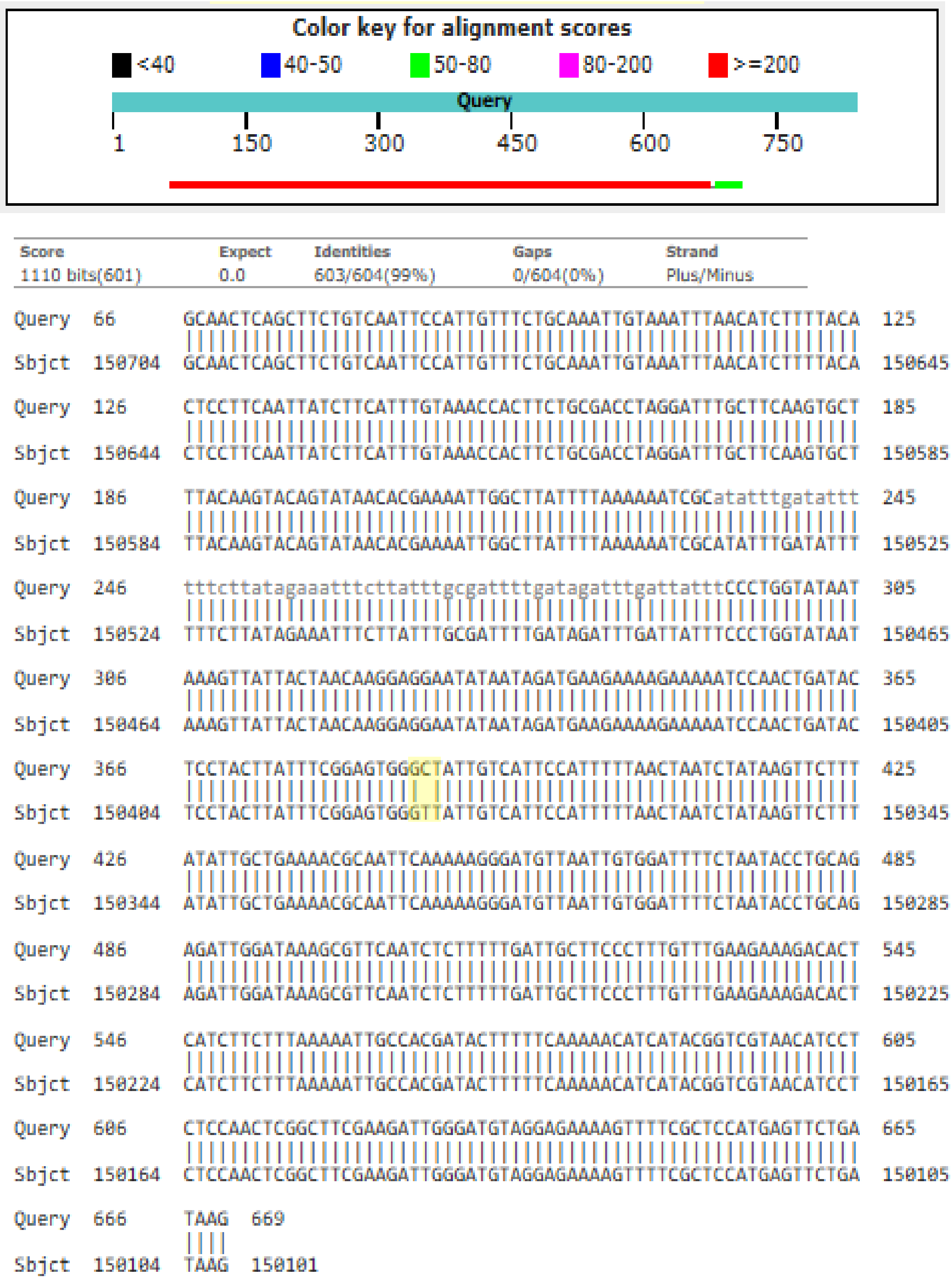

```
Score            Expect   Identities      Gaps        Strand
1110 bits(601)   0.0      603/604(99%)    0/604(0%)   Plus/Minus

Query  66      GCAACTCAGCTTCTGTCAATTCCATTGTTTCTGCAAATTGTAAATTTAACATCTTTTACA  125
               ||||||||||||||||||||||||||||||||||||||||||||||||||||||||||||
Sbjct  150704  GCAACTCAGCTTCTGTCAATTCCATTGTTTCTGCAAATTGTAAATTTAACATCTTTTACA  150645

Query  126     CTCCTTCAATTATCTTCATTTGTAAACCACTTCTGCGACCTAGGATTTGCTTCAAGTGCT  185
               ||||||||||||||||||||||||||||||||||||||||||||||||||||||||||||
Sbjct  150644  CTCCTTCAATTATCTTCATTTGTAAACCACTTCTGCGACCTAGGATTTGCTTCAAGTGCT  150585

Query  186     TTACAAGTACAGTATAACACGAAAATTGGCTTATTTTAAAAAATCGCatatttgatattt  245
               ||||||||||||||||||||||||||||||||||||||||||||||||||||||||||||
Sbjct  150584  TTACAAGTACAGTATAACACGAAAATTGGCTTATTTTAAAAAATCGCATATTTGATATTT  150525

Query  246     tttcttatagaaatttcttatttgcgattttgatagatttgattatttCCCTGGTATAAT  305
               ||||||||||||||||||||||||||||||||||||||||||||||||||||||||||||
Sbjct  150524  TTTCTTATAGAAATTTCTTATTTGCGATTTTGATAGATTTGATTATTTCCCTGGTATAAT  150465

Query  306     AAAGTTATTACTAACAAGGAGGAATATAATAGATGAAGAAAAGAAAAATCCAACTGATAC  365
               ||||||||||||||||||||||||||||||||||||||||||||||||||||||||||||
Sbjct  150464  AAAGTTATTACTAACAAGGAGGAATATAATAGATGAAGAAAAGAAAAATCCAACTGATAC  150405

Query  366     TCCTACTTATTTCGGAGTGGGCTATTGTCATTCCATTTTTAACTAATCTATAAGTTCTTT  425
               ||||||||||||||||||||| ||||||||||||||||||||||||||||||||||||||
Sbjct  150404  TCCTACTTATTTCGGAGTGGGTTATTGTCATTCCATTTTTAACTAATCTATAAGTTCTTT  150345

Query  426     ATATTGCTGAAAACGCAATTCAAAAAGGGATGTTAATTGTGGATTTTCTAATACCTGCAG  485
               ||||||||||||||||||||||||||||||||||||||||||||||||||||||||||||
Sbjct  150344  ATATTGCTGAAAACGCAATTCAAAAAGGGATGTTAATTGTGGATTTTCTAATACCTGCAG  150285

Query  486     AGATTGGATAAAGCGTTCAATCTCTTTTTGATTGCTTCCCTTTGTTTGAAGAAAGACACT  545
               ||||||||||||||||||||||||||||||||||||||||||||||||||||||||||||
Sbjct  150284  AGATTGGATAAAGCGTTCAATCTCTTTTTGATTGCTTCCCTTTGTTTGAAGAAAGACACT  150225

Query  546     CATCTTCTTTAAAAATTGCCACGATACTTTTTCAAAAACATCATACGGTCGTAACATCCT  605
               ||||||||||||||||||||||||||||||||||||||||||||||||||||||||||||
Sbjct  150224  CATCTTCTTTAAAAATTGCCACGATACTTTTTCAAAAACATCATACGGTCGTAACATCCT  150165

Query  606     CTCCAACTCGGCTTCGAAGATTGGGATGTAGGAGAAAAGTTTTCGCTCCATGAGTTCTGA  665
               ||||||||||||||||||||||||||||||||||||||||||||||||||||||||||||
Sbjct  150164  CTCCAACTCGGCTTCGAAGATTGGGATGTAGGAGAAAAGTTTTCGCTCCATGAGTTCTGA  150105

Query  666     TAAG  669
               ||||
Sbjct  150104  TAAG  150101
```

(L) Modified *shp144*W16A with its putative promoter [Tryptophan (TGG) changed to alanine (GCG)]

Alignment with Mal/F primer

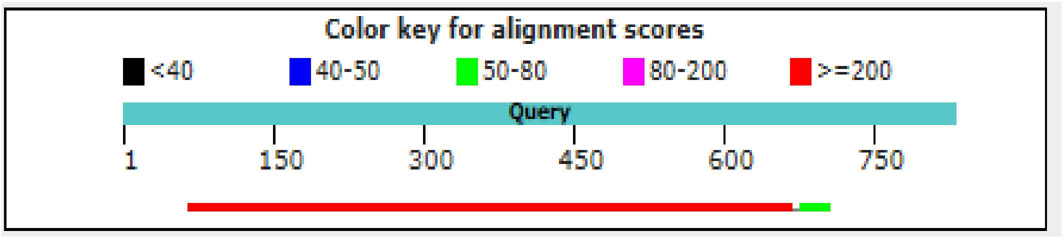

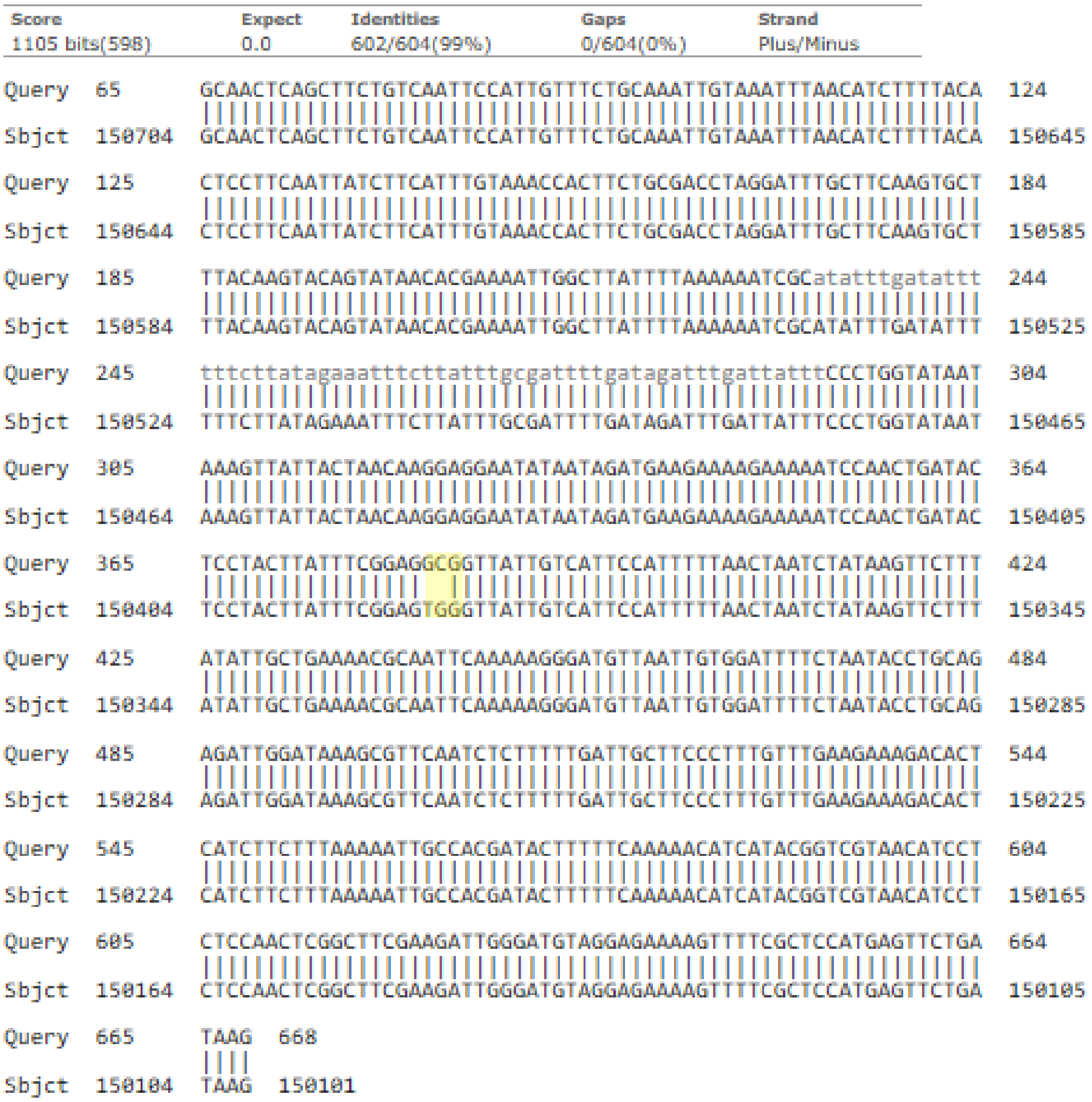

```
Score             Expect   Identities      Gaps        Strand
1105 bits(598)    0.0      602/604(99%)    0/604(0%)   Plus/Minus

Query  65      GCAACTCAGCTTCTGTCAATTCCATTGTTTCTGCAAATTGTAAATTTAACATCTTTTACA  124
               ||||||||||||||||||||||||||||||||||||||||||||||||||||||||||||
Sbjct  150704  GCAACTCAGCTTCTGTCAATTCCATTGTTTCTGCAAATTGTAAATTTAACATCTTTTACA  150645

Query  125     CTCCTTCAATTATCTTCATTTGTAAACCACTTCTGCGACCTAGGATTTGCTTCAAGTGCT  184
               ||||||||||||||||||||||||||||||||||||||||||||||||||||||||||||
Sbjct  150644  CTCCTTCAATTATCTTCATTTGTAAACCACTTCTGCGACCTAGGATTTGCTTCAAGTGCT  150585

Query  185     TTACAAGTACAGTATAACACGAAAATTGGCTTATTTTAAAAAATCGCatatttgatattt  244
               ||||||||||||||||||||||||||||||||||||||||||||||||||||||||||||
Sbjct  150584  TTACAAGTACAGTATAACACGAAAATTGGCTTATTTTAAAAAATCGCATATTTGATATTT  150525

Query  245     tttcttatagaaatttcttatttgcgattttgatagatttgattatttCCCTGGTATAAT  304
               ||||||||||||||||||||||||||||||||||||||||||||||||||||||||||||
Sbjct  150524  TTTCTTATAGAAATTTCTTATTTGCGATTTTGATAGATTTGATTATTTCCCTGGTATAAT  150465

Query  305     AAAGTTATTACTAACAAGGAGGAATATAATAGATGAAGAAAAGAAAAATCCAACTGATAC  364
               ||||||||||||||||||||||||||||||||||||||||||||||||||||||||||||
Sbjct  150464  AAAGTTATTACTAACAAGGAGGAATATAATAGATGAAGAAAAGAAAAATCCAACTGATAC  150405

Query  365     TCCTACTTATTTCGGAGGCGGTTATTGTCATTCCATTTTTAACTAATCTATAAGTTCTTT  424
               |||||||||||||||||  |||||||||||||||||||||||||||||||||||||||||
Sbjct  150404  TCCTACTTATTTCGGAGTGGGTTATTGTCATTCCATTTTTAACTAATCTATAAGTTCTTT  150345

Query  425     ATATTGCTGAAAACGCAATTCAAAAAGGGATGTTAATTGTGGATTTTCTAATACCTGCAG  484
               ||||||||||||||||||||||||||||||||||||||||||||||||||||||||||||
Sbjct  150344  ATATTGCTGAAAACGCAATTCAAAAAGGGATGTTAATTGTGGATTTTCTAATACCTGCAG  150285

Query  485     AGATTGGATAAAGCGTTCAATCTCTTTTTGATTGCTTCCCTTTGTTTGAAGAAAGACACT  544
               ||||||||||||||||||||||||||||||||||||||||||||||||||||||||||||
Sbjct  150284  AGATTGGATAAAGCGTTCAATCTCTTTTTGATTGCTTCCCTTTGTTTGAAGAAAGACACT  150225

Query  545     CATCTTCTTTAAAAATTGCCACGATACTTTTTCAAAAACATCATACGGTCGTAACATCCT  604
               ||||||||||||||||||||||||||||||||||||||||||||||||||||||||||||
Sbjct  150224  CATCTTCTTTAAAAATTGCCACGATACTTTTTCAAAAACATCATACGGTCGTAACATCCT  150165

Query  605     CTCCAACTCGGCTTCGAAGATTGGGATGTAGGAGAAAAGTTTTCGCTCCATGAGTTCTGA  664
               ||||||||||||||||||||||||||||||||||||||||||||||||||||||||||||
Sbjct  150164  CTCCAACTCGGCTTCGAAGATTGGGATGTAGGAGAAAAGTTTTCGCTCCATGAGTTCTGA  150105

Query  665     TAAG  668
               ||||
Sbjct  150104  TAAG  150101
```

(M) Modified *shp144*E15A with its putative promoter [Glutamate (GAG) changed to alanine (GCG)]

Alignment with Mal/F primer

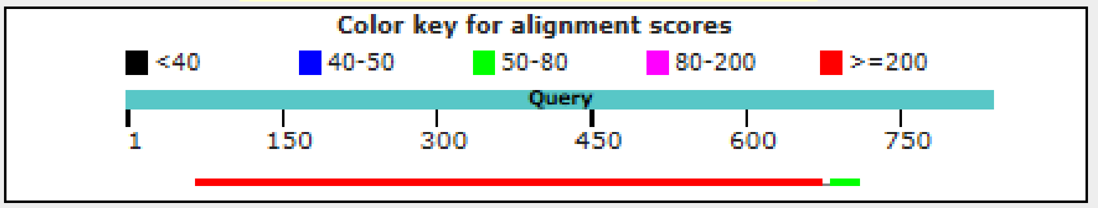

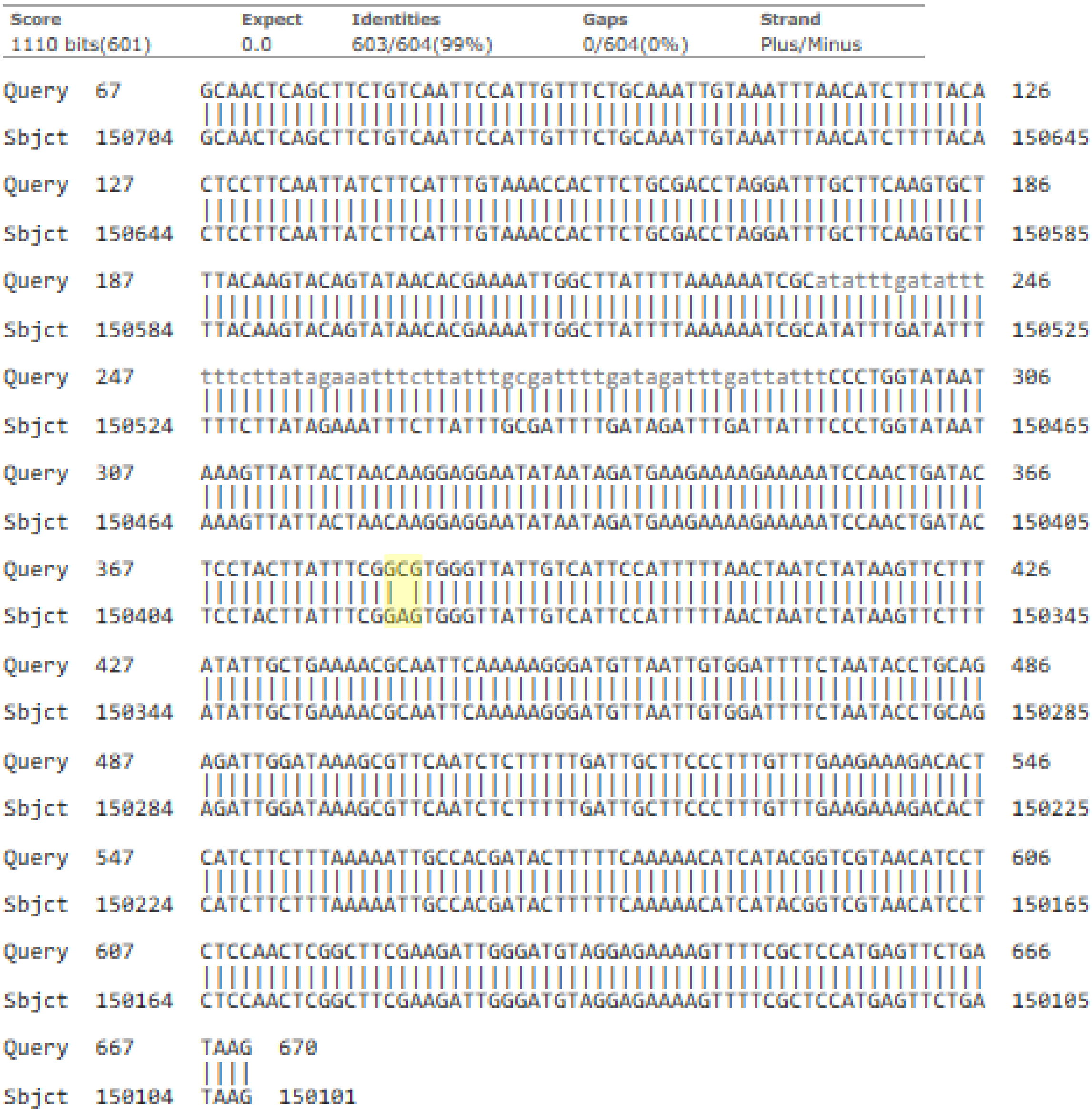

Score	Expect	Identities	Gaps	Strand
1110 bits(601)	0.0	603/604(99%)	0/604(0%)	Plus/Minus

```
Query  67      GCAACTCAGCTTCTGTCAATTCCATTGTTTCTGCAAATTGTAAATTTAACATCTTTTACA  126
               ||||||||||||||||||||||||||||||||||||||||||||||||||||||||||||
Sbjct  150704  GCAACTCAGCTTCTGTCAATTCCATTGTTTCTGCAAATTGTAAATTTAACATCTTTTACA  150645

Query  127     CTCCTTCAATTATCTTCATTTGTAAACCACTTCTGCGACCTAGGATTTGCTTCAAGTGCT  186
               ||||||||||||||||||||||||||||||||||||||||||||||||||||||||||||
Sbjct  150644  CTCCTTCAATTATCTTCATTTGTAAACCACTTCTGCGACCTAGGATTTGCTTCAAGTGCT  150585

Query  187     TTACAAGTACAGTATAACACGAAAATTGGCTTATTTTAAAAAATCGCatatttgatattt  246
               ||||||||||||||||||||||||||||||||||||||||||||||||||||||||||||
Sbjct  150584  TTACAAGTACAGTATAACACGAAAATTGGCTTATTTTAAAAAATCGCATATTTGATATTT  150525

Query  247     tttcttatagaaatttcttatttgcgattttgatagatttgattatttCCCTGGTATAAT  306
               ||||||||||||||||||||||||||||||||||||||||||||||||||||||||||||
Sbjct  150524  TTTCTTATAGAAATTTCTTATTTGCGATTTTGATAGATTTGATTATTTCCCTGGTATAAT  150465

Query  307     AAAGTTATTACTAACAAGGAGGAATATAATAGATGAAGAAAAGAAAAATCCAACTGATAC  366
               ||||||||||||||||||||||||||||||||||||||||||||||||||||||||||||
Sbjct  150464  AAAGTTATTACTAACAAGGAGGAATATAATAGATGAAGAAAAGAAAAATCCAACTGATAC  150405

Query  367     TCCTACTTATTTCGGCGTGGGTTATTGTCATTCCATTTTTAACTAATCTATAAGTTCTTT  426
               ||||||||||||||| ||||||||||||||||||||||||||||||||||||||||||||
Sbjct  150404  TCCTACTTATTTCGGAGTGGGTTATTGTCATTCCATTTTTAACTAATCTATAAGTTCTTT  150345

Query  427     ATATTGCTGAAAACGCAATTCAAAAAGGGATGTTAATTGTGGATTTTCTAATACCTGCAG  486
               ||||||||||||||||||||||||||||||||||||||||||||||||||||||||||||
Sbjct  150344  ATATTGCTGAAAACGCAATTCAAAAAGGGATGTTAATTGTGGATTTTCTAATACCTGCAG  150285

Query  487     AGATTGGATAAAGCGTTCAATCTCTTTTTGATTGCTTCCCTTTGTTTGAAGAAAGACACT  546
               ||||||||||||||||||||||||||||||||||||||||||||||||||||||||||||
Sbjct  150284  AGATTGGATAAAGCGTTCAATCTCTTTTTGATTGCTTCCCTTTGTTTGAAGAAAGACACT  150225

Query  547     CATCTTCTTTAAAAATTGCCACGATACTTTTTCAAAAACATCATACGGTCGTAACATCCT  606
               ||||||||||||||||||||||||||||||||||||||||||||||||||||||||||||
Sbjct  150224  CATCTTCTTTAAAAATTGCCACGATACTTTTTCAAAAACATCATACGGTCGTAACATCCT  150165

Query  607     CTCCAACTCGGCTTCGAAGATTGGGATGTAGGAGAAAAGTTTTCGCTCCATGAGTTCTGA  666
               ||||||||||||||||||||||||||||||||||||||||||||||||||||||||||||
Sbjct  150164  CTCCAACTCGGCTTCGAAGATTGGGATGTAGGAGAAAAGTTTTCGCTCCATGAGTTCTGA  150105

Query  667     TAAG  670
               ||||
Sbjct  150104  TAAG  150101
```

(N) Modified *shp144*S14A with its putative promoter [Serine (TCG) changed to alanine (GCG)]

Alignment with Mal/F primer

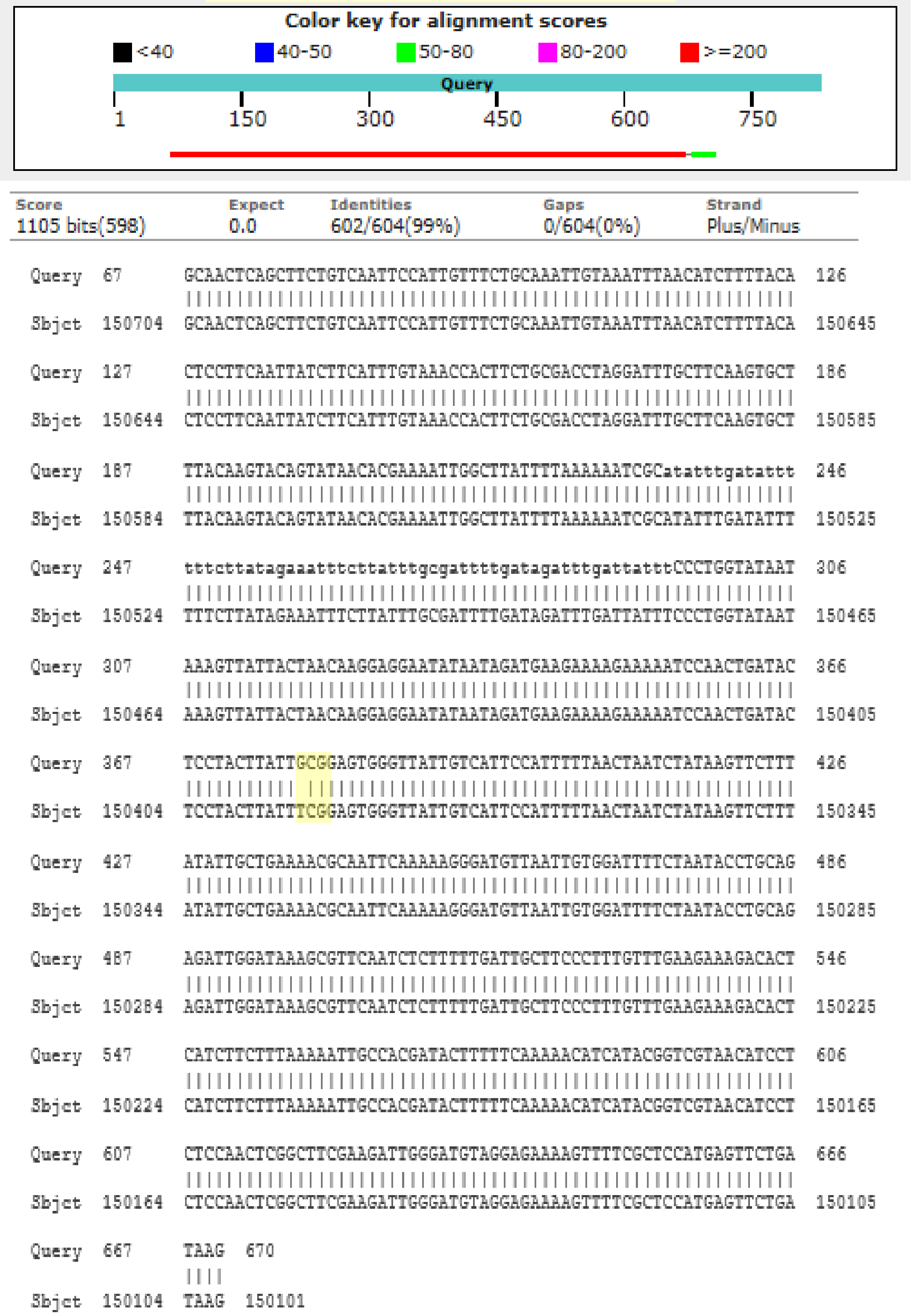

Color key for alignment scores

⬛ <40 🟦 40-50 🟩 50-80 🟪 80-200 🟥 >=200

Score	Expect	Identities	Gaps	Strand
1105 bits(598)	0.0	602/604(99%)	0/604(0%)	Plus/Minus

```
Query  67      GCAACTCAGCTTCTGTCAATTCCATTGTTTCTGCAAATTGTAAATTTAACATCTTTTACA  126
               ||||||||||||||||||||||||||||||||||||||||||||||||||||||||||||
Sbjct  150704  GCAACTCAGCTTCTGTCAATTCCATTGTTTCTGCAAATTGTAAATTTAACATCTTTTACA  150645

Query  127     CTCCTTCAATTATCTTCATTTGTAAACCACTTCTGCGACCTAGGATTTGCTTCAAGTGCT  186
               ||||||||||||||||||||||||||||||||||||||||||||||||||||||||||||
Sbjct  150644  CTCCTTCAATTATCTTCATTTGTAAACCACTTCTGCGACCTAGGATTTGCTTCAAGTGCT  150585

Query  187     TTACAAGTACAGTATAACACGAAAATTGGCTTATTTTAAAAAATCGCatatttgatattt  246
               ||||||||||||||||||||||||||||||||||||||||||||||||||||||||||||
Sbjct  150584  TTACAAGTACAGTATAACACGAAAATTGGCTTATTTTAAAAAATCGCATATTTGATATTT  150525

Query  247     tttcttatagaaatttcttatttgcgattttgatagatttgattatttCCCTGGTATAAT  306
               ||||||||||||||||||||||||||||||||||||||||||||||||||||||||||||
Sbjct  150524  TTTCTTATAGAAATTTCTTATTTGCGATTTTGATAGATTTGATTATTTCCCTGGTATAAT  150465

Query  307     AAAGTTATTACTAACAAGGAGGAATATAATAGATGAAGAAAAGAAAAATCCAACTGATAC  366
               ||||||||||||||||||||||||||||||||||||||||||||||||||||||||||||
Sbjct  150464  AAAGTTATTACTAACAAGGAGGAATATAATAGATGAAGAAAAGAAAAATCCAACTGATAC  150405

Query  367     TCCTACTTATTGCGGAGTGGGTTATTGTCATTCCATTTTTAACTAATCTATAAGTTCTTT  426
               ||||||||||| ||||||||||||||||||||||||||||||||||||||||||||||||
Sbjct  150404  TCCTACTTATTTCGGAGTGGGTTATTGTCATTCCATTTTTAACTAATCTATAAGTTCTTT  150345

Query  427     ATATTGCTGAAAACGCAATTCAAAAAGGGATGTTAATTGTGGATTTTCTAATACCTGCAG  486
               ||||||||||||||||||||||||||||||||||||||||||||||||||||||||||||
Sbjct  150344  ATATTGCTGAAAACGCAATTCAAAAAGGGATGTTAATTGTGGATTTTCTAATACCTGCAG  150285

Query  487     AGATTGGATAAAGCGTTCAATCTCTTTTTGATTGCTTCCCTTTGTTTGAAGAAAGACACT  546
               ||||||||||||||||||||||||||||||||||||||||||||||||||||||||||||
Sbjct  150284  AGATTGGATAAAGCGTTCAATCTCTTTTTGATTGCTTCCCTTTGTTTGAAGAAAGACACT  150225

Query  547     CATCTTCTTTAAAAATTGCCACGATACTTTTTCAAAAACATCATACGGTCGTAACATCCT  606
               ||||||||||||||||||||||||||||||||||||||||||||||||||||||||||||
Sbjct  150224  CATCTTCTTTAAAAATTGCCACGATACTTTTTCAAAAACATCATACGGTCGTAACATCCT  150165

Query  607     CTCCAACTCGGCTTCGAAGATTGGGATGTAGGAGAAAAGTTTTCGCTCCATGAGTTCTGA  666
               ||||||||||||||||||||||||||||||||||||||||||||||||||||||||||||
Sbjct  150164  CTCCAACTCGGCTTCGAAGATTGGGATGTAGGAGAAAAGTTTTCGCTCCATGAGTTCTGA  150105

Query  667     TAAG  670
               ||||
Sbjct  150104  TAAG  150101
```

Appendix 3

Genetic map of pLEICS-01 (PROTEX, University of Leicester) with 6His-Tag for cloning and protein expression analysis.

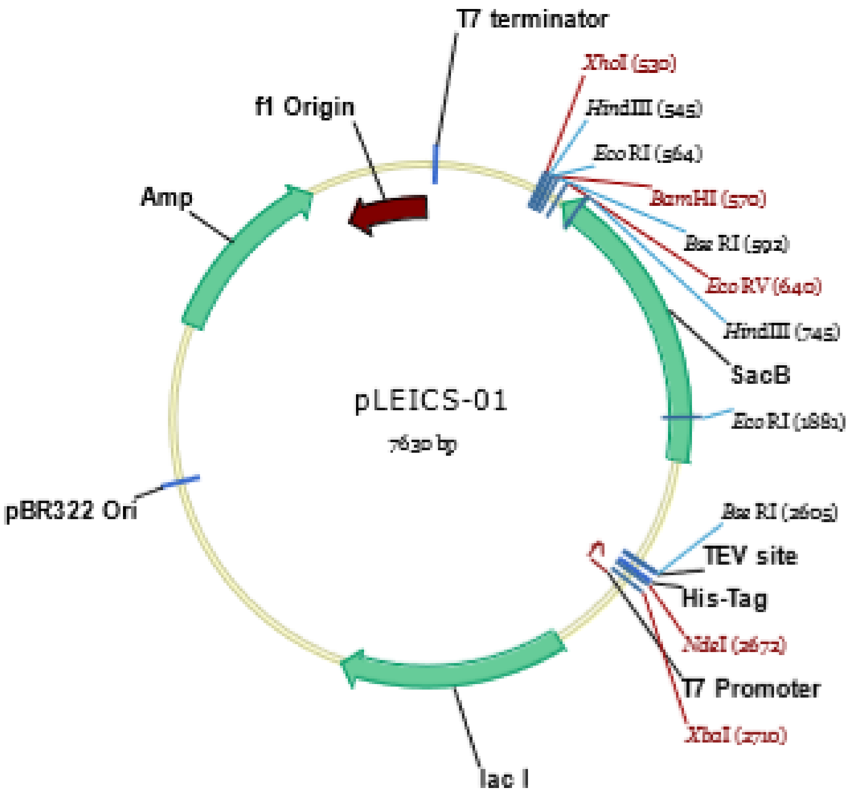

Appendix 4

(A-B) Schematic diagrams and DNA sequence analysis of recombinant pLEICS-01 constructs (full length and truncated recombinant Rgg144) for protein expression analysis.

(A) Full length Rgg144 (SPD_0144)

Alignment with T7 promoter

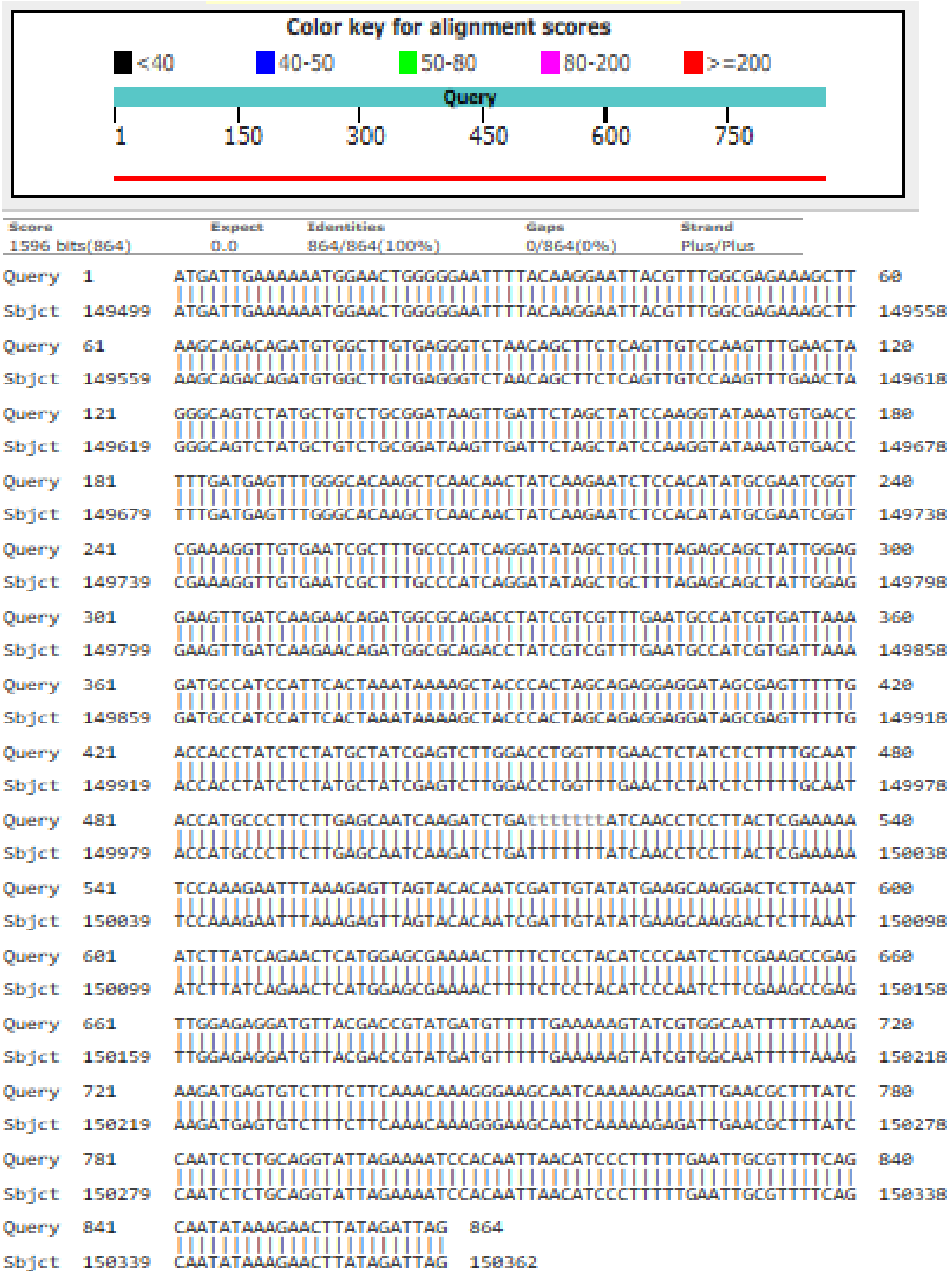

```
Score             Expect   Identities        Gaps         Strand
1596 bits(864)    0.0      864/864(100%)     0/864(0%)    Plus/Plus

Query  1       ATGATTGAAAAAATGGAACTGGGGGAATTTTACAAGGAATTACGTTTGGCGAGAAAGCTT  60
               ||||||||||||||||||||||||||||||||||||||||||||||||||||||||||||
Sbjct  149499  ATGATTGAAAAAATGGAACTGGGGGAATTTTACAAGGAATTACGTTTGGCGAGAAAGCTT  149558

Query  61      AAGCAGACAGATGTGGCTTGTGAGGGTCTAACAGCTTCTCAGTTGTCCAAGTTTGAACTA  120
               ||||||||||||||||||||||||||||||||||||||||||||||||||||||||||||
Sbjct  149559  AAGCAGACAGATGTGGCTTGTGAGGGTCTAACAGCTTCTCAGTTGTCCAAGTTTGAACTA  149618

Query  121     GGGCAGTCTATGCTGTCTGCGGATAAGTTGATTCTAGCTATCCAAGGTATAAATGTGACC  180
               ||||||||||||||||||||||||||||||||||||||||||||||||||||||||||||
Sbjct  149619  GGGCAGTCTATGCTGTCTGCGGATAAGTTGATTCTAGCTATCCAAGGTATAAATGTGACC  149678

Query  181     TTTGATGAGTTTGGGCACAAGCTCAACAACTATCAAGAATCTCCACATATGCGAATCGGT  240
               ||||||||||||||||||||||||||||||||||||||||||||||||||||||||||||
Sbjct  149679  TTTGATGAGTTTGGGCACAAGCTCAACAACTATCAAGAATCTCCACATATGCGAATCGGT  149738

Query  241     CGAAAGGTTGTGAATCGCTTTGCCCATCAGGATATAGCTGCTTTAGAGCAGCTATTGGAG  300
               ||||||||||||||||||||||||||||||||||||||||||||||||||||||||||||
Sbjct  149739  CGAAAGGTTGTGAATCGCTTTGCCCATCAGGATATAGCTGCTTTAGAGCAGCTATTGGAG  149798

Query  301     GAAGTTGATCAAGAACAGATGGCGCAGACCTATCGTCGTTTGAATGCCATCGTGATTAAA  360
               ||||||||||||||||||||||||||||||||||||||||||||||||||||||||||||
Sbjct  149799  GAAGTTGATCAAGAACAGATGGCGCAGACCTATCGTCGTTTGAATGCCATCGTGATTAAA  149858

Query  361     GATGCCATCCATTCACTAAATAAAAGCTACCCACTAGCAGAGGAGGATAGCGAGTTTTTG  420
               ||||||||||||||||||||||||||||||||||||||||||||||||||||||||||||
Sbjct  149859  GATGCCATCCATTCACTAAATAAAAGCTACCCACTAGCAGAGGAGGATAGCGAGTTTTTG  149918

Query  421     ACCACCTATCTCTATGCTATCGAGTCTTGGACCTGGTTTGAACTCTATCTCTTTTGCAAT  480
               ||||||||||||||||||||||||||||||||||||||||||||||||||||||||||||
Sbjct  149919  ACCACCTATCTCTATGCTATCGAGTCTTGGACCTGGTTTGAACTCTATCTCTTTTGCAAT  149978

Query  481     ACCATGCCCTTCTTGAGCAATCAAGATCTGAtttttttATCAACCTCCTTACTCGAAAAA  540
               ||||||||||||||||||||||||||||||||||||||||||||||||||||||||||||
Sbjct  149979  ACCATGCCCTTCTTGAGCAATCAAGATCTGATTTTTTTATCAACCTCCTTACTCGAAAAA  150038

Query  541     TCCAAAGAATTTAAAGAGTTAGTACACAATCGATTGTATATGAAGCAAGGACTCTTAAAT  600
               ||||||||||||||||||||||||||||||||||||||||||||||||||||||||||||
Sbjct  150039  TCCAAAGAATTTAAAGAGTTAGTACACAATCGATTGTATATGAAGCAAGGACTCTTAAAT  150098

Query  601     ATCTTATCAGAACTCATGGAGCGAAAACTTTTCTCCTACATCCCAATCTTCGAAGCCGAG  660
               ||||||||||||||||||||||||||||||||||||||||||||||||||||||||||||
Sbjct  150099  ATCTTATCAGAACTCATGGAGCGAAAACTTTTCTCCTACATCCCAATCTTCGAAGCCGAG  150158

Query  661     TTGGAGAGGATGTTACGACCGTATGATGTTTTTGAAAAAGTATCGTGGCAATTTTTAAAG  720
               ||||||||||||||||||||||||||||||||||||||||||||||||||||||||||||
Sbjct  150159  TTGGAGAGGATGTTACGACCGTATGATGTTTTTGAAAAAGTATCGTGGCAATTTTTAAAG  150218

Query  721     AAGATGAGTGTCTTTCTTCAAACAAAGGGAAGCAATCAAAAAGAGATTGAACGCTTTATC  780
               ||||||||||||||||||||||||||||||||||||||||||||||||||||||||||||
Sbjct  150219  AAGATGAGTGTCTTTCTTCAAACAAAGGGAAGCAATCAAAAAGAGATTGAACGCTTTATC  150278

Query  781     CAATCTCTGCAGGTATTAGAAAATCCACAATTAACATCCCTTTTTGAATTGCGTTTTCAG  840
               ||||||||||||||||||||||||||||||||||||||||||||||||||||||||||||
Sbjct  150279  CAATCTCTGCAGGTATTAGAAAATCCACAATTAACATCCCTTTTTGAATTGCGTTTTCAG  150338

Query  841     CAATATAAAGAACTTATAGATTAG  864
               ||||||||||||||||||||||||
Sbjct  150339  CAATATAAAGAACTTATAGATTAG  150362
```

(B) Truncated Rgg144 (SPD_0144)

Alignment with T7 promoter

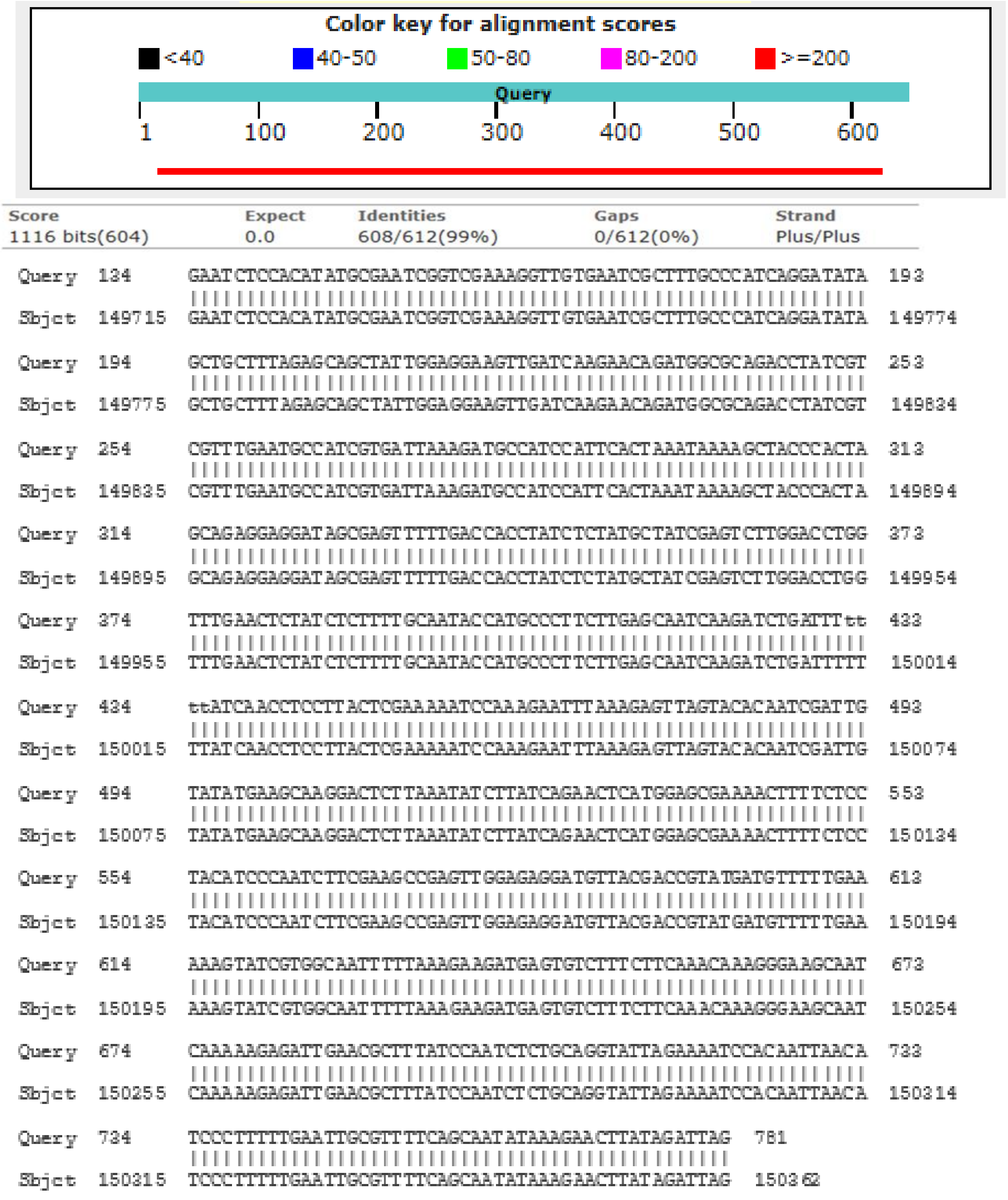

```
Score            Expect   Identities      Gaps         Strand
1116 bits(604)   0.0      608/612(99%)    0/612(0%)    Plus/Plus

Query  134     GAATCTCCACATATGCGAATCGGTCGAAAGGTTGTGAATCGCTTTGCCCATCAGGATATA  193
               ||||||||||||||||||||||||||||||||||||||||||||||||||||||||||||
Sbjct  149715  GAATCTCCACATATGCGAATCGGTCGAAAGGTTGTGAATCGCTTTGCCCATCAGGATATA  149774

Query  194     GCTGCTTTAGAGCAGCTATTGGAGGAAGTTGATCAAGAACAGATGGCGCAGACCTATCGT  253
               ||||||||||||||||||||||||||||||||||||||||||||||||||||||||||||
Sbjct  149775  GCTGCTTTAGAGCAGCTATTGGAGGAAGTTGATCAAGAACAGATGGCGCAGACCTATCGT  149834

Query  254     CGTTTGAATGCCATCGTGATTAAAGATGCCATCCATTCACTAAATAAAAGCTACCCACTA  313
               ||||||||||||||||||||||||||||||||||||||||||||||||||||||||||||
Sbjct  149835  CGTTTGAATGCCATCGTGATTAAAGATGCCATCCATTCACTAAATAAAAGCTACCCACTA  149894

Query  314     GCAGAGGAGGATAGCGAGTTTTTGACCACCTATCTCTATGCTATCGAGTCTTGGACCTGG  373
               ||||||||||||||||||||||||||||||||||||||||||||||||||||||||||||
Sbjct  149895  GCAGAGGAGGATAGCGAGTTTTTGACCACCTATCTCTATGCTATCGAGTCTTGGACCTGG  149954

Query  374     TTTGAACTCTATCTCTTTTGCAATACCATGCCCTTCTTGAGCAATCAAGATCTGATTTtt  433
               ||||||||||||||||||||||||||||||||||||||||||||||||||||||||||||
Sbjct  149955  TTTGAACTCTATCTCTTTTGCAATACCATGCCCTTCTTGAGCAATCAAGATCTGATTTTT  150014

Query  434     ttATCAACCTCCTTACTCGAAAAATCCAAAGAATTTAAAGAGTTAGTACACAATCGATTG  493
               ||||||||||||||||||||||||||||||||||||||||||||||||||||||||||||
Sbjct  150015  TTATCAACCTCCTTACTCGAAAAATCCAAAGAATTTAAAGAGTTAGTACACAATCGATTG  150074

Query  494     TATATGAAGCAAGGACTCTTAAATATCTTATCAGAACTCATGGAGCGAAAACTTTTCTCC  553
               ||||||||||||||||||||||||||||||||||||||||||||||||||||||||||||
Sbjct  150075  TATATGAAGCAAGGACTCTTAAATATCTTATCAGAACTCATGGAGCGAAAACTTTTCTCC  150134

Query  554     TACATCCCAATCTTCGAAGCCGAGTTGGAGAGGATGTTACGACCGTATGATGTTTTTGAA  613
               ||||||||||||||||||||||||||||||||||||||||||||||||||||||||||||
Sbjct  150135  TACATCCCAATCTTCGAAGCCGAGTTGGAGAGGATGTTACGACCGTATGATGTTTTTGAA  150194

Query  614     AAAGTATCGTGGCAATTTTTAAAGAAGATGAGTGTCTTTCTTCAAACAAAGGGAAGCAAT  673
               ||||||||||||||||||||||||||||||||||||||||||||||||||||||||||||
Sbjct  150195  AAAGTATCGTGGCAATTTTTAAAGAAGATGAGTGTCTTTCTTCAAACAAAGGGAAGCAAT  150254

Query  674     CAAAAAGAGATTGAACGCTTTATCCAATCTCTGCAGGTATTAGAAAATCCACAATTAACA  733
               ||||||||||||||||||||||||||||||||||||||||||||||||||||||||||||
Sbjct  150255  CAAAAAGAGATTGAACGCTTTATCCAATCTCTGCAGGTATTAGAAAATCCACAATTAACA  150314

Query  734     TCCCTTTTTGAATTGCGTTTTCAGCAATATAAAGAACTTATAGATTAG  781
               ||||||||||||||||||||||||||||||||||||||||||||||||
Sbjct  150315  TCCCTTTTTGAATTGCGTTTTCAGCAATATAAAGAACTTATAGATTAG  150362
```

Appendix 5

(A-B) Confirmation the identity of recombinant full length and truncated Rgg144 proteins using MALDI-TOF mass spectrometry.

(A) Full length Rgg144 protein

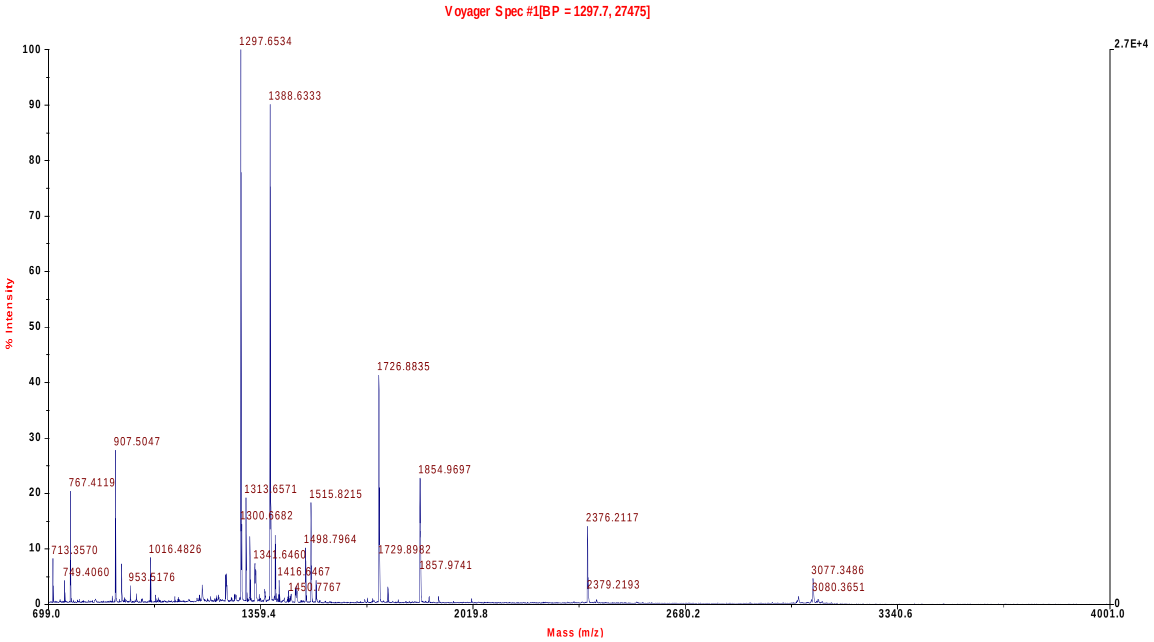

(B) Truncated Rgg144 protein

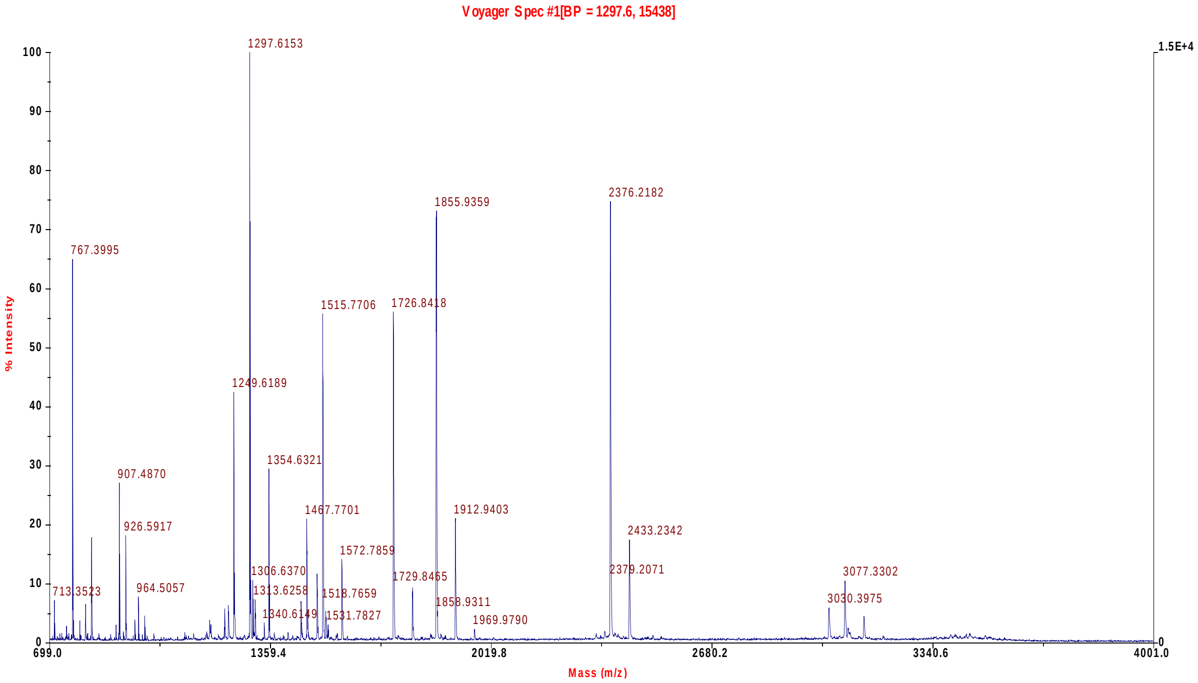

Appendix 6

(A-B) Identification the molecular weight of full length and truncated Rgg144 recombinant proteins using Electrospray LC-MS at PNACL.

(A) Full length Rgg144 protein

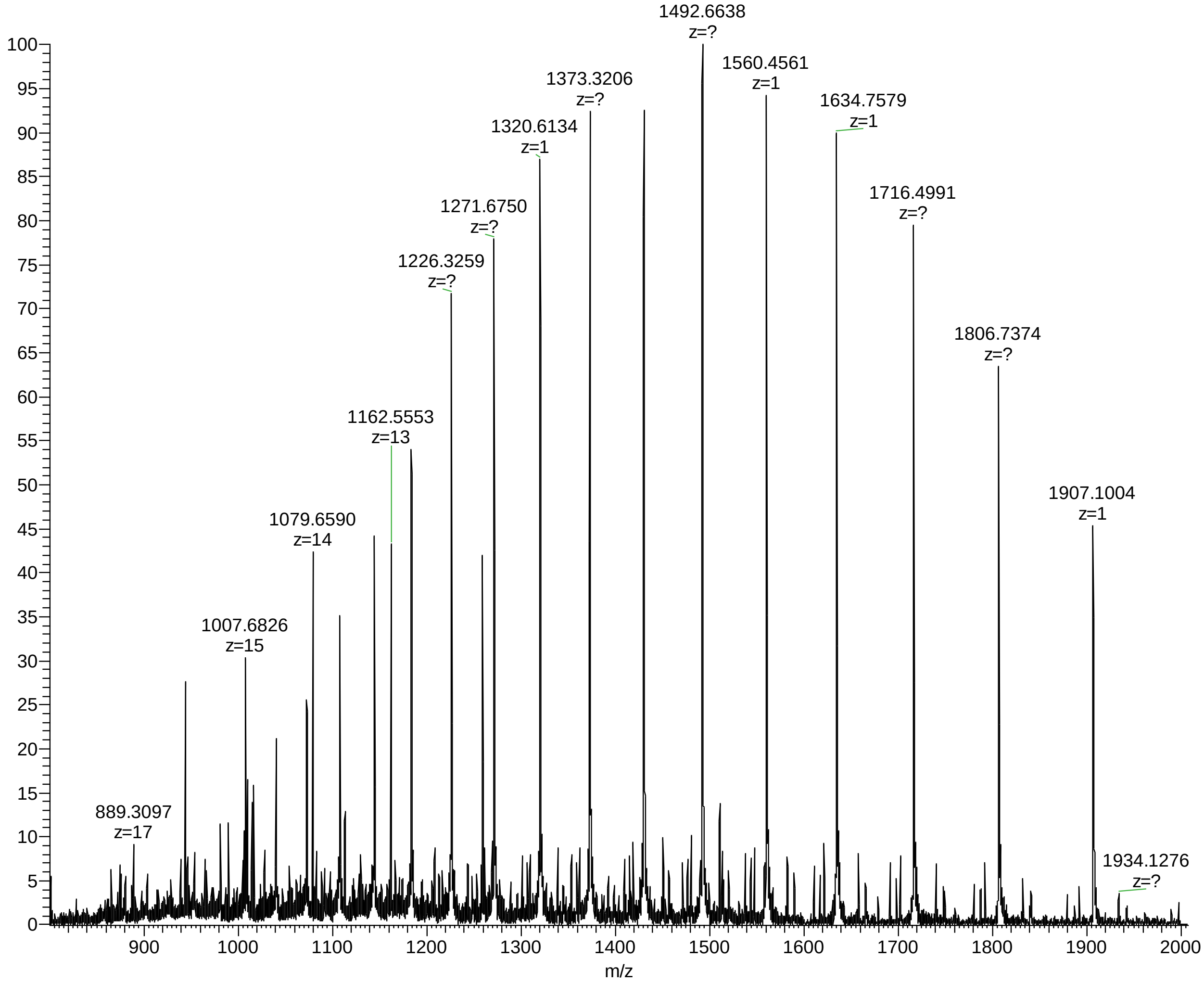

Full length Rgg144 protein

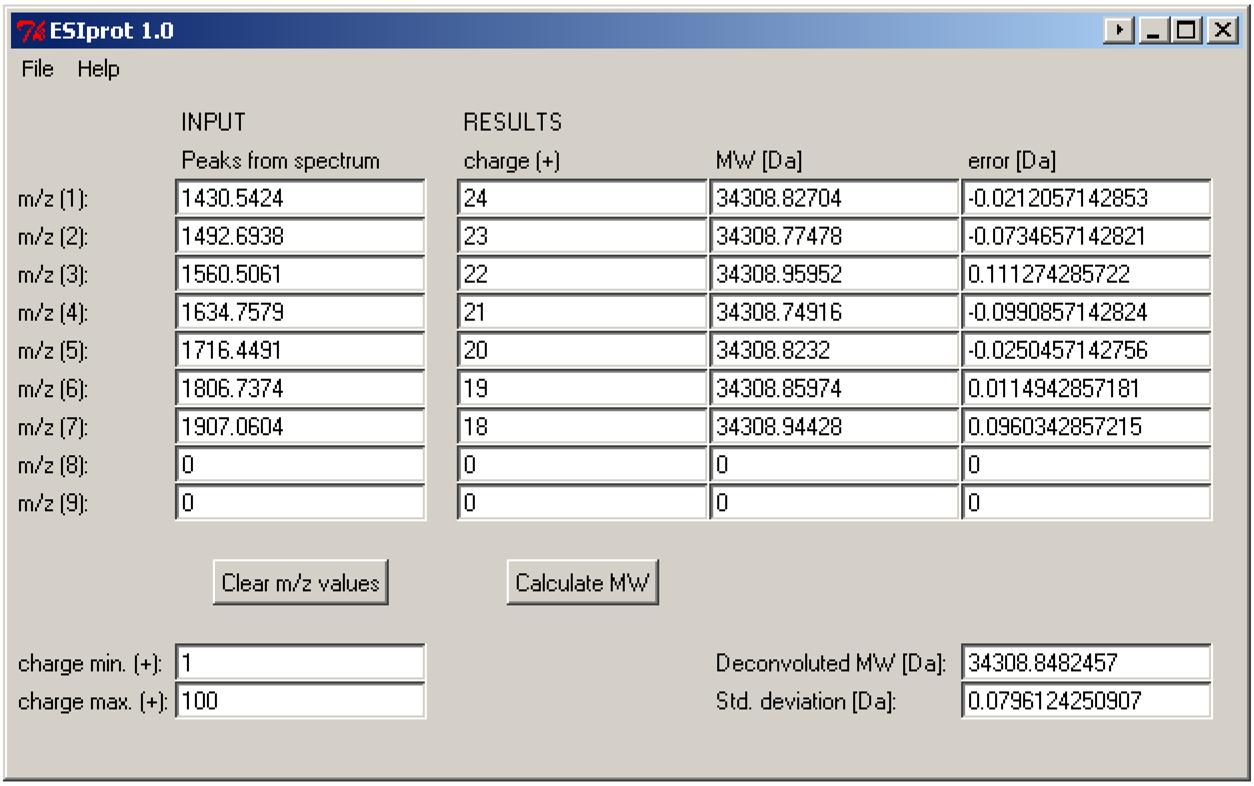

	INPUT	RESULTS		
	Peaks from spectrum	charge (+)	MW [Da]	error [Da]
m/z (1):	1430.5424	24	34308.82704	-0.0212057142853
m/z (2):	1492.6938	23	34308.77478	-0.0734657142821
m/z (3):	1560.5061	22	34308.95952	0.111274285722
m/z (4):	1634.7579	21	34308.74916	-0.0990857142824
m/z (5):	1716.4491	20	34308.8232	-0.0250457142756
m/z (6):	1806.7374	19	34308.85974	0.0114942857181
m/z (7):	1907.0604	18	34308.94428	0.0960342857215
m/z (8):	0	0	0	0
m/z (9):	0	0	0	0

charge min. (+): 1
charge max. (+): 100

Deconvoluted MW [Da]: 34308.8482457
Std. deviation [Da]: 0.0796124250907

Experimentally Determined Molecular Weight (average) = 34308.84 +- 0.08 Da

(B) Truncated Rgg144 protein

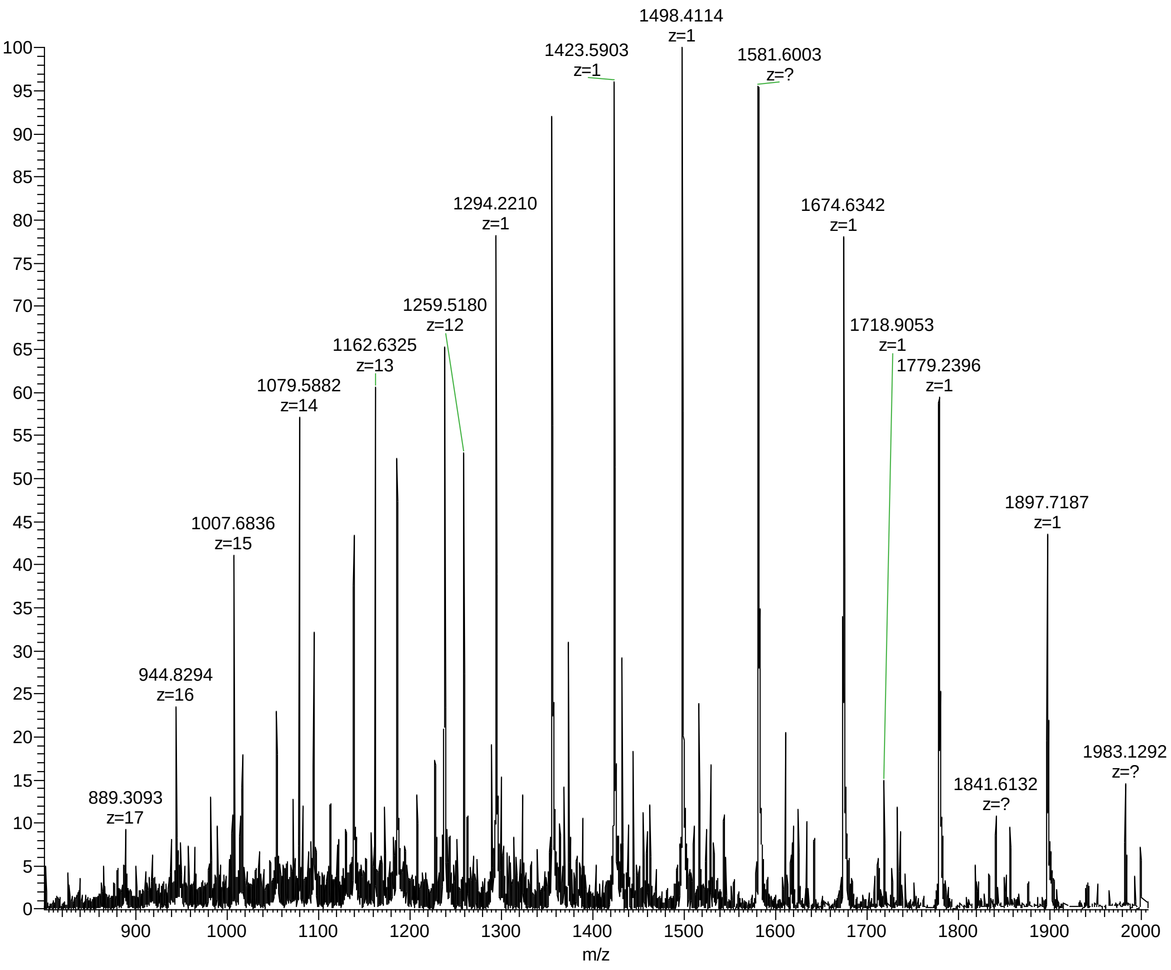

Truncated Rgg144 protein

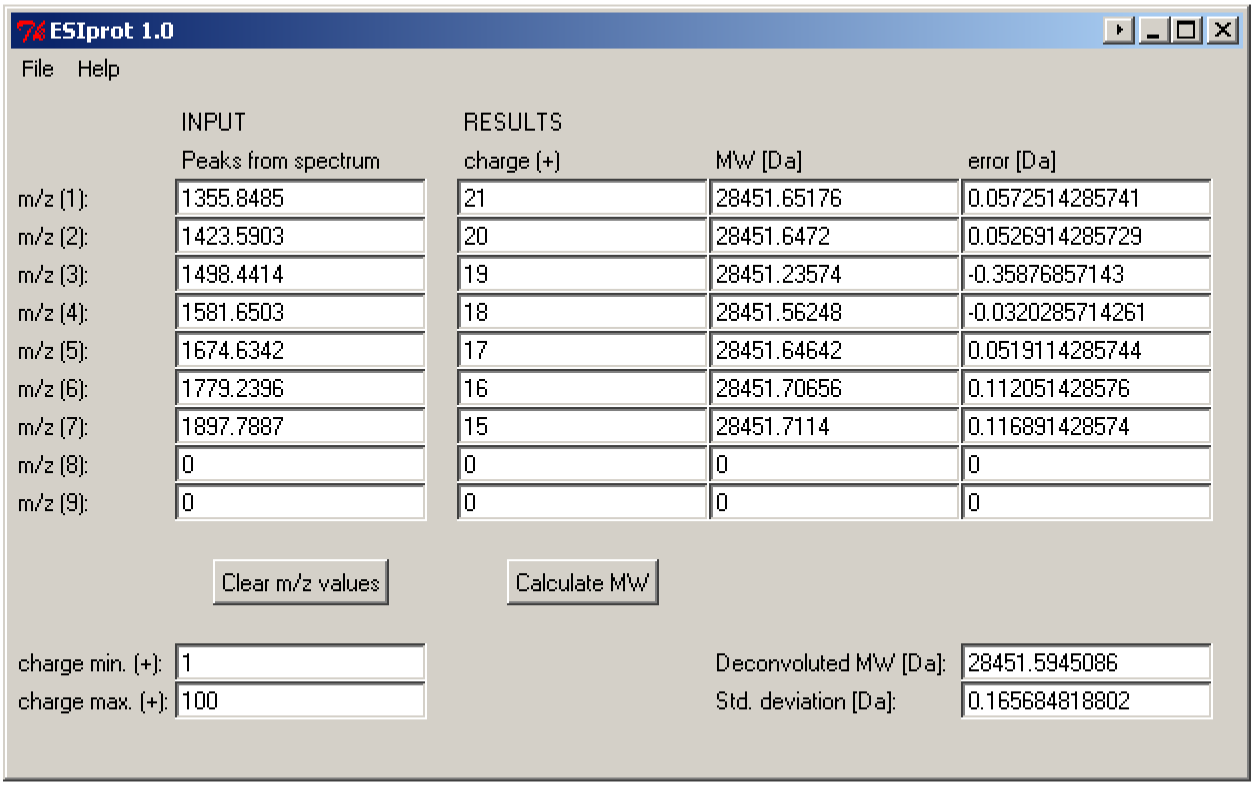

	INPUT	RESULTS		
	Peaks from spectrum	charge (+)	MW [Da]	error [Da]
m/z (1):	1355.8485	21	28451.65176	0.0572514285741
m/z (2):	1423.5903	20	28451.6472	0.0526914285729
m/z (3):	1498.4414	19	28451.23574	-0.35876857143
m/z (4):	1581.6503	18	28451.56248	-0.0320285714261
m/z (5):	1674.6342	17	28451.64642	0.0519114285744
m/z (6):	1779.2396	16	28451.70656	0.112051428576
m/z (7):	1897.7887	15	28451.7114	0.116891428574
m/z (8):	0	0	0	0
m/z (9):	0	0	0	0

charge min. (+): 1
charge max. (+): 100

Deconvoluted MW [Da]: 28451.5945086
Std. deviation [Da]: 0.165684818802

Experimentally Determined Molecular Weight (average) = 28451.59 +- 0.17 Da

Appendix 7

Multiple sequence alignment of streptococcal SHPs using Clustal Omega software.

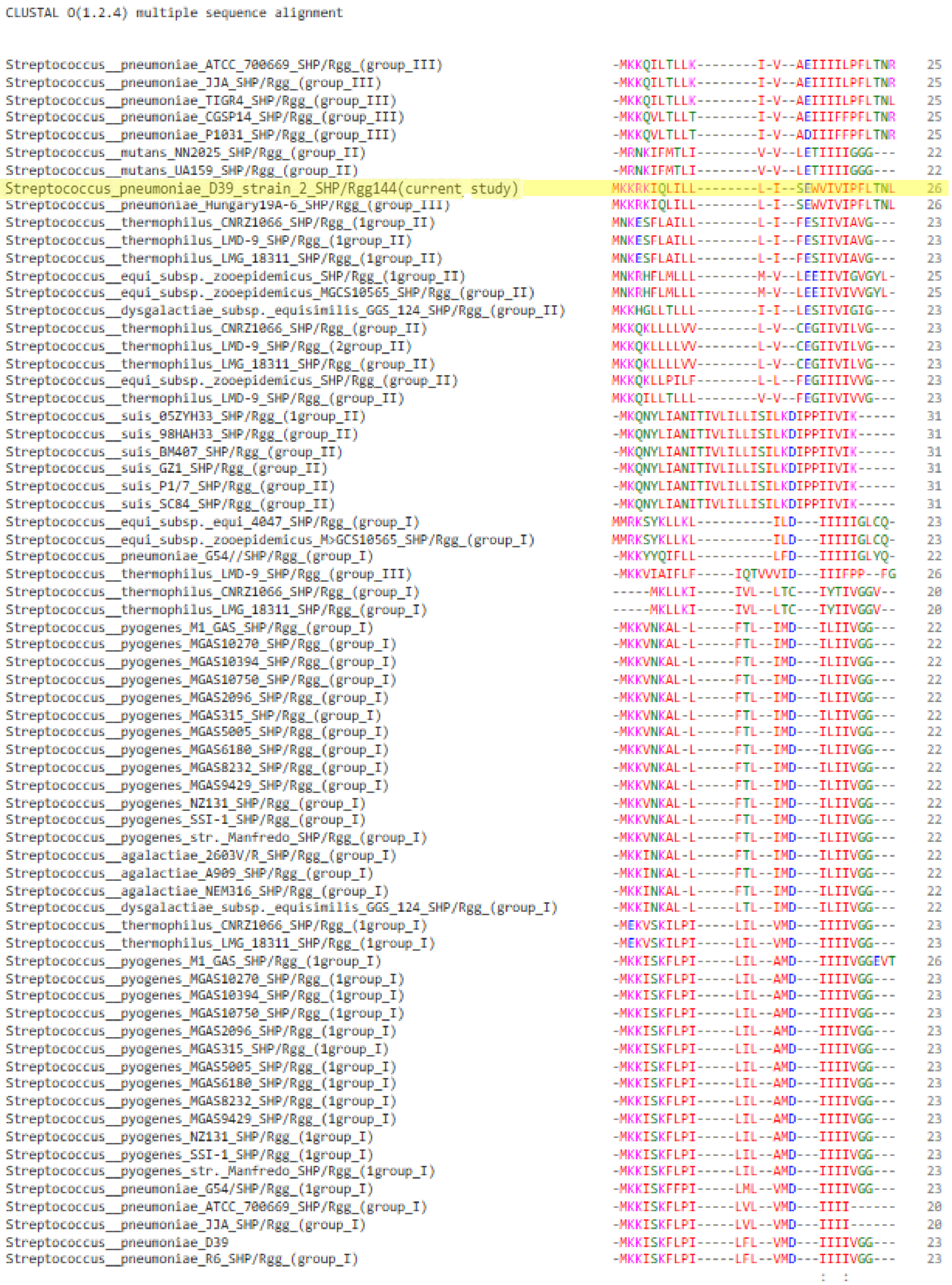

```
CLUSTAL O(1.2.4) multiple sequence alignment


Streptococcus__pneumoniae_ATCC_700669_SHP/Rgg_(group_III)                              -MKKQILTLLK--------I-V--AEIIIILPFLTNR     25
Streptococcus__pneumoniae_JJA_SHP/Rgg_(group_III)                                      -MKKQILTLLK--------I-V--AEIIIILPFLTNR     25
Streptococcus__pneumoniae_TIGR4_SHP/Rgg_(group_III)                                    -MKKQILTLLK--------I-V--AEIIIILPFLTNL     25
Streptococcus__pneumoniae_CGSP14_SHP/Rgg_(group_III)                                   -MKKQVLTLLT--------I-V--AEIIIFFPFLTNR     25
Streptococcus__pneumoniae_P1031_SHP/Rgg_(group_III)                                    -MKKQVLTLLT--------I-V--ADIIIFFPFLTNR     25
Streptococcus__mutans_NN2025_SHP/Rgg_(group_II)                                        -MRNKIFMTLI--------V-V--LETIIIIGGG---     22
Streptococcus__mutans_UA159_SHP/Rgg_(group_II)                                         -MRNKIFMTLI--------V-V--LETIIIIGGG---     22
Streptococcus_pneumoniae_D39_strain_2_SHP/Rgg144(current study)                        MKKRKIQLILL--------L-I--SEWVIVIPFLTNL     26
Streptococcus__pneumoniae_Hungary19A-6_SHP/Rgg_(group_III)                             MKKRKIQLILL--------L-I--SEWVIVIPFLTNL     26
Streptococcus__thermophilus_CNRZ1066_SHP/Rgg_(1group_II)                               MNKESFLAILL--------L-I--FESIIVIAVG---     23
Streptococcus__thermophilus_LMD-9_SHP/Rgg_(1group_II)                                  MNKESFLAILL--------L-I--FESIIVIAVG---     23
Streptococcus__thermophilus_LMG_18311_SHP/Rgg_(1group_II)                              MNKESFLAILL--------L-I--FESIIVIAVG---     23
Streptococcus__equi_subsp._zooepidemicus_SHP/Rgg_(1group_II)                           MNKRHFLMLLL--------M-V--LEEIIVIGVGYL-     25
Streptococcus__equi_subsp._zooepidemicus_MGCS10565_SHP/Rgg_(group_II)                  MNKRHFLMLLL--------M-V--LEEIIVIVVGYL-     25
Streptococcus__dysgalactiae_subsp._equisimilis_GGS_124_SHP/Rgg_(group_II)              MKKHGLLTLLL--------I-I--LESIIVIGIG---     23
Streptococcus__thermophilus_CNRZ1066_SHP/Rgg_(group_II)                                MKKQKLLLLVV--------L-V--CEGIIVILVG---     23
Streptococcus__thermophilus_LMD-9_SHP/Rgg_(2group_II)                                  MKKQKLLLLVV--------L-V--CEGIIVILVG---     23
Streptococcus__thermophilus_LMG_18311_SHP/Rgg_(group_II)                               MKKQKLLLLVV--------L-V--CEGIIVILVG---     23
Streptococcus__equi_subsp._zooepidemicus_SHP/Rgg_(group_II)                            MKKQKLLPILF--------L-L--FEGIIIIVVG---     23
Streptococcus__thermophilus_LMD-9_SHP/Rgg_(group_II)                                   MKKQILLTLLL--------V-V--FEGIIVIVVG---     23
Streptococcus__suis_05ZYH33_SHP/Rgg_(1group_II)                                        -MKQNYLIANITIVLILLISILKDIPPIIVIK-----     31
Streptococcus__suis_98HAH33_SHP/Rgg_(group_II)                                         -MKQNYLIANITIVLILLISILKDIPPIIVIK-----     31
Streptococcus__suis_BM407_SHP/Rgg_(group_II)                                           -MKQNYLIANITIVLILLISILKDIPPIIVIK-----     31
Streptococcus__suis_GZ1_SHP/Rgg_(group_II)                                             -MKQNYLIANITIVLILLISILKDIPPIIVIK-----     31
Streptococcus__suis_P1/7_SHP/Rgg_(group_II)                                            -MKQNYLIANITIVLILLISILKDIPPIIVIK-----     31
Streptococcus__suis_SC84_SHP/Rgg_(group_II)                                            -MKQNYLIANITIVLILLISILKDIPPIIVIK-----     31
Streptococcus__equi_subsp._equi_4047_SHP/Rgg_(group_I)                                 MMRKSYKLLKL----------ILD---IIIIIGLCQ-     23
Streptococcus__equi_subsp._zooepidemicus_M>GCS10565_SHP/Rgg_(group_I)                  MMRKSYKLLKL----------ILD---IIIIIGLCQ-     23
Streptococcus__pneumoniae_G54//SHP/Rgg_(group_I)                                       -MKKYYQIFLL----------LFD---IIIIIGLYQ-     22
Streptococcus__thermophilus_LMD-9_SHP/Rgg_(group_III)                                  -MKKVIAIFLF-----IQTVVVID---IIIFPP--FG     26
Streptococcus__thermophilus_CNRZ1066_SHP/Rgg_(group_I)                                 -----MKLLKI-----IVL--LTC---IYTIVGGV--     20
Streptococcus__thermophilus_LMG_18311_SHP/Rgg_(group_I)                                -----MKLLKI-----IVL--LTC---IYIIVGGV--     20
Streptococcus__pyogenes_M1_GAS_SHP/Rgg_(group_I)                                       -MKKVNKAL-L-----FTL--IMD---ILIIVGG---     22
Streptococcus__pyogenes_MGAS10270_SHP/Rgg_(group_I)                                    -MKKVNKAL-L-----FTL--IMD---ILIIVGG---     22
Streptococcus__pyogenes_MGAS10394_SHP/Rgg_(group_I)                                    -MKKVNKAL-L-----FTL--IMD---ILIIVGG---     22
Streptococcus__pyogenes_MGAS10750_SHP/Rgg_(group_I)                                    -MKKVNKAL-L-----FTL--IMD---ILIIVGG---     22
Streptococcus__pyogenes_MGAS2096_SHP/Rgg_(group_I)                                     -MKKVNKAL-L-----FTL--IMD---ILIIVGG---     22
Streptococcus__pyogenes_MGAS315_SHP/Rgg_(group_I)                                      -MKKVNKAL-L-----FTL--IMD---ILIIVGG---     22
Streptococcus__pyogenes_MGAS5005_SHP/Rgg_(group_I)                                     -MKKVNKAL-L-----FTL--IMD---ILIIVGG---     22
Streptococcus__pyogenes_MGAS6180_SHP/Rgg_(group_I)                                     -MKKVNKAL-L-----FTL--IMD---ILIIVGG---     22
Streptococcus__pyogenes_MGAS8232_SHP/Rgg_(group_I)                                     -MKKVNKAL-L-----FTL--IMD---ILIIVGG---     22
Streptococcus__pyogenes_MGAS9429_SHP/Rgg_(group_I)                                     -MKKVNKAL-L-----FTL--IMD---ILIIVGG---     22
Streptococcus__pyogenes_NZ131_SHP/Rgg_(group_I)                                        -MKKVNKAL-L-----FTL--IMD---ILIIVGG---     22
Streptococcus__pyogenes_SSI-1_SHP/Rgg_(group_I)                                        -MKKVNKAL-L-----FTL--IMD---ILIIVGG---     22
Streptococcus__pyogenes_str._Manfredo_SHP/Rgg_(group_I)                                -MKKVNKAL-L-----FTL--IMD---ILIIVGG---     22
Streptococcus__agalactiae_2603V/R_SHP/Rgg_(group_I)                                    -MKKINKAL-L-----FTL--IMD---ILIIVGG---     22
Streptococcus__agalactiae_A909_SHP/Rgg_(group_I)                                       -MKKINKAL-L-----FTL--IMD---ILIIVGG---     22
Streptococcus__agalactiae_NEM316_SHP/Rgg_(group_I)                                     -MKKINKAL-L-----FTL--IMD---ILIIVGG---     22
Streptococcus__dysgalactiae_subsp._equisimilis_GGS_124_SHP/Rgg_(group_I)               -MKKINKAL-L-----LTL--IMD---ILIIVGG---     22
Streptococcus__thermophilus_CNRZ1066_SHP/Rgg_(1group_I)                                -MEKVSKILPI-----LIL--VMD---IIIIVGG---     23
Streptococcus__thermophilus_LMG_18311_SHP/Rgg_(1group_I)                               -MEKVSKILPI-----LIL--VMD---IIIIVGG---     23
Streptococcus__pyogenes_M1_GAS_SHP/Rgg_(1group_I)                                      -MKKISKFLPI-----LIL--AMD---IIIIVGGEVT     26
Streptococcus__pyogenes_MGAS10270_SHP/Rgg_(1group_I)                                   -MKKISKFLPI-----LIL--AMD---IIIIVGG---     23
Streptococcus__pyogenes_MGAS10394_SHP/Rgg_(1group_I)                                   -MKKISKFLPI-----LIL--AMD---IIIIVGG---     23
Streptococcus__pyogenes_MGAS10750_SHP/Rgg_(1group_I)                                   -MKKISKFLPI-----LIL--AMD---IIIIVGG---     23
Streptococcus__pyogenes_MGAS2096_SHP/Rgg_(1group_I)                                    -MKKISKFLPI-----LIL--AMD---IIIIVGG---     23
Streptococcus__pyogenes_MGAS315_SHP/Rgg_(1group_I)                                     -MKKISKFLPI-----LIL--AMD---IIIIVGG---     23
Streptococcus__pyogenes_MGAS5005_SHP/Rgg_(1group_I)                                    -MKKISKFLPI-----LIL--AMD---IIIIVGG---     23
Streptococcus__pyogenes_MGAS6180_SHP/Rgg_(1group_I)                                    -MKKISKFLPI-----LIL--AMD---IIIIVGG---     23
Streptococcus__pyogenes_MGAS8232_SHP/Rgg_(1group_I)                                    -MKKISKFLPI-----LIL--AMD---IIIIVGG---     23
Streptococcus__pyogenes_MGAS9429_SHP/Rgg_(1group_I)                                    -MKKISKFLPI-----LIL--AMD---IIIIVGG---     23
Streptococcus__pyogenes_NZ131_SHP/Rgg_(1group_I)                                       -MKKISKFLPI-----LIL--AMD---IIIIVGG---     23
Streptococcus__pyogenes_SSI-1_SHP/Rgg_(1group_I)                                       -MKKISKFLPI-----LIL--AMD---IIIIVGG---     23
Streptococcus__pyogenes_str._Manfredo_SHP/Rgg_(1group_I)                               -MKKISKFLPI-----LIL--AMD---IIIIVGG---     23
Streptococcus__pneumoniae_G54/SHP/Rgg_(1group_I)                                       -MKKISKFFPI-----LML--VMD---IIIIVGG---     23
Streptococcus__pneumoniae_ATCC_700669_SHP/Rgg_(group_I)                                -MKKISKFLPI-----LVL--VMD---IIII------     20
Streptococcus__pneumoniae_JJA_SHP/Rgg_(group_I)                                        -MKKISKFLPI-----LVL--VMD---IIII------     20
Streptococcus__pneumoniae_D39                                                          -MKKISKFLPI-----LFL--VMD---IIIIVGG---     23
Streptococcus__pneumoniae_R6_SHP/Rgg_(group_I)                                         -MKKISKFLPI-----LFL--VMD---IIIIVGG---     23
                                                                                                                  :  :
```

References

Adams, P.D., Afonine, P.V., Bunkoczi, G., Chen, V.B., Davis, I.W., Echols, N., Headd, J.J., Hung, L., Kapral, G.J., Grosse-Kunstleve, R., McCoy, A.J., *et al.* (2010). PHENIX: a comprehensive Python-based system for macromolecular structure solution. *Acta Crystallographica Section D*, **66**(2), 213-221.

Adrian, P.V. and Klugman, K.P. (1997). Mutations in the dihydrofolate reductase gene of trimethoprim-resistant isolates of *Streptococcus pneumoniae*. *Antimicrobial agents and chemotherapy*, **41**(11), 2406-2413.

Aggarwal, C., Jimenez, J.C., Nanavati, D. and Federle, M.J. (2014). Multiple length peptide-pheromone variants produced by *Streptococcus pyogenes* directly bind Rgg proteins to confer transcriptional regulation. *Journal of Biological Chemistry*, **289**(32), 22427–22436.

Aggarwal, S.D., Eutsey, R., West-Roberts, J., Domenech, A., Xu, W., Abdullah, I.T., Mitchell, A.P., Veening, J.W., Yesilkaya, H. and Hiller, N.L. (2018). Function of BriC peptide in the pneumococcal competence and virulence portfolio. *PLoS Pathogens*, **14**(10), e1007328.

Akerley, B.J., Rubin, E.J., Novick, V.L., Amaya, K., Judson, N. and Mekalanos, J.J. (2002). A genome-scale analysis for identification of genes required for growth or survival of *Haemophilus influenzae*. *Proceedings of the National Academy of Sciences of the United States of America*, **99**(2), 966-971.

Albani, J.R. (2007). Principles and Applications of Fluorescence Spectroscopy. *Blackwell Science Ltd*, Oxford, UK.

Al-Bayati, F.A., Kahya, H.F., Damianou, A., Shafeeq, S., Kuipers, O.P., Andrew, P.W. and Yesilkaya, H. (2017). Pneumococcal galactose catabolism is controlled by multiple regulators acting on pyruvate formate lyase. *Scientific Reports*, **7**, 43587.

Allen, R.C., Popat, R., Diggle, S.P. and Brown, S.P. (2014) Targeting virulence: can we make evolution-proof drugs? *Nature Reviews Microbiology*, **12**(4), 300-308.

Alloing, G., Trombe, M.C. and Claverys, J.P. (1990). The *ami* locus of the Gram-positive bacterium *Streptococcus pneumoniae* is similar to binding protein-dependent transport operons of Gram-negative bacteria. *Molecular Microbiology*, **4**(4), 633-644.

AlonsoDeVelasco, E., Verheul, A.F., Verhoef, J. and Snippe, H. (1995). *Streptococcus pneumoniae*: virulence factors, pathogenesis, and vaccines. *Microbiological Reviews*, **59**(4), 591-603.

Alper, H. and Stephanopoulos, G. (2007). Global transcription machinery engineering: a new approach for improving cellular phenotype. *Metabolic Engineering*, **9**(3), 258-267.

Andisi, V.F., Hinojosa, C.A., de Jong, A., Kuipers, O.P., Orihuela, C.J. and Bijlsma, J.J. (2012). Pneumococcal gene complex involved in resistance to extracellular oxidative stress. *Infection and Immunity*, **80**(3), 1037-1049.

Aprianto, R., Slager, J., Holsappel, S. and Veening, J.W. (2018). High-resolution analysis of the pneumococcal transcriptome under a wide range of infection-relevant conditions. *Nucleic Acids Research*, **46**(19), 9990-10006.

Attali, C., Durmort, C., Vernet, T. and Di Guilmi, A.M. (2008). The interaction of *Streptococcus pneumoniae* with plasmin mediates transmigration across endothelial and epithelial monolayers by intercellular junction cleavage. *Infection and Immunity*, **76**(11), 5350-5356.

Auzat, I., Chapuy-Regaud, S., Le Bras, G., Dos Santos, D., Ogunniyi, A.D., Le Thomas, I., Garel, J., R., Paton, J.C. and Trombe, M.C. (1999). The NADH oxidase of *Streptococcus pneumoniae*: its involvement in competence and virulence. *Molecular Microbiology*, **34**(5), 1018-1028.

Bai, A.J. and Rai, V.R. (2011). Bacterial quorum sensing and food industry. *Comprehensive Reviews in Food Science and Food Safety*, **10**(3), 183-193.

Balachandran, P., Hollingshead, S.K., Paton, J.C. and Briles, D.E. (2001). The autolytic enzyme LytA of *Streptococcus pneumoniae* is not responsible for releasing pneumolysin. *Journal of Bacteriology*, **183**(10), 3108-3116.

Banerjee, G. and Ray, A.K. (2017). Quorum-sensing network-associated gene regulation in Gram-positive bacteria. *Acta Microbiologica et Immunologica Hungarica*, **64**(4), 439-453.

Bartilson, M., Marra, A., Christine, J., Asundi, J.S., Schneider, W.P. and Hromockyj, A.E. (2001). Differential fluorescence induction reveals *Streptococcus pneumoniae* loci regulated by competence stimulatory peptide. *Molecular Microbiology*, **39**(1), 126-135.

Beier, D. and Gross, R. (2006). Regulation of bacterial virulence by two-component systems. *Current Opinion in Microbiology*, **9**(2), 143-152.

Bergman, N.H., Anderson, E.C., Swenson, E.E., Janes, B.K., Fisher, N., Niemeyer, M.M., Miyoshi, A.D. and Hanna, P.C. (2007). Transcriptional profiling of Bacillus anthracis during infection of host macrophages. *Infection and Immunity*, **75**(7), 3434-3444.

Berry, A.M. and Paton, J.C. (2000). Additive attenuation of virulence of *streptococcus pneumoniae* by mutation of the genes encoding pneumolysin and other putative pneumococcal virulence proteins. *Infection and Immunity*, **68**(1), 133-140.

Berry, A.M., Lock, R.A. and Paton, J.C. (1996). Cloning and characterization of *nanB*, a second *Streptococcus pneumoniae* neuraminidase gene, and purification of the NanB enzyme from recombinant *Escherichia coli*. *Journal of Bacteriology*, **178**(16), 4854-4860.

Betts, M.J. and Russell, R.B. (2003). Amino Acid Properties and Consequences of Substitution. In: *Bioinformatics for Geneticists* (ed. by Barnes, M.R. and Gray, I.C.). *John Wiley & Sons Ltd*, Chichester, UK, pp. 289-316.

Bidossi, A., Mulas, L., Decorosi, F., Colomba, L., Ricci, S., Pozzi, G., Deutscher, J., Viti, C. and Oggioni, M.R. (2012). A functional genomics approach to establish the complement of carbohydrate transporters in *Streptococcus pneumoniae*. *PLoS One*, **7**(3), e33320.

Blanchette, K.A., Shenoy, A.T., Milner, J., Gilley, R.P., McClure, E., Hinojosa, C.A., Kumar, N., Daughtery, S.C., Tallon, L.J. and Ott, S. (2016). Neuraminidase A exposed galactose promotes *Streptococcus pneumoniae* biofilm formation during colonization. *Infection and Immunity*, **84**(10), 2922–2932.

Blanchette-Cain, K., Hinojosa, C.A., Babu, R.A.S., Lizcano, A., Gonzalez-Juarbe, N., Munoz-Almagro, C., Sanchez, C.J., Bergman, M.A. and Orihuela, C.J. (2013). *Streptococcus pneumoniae* biofilm formation is strain dependent, multifactorial, and associated with reduced invasiveness and immunoreactivity during colonization. *mBio*, **4**(5), e00745-13.

Blue, C.E. and Mitchell, T.J. (2003). Contribution of a response regulator to the virulence of *Streptococcus pneumoniae* is strain dependent. *Infection and Immunity*, **71**(8), 4405-4413.

Boersma, M.D., Sadowsky, J.D., Tomita, Y.A. and Gellman, S.H. (2008). Hydrophile scanning as a complement to alanine scanning for exploring and manipulating protein–protein recognition: application to the Bim BH3 domain. *Protein Science*, **17**(7), 1232-1240.

Bogaert, D., de Groot, R. and Hermans, P. (2004). *Streptococcus pneumoniae* colonisation: the key to pneumococcal disease. *The Lancet infectious diseases*, **4**(3), 144-154.

Bojang, A., Jafali, J., Egere, U.E., Hill, P.C., Antonio, M., Jeffries, D., Greenwood, B.M. and Roca, A. (2015). Seasonality of pneumococcal nasopharyngeal carriage in rural Gambia determined within the context of a cluster randomized pneumococcal vaccine trial. *PLoS One*, **10**(7), e0129649.

Bongiorni, C., Ishikawa, S., Stephenson, S., Ogasawara, N. and Perego, M. (2005). Synergistic regulation of competence development in *Bacillus subtilis* by two Rap-Phr systems. *Journal of Bacteriology*, **187**(13), 4353-4361.

Bortoni, M.E., Terra, V.S., Hinds, J., Andrew, P.W. and Yesilkaya, H. (2009). The pneumococcal response to oxidative stress includes a role for Rgg. *Microbiology*, **155**(12), 4123-4134.

Bouillaut, L., Perchat, S., Arold, S., Zorrilla, S., Slamti, L., Henry, C., Gohar, M., Declerck, N. and Lereclus, D. (2008). Molecular basis for group-specific activation of the virulence regulator PlcR by PapR heptapeptides. *Nucleic acids research*, **36**(11), 3791-3801.

Brackman, G., Cos, P., Maes, L., Nelis, H.J. and Coenye, T. (2011). Quorum sensing inhibitors increase the susceptibility of bacterial biofilms to antibiotics *in vitro* and *in vivo*. *Antimicrobial Agents and Chemotherapy*, **55**(6), 2655-2661.

Bradford, M.M. (1976). A rapid and sensitive method for the quantitation of microgram quantities of protein utilizing the principle of protein-dye binding. *Analytical Biochemistry*, **72**(1-2), 248-254.

Bricker, A.L. and Camilli, A. (1999). Transformation of a type 4 encapsulated strain of *Streptococcus pneumoniae*. *FEMS Microbiology Letters*, **172**(2), 131-135.

Bridy-Pappas, A.E., Margolis, M.B., Center, K.J. and Isaacman, D.J. (2005). *Streptococcus pneumoniae*: description of the pathogen, disease epidemiology, treatment, and prevention. Pharmacotherapy. *The Journal of Human Pharmacology and Drug Therapy*, **25**(9), 1193-1212.

Brittan, J.L., Buckeridge, T.J., Finn, A., Kadioglu, A. and Jenkinson, H.F. (2012). Pneumococcal neuraminidase A: an essential upper airway colonization factor for *Streptococcus pneumoniae*. *Molecular Oral Microbiology*, **27**(4), 270-283.

Bronstein, I., Fortin, J., Stanley, P.E., Stewart, G.S.A.B. and Kricka, L.J. (1994). Chemiluminescent and bioluminescent reporter gene assays. *Analytical Biochemistry*, **219**(2), 169-181.

Brooks, B.D. and Brooks, A.E. (2014). Therapeutic strategies to combat antibiotic resistance. *Advanced Drug Delivery Reviews,* **78**, 14-27.

Brooks, L.R.K. and Mias, G.I. (2018). *Streptococcus pneumoniae*'s virulence and host immunity: aging, diagnostics and prevention. *Frontiers in Immunology*, **9**, 1366.

Brooks-Walter, A., Briles, D.E. and Hollingshead, S.K. (1999). The *pspC* gene of *Streptococcus pneumoniae* encodes a polymorphic protein, PspC, which elicits cross-reactive antibodies to PspA and provides immunity to pneumococcal bacteremia. *Infection and Immunity*, **67**(12), 6533-6542.

Browning, D.F. and Busby, S.J.W. (2004). The regulation of bacterial transcription initiation. *Nature Reviews Microbiology*, **2**(1), 57.

Browning, D.F. and Busby, S.J.W. (2016). Local and global regulation of transcription initiation in bacteria. *Nature Reviews Microbiology,* **14**(10), 638.

Bryant, J.C., Dabbs, R.C., Oswalt, K.L., Brown, L.R., Rosch, J.W., Seo, K.S., Donaldson, J.R., McDaniel, L.S. and Thornton, J.A. (2016). Pyruvate oxidase of *Streptococcus pneumoniae* contributes to pneumolysin release. *BMC Microbiology*, **16**(1), 271.

Buckwalter, C.M. and King, S.J. (2012). Pneumococcal carbohydrate transport: food for thought. *Trends in Microbiology*, **20**(11), 517-522.

Burke, T.J., Loniello, K.R., Beebe, J.A. and Ervin, K.M. (2003). Development and application of fluorescence polarization assays in drug discovery. *Combinatorial Chemistry and High Throughput Screening*, **6**(3), 183-194.

Burnaugh, A.M., Frantz, L.J. and King, S.J. (2008). Growth of *Streptococcus pneumoniae* on human glycoconjugates is dependent upon the sequential activity of bacterial exoglycosidases. *Journal of Bacteriology*, **190**(1), 221-230.

Calne, R. (2004). Cyclosporine as a milestone in immunosuppression. *Transplantation Proceedings*, **36** (Suppl. 2S), S13-S15.

Camilli, R., D'Ambrosio, F., Del Grosso, M., de Araujo, F.P., Caporali, M.G., Del Manso, M., Gherardi, G., D'Ancona, F., Pantosti, A. and Group, P.S. (2017). Impact of pneumococcal conjugate vaccine (PCV7 and PCV13) on pneumococcal invasive diseases in Italian children and insight into evolution of pneumococcal population structure. *Vaccine*, **35**(35), 4587-4593.

Canovas, J., Baldry, M., Bojer, M.S., Andersen, P.S., Gless, B.H., Grzeskowiak, P.K., Stegger, M., Damborg, P., Olsen, C.A. and Ingmer, H. (2016). Cross-talk between *Staphylococcus aureus* and other Staphylococcal species via the *agr* quorum sensing system. *Frontiers in Microbiology*, **7**, 1733.

Carvalho, S.M., Kuipers, O.P. and Neves, A.R. (2013a). Environmental and nutritional factors that affect growth and metabolism of the pneumococcal serotype 2 strain D39 and its no encapsulated derivative strain R6. *PLoS One*, **8**(3), e58492.

Carvalho, S.M., Andisi, V.F., Gradstedt, H., Neef, J., Kuipers, O.P., Neves, A.R. and Bijlsma, J.J.E. (2013b). Pyruvate oxidase influences the sugar utilization pattern and capsule production in *Streptococcus pneumoniae*. *PLoS One*, **8**(7), e68277.

Carvalho, S.M., Kloosterman, T.G., Kuipers, O.P. and Neves, A.R. (2011). CcpA ensures optimal metabolic fitness of *Streptococcus pneumoniae*. *PLoS One*, **6**(10), e26707.

Casino, P., Rubio, V. and Marina, A. (2009). Structural insight into partner specificity and phosphoryl transfer in two-component signal transduction. *Cell*, **139**(2), 325-336.

Cassone, M., Gagne, A.L., Spruce, L.A., Seeholzer, S.H. and Sebert, M.E. (2012). The HtrA protease from *Streptococcus pneumoniae* digests both denatured proteins and the competence-stimulating peptide. *Journal of Biological Chemistry*, **287**(46), 38449-38459.

Centers for Disease Control and Prevention (2016). Active Bacterial Core Surveillance Report, Emerging Infections Program Network, *Streptococcus pneumoniae*. Available at: http://www.cdc.gov/abcs/reportsfindings/survreports/spneu16.html.

Chalmers, J.D., Campling, J., Dicker, A., Woodhead, M. and Madhava, H. (2016). A systematic review of the burden of vaccine preventable pneumococcal disease in UK adults. *BMC Pulmonary Medicine*, **16**(1), 77.

Chan, F.T.S., Pinotsi, D., Gabriele, S., Kaminski-Schierle, G.S. and Kaminski, C.F. (2014). Structure-Specific Intrinsic Fluorescence of Protein Amyloids Used to Study their Kinetics of Aggregation. In: *Bio-nanoimaging: Protein Misfolding and Aggregation* (ed. by Uversky, V.N. and Lyubchenko, Y.L.). *Elsevier Inc*, pp. 147-155.

Chandler, J.R., Flynn, A.R., Bryan, E.M. and Dunny, G.M. (2005). Specific control of endogenous cCF10 pheromone by a conserved domain of the pCF10-encoded regulatory protein PrgY in *Enterococcus faecalis*. *Journal of Bacteriology*, **187**(14), 4830-4843.

Chang, J.C. and Federle, M.J. (2016). PptAB exports Rgg quorum-sensing peptides in *Streptococcus*. *PLoS One*, **11**(12), e0168461.

Chang, J.C., Jimenez, J.C. and Federle, M.J. (2015). Induction of a quorum sensing pathway by environmental signals enhances group A streptococcal resistance to lysozyme. *Molecular Microbiology*, **97**(6), 1097-1113.

Chang, J.C., LaSarre, B., Jimenez, J.C., Aggarwal, C. and Federle, M.J. (2011). Two group A streptococcal peptide pheromones act through opposing Rgg regulators to control biofilm development. *PLoS Pathogens*, **7**(8), e1002190.

Chao, Y., Marks, L.R., Pettigrew, M.M. and Hakansson, A.P. (2015). *Streptococcus pneumoniae* biofilm formation and dispersion during colonization and disease. *Frontiers in Cellular and Infection Microbiology*, **4**, 194.

Chatterjee, A., Cook, L.C., Shu, C.C., Chen, Y., Manias, D.A., Ramkrishna, D., Dunny, G.M. and Hu, W.S. (2013). Antagonistic self-sensing and mate-sensing signaling controls antibiotic-resistance transfer. *Proceedings of the National Academy of Sciences of the United States of America*, **110**(17), 7086-7090.

Chaussee, M.A., Callegari, E.A. and Chaussee, M.S. (2004). Rgg regulates growth phase-dependent expression of proteins associated with secondary metabolism and stress in *Streptococcus pyogenes*. *Journal of Bacteriology*, **186**(21), 7091-7099.

Chaussee, M.S., Ajdic, D. and Ferretti, J.J. (1999). The *rgg* gene of *Streptococcus pyogenes* NZ131 positively influences extracellular SPE B production. *Infection and Immunity*, **67**(4), 1715-1722.

Chaussee, M.S., Somerville, G.A., Reitzer, L. and Musser, J.M. (2003). Rgg coordinates virulence factor synthesis and metabolism in *Streptococcus pyogenes*. *Journal of Bacteriology*, **185**(20), 6016-6024.

Chen, F., Gao, Y., Chen, X., Yu, Z. and Li, X. (2013). Quorum quenching enzymes and their application in degrading signal molecules to block quorum sensing-dependent infection. *International Journal of Molecular Sciences,* **14**(9), 17477-17500.

Chiavolini, D., Pozzi, G. and Ricci, S. (2008). Animal models of *Streptococcus pneumoniae* disease. *Clinical Microbiology Reviews*, **21**(4), 666-685.

Cho, S., Law, J. and Ng, C.K. (2009). Effect of Growth at Sub-lethal Concentrations of Kanamycin on the Cell Membrane Integrity and Amount of Capsular Glucuronic Acid in Wild-type *Escherichia coli* and Strain with a *cpsB* Mutation. *Journal of Experimental Microbiology and Immunology*, **13**, 29-35.

Christensen, L.D., van Gennip, M., Jakobsen, T.H., Alhede, M., Hougen, H.P., Høiby, N., Bjarnsholt, T. and Givskov, M. (2012). Synergistic antibacterial efficacy of early combination treatment with tobramycin and quorum-sensing inhibitors against *Pseudomonas aeruginosa* in an intraperitoneal foreign-body infection mouse model. *Journal of Antimicrobial Chemotherapy*, **67**(5), 1198-1206.

Chuang, O.N., Schlievert, P.M., Wells, C.L., Manias, D.A., Tripp, T.J. and Dunny, G.M. (2009). Multiple functional domains of *Enterococcus faecalis* aggregation substance Asc10 contribute to endocarditis virulence. *Infection and Immunity*, **77**(1), 539-548.

Chuang-Smith, O., Wells, C.L., Henry-Stanley, M. and Dunny, G.M. (2010). Acceleration of *Enterococcus faecalis* biofilm formation by aggregation substance expression in an *ex vivo* model of cardiac valve colonization. *PLoS One*, **5**(12), e15798.

Clatworthy, A.E., Pierson, E. and Hung, D.T. (2007). Targeting virulence: a new paradigm for antimicrobial therapy. *Nature Chemical Biology*, **3**(9), 541.

Clausen, V.A., Bae, W., Throup, J., Burnham, M.K.R., Rosenberg, M. and Wallis, N.G. (2003). Biochemical characterization of the first essential two-component signal transduction system from *Staphylococcus aureus* and *Streptococcus pneumoniae*. *Journal of Molecular Microbiology and Biotechnology*, **5**(4), 252-260.

Claverys, J.P., Martin, B. and Håvarstein, L.S. (2007). Competence-induced fratricide in streptococci. *Molecular Microbiology*, **64**(6), 1423-1433.

Coffey, T.J., Dowson, C.G., Daniels, M. and Spratt, B.G. (1995). Genetics and molecular biology of β-Lactam-resistant pneumococci. *Microbial Drug Resistance*, **1**(1), 29-34.

Collaborative Computational Project, Number 4 (1994). The CCP4 suite: programs for protein crystallography. *Acta crystallographica. Section D, Biological crystallography*, **50**(5), 760-763.

Conklin, L., Loo, J.D., Kirk, J., Fleming-Dutra, K., Deloria Knoll, M., Park, D.E., Goldblatt, D., O'Brien, K.L. and Whitney, C.G. (2014). Systematic review of the effect of pneumococcal conjugate vaccine dosing schedules on vaccine-type invasive pneumococcal disease among young children. *The Paediatric Infectious Disease Journal*, **33**(Suppl. 2), S109-S118.

Cook, L.C. and Federle, M.J. (2014). Peptide pheromone signaling in *Streptococcus* and *Enterococcus*. *FEMS Microbiology Reviews*, **38**(3), 473-492.

Cook, L.C., LaSarre, B. and Federle, M.J. (2013). Interspecies communication among commensal and pathogenic streptococci. *mBio*, **4**(4), e00382-13.

Core, L. and Perego, M. (2003). TPR-mediated interaction of RapC with ComA inhibits response regulator-DNA binding for competence development in *Bacillus subtilis*. *Molecular Microbiology*, **49**(6), 1509-1522.

Cornick, J.E. and Bentley, S.D. (2012). *Streptococcus pneumoniae*: the evolution of antimicrobial resistance to beta-lactams, fluoroquinolones and macrolides. *Microbes and Infection*, **14**(7-8), 573-583.

Cortes, P.R., Piñas, G.E., Cian, M.B., Yandar, N. and Echenique, J. (2015). Stress-triggered signaling affecting survival or suicide of *Streptococcus pneumoniae*. *International Journal of Medical Microbiology*, **305**(1), 157-169.

Costa, S., Almeida, A., Castro, A. and Domingues, L. (2014). Fusion tags for protein solubility, purification and immunogenicity in *Escherichia coli*: the novel Fh8 system. *Frontiers in Microbiology*, **5**, 63.

Cuevas, R.A., Eutsey, R., Kadam, A., West-Roberts, J., Woolford, C.A., Mitchell, A.P., Mason, K.M. and Hiller, N.L. (2017). A novel streptococcal cell-cell communication peptide promotes pneumococcal virulence and biofilm formation. *Molecular Microbiology*, **105**(4), 554-571.

Dagkessamanskaia, A., Moscoso, M., Hénard, V., Guiral, S., Overweg, K., Reuter, M., Martin, B., Wells, J. and Claverys, J. (2004). Interconnection of competence, stress and CiaR regulons in *Streptococcus pneumoniae*: competence triggers stationary phase autolysis of *ciaR* mutant cells. *Molecular Microbiology*, **51**(4), 1071-1086.

Daniels, C.C., Rogers, P.D. and Shelton, C.M. (2016). A Review of Pneumococcal Vaccines: Current Polysaccharide Vaccine Recommendations and Future Protein Antigens. *Journal of Pediatric Pharmacology Therapeutics*, **21**(1), 27-35.

Darrieux, M., Goulart, C., Briles, D. and Leite, L.C.d.C. (2015). Current status and perspectives on protein-based pneumococcal vaccines. *Critical Reviews in Microbiology*, **41**(2), 190-200.

de Vos, A.F., Dessing, M.C., Lammers, A.J.J., de Porto, A.P.N.A., Florquin, S., de Boer, O. J., de Beer, R., Terpstra, S., Bootsma, H.J., Hermans, P.W., van 't Veer, C. and van der Poll, T. (2015). The polysaccharide capsule of *Streptococcus pneumonia* partially impedes MyD88-mediated immunity during pneumonia in mice. *PLoS One*, **10**(2), e0118181.

Deber, C.M.B., Brodsky, B. and Rath, A. (2010). Proline Residues in Proteins. *John Wiley & Sons Ltd,* Chichester.

Declerck, N., Bouillaut, L., Chaix, D., Rugani, N., Slamti, L., Hoh, F., Lereclus, D. and Arold, S.T. (2007). Structure of PlcR: Insights into virulence regulation and evolution of quorum sensing in Gram-positive bacteria. *Proceedings of the National Academy of Sciences of the United States of America*, **104**(47), 18490-18495.

Dessau, M.A. and Modis, Y. (2011). Protein crystallization for X-ray crystallography. *Journal of Visualized Experiments*, (47), 2285.

Detmers, F.J.M., Lanfermeijer, F.C., Abele, R., Jack, R.W., Tampe, R., Konings, W.N. and Poolman, B. (2000). Combinatorial peptide libraries reveal the ligand-binding mechanism of the oligopeptide receptor OppA of *Lactococcus lactis*. *Proceedings of the National Academy of Sciences of the United States of America*, **97**(23), 12487-12492.

Deutscher, J. (2008). The mechanisms of carbon catabolite repression in bacteria. *Current Opinion in Microbiology*, **11**(2), 87-93.

Deutscher, J., Francke, C. and Postma, P.W. (2006). How phosphotransferase system-related protein phosphorylation regulates carbohydrate metabolism in bacteria. *Microbiology and Molecular Biology Reviews*, **70**(4), 939-1031.

Do, H. and Kumaraswami, M. (2016). Structural mechanisms of peptide recognition and allosteric modulation of gene regulation by the RRNPP family of quorum-sensing regulators. *Journal of Molecular Biology*, **428**(14), 2793-2804.

Dong, Y., Wang, L. and Zhang, L. (2007). Quorum-quenching microbial infections: mechanisms and implications. *Philosophical Transactions of the Royal Society B: Biological Sciences*, **362**(1483), 1201-1211.

Dong, Y., Wang, L., Xu, J., Zhang, H., Zhang, X. and Zhang, L. (2001). Quenching quorum-sensing-dependent bacterial infection by an N-acyl homoserine lactonase. *Nature*, **411**(6839), 813.

Duan, C., Zhu, L., Xu, Y. and Lau, G.W. (2012). Saturated alanine scanning mutagenesis of the pneumococcus competence stimulating peptide identifies analogs that inhibit genetic transformation. *PLoS One*, **7**(9), e44710.

Duane, P.G., Rubins, J.B., Weisel, H.R. and Janoff, E.N. (1993). Identification of hydrogen peroxide as a *Streptococcus pneumoniae* toxin for rat alveolar epithelial cells. *Infection and Immunity*, **61**(10), 4392-4397.

Dubois, T., Faegri, K., Perchat, S., Lemy, C., Buisson, C., Nielsen-LeRoux, C., Gohar, M., Jacques, P., Ramarao, N. and Kolstø, A. and Lereclus, D. (2012). Necrotrophism is a quorum-sensing-regulated lifestyle in *Bacillus thuringiensis*. *PLoS Pathogens*, **8**(4), e1002629.

Dubois, T., Perchat, S., Verplaetse, E., Gominet, M., Lemy, C., Aumont-Nicaise, M., Grenha, R., Nessler, S. and Lereclus, D. (2013). Activity of the *Bacillus thuringiensis* NprR-NprX cell-cell communication system is co-ordinated to the physiological stage through a complex transcriptional regulation. *Molecular Microbiology*, **88**(1), 48-63.

Dunny, G.M. and Berntsson, R.P.A. (2016). Enterococcal sex pheromones: evolutionary pathways to complex, two-signal systems. *Journal of Bacteriology*, **198**(11), 1556-1562.

Durando, P., Faust, S.N., Fletcher, M., Krizova, P., Torres, A. and Welte, T. (2013). Experience with pneumococcal polysaccharide conjugate vaccine (conjugated to CRM197 carrier protein) in children and adults. *Clinical Microbiology and Infection*, **19**, 1-9.

Eggink, D., Berkhout, B. and Sanders, R.W. (2010). Inhibition of HIV-1 by fusion inhibitors. *Current Pharmaceutical Design*, **16**(33), 3716-3728.

Eliopoulos, G.M. (2004). Quinolone resistance mechanisms in *pneumococci*. *Clinical Infectious Diseases*, **38**(Suppl 4), S350-S356.

Engholm, D.H., Kilian, M., Goodsell, D.S., Andersen, E.S. and Kjærgaard, R.S. (2017). A visual review of the human pathogen *Streptococcus pneumoniae*. *FEMS Microbiology Reviews*, **41**(6), 854-879.

Engstrom, M.D. and Pfleger, B.F. (2017). Transcription control engineering and applications in synthetic biology. *Synthetic and Systems Biotechnology*, **2**(3), 176-191.

Ernst, W. (2016). Humanized mice in infectious diseases. *Comparative Immunology, Microbiology and Infectious Diseases*, **49**, 29-38.

Favre-Bonte, S., Joly, B. and Forestier, C. (1999). Consequences of reduction of *Klebsiella pneumoniae* capsule expression on interactions of this bacterium with epithelial cells. *Infection and Immunity*, **67**(2), 554-561.

Feldman, C. and Anderson, R. (2014). Current and new generation pneumococcal vaccines. *Journal of Infection*, **69**(4), 309-325.

Feldman, C., Anderson, R., Cockeran, R., Mitchell, T., Cole, P. and Wilson, R. (2002). The effects of pneumolysin and hydrogen peroxide, alone and in combination, on human ciliated epithelium *in vitro*. *Respiratory Medicine*, **96**(8), 580-585.

Fernandez, A., Borges, F., Gintz, B., Decaris, B. and Leblond-Bourget, N. (2006). The *rggC* locus, with a frame shift mutation, is involved in oxidative stress response by *Streptococcus thermophilus*. *Archives of Microbiology*, **186**(3), 161-169.

Fetzner, S. (2015). Quorum quenching enzymes. *Journal of Biotechnology*, **201**, 2-14.

Fleming, E., Lazinski, D.W. and Camilli, A. (2015). Carbon catabolite repression by seryl phosphorylated HPr is essential to *Streptococcus pneumoniae* in carbohydrate-rich environments. *Molecular Microbiology*, **97**(2), 360-380.

Fletcher, M.A. and Fritzell, B. (2012). Pneumococcal conjugate vaccines and otitis media: an appraisal of the clinical trials. *International Journal of Otolaryngology*, **2012**, 312935.

Fleuchot, B., Gitton, C., Guillot, A., Vidic, J., Nicolas, P., Besset, C., Fontaine, L., Hols, P., Leblond-Bourget, N., Monnet, V. and Gardan, R. (2011). Rgg proteins associated with internalized small hydrophobic peptides: a new quorum-sensing mechanism in streptococci. *Molecular Microbiology*, **80**(4), 1102-1119.

Fleuchot, B., Guillot, A., Mezange, C., Besset, C., Chambellon, E., Monnet, V. and Gardan, R. (2013). Rgg-associated SHP signaling peptides mediate cross-talk in Streptococci. *PLoS One*, **8**(6), e66042.

Fontaine, L., Boutry, C., de Frahan, M.H., Delplace, B., Fremaux, C., Horvath, P., Boyaval, P. and Hols, P. (2010). A novel pheromone quorum-sensing system controls the development of natural competence in *Streptococcus thermophilus* and *Streptococcus salivarius*. *Journal of Bacteriology*, **192**(5), 1444-1454.

Fontaine, L., Goffin, P., Dubout, H., Delplace, B., Baulard, A., Lecat-Guillet, N., Chambellon, E., Gardan, R. and Hols, P. (2013). Mechanism of competence activation by the ComRS signalling system in streptococci. *Molecular Microbiology*, **87**(6), 1113-1132.

Fosgerau, K. and Hoffmann, T. (2015). Peptide therapeutics: current status and future directions. *Drug Discovery Today*, **20**(1), 122-128.

Frederix, M. and Downie, J.A. (2011). Quorum sensing: regulating the regulators. *Advances in Microbial Physiology*. *Elsevier Inc*, 23-80.

Fujiwara, T., Hoshino, T., Ooshima, T., Sobue, S. and Hamada, S. (2000). Purification, Characterization, and Molecular Analysis of the Gene Encoding Glucosyltransferase from *Streptococcus oralis. Infection and Immunity,* **68**(5), 2475-2483.

Fuqua, C., Parsek, M.R. and Greenberg, E.P. (2001). Regulation of gene expression by cell-to-cell communication: acyl-homoserine lactone quorum sensing. *Annual Review of Genetics*, **35**(1), 439-468.

Galán-Bartual, S., Pérez-Dorado, I., García, P. and Hermoso, J. A. (2015). Structure and Function of Choline-Binding Proteins. In: *Streptococcus pneumoniae Molecular Mechanisms of Host-Pathogen Interactions* (ed. by Brown, J., Hammerschmidt, S. and Orihuela, .C.). *Elsevier Inc*, pp. 207-230.

Gallego del Sol, F. and Marina, A. (2013). Structural basis of Rap phosphatase inhibition by Phr peptides. *PLoS Biology*, **11**(3), e1001511.

Gamez, G. and Hammerschmidt, S. (2012). Combat pneumococcal infections: adhesins as candidates for protein-based vaccine development. *Current Drug Targets*, **13**(3), 323-337.

Gaspar, P., Al-Bayati, F., Andrew, P.W., Neves, A.R. and Yesilkaya, H. (2014). Lactate dehydrogenase is the key enzyme for pneumococcal pyruvate metabolism and pneumococcal survival in blood. *Infection and Immunity*, **82**(12), 5099–5109.

Geno, K.A., Gilbert, G.L., Song, J.Y., Skovsted, I.C., Klugman, K.P., Jones, C., Konradsen, H.B. and Nahm, M.H. (2015). Pneumococcal Capsules and Their Types: Past, Present, and Future. *Clinical Microbiology Reviews*, **28**(3), 871-899.

Ghisaidoobe, A.B.T. and Chung, S.J. (2014). Intrinsic tryptophan fluorescence in the detection and analysis of proteins: a focus on Förster resonance energy transfer techniques. *International Journal of Molecular Sciences,* **15**(12), 22518-22538.

Giammarinaro, P. and Paton, J.C. (2002). Role of RegM, a homologue of the catabolite repressor protein CcpA, in the virulence of *Streptococcus pneumoniae*. *Infection and Immunity,* **70**(10), 5454-5461.

Glanville, D.G., Han, L., Maule, A.F., Woodacre, A., Thanki, D., Abdullah, I.T., Morrissey, J.A., Clarke, T.B., Yesilkaya, H. and Silvaggi, N.R. (2018). RitR is an archetype for a novel family of redox sensors in the streptococci that has evolved from two-component response regulators and is required for pneumococcal colonization. *PLoS Pathogens,* **14**(5), e1007052.

Gogos, A., Jimenez, J.C., Chang, J.C., Wilkening, R.V. and Federle, M.J. (2018). A quorum sensing-regulated protein binds cell-wall component and enhances lysozyme resistance in *Streptococcus pyogenes*. *Journal of Bacteriology*, **200**(11), 00701-17.

Gohar, M., Faegri, K., Perchat, S., Ravnum, S., Økstad, O.A., Gominet, M., Kolstø, A. and Lereclus, D. (2008). The PlcR virulence regulon of *Bacillus cereus*. *PLoS One,* **3**(7), e2793.

Gómez-Mejia, A., Gámez, G. and Hammerschmidt, S. (2018). *Streptococcus pneumoniae* two-component regulatory systems: The interplay of the pneumococcus with its environment. *International Journal of Medical Microbiology*, **308**(6), 722-737.

Gopal, G.J. and Kumar, A. (2013). Strategies for the production of recombinant protein in *Escherichia coli*. *The protein Journal*, **32**(6), 419-425.

Görke, B. and Stülke, J. (2008). Carbon catabolite repression in bacteria: many ways to make the most out of nutrients. *Nature Reviews Microbiology,* **6**(8), 613-624.

Gorman, C.M., Moffat, L.F. and Howard, B.H. (1982). Recombinant genomes which express chloramphenicol acetyltransferase in mammalian cells. *Molecular and Cellular Biology,* **2**(9), 1044-1051.

Govindarajan, S. and Amster-Choder, O. (2014). Transcription Regulation in Bacteria. *Reference Module in Biomedical Sciences, Elsevier Inc.*

Grandclément, C., Tannières, M., Moréra, S., Dessaux, Y. and Faure, D. (2016). Quorum quenching: role in nature and applied developments. *FEMS Microbiology Reviews*, **40**(1), 86-116.

Gratz, N., Loh, L.N. and Tuomanen, E. (2015). Pneumococcal Invasion: Development of Bacteremia and Meningitis. In: *Streptococcus pneumoniae Molecular Mechanisms of Host-Pathogen Interactions* (eds. by Brown, J., Hammerschmidt, S. and Orihuela, .C.). *Elsevier Inc,* pp. 433-451.

Green, R., and Rogers, E.J. (2013). Transformation of chemically competent *E. coli*. *Methods in Enzymology*, **529**, 329–336.

Grenha, R., Slamti, L., Nicaise, M., Refes, Y., Lereclus, D. and Nessler, S. (2013). Structural basis for the activation mechanism of the PlcR virulence regulator by the quorum-sensing signal peptide PapR. *Proceedings of the National Academy of Sciences of the United States of America*, **110**(3), 1047-1052.

Gualdi, L., Hayre, J.K., Gerlini, A., Bidossi, A., Colomba, L., Trappetti, C., Pozzi, G., Docquier, J.D., Andrew, P., Ricci, S. and Oggioni, M.R. (2012). Regulation of neuraminidase expression in *Streptococcus pneumoniae*. *BMC Microbiology*, **12**, 200.

Guenzi, E., Gasc, A.M., Sicard, M.A. and Hakenbeck, R. (1994). A two-component signal-transducing system is involved in competence and penicillin susceptibility in laboratory mutants of *Streptococcus pneumoniae*. *Molecular Microbiology*, **12**(3), 505-515.

Guiral, S., Henard, V., Laaberki, M., Granadel, C., Prudhomme, M., Martin, B. and Claverys, J. (2006). Construction and evaluation of a chromosomal expression platform (CEP) for ectopic, maltose-driven gene expression in *Streptococcus pneumoniae*. *Microbiology*, **152**(2), 343-349.

Guiral, S., Mitchell, T.J., Martin, B. and Claverys, J.P. (2005). Competence-programmed predation of noncompetent cells in the human pathogen *Streptococcus pneumoniae*: genetic requirements. *Proceedings of the National Academy of Sciences of the United States of America*, **102**(24), 8710-8715.

Gut, H., King, S.J. and Walsh, M.A. (2008). Structural and functional studies of *Streptococcus pneumoniae* neuraminidase B: An intramolecular trans-sialidase. *FEBS Letters*, **582**(23-24), 3348-3352.

Hajaj, B., Yesilkaya, H., Benisty, R., David, M., Andrew, P.W. and Porat, N. (2012). Thiol peroxidase is an important component of *Streptococcus pneumoniae* in oxygenated environments. *Infection and Immunity*, **80**(12), 4333-4343.

Hajaj, B., Yesilkaya, H., Shafeeq, S., Zhi, X., Benisty, R., Tchalah, S., Kuipers, O.P. and Porat, N. (2017). CodY Regulates Thiol Peroxidase Expression as Part of the Pneumococcal Defense Mechanism against H(2)O(2) Stress. *Frontiers in Cellular and Infection Microbiology*, **7**, 210.

Hakenbeck, R., Bruckner, R., Denapaite, D. and Maurer, P. (2012). Molecular mechanisms of beta-lactam resistance in *Streptococcus pneumoniae*. *Future Microbiology*, **7**(3), 395-410.

Hakenbeck, R., Grebe, T., Zahner, D. and Stock, J.B. (1999). β-Lactam resistance in *Streptococcus pneumoniae*: penicillin-binding proteins and non-penicillin-binding proteins. *Molecular Microbiology*, **33**(4), 673-678.

Halfmann, A., Kovacs, M., Hakenbeck, R. and Bruckner, R. (2007a). Identification of the genes directly controlled by the response regulator CiaR in *Streptococcus pneumoniae*: five out of 15 promoters drive expression of small non-coding RNAs. *Molecular Microbiology*, **66**(1), 110-126.

Halfmann, A., Hakenbeck, R. and Brückner, R. (2007b). A new integrative reporter plasmid for *Streptococcus pneumoniae*. *FEMS Microbiology Letters*, **268**(2), 217-224.

Hall, M.D., Yasgar, A., Peryea, T., Braisted, J.C., Jadhav, A., Simeonov, A. and Coussens, N.P. (2016). Fluorescence polarization assays in high-throughput screening and drug discovery: a review. *Methods and Applications in Fluorescence*, **4**(2), 022001.

Hammerschmidt, S., Wolff, S., Hocke, A., Rosseau, S., Müller, E. and Rohde, M. (2005). Illustration of pneumococcal polysaccharide capsule during adherence and invasion of epithelial cells. *Infection and Immunity,* **73**(8), 4653-4667.

Hand, N.J. and Silhavy, T.J. (2000). A practical guide to the construction and use of *lac* fusions in *Escherichia coli*. *Methods in Enzymology,* **326**,11-35.

Harapanahalli, A.K., Younes, J.A., Allan, E., van, d.M. and Busscher, H.J. (2015). Chemical Signals and Mechanosensing in Bacterial Responses to Their Environment. *PLoS Pathogens*, **11**(8), e1005057.

Haugen, S.P., Ross, W. and Gourse, R.L. (2008). Advances in bacterial promoter recognition and its control by factors that do not bind DNA. *Nature Reviews Microbiology,* **6**(7), 507-519.

Hava, D.L. and Camilli, A. (2002). Large-scale identification of serotype 4 *Streptococcus pneumoniae* virulence factors. *Molecular Microbiology,* **45**(5), 1389-1406.

Håvarstein, L.S., Coomaraswamy, G. and Morrison, D.A. (1995). An unmodified heptadecapeptide pheromone induces competence for genetic transformation in *Streptococcus pneumoniae*. *Proceedings of the National Academy of Sciences of the United States of America*, **92**(24), 11140-11144.

Håvarstein, L.S., Holo, H. and Nes, I.F. (1994). The leader peptide of colicin V shares consensus sequences with leader peptides that are common among peptide bacteriocins produced by gram-positive bacteria. *Microbiology*, **140**(Pt 9), 2383-2389.

Hayashi, K., Kensuke, T., Kobayashi, K., Ogasawara, N. and Ogura, M. (2006). *Bacillus subtilis* RghR (YvaN) represses *rapG* and *rapH*, which encode inhibitors of expression of the *srfA* operon. *Molecular Microbiology,* **59**(6), 1714-1729.

Hayes, B.M., Jewett, M.W. and Rosa, P.A. (2010). *lacZ* reporter system for use in *Borrelia burgdorferi*. *Applied and Environmental Microbiology*, **76**(22), 7407-7412.

Heckman, K.L. and Pease, L.R. (2007). Gene splicing and mutagenesis by PCR-driven overlap extension. *Nature protocols,* **2**(4), 924.

Hemsley, C., Joyce, E., Hava, D.L., Kawale, A. and Camilli, A. (2003). MgrA, an orthologue of Mga, Acts as a transcriptional repressor of the genes within the *rlrA* pathogenicity islet in *Streptococcus pneumoniae*. *Journal of Bacteriology*, **185**(22) , 6640-6647.

Hendriksen, W.T. (2010). Gene regulation in *Streptococcus pneumoniae*: interplay between nutrition and virulence. PhD Thesis. *Department of Pediatrics, Erasmus University Rotterdam,* Netherlands.

Hendriksen, W.T., Bootsma, H.J., Estevao, S., Hoogenboezem, T., de Jong, A., de Groot, R., Kuipers, O.P. and Hermans, P.W. (2008a). CodY of *Streptococcus pneumoniae*: link between nutritional gene regulation and colonization. *Journal of Bacteriology,* **190**(2), 590-601.

Hendriksen, W.T., Kloosterman, T.G., Bootsma, H.J., Estevao, S., de Groot, R., Kuipers, O.P. and Hermans, P.W. (2008b). Site-specific contributions of glutamine-dependent regulator GlnR and GlnR-regulated genes to virulence of *Streptococcus pneumoniae*. *Infection and Immunity*, **76**(3), 1230-1238.

Hendriksen, W.T., Silva, N., Bootsma, H.J., Blue, C.E., Paterson, G.K., Kerr, A.R., de Jong, A., Kuipers, O.P., Hermans, P.W. and Mitchell, T.J. (2007). Regulation of gene expression in *Streptococcus pneumoniae* by response regulator 09 is strain dependent. *Journal of Bacteriology*, **189**(4), 1382-1389.

Henkin, T.M. (1996). The role of the CcpA transcriptional regulator in carbon metabolism in *Bacillus subtilis*. *FEMS Microbiology Letters*, **135**(1), 9-15.

Henriques-Normark, B. and Tuomanen, E.I. (2013). The pneumococcus: epidemiology, microbiology, and pathogenesis. *Cold Spring Harbor Perspectives in Medicine*, **3**(7), a010215.

Henry, R., Bruneau, E., Gardan, R., Bertin, S., Fleuchot, B., Decaris, B. and Leblond-Bourget, N. (2011). The *rgg0182* gene encodes a transcriptional regulator required for the full *Streptococcus thermophilus*LMG18311 thermal adaptation. *BMC Microbiology*, **11**(1), 223.

Hentzer, M. and Givskov, M. (2003). Pharmacological inhibition of quorum sensing for the treatment of chronic bacterial infections. *The Journal of Clinical Investigation*, **112**(9), 1300-1307.

Heras, B., Scanlon, M.J. and Martin, J.L. (2015). Targeting virulence not viability in the search for future antibacterials. *British Journal of Clinical Pharmacology*, **79**(2), 208-215.

Hicks, L.A., Chien, Y.W., Taylor, T.H., J., Haber, M. and Klugman, K.P. (2011). Outpatient antibiotic prescribing and nonsusceptible *Streptococcus pneumoniae* in the United States, 1996-2003. *Clinical Infectious Diseases*, **53**(7), 631-639.

Hirst, R.A., Gosai, B., Rutman, A., Guerin, C.J., Nicotera, P., Andrew, P.W. and O'Callaghan, C. (2008). *Streptococcus pneumoniae* deficient in pneumolysin or autolysin has reduced virulence in meningitis. *The Journal of Infectious Diseases*, **197**(5), 744-751.

Hirt, H., Erlandsen, S. and Dunny, G. (2000). Heterologous inducible expression of *Enterococcus faecalis* pCF10 aggregation substance Asc10 in *Lactococcus lactis* and *Streptococcus gordonii* contributes to cell hydrophobicity and adhesion to fibrin. *Journal of Bacteriology*, **182**(8), 2299-2306.

Hoang, T.T. and Schweizer, H.P. (1999). Characterization of *Pseudomonas aeruginosa* enoyl-acyl carrier protein reductase (FabI): a target for the antimicrobial triclosan and its role in acylated homoserine lactone synthesis. *Journal of Bacteriology*, **181**(17), 5489-5497.

Hodder, S.L., Chew, D. and Swaminathan, S. (2010). Adult Immunization in Women and Men. In: *Principles of Gender-Specific Medicine* (Second Edition) (ed. by Legato, M.J.). *Elsevier Inc*, pp. 563-582.

Holmes, A.R., McNab, R., Millsap, K.W., Rohde, M., Hammerschmidt, S., Mawdsley, J.L. and Jenkinson, H.F. (2001). The *pavA* gene of *Streptococcus pneumoniae* encodes a fibronectin-binding protein that is essential for virulence. *Molecular Microbiology*, **41**(6), 1395-1408.

Hong, L., Koelsch, G., Lin, X., Wu, S., Terzyan, S., Ghosh, A.K., Zhang, X.C. and Tang, J. (2000). Structure of the protease domain of memapsin 2 (β-Secretase) complexed with inhibitor. *Science*, **290**(5489), 150-153.

Hoover, S.E., Perez, A.J., Tsui, H.T., Sinha, D., Smiley, D.L., DiMarchi, R.D., Winkler, M.E. and Lazazzera, B.A. (2015). A new quorum-sensing system (TprA/PhrA) for *Streptococcus pneumoniae* D 39 that regulates a lantibiotic biosynthesis gene cluster. *Molecular Microbiology*, **97**(2), 229-243.

Horton, R.M. (1995). PCR-mediated recombination and mutagenesis. *Molecular Biotechnology*, **3**(2), 93-99.

Horton, R.M., Ho, S.N., Pullen, J.K., Hunt, H.D., Cai, Z. and Pease, L.R. (1993). Gene splicing by overlap extension. *Methods in Enzymology*, **217**, 270-279.

Hoskins, J., Alborn, W.E., J., Arnold, J., Blaszczak, L.C., Burgett, S., DeHoff, B.S., Estrem, S.T., Fritz, L., Fu, D.J., Fuller, W., Geringer, C., *et al*. (2001). Genome of the bacterium *Streptococcus pneumoniae* strain R6. *Journal of Bacteriology*, **183**(19), 5709-5717.

Hussey, S.J., Purves, J., Allcock, N., Fernandes, V.E., Monks, P.S., Ketley, J.M., Andrew, P.W. and Morrissey, J.A. (2017). Air pollution alters *Staphylococcus aureus* and *Streptococcus pneumoniae* biofilms, antibiotic tolerance and colonisation. *Environmental Microbiology,* **19**(5), 1868-1880.

Hyams, C., Camberlein, E., Cohen, J.M., Bax, K. and Brown, J.S. (2010). The *Streptococcus pneumoniae* capsule inhibits complement activity and neutrophil phagocytosis by multiple mechanisms. *Infection and Immunity*, **78**(2), 704-715.

Ibrahim, M., Nicolas, P., Bessieres, P., Bolotin, A., Monnet, V. and Gardan, R. (2007a). A genome-wide survey of short coding sequences in streptococci. *Microbiology,* **153**, 3631-3644.

Ibrahim, M., Guillot, A., Wessner, F., Algaron, F., Besset, C., Courtin, P., Gardan, R. and Monnet, V. (2007b). Control of the transcription of a short gene encoding a cyclic peptide in *Streptococcus thermophilus*: a new quorum-sensing system? *Journal of Bacteriology*, **189**(24), 8844-8854.

Ibrahim, Y.M., Kerr, A.R., McCluskey, J. and Mitchell, T.J. (2004a). Control of virulence by the two-component system CiaR/H is mediated via HtrA, a major virulence factor of *Streptococcus pneumoniae*. *Journal of Bacteriology*, **186**(16), 5258-5266.

Ibrahim, Y.M., Kerr, A.R., McCluskey, J. and Mitchell, T.J. (2004b). Role of HtrA in the virulence and competence of *Streptococcus pneumoniae*. *Infection and Immunity*, **72**(6), 3584-3591.

Iyer, R., Baliga, N.S. and Camilli, A. (2005). Catabolite control protein A (CcpA) contributes to virulence and regulation of sugar metabolism in *Streptococcus pneumoniae*. *Journal of Bacteriology*, **187**(24), 8340-8349.

Izurieta, P., Bahety, P., Adegbola, R., Clarke, C. and Hoet, B. (2018). Public health impact of pneumococcal conjugate vaccine infant immunization programs: assessment of invasive pneumococcal disease burden and serotype distribution. *Expert Review of Vaccines*, **17**(6), 479-493.

Jakobsen, T.H., Bragason, S.K., Phipps, R.K., Christensen, L.D., van Gennip, M., Alhede, M., Skindersoe, M., Larsen, T.O., Høiby, N., Bjarnsholt, T. and Givskov, M. (2012). Food as a source for QS inhibitors: iberin from horseradish revealed as a quorum sensing inhibitor of *Pseudomonas aeruginosa*. *Applied and Environmental Microbiology,* **78**(7), 2410-2421.

Janapatla, R.P., Hsu, M.H., Hsieh, Y.C., Lee, H.Y., Lin, T.Y. and Chiu, C.H. (2013). Necrotizing pneumonia caused by nanC-carrying serotypes is associated with pneumococcal haemolytic uraemic syndrome in children. *Clinical Microbiology and Infection*, **19**(5), 480-486.

Janoff, E.N. and Musher, D.M. (2015). *Streptococcus pneumoniae*. In: *Mandell, Douglas, and Bennett's Principles and Practice of Infectious Diseases* (Eighth Edition) (ed. by Bennett, J.E., Dolin, R. and Blaser, M.J.). *Elsevier Inc*, pp. 2310-2327.

Jedrzejas, M.J. (2001). Pneumococcal virulence factors: structure and function. *Microbiology and Molecular Biology Reviews*, **65**(2), 187-207.

Jedrzejas, M.J. (2007). Unveiling molecular mechanisms of bacterial surface proteins: *Streptococcus pneumoniae* as a model organism for structural studies. *Cellular and Molecular Life Sciences*, **64**(21), 2799-2822.

Jefferies, J.M., Macdonald, E., Faust, S.N. and Clarke, S.C. (2011). 13-valent pneumococcal conjugate vaccine (PCV13). *Human Vaccines*, **7**(10), 1012-1018.

Jefferson, R.A., Kavanagh, T.A. and Bevan, M.W. (1987). GUS fusions: B-glucuronidase as a sensitive and versatile gene fusion marker in higher plants. *The EMBO journal,* **6**(13), 3901-3907.

Jensch, I., Gamez, G., Rothe, M., Ebert, S., Fulde, M., Somplatzki, D., Bergmann, S., Petruschka, L., Rohde, M., Nau, R. and Hammerschmidt, S. (2010). PavB is a surface-exposed adhesin of *Streptococcus pneumoniae* contributing to nasopharyngeal colonization and airways infections. *Molecular Microbiology,* **77**(1), 22-43.

Jensen, A., Valdórsson, O., Frimodt- Møller, N., Hollingshead, S. and Kilian, M. (2015). Commensal streptococci serve as a reservoir for β-Lactam resistance genes in *Streptococcus pneumoniae*. *Antimicrobial Agents and Chemotherapy,* **59**(6), 3529–3540.

Jeong, J.K., Kwon, O., Lee, Y.M., Oh, D.B., Lee, J.M., Kim, S., Kim, E.H., Le, T.N., Rhee, D.K. and Kang, H.A. (2009). Characterization of the *Streptococcus pneumoniae* BgaC protein as a novel surface β-galactosidase with specific hydrolysis activity for the Galβ1-3GlcNAc moiety of oligosaccharides. *Journal of Bacteriology,* **191**(9), 3011-3023.

Jia, B. and Jeon, C.O. (2016). High-throughput recombinant protein expression in *Escherichia coli*: current status and future perspectives. *Open Biology,* **6**(8), 160196.

Jiang, M., Grau, R. and Perego, M. (2000). Differential processing of propeptide inhibitors of Rap phosphatases in *Bacillus subtilis*. *Journal of Bacteriology,* **182**(2), 303-310.

Jimenez, J.C. and Federle, M.J. (2014). Quorum sensing in group A Streptococcus. *Frontiers in Cellular and Infection Microbiology,* **4**, 127.

Jimenez, P.N., Koch, G., Thompson, J.A., Xavier, K.B., Cool, R.H. and Quax, W.J. (2012). The multiple signaling systems regulating virulence in *Pseudomonas aeruginosa*. *Microbiology and Molecular Biology Reviews*, **76**(1), 46-65.

Johnson, H.L., Deloria-Knoll, M., Levine, O.S., Stoszek, S.K., Freimanis Hance, L., Reithinger, R., Muenz, L.R. and O'Brien, K.L. (2010). Systematic evaluation of serotypes causing invasive pneumococcal disease among children under five: the pneumococcal global serotype project. *PLoS Medicine*, **7**(10), e1000348.

Johnston, C., Bootsma, H.J., Aldridge, C., Manuse, S., Gisch, N., Schwudke, D., Hermans, P.W., Grangeasse, C., Polard, P., Vollmer, W. and Claverys, J.P. (2015). Co-Inactivation of GlnR and CodY Regulators Impacts Pneumococcal Cell Wall Physiology. *PLoS One*, **10**(4), e0123702.

Junges, R., Salvadori, G., Shekhar, S., Amdal, H.A., Periselneris, J.N., Chen, T., Brown, J.S. and Petersen, F.C. (2017). A quorum-sensing system that regulates *Streptococcus pneumoniae* biofilm formation and surface polysaccharide production. *mSphere*, **2**(5), e00324-17.

Kadam, A., Eutsey, R.A., Rosch, J., Miao, X., Longwell, M., Xu, W., Woolford, C.A., Hillman, T., Motib, A.S., Yesilkaya, H., Mitchell, A.P. and Hiller, N.L. (2017). Promiscuous signaling by a regulatory system unique to the pandemic PMEN1 pneumococcal lineage. *PLoS Pathogens*, **13**(5), e1006339.

Kadioglu, A. and Andrew, P.W. (2005). Susceptibility and resistance to pneumococcal disease in mice. *Briefings in Functional Genomics and Proteomics*, **4**(3), 241-247.

Kadioglu, A., Brewin, H., Hartel, T., Brittan, J.L., Klein, M., Hammerschmidt, S. and Jenkinson, H.F. (2010). Pneumococcal protein PavA is important for nasopharyngeal carriage and development of sepsis. *Molecular Oral Microbiology*, **25**(1), 50-60.

Kadioglu, A., Taylor, S., Iannelli, F., Pozzi, G., Mitchell, T.J. and Andrew, P.W. (2002). Upper and lower respiratory tract infection by *Streptococcus pneumoniae* is affected by pneumolysin deficiency and differences in capsule type. *Infection and Immunity*, **70**(6), 2886-2890.

Kadioglu, A., Weiser, J.N., Paton, J.C. and Andrew, P.W. (2008). The role of *Streptococcus pneumoniae* virulence factors in host respiratory colonization and disease. *Nature Reviews Microbiology*, **6**(4), 288-301.

Kahya, H.F., Andrew, P.W. and Yesilkaya, H. (2017). Deacetylation of sialic acid by esterases potentiates pneumococcal neuraminidase activity for mucin utilization, colonization and virulence. *PLoS Pathogens*, **13**(3), e1006263.

Kalia, V.C. (2013). Quorum sensing inhibitors: an overview. *Biotechnology Advances*, **31**(2), 224-245.

Kaplan, S.L. (2004). Review of antibiotic resistance, antibiotic treatment and prevention of pneumococcal pneumonia. *Paediatric Respiratory Reviews*, **5** (Suppl. A), S153-S158.

Karatan, E. and Watnick, P. (2009). Signals, regulatory networks, and materials that build and break bacterial biofilms. *Microbiology and Molecular Biology Reviews*, **73**(2), 310-347.

Karathanasi, G., Bojer, M.S., Baldry, M., Johannessen, B., Wolff, S., Greco, I., Kilstrup, M., Hansen, P.R. and Ingmer, H. (2018). Linear peptidomimetics as potent antagonists of *Staphylococcus aureus* agr quorum sensing. *Scientific Reports*, **8**(1), 3562.

Kashmiri, Z.N. and Mankar, S.A. (2014). Free radicals and oxidative stress in bacteria. *International Journal of Current Microbiology and Applied Sciences*, **3**(9), 34-40.

Kastenbauer, S. and Pfister, H.W. (2003). Pneumococcal meningitis in adults: spectrum of complications and prognostic factors in a series of 87 cases. *Brain*, **126**, 1015-1025.

Kaufman, G.E. and Yother, J. (2007). CcpA-dependent and-independent control of beta-galactosidase expression in *Streptococcus pneumoniae* occurs via regulation of an upstream phosphotransferase system-encoding operon. *Journal of Bacteriology,* **189**(14), 5183-5192.

Kaufmann, G.F., Sartorio, R., Lee, S., Mee, J.M., Altobell, L.J., Kujawa, D.P., Jeffries, E., Clapham, B., Meijler, M.M. and Janda, K.D. (2006). Antibody interference with N-acyl homoserine lactone-mediated bacterial quorum sensing. *Journal of the American Chemical Society*, **128**(9), 2802-2803.

Kavanaugh, J.S., Thoendel, M. and Horswill, A.R. (2007). A role for type I signal peptidase in *Staphylococcus aureus* quorum sensing. *Molecular Microbiology*, **65**(3), 780-798.

Kay, E.J., Yates, L.E., Terra, V.S., Cuccui, J. and Wren, B.W. (2016). Recombinant expression of *Streptococcus pneumoniae* capsular polysaccharides in *Escherichia coli*. *Open Biology,* **6**(4), 150243.

Kietzman, C.C. and Rosch, J.W. (2015). Regulatory Strategies of the Pneumococcus. In: *Streptococcus pneumoniae Molecular Mechanisms of Host-Pathogen Interactions* (ed. by Brown, J., Hammerschmidt, S. and Orihuela, C.). *Elsevier Inc*, pp. 109-128.

Kim, J.O. and Weiser, J.N. (1998). Association of intrastrain phase variation in quantity of capsular polysaccharide and teichoic acid with the virulence of *Streptococcus pneumoniae*. *The Journal of Infectious Diseases*, **177**(2), 368-377.

Kimaro Mlacha, S.Z., Romero-Steiner, S., Hotopp, J.C., Kumar, N., Ishmael, N., Riley, D.R., Farooq, U., Creasy, T.H., Tallon, L.J., Liu, X., Goldsmith, C.S., *et al.* (2013). Phenotypic, genomic, and transcriptional characterization of *Streptococcus pneumoniae* interacting with human pharyngeal cells. *BMC Genomics*, **14**, 383.

King, S.J. (2010). Pneumococcal modification of host sugars: a major contributor to colonization of the human airway? *Molecular Oral Microbiology*, **25**(1), 15-24.

King, S.J., Hippe, K.R. and Weiser, J.N. (2006). Deglycosylation of human glycoconjugates by the sequential activities of exoglycosidases expressed by *Streptococcus pneumoniae*. *Molecular Microbiology*, **59**(3), 961-974.

King, S.J., Hippe, K.R., Gould, J.M., Bae, D., Peterson, S., Cline, R.T., Fasching, C., Janoff, E.N. and Weiser, J.N. (2004). Phase variable desialylation of host proteins that bind to *Streptococcus pneumoniae in vivo* and protect the airway. *Molecular Microbiology,* **54**(1), 159-171.

Kloosterman, T.G., Hendriksen, W.T., Bijlsma, J.J., Bootsma, H.J., van Hijum, S.A., Kok, J., Hermans, P.W. and Kuipers, O.P. (2006a). Regulation of glutamine and glutamate metabolism by GlnR and GlnA in *Streptococcus pneumoniae*. *Journal of Biological Chemistry*, **281**(35), 25097-25109.

Kloosterman, T.G., Bijlsma, J.J.E., Kok, J. and Kuipers, O.P. (2006b). To have neighbour's fare: extending the molecular toolbox for *Streptococcus pneumoniae*. *Microbiology*, **152**(2), 351-359.

Koliou, M.G., Andreou, K., Lamnisos, D., Lavranos, G., Iakovides, P., Economou, C. and Soteriades, E.S. (2018). Risk factors for carriage of *Streptococcus pneumoniae* in children. *BMC Pediatrics*, **18**(1), 144.

Kostyukova, N.N., Volkova, M.O., Ivanova, V.V. and Kvetnaya, A.S. (1995). A study of pathogenic factors of *Streptococcus pneumoniae* strains causing meningitis. *FEMS Immunology and Medical Microbiology*, **10**(2), 133-137.

Kozlowicz, B.K., Shi, K., Gu, Z.Y., Ohlendorf, D.H., Earhart, C.A. and Dunny, G.M. (2006). Molecular basis for control of conjugation by bacterial pheromone and inhibitor peptides. *Molecular Microbiology*, **62**(4), 958-969.

Kreikemeyer, B., McIver, K.S. and Podbielski, A. (2003). Virulence factor regulation and regulatory networks in *Streptococcus pyogenes* and their impact on pathogen-host interactions. *Trends in Microbiology*, **11**(5), 224-232.

Kyaw, M.H., Lynfield, R., Schaffner, W., Craig, A.S., Hadler, J., Reingold, A., Thomas, A.R., Harrison, L.H., Bennett, N.M., Farley, M.M., Facklam, R.R., Jorgensen, J.H., Besser, J., Zell, E.R., Schuchat, A. and Whitney, C.G. (2006). Effect of Introduction of the Pneumococcal Conjugate Vaccine on Drug-Resistant *Streptococcus pneumoniae*. *New England Journal of Medicine*, **354**(14), 1455-1463.

Lai, Y., Peng, H. and Chang, H. (2003). RmpA2, an activator of capsule biosynthesis in *Klebsiella pneumoniae* CG43, regulates K2 *cps* gene expression at the transcriptional level. *Journal of Bacteriology*, **185**(3), 788-800.

Lakowicz, J.R. (2006). Principles of Fluorescence Spectroscopy, Third edition. *Springer Science and Business Media*, Berlin, pp. 529-606.

Lange, R., Wagner, C., de Saizieu, A., Flint, N., Molnos, J., Stieger, M., Caspers, P., Kamber, M., Keck, W. and Amrein, K.E. (1999). Domain organization and molecular characterization of 13 two-component systems identified by genome sequencing of *Streptococcus pneumoniae*. *Gene*, **237**(1), 223-234.

LaSarre, B. and Federle, M.J. (2013). Exploiting quorum sensing to confuse bacterial pathogens. *Microbiology and Molecular Biology Reviews*, **77**(1), 73-111.

LaSarre, B., Aggarwal, C. and Federle, M.J. (2012). Antagonistic Rgg regulators mediate quorum sensing via competitive DNA binding in *Streptococcus pyogenes*. *mBio*, **3**(6), e00333-12.

Lau, G.W., Haataja, S., Lonetto, M., Kensit, S.E., Marra, A., Bryant, A.P., McDevitt, D., Morrison, D.A. and Holden, D.W. (2001). A functional genomic analysis of type 3 *Streptococcus pneumoniae* virulence. *Molecular Microbiology*, **40**(3), 555-571.

Lazazzera, B.A., Solomon, J.M. and Grossman, A.D. (1997). An exported peptide functions intracellularly to contribute to cell density signaling in *B. subtilis*. *Cell*, **89**(6), 917-925.

Lea, W.A. and Simeonov, A. (2011). Fluorescence polarization assays in small molecule screening. *Expert Opinion on Drug Discovery*, **6**(1), 17-32.

Lee, J., Lee, H., Shin, M. and Ryu, W. (2004). Versatile PCR-mediated insertion or deletion mutagenesis. *BioTechniques*, **36**(3), 398-400.

Leonard, B.A., Podbielski, A., Hedberg, P.J. and Dunny, G.M. (1996). *Enterococcus faecalis* pheromone binding protein, PrgZ, recruits a chromosomal oligopeptide permease system to import sex pheromone cCF10 for induction of conjugation. *Proceedings of the National Academy of Sciences of the United States of America*, **93**(1), 260-264.

Lereclus, D., Agaisse, H., Gominet, M., Salamitou, S. and Sanchis, V. (1996). Identification of a *Bacillus thuringiensis* gene that positively regulates transcription of the phosphatidylinositol-specific phospholipase C gene at the onset of the stationary phase. *Journal of Bacteriology*, **178**(10), 2749-2756.

Li, Z. and Nair, S.K. (2012). Quorum sensing: how bacteria can coordinate activity and synchronize their response to external signals? *Protein Science*, **21**(10), 1403-1417.

Liang, S.T., Dennis, P.P. and Bremer, H. (1998). Expression of *lacZ* from the Promoter of the *Escherichia coli spc* Operon Cloned into Vectors Carrying the W205 *trp-lac* Fusion. *Journal of Bacteriology*, **180**(23), 6090-6100.

Lin, H., Peng, Y., Lin, Z., Zhang, S. and Guo, Y. (2015). Development of a conjugate vaccine against invasive pneumococcal disease based on capsular polysaccharides coupled with PspA/family 1 protein of *Streptococcus pneumoniae*. *Microbial Pathogenesis*, **83-84**, 35-40.

Lin, Y., Xu, J., Hu, J., Wang, L., Ong, S.L., Leadbetter, J.R. and Zhang, L. (2003). Acyl-homoserine lactone acylase from Ralstonia strain XJ12B represents a novel and potent class of quorum-quenching enzymes. *Molecular Microbiology*, **47**(3), 849-860.

Liñares, J., Ardanuy, C., Pallares, R. and Fenoll, A. (2010). Changes in antimicrobial resistance, serotypes and genotypes in *Streptococcus pneumoniae* over a 30-year period. *Clinical Microbiology and Infection*, **16**(5), 402-410.

Lindén, S.K., Sutton, P., Karlsson, N.G., Korolik, V. and McGuckin, M.A. (2008). Mucins in the mucosal barrier to infection. *Mucosal Immunology*, **1**(3), 183-197.

Liochev, S.I. and Fridovich, I. (2007). The effects of superoxide dismutase on H_2O_2 formation. *Free Radical Biology and Medicine*, **42**(10), 1465-1469.

Lixa, C., Mujo, A., Anobom, C.D. and Pinheiro, A.S. (2015). A structural perspective on the mechanisms of quorum sensing activation in bacteria. *Annals of the Brazilian Academy of Sciences*, **87**(4), 2189-2203.

Long, J.P., Tong, H.H. and DeMaria, T.F. (2004). Immunization with native or recombinant *Streptococcus pneumoniae* neuraminidase affords protection in the chinchilla otitis media model. *Infection and Immunity*, **72**(7), 4309-4313.

Loose, M., Hudel, M., Zimmer, K.P., Garcia, E., Hammerschmidt, S., Lucas, R., Chakraborty, T. and Pillich, H. (2015). Pneumococcal hydrogen peroxide-induced stress signaling regulates inflammatory genes. *The Journal of Infectious Diseases*, **211**(2), 306-316.

Lulko, A.T., Buist, G., Kok, J. and Kuipers, O.P. (2007). Transcriptome analysis of temporal regulation of carbon metabolism by CcpA in *Bacillus subtilis* reveals additional target genes. *Journal of Molecular Microbiology and Biotechnology*, **12**(1-2), 82-95.

Luo, P. and Morrison, D.A. (2003). Transient association of an alternative sigma factor, ComX, with RNA polymerase during the period of competence for genetic transformation in *Streptococcus pneumoniae*. *Journal of Bacteriology*, **185**(1), 349-358.

Lyon, G.J., Mayville, P., Muir, T.W. and Novick, R.P. (2000). Rational design of a global inhibitor of the virulence response in *Staphylococcus aureus*, based in part on localization of the site of inhibition to the receptor-histidine kinase, AgrC. *Proceedings of the National Academy of Sciences of the United States of America*, **97**(24), 13330-13335.

Maestro, B. and Sanz, J.M. (2016). Choline binding proteins from *Streptococcus pneumoniae*: A dual role as enzybiotics and targets for the design of new antimicrobials. *Antibiotics*, **5**(2), 21.

Maidin, M.S.T., Song, A.A., Jalilsood, T., Sieo, C.C., Yusoff, K. and Rahim, R.A. (2014). Construction of a novel inducible expression vector for *Lactococcus lactis* M4 and *Lactobacillus plantarum* Pa21. *Plasmid*, **74**, 32-38.

Malley, R., Henneke, P., Morse, S.C., Cieslewicz, M.J., Lipsitch, M., Thompson, C.M., Kurt-Jones, E., Paton, J.C., Wessels, M.R. and Golenbock, D.T. (2003). Recognition of pneumolysin by Toll-like receptor 4 confers resistance to pneumococcal infection. *Proceedings of the National Academy of Sciences of the United States of America*, **100**(4), 1966-1971.

Manco, S., Hernon, F., Yesilkaya, H., Paton, J.C., Andrew, P.W. and Kadioglu, A. (2006). Pneumococcal neuraminidases A and B both have essential roles during infection of the respiratory tract and sepsis. *Infection and Immunity*, **74**(7), 4014-4020.

Manefield, M., Rasmussen, T.B., Henzter, M., Andersen, J.B., Steinberg, P., Kjelleberg, S. and Givskov, M. (2002). Halogenated furanones inhibit quorum sensing through accelerated LuxR turnover. *Microbiology*, **148**(4), 1119-1127.

Mansson, M., Nielsen, A., Kjærulff, L., Gotfredsen, C.H., Wietz, M., Ingmer, H., Gram, L. and Larsen, T.O. (2011). Inhibition of virulence gene expression in *Staphylococcus aureus* by novel depsipeptides from a marine photobacterium. *Marine drugs*, **9**(12), 2537-2552.

Marion, C., Burnaugh, A.M., Woodiga, S.A. and King, S.J. (2011). Sialic acid transport contributes to pneumococcal colonization. *Infection and Immunity*, **79**(3), 1262-1269.

Marion, C., Limoli, D.H., Bobulsky, G.S., Abraham, J.L., Burnaugh, A.M. and King, S.J. (2009). Identification of a pneumococcal glycosidase that modifies O-linked glycans. *Infection and Immunity*, **77**(4), 1389-1396.

Marion, C., Stewart, J.M., Tazi, M.F., Burnaugh, A.M., Linke, C.M., Woodiga, S.A. and King, S.J. (2012). *Streptococcus pneumoniae* can utilize multiple sources of hyaluronic acid for growth. *Infection and Immunity*, **80**(4), 1390-1398.

Marketon, M.M., Gronquist, M.R., Eberhard, A. and Gonzalez, J.E. (2002). Characterization of the *Sinorhizobium meliloti sinR/sinI* locus and the production of novel *N*-acyl homoserine lactones. *Journal of Bacteriology*, **184**(20), 5686-5695.

Marks, L.R., Davidson, B.A., Knight, P.R. and Hakansson, A.P. (2013). Interkingdom signaling induces *Streptococcus pneumoniae* biofilm dispersion and transition from asymptomatic colonization to disease. *mBio*, **4**(4), e00438-13.

Marks, L.R., Parameswaran, G.I. and Hakansson, A.P. (2012). Pneumococcal interactions with epithelial cells are crucial for optimal biofilm formation and colonization *in vitro* and *in vivo*. *Infection and Immunity*, **80**(8), 2744–2760.

Marshall, J.E., Faraj, B.H., Gingras, A.R., Lonnen, R., Sheikh, M.A., El-Mezgueldi, M., Moody, P.C., Andrew, P.W. and Wallis, R. (2015). The Crystal Structure of Pneumolysin at 2.0 A Resolution Reveals the Molecular Packing of the Pre-pore Complex. *Scientific Reports*, **5**, 13293.

Martin, B., Granadel, C., Campo, N., Henard, V., Prudhomme, M. and Claverys, J.P. (2010). Expression and maintenance of ComD-ComE, the two-component signal-transduction system that controls competence of *Streptococcus pneumoniae*. *Molecular Microbiology*, **75**(6), 1513-1528.

Mascher, T., Helmann, J.D. and Unden, G. (2006). Stimulus perception in bacterial signal-transducing histidine kinases. *Microbiology and Molecular Biology Reviews*, **70**(4), 910-938.

Mascher, T., Zähner, D., Merai, M., Balmelle, N., de Saizieu, A.B. and Hakenbeck, R. (2003). The *Streptococcus pneumoniae cia* regulon: CiaR target sites and transcription profile analysis. *Journal of Bacteriology*, **185**(1), 60-70.

Mashburn-Warren, L., Morrison, D.A. and Federle, M.J. (2010). A novel double-tryptophan peptide pheromone controls competence in *Streptococcus* spp. via an Rgg regulator. *Molecular Microbiology*, **78**(3), 589-606.

Maskell, J.P., Sefton, A.M. and Hall, L.M. (1997). Mechanism of sulfonamide resistance in clinical isolates of *Streptococcus pneumoniae*. *Antimicrobial Agents Chemotherapy*, **41**(10), 2121-2126.

Mayville, P., Ji, G., Beavis, R., Yang, H., Goger, M., Novick, R.P. and Muir, T.W. (1999). Structure-activity analysis of synthetic autoinducing thiolactone peptides from *Staphylococcus aureus* responsible for virulence. *Proceedings of the National Academy of Sciences of the United States of America*, **96**(4), 1218-1223.

McGee, L., Pletz, M.W., Fobiwe, J.P. and Klugman, K.P. (2015). Antibiotic Resistance of Pneumococci. In: *Streptococcus pneumoniae Molecular Mechanisms of Host-Pathogen Interactions* (ed. by Brown, J., Hammerschmidt, S. and Orihuela, C.). *Elsevier Inc*, pp. 21-40.

McIver, K.S. (2009). Stand-alone response regulators controlling global virulence networks in *Streptococcus pyogenes*. *Contributions to Microbiology*, **16**, 103-119.

MDowell, P., Affas, Z., Reynolds, C., Holden, M.T.G., Wood, S.J., Saint, S., Cockayne, A., Hill, P.J., Dodd, C.E.R. Bycroft, B.W., Chan, W.C. and Williams, P. (2001). Structure, activity and evolution of the group I thiolactone peptide quorum-sensing system of *Staphylococcus aureus*. *Molecular Microbiology*, **41**(2), 503-512.

Mellroth, P., Daniels, R., Eberhardt, A., Ronnlund, D., Blom, H., Widengren, J., Normark, S. and Henriques-Normark, B. (2012). LytA, major autolysin of *Streptococcus pneumoniae*, requires access to nascent peptidoglycan. *Journal of Biological Chemistry*, **287**(14), 11018-11029.

Miles, A.A., Misra, S.S. and Irwin, J.O. (1938). The estimation of the bactericidal power of the blood. *The Journal of Hygiene*, **38**(6), 732–749.

Miller, J.H. (1972). Experiments in molecular genetics. *Cold Spring Harbor Laboratory*, pp. 352–355.

Mitchell, A.M. and Mitchell, T.J. (2010). *Streptococcus pneumoniae*: virulence factors and variation. *Clinical Microbiology and Infection*, **16**(5), 411-418.

Mitchell, T.J., Alexander, J.E., Morgan, P.J. and Andrew, P.W. (1997). Molecular analysis of virulence factors of *Streptococcus pneumoniae. Journal of Applied Microbiology Symposium Supplement*, **83**, 62S-71S.

Mitchell, T.J., Andrew, P.W., Saunders, F.K., Smith, A.N. and Boulnois, G.J. (1991). Complement activation and antibody binding by pneumolysin via a region of the toxin homologous to a human acute-phase protein. *Molecular Microbiology*, **5**(8), 1883-1888.

Miyaji, E.N., Vadesilho, C.F.M., Oliveira, M.L.S., Zelanis, A., Briles, D.E. and Ho, P.L. (2015). Evaluation of a vaccine formulation against *Streptococcus pneumoniae* based on choline-binding proteins. *Clinical and Vaccine Immunology*, **22**(2), 213-220.

Moerke, N.J. (2009). Fluorescence polarization (FP) assays for monitoring peptide-protein or nucleic acid-protein binding. *Current protocols in Chemical Biology*, **1**(1), 1-15.

Moffitt, K.L. and Malley, R. (2011). Next generation pneumococcal vaccines. *Current Opinion in Immunology*, **23**(3), 407-413.

Mohawk, K.L. and O'Brien, A.D. (2011). Mouse models of *Escherichia coli* O157:H7 infection and shiga toxin injection. *Journal of Biomedicine and Biotechnology*, **2011**, 258185.

Mohedano, M.L., Overweg, K., de, l.F., Reuter, M., Altabe, S., Mulholland, F., de Mendoza, D., Lopez, P. and Wells, J.M. (2005). Evidence that the essential response regulator YycF in *Streptococcus pneumoniae* modulates expression of fatty acid biosynthesis genes and alters membrane composition. *Journal of Bacteriology*, **187**(7), 2357-2367.

Monedero, V., Revilla-Guarinos, A. and Zuniga, M. (2017). Physiological Role of Two-Component Signal Transduction Systems in Food-Associated Lactic Acid Bacteria. *Advances in Applied Microbiology*, **99**, 1-51.

Monnet, V. and Gardan, R. (2015). Quorum-sensing regulators in Gram-positive bacteria: 'cherchez le peptide'. *Molecular Microbiology*, **97**(2), 181-184.

Monnet, V., Juillard, V. and Gardan, R. (2016). Peptide conversations in Gram-positive bacteria. *Critical Reviews in Microbiology*, **42**(3), 339-351.

Mookherjee, A., Singh, S. and Maiti, M.K. (2018). Quorum sensing inhibitors: can endophytes be prospective sources? *Archives of Microbiology*, **200** (2), 355-369.

Mook-Kanamori, B.B., Geldhoff, M., van der Poll, T. and van de Beek, D. (2011). Pathogenesis and pathophysiology of pneumococcal meningitis. *Clinical Microbiology Reviews*, **24**(3), 557-591.

Moscoso, M., García, E. and López, R. (2006). Biofilm formation by *Streptococcus pneumoniae*: role of choline, extracellular DNA, and capsular polysaccharide in microbial accretion. *Journal of Bacteriology,* **188**(22), 7785-7795.

Motib, A., Guerreiro, A., Al-Bayati, F., Piletska, E., Manzoor, I., Shafeeq, S., Kadam, A., Kuipers, O., Hiller, L.,Cowen, T., Piletska, S., Andrew,.P.W. and Yesilkaya, H. (2017). Modulation of Quorum Sensing in a Gram-Positive Pathogen by Linear Molecularly Imprinted Polymers with Anti-infective Properties. *Angewandte Chemie International Edition*, **56**(52), 16555-16558.

Munishkina, L.A. and Fink, A.L. (2007). Fluorescence as a method to reveal structures and membrane-interactions of amyloidogenic proteins. *Biochimica et Biophysica Acta*, **1768**(8), 1862-1885.

Muñoz-Elías, E.J., Marcano, J. and Camilli, A. (2008). Isolation of *Streptococcus pneumoniae* biofilm mutants and their characterization during nasopharyngeal colonization. *Infection and Immunity*, **76**(11), 5049-5061.

Murshudov, G.N., Vagin, A.A. and Dodson, E.J. (1997). Refinement of macromolecular structures by the maximum-likelihood method. *Acta Crystallographica Section D Biological Crystallography*, **53**(3), 240-255.

Musher, D.M. (1992). Infections caused by *Streptococcus pneumoniae*: clinical spectrum, pathogenesis, immunity, and treatment. *Clinical Infectious Diseases*, **14**(4), 801-807.

Nakayama, J., Cao, Y., Horii, T., Sakuda, S., Akkermans, A.D., de Vos, W.M. and Nagasawa, H. (2001). Gelatinase biosynthesis-activating pheromone: a peptide lactone that mediates a quorum sensing in *Enterococcus faecalis*. *Molecular Microbiology*, **41**(1), 145-154.

Nakayama, J., Uemura, Y., Nishiguchi, K., Yoshimura, N., Igarashi, Y. and Sonomoto, K. (2009). Ambuic acid inhibits the biosynthesis of cyclic peptide quormones in gram-positive bacteria. *Antimicrobial Agents and Chemotherapy*, **53**(2), 580-586.

Navarro, A., Wu, H. and Wang, S.S. (2009). Engineering problems in protein crystallization. *Separation and Purification Technology*, **68**(2), 129-137.

Neely, M.N., Lyon, W.R., Runft, D.L. and Caparon, M. (2003). Role of RopB in growth phase expression of the SpeB cysteine protease of *Streptococcus pyogenes*. *Journal of Bacteriology*, **185**(17), 5166-5174.

Neidhardt, F.C., Ingraham, J.L. and Schaechter, M. (1990). Physiology of the Bacterial cell: A Molecular Approach. *Sinauer Associates Inc*, Sunderland.

Nelson, A.L., Roche, A.M., Gould, J.M., Chim, K., Ratner, A.J. and Weiser, J.N. (2007). Capsule enhances pneumococcal colonization by limiting mucus-mediated clearance. *Infection and Immunity*, **75**(1), 83-90.

Ng, W. and Bassler, B.L. (2009). Bacterial quorum-sensing network architectures. *Annual Review of Genetics*, **43**, 197-222.

Ng, W.L., Kazmierczak, K.M. and Winkler, M.E. (2004). Defective cell wall synthesis in *Streptococcus pneumoniae* R6 depleted for the essential PcsB putative murein hydrolase or the VicR (YycF) response regulator. *Molecular Microbiology*, **53**(4), 1161-1175.

Ng, W.L., Tsui, H.C. and Winkler, M.E. (2005). Regulation of the *pspA* virulence factor and essential *pcsB* murein biosynthetic genes by the phosphorylated VicR (YycF) response regulator in *Streptococcus pneumoniae*. *Journal of Bacteriology*, **187**(21), 7444-7459.

Nguyen, C.T., Park, S.S. and Rhee, D.K. (2015). Stress responses in *Streptococcus* species and their effects on the host. *Journal of Microbiology*, **53**(11), 741-749.

Novick, R.P. (2003). Autoinduction and signal transduction in the regulation of staphylococcal virulence. *Molecular Microbiology*, **48**(6), 1429-1449.

Novick, R.P. and Geisinger, E. (2008). Quorum sensing in staphylococci. *Annual Review of Genetics*, **42**, 541-564.

Obaro, S. and Adegbola, R. (2002). The pneumococcus: carriage, disease and conjugate vaccines. *Journal of Medical Microbiology*, **51**(2), 98-104.

O'Brien, K.L., Ramakrishnan, M., Finn, A. and Malley, R. (2016). Pneumococcus, Pneumococcal Disease, and Prevention. In: The Vaccine Book (Second Edition) (ed. by Bloom, B.R. and Lambert, P.). *Elsevier Inc*, pp. 225-243.

O'Brien, K.L., Wolfson, L.J., Watt, J.P., Henkle, E., Deloria-Knoll, M., McCall, N., Lee, E., Mulholland, K., Levine, O.S. and Cherian, T. (2009). Burden of disease caused by *Streptococcus pneumoniae* in children younger than 5 years: global estimates. *Lancet*, **374**(9693), 893-902.

Ogunniyi, A.D. and Paton, J.C. (2015). Vaccine Potential of Pneumococcal Proteins. In: *Streptococcus pneumoniae Molecular Mechanisms of Host-Pathogen Interactions* (ed. by Brown, J., Hammerschmidt, S. and Orihuela, C.). *Elsevier Inc*, pp. 59-78.

Ogunniyi, A.D., Mahdi, L.K., Trappetti, C., Verhoeven, N., Mermans, D., Van der Hoek, M.B., Plumptre, C.D. and Paton, J.C. (2012). Identification of genes that contribute to the pathogenesis of invasive pneumococcal disease by *in vivo* transcriptomic analysis. *Infection and Immunity*, **80**(9), 3268-3278.

Olarte, L., Barson, W.J., Barson, R.M., Romero, J.R., Bradley, J.S., Tan, T.Q., Givner, L.B., Hoffman, J.A., Lin, P.L., Hultén, K.G., Mason, E.O. and Kaplan, S.L. (2017). Pneumococcal Pneumonia Requiring Hospitalization in US Children in the 13-Valent Pneumococcal Conjugate Vaccine Era. *Clinical Infectious Diseases*, **64**(12), 1699-1704.

Ong, C.L., Potter, A.J., Trappetti, C., Walker, M.J., Jennings, M.P., Paton, J.C. and McEwan, A.G. (2013). Interplay between manganese and iron in pneumococcal pathogenesis: role of the orphan response regulator RitR. *Infection and Immunity*, **81**(2), 421-429.

Orihuela, C.J., Gao, G., Francis, K.P., Yu, J. and Tuomanen, E.I. (2004). Tissue-specific contributions of pneumococcal virulence factors to pathogenesis. *The Journal of Infectious Diseases*, **190**(9), 1661-1669.

Orihuela, C.J., Mahdavi, J., Thornton, J., Mann, B., Wooldridge, K.G., Abouseada, N., Oldfield, N.J., Self, T., Ala'Aldeen, D.A. and Tuomanen, E.I. (2009). Laminin receptor initiates bacterial contact with the blood brain barrier in experimental meningitis models. *Journal of Clinical Investigation*, **119**(6), 1638-1646.

Oster, C.J. and Phillips, G.J. (2011). Vectors for ligation-independent construction of *lacZ* gene fusions and cloning of PCR products using a nicking endonuclease. *Plasmid*, **66**(3), 180-185.

Owicki, J.C. (2000). Fluorescence polarization and anisotropy in high throughput screening: perspectives and primer. *Journal of Biomolecular Screening*, **5**(5), 297-306.

Paixão, L., Caldas, J., Kloosterman, T.G., Kuipers, O.P., Vinga, S. and Neves, A.R. (2015a). Transcriptional and metabolic effects of glucose on *Streptococcus pneumoniae* sugar metabolism. *Frontiers in Microbiology*, **6**, 1041.

Paixão, L., Oliveira, J., Veríssimo, A., Vinga, S., Lourenço, E.C., Ventura, M.R., Kjos, M., Veening, J.W., Fernandes, V.E., Andrew, P.W., Yesilkaya, H. and Neves, A.R. (2015b). Host glycan sugar-specific pathways in *Streptococcus pneumonia*: galactose as a key sugar in colonisation and infection. *PLoS One*, **10**(4), e0127483.

Pan, X., Ge, J., Li, M., Wu, B., Wang, C., Wang, J., Feng, Y., Yin, Z., Zheng, F. and Cheng, G. (2009). The orphan response regulator CovR: a globally negative modulator of virulence in *Streptococcus suis* serotype 2. *Journal of Bacteriology*, **191**(8), 2601-2612.

Papenfort, K. and Bassler, B.L. (2016). Quorum sensing signal–response systems in Gram-negative bacteria. *Nature Reviews Microbiology*, **14**(9), 576-588.

Parashar, V., Aggarwal, C., Federle, M.J. and Neiditch, M.B. (2015). Rgg protein structure-function and inhibition by cyclic peptide compounds. *Proceedings of the National Academy of Sciences of the United States of America*, **112**(16), 5177-5182.

Parashar, V., Jeffrey, P.D. and Neiditch, M.B. (2013). Conformational change-induced repeat domain expansion regulates Rap phosphatase quorum-sensing signal receptors. *PLoS Biology*, **11**(3), e1001512.

Park, H., Lee, K., Yeo, S., Shin, H. and Holzapfel, W.H. (2017). Autoinducer-2 quorum sensing influences viability of *Escherichia coli* O157:H7 under osmotic and *in vitro* gastrointestinal stress conditions. *Frontiers in Microbiology*, **8**, 1077.

Park, J., Jagasia, R., Kaufmann, G.F., Mathison, J.C., Ruiz, D.I., Moss, J.A., Meijler, M.M., Ulevitch, R.J. and Janda, K.D. (2007). Infection control by antibody disruption of bacterial quorum sensing signalling. *Chemistry and Biology*, **14**(10), 1119-1127.

Parsek, M.R., Val, D.L., Hanzelka, B.L., Cronan, J.E. Jr and Greenberg, E.P. (1999). Acyl homoserine-lactone quorum-sensing signal generation. *Proceedings of the National Academy of Sciences of the United States of America*, **96**(8), 4360-4365.

Paterson, G.K. and Orihuela, C.J. (2010). Pneumococcal microbial surface components recognizing adhesive matrix molecules targeting of the extracellular matrix. *Molecular Microbiology,* **77**(1), 1-5.

Paterson, G.K., Blue, C.E. and Mitchell, T.J. (2006a). An operon in *Streptococcus pneumoniae* containing a putative alkylhydroperoxidase D homologue contributes to virulence and the response to oxidative stress. *Microbial Pathogenesis,* **40**(4), 152-160.

Paterson, G.K., Blue, C.E. and Mitchell, T.J. (2006b). Role of two-component systems in the virulence of *Streptococcus pneumoniae*. *Journal of Medical Microbiology,* **55**, 355-363.

Paton, J.C. (1998). Novel pneumococcal surface proteins: role in virulence and vaccine potential. *Trends in Microbiology,* **6**(3), 85-7.

Perchat, S., Dubois, T., Zouhir, S., Gominet, M., Poncet, S., Lemy, C., Aumont-Nicaise, M., Deutscher, J., Gohar, M., Nessler, S. and Lereclus, D. (2011). A cell-cell communication system regulates protease production during sporulation in bacteria of the *Bacillus cereus* group. *Molecular Microbiology,* **82**(3), 619-633.

Perego, M. (1997). A peptide export-import control circuit modulating bacterial development regulates protein phosphatases of the phosphorelay. *Proceedings of the National Academy of Sciences of the United States of America*, **94**(16), 8612-8617.

Perego, M. and Brannigan, J.A. (2001). Pentapeptide regulation of aspartyl-phosphate phosphatases. *Peptides,* **22**(10), 1541-1547.

Perego, M., Hanstein, C., Welsh, K.M., Djavakhishvili, T., Glaser, P. and Hoch, J.A. (1994). Multiple protein-aspartate phosphatases provide a mechanism for the integration of diverse signals in the control of development in *B. subtilis*. *Cell,* **79**(6), 1047-1055.

Pereira, C.S., Thompson, J.A. and Xavier, K.B. (2013). AI-2-mediated signalling in bacteria. *FEMS Microbiology Reviews,* **37**(2), 156-181.

Pérez Morales, T.G., Ratia, K., Wang, D.S., Gogos, A., Driver, T.G. and Federle, M.J. (2018). A novel chemical inducer of *Streptococcus* quorum sensing acts by inhibiting the pheromone-degrading endopeptidase PepO. *Journal of Biological Chemistry,* **293**(3), 931-940.

Pérez-Pascual, D., Gaudu, P., Fleuchot, B., Besset, C., Rosinski-Chupin, I., Guillot, A., Monnet, V. and Gardan, R. (2015). RovS and its associated signaling peptide form a cell-to-cell communication system required for *Streptococcus agalactiae* pathogenesis. *mBio,* **6**(1), e02306-14.

Perez-Pascual, D., Monnet, V. and Gardan, R. (2016). Bacterial Cell-Cell Communication in the Host via RRNPP Peptide-Binding Regulators. *Frontiers in Microbiology,* **7**, 706.

Perez-Rueda, E., Hernandez-Guerrero, R., Martinez-Nuñez, M., Armenta-Medina, D., Sanchez, I. and Ibarra, J.A. (2018). Abundance, diversity and domain architecture variability in prokaryotic DNA-binding transcription factors. *PLoS One*, **13**(4), e0195332.

Pericone, C.D., Bae, D., Shchepetov, M., McCool, T. and Weiser, J.N. (2002). Short-sequence tandem and nontandem DNA repeats and endogenous hydrogen peroxide production contribute to genetic instability of *Streptococcus pneumoniae*. *Journal of Bacteriology*, **184**(16), 4392-4399.

Pericone, C.D., Overweg, K., Hermans, P.W.M. and Weiser, J.N. (2000). Inhibitory and bactericidal effects of hydrogen peroxide production by *Streptococcus pneumoniae* on other inhabitants of the upper respiratory tract. *Infection and Immunity*, **68**(7), 3990-3997.

Pericone, C.D., Park, S., Imlay, J.A. and Weiser, J.N. (2003). Factors contributing to hydrogen peroxide resistance in *Streptococcus pneumoniae* include pyruvate oxidase (SpxB) and avoidance of the toxic effects of the Fenton reaction. *Journal of Bacteriology*, **185**(23), 6815-6825.

Peterson, S.N., Sung, C.K., Cline, R., Desai, B.V., Snesrud, E.C., Luo, P., Walling, J., Li, H., Mintz, M., Tsegaye, G., Burr, P.C., Do, Y., Ahn, S., Gilbert, J., Fleischmann, R.D. and Morrison, D.A. (2004). Identification of competence pheromone responsive genes in *Streptococcus pneumoniae* by use of DNA microarrays. *Molecular Microbiology*, **51**(4), 1051-1070.

Pettigrew, M.M., Fennie, K.P., York, M.P., Daniels, J. and Ghaffar, F. (2006). Variation in the presence of neuraminidase genes among *Streptococcus pneumoniae* isolates with identical sequence types. *Infection and Immunity*, **74**(6), 3360-3365.

Philips, B.J., Meguer, J.X., Redman, J. and Baker, E.H. (2003). Factors determining the appearance of glucose in upper and lower respiratory tract secretions. *Intensive Care Medicine*, **29**(12), 2204-2210.

Phillips, G.J. (2001). Green fluorescent protein--a bright idea for the study of bacterial protein localization. *FEMS Microbiology Letters*, **204**(1), 9-18.

Pletz, M.W. and Welte, T. (2015). Pneumococcal conjugate vaccine for adults: "It's tough to make predictions, ...". *European Respiratory Journal*, **46**(5), 1265-1268.

Pletz, M.W., Maus, U., Krug, N., Welte, T. and Lode, H. (2008). Pneumococcal vaccines: mechanism of action, impact on epidemiology and adaption of the species. *International Journal of Antimicrobial Agents*, **32**(3), 199-206.

Podbielski, A. and Kreikemeyer, B. (2004). Cell density-dependent regulation: basic principles and effects on the virulence of Gram-positive cocci. *International Journal of Infectious Diseases*, **8**(2), 81-95.

Pomerantsev, A.P., Pomerantseva, O.M., Camp, A.S., Mukkamala, R., Goldman, S. and Leppla, S.H. (2009). PapR peptide maturation: role of the NprB protease in *Bacillus cereus* 569 PlcR/PapR global gene regulation. *FEMS Immunology and Medical Microbiology*, **55**(3), 361-377.

Postma, P.W. and Lengeler, J.W. (1985). Phosphoenolpyruvate:carbohydrate phosphotransferase system of bacteria. *Microbiological Reviews*, **49**(3), 232-269.

Pottathil, M. and Lazazzera, B.A. (2003). The extracellular Phr peptide-Rap phosphatase signaling circuit of *Bacillus subtilis*. *Frontiers in Bioscience*, **8**, d32-45.

Potter, A.J., Kidd, S.P., McEwan, A.G. and Paton, J.C. (2010). The MerR/NmlR family transcription factor of *Streptococcus pneumoniae* responds to carbonyl stress and modulates hydrogen peroxide production. *Journal of Bacteriology*, **192**(15), 4063-4066.

Potter, A.J., Trappetti, C. and Paton, J.C. (2012). *Streptococcus pneumoniae* uses glutathione to defend against oxidative stress and metal ion toxicity. *Journal of Bacteriology*, **194**(22), 6248-6254.

Prato, R., Fortunato, F. and Martinelli, D. (2016). Pneumococcal pneumonia prevention among adults: is the herd effect of pneumococcal conjugate vaccination in children as good a way as the active immunization of the elderly? *Current Medical Research and Opinion*, **32**(3), 543-545.

Prymula, R. and Schuerman, L. (2009). 10-valent pneumococcal nontypeable *Haemophilus influenzae* PD conjugate vaccine: Synflorix™. *Expert Review of Vaccines*, **8**(11), 1479-1500.

Qi, F., Chen, P. and Caufield, P.W. (1999). Functional analyses of the promoters in the lantibiotic mutacin II biosynthetic locus in *Streptococcus mutans*. *Applied and Environmental Microbiology*, **65**(2), 652-658.

Qin, L., Kida, Y., Imamura, Y., Kuwano, K. and Watanabe, H. (2013). Impaired capsular polysaccharide is relevant to enhanced biofilm formation and lower virulence in *Streptococcus pneumoniae*. *Journal of Infection and Chemotherapy*, **19**(2), 261-271.

Qiu, R., Pei, W., Zhang, L., Lin, J. and Ji, G. (2005). Identification of the putative staphylococcal AgrB catalytic residues involving the proteolytic cleavage of AgrD to generate autoinducing peptide. *Journal of Biological Chemistry*, **280**(17), 16695-16704.

Qu, H., Ricklin, D., Bai, H., Chen, H., Reis, E.S., Maciejewski, M., Tzekou, A., DeAngelis, R.A., Resuello, R.R.G. and Lupu, F. (2013). New analogs of the clinical complement inhibitor compstatin with subnanomolar affinity and enhanced pharmacokinetic properties. *Immunobiology*, **218**(4), 496-505.

Queck, S.Y., Jameson-Lee, M., Villaruz, A.E., Bach, T.H.L., Khan, B.A., Sturdevant, D.E., Ricklefs, S.M., Li, M. and Otto, M. (2008). RNAIII-independent target gene control by the agr quorum-sensing system: insight into the evolution of virulence regulation in *Staphylococcus aureus*. *Molecular Cell*, **32**(1), 150-158.

Raineri, D. (2001). Introduction to molecular biology. *Blackwell Science, Inc*.

Ramos-Sevillano, E., Moscoso, M., García, P., García, E. and Yuste, J. (2011). Nasopharyngeal colonization and invasive disease are enhanced by the cell wall hydrolases LytB and LytC of *Streptococcus pneumoniae*. *PLoS One*, **6**(8), e23626.

Rasmussen, T.B. and Givskov, M. (2006). Quorum-sensing inhibitors as anti-pathogenic drugs. *International Journal of Medical Microbiology*, **296**(2-3), 149-161.

Rawlinson, E.L., Nes, I.F. and Skaugen, M. (2002). LasX, a transcriptional regulator of the lactocin S biosynthetic genes in *Lactobacillus sakei* L45, acts both as an activator and a repressor. *Biochimie*, **84**(5-6), 559-567.

Regev-Yochay, G., Trzcinski, K., Thompson, C.M., Lipsitch, M. and Malley, R. (2007). SpxB is a suicide gene of *Streptococcus pneumoniae* and confers a selective advantage in an in vivo competitive colonization model. *Journal of Bacteriology*, **189**(18), 6532-6539.

Reinert, R.R. (2009). The antimicrobial resistance profile of *Streptococcus pneumoniae*. *Clinical Microbiology and Infection*, **15** (Suppl. 3), 7-11.

Reinert, R.R., Paradiso, P. and Fritzell, B. (2010). Advances in pneumococcal vaccines: the 13-valent pneumococcal conjugate vaccine received market authorization in Europe. *Expert Review of Vaccines*, **9**(3), 229-236.

Reller, L.B., Weinstein, M.P., Werno, A.M. and Murdoch, D.R. (2008). Laboratory Diagnosis of Invasive Pneumococcal Disease. *Clinical Infectious Diseases*, **46**(6), 926-932.

Reyrat, J., Pelicic, V., Gicquel, B. and Rappuoli, R. (1998). Counterselectable markers: untapped tools for bacterial genetics and pathogenesis. *Infection and Immunity*, **66**(9), 4011-4017.

Rice, A.J., Woo, J.K., Khan, A., Szypulinski, M.Z., Johnson, M.E., Lee, H. and Lee, H. (2016). Over-expression, purification, and confirmation of *Bacillus anthracis* transcriptional regulator NprR. *Protein Expression and Purification*, **125**, 83-89.

Richards, L., Ferreira, D.M., Miyaji, E.N., Andrew, P.W. and Kadioglu, A. (2010). The immunising effect of pneumococcal nasopharyngeal colonisation; protection against future colonisation and fatal invasive disease. *Immunobiology*, **215**(4), 251-263.

Ring, A., Weiser, J.N. and Tuomanen, E.I. (1998). Pneumococcal trafficking across the blood-brain barrier. Molecular analysis of a novel bidirectional pathway. *The Journal of Clinical Investigation*, **102**(2), 347-360.

Robb, M., Hobbs, J.K., Woodiga, S.A., Shapiro-Ward, S., Suits, M.D.L., McGregor, N., Brumer, H., Yesilkaya, H., King, S.J. and Boraston, A.B. (2017). Molecular Characterization of N-glycan degradation and transport in *Streptococcus pneumoniae* and its contribution to virulence. *PLoS Pathogens*, **13**(1), e1006090.

Rocha-Estrada, J., Aceves-Diez, A.E., Guarneros, G. and de la Torre, M. (2010). The RNPP family of quorum-sensing proteins in Gram-positive bacteria. *Applied Microbiology and Biotechnology*, **87**(3), 913-923.

Rose, M.C. and Voynow, J.A. (2006). Respiratory tract mucin genes and mucin glycoproteins in health and disease. *Physiological Reviews*, **86**(1), 245-278.

Rossi, A.M. and Taylor, C.W. (2011). Analysis of protein-ligand interactions by fluorescence polarization. *Nature Protocols*, **6**(3), 365.

Rubins, J.B. and Janoff, E.N. (1998). Pneumolysin: a multifunctional pneumococcal virulence factor. *Journal of Laboratory and Clinical Medicine*, **131**(1), 21-27.

Ruby, E.G. (1996). Lessons from a cooperative, bacterial-animal association: The *Vibrio fischeri-Euprymna scolopes* light organ symbiosis. *Annual Reviews of Microbiology*, **50**(1), 591-624.

Rutherford, S.T. and Bassler, B.L. (2012). Bacterial quorum sensing: its role in virulence and possibilities for its control. *Cold Spring Harbor Perspectives in Medicine*, **2**(11), a012427.

Saito, H. and Miura, K. (1963). Preparation of transforming deoxyribonucleic acid by phenol treatment. *Biochimica et Biophysica Acta*, **72**, 619-629.

Saleh, M., Bartual, S.G., Abdullah, M.R., Jensch, I., Asmat, T.M., Petruschka, L., Pribyl, T., Gellert, M., Lillig, C.H., Antelmann, H., Hermoso, J.A. and Hammerschmidt, S. (2013). Molecular architecture of *Streptococcus pneumoniae* surface thioredoxin-fold lipoproteins crucial for extracellular oxidative stress resistance and maintenance of virulence. *EMBO Molecular Medicine*, **5**(12), 1852-1870.

Sambrook, J., Fritsch, E.F. and Maniatis, T. (1989). Molecular Cloning: A Laboratory Manual. *Cold Spring Harbor Laboratory Press*, New York.

Samen, U.M., Eikmanns, B.J. and Reinscheid, D.J. (2006). The transcriptional regulator RovS controls the attachment of *Streptococcus agalactiae* to human epithelial cells and the expression of virulence genes. *Infection and Immunity*, **74**(10), 5625-5635.

Sanders, J.W., Leenhouts, K., Burghoorn, J., Brands, J.R., Venema, G. and Kok, J. (1998). A chloride-inducible acid resistance mechanism in *Lactococcus lactis* and its regulation. *Molecular Microbiology*, **27**(2), 299-310.

Sanford, M. (2012). Pneumococcal polysaccharide conjugate vaccine (13-valent, adsorbed): in older adults. *Drugs*, **72**(9), 1243-1255.

Schauder, S., Shokat, K., Surette, M.G. and Bassler, B.L. (2001). The LuxS family of bacterial autoinducers: biosynthesis of a novel quorum-sensing signal molecule. *Molecular Microbiology*, **41**(2), 463-476.

Sebert, M.E., Palmer, L.M., Rosenberg, M. and Weiser, J.N. (2002). Microarray-based identification of *htrA*, a *Streptococcus pneumoniae* gene that is regulated by the CiaRH two-component system and contributes to nasopharyngeal colonization. *Infection and Immunity*, **70**(8), 4059-4067.

Seitz, P. and Blokesch, M. (2014). DNA transport across the outer and inner membranes of naturally transformable *Vibrio cholerae* is spatially but not temporally coupled. *mBio*, **5**(4), e01409-14.

Seshasayee, A.S.N., Sivaraman, K. and Luscombe, N.M. (2011). An overview of prokaryotic transcription factors : A Summary of Function and Occurrence in Bacterial Genomes. In: A Handbook of Transcription Factors (ed. by Hughes, T.R.). Sub-cellular Biochemistry, vol 52. *Springer*, *Dordrecht*, pp. 7-23.

Shak, J.R., Ludewick, H.P., Howery, K.E., Sakai, F., Yi, H., Harvey, R.M., Paton, J.C., Klugman, K.P. and Vidal, J.E. (2013). Novel role for the *Streptococcus pneumoniae* toxin pneumolysin in the assembly of biofilms. *mBio*, **4**(5), e00655-13.

Shakhnovich, E.A., King, S.J. and Weiser, J.N. (2002). Neuraminidase expressed by *Streptococcus pneumoniae* desialylates the lipopolysaccharide of *Neisseria meningitidis* and *Haemophilus influenzae*: a paradigm for interbacterial competition among pathogens of the human respiratory tract. *Infection and Immunity*, **70**(12), 7161-7164.

Shapiro, J.A. (1969). Mutations caused by the insertion of genetic material into the galactose operon of *Escherichia coli*. *Journal of Molecular Biology*, **40**(1), 93-105.

Shi, K., Brown, C.K., Gu, Z.Y., Kozlowicz, B.K., Dunny, G.M., Ohlendorf, D.H. and Earhart, C.A. (2005). Structure of peptide sex pheromone receptor PrgX and PrgX/pheromone complexes and regulation of conjugation in *Enterococcus faecalis*. *Proceedings of the National Academy of Sciences of the United States of America*, **102**(51), 18596-18601.

Shiri, T., Datta, S., Madan, J., Tsertsvadze, A., Royle, P., Keeling, M.J., McCarthy, N.D. and Petrou, S. (2017). Indirect effects of childhood pneumococcal conjugate vaccination on invasive pneumococcal disease: a systematic review and meta-analysis. *The Lancet Global Health*, **5**(1), e51-e59.

Short, K. R. and Diavatopoulos, D. A. (2015). Nasopharyngeal Colonization with *Streptococcus pneumoniae*. In: *Streptococcus pneumoniae* Molecular Mechanisms of Host-Pathogen Interactions (ed. by Brown, J., Hammerschmidt, S. and Orihuela, .C.). *Elsevier Inc*, pp. 279–291.

Short, K.R., Habets, M.N., Hermans, P.W. and Diavatopoulos, D.A. (2012). Interactions between *Streptococcus pneumoniae* and influenza virus: a mutually beneficial relationship? *Future Microbiology*, **7**(5), 609-624.

Shrestha, S., Foxman, B., Weinberger, D.M., Steiner, C., Viboud, C. and Rohani, P. (2013). Identifying the interaction between influenza and pneumococcal pneumonia using incidence data. *Science Translational Medicine*, **5**(191), 191ra84.

Siehnel, R., Traxler, B., An, D.D., Parsek, M.R., Schaefer, A.L. and Singh, P.K. (2010). A unique regulator controls the activation threshold of quorum-regulated genes in *Pseudomonas aeruginosa*. *Proceedings of the National Academy of Sciences of the United States of America*, **107**(17), 7916-7921.

Sifri, C.D. (2008). Quorum sensing: bacteria talk sense. *Clinical Infectious Diseases*, **47**(8), 1070-1076.

Singh, A. and Dutta, A.K. (2018). Pneumococcal Vaccines - How Many Serotypes are Enough? *The Indian Journal of Pediatrics*, **85**(1), 47-52.

Singh, A., Upadhyay, V., Upadhyay, A.K., Singh, S.M. and Panda, A.K. (2015). Protein recovery from inclusion bodies of *Escherichia coli* using mild solubilization process. *Microbial Cell Factories*, **14**(1), 41.

Singh, S.M. and Panda, A.K. (2005). Solubilization and refolding of bacterial inclusion body proteins. *Journal of Bioscience and Bioengineering*, **99**(4), 303-310.

Sings, H.L. (2017). Pneumococcal conjugate vaccine uses in adults - Addressing an unmet medical need for non-bacteremic pneumococcal pneumonia. *Vaccine*, **35**(40), 5406-5417.

Skaugen, M., Andersen, E.L., Christie, V.H. and Nes, I.F. (2002). Identification, characterization, and expression of a second, bicistronic, operon involved in the production of lactocin S in *Lactobacillus sakei* L45. *Applied and Environmental Microbiology*, **68**(2), 720-727.

Slamti, L. and Lereclus, D. (2002). A cell-cell signaling peptide activates the PlcR virulence regulon in bacteria of the *Bacillus cereus* group. *The EMBO Journal*, **21**(17), 4550-4559.

Snyder, L., Peters, J.E., Henkin, T.M. and Champness, W. (2013). Molecular Genetics of Bacteria, Fourth Edition. *American Society of Microbiology*, Washington, DC.

Solano-Collado, M.V. (2014). Molecular characterization of the MgaSpn transcriptional regulator of *Streptcoccus pneumoniae.* PhD Thesis. *Complutense University of Madrid*, Spain.

Solovyev, V. and Salamov, A. (2011). Automatic Annotation of Microbial Genomes and Metagenomic Sequences. In: *Metagenomics and its applications in agriculture, Biomedicine and Environmental Studies* (ed. by Li, R.W.). *Nova Science Publishers*, pp. 61-78.

Sonenshein, A.L. (2007). Control of key metabolic intersections in *Bacillus subtilis*. *Nature Reviews Microbiology*, **5**(12), 917.

Southward, C.M. and Surette, M.G. (2002). The dynamic microbe: green fluorescent protein brings bacteria to light. *Molecular Microbiology*, **45**(5), 1191-1196.

Spellerberg, B., Cundell, D.R., Sandros, J., Pearce, B.J., Idanpaan-Heikkila, I., Rosenow, C. and Masure, H.R. (1996). Pyruvate oxidase, as a determinant of virulence in *Streptococcus pneumoniae*. *Molecular Microbiology*, **19**(4), 803-813.

Srivastava, S. and Srivastava, P.S. (2003). Understanding bacteria. *Springer Science & Business Media, B.Y.*

Stewart, G.S.A.B. and Williams, P. (1992). *lux* genes and the applications of bacterial bioluminescence. *Microbiology*, **138**(7), 1289-1300.

Straume, D., Stamsås, G.A. and Håvarstein, L.S. (2015). Natural transformation and genome evolution in *Streptococcus pneumoniae*. *Infection, Genetics and Evolution*, **33**, 371-380.

Stroeher, U.H., Kidd, S.P., Stafford, S.L., Jennings, M.P., Paton, J.C. and McEwan, A.G. (2007). A pneumococcal MerR-like regulator and S-nitrosoglutathione reductase are required for systemic virulence. *The Journal of Infectious Diseases*, **196**(12), 1820-1826.

Sulavik, M.C. and Clewell, D.B. (1996). Rgg is a positive transcriptional regulator of the *Streptococcus gordonii gtfG* gene. *Journal of Bacteriology*, **178**(19), 5826-5830.

Sulavik, M.C., Tardif, G. and Clewell, D.B. (1992). Identification of a gene, *rgg*, which regulates expression of glucosyltransferase and influences the Spp phenotype of *Streptococcus gordonii* Challis. *Journal of Bacteriology*, **174**(11), 3577-3586.

Sully, E.K., Malachowa, N., Elmore, B.O., Alexander, S.M., Femling, J.K., Gray, B.M., DeLeo, F.R., Otto, M., Cheung, A.L., Edwards, B.S., Sklar, L.A., Horswill, A.R., Hall, P.R. and Gresham, H.D. (2014). Selective chemical inhibition of *agr* quorum sensing in *Staphylococcus aureus* promotes host defense with minimal impact on resistance. *PLoS Pathogens*, **10**(6), e1004174.

Syvitski, R.T., Tian, X., Sampara, K., Salman, A., Lee, S.F., Jakeman, D.L. and Li, Y. (2007). Structure-activity analysis of quorum-sensing signaling peptides from *Streptococcus mutans*. *Journal of Bacteriology*, **189**(4), 1441-1450.

Terra, V.S., Homer, K.A., Rao, S.G., Andrew, P.W. and Yesilkaya, H. (2010). Characterization of novel β-Galactosidase activity that contributes to glycoprotein degradation and virulence in *Streptococcus pneumoniae*. *Infection and Immunity*, **78**(1), 348-357.

Terra, V.S. (2011). Pneumococcal interactions with mucin. PhD Thesis. *Department of Infection, Immunity and Inflammation, University of Leicester*, UK.

Tettelin, H., Nelson, K.E., Paulsen, I.T., Eisen, J.A., Read, T.D., Peterson, S., Heidelberg, J., DeBoy, R.T., Haft, D.H., Dodson, R.J., Durkin, A.S., *et al.* (2001). Complete genome sequence of a virulent isolate of *Streptococcus pneumoniae*. *Science*, **293**(5529), 498-506.

Thoendel, M. and Horswill, A.R. (2009). Identification of *Staphylococcus aureus* AgrD residues required for autoinducing peptide biosynthesis. *Journal of Biological Chemistry*, **284**(33), 21828-21838.

Thoendel, M., Kavanaugh, J.S., Flack, C.E. and Horswill, A.R. (2011). Peptide signaling in the staphylococci. *Chemical Reviews*, **111**(1), 117-151.

Throup, J.P., Koretke, K.K., Bryant, A.P., Ingraham, K.A., Chalker, A.F., Ge, Y., Marra, A., Wallis, N.G., Brown, J.R., Holmes, D.J., Rosenberg, M. and Burnham, M.K. (2000). A genomic analysis of two-component signal transduction in *Streptococcus pneumoniae*. *Molecular Microbiology*, **35**(3), 566-576.

Titgemeyer, F. and Hillen, W. (2002). Global control of sugar metabolism: a Gram-positive solution. *Antonie van Leeuwenhoek*, **82**(1-4), 59–71.

Tong, H.H., Blue, L.E., James, M.A. and DeMaria, T.F. (2000). Evaluation of the virulence of a *Streptococcus pneumoniae* neuraminidase-deficient mutant in nasopharyngeal colonization and development of otitis media in the chinchilla model. *Infection and Immunity*, **68**(2), 921-924.

Trappetti, C. and Oggioni, M.R. (2015). Biofilm Formation Under *In Vitro* Conditions. In: *Streptococcus Pneumoniae Molecular Mechanisms of Host-Pathogen Interactions* (ed. by Brown, J., Hammerschmidt, S. and Orihuela, C.). *Elsevier Inc*, pp. 245-255.

Trappetti, C., Kadioglu, A., Carter, M., Hayre, J., Iannelli, F., Pozzi, G., Andrew, P.W. and Oggioni, M.R. (2009). Sialic acid: a preventable signal for pneumococcal biofilm formation, colonization, and invasion of the host. *The Journal of Infectious Diseases*, **199**(10), 1497-1505.

Trappetti, C., van der Maten, E., Amin, Z., Potter, A.J., Chen, A.Y., van Mourik, P.M., Lawrence, A.J., Paton, A.W. and Paton, J.C. (2013). Site of isolation determines biofilm formation and virulence phenotypes of *Streptococcus pneumoniae* serotype 3 clinical isolates. *Infection and Immunity*, **81**(2), 505-513.

Tretiakova, A.P., Little, C.S., Blank, K.J. and Jameson, B.A. (2000). Rational design of cytotoxic T-cell inhibitors. *Nature Biotechnology*, **18**(9), 984.

Tuomanen, E. (2006). *Streptococcus pneumoniae*. In: *The Prokaryotes* (ed. by Dworkin, M., Falkow, S., Rosenberg, E., Schleifer, KH. and Stackebrandt, E.). *Springer US*, New York, NY, pp. 149–162.

Turan, N. B., Chormey, D. S., Büyükpınar, Ç., Engin, G. O. and Bakirdere, S. (2017). Quorum sensing: little talks for an effective bacterial coordination. *TrAC Trends in Analytical Chemistry*, **91**, 1-11.

Uchiyama, S., Carlin, A.F., Khosravi, A., Weiman, S., Banerjee, A., Quach, D., Hightower, G., Mitchell, T.J., Doran, K.S. and Nizet, V. (2009). The surface-anchored NanA protein promotes pneumococcal brain endothelial cell invasion. *Journal of Experimental Medicine*, **206**(9), 1845-1852.

Uliczka, F., Pisano, F., Kochut, A., Opitz, W., Herbst, K., Stolz, T. and Dersch, P. (2011). Monitoring of gene expression in bacteria during infections using an adaptable set of bioluminescent, fluorescent and colorigenic fusion vectors. *PLoS One*, **6**(6), e20425.

Ulijasz, A.T., Andes, D.R., Glasner, J.D. and Weisblum, B. (2004). Regulation of iron transport in *Streptococcus pneumoniae* by RitR, an orphan response regulator. *Journal of Bacteriology*, **186**(23), 8123-8136.

Ulijasz, A.T., Falk, S.P. and Weisblum, B. (2009). Phosphorylation of the RitR DNA-binding domain by a Ser-Thr phosphokinase: implications for global gene regulation in the streptococci. *Molecular Microbiology*, **71**(2), 382-390.

Uroz, S., Chhabra, S.R., Cámara, M., Williams, P., Oger, P. and Dessaux, Y. (2005). *N*-Acylhomoserine lactone quorum-sensing molecules are modified and degraded by *Rhodococcus erythropolis* W2 by both amidolytic and novel oxidoreductase activities. *Microbiology*, **151**, 3313-3322.

Vallejo, L.F. and Rinas, U. (2004). Strategies for the recovery of active proteins through refolding of bacterial inclusion body proteins. *Microbial Cell Factories*, **3**(1), 11.

van de Rijn, I. and Kessler, R.E. (1980). Growth characteristics of group A streptococci in a new chemically defined medium. *Infection and Immunity*, **27**(2), 444-448.

van der Poll, T. and Opal, S.M. (2009). Pathogenesis, treatment, and prevention of pneumococcal pneumonia. *The Lancet*, **374**(9700), 1543-1556.

Verbeke, F., De Craemer, S., Debunne, N., Janssens, Y., Wynendaele, E., Van de Wiele, C. and De Spiegeleer, B. (2017). Peptides as quorum sensing molecules: measurement techniques and obtained levels *in vitro* and *in vivo*. *Frontiers in Neuroscience*, **11**, 183.

Verma, R. and Khanna, P. (2012). Pneumococcal conjugate vaccine: a newer vaccine available in India. *Human Vaccines and Immunotherapeutics*, **8**(9), 1317-1320.

Vickerman, M.M. and Minick, P.E. (2002). Genetic analysis of the *rgg-gtfG* junctional region and its role in *Streptococcus gordonii* glucosyltransferase activity. *Infection and Immunity*, **70**(4), 1703-1714.

Wang, D., Lu, J., Yu, J., Hou, H., Leenhouts, K., Van Roosmalen, M.L., Gu, T., Jiang, C., Kong, W. and Wu, Y. (2018). A novel PspA protein vaccine intranasal delivered by bacterium-like particles provides broad protection against pneumococcal pneumonia in mice. *Immunological Investigations*, **47**(4), 403-415.

Wardal, E., Sadowy, E. and Hryniewicz, W. (2010). Complex nature of enterococcal pheromone-responsive plasmids. *Polish Journal of Microbiology*, **59**(2), 79-87.

Warner, J.B. and Lolkema, J.S. (2003). CcpA-dependent carbon catabolite repression in bacteria. *Microbiology and Molecular Biology Reviews*, **67**(4), 475-490.

Waters, C.M. and Bassler, B.L. (2005). Quorum sensing: cell-to-cell communication in bacteria. *Annual Review of Cell and Developmental Biology*, **21**, 319-346.

Widdel, F. (2007). Theory and measurement of bacterial growth. *Grundpraktikum Mikrobiologie, Universität Bremen*, **4**(11), 1-11.

Widdowson, C.A., Klugman, K.P. and Hanslo, D. (1996). Identification of the tetracycline resistance gene, tet(O), in *Streptococcus pneumoniae*. *Antimicrobial agents and chemotherapy*, **40**(12), 2891-2893.

Willenborg, J., Greeff, A., Jarek, M., Valentin-Weigand, P. and Goethe, R. (2014). The CcpA regulon of *Streptococcus suis* reveals novel insights into the regulation of the streptococcal central carbon metabolism by binding of CcpA to two distinct binding motifs. *Molecular Microbiology*, **92**(1), 61-83.

Wohlleben, W., Mast, Y., Stegmann, E. and Ziemert, N. (2016). Antibiotic drug discovery. *Microbial Biotechnology*, **9**(5), 541-548.

World Health Organization (2007). Pneumococcal conjugate vaccine for childhood immunization--WHO position paper. *Weekly epidemiological record*, **82**(12), 93-104.

World Health Organization (2008). 23-valent pneumococcal polysaccharide vaccine: WHO position paper. *Weekly epidemiological record*, **83**(42), 373-384.

World Health Organization (2012). Pneumococcal vaccines WHO position paper-2012-recommendations. *Vaccine*, **30**(32), 4717- 4718.

Xu, G., Li, X., Andrew, P.W. and Taylor, G.L. (2008a). Structure of the catalytic domain of *Streptococcus pneumoniae* sialidase NanA. *Acta Crystallographica Section F Structural Biology and Crystallization Communications*, 64(Pt 9), 772-775.

Xu, G., Potter, J.A., Russell, R.J.M., Oggioni, M.R., Andrew, P.W. and Taylor, G.L. (2008b). Crystal Structure of the NanB Sialidase from *Streptococcus pneumoniae*. *Journal of Molecular Biology*, **384**(2), 436-449.

Yang, J., Evans, B.A. and Rozen, D.E. (2010). Signal diffusion and the mitigation of social exploitation in pneumococcal competence signalling. *Proceedings of the Royal Society B: Biological Sciences*, **277**(1696), 2991–2999.

Yesilkaya, H., Andisi, V.F., Andrew, P.W. and Bijlsma, J.J. (2013). *Streptococcus pneumoniae* and reactive oxygen species: an unusual approach to living with radicals. *Trends in Microbiology*, **21**(4), 187-195.

Yesilkaya, H., Kadioglu, A., Gingles, N., Alexander, J.E., Mitchell, T.J. and Andrew, P.W. (2000). Role of manganese-containing superoxide dismutase in oxidative stress and virulence of *Streptococcus pneumoniae*. *Infection and Immunity,* **68**(5), 2819-2826.

Yesilkaya, H., Manco, S., Kadioglu, A., Terra, V.S. and Andrew, P.W. (2008). The ability to utilize mucin affects the regulation of virulence gene expression in *Streptococcus pneumoniae*. *FEMS Microbiology Letters*, **278**(2), 231-235.

Yesilkaya, H., Spissu, F., Carvalho, S.M., Terra, V.S., Homer, K.A., Benisty, R., Porat, N., Neves, A.R. and Andrew, P.W. (2009). Pyruvate formate lyase is required for pneumococcal fermentative metabolism and virulence. *Infection and Immunity,* **77**(12), 5418-5427.

Yildirim, I., Shea, K.M. and Pelton, S.I. (2015). Pneumococcal Disease in the Era of Pneumococcal Conjugate Vaccine. *Infectious Disease Clinics of North America* , **29**(4), 679-697.

Yu, J., Bryant, A.P., Marra, A., Lonetto, M.A., Ingraham, K.A., Chalker, A.F., Holmes, D.J., Holden, D., Rosenberg, M. and McDevitt, D. (2001). Characterization of the *Streptococcus pneumoniae* NADH oxidase that is required for infection. *Microbiology,* **147**, 431-438.

Zhang, D., Luo, G., Ding, X. and Lu, C. (2012). Preclinical experimental models of drug metabolism and disposition in drug discovery and development. *Acta Pharmaceutica Sinica B,* **2**(6), 549-561.

Zhang, L., Gray, L., Novick, R.P. and Ji, G. (2002). Transmembrane topology of AgrB, the protein involved in the post-translational modification of AgrD in *Staphylococcus aureus*. *The Journal of Biological Chemistry,* **277**(38), 34736-34742.

Zhang, X. and Bremer, H. (1995). Control of the *Escherichia coli rrnB* P1 promoter strength by ppGpp. *The Journal of Biological Chemistry*, **270**(19), 11181-11189.

Zheng, F., Ji, H., Cao, M., Wang, C., Feng, Y., Li, M., Pan, X., Wang, J., Qin, Y., Hu, F. and Tang, J. (2011). Contribution of the Rgg transcription regulator to metabolism and virulence of *Streptococcus suis* serotype 2. *Infection and Immunity*, **79**(3), 1319-1328.

Zhi, X. (2017). Investigation in to the functional role of Rgg Quorum Sensing Systems in *Streptococcus pneumoniae*. PhD Thesis. *Department of Infection, Immunity and Inflammation, University of Leicester*, UK.

Zhi, X., Abdullah, I.T., Gazioglu, O., Manzoor, I., Shafeeq, S., Kuipers, O.P., Hiller, N.L., Andrew, P.W. and Yesilkaya, H. (2018). Rgg-Shp regulators are important for pneumococcal colonization and invasion through their effect on mannose utilization and capsule synthesis. *Scientific Reports,* **8**(1), 6369.

Zhu, L. and Lau, G.W. (2011). Inhibition of competence development, horizontal gene transfer and virulence in *Streptococcus pneumoniae* by a modified competence stimulating peptide. *PLoS Pathogens,* **7**(9), e1002241.

Zhu, L., Lin, J., Kuang, Z., Vidal, J.E. and Lau, G.W. (2015). Deletion analysis of *Streptococcus pneumoniae* late competence genes distinguishes virulence determinants that are dependent or independent of competence induction. *Molecular Microbiology*, **97**(1), 151-165.

Zomer, A.L., Buist, G., Larsen, R., Kok, J. and Kuipers, O.P. (2007). Time-resolved determination of the CcpA regulon of *Lactococcus lactis* subsp. *cremoris* MG1363. *Journal of Bacteriology*, **189**(4), 1366-1381.

Zouhir, S., Perchat, S., Nicaise, M., Perez, J., Guimaraes, B., Lereclus, D. and Nessler, S. (2013). Peptide-binding dependent conformational changes regulate the transcriptional activity of the quorum-sensor NprR. *Nucleic Acids Research*, **41**(16), 7920-7933.

Zwijnenburg, P.J., van der Poll, T., Florquin, S., van Deventer, S.J., Roord, J.J. and van Furth, A.M. (2001). Experimental pneumococcal meningitis in mice: a model of intranasal infection. *The Journal of Infectious Diseases*, **183**(7), 1143-1146.